CALIFORNIA COOPERATIVE OCEANIC FISHERIES INVESTIGATIONS

Reports

VOLUME 52
JANUARY 1 TO DECEMBER 31, 2011

Cooperating Agencies:

CALIFORNIA DEPARTMENT OF FISH AND GAME
UNIVERSITY OF CALIFORNIA, SCRIPPS INSTITUTION OF OCEANOGRAPHY
NATIONAL OCEANIC AND ATMOSPHERIC ADMINISTRATION, NATIONAL MARINE FISHERIES SERVICE

CALCOFI COORDINATOR John N. Heine
EDITOR John N. Heine

Printed and distributed December 2011, La Jolla, California
ISSN 0575-3317

CONTENTS

Part I

REPORTS, REVIEW, AND PUBLICATIONS

REPORT OF THE CALCOFI COMMITTEE 2010

SIO HIGHLIGHTS

Four CalCOFI cruises were carried out successfully over the last 12 months. The standard CalCOFI measurements were made on all 4 cruises, with the addition of pelagic trawl samples on the Scripps cruises collected to a depth of 750 m using a Motoda-Oozeki-Hu trawl (MOHT) with 5 m^2 mouth opening and 1.7 mm mesh. The net samples primarily the micronekton (krill and midwater fauna), as well as larger fish larvae and juvenile fishes. The trawl sampling complements the multifrequency acoustic sampling on the Scripps CalCOFI cruises, providing ground-truth data on species and size composition. In 2011, an MOHT opening-closing system (MOHTOCS) will be added to the summer cruise based on a Hydrobios mini multinet sampler with 5 cod ends, which will enable depth stratified sampling of acoustic targets to 1000 m depth. The acoustic and trawl sampling system was funded by a grant from the Gordon and Betty Moore Foundation. The California Current Ecosystem Long-Term Ecological Research (CCE LTER) program will provide funding for the ship-time for trawl sampling.

The CCE LTER program continues to use CalCOFI cruises to further characterize the biogeochemical cycles and populations of planktonic organisms. This year CCE purchased an advanced laser fluorometry system that uses seawater from the ship's flow-through system to characterize the phytoplankton community structure and probe the physiological health of the phytoplankton. It is hoped that this system will provide insight into spatial patterns of phytoplankton community structure and physiological state on scales smaller than the station spacing.

Since July 2009 we have been deploying drifters on CalCOFI cruises from the Institute for Computational Earth System Science (ICESS). The objective of this project is to observe and study near-shore ocean circulation off the southern California coast. The drifters record their position with GPS every 10 minutes and transmit their position data in near real-time to a web-based host computer. This sort of time and space resolution enables characteristic nearshore circulation patterns to be properly resolved. Links to tracks of drifters deployed on recent cruises can be found on the CalCOFI Web site.

The most interesting oceanographic event during 2010/2011 was the transition from El Niño conditions to La Niña conditions. Even though these events were among the strongest equatorial events, their effects on oceanographic conditions off southern California were relatively small, in contrast to the 1998/9 event.

Starting in 2011, NOAA funding for the Scripps CalCOFI program will be carried out through the new Cooperative Institute for Marine Ecosystems and Climate (CIMEC). This entails a significant increase in the overhead rate charged for nonship and equipment items from 16.7% to 54.5%. This places considerable strain on our NOAA funders in the current fiscal climate.

The CalCOFI program submitted a proposal to the South Coast Marine Protected Areas (MPA) Baseline Monitoring Program, "An integrated monitoring and assessment program for southern California Marine Protected Areas". The proposed study would monitor fish communities, seabirds and marine mammals within and outside south coast MPAs through Continuous Underway Fish Egg Sampling (CUFES), net tows for the ichthyoplankton, acoustics, and seabird and marine mammal observations. The proposal was led by PI Tony Koslow (SIO) and co-PIs Ralf Goericke (SIO), Andrew Thompson (SWFSC), and Bill Sydeman (Farallon Institute).

The past year has seen increased interest in changing oxygen levels in the California Current and their ecological impacts. Based on analysis of the CalCOFI oxygen time series, McClatchie et al. (2010) reported that midwater oxygen concentrations were about 20% lower in the early and most recent decades of the record. Koslow et al. (in press) examined patterns in the CalCOFI ichthyoplankton time series and observed that the dominant pattern was the coherent response of a broad suite of mesopelagic and, to a lesser extent, demersal species to these changes in oxygen levels. The larval abundance for 24 species of mesopelagic fishes was lower by a factor of 2.6 in the 1950s and 1960s and since 2000. There was a highly significant correlation ($r = 0.74$) with midwater oxygen concentrations. Global climate models predict a 20%–40% decline in midwater oxy-

gen levels in the coming century due to the impacts of global warming, which will increase stratification of near-surface waters and reduce ventilation of the deep ocean. This is the first report of its potential ecological impact. These midwater fishes serve as important forage for a variety of piscivorous fishes, squids, marine mammals and seabirds.

CDFG HIGHLIGHTS

Marine Regulatory Changes

In 2010, the Commission undertook ten rule-making actions that addressed marine and anadromous species' aquaculture. In 2010, Fish and Game unveiled its new Automated License Data System (ALDS) for sport fishing and commercial licensing and fees. The new system will create an accurate customer database, reduce the risk of fraud, improve DFG's ability to manage resources, as well as meet state and federal mandates for tracking customer data. The Commission adopted changes to the herring, rock crab, and groundfish commercial fisheries and sport fishing regulations related to salmon, lobster hoop nets, and groundfish. Permits and procedures for aquaculture-restricted species were revised and updated as were sport fishing and commercial licensing requirements.

Marine Life Protection Act

The FG Commission adopted a network of 36 Marine Protected Areas (MPAs) encompassing approximately 187 square miles in the south coast region, defined as state waters between Point Conception (Santa Barbara County) and the California border with Mexico under the Marine Life Protection Act (MLPA). The MLPA requires California to reexamine and redesign its system of MPAs with the goals to, increase their effectiveness in protecting the state's marine life and habitats, marine ecosystems, and marine natural heritage. In addition, emergency action was taken to establish a portion of the Stewarts Point State Marine Reserve in Sonoma County along the north central coast as a State Marine Conservation to allow for the recreational take from shore of specified marine aquatic plants, finfish and marine invertebrates including red abalone with specified gear types. This emergency action was taken to avoid serious harm to the health, safety and general welfare of the Kashia Band of Pomo Indians of the Stewarts Point Rancheria.

Aquaculture and Bay Management

The Aquaculture and Bay Management Project completed the California Pacific Herring Commercial Fishing Regulations Supplemental Environmental Document (SED) for the 2010–11 season. The SED included herring spawning biomass estimates, as well as spawning population, and commercial catch assessments. The SED evaluated DFG's recommendation to reopen the commercial herring season with a quota equal to 5% of the 2009–10 spawning biomass estimate. The spawning population increased from the historic low in 2008–09, primarily due to favorable estuarine and oceanic conditions. The spawning biomass estimate for the 2009–10 season is 38,409 tons, which is below the historic average (1978–79 to present) of 49,428 tons. However, this is a significant increase over the 2008–09 season estimate of 4,833 tons, which demonstrates the potential for stock recovery with conservative management of the fishery.

Staff worked collaboratively with the newly formed San Francisco Bay Herring Research Association. The Association was formed by the fishing industry with funds set aside from the Cosco-Busan oil spill settlement dedicated for Pacific herring research.

Invertebrate Fisheries Management

Project staff have been working to develop a stock assessment model for lobster in California. A surplus production model with size/age structure information was evaluated for its use in stock assessment. The NOAA fishery toolbox version of this model, ASPIC, failed with the datasets available. Currently, a model based on Beverton and Holt Invariant methods, used to evaluate the Baja fishery, is being evaluated for its use in estimating California stocks. Furthermore, staff worked with Ocean Protection Council funds to digitize 20 years of commercial logbook information as well as the newly introduced recreational lobster report card data. Project biologists completed a joint study with San Diego State University examining lobster movement patterns in San Diego Bay. The size of the lobster population in the bay was estimated at 94,000 to 108,000 lobsters. Tagging suggests that 75% of the lobsters reside near the bay mouth and 25% residing within the submerged rocky structures and seagrass beds along North Island and Shelter Island. There were no patterns of movement toward the mouth or away from the interior of the bay.

The abalone project continued stock assessment work in northern and southern California. The southern Pink/Green AbaloneTranslocation/Aggregation Study began in 2008 with funding from NOAA Protected Resources. Study sites were established at San Clemente and Santa Catalina Islands in 2009 and 2010, and monitoring is ongoing. Abalone were tagged with both a PIT tag and external-numbered tag so that each abalone could be individually identified. Green abalone were translocated at both Santa Catalina and San Clemente Islands at two sites on each island with two additional sites as controls. The white abalone restoration project funded by

a NOAA Section 6 Protected Species grant began this year. This three year collaborative project will focus on developing and implementing restoration tools for the critically endangered white abalone working with the captive breeding program at the Bodega Marine Lab, University of California, Davis.

A status report on the northern California red abalone recreational fishery was completed and submitted to the Fish and Game Commission. The main finding was the average density of red abalone at eight index sites was near the Abalone Recovery and Management Plan trigger which would require a reduction in the Total Allowable Catch (TAC) from the current level approximately 280,000 red abalone per year. Abalone staff completed surveys at Stornetta Ranch an area that had been a "defacto" reserve as access was restricted due to private property but was opened to the public in 2005. In 2010, the site was once again closed to abalone fishing as part of the MLPA process and there was a modest increase in abalone density at the site.

Dungeness crab megalopae trapping continued in Bodega Bay and Humboldt Bay. This monitoring of recruitment will be used to develop a predictive population abundance index for the fishery, complementing a similar index in Oregon. In 2010, Humboldt Bay clam creel survey results were published which used bootstrap methods, to compare with historic surveys. The 2008 survey revealed an important shift in the species composition of clams in the fishery, a decrease in fishing effort, and unique methods of take within Humboldt Bay, compared to the historical survey period of 1975–1989.

Ocean Salmon

In 2010, California ocean salmon fisheries were open for the first time in two years due to an increase in the abundance of Sacramento River Fall Chinook (SRFC). Despite the opening, fisheries were still constrained to satisfy both the National Marine Fisheries Service and the Pacific Fishery Management Council's guidance to target the upper end of the SRFC's conservation objective of 122,000–180,000 hatchery and natural adults to return to spawn the following fall. Commercial ocean salmon fisheries were opened for the first time since 2007 for a 70 day season. Estimated total commercial landings were 15,100 Chinook salmon (103 mt). Average nominal ex-vessel price was $12.00/kg ($5.50/lb), with an ex-vessel value of $1.2 million. The recreational fishing season increased significantly for a season total of 500 days across four major port areas. In 2009, only a 10-day sport fishery was allowed in northern California. An estimated 14,700 Chinook were landed in 2010, compared to 700 salmon landed in 2009. Approximately 48,800 anglers fished for salmon in 2010 compared to 5,400 salmon anglers in 2009.

Groundfish

New recreational and commercial groundfish regulations were developed for 2011–2012 and approved by the Pacific Fishery Management Council (Council) in June 2010. However, following revisions by the National Marine Fisheries Service (NMFS) and delays in the federal rulemaking process, the new regulations did not go into effect until June 9, 2011 in state waters. Key recreational regulation changes include: simplified gear restrictions, renamed management areas, and liberalized lingcod seasons and size limits, cabezon bag limits, California scorpionfish depth restrictions, and central California season and depth restrictions.

Commercial management strategy highlights for 2010 included preparing environmental documents for the Trawl Rationalization Program, federal commercial regulations, and federal Groundfish Fishery Management Plan amendments. In addition, staff provided updated sections for the regulatory package that increased the statewide cabezon total allowable catch for both the commercial and recreational sectors as indicated by the Council and NMFS, based upon the results of the 2009 cabezon stock assessment. Groundfish staff also collaborated with NMFS to complete a historical catch reconstruction of recreational and commercial landings information, and completed a set of California sheephead research maps for California and Mexico to summarize existing research and to help identify information gaps. Completion of both tasks will contribute information to future stock assessments.

For the 2010 recreational outreach program, groundfish project staff disseminated regulation information to anglers and the public at 12 ports from Crescent City to Morro Bay. Statewide, staff distributed approximately 5,000 rockfish identification flyers and barotrauma information flyers to anglers, license vendors, tackle shops, CDFG wardens and CDFG offices. Lastly, staff helped hire, train, equip, schedule and supervise new California Recreational Fisheries Survey staff in preparation for the new Department program implementation in 2011.

Recreational Fisheries

The California Recreational Fisheries Survey (CRFS) began in January 2004 to provide catch and effort estimates for marine recreational finfish fisheries. The CRFS generates monthly estimates of total recreational catch for four modes of fishing (beach/bank and shore, piers and jetties, commercial passenger fishing vessels, and private vessels launched from public launch ramps) for six geographic districts along California's 1,100 miles of coast. The data are used by state and federal regulators to craft regulations to protect fish stocks and provide recreational fishing opportunities. This is a multipart sur-

vey which uses field sampling and telephone surveys. In 2010, approximately 45 samplers worked to gather the field data. The CRFS samplers interviewed more than 73,000 anglers at over 500 sites, and examined more than 146,000 fish. The licensed angler telephone survey completed almost 26,000 interviews. For more information, go the CDFG's Marine Region Website: http://www.dfg.ca.gov/marine/crfs.asp.

Fishery-Independent SCUBA Assessment

In southern California, project staff published their analysis of historic Department barred sand bass tag and recapture data collected in the 1960s and 1990s. Staff also collaborated with researchers at California State University, Long Beach on a study that utilized active acoustic telemetry to quantify the fine-scale movement patterns of barred sand bass, *Paralabrax nebulifer*, within the spawning aggregations on Huntington Beach Flats.

In central California, project staff have completed three years of study using traps, hook and line, and mark-recapture methods to determine relative abundance, size, and movements of several nearshore groundfishes in Carmel Bay. Data were collected at several sites, including the newly created Carmel Pinnacles State Marine Reserve. In total, 5,632 fish were tagged and ~3% were recaptured or visually resighted during scuba surveys. Gopher rockfish (*Sebastes carnatus*), black-and-yellow rockfish (*S. chrysomelas*), kelp greenling (*Hexagrammos decagrammus*) and cabezon (*Scorpaenichthys marmoratus*) were the most abundant species caught by traps. Blue rockfish (*Sebastes mystinus*), gopher rockfish, olive rockfish (*Sebastes serranoides*) and kelp rockfish (*Sebastes atrovirens*) were the most abundant species caught using hook and line gear. Age, growth, and maturity information were collected for kelp greening from 2008 to 2010. Maturity data collected indicates that kelp greenling spawn from September to January. Preliminary estimates of size at 50% maturity are 275 mm TL for females and 215 mm TL for males. For more information see http://www.dfg.ca.gov/marine/scuba/index.asp.

NOAA HIGHLIGHTS

2010 CalCOFI Field Season

The field season of 2010 will be noted and remembered for two significant milestones. On August 3, 2010 we officially said goodbye to the NOAA ship *David Starr Jordan* as she was decommissioned during ceremonies conducted at the NOAA Fisheries facility on Lake Washington in Seattle. The *David Starr Jordan* was built by the Christy Corporation in Sturgeon Bay, Wisconsin, and launched in 1964 for the U.S. Bureau of Commercial Fisheries, which later became part of NOAA as the National Marine Fisheries Service. Since her commissioning in 1966 in San Diego, over 1.3 million nautical miles have passed under the *Jordan*'s keel during almost 9,000 days at sea. Many of those miles were earned during CalCOFI surveys.

Shortly after we witnessed the *Jordan*'s decommissioning, the newest member of the NOAA fleet, the *Bell M. Shimada,* was commissioned on August 25, 2010 in Puget Sound, Washington. The *Shimada* is the fourth ship of the FSV (Fisheries Survey Vessel) class built in Moss Point, Mississippi, by V.T. Halter. The 208 foot vessel represents the latest in state-of-the-art technology with a suite of scientific acoustic sensors mounted on an acoustically quiet platform. The *Shimada* will serve West Coast scientists to support NOAA's mission to protect, restore and manage living marine, coastal and ocean resources. The *Bell M. Shimada* is scheduled to conduct the spring CalCOFI survey beginning in March of 2011.

The beginning of the field season for CalCOFI's 61st year saw the remnants of a moderate equatorial El Niño which persisted into May of 2010. Positive equatorial SST anomalies became negative by June as a weak La Niña system established itself and persisted through the remainder of 2010. Local anomalies within the CCLME remained neutral to negative throughout the year. The 2010 field season saw the successful completion of the standard quarterly CalCOFI surveys and the Pacific sardine (*Sardinops sagax*) biomass survey using a total of three different research vessels but also was noted for additional activities towards the latter part of the year.

Over the course of the 2010 calendar year a total of four individual surveys were completed using three different vessels: SIO's R/V *New Horizon*, the NOAA ship *Miller Freeman*, and the chartered fishing vessel F/V *Frosti*. Throughout these combined surveys a total of 407 Bongo tows, 349 Pairovet tows, 271 Manta tows, 421 CTD casts, 43 Oozeki trawls and 1,898 CUFES samples were collected during the field season. Also collected during the season were approximately 2,900 hours of acoustic measurements, 1,200 hours of marine mammal and bird observations and 52 satellite-tracked current drifters were deployed. In addition, 98 surface trawls were conducted netting approximately 270 kilograms of adult and juvenile Pacific sardine for the annual spawning biomass estimate.

Sandwiched in between the summer and fall surveys, members of the CalCOFI seagoing group and SWFSC scientists were given the opportunity to put the recently commissioned NOAA ship *Bell M. Shimada* through her paces. Over two five-day periods the ship conducted an abbreviated CalCOFI survey within the Southern California Bight and performed high resolution sampling of a glider identified mesoscale front over the Santa Rosa Ridge. Between these two short surveys, researchers were able to able to identify strengths and weaknesses

of the new platform and present suggestions which will hopefully benefit users and operators before the ship goes into full operation next year.

California Current Ecosystem Surveys

During spring 2010, the Fisheries Resources Division of the Southwest Fisheries Science Center conducted a survey of the California Current Ecosystem (CCE) off the U.S. West Coast, from the Mexican to Canadian borders. The cruise was an expansion of the standard CalCOFI sampling and was conducted during April and May using the NOAA ship *Miller Freeman* and the contract vessel F/V *Frosti*.

The survey was conducted in an anomalously warm year, when the spring spawning Pacific sardine (*Sardinops sagax*) were subjected to El Niño conditions. Prior to the survey, during March 2010, sea-surface temperatures, averaged along the entire West Coast, were 0.5 to 1 degree Celsius (0.9 to 1.8 Fahrenheit) warmer than normal, and at points off southern California were as much as 1.6 degrees Celsius (2.9 degrees Fahrenheit) higher than normal. The most unusually high temperatures were mapped around Santa Catalina and San Clemente islands. Spawn of sardine was only observed north of the Channel Islands and was concentrated off the central California coast. No evidence of sardine spawn was found off northern California, Oregon, or Washington during the survey.

Acoustic data provided a wealth of information on the distributions of euphausiids and fish, particularly Pacific sardine and jack and Pacific mackerel. This information is relevant to stock assessments and ecosystem investigations, for example seabird-prey interactions. Consistent with the aforementioned observations of sardine spawn, sardine were acoustically mapped south of San Francisco and north of the Channel Islands. Again, consistent with their seasonal migration pattern, no sardine were sampled north of California with the acoustic-trawl method.

Mammal and seabird observations were conducted only from the NOAA ship *Miller Freeman*, between San Diego and San Francisco. A notable feature of the marine mammal sightings was a school of approximately 850 Pacific white-sided dolphin (*Lagenorhynchus obliquidens*) and about 650 northern right whale dolphins (*Lissodelphis borealis*). Observations of this megapod of mixed dolphin species spanned over six miles, nearshore, south of Monterey. By far, the most numerous seabird species encountered by the *Miller Freeman* was red-necked phalarope, accounting for more than 75% of the total. On 12 April, an estimated 10,000 birds of this species were encountered in less than one hour, spanning about 10 nm, just north of the Channel Islands. Cassin's auklets and humpback whales were also observed feeding in the area. A NOAA Technical Memorandum is planned to summarize the preliminary results from the spring 2010 CCE survey.

CalCOFI Ichthyoplankton Update

During the past year the SWFSC Ichthyoplankton Ecology continued to retroactively update to current standards larval fish identifications from 1951 to the present. Identification of Pacific whiting (hake) and jack and Pacific mackerels collected in the CalCOFI bongo net samples are now complete from 1986 to the present for the eggs and 1966 to the present for the larvae.

We have identified market squid paralarvae from CalCOFI bongo samples dating back to 1997 and from neuston samples dating back to 1981. All cephalopod paralarvae have been identified in all samples and included in the database since 2008. Additional cephalopod paralarvae species were identified sporadically from CalCOFI samples from 1997 to 2007. The presence or absence of jumbo squid paralarvae has been of particular interest in recent years; ommastrephid paralarvae are rare in CalCOFI collections, and none have been collected since summer of 2008.

We collaborated with Ron Burton and his students at SIO on the development of a high-throughput system for molecular identification of ichthyoplankton in the California Current Ecosystem. The ultimate aim of this project is to provide accurate, near real-time identifications of fish eggs, which often are difficult or impossible to identify to species using traditional morphological characters. When fully developed, this method will be enable us to identify with accuracy the spawning locations of several taxa of that are valuable to sport or commercial fisheries such as Pacific hake, Pacific mackerel, white seabass and California barracuda.

We analyzed the larval fish assemblage from the winter CalCOFI cruises in 2002–2004. These cruises coincided with detailed sampling within the Cowcod Conservation Area (CCA), a marine reserves embedded within the core CalCOFI sample frame. We evaluated simultaneously assemblage dynamics from the relatively large (CalCOFI) and small (CCA) spatial scales. We found that the larval fish assemblage changed significantly during a transition from La Nina (2002) to El Niño conditions (2003–2004) at the smaller scale, but was relatively stable through time at the larger scale. A manuscript describing these results is being prepared.

PaCOOS—Pacific Coast Ocean Observing System

In 2010 the focus for PaCOOS was to continue to serve biological data via the Internet as well as increase survey coverage in support of the California Current (CC) ecological observing system. Data access and data

interoperability underlie ecological forecasts and integrated ecosystem assessments in the California Current. Collaboration and partnerships within NOAA and between NOAA and academic scientists remains the primary means of developing these forecasts and assessments.

Data management activities in 2010 centered on merging and access to the historical CalCOFI biological and physical data housed at the Southwest Fisheries Science Center and the Scripps Institution of Oceanography, respectively. Currently, PaCOOS is developing a map with a series of overlays of ongoing ocean surveys carried out in the California Current Large Marine Ecosystem. The surveys include government, academic and other research nonprofit organizations from Mexico to Canada. The final activity to highlight is the quarterly reporting of climate and ecosystem science and management activities in the California Current that started in 2008. The quarterlies can also be accessed on the PaCOOS Web site.

The 2011 plans for PaCOOS include continued coordination with the Regional Associations on joint proposal development with an emphasis on data management, ecological forecasting and assessment, and increasing ocean observing data when opportunities arise.

Other Surveys Conducted in the California Current

Lines 60 and 67. MBARI, NPS, and UCSC scientists continue to occupy Line 67 off Monterey and Line 60 off San Francisco with NOAA and MBARI funding. A consistent suite of samples has now been collected quarterly along Line 67 since 1997, and nearshore since 1989. In recent years this shipboard work has been augmented by mooring, AUV, and glider programs. The focus has been on: 1) seasonal/interannual/decadal temporal variations; and 2) Monterey Bay/upwelling system/California Current spatial variations. The data document California Current and Upwelling System dynamics over several ENSO cycles as well as a decadal to multidecadal shift.

In 2010 we were able to occupy Line 67 five times. The first two cruises (winter and spring) were in association with southern CalCOFI. The first cruise was on the F/V *New Horizon* in February (S110) and the second on the NOAA ship *Miller Freeman* in April (S210). MBARI and UCSC personnel collected nutrient, phytoplankton and zooplankton samples during a summer cruise aboard the NOAA ship *McArthur II* in July (S310) with support from the Monterey Bay National Marine Sanctuary. A fall cruise out to 67–135 (400 km from shore) was made aboard the MBARI vessel *Western Flyer* in September (S410). Finally, a cruise was made aboard the Point Sur in November (S510). Data from the three cruises have been processed and quality-controlled, and are available both in the MBARI Biological Oceanography database and online. 2010 was a near-normal year, although with warmer than average start due to the effects of the 2009–10 El Niño. MBARI moorings documented warmer than average and fresher conditions during the first 4 months of the year. Lower than average surface chlorophyll and higher than average deep chlorophyll accompanied the warmer and fresher conditions. The last 8 months of the year were average or slightly cooler and saltier than average. As analysis and publication proceed, the 2010 work will enable data-based exploration of: 1) the 2009–10 El Niño; 2) the putative decadal shift to cool conditions after 1998; and 3) secular climate change.

Trinidad Head Line. NOAA's National Marine Fisheries Service, Southwest Fisheries Science Center and Humboldt State University continue collaborative ocean observing efforts off northern California. Data are collected at roughly monthly intervals along the Trinidad Head line, which consists of six stations along a transect extending approximately 27 nm due west from Trinidad Head. Standard sampling protocols include CTD casts to a maximum depth of 150 m, collection of zooplankton samples by oblique bongo tows (505 μm to formalin and 335 μm mesh to EtOH) from a maximum depth of 100 m and vertical 0.5 m ring net tows from a maximum depth of 100 m (200 μm mesh to formalin). These observations are being augmented by CTD data and ring net samples collected at the first five stations during research cruises lead by Dr. Jeff Abell (HSU, Oceanography) to quantify ocean acidity and other hydrographic and chemical parameters under a grant funded through the Ocean Protection Council. All cruises in 2010 and into 2011 were conducted aboard Humboldt State University's R/V *Coral Sea*. On NMFS-HSU PaCOOS cruises, sampling of offshore stations occurs after dark, but sampling over the shelf is conducted during daylight hours. Sampling on OPC cruises is typically conducted during daylight hours.

Here we report hydrographic and chemical data for Station TH02 (41°3.50'N, 124°16.00'W). These data show the dissipation of coastal effects of the 2009–2010 El Niño as strong upwelling resumed in the late spring and summer of 2010. Modest warming occurred in late summer and fall 2010, but was not nearly as pervasive as during the previous year's. Observations into 2011 indicate the effects of variable upwelling and downwelling during winter and early spring.

Shark Surveys

The SWFSC's shark research group is responsible for collecting data to support the management of blue (*Prionace glauca*), shortfin mako (*Isurus oxyrinchus*) and common thresher sharks (*Alopias vulpinus*), all of which are

common in off the U.S. West Coast and taken in regional fisheries, primarily as juveniles. Common thresher and mako sharks have the greatest commercial value and are also targeted by sport fishers. Although the blue shark has little market importance in the United States, it is a leading bycatch species in a number of U.S. fisheries and is targeted in Mexico. One of the primary methods used by NOAA Fisheries to collect data on the three species is fisheries independent surveys. These surveys provide catch data that allow us to track trends in abundance. Use of fisheries data alone for estimating population status is complicated by changes in regulations, fishing methods, and areas over time. The surveys also provide the opportunity to deploy conventional and electronic tags, obtain biological samples and conduct studies on age and growth.

Juvenile Mako and Blue Shark Survey. In 2010, the SWFSC conducted its seventeenth juvenile shark survey for mako and blue sharks since 1994. The annual abundance survey was completed between July 14 and August 12, 2010. Working aboard F/V *Ventura II*, a team of scientists and volunteers fished a total of 5,956 hooks during 29 daytime sets inside seven focal areas within the Southern California Bight. Survey catch totaled 13 shortfin makos, 25 blue sharks, 18 pelagic rays (*Pteroplatytrygon violacea*), 10 opah (*Lampris guttatus*), and 1 mola (*Mola mola*). The preliminary data indicate that the nominal survey catch rate was 0.057 per 100 hook-hours for shortfin mako and 0.105 per 100 hook-hours for blue sharks. The nominal CPUE for both blue and shortfin mako sharks were the lowest in survey history. There is a declining trend in nominal CPUE for both species over the time series of the survey.

Additional research projects were also conducted during the cruise. An experiment begun in 2009 was continued to examine the potential for using a composite of rare earth metals to reduce shark bycatch. The metals were secured close to the baited hooks and catch rates on treatment and control hooks were compared. Thirteen sets were completed for the experiment during the 2010 cruise to add to the 25 sets conducted in 2009. Preliminary results indicate that the rare earth metals did not affect the catch rate of shortfin mako or blue sharks as they were caught on the experimental hooks and control hooks in almost equal numbers. These results differ from those found on some coastal shark species where the deterrents proved effective at lowering catch rates. The data are being further examined based on size, sex, and other potential factors before drawing final conclusions.

Other objectives of the cruise were to deploy satellite and conventional tags, and to collect biological samples from sharks and swordfish. A total of 242 conventional tags were deployed on 50 shortfin mako sharks and 192 blue sharks. A total of 310 DNA samples were collected including samples from 53 shortfin mako and 244 blue sharks. In a cooperative effort with TOPP (Tagging of Pacific Pelagics), 10 electronic tags were deployed on sharks to examine the habitat-use patterns in the California Current system. Four shortfin mako sharks ranging from 147 to 203 cm fork length were released with a radio position transmitting tag (SPOT). Six blue sharks ranging from 175 to 221 cm fork length were also released with SPOT tags. Satellite tagging of mako and blue sharks has been ongoing since 2002 and reveals site fidelity of both species to the Southern California Bight waters in the summer months with excursions throughout the entire temperate Eastern Pacific Ocean during other seasons.

Neonate Common Thresher Shark Survey. The common thresher shark pre-recruit index and nursery ground survey was initiated in 2003 to develop a fisheries-independent index of pre-recruit abundance and has been conducted in each year since. Common thresher sharks are the most valuable sharks taken in commercial fisheries off California and are also frequently caught by recreational fishermen. In September 2010, the SWFSC team worked aboard the F/V *Outer Banks.* Forty-eight longline sets were made in relatively shallow, nearshore waters and a total of 4,800 hooks were fished during the 18-day cruise. Shark catch included 295 common thresher, 5 smoothhound (*Mustelus*), 2 spiny dogfish (*Squalus acanthias*), and 1 leopard (*Triakis semifasciata*) shark. Two hundred and sixty-eight sharks were tagged with conventional tags and 280 DNA samples were collected.

The preliminary survey data indicate that the average nominal catch rate by set was 3.75 per 100 hook-hours for common thresher sharks. This is the highest catch rate since the inception of the survey. The distribution of common threshers is very patchy and areas of high abundance are not consistent across years. In all years, a large percentage of the catch has been neonates, which were found in all areas surveyed. In addition to providing important information on abundance and distributions, the thresher shark pre-recruit survey enhances other ongoing research at SWFSC, including age and growth, feeding, and habitat utilization studies.

West Coast Midwater Trawl Survey. The twenty-ninth annual West Coast midwater trawl survey was conducted during the peak of the upwelling season from May 2 through May 26, 2011. The survey targets pelagic juvenile rockfish for fisheries oceanography studies and for developing indices of year class strength for stock assessments, although in recent years the focus of the survey has expanded to encompass an ecosystem survey focusing on the productivity and distribution of the forage assemblage (particularly krill).

Although in recent years the survey has typically

been conducted on larger research vessels over a 6 week period, and spanned the region from Cape Mendocino to the U.S./Mexico border, budget constraints led to a cancellation of the anticipated cruise on the newly christened NOAA ship *Bell M. Shimada*, and a very abbreviated (over time and space) survey was conducted onboard the chartered fishing vessel F/V *Excalibur*. As a result, research activities did not include daytime oceanographic or seabird/marine mammal surveys (for the first time since 1985), nor was it possible to collect multibeam acoustic data, and the duration and spatial extent of the survey was truncated considerably. High winds during much of the survey and an abundance of jellyfish in many areas also constrained the survey. Consequently, a reduced number of trawls (66) and CTD casts (70) were conducted in 2011. By contrast, from 2003–2010 the average number of tows per year was 144, with an average of 251 CTD casts. Future surveys are anticipated to take place on the NOAA ship *Bell M. Shimada*, which should result in a return to greater spatial and temporal resolution and data availability. A companion survey north of Cape Mendocino also took place in 2011, consistent with a collaborative survey run by the NWFSC and the Pacific Whiting Conservation Cooperative surveys conducted from 2001–2009. Efforts to standardize and pool the results of these surveys for the development of coastwide indices of abundance are ongoing.

Sampling is focused on young-of-the-year (YOY) groundfish, particularly rockfishes (*Sebastes* spp.), Pacific whiting (*Merluccius productus*), lingcod (*Ophiodon elongatus*), rex sole (*Glyptocephalus zachirus*), and sanddabs (*Citharichthys* spp.). Data are used in stock assessments for several of these species. In addition, a wide variety of other epipelagic micronekton are captured and enumerated, including krill (*Euphausia pacifica* and *Thysanoessa spinifera*), market squid (*Loligo opalescens*), lanternfishes (*Diaphus theta*, *Tarletonbeania crenularis*, *Stenobrachius leucopsarus, Lampanyctus* spp.), northern anchovy (*Engraulis mordax*), and Pacific sardine (*Sardinops sagax*). The entire assemblage is analyzed to develop indicators of ecosystem state and productivity, which relates the productivity of higher trophic level species that forage on much or all of this assemblage. As with the 2009 and 2010 data, results from 2011 continue to represent a return to cool, high productivity conditions similar to the 1999 to 2003 period for many groups, with the highest catches since this period being observed for juvenile rockfish, sanddabs and market squid in particular. Additional information on these data and efforts are reported in the State of the California Current report in this volume.

REVIEW OF SELECTED CALIFORNIA FISHERIES FOR 2010: COASTAL PELAGIC FINFISH, MARKET SQUID, OCEAN SALMON, GROUNDFISH, HIGHLY MIGRATORY SPECIES, DUNGENESS CRAB, SPINY LOBSTER, SPOT PRAWN, KELLET'S WHELK, AND WHITE SEABASS

CALIFORNIA DEPARTMENT OF FISH AND GAME
Marine Region
8604 La Jolla Shores Drive
La Jolla, CA 92037
DSweetnam@dfg.ca.gov

SUMMARY

In 2010, commercial fisheries landed an estimated 197,956 metric tons (t) of fish and invertebrates from California ocean waters (fig. 1). This represents an increase of 23% from the 160,615 t landed in, and a nearly 22% decline from the peak landings of 252,568 t observed in 2000. The preliminary ex-vessel economic value of commercial landings in 2010 was nearly $175 million, an increase of 56% from the $112 million in 2009.

California market squid once again emerged as the largest volume and highest value fishery in the state with over nearly 130,000 t landed and an ex-vessel value of approximately $73.8 million, a 30% increase from the $56.9 million of 2009. Such increases can be attributed to favorable environmental conditions.

Pacific sardine landings experienced a 10% decrease in volume during 2010. This was largely due to a more restrictive harvest guideline (HG) based on declining stock abundance. Similar to 2008, the fishery exhibited the characteristics of a "derby." Other coastal pelagic finfish that also experienced a drop in landings were Pacific mackerel and northern anchovy. Jack mackerel, on the other hand, registered an increase in landings.

In 2010, 9,960 t of commercial groundfish were landed in California, a slight decrease over 2009 landings. However, the ex-vessel value of the fishery of $20.8 million saw an increase over 2009 values.

In terms of highly migratory species, 367 t of swordfish with an ex-vessel value of $2.2 million were landed in 2010, a 10% decline from landings in 2009 of 407 t. Albacore was the most abundant tuna caught in California waters, as well as along the West Coast. Commercial landings totaled 11,855 t with an ex-vessel value $1.8 million. Recreational albacore landings in California from Commercial Passenger Fishing Vessels (CPFV) totaled 33,679 fish.

Dungeness crab landings more than doubled in 2010 compared to 2009, and remained one of the more valuable state fisheries with an ex-vessel value of $34.2 million. Concerns regarding increased effort in the fishery have prompted strong support for a statewide, tiered trap limit program. As of May 2011, legislation is pending on creation of a trap limit program.

A total of 319 t, the California spiny lobster (*Panulirus interruptus*) was commercially landed in 2010. While substantially lower than the recent peak of 403 t in 2006, the 2010 landing total continues a trend of 300 t, or more, lobsters landed per calendar year since 2000. The 2010 ex-vessel value of the lobster fishery was a record $11.13 million.

Spot prawn landings in 2010 were 110 t, a 14% decrease from 2009 although market demand was high. The decrease in landings is most likely due to the poor weather and sea conditions that characterized 2010.

Kellet's whelk supports a growing commercial fishery, but is not important recreationally with 67.5 t landed in 2010 with an ex-vessel value of $117,000. The California Fish and Game Commission (Commission) has identified Kellet's whelk as an emerging fishery because both landings and the number of participants in this fishery have increased dramatically since 1993.

White seabass is the target of both a commercial and recreational fishery. The commercial white seabass fishery landed 243 t in 2010, a 39% increase from the 2009 total of 175 t, while the recreational take increased by 56% to 121 t in 2010 from the previous year's total of 77 t. The commercial ex-vessel value in 2010 was $1,528,913.

In 2010, the Commission undertook nine rulemaking actions that addressed marine and anadromous species. The Commission adopted changes to commercial or sport fishing regulations that include Central Valley and ocean salmon, rock crab, lobster hoop net, and herring. The Department also began implementing an Automated License Data System which allows for the purchase of commercial and recreational fishing licenses online. It also creates a customer information database that satisfies the federal mandate of establishing a National Saltwater Angler Registry.

On 15 December 2010 the Commission adopted regulations to create a suite of marine protected areas (MPAs) in southern California from Point Conception to the California/Mexico border. Developed under the Marine Life Protection Act planning process, the network of 49 MPAs and 3 special closures (including 13 MPAs and 3 special closures previously established at

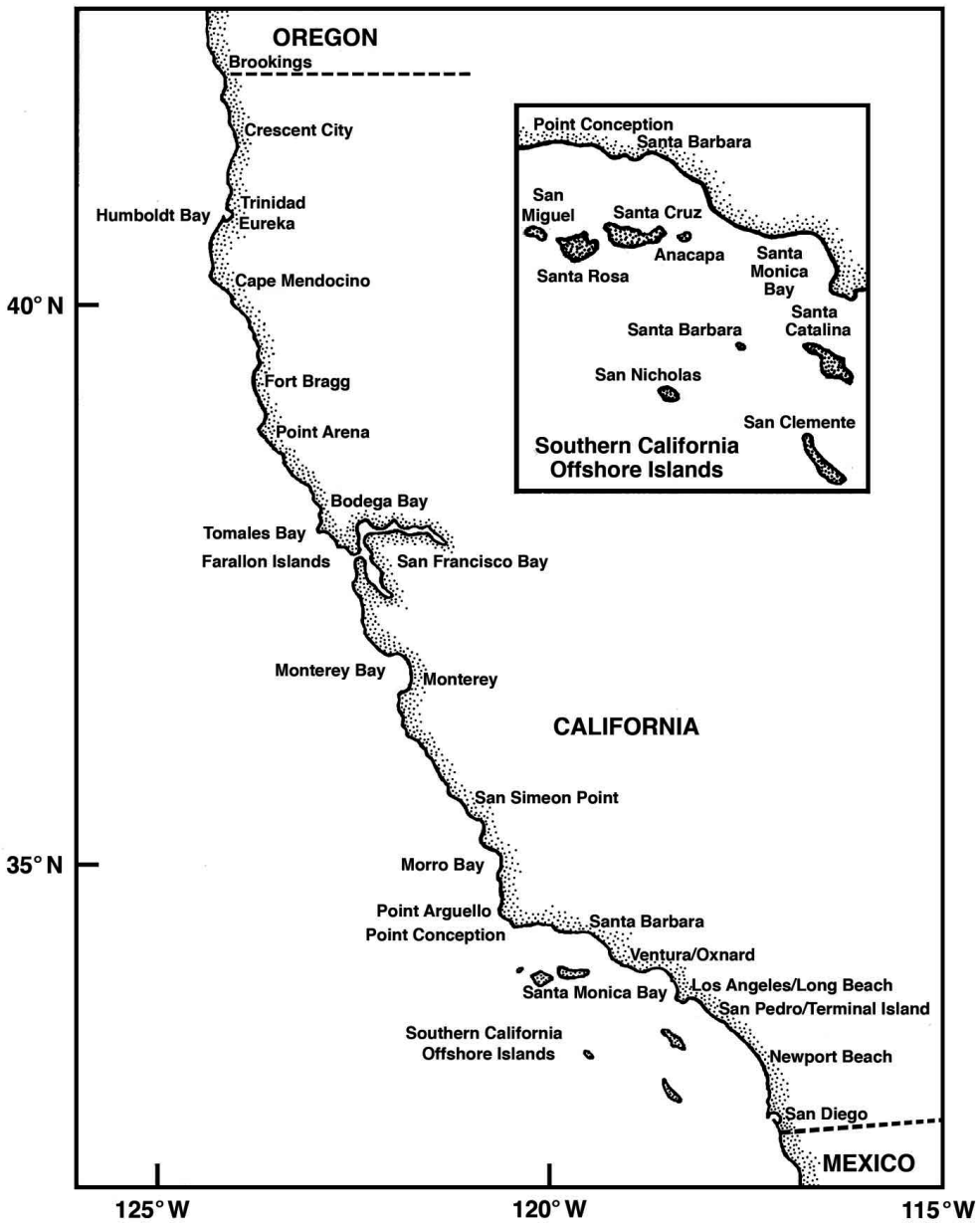

Figure 1. California ports and fishing areas.

the northern Channel Islands) covers approximately 354 square miles of state waters and represents approximately 15% of the region. These new MPAs will go into effect on 1 October 2011.

Coastal Pelagic Finfish

Pacific sardine (*Sardinops sagax*), Pacific mackerel (*Scomber japonicus*), jack mackerel (*Trachurus symmetricus*), and northern anchovy (*Engraulis mordax*) form a finfish complex known as coastal pelagic species (CPS). These species are jointly managed by the Pacific Fishery Management Council (Council) and the National Marine Fisheries Service (NMFS). In 2010, total commercial landings for these species equaled 37,050 t (table 1), and was worth nearly $5.2 million in ex-vessel value. Compared to landings in 2009, this represents an 18% and 25% decrease in quantity and value, respectively. Once again Pacific sardine ranks as the largest fishery among these four species, contributing 91% of the combined quantity and 82% of the combined value.

Pacific Sardine. In 2010, the total tonnage of Pacific sardine landed, 33,658 t, was 10% lower than in 2009 (37,578 t). California landings of Pacific sardine generated an ex-vessel value of approximately $4.3 million. Commercial landings of sardine averaged 48,050 t over the ten-year period from 2001–2010 (fig. 2). Nearly all

TABLE 1
Landings of Coastal Pelagic Species in California (metric tons)

Year	Pacific sardine	Northern anchovy	Pacific mackerel	Jack mackerel	Unspecified mackerel	Pacific herring	Herring roe	Market squid	Total
1977	2	101,132	3,316	47,615		5,286		12,811	170,163
1978	1	11,439	8,241	34,349	48	4,473		17,145	75,696
1979	51	48,880	22,404	21,548	301	4,257		19,982	117,424
1980	21	42,946	25,739	24,181	56	8,061		15,385	116,389
1981	34	52,308	35,257	17,778	132	5,961		23,510	134,980
1982	2	42,150	17,667	19,618	18,398	10,604		16,308	124,747
1983	1	4,427	17,812	9,829	23,659	8,024		1,824	65,576
1984	1	2,889	26,043	9,149	18,038	3,847		564	60,532
1985	6	1,626	18,149	6,876	19,624	7,984		10,275	64,540
1986	388	1,535	22,095	4,777	25,995	7,658		21,278	83,727
1987	439	1,390	26,941	8,020	19,783	8,420		19,984	84,978
1988	1,188	1,478	30,127	5,068	20,736	8,641		37,233	104,471
1989	837	2,449	21,067	10,746	26,661	9,296		40,893	111,950
1990	1,664	3,208	31,077	3,223	9,039	7,436		28,447	84,094
1991	7,587	4,014	31,680	1,693	339	7,347		37,389	90,048
1992	17,950	1,124	18,574	1,209	3	6,319		13,110	58,289
1993	15,346	1,958	11,798	1,673		3,846	0	42,722	77,345
1994	11,644	1,789	10,008	2,704	0	77	2,874	55,508	84,603
1995	40,328	1,886	8,625	1,728		3	4,664	72,433	129,667
1996	32,559	4,421	9,597	2,178	4	249	5,162	80,784	134,954
1997	43,246	5,718	18,398	1,160	1	0	9,147	70,387	148,057
1998	42,956	1,457	20,515	824		0	2,009	2,895	70,656
1999	59,493	5,179	8,688	953	0		2,279	91,950	168,542
2000	53,612	11,754	21,916	1,269	0	26	3,450	118,816	210,843
2001	51,894	19,277	6,925	3,624	1	0	2,768	86,385	170,873
2002	58,354	4,643	3,367	1,006	2	0	3,324	72,920	143,615
2003	34,732	1,676	3,999	156	0	34	1,808	45,061	87,467
2004	44,305	6,793	3,570	1,027	0	60	1,581	41,026	98,362
2005	34,633	11,182	3,244	199		219	136	58,391	108,005
2006	46,577	12,791	5,891	1,167	0	37	694	49,159	116,316
2007	80,981	10,390	5,018	630	1	336	261	49,474	147,091
2008	57,806	14,285	3,530	274	0	131	626	38,101	114,754
2009	37,578	2,668	5,079	119	1	74	460	92,338	138,317
2010	33,658	1,026	2,056	310	0			129,904	166,954

Data Source: Commercial Fisheries Information System (CFIS)

(96%) of California's 2010 sardine catch was landed in Los Angeles (83%, 27,809 t) and Monterey (13%, 4,305 t) port areas (table 2).

The Pacific sardine fishery ranges from British Columbia, Canada, southward to Baja California, Mexico (BCM). Since the resurgence of sardines in the 1980s, the majority of landings have occurred in southern California and northern Baja California. However, since the expansion of the sardine fishery in 1999, landings have steadily increased in the Pacific Northwest and Canada. The combined landings of Pacific sardine for California, Oregon, and Washington totaled 66,920 t, a slight decrease from the 67,050 t landed in 2009. The Pacific sardine harvest guideline (HG) for each calendar year is determined from the previous year's stock biomass estimate (of ≥1-year-old fish on 1 July) in U.S. and Mexican waters. The recommended HG for the 2010 season was 67,039 t based on a biomass estimate of 702,204 t. The Pacific sardine HG was apportioned coastwide through the year with 35% allocated from 1 January through 30 June, 40% plus any portion not harvested allocated from 1 July through 15 September, and the last 25%, plus any portion not harvested from the first two allocations, released on 15 September.

In 2010, U.S. West Coast fisheries harvested nearly all (99.8%) of the HG, same as the previous year (100%). The 1st allocation (Jan 1–June 30) lasted 163 days. This was markedly longer than the 2nd (July 1–Sept 14) and 3rd (Sept 15–Dec 31) allocations which lasted 22 and 10 days, respectively. Increased fishing efforts, such as multiple landings per day, were observed during all allocation periods. During the 2nd and 3rd allocations, fishing effort continued during weekends, a period normally not fished. Since the 2008 reduction in the HG, the fishery has become a "derby," resulting in early closures of each allocation period. The directed Pacific sardine fishery was officially closed by the NMFS on September 24, 2010.

The steady increase of sardines landed in Oregon since 1999 may have leveled off in the last 3 years (fig. 3). Oregon landings of sardine totaled 20,852 t in 2010, a slight decrease from 2009 (21,481 t). In 2010, Oregon

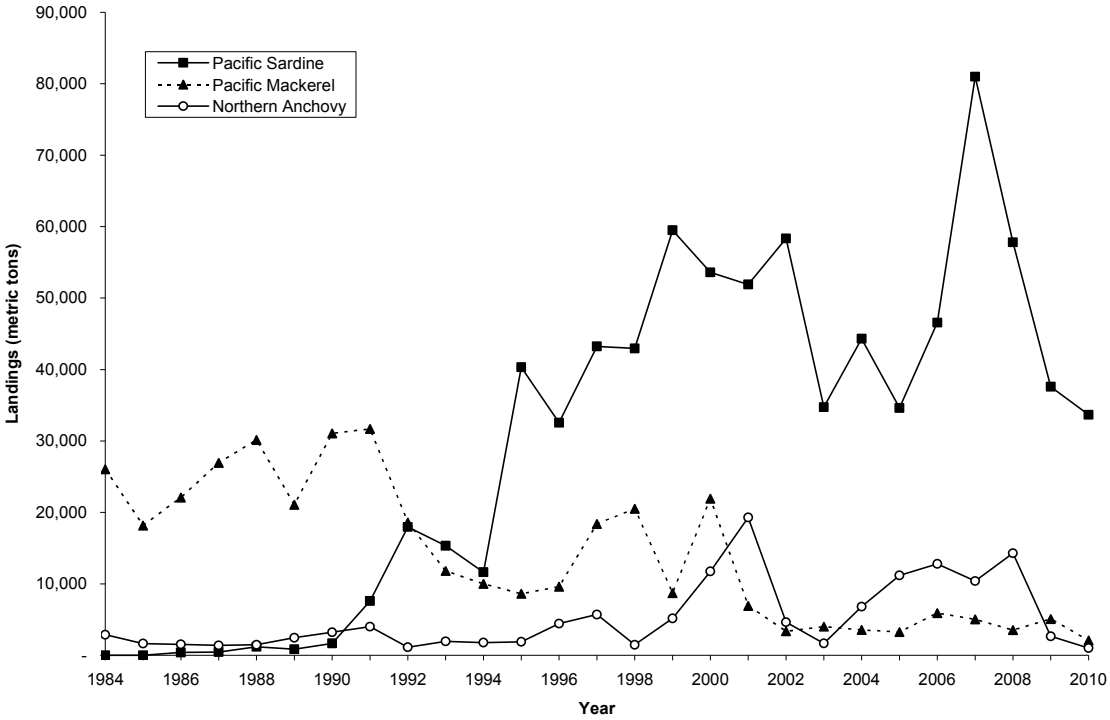

Figure 2. California commercial landings of Pacific sardine (*Sardinops sagax*), Pacific mackerel (*Scomber japonicus*), and northern anchovy (*Engraulis mordax*), 1984–2010.

exported 646 t of sardine product worth a little over $555,000.

Washington landings of Pacific sardine totaled 12,381 t in 2010, an increase of 54% from 2009 (8,026 t). Washington exported more sardine (35,764 t) than was landed; the product was most likely sardine landed in Oregon or the previous year.

In November 2010, the Council adopted a HG of 50,526 t for the 2011 Pacific sardine fishery based on a biomass estimate of 537,173 t and the harvest control rule in the Coastal Pelagic Species Fishery Management Plan (CPS FMP). This HG would be a 30% reduction from that of 2010. It would also incorporate a 4,200 t set-aside allocated for dedicated Pacific sardine research activities in 2011.

The 2010 recreational Pacific sardine catch as sampled from the California Recreational Fisheries Survey (CRFS) was 50 t (886,000 fish), similar to that of 2009 (20% increase, by number of fish). The majority of the fish landed were from man-made structures, such as piers.

Pacific Mackerel. In 2010, 2,056 t of Pacific mackerel were landed in California (table 1, fig. 2). The majority of landings were made in southern California port areas (table 2). The total ex-vessel value generated for Pacific mackerel in 2010 was $410,800. Industry exported 552 t of mackerel product, valued at nearly $5,877,000, to 15 countries. Egypt (168 t), Peru (88 t), and Jamaica (72 t) received over 59% of this product.

TABLE 2
Landings (metric tons) of Pacific sardine (*Sardinops sagax*) and Pacific mackerel (*Scomber japonicus*) at California port areas in 2010.

	Pacific sardine		Pacific mackerel	
Area	Landings	% Total	Landings	% Total
Monterey	4,305	12.8	0.0	0.0
Santa Barbara	1,524	4.5	9.4	0.5
Los Angeles	27,809	82.7	2,045.2	99.5
Total	33,638	100	2,054.6	100

Oregon reported 49 t of Pacific mackerel landed there in 2010 for a total ex-vessel value of $2,872. This is slightly less than the 2009 catch of 53 t. No landings of mackerel have been reported in Washington since 2005. Washington landings of Pacific mackerel are typically low, with the greatest landings occurring in 2001 (371 t).

Similar to sardines, the majority of Pacific mackerel landings occur in southern California and Ensenada, BCM. In the U.S., the fishing season for Pacific mackerel is 1 July to 30 June the following year. At the start of the 2010–2011 season, based on an estimated biomass of 282,049 t, the PMFC set the HG at 11,000 t, with a 3,000 t set-aside for incidental landings in other fisheries. Landings above the HG would be constrained by an incidental catch rate of 45% by weight when landed with other CPS.

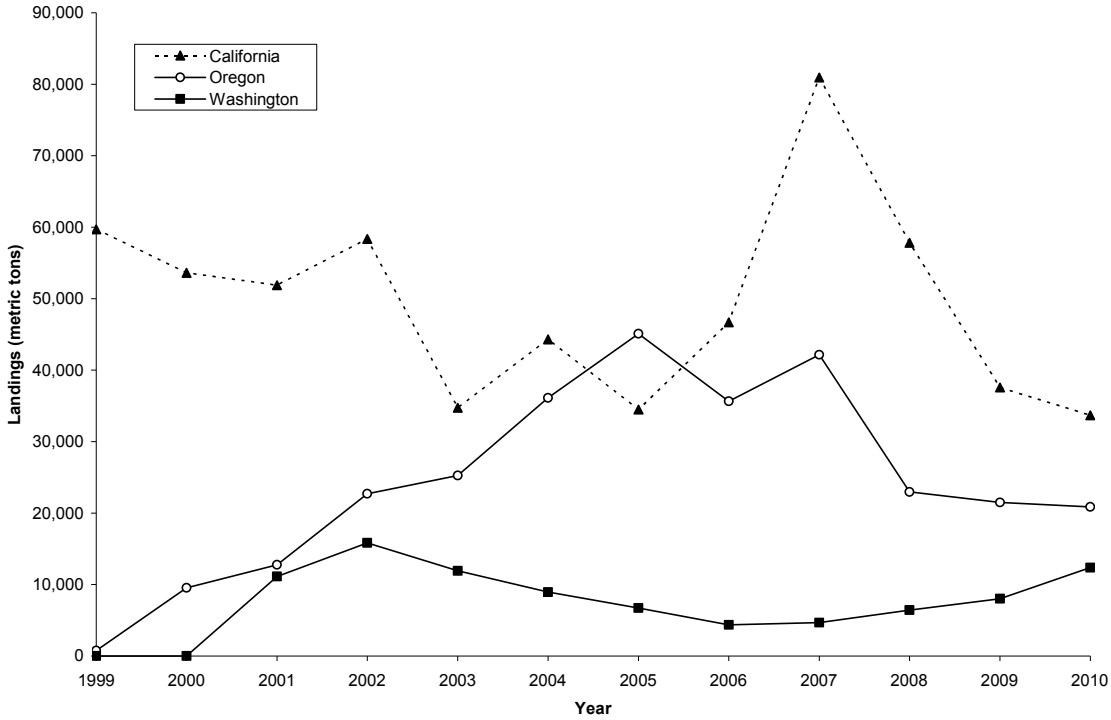

Figure 3. Commercial landings of Pacific sardine (*Sardinops sagax*) in California, Oregon, and Washington, 1999–2010.

The 2010 recreational Pacific mackerel catch as sampled from CRFS was 233 t (1,168,000 fish), a 97% (77%, by number of fish) increase from 2009. A total of 27,205 fish were reported landed on CPFVs.

Jack Mackerel. In 2010, jack mackerel landings represented less than 1% of the total catch of federally managed CPS finfish in California with 310 t landed. The ex-vessel revenue for jack mackerel was $62,355 for California. Landings in Oregon continue to be low with 3 t landed in 2010 (no ex-vessel value). Washington reported no landings of jack mackerel during 2010.

The 2010 recreational jack mackerel catch as sampled from CRFS was 17 t (276,000 fish), a 325% (500%, by number of fish) increase from 2009. A total of 2,017 fish were landed on CPFVs.

Northern Anchovy. Landings of northern anchovy in California have been reported since 1916. Historically, anchovy was reduced to oil or fish meal and the fishery was modest compared to Pacific sardine and Pacific mackerel. However, periods of low sardine abundance saw increased anchovy landings. Peak landings were seen in the early to mid 1970s with total annual harvest exceeding 100,000 t at times. Presently, landings of northern anchovy are modest, averaging about 8,500 t per year over the last 10 years (fig. 2). The vast majority of northern anchovy are landed in California, with occasional landings in Oregon and Washington. Anchovy are currently used for human consumption, animal food, live bait, and reduction.

Three stocks of northern anchovy are identified: northern, central and southern. California fishery harvests are taken from the central stock which ranges from northern Baja to San Francisco. Studies of scale deposits on the sea floor suggest that anchovy abundance can be quite high at times. Currently, northern anchovy are a monitored species under the CPS FMP.

California landings of northern anchovy in 2010 amounted to 1,026 t with an ex-vessel value of nearly $462,700 (table 1). This is a 62% decrease from 2009 landings (2,668 t). Exports of northern anchovy product from California totaled 11 t for an export value of $68,877. Three countries received anchovy product from California; Taiwan received the majority at 91%.

For 2010, Oregon reported landings totaling 138 t with an ex-vessel value of $31,869. No exports of northern anchovy were reported. Washington reported no landings of anchovy for 2010.

Pacific Bonito. From 2001 to 2010, annual Pacific bonito (*Sarda chiliensis lineolata*) landings averaged 607 t, a small percentage of the total CPS quantity landed in California. In 2010, landings decreased drastically from last year's high of 2,133 t to 18 t. The landings generated an ex-vessel value of $14,373. No landings of Pacific bonito were reported from Oregon or Washington in 2010. The California recreational catch for Pacific bonito in 2010 was 81 t (78,000 fish), a 45% decrease from 2009. A total of 38,528 fish were landed on CPFVs.

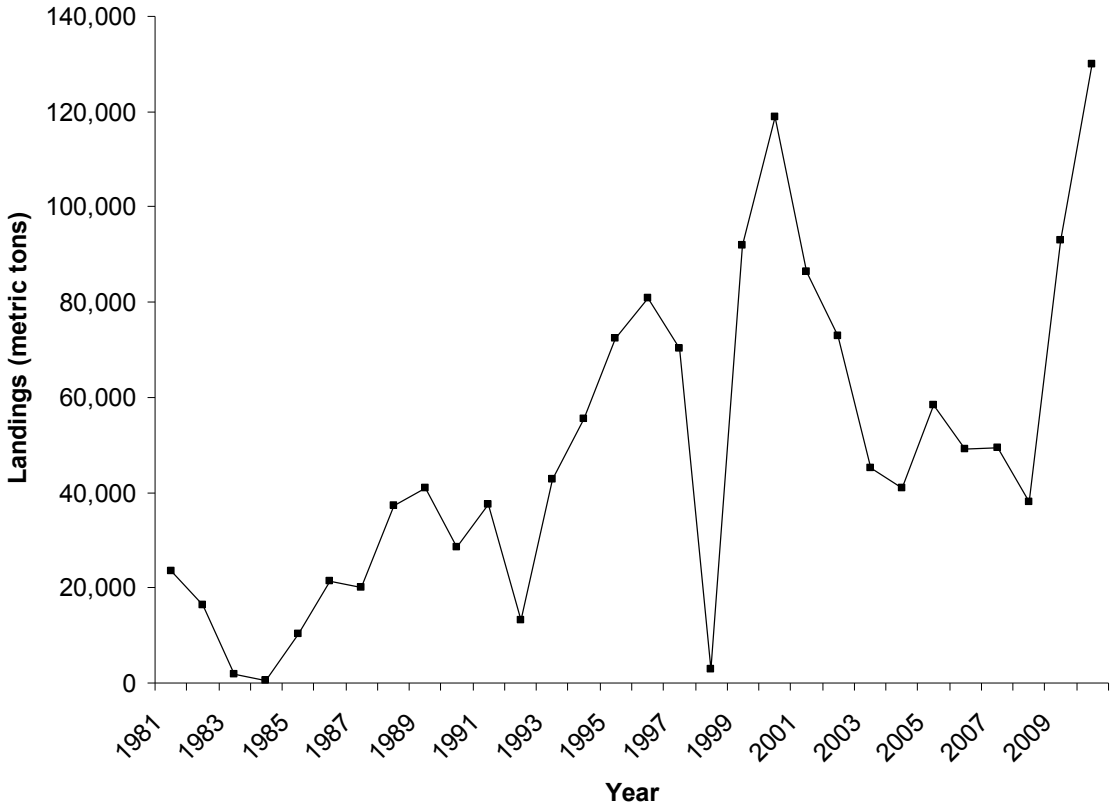

Figure 4. California commercial market squid (*Loligo opalescens*) landings, 1981-2010.

California Market Squid

In 2010, market squid, *Doryteuthis opalescens*, (formerly *Loligo opalescens*) dominated commercial landings of marine species in California, contributing about 66% of the total tonnage and 41% of total ex-vessel value of all species landed. Landings of market squid in 2010 increased 45% of 2009 landings, from 93,106 t to 129,904 t (fig. 4). Ex-vessel value increased 30% from $56.9 million in 2009 to $73.8 million in 2010. California fish businesses exported 92,559 t of market squid to 42 countries for a value of $107 million in 2010. The majority (90%) was shipped to just five countries but most (76%) went to China.

For the first time since the inception of the Market Squid Fishery Management Plan in 2005, market squid landings were projected to reach the seasonal catch limit of 107,048 metric tons (t). Accordingly, the Department of Fish and Game (Department) closed the fishery on 17 December 2010 for a total of 119,482 t landed for the open portion of the 2010/2011 season.

Commercial fishing for market squid is limited by fishery control rules set forth in the Market Squid Fishery Management Plan. Vessels are required to have a permit to possess or land over 1.8 t of squid, except when fishing for them to use as live bait. Permits are valid for the management season, from 1 April to 31 March the following year. In 2010, there were 83 market squid vessel (purse seine), 60 light boat (attracting), and 26 brail (or dip net) permits issued. Of the 83 vessel permits, 73 vessels were active in the fishery with 56 vessels contributing 95% of the landings. Other fishery control rules include an annual catch limit, weekend closures, spatial closures, and lighting restrictions.

Although the fishery has its historical origins in Monterey Bay, the fishery has been dominated by the southern California landings (fig. 5). Of note is the increase in landings for Monterey, which has seen less than 1,000 t in four of the last 5 seasons.

Market squid live less than a year and have been found in nearshore waters of the eastern Pacific Ocean from Baja California to the Gulf of Alaska. The population appears to fluctuate widely in abundance in response to short-term oceanographic events, like the El Niño Southern Oscillation. Ecologically, they are considered important as forage for other species, including predatory fishes, marine mammals, and seabirds.

A live bait fishery exists for market squid; however, the amount of market squid harvested and the value of the fishery is largely unknown, as there are no permitting and reporting requirements. The live bait fishery is likely a low-volume, high-value endeavor, as recreational anglers are willing to pay up to $85 for a "scoop" of live squid.

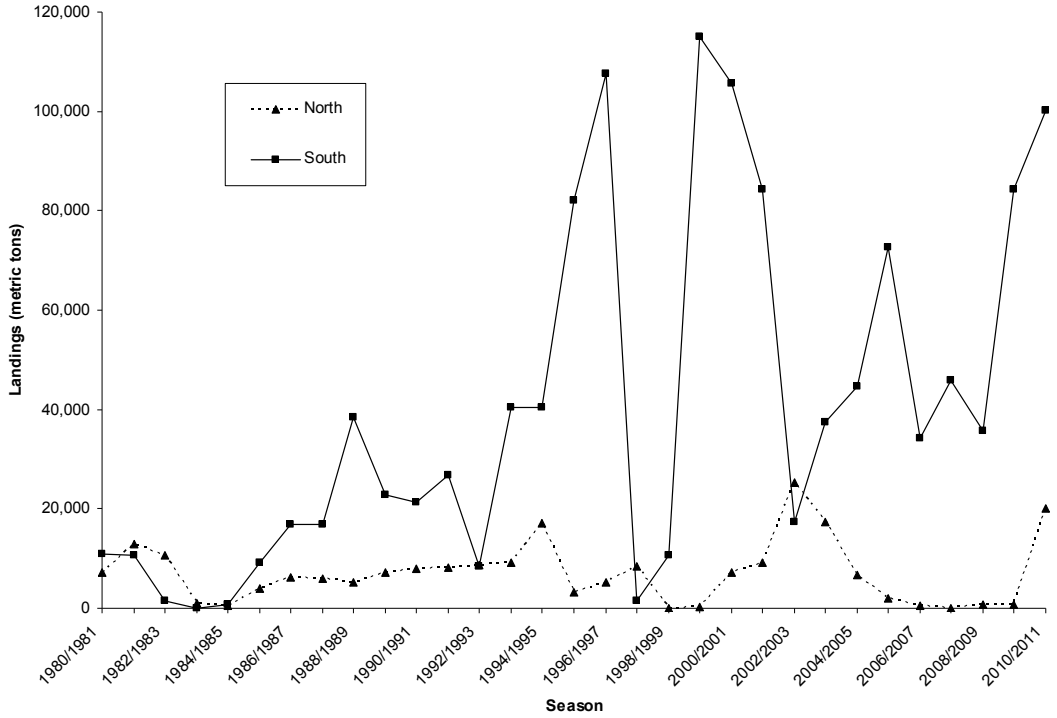

Figure 5. Comparison of market squid landings for northern and southern fisheries by fishing season (1 April–31 March), from 1980–81 to 2010–11 seasons.

Ocean Salmon

Ocean salmon fisheries in California primarily target Chinook salmon (*Oncorhynchus tshawytscha*). The retention of coho salmon (*O. kisutch*) has been prohibited in the commercial and recreational fisheries since 1993 and 1996, respectively. Pink salmon (*O. gorbuscha*) are taken occasionally in the fisheries, usually in odd years. Each season, the Council and the Commission regulate California's ocean salmon fisheries to meet the conservation objectives for Klamath River fall Chinook and Sacramento River fall Chinook (SRFC) stocks as described in the Salmon Fishery Management Plan (FMP). In addition, the fisheries must meet the NMFS Endangered Species Act (ESA) consultation standards for listed stocks, including Sacramento River winter Chinook (endangered), Central Valley spring Chinook (threatened), California coastal Chinook (threatened), Central California coast coho (endangered), and Southern Oregon/Northern California coho stocks (threatened).

In 2010, California ocean salmon fisheries were constrained to satisfy both NMFS and the Council's guidance to target the upper end of the FMP conservation goal range of 122,000–180,000 hatchery and natural adult SRFC spawners. In 2009, SRFC failed to meet its conservation goal for the third consecutive year, thereby trigging an Overfishing Concern under the terms of the FMP. SRFC generally contribute 80–90% of California's ocean salmon landings.

In 2010, the commercial ocean salmon fishery was opened for the first time since 2007. The commercial season was open for 8 days in July from Horse Mountain to the U.S. Mexico border. Additionally the Fort Bragg area had two quota fisheries, one at the end of July (18,000 Chinook quota) and one in August (9,375 Chinook quota), for a season total of 70 days (days open in each of four management areas combined).

An estimated 15,100 Chinook salmon (103 t) were landed during the 2010 commercial season (fig. 6). The average weight per fish was 6.85 kg (15.10 lbs). The average price was $12.00/kg ($5.50/lb), the highest nominal price on record. The total ex-vessel value of the fishery in 2010 was estimated to be $1.2 million. Total commercial effort was estimated to be 2,000 days fished in 2010. The Fort Bragg quota fisheries did not reach the quota allotments and remained open for the entire length of the fishery.

In 2010, the recreational fishing season increased significantly compared to the 10 day fishery in 2009, for a season total of 500 days (days open in each of four management areas combined). An estimated 14,700 Chinook were landed in 2010 compared to 700 salmon in 2009 (fig. 7). There were an estimated 48,800 angler days in 2010 compared to 5,400 angler days in 2009. The bag and possession limit was two salmon per day of any species except coho, and anglers were required to use no more than two single-point, single-shank barb-

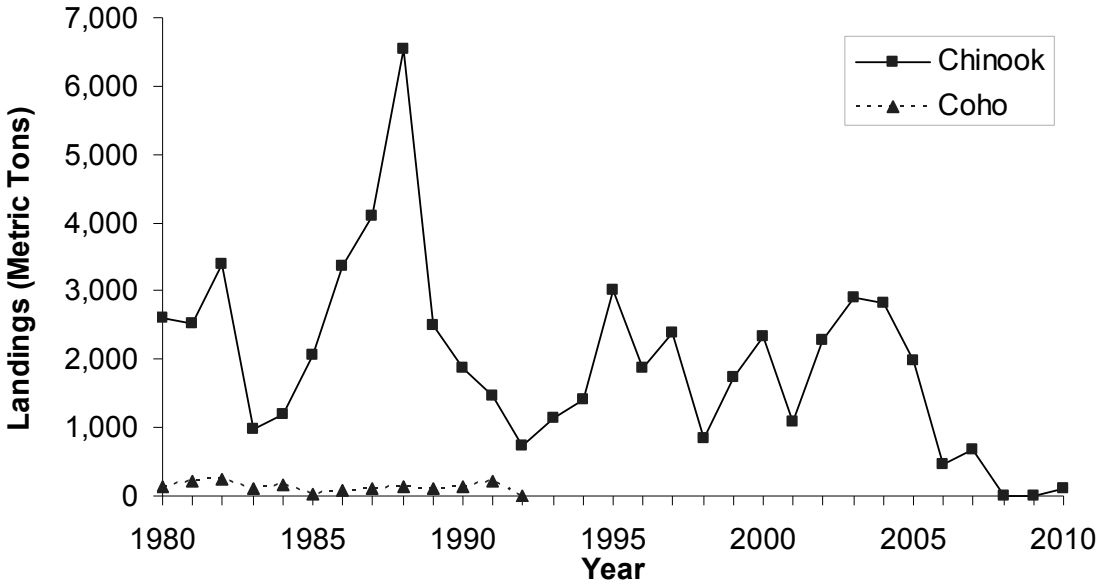

Figure 6. California commercial landings of Chinook (*Oncorhynchus tshawytscha*) and coho (*O. kisutch*) salmon, 1980–2010.

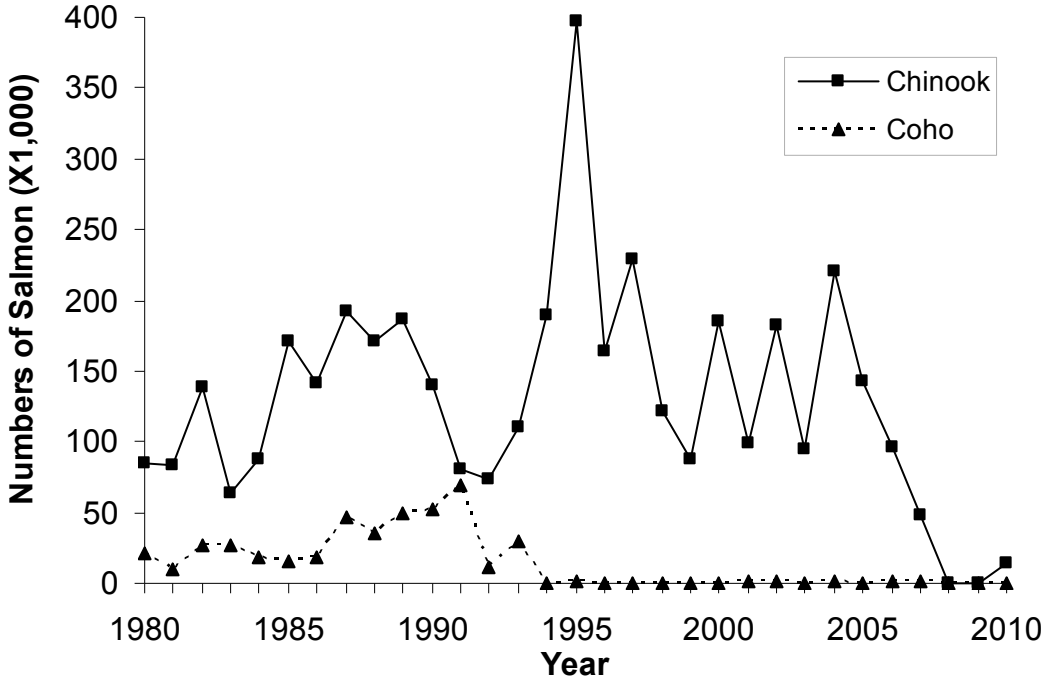

Figure 7. California recreational landings of Chinook and coho salmon, 1980–2010.

less hooks when fishing for salmon. The minimum size limit was 20 inches (508 mm) total length (TL) in April and increased to 24 inches (610 mm) TL in May, to protect the generally smaller-sized endangered winter run Chinook. Approximately 200 coho were landed illegally during 2010, presumably by anglers who misidentified their salmon as Chinook.

In fall 2010, SRFC met the lower range of the conservation goal of 122,000–180,000 hatchery and natural adult spawners for the first time since 2006. Nearly 125,400 SRFC adults returned to spawn in the Sacramento River basin. A total of 27,500 jacks (age-2 fish) returned. Based on these data, the Sacramento Index of ocean abundance forecast for 2011 is 729,900 SRFC, without any additional ocean or in-river fishing.

In April 2011, the Council and Commission approved substantial recreational and commercial salmon fisheries off California and southern Oregon. The SRFC conservation goal, and the 2011 NMFS guidance to target the upper end of the conservation goal, is satisfied

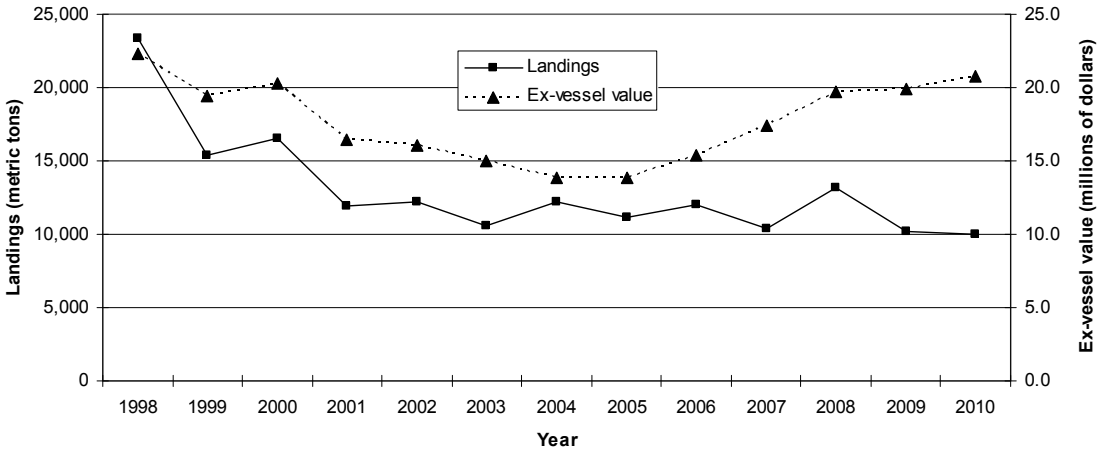

Figure 8. California commercial landings of total groundfish by all gears, 1998–2010.

by the adopted season structures. For more information on the 2011 fisheries, see the Council's Web site (www.pcouncil.org) "Preseason Report III, Analysis of Council Adopted Management Measures for 2011 Ocean Salmon Fisheries," which was compiled by the Council's Salmon Technical Team and Council staff.

Groundfish

More than 90 species of bottom-dwelling marine finfish are included in the federally-managed groundfish fishery. The species that comprise the groundfish fishery are diverse and complex; their primary distributions range from nearshore depths to deep offshore habitats. "Groundfish" species include all rockfishes in the Scorpaenidae family, flatfishes such as Dover sole (*Microstomus pacificus*) and petrale sole (*Eopsetta jordani*), roundfishes such as sablefish (*Anoplopoma fimbria*) and lingcod (*Ophiodon elongatus*), and various sharks and skates. Of the 90+ groundfish species, approximately 50 are consistently harvested and require management measures that balance biological and economical goals.

Commercial Fishery. In 2010, 9,960 t of commercial groundfish were landed in California with an estimated ex-vessel value of $20.8 million. Compared to the 2009 fishing year, this was an overall decline of 3% of the landings (10,191 t) and a 4% increase of the ex-vessel value ($19.9 million). During the last decade, the volume of landed groundfish has declined by 45% when the current 2010 landings are compared to the 2000 landings (16,561 t). Conversely, the ex-vessel value of the groundfish fishery experienced some downward fluctuation but continued to increase in total value despite lower landings (fig. 8). The area from the California/Oregon border to the Monterey Bay port complex accounted for 85% (8,503 t) of the groundfish landed in California and 63% of the ex-vessel value ($13.3 million). The groundfish fishery primarily operates using trawl gear, accounting for 77% of the landings, followed by hook-and-line and trap gear (23%). Gill net and seining gear comprise the remainder. Dover sole (2,622 t), sablefish (2,449 t), Pacific whiting (*Merluccius productus*) (2,427 t), and the thornyhead complex—*Sebastolobus altivelis* (552 t) and *Sebastolobus alascanus* (474 t)—continued to dominate as the top five species landed in 2010. These five species comprised 85% of the total groundfish landings. Collectively, the flatfishes accounted for 31%, roundfishes 50%, the thornyhead complex 10% and rockfishes 8% of the total landed groundfish. The "other" groundfish species category is 99.9% comprised of grenadier (*Macrouridae*) which accounted for 95 t (table 3). Contrary to high-volume high-priced species such as sablefish, nearshore rockfishes are generally a low-volume high-priced commodity in California—gopher rockfish (*Sebastes carnatus*), brown rockfish (*Sebastes auriculatus*) and grass rockfish (*Sebates rastrelliger*) earned a combined ex-vessel value of $991,697, and 28 t, 27 t and 12 t were landed respectively. The highest volume rockfish was chilipepper (*Sebastes goodei*) with 342 t landed and an ex-vessel value of $457,029. Over the last decade, management measures such as limiting access and restricting landings have been used to protect vulnerable nearshore rockfish stocks. This limitation on the fishery, in addition to the live fish market that developed in the late 1980s and continues to thrive today, contributes to the high market value of the nearshore fishery. In 2010, grass rockfish earned an average of $19,341/t followed by China rockfish ($16,274/t) and gopher rockfish ($14,618/t). By contrast, chilipepper earned an average of $1,903/t.

Overfished rockfish species accounted for less than 1% (32 t) of the total landings in 2010 which is less than 2009 when 1% (57 t) were taken; the predominant species taken was widow rockfish (*Sebastes entomelas*) in both years.

TABLE 3
California commercial groundfish landings (in metric tons) and ex-vessel value in 2010 with comparisons to 2009. The top five species by weight for the Flatfishes and Rockfishes are represented in the table.

	2010		2009		% change from 2009	% change from 2009
	Harvest (t)	Value ($)	Harvest (t)	Value ($)	(t)	($)
Flatfishes						
Dover sole	2,622	$1,798,113	3,167	$2,571,883	–17	–30
Petrale sole	213	$557,412	532	$1,146,206	–60	–51
Arrowtooth flounder	68	$14,921	45	$10,132	51	47
Sanddabs	56	$91,722	107	$115,136	–48	–20
Rex sole	55	$43,385	107	$84,897	–49	–49
English sole	24	$21,091	73	$55,414	–67	–62
Other flatfishes	33	$60,601	37	$54,239	–11	12
Total Flatfishes	3,071	$2,587,246	4,069	$4,037,907	–25	–36
Rockfishes						
Chilipepper	342	$457,029	241	$329,784	42	39
Blackgill rockfish	96	$247,963	95	$257,122	1	–4
Group slope rockfish	78	$108,166	75	$102,651	4	5
Splitnose rockfish	64	$48,403	57	$46,065	12	5
Black rockfish	53	$219,347	94	$398,010	–44	–45
Gopher rockfish	28	$412,792	24	$372,535	17	11
Other rockfishes	88	$982,306	143	$1,164,564	–38	–16
Overfished species						
Bocaccio	4	$9,299	6	$15,476	–33	–40
Canary rockfish	0.44	$637	1.1	$1,437	–60	–56
Cowcod	0.03	$132	0.06	$588	–50	–78
Darkblotched rockfish	17	$21,750	46	$59,366	–63	–63
Pacific ocean perch	0.04	$47	0.78	$771	–95	–94
Widow rockfish	10	$8,937	4.04	$6,288	148	42
Yelloweye rockfish	0	$8	0.04	$303	—	—
Total Rockfishes	781	$2,516,817	787	$2,754,961	–1	–9
Roundfishes						
Sablefish	2,449	$11,501,299	2,249	9,782,141	9	18
Pacific whiting	2,427	$694,248	1,792	206,193	35	237
Lingcod	47	$173,276	57	187,842	–18	–8
Cabezon	23	$266,032	18	231,421	28	15
Kelp greenling	2	$22,154	1	19,973	100	11
Total Roundfishes	4,947	$12,657,009	4,117	$10,427,570	20	21
Scorpionfish, California	3	$26,734	3	$29,669	0	–10
Sharks & Skates	35	$28,834	117	$83,478	–70	–65
Thornyheads	1,026	$2,957,617	1,027	$2,612,205	0	13
Other Groundfish	95	$44,453	71	$29,474	34	51
Total Groundfish	9,960	$20,818,711	10,191	$19,975,264	–2	1

Data Source: CFIS (CMASTR) Extraction Date: 05-12-2011

Recreational Fishery. The Recreational Fisheries Information Network (RecFIN) Program houses recreational data from California, Oregon, and Washington. The California data, available from 1980 to the present, provide the best available information regarding recreational catch off California. RecFIN incorporates data from two recreational fishery sampling programs: the Marine Recreational Fisheries Statistical Survey (MRFSS), which sampled catch from 1980 to 2003; and the CRFS, initiated by the Department in 2004. Due to modifications in sampling protocols and differences in data estimation procedures, these two surveys are not directly comparable to each other. Information from CRFS indicates that in 2010, California anglers targeting groundfish participated in an estimated 1,074,000 angler trips. This is a 6% increase from 2009 (1,005,000 angler trips) and a 26% increase from 2008 (805,000 angler trips). The recreational groundfish fishery in California is predominantly a hook and line fishery with little being taken by spear.

An estimated 1,067 t of groundfish were taken by the recreational fishery in 2010 (table 4), a 15% decrease from 2009 (1,250 t) but an 11% increase from 2008 (945 t). The top five species were: black and vermilion rockfishes, lingcod, and gopher and brown rockfishes, accounting for approximately 51% of the total groundfish estimated catch by weight. The same five species dominated catches in 2009, accounting for 49% of the total weight. In 2010, 33% of the groundfish effort occurred in southern California (south of Point Conception), with California scorpionfish (*Scorpaena guttata*) and Pacific sanddab (*Citharichthys sordidus*) dominating

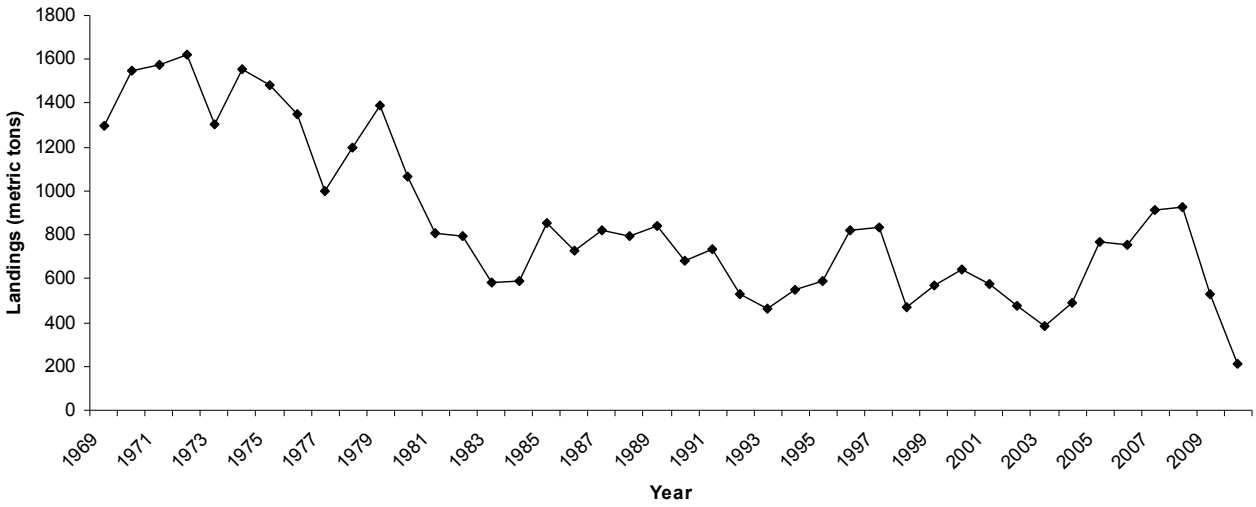

Figure 9. California commercial landings of petrale sole (*Eopsetta jordani*) by all gears, 1969–2010.

TABLE 4
California recreational groundfish landings (A+B1) greater than 5 metric tons in 2010 with 2009 comparisons

	2010 Harvest (t)	2009 Harvest (t)	% Change from 2009
Black rockfish	180	243	–26
Vermilion rockfish	139	130	7
Lingcod	94	128	–27
Gopher rockfish	76	57	33
Brown rockfish	69	60	15
CA scorpionfish	63	66	–5
Bocaccio	57	46	24
Copper rockfish	48	60	–20
Blue rockfish	46	45	2
Pacific sanddab	43	28	54
Leopard shark	35	35	0
Yellowtail rockfish	24	49	–51
Cabezon	24	32	–25
CA sheephead	20	32	–38
Starry rockfish	19	24	–21
China rockfish	17	20	–15
Canary rockfish	13	15	–13
Olive rockfish	12	24	–50
Greenspotted rockfish	11	15	–27
Black-and-yellow rockfish	11	12	–8
Kelp greenling	10	15	–33
Speckled rockfish	7	7	0
Kelp rockfish	6	4	50
Grass rockfish	6	9	–33
Other rockfishes	30	41	–27
Total Groundfish	1,067	1,250	–15
Angler Trips			
Bottomfish Effort	1,074,000	1,005,000	5

Rockfish species of concern including yelloweye rockfish (1.3 t), cowcod (0.03 t) are included in the "Other" category.

Data source: RecFIN Date Extracted: 6-3-2011

the catch. Central California (Point Conception to Cape Mendocino) accounted for 50% of the total groundfish effort and was dominated by vermilion, gopher and brown rockfishes. Lastly, northern California (Point Mendocino to the California Oregon border) accounted for 18% of the estimated catch; the majority was black rockfish followed by moderate amounts of lingcod and vermilion rockfish.

Petrale Sole Fishery. Petrale sole is a larger flatfish and among the most valuable commercial flatfish found throughout the state of California. Petrale sole landings have been documented in California as far back as the late 1800s but were only officially recorded by the Department since 1969 (fig. 9). Over the last decade, petrale sole had an average ex-vessel value of $1.3 million annually followed by a drop in 2010 (due to regulation changes—see below) with an ex-vessel value of $557,411. It is primarily a trawl-caught species and the fishery is characterized by a strong winter and summer seasonality. During winter months, petrale sole aggregate in deep water for spawning and the trawl fleet harvests greater volume with less catch of associated groundfish species (such as chilipepper). Conversely, during spring and summer petrale sole are found in shallower water spread out over the continental shelf where they are harvested with a large mixture of slope rockfish species. It is commonly caught with sablefish, Dover sole and other flatfishes throughout the year.

In the recreational fishery, petrale sole is not a targeted species but is taken while prosecuting other species. An evaluation of both MRFSS and CRFS data suggests that since 1980 estimated annual recreational catch of petrale sole averaged 43 t.

Petrale Sole Stock Assessment and Management. Because of the economic and biological importance of petrale sole, periodic stock assessments are conducted. In 2009, the Council adopted a new full stock assessment for the stock along the Pacific West Coast of Washington, Oregon and California. The assessment indicated the stock

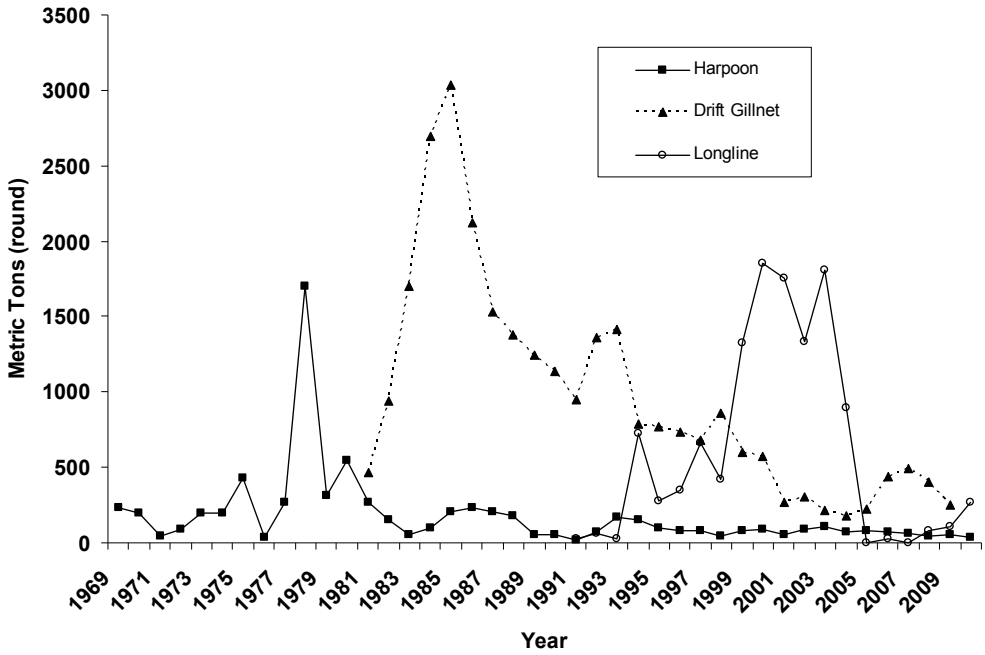

Figure 10. California landings (round weight) of swordfish by gear type 1969–2010.

was at 11.6% of its unfished biomass and officially "overfished" (under the NMFS newly revised threshold reference point for flatfish at 12.5% of unfished biomass.) This prompted the Council to recommend immediate action to decrease the fishing pressure on petrale sole in the 2010 season by limiting access to winter fishing grounds and reducing trip limits. These restrictions led to the 60% decrease in petrale sole landings and 51% decrease in ex-vessel value from 2009 to 2010. To offset this lost opportunity, the Council also recommended increased harvest amounts for other species of healthy groundfish such as sablefish, longspine and shortspine thornyheads, slope rockfishes and Dover sole. Stocks declared overfished have been given a standard of 10 years to rebuild and require strict management measures in both state and federal waters, including strict annual catch limits. Because petrale sole grow quickly and reach maturity at a young age the recommended management changes lead to a projection of petrale sole to be rebuilt by 2016, well within the 10 year goal. In addition, the NMFS implemented the Shorebased Individual Fishing Quota program in early 2011, which is expected to keep landings of petrale sole (and all other groundfish trawl species) within the trawl allocation limits that have been established.

Highly Migratory Species

Swordfish. Swordfish (*Xiphias gladius*) is the most valuable highly migratory species (HMS) taken in California, in both price-per-kilogram and total revenue; most landings take place in California. In 2010, 367 t of swordfish with an ex-vessel value of $2.2 million were landed in California, a 10% decline from landings in 2009 of 407 t. For 2010, 10% were taken by harpoon gear, 16% were taken by drift gill net gear, and 74% were taken by hook and line gears (mostly Hawaiian vessels fishing outside the Exclusive Economic Zone). Swordfish landings have been affected dramatically by the gear used and management measures implemented over the decades. The 1970s were dominated by harpoon, the 1980s and 1990s by drift gill net gear, and the 2000s by longline gear (fig. 10). Revenues for swordfish peaked in 2000 at $11.3 million and have varied with management measure and gear type. Generally, annual revenues have averaged about $800,000 for harpoon, $3.2 million for drift gill net, and $2.2 million for longline since the fisheries started (fig. 11).

In 2010, the Council decided to change regulations involving the possession and landing of incidentally caught swordfish in the deep-set tuna longline fishery off the West Coast. Formerly, only 10 swordfish were allowed to be retained; the regulation change would allow a 10 fish trip limit if fishing with J-hooks, a 25 fish trip limit if fishing with circle hooks, and no limit if the vessel were carrying an observer. These regulation changes are more consistent with those in the Hawaiian deep-set tuna fishery, and came into effect in April 2011.

Recreationally caught swordfish are an extremely rare occurrence along the West Coast. Since 2003, swordfish have only been caught recreationally in California in 2007; none were recorded in 2010.

Albacore. Albacore (*Thunnus alalunga*) is the most

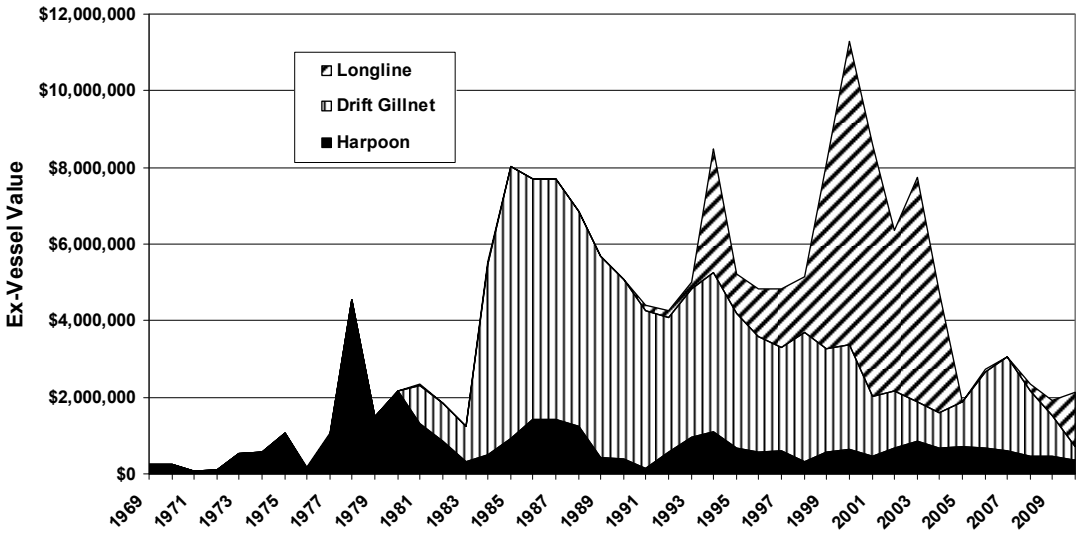

Figure 11. Annual ex-vessel revenue of CA swordfish by gear type 1969–2010.

abundant tuna caught in commercial fisheries and recreational fisheries in California and along the West Coast. In the commercial fishery albacore are caught primarily using hook and line gear (jigs, bait, or trolling), but they are also taken in drift gill nets or purse seines. Along the entire West Coast 11,855 t were landed in 2010, a decrease of 4% coastwide from 2009, when 12,307 t were landed. However, California landings nearly doubled from last year at 742 t. In 2010 the ex-vessel value in California was $1.8 million with a price-per-kilogram of $2.42/kg ($1.10/lb), a few cents lower than the coastwide average. Albacore was the only HMS to be landed in Oregon (4,854 t) and Washington (6,259 t), although in volume it made up 90% of all HMS landed on the West Coast.

Estimates from RecFIN indicate that anglers landed about 10,000 albacore in California, out of 80,000 caught coastwide, mostly in the private/rental boat mode; 38,000 were taken in Oregon and 32,000 in Washington.

Yellowfin Tuna. Landings of yellowfin tuna (*Thunnus albacares*) declined further over 2009's low of 45 t to less than 1 ton landed in 2010, with an ex-vessel value of $6,861; however the price-per-kilogram was $9.04, presumably because of scarcity, as compared with $1.11/kg in 2009. All yellowfin was landed in California by longline gear. About 18 t of fresh yellowtail was exported to Canada and Thailand. CPFV logbooks reported anglers caught 30,961 yellowfin tuna in 2010, with 85% of those fish taken in Mexican waters; this is a 64% drop from 87,064 fish reported in 2009.

Skipjack Tuna. Commercial landings of skipjack tuna (*Kastuwonus pelamis*) in 2010 cannot be reported due to confidentiality requirements and there were no exports. There were 5 t landed in 2009. No skipjack tuna were sampled in 2010 by RecFIN, although California CPFV logs reported 318 fish taken, 98% of which were caught on trips to Mexican waters. This is a 96% drop from 2009, when nearly 7,000 skipjack were taken by CPFV anglers (78% from Mexico).

Bluefin Tuna. Commercial landings of bluefin tuna (*Thunnus thynnus*) also sharply declined in 2010 with only 1 t landed in California. Landings in 2009 had been a five year high at nearly 500 t coastwide (415 t in California and 75 t in Oregon). Ex-vessel price increased to $4.38/kg in 2010, from 1.54/kg in 2009. Nearly all of bluefin caught in 2010 was taken in drift gill nets, in comparison to 2009, when most of the landings came from purse seine gear. Three tons of frozen bluefin tuna was exported to Canada. RecFIN estimates sport anglers took only 20 bluefin tuna in 2010, whereas in 2009 almost ten times as many were landed. CPFV logs report about 8,173 bluefin taken in 2010, with 95% of that occurring in Mexican waters, declining 32% from 2009, when anglers took 12,037 fish (78% from Mexican waters).

Common Thresher Shark. Common thresher shark (*Alopias vulpinus*) is the most common and most valuable shark taken in HMS fisheries. As in 2009, 90% of commercially-caught thresher shark was taken in gill net fisheries in 2010. Landings of common thresher shark declined by 11% from 107 t in 2009 to 95 t in 2010. Ex-vessel value was $154,835 at an average of $2.77/kilogram dressed weight ($1.26/lb), decreasing from $3.14/kg ($1.43/lb) in 2009. California CPFV logs reported 70 threshers caught. RecFIN landings, which include private boats, estimate anglers landed about 1300 thresher sharks in California (less than 10 in Oregon); a decrease from the estimated 2000 last year.

Shortfin Mako Shark. Shortfin mako shark (*Isurus oxyrhincus*) is the second most common shark landed in California HMS fisheries; 87% of were taken by gill net

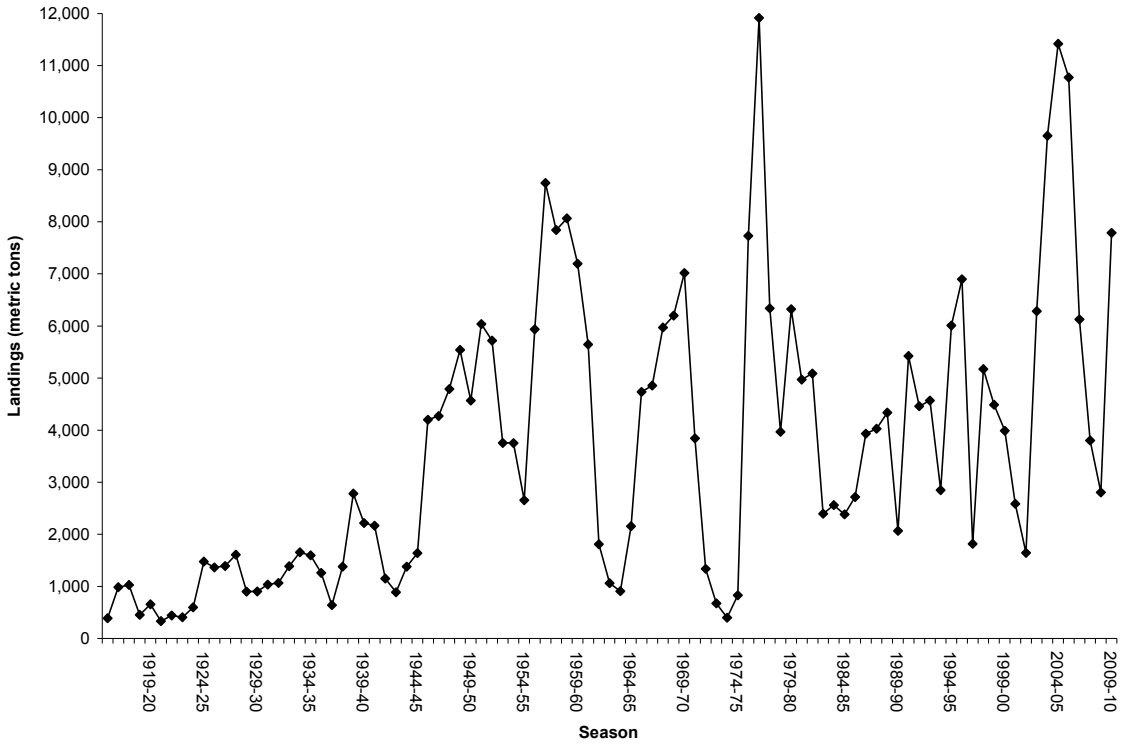

Figure 12. California commercial Dungeness crab (*Metacarcinus magister*) landings, 1915–16 to 2009–10.

gear in 2010, with 13% taken by hook and line gear. Mako shark landings decreased 29% from 2009's landings of 30 t to 21 t in 2010. Ex-vessel revenue was $35,565, with an average price-per-kilogram of $2.44 ($1.11/lb) dressed weight, a slight decrease from $2.64/kg ($1.20/lb) in 2009. CPFV logs reported 268 mako sharks taken in 2010, a decrease of 26% from 359 in 2009, while RecFIN estimated 361 taken by primarily private vessels.

Dorado (dolphinfish). Commercial landings of dorado (*Coryphaena hippurus*) increased to 3.7 t in 2010, more than five times the amount landed in 2009. The ex-vessel revenue was $15,851, at $4.73/kg, 24% less than 2009's price-per-kilogram of $6.25/kg. In contrast, CPFV logs recorded a decrease in landings in 2010, with 1,317 fish landed, only 7% of the previous year when anglers took 18,981 fish; 86% of dorado taken by CPFVs in 2010 were from Mexican waters.

HMS Management. In light of the Magnusson Act Reauthorization, the Council approved Amendment 2 to the Highly Migratory Species Fishery Management Plan (HMS FMP) on Annual Catch Limits for HMS. As part of this decision, management unit species were redefined as albacore tuna, bigeye tuna, skipjack tuna, bluefin tuna, yellowfin tuna, striped marlin, swordfish, blue shark, common thresher shark, shortfin mako shark and dorado. Bigeye thresher shark and pelagic thresher sharks were moved from management unit species to ecosystem component species, that is, species which are occasionally incidentally caught, but either in limited amounts or seldom retained. These also included common mola, escolar, lancetfishes, louvar, pelagic stingray, and wahoo. The Council included language: 1) to apply the international exception to all management species (i.e., to be managed according to measures of international Regional Fishery Management Organizations); 2) on the need to coordinate with the Western Pacific Fishery Management Council as to lead roles for particular species; 3) that estimates of maximum sustainable yield (MSY) and optimum yield (OY) can be adjusted as new data become available, but in the interim will be used as currently described in the FMP.

Dungeness Crab

The fishery for Dungeness crab, *Metacarcinus magister,* (formerly *Cancer magister*) is highly cyclical and spans the West Coast of North America from Alaska to Point Conception, California. California commercial landings of Dungeness crab for the 2009–10 season totaled 7,789 t, more than double the catch of the 2008–09 season, and just above both the 10-season and 50-season moving averages of 6,288 t and 4,535 t, respectively (fig. 12). The 2009–10 season marked the beginning of an upturn in the catch cycle from a low of 2,807 t the previous season. The average price paid to fishermen was $4.39/kg ($1.99/lb) resulting in a total ex-vessel value of $34.2 million. Value increased by 133% from the previous sea-

son, which was worth an estimated $14.7 million. The rate of increase in landings and value over the previous season was relatively even between the two fishing regions of northern and central California. During the past decade, northern California landings have averaged three times the amount of central California catches, with the regional boundary at the Sonoma/Mendocino county line. Initial data from the first six weeks of the 2010–11 season ending on Dec 31, 2010, indicate a dramatic and unprecedented shift in catch to the central coast, with 6,145 t landed in central California out of a statewide total of 8,187 t, already exceeding the previous season's total catch.

Dungeness crab is one of California's largest and most valuable commercial fisheries, managed through the state legislature, and is also the basis of a robust sport fishery, managed through the Commission. The commercial fishery regulations are comprised of size, sex and seasonal restrictions, along with restricted access to the fishery. Only male crabs larger than 159 mm (6.25 in) carapace width are harvested commercially. The minimum size limit is designed to protect sexually mature male crabs from harvest for at least one season. This provision seems successful because studies have shown that, despite the presumption that nearly all legal sized male crabs are harvested each season, most sexually mature female crabs are fertilized each year. The central California season, south of the Mendocino/Sonoma County line, begins 15 November and ends 30 June. The northern California season, north of the line, conditionally begins on 1 December and ends 15 July. The timing of the seasons avoids the portion of the lifecycle when most crabs are molting or soft-shelled, and thus vulnerable to predation and handling mortality.

Mature males molt annually in the summer and then begin gaining weight in their new shells. The timing of this molt varies, but the 1 December fishery opening along most of the West Coast usually results in adequately filled out crab reaching the popular holiday markets. However, commencing in the 1995–96 season the state legislature authorized an industry-funded preseason crab quality test to ensure crab are ready for harvest on the target opening date. The test is conducted in concert with tests in Washington and Oregon. The states then mutually agree, through the Tri-state Crab Committee, on whether to delay the opening of the season in order to let the crabs accumulate more body meat weight. Thus far, only the 2005–06 northern California season has been delayed via this process. The 2010–11 season was delayed unofficially until December 10, north of Sonoma County, by mutual agreement of fishermen and processors, but not by action of the state agencies. Central California coast crab typically molt earlier than northern crab, and the area is not included in the testing procedure or subject to opening delays. In case of a northern season delay, "fair start" statutes mandate that anyone fishing in the central area must wait 30-days after the delayed northern season opener to fish in those northern waters.

The sport fishery is mainly controlled through size, season, and bag limit regulations. The minimum size for sport fishing is 146 mm (5.75 in) and, unlike the commercial fishery, the take is not legally limited to male crabs. The daily bag limit and possession limit is ten crabs. Sport fishers on CPFVs, a growing trend in the last decade, are generally subject to the same regulations, except that when fishing from Sonoma County and south, the bag limit is reduced to six and the size limit is 152 mm (6.0 in). In November 2009, the CRFS began sampling Dungeness crab sport fishing from shore and private, rental and CPFV vessels. CRFS estimated that for the 2009–10 recreational season, 365,000 Dungeness crabs were caught—mostly using vessels. This represents less than 250 t based on an estimated weight of 0.68 kg (1.5 lb) per crab, or about 3% of the commercial catch during this time period.

Of the approximately 585 vessels with a 2010 commercial Dungeness Crab Vessel Permit, 397 boats made at least one landing in the 2009–10 season. The Dungeness crab fishery can be characterized as a derby-type fishery where much of the total catch is caught in a relatively short period of time at the beginning of the season. For example, in the 2009–10 season, 80% of the statewide catch was landed by 1 January—only six weeks after the northern season opened in central California. There is no limit to the number of traps a vessel may fish or the frequency with which they are fished, and no reliable estimates of either effort level. As the groundfish industry has declined, larger multipurpose vessels have devoted more effort to Dungeness crab. According to a 2003 CalCOFI report based on a fisherman survey, there were at least 172,000 traps being fished in California during the 2001–2002 season. In Oregon's comparable Dungeness crab fishery, the estimated number of traps soared from 150,000 in 2002 to 200,000 in 2005 before implementation of a trap limit program. Complaints of overcrowded fishing grounds, in central California in particular, have escalated in recent years.

Concerns over effort in terms of crab traps, deployed in both central and northern California, led to multiple unsuccessful legislative attempts by California fishermen to create a trap limit program for their district. Failures to reform the fishery in the past were generally attributed to lack of agreement between fishermen in the two regions. In 2008, a small group of crab fishermen, with assistance from an environmental non-profit organization, prompted the passage of legislation which mandated the formation of a Dungeness Crab Task Force

Figure 13. California commercial spiny lobster (*Panulirus interruptus*) landings by weight, 1916–2010.

(DCTF) comprised of commercial and sport fishing representatives along with non-governmental and government agency advisors. A total of 24 recommendations and five objectives were included in two final reports produced by the Task Force in January 2010. Recommendations included support for controlling total allowable commercial effort, defining latent permits, putting special restrictions on latent permits, defining vessel size expansion, preventing permit transfers to fish processors, continuing current management schemes (size, sex, season), and—most notably—a strong recommendation for an industry funded, statewide, tiered trap limit program. As of May 2011, a bill extending the existence of the DCTF and creating a trap limit program was moving forward through the legislative process.

California Spiny Lobster

A total of 319 t the California spiny lobster (*Panulirus interruptus*) was commercially landed in 2010, a 1 t less than in 2009 (fig. 13). While substantially lower than the recent peak of 403 t in 2006, the 2010 landing total continues a trend of 300 t, or more, lobsters landed per calendar year since 2000. The 2010 ex-vessel value of the lobster fishery was $11.13 million, up from the $7.89 million in 2009, and greatly surpassing the previous high of $8.06 million set in 2006.

The commercial and recreational seasons for harvesting California spiny lobster begin in late September and extend to the middle of March. Essential commercial fishery information is collected using fishermen logbooks and dealer landing receipts. Logbooks record location and date of catch, number of traps pulled, and number of lobster kept and released. Landing receipts record catch location, size of catch in pounds, and the price paid per pound. The recreational season is monitored through the use of a lobster report card introduced at the beginning of the 2008–09 recreational season and from data collected by California Recreational Fisheries Survey samplers.

The commercial lobster fishery is managed by a restricted access program. In 2010, there were 200 lobster operator permits and three-quarters of those permits are transferable. Since April 1, 2008, there have been no restrictions on the number of transferable permits that can be transferred. Seventeen permit transfers took place in calendar year 2010. In the 2009–10 season, the number of active fishermen numbered 152, almost equal to the 151 fishermen that were active during 2008–09.

Currently, there are no limits on the amount of lobster that permittees can land or the number of traps they can use. Traps are generally set along depth contours in the vicinity of kelp beds along the mainland and at all the Channel Islands. Typically, between 100 and 300 traps are set at a time although operators with larger boats or a crewmember may set more. Soak times in 2009–10 averaged three days. The total number of trap pulls in the 2009–10 season is estimated at 859,000 resulting in a catch of approximately 1.7 million lobsters, of which 28% were retained which translates to a preliminary landing weight of approximately 319 t. The landing weight of the 2008–09 season was higher than that of the 2009–10 season at 330 t.

The median ex-vessel price for the 2009–10 season was $26.46/kg ($12.00/lb). The median ex-vessel price for the 2010 calendar year, however, jumped to $35.27/kg ($16.00/lb) due to a dramatic increase in price paid

for lobster that began with the arrival of the 2010–11 season. The ex-vessel price ranged from $17.64/kg ($8.00/lb) to $37.48/kg ($17.00/lb) for the 2009–10 season and from $17.64/kg ($8.00/lb) to $40.79/kg ($18.50/lb) for the 2010 calendar year. The ex-vessel value of the 2009–10 lobster season was $9 million. Point Loma landings had the highest ex-vessel value at $1.39 million representing 15% of the total season value.

Recreational fishermen are allowed to catch lobster by hand when snorkeling or scuba diving, or by using baited hoop nets. Up to five baited hoop nets per person, with a maximum of ten hoop nets per boat, can be used. There is a daily bag and possession limit of seven lobsters per fisherman. In both the recreational fishery as well as the commercial fishery, lobsters must exceed a carapace length of 82.6 mm (3.25 in) to be kept. A 1992 Department creel survey involving four sites in San Diego and Ventura counties during the first two weekends of the season revealed that approximately 80% of the interviewed lobster fishermen used scuba gear to catch lobsters; 20% used hoop nets. A 2007 creel survey was conducted at the same 1992 survey sites during the first 10 weeks of the 2007–08 lobster season. Using data from the first two weekends, this creel survey found the opposite: approximately 80% of the fishermen used hoop nets while only 20% used scuba gear. Recent years have seen the introduction of a more efficient hoop net into the fishery which a Department study showed can catch 57% more lobster than a traditional hoop net with the same effort.

A lobster report card, which is issued for the calendar year like the annual fishing license, was introduced in fall 2008. Fisherman fishing for lobster are to record the time, location, gear, and retained catch, if any, by trip. There were approximately 27,500 cards sold in 2008, 31,000 cards sold in 2009, and 29,000 cards sold in 2010. These numbers estimate the potential extent of recreational fishery effort; however there is an additional and unquantified population of poachers retaining lobsters illegally. The return rate of cards has precipitously fallen—from 22% of 2008 cards, to 14% of 2009 cards, to 11% of 2010 cards. Due to low return rates of cards, certain assumptions are made by the Department and the true ratio of hoopnetters to divers remains unknown although some constants can be seen in the first few years of report card data. The % of returned report cards indicate that lobster fishing effort has remained at about 86%. The % of fishing trips that caught zero lobsters has remained fairly constant at 36–40%. The mean number of trips per card has fluctuated from 4.4 trips per card in 2008, to 5.3 trips per card in 2009, and 5.1 trips per card in 2010. Catch per trip and catch per card have remained constant. From 2008–2010, catch per trip only varied from 2.1 to 2.2 lobsters per trip. During the same time period, catch per card has varied from 9.1 lobsters in 2008, to 11.6 lobsters in 2009, to 10.5 lobsters per card in 2010.

Department biologists extrapolated the available report card data to obtain estimates of the 24,000 lobster fishermen that actually fished in 2008, the 26,500 that fished in 2009, and the 25,000 that fished in 2010. An estimated 219,300 lobsters were retained in 2008, 308,400 in 2009, and 262,100 in 2010 by the recreational fishery. Department creel survey data indicates that a legal sized (83 mm) lobster weighs on average 0.59 kg (1.3 lbs), allowing a total retained weight of the recreational catch to be estimated. For 2008, total retained catch was estimated at 129 t (285,000 lbs), 2009 total retained catch was estimated at 182 t (401,000 lbs), and 2010 total retained catch was estimated at 155 t (341,000 lbs). The recreational fishery landed an amount of lobsters equal to 39% of commercial landings in 2008, 57% of the commercial total in 2009, and 49% of the commercial total in 2010. The establishment of the lobster report card has allowed the Department to estimate the size of the recreational fishery and to determine that it is indeed a significant portion of the total lobster harvest in California.

In 2009, spiny lobster were identified within the Department as a high-priority for the development of a fishery management plan (FMP). As an early part of the FMP process, a stock assessment was initiated. First, data sources were identified and evaluated for use in the effort. Since there is currently no fishery-independent index of abundance for spiny lobster north of the Mexican border that covers the full range of the stock, an effort was made to concentrate on data sets that cover the entire Southern California Bight. The Department digitized over 20 years of commercial logbook information as well as the newly introduced recreational lobster report cards. Data entry occurred in parallel with the stock assessment efforts that continue to this day. The assessment effort initially concentrated on the development of models and approaches that could provide reference points for the FMP, focusing primarily on using a surplus production model (ASPIC). Preliminary steps were also taken to develop size/age structure information for use in more sophisticated approaches. Ultimately, the ASPIC model failed with the datasets available. A model based on Beverton and Holt invariant methods, used to evaluate the Baja fishery, could provide valuable information and reference points, and will be evaluated in 2011.

Spot Prawn

Preliminary 2010 spot prawn (*Pandalus platyceros*) landings were 110 t, a 14% decrease from 2009 (128 t) (fig. 14). Market demand for spot prawn is high, and

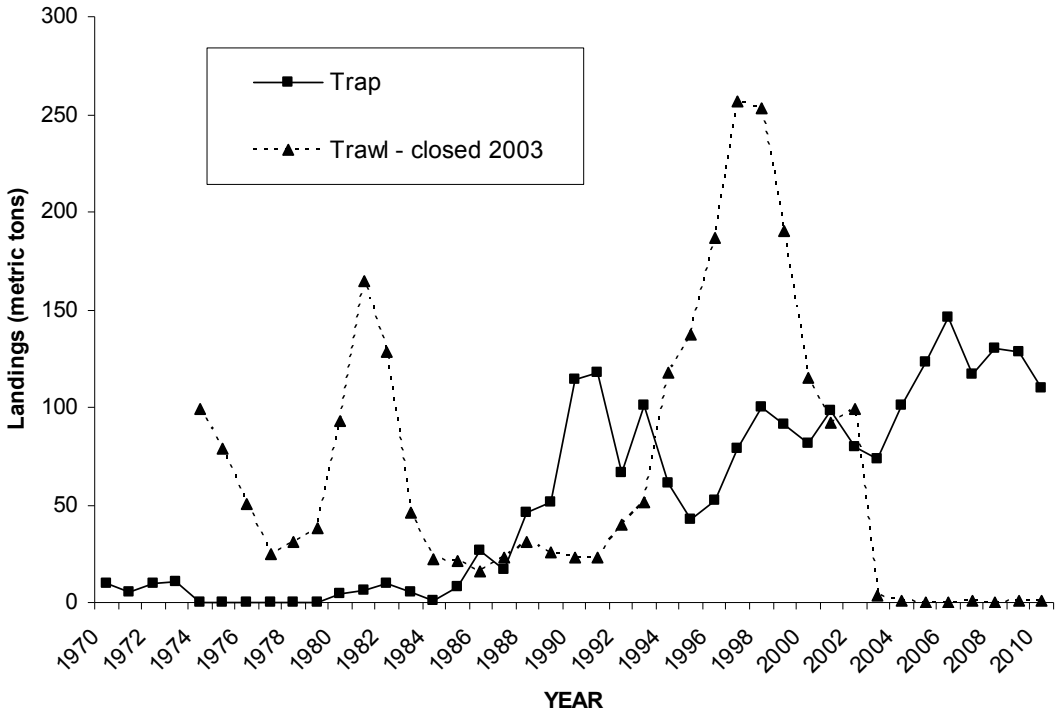

Figure 14. California spot prawn (*Pandalus platyceros*) landings, 1970–2010.

the decrease in landings is most likely due to the poor weather and sea conditions that characterized 2010. The spot prawn fishery originated in Monterey Bay as an incidental catch in octopus traps. In 1974, a trawl fishery targeting spot prawns developed off Santa Barbara. Until 2002, spot prawn were harvested by trawl and trap gear. In 2003, the use of trawl gear for the take of spot prawn was outlawed because of the bycatch of rockfish, particularly bocaccio, an overfished species. Consequently, 2003 spot prawn landings were the lowest since 1987 when trapping was just getting underway in southern California. The annual trap harvest has averaged 122 t since 2004, and appears to be sustainable.

Spot prawn is currently caught only with trap gear, although a small amount shows up as bycatch in the ridgeback prawn trawl fishery. Spot prawn traps are required to be made of mesh with a minimum inside measurement of 2.22 x 2.22 cm (7/8 × 7/8 in). The traps may not exceed 1.8 m (6 ft) in any dimension. The baited traps are fished in strings at depths of 174–302 m (95–165 fathoms) along submarine canyons or shelf breaks. Each string consists of a groundline with anchors and a buoy at one or both ends, and 10 to 30 traps attached. No other species may be taken in a prawn trap, so all bycatch is returned to the water immediately. Fishermen are required to fill out a logbook.

A two-tiered restricted access trap vessel permit program was initiated in 2002. Tier 1 permittees may use no more than 500 traps, unless fishing in state waters north of Point Arguello where they are only allowed the use of 300 traps. Tier 1 permits became transferable on April 1, 2005, and there are currently 17 vessels in Tier 1. The Tier 1 vessel permits are sold on the open market and are the highest priced permit in California fisheries. The Department receives a transfer fee of $50.00 when a permit is transferred to the new vessel owner.

Tier 2 vessel permittees made a smaller number of qualifying trap landings, and are limited to an annual harvest quota of just over 2 t. Permittees may use no more than 150 traps and the permits are non-transferable. There are three Tier 2 vessels.

When the use of trawl gear for the take of spot prawn was prohibited, the Commission directed the Department to develop a conversion program for the trawl fleet. A conversion program went into effect in 2005, which allowed the owners of a dozen former spot prawn trawl vessels to purchase Tier 3 spot prawn trap vessel permits that year. Tier 3 permits have the same restrictions as Tier 1 permits with the major exception of the permits being non-transferable. Eight Tier 3 vessels remain. In 2010, the fee for the Tier 3 permit was $1,269.00, whereas both Tier 1 and Tier 2 vessel permits were $317. Permits must be renewed annually or they are lost.

In 2010, 19 trap permittees landed spot prawn. Four of the 19 permittees fished north of Point Conception, mainly in the vicinity of Monterey Bay Canyon. The remaining 15 vessels fished in southern California, fre-

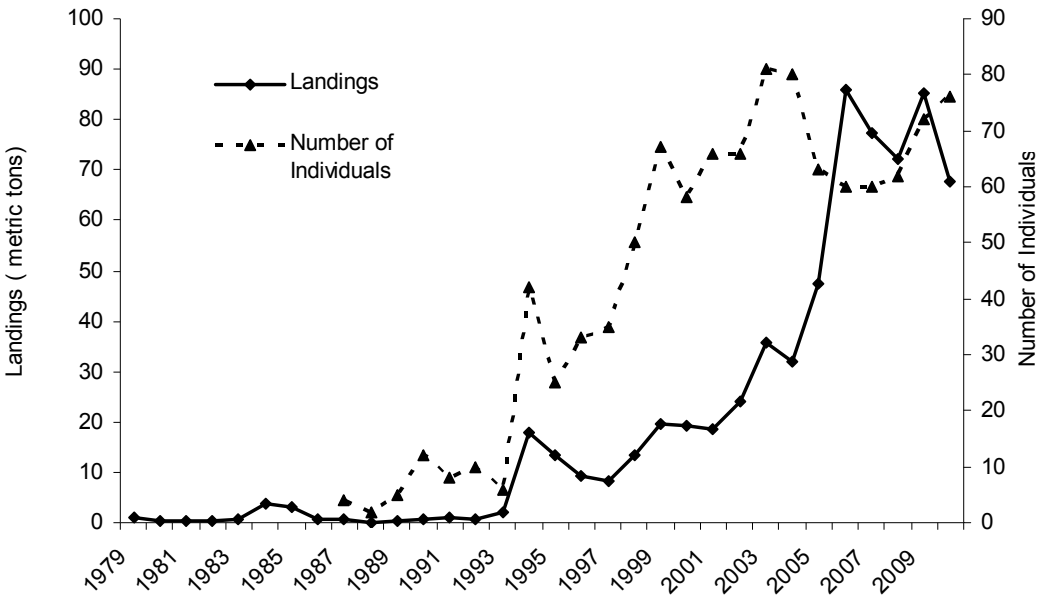

Figure 15. California commercial landings of Kellet's whelk (*Kelletia kelletii*), 1979–2010.

quently off one of the Channel Islands. This fishing pattern has been stable for the past five years.

Fifteen of the 17 Tier 1 trappers landed 86% of the catch, with each vessel landing an average of 6.3 t. All three Tier 2 fishermen fished, and only one of the Tier 3 permittees went fishing. The other seven Tier 3 permittees have not had the capital necessary to purchase a vessel more suitable for trapping, or the necessary traps and associated ground tackle. A 22.7 kg (50 lbs.) allowance of spot prawn while trawling for ridgeback prawn is still legal, but spot prawn may not be landed as bycatch when trawling for pink shrimp.

Almost all spot prawn harvested is sold live, with ex-vessel prices ranging from $22 to $31/kg ($10.00 to $14.00/lb). Fresh dead spot prawn generally sells for half the price of live. Most trap permittees have invested in live tanks and chillers on their vessels to keep the prawns in top condition for the live market. The trap fishery in southern California (south of Point Arguello) is closed from 1 November to 31 January to provide protection for ovigerous females. North of Point Arguello, the spot prawn trap season is closed from 1 May to 31 July, an accommodation to prevent serious fishing gear conflicts in the Monterey Bay area.

Kellet's Whelk

Kellet's whelk (*Kelletia kelletii*) supports a growing commercial fishery, but is not important recreationally. Commercial landings increased steadily from insignificant levels in the early 1990s to nearly 80 t in 2006 (fig. 15). During the most recent five years, catches have averaged 78.8 t. Landings in 2010 were 67.5 t with an ex-vessel value of $117,000.

The Kellet's whelk is a large predatory gastropod in the family Buccinidae. Kellet's whelk shells can reach nearly 179 mm (7 inches) with conspicuous whorls, conchlike in appearance and tan to white or green coloration. Whelks inhabit subtidal rocky substrates from the intertidal to depths of 70 m. The historic distribution of whelks extends from Isla Asuncion in Baja California, Mexico to Point Conception north of Santa Barbara, California. In the 1980s whelk expanded their historic range when they were observed north of Point Conception in Monterey Bay, California.

Little is known about the population status of Kellet's whelk. Several subtidal monitoring programs quantify whelks since they are large conspicuous snails. One trend that has been quantified is that whelk in the historic portion of their range in the Southern California Bight are at higher densities than at the northern end of the new range north of Point Conception. One study found densities of adult whelk tenfold greater at sites south of Point Conception compared with newly inhabited sites north of Point Conception. Furthermore, sites to the north lack small whelks in some years suggesting there may be irregular recruitment.

The number of annual participants in the commercial fishery has fluctuated around seventy individuals during the past decade, following a steady increase in the 1990s. The average whelk in the fishery weighing 150 g, which equates to roughly 2.65 million whelk taken since 2006. Whelk are commercially caught in southern California incidentally in lobster and crab traps, and are also targeted with a small dive fishery. In 2010, the dive fishery landed just 1% of the catch. The peak year for the dive fishery was 2003 when the fishery landed 8.4 t, account-

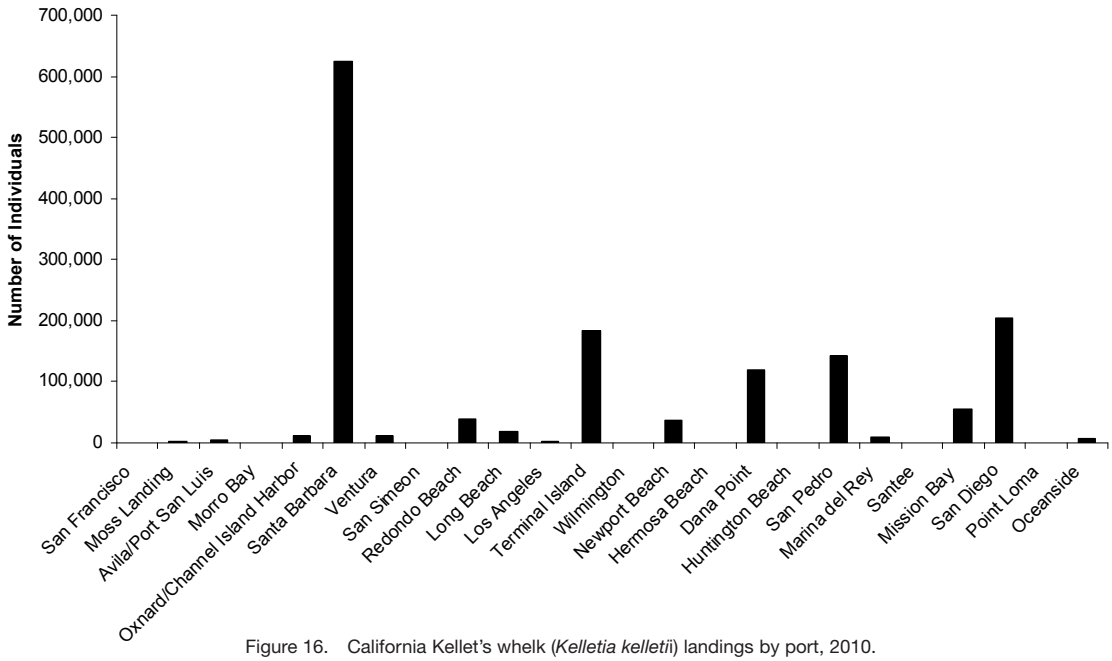

Figure 16. California Kellet's whelk (*Kelletia kelletii*) landings by port, 2010.

ing for 24% of the total catch. Since then, the dive fishery has decreased in importance, comprising only 3% of the total landings over the past five years. Whelk landings in the fishery are spread evenly across the 12 months of the year.

Whelk are taken in the southern California rock crab fishery which is open year round and the lobster fishery which is open from October to mid-March. Whelk may not be taken in the tidal invertebrate zone between the high tide mark and 1,000 feet beyond the low tide mark. In addition, commercial divers must hold a commercial dive permit and recreational divers must adhere to the distance restrictions while obeying a 35 whelk per day bag limit. Scientific collectors during the four year period from 2003–2006 took a total of 2,066 whelk.

Most whelk are landed in five ports in the Southern California Bight (fig. 16). The top port is Santa Barbara, followed by San Diego, Terminal Island, San Pedro and Dana Point. These top five ports account for 86% of the catch. Kellet's whelk are fished for human consumption and sold live in fresh fish markets. Ex-vessel value in the fishery closely tracks landings over time with the highest values during the years of the highest landings. The value of the fishery in 2010 was $117,000 with the average of the last five years slightly higher at $134,000.

Emerging Fishery Status. In April 2011, Kellet's whelk was named an emerging fishery by the Fish and Game Commission. A fishery can be designated as an emerging fishery as outlined in Fish and Game Code if the landings or the number of participants increases or if the gear efficiency increases such that "*the existing regulations are not sufficient to insure a stable, sustainable fishery*." Both landings and the number of participants in this fishery have increased dramatically since 1993. In addition, there is concern that the new transferability of the southern rock crab trap permits may also lead to an increase in Kellet's whelk landings. Furthermore, rock crab trap permits are relatively inexpensive ($350) and transfer fees are $1,000. However transferable permits on the open market can sell for more than 10 times this amount. Therefore, the whelk fishery was deemed to meet the conditions necessary for listing as an emerging fishery.

Management Considerations. Although currently there are no management measures in place for Kellet's whelk, there are a number of options available for consideration. One possibility is size limits structured to allow for a number of spawning seasons prior to entry into the fishery. Implementation of size limits would require site-specific information about size-frequency distributions. Season closures could be established to avoid months when mating and spawning takes place to protect reproduction. Since the fishery operates during all months, biological spawning considerations could help guide season closures. Catch limits could be implemented in the fishery to conserve the resource and provide for a sustainable fishery. More work quantifying the density of whelks at numerous sites could be conducted to inform decisions about possible regulations. Finally, gear restrictions and or depth restrictions could be implemented in the fishery. Depth limits could be implemented to ban the catch of whelk in traps at certain depths providing a refuge in depth from fishing mortality. This approach is currently used in the recreational red abalone fishery in northern California where

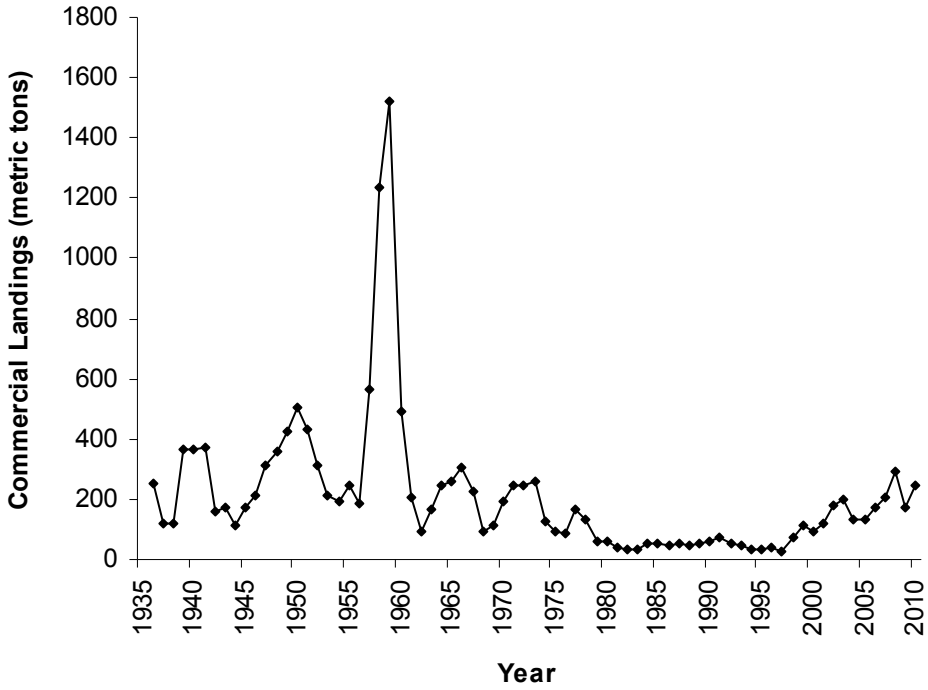

Figure 17. California commercial white seabass (*Atractoscion nobilis*) landings, 1935–2010.

only free divers are permitted to fish, which in effect excludes abalone in the deeper habitat from the fishery.

White Seabass

The white seabass (*Atractoscion nobilis*) is the largest member of the Sciaenid family found in California waters. In addition to being a popular sport fish, white seabass is also targeted by a commercial fishery. The commercial white seabass fishery landed 243 t in 2010 (fig. 17), a 39% increase from the 2009 total of 175 t. Estimates of recreational take for 2010 are generated from the CRFS for the private boat and shore-based modes. The estimate of recreational take increased by 56% to 121 t in 2010 from the previous year's total of 77 t. The recreational catch estimates prior to 2004 are from a different survey and are not directly comparable to the estimates from the CRFS (see Groundfish, Recreational Fishery, above). However, historical trends in the recreational catch of white seabass can be determined from CPFV logbook data (fig. 18). The combined commercial and recreational catch for 2010 was 364 t.

Commercial and recreational fisheries for white seabass in California have existed since the 1890s. Historically, commercial landings have fluctuated widely, including the landings of white seabass taken in Mexican waters by California commercial fishermen. In 1959, the white seabass commercial take in Mexican waters was 1% of California's white seabass annual landings, while in 1981, it reached 89% of the total annual catch (fig. 19). Since this time, the Mexican government has prohibited access permits to the U.S commercial fleet.

Beginning in 1994, the use of set and drift gill nets within 3 nautical miles of the mainland shore from Point Arguello to the U.S. Mexico border and in waters less than 70 fathoms or within 1 mile (whichever is less) of the Channel Islands was prohibited. In April 2002, the use of gill and trammel nets in depths of 60 fathoms or less was prohibited from Point Reyes to Point Arguello. Despite such restrictions, most commercial white seabass landings are still taken with set and drift gill nets. In 2010, set and drift gill nets accounted for 76% of the commercial landings by weight, while hook and line vessels accounted for 22%. Although the hook and line fishery, as well as trawl and other incidental gears (trap), continues to be a minor component of the commercial fishery, the number of hook-and-line vessels targeting white seabass has increased by 266% since 2008. Almost half of these vessels, however, made less than three landings in 2010, indicating that the majority of hook and line vessels opportunistically catch white seabass when available along the coast.

The minimum legal size limit for white seabass in the commercial and recreational fisheries is 710 mm (28 in.). The commercial fishery for white seabass is closed between Point Conception and the U.S. Mexico border from 15 March to 15 June, except one fish not less than 710 mm in total length may be taken, possessed, or sold by a vessel each day if taken incidental to gill and trammel net fishing operations. In 2010, the average ex-vessel value paid by dealers was $2.76/lb. The total ex-vessel value in 2010 was $1,528,913, approximately 76% more than in 2009.

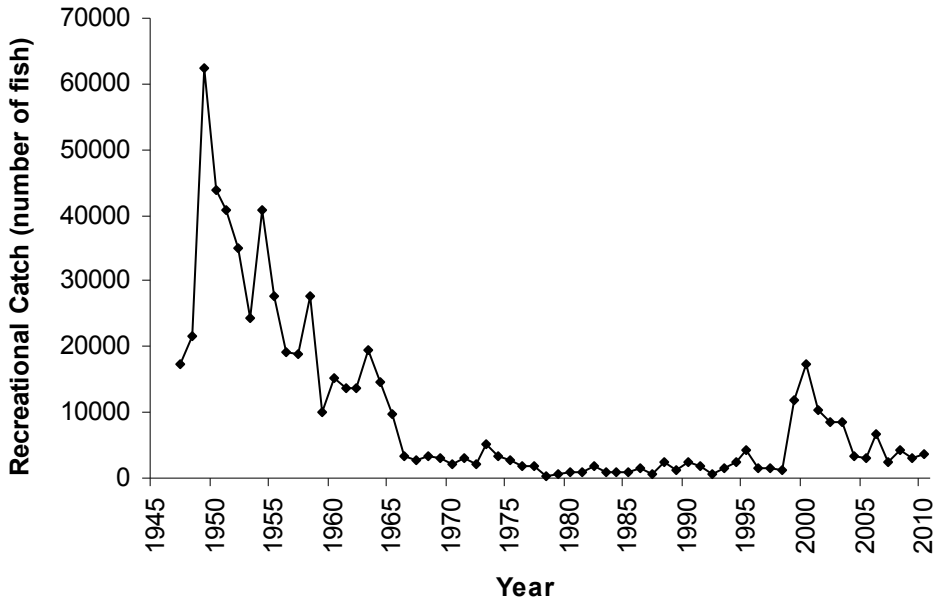

Figure 18. California recreational white seabass (*Atractoscion nobilis*) landings, from Commercial Passenger Fishing Vessel logbooks, 1947–2010.

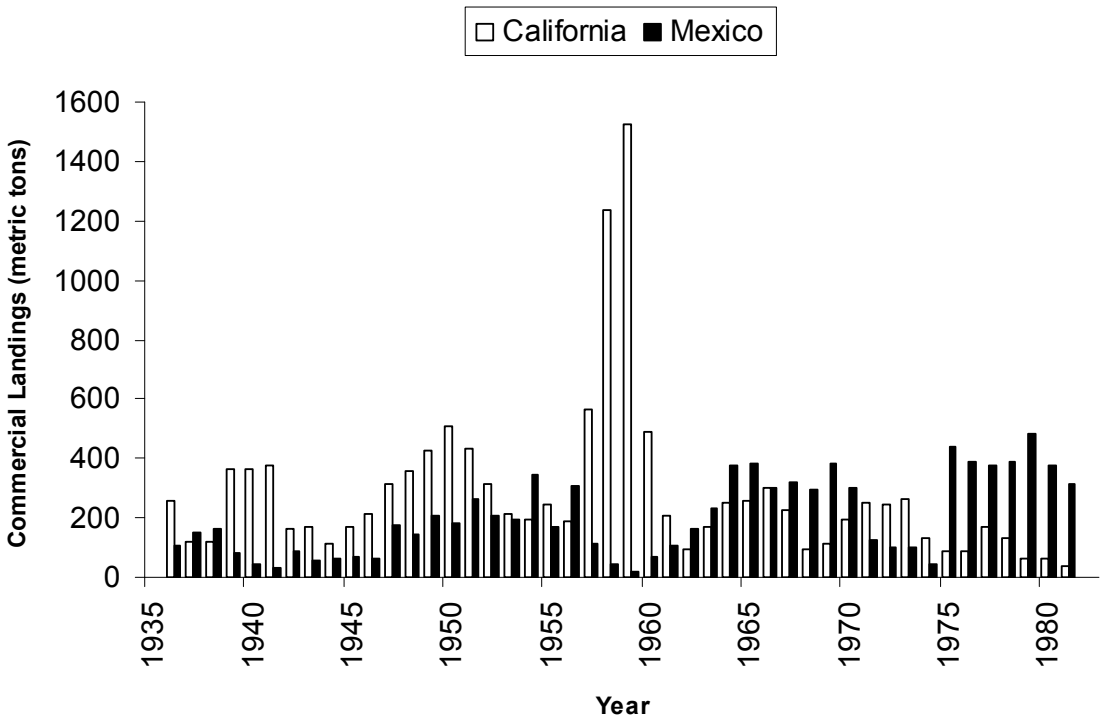

Figure 19. Comparison of landings of white seabass (*Atractoscion nobilis*) taken in California and Mexican waters by California commercial fishermen, 1936–1981.

The recreational fishery for white seabass occurs almost entirely south of Point Arguello. Typically, 95% to 99% of the catch is caught south of this point; however, in 2010, only 62% of the catch occurred south of Point Arguello, while 38% occurred within northern California. This increase of the northern catch is attributed to the high numbers of white seabass available within Monterey Bay from August to October 2010. The fishery is open all year, but the majority of the recreational take occurs between March and September. The daily bag limit is three fish, except from 15 March through 15 June when the daily bag limit is one fish. Most fish are caught by hook and line anglers onboard CPFVs and private boats.

In 1982, the California Legislature established the Ocean Resources Enhancement and Hatchery Program (OREHP). This legislation was adopted to fund research into the artificial propagation of marine finfish species whose populations had become depleted. The ultimate goal is to enhance populations of marine finfish species important to California for their recreational and commercial fishing value. Initially, research was focused on California halibut and white seabass; however, white seabass was eventually chosen as the primary focus because of the depressed condition of the stock at the time and its higher value to recreational and commercial fishermen.

The Department manages the OREHP with the assistance of an advisory panel that consists of academic and management agency scientists, representatives of both commercial and recreational fishing groups, and the aquaculture industry. The program is funded through the sale of recreational and commercial marine enhancement stamps for all saltwater anglers south of Point Arguello. In 1995, the OREHP completed construction of the Leon Raymond Hubbard, Jr. Marine Fish Hatchery in Carlsbad, California. The primary function of the hatchery, which is operated by the Hubbs-SeaWorld Research Institute (HSWRI), is to provide juvenile white seabass, approximately 4 inches (100 mm) total length (TL), growout pens operated by volunteer fishermen and nonprofit organizations. Currently, the hatchery and growout pens may release up to 350,000 juvenile white seabass per year.

There are 13 growout pens located in bays and marinas from Santa Barbara to San Diego in southern California. At the growout pens, juvenile white seabass are reared to 200–250 mm TL before they are released at or near the growout site. In 2010, 89,002 hatchery-raised white seabass were released, approximately 42% of last year's release of 152,658 fish. This decline in production was due to disease issues within the hatchery and growout facilities. Since 1986, over 1.7 million white seabass, each implanted with a coded wire tag (CWT), have been released from the OREHP facilities.

Since the mid-late1980s, the OREHP has contracted with researchers to develop juvenile and adult sampling programs to assess the proportion of hatchery-raised fish to the wild population. In the late 1990s, HSWRI researchers developed a sampling program to recover adult hatchery-raised white seabass from the commercial and recreational fisheries. The program, which is ongoing, is aimed at scanning white seabass for the presence of a CWT. Since the inception of both programs, 1,400 hatchery-raised juvenile white seabass have been recovered in the juvenile gill net studies while 171 tagged adult white seabass (legal-size) have been recovered from the recreational and commercial fisheries.

In June 2010, the Department submitted the White Seabass Enhancement Plan (WSEP) to the Commission, which it approved on 21 October 2010. The WSEP provides a framework for managing the OREHP in an environmentally sustainable manner and establishes best management practices (BMPs) for hatchery and growout operations, fish health, genetics, and benthic monitoring.

To manage the state's commercial and recreational fisheries for white seabass, the Commission adopted a White Seabass Fishery Management Plan (WSFMP) in 1996. To implement the WSFMP, the Commission adopted regulations in 2002 to establish a fishing season of September 1 through August 31 of the following year. The Commission also adopted an optimum yield (OY) in 2002. The OY is based on a maximum sustainable yield proxy of the unfished biomass and is currently set at 540 t (1.2 million pounds). The OY has never been reached since its implementation, but came close in the 2001–02 fishing season when combined landings reached 530 t (1,177,781 pounds). In the 2009–10 fishing season, the total recreational and commercial harvest was 305 t (678,262 pounds), 57% of the allowable catch.

Editor:
D. Sweetnam

Contributors:
K. Barsky, Spot prawn
T. Buck, Lobster
P. Kalvass, Dungeness crab
L. Laughlin, Highly migratory species
C. McKnight, Groundfish
B. Miller, Market squid
J. Phillips, Ocean salmon
L. Rogers-Bennett, Kellet's whelk
V. Taylor, White seabass
P. Ton, Coastal pelagic finfish

STATE OF THE CALIFORNIA CURRENT 2010–2011: REGIONALLY VARIABLE RESPONSES TO A STRONG (BUT FLEETING?) LA NIÑA

ERIC P. BJORKSTEDT
NOAA Fisheries Service
Southwest Fisheries Science Center
Fisheries Ecology Division and
Department of Fisheries Biology
Humboldt State University
P.O. Box 690
Trinidad, CA 95570

RALF GOERICKE
Scripps Institution of Oceanography
University of California, San Diego
9500 Gilman Drive
La Jolla, CA 92093-0205

SAM MCCLATCHIE, ED WEBER,
WILLIAM WATSON, NANCY LO
NOAA Fisheries Service
Southwest Fisheries Science Center
8604 La Jolla Shores Drive
La Jolla, CA 92037-1508

BILL PETERSON, BOB EMMETT,
RIC BRODEUR
NOAA Fisheries Service
Northwest Fisheries Science Center
Hatfield Marine Science Center
Newport, OR 97365

JAY PETERSON, MARISA LITZ
Cooperative Institute for
Marine Resource Studies
Oregon State University
Hatfield Marine Science Center
Newport, OR 97365

JOSÉ GÓMEZ-VALDÉS,
GILBERTO GAXIOLA-CASTRO,
BERTHA LAVANIEGOS
Centro de Investigación Científica y de
Educación Superior de Ensenada (CICESE)
División de Oceanología
Carretera Ensenada-Tijuana #3918
Zona Playitas, Ensenada, B.C., Mexico

FRANCISCO CHAVEZ
Monterey Bay Aquarium Research Institute
7700 Sandholdt Road
Moss Landing, CA 95039

CURTIS A. COLLINS
Naval Postgraduate School
Monterey, CA 93943

JOHN FIELD, KEITH SAKUMA
NOAA Fisheries Service
Southwest Fisheries Science Center
Fisheries Ecology Division
110 Shaffer Road
Santa Cruz, CA 95060

STEVEN J. BOGRAD,
FRANKLIN B. SCHWING
NOAA Fisheries Service
Southwest Fisheries Science Center
Environmental Research Division
1352 Lighthouse Avenue
Pacific Grove, CA 93950-2020

PETE WARZYBOK, RUSSELL BRADLEY,
JAIME JAHNCKE
PRBO Conservation Science
3820 Cypress Drive #11
Petaluma, CA 94954

GREGORY S. CAMPBELL,
JOHN A. HILDEBRAND
Scripps Institution of Oceanography
University of California San Diego
9500 Gilman Drive
La Jolla, CA 92093-0205

WILLIAM J. SYDEMAN,
SARAH ANN THOMPSON
Farallon Institute for
Advanced Ecosystem Research
Petaluma, CA 94952

JOHN L. LARGIER, CHRIS HALLE
University of California, Davis
Bodega Marine Laboratory
P.O. Box 247
Bodega Bay, CA 94923

SUNGYONG KIM
Scripps Institution of Oceanography
University of California San Diego
9500 Gilman Drive
La Jolla, CA 92093-0205

JEFF ABELL
Department of Oceanography
Humboldt State University
1 Harpst Street
Arcata, CA 95521

ABSTRACT

The state of the California Current system (CCS) since spring 2010 has evolved in response to the development of cooler La Niña following the dissipation of the relatively weak and short-lived El Niño event of 2009–2010. The 2009–2010 El Niño appears to have dissipated quite rapidly in early spring 2010, yet the transition to anomalously cool conditions followed somewhat later with the onset of anomalously strong upwelling throughout the CCS in summer 2010 and the development of unusually—in some cases record—cool conditions throughout the CCS. However, following the fairly consistent emergence of cooler La Niña conditions across the CCS going into summer 2010, regional contrasts were apparent. Off southern California, the effects of both the 2009–2010 El Niño and subsequent return to La Niña conditions appear to have had modest effects on the system, and the patterns that attract interest appear to be unfolding over longer time scales (e.g., freshening of upper water column and trends in nitrate and oxygen concentrations). In contrast, the northern California Current has exhibited much more dramatic short-term changes over the past two years, due in part to greater variability in environmental forcing affecting this region. Ecosystem responses also varied across the CCS. The pelagic ecosystem off central and southern California showed evidence of enhanced productivity, in terms of rockfish recruitment, seabird abundance and reproductive success, etc., and the planktonic assemblage off Baja California indicated a resurgence of crustacean zooplankton following a period dominated by gelatinous zooplankton. Off northern California and Oregon, however, the return to La Niña conditions did not entirely reverse changes in the copepod assemblage arising during the 2009–2010 El Niño, which may have contributed to low at-sea survival of juvenile salmon. At the time of writing, tropical conditions are ENSO-neutral and forecast to remain so into fall 2011 and possibly into early 2012, yet the PDO remained strongly negative into summer 2011. It is uncertain whether the return to cool conditions observed in the past year will continue to govern the state of the California Current.

INTRODUCTION

This report reviews oceanographic conditions and ecosystem responses in the California Current system (CCS) from spring 2010 through spring 2011. This review is based on observations collected and analyzed by a diverse range of government, academic, and private research programs and voluntarily contributed in response to an open solicitation for contributions. Programs or institutions that have contributed data and analysis to this and previous reports in this series include the Environmental Research Division, Fisheries Resources Division and Fisheries Ecology Division of the Southwest Fisheries Science Center (SWFSC) of NOAA's National Marine Fisheries Service (NMFS), Humboldt State University, the California Cooperative Oceanic Fisheries Investigations (CalCOFI) program off southern California, the Investigaciónes Mexicanas de la Corriente de California (IMECOCAL) program off Baja California, the Monterey Bay Aquarium Research Institute (MBARI) off central California, the Naval Postgraduate School (NPS), the Fisheries Ecology Division of NOAA's Northwest Fisheries Science Center (NWFSC), PRBO Conservation Science, the Farallon Institute for Advanced Ecosystem Research, and the Coastal Ocean Currents Monitoring Program (COCMP) which includes several academic institutions along the coast (see Acknowledgements). Data continue to be collected along the Bodega Line and will be included in future reports.

As in previous reports in this series, the focus here is on reviewing recent observations in the context of historical patterns as a means of identifying changes in the state of the CCS ostensibly related to changing climatic conditions. This review emphasizes evaluation of augmented or new time series of observations. Where necessary for additional context, insights from spatial patterns are described in general terms in the text; supporting maps and other "snapshots" of the CCS, including more detailed information on specific cruises, are available online at observing programs' Web sites (indicated below). The data sets reviewed herein are the subject of ongoing research to understand links between climate and ecosystem processes, work that is well beyond the scope of the present paper. This review focuses on description and preliminary synthesis of available observations, and offers only sparse information on methods related to data collection (primarily in footnotes). For many ongoing observing programs, more detailed descriptions of methods are available in previous State of the California Current reports or online.

The report is organized as follows. First, we review recent historical conditions and long-term indices of large-scale climate modes (e.g., the Pacific Decadal Oscillation or PDO), followed by more detailed, recent, basin-scale information from the tropical and northern Pacific Ocean. This review provides a broad temporal and spatial context for observations that focus more specifically on patterns and structure in physical forcing and responses at scales that span the entire CCS. Second, proceeding from south to north, we summarize the state of the CCS based on physical, chemical and biological observations collected in the course of repeated ship-based surveys that occupy designated stations at more or less regular intervals throughout the year (fig. 1). Third, we summarize information on the status of higher trophic levels whether derived from data collected on one (or rarely two) targeted large-scale surveys, as part of seasonal sampling programs, in conjunction with ongoing large-scale surveys of the CCS, or aggregated from a suite of survey-based, fishery-based, and other sources. In reviewing these diverse data sets, it is important to remember that responses to climate forcing may be relatively rapid or may include substantial lags, particularly in variables that require time to accumulate the effects of changes in forcing or in variables that scale with species' life histories or phenology. Finally, in the Discussion, we summarize the evolution of the state of the CCS through the last year.

RECENT EVOLUTION OF THE STATE OF THE CALIFORNIA CURRENT

A shift to cool conditions following the 1997–1998 El Niño (Bograd et al. 2000; Peterson and Schwing 2003) drove ecosystem responses consistent with those expected for such a transition, e.g., increased zooplankton production, as well as occasional shifts in zooplankton community structure (Brinton and Townsend 2003; Lavaniegos and Ohman 2003). Two events impinged on the CCS in 2002–2003: an intrusion of subarctic waters (the signature of which was detectable in parts of the CCS into 2007), and a mild tropical El Niño (Venrick et al. 2003). Strong ecosystem responses to the intrusion of anomalously cool, fresh, and nutrient-rich waters (e.g., enhanced productivity) were observed only in the northern CCS (e.g., off Oregon); it is thought that the effects of El Niño were likely to have countered any similar responses off southern California and Baja California (Venrick et al. 2003; Wheeler et al. 2003; Bograd and Lynn 2003; Goericke et al. 2004). Since 2004, regional variability has dominated over coherent CCS-wide patterns (Goericke et al. 2005; Peterson et al. 2006; Goericke et al. 2007; McClatchie et al. 2008, 2009; Bjorkstedt et al. 2010). The late onset of upwelling in 2005 and 2006 led to delayed spin-up of productivity in coastal waters, with strongly negative consequences for higher trophic levels in the northern CCS (Peterson et al. 2006; Sydeman et al. 2006; Goericke et al. 2007; Lindley et al. 2009). Cool conditions associated with La Niña

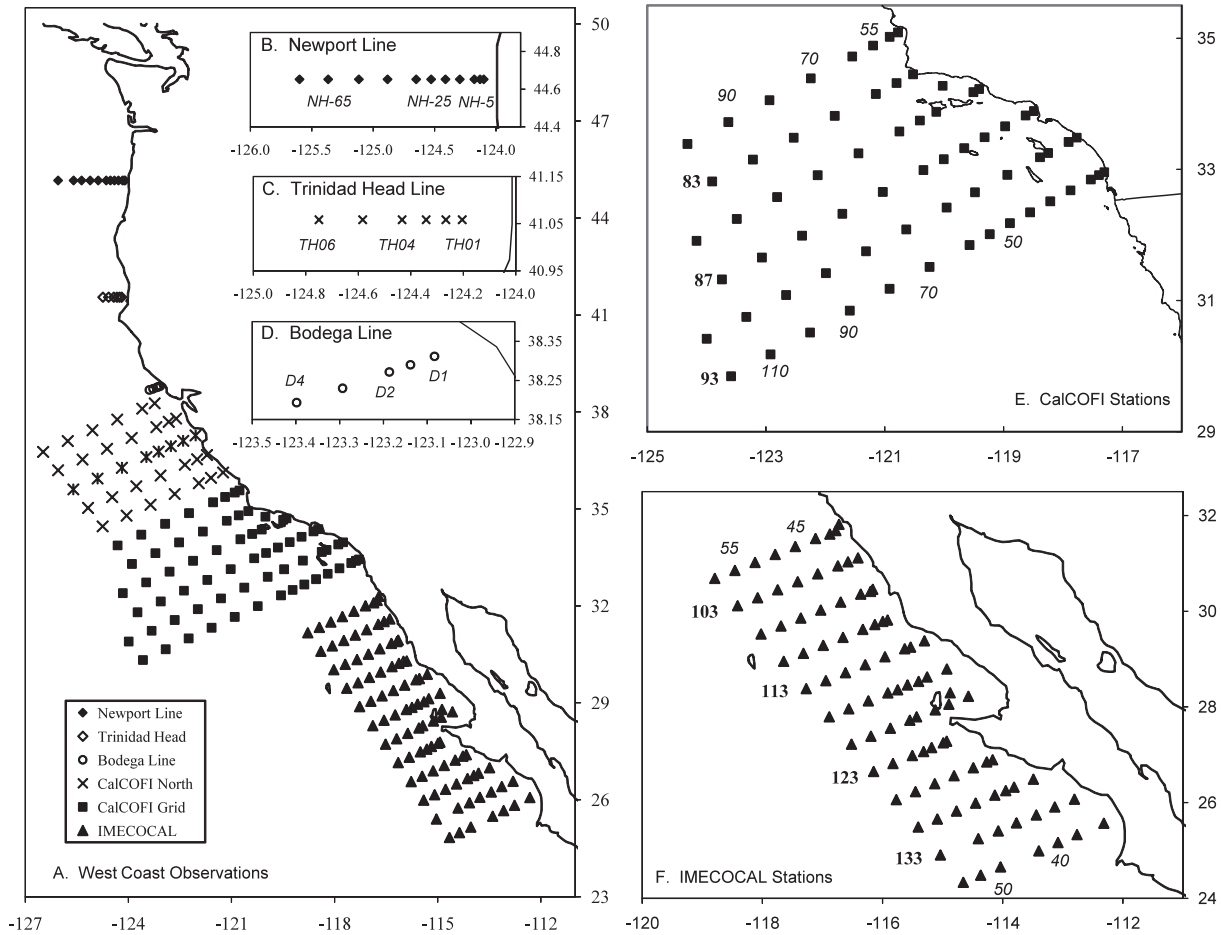

Figure 1. (Panel A) Location of stations for year-round ship-based observing programs that contributed data to this year's report. (Panel B–F) Exploded views of each region or line.Observational lines are labeled using bold numbers positioned west of the line terminus; stations are labeled using numbers in italics immediately below or above the respective stations. Line and station numbers for the IMECOCAL (panel F) and CalCOFI (panel E) programs follow the CalCOFI line and station nomenclature. The Newport Line (panel B) station names designate distance (nm) from shore. The 66 standard CalCOFI stations (black squares in A and E) are occupied on all cruises, weather permitting. During the winter and spring cruises the pattern is extended north for observations of hydrographic properties and distributions of fish eggs and larvae (crosses). The Monterey Bay Aquarium Research Institute monitors conditions along line 67 off Monterey Bay. The Newport Line is sampled biweekly out to St 25 and occasionally further offshore. The Trinidad Head Line (panel C) is occupied at monthly or shorter intervals. The Bodega Line (panel D) is occupied at quarterly or shorter intervals; data for the Bodega Line were not available for this year's report, but will be included in future reports.

prevailed from mid-2007 through 2008 into early 2009, but regional variability was again dominant: increases in productivity in the northern CCS were not matched by similar responses off southern California and Baja California despite evidence of hydrographic effects of La Niña (McClatchie et al. 2008, 2009).The general pattern of substantial contrasts between the northern and southern regions of the CCS persisted into the short-lived, relatively weak El Niño event in late 2009 through early 2010 (Bjorkstedt et al. 2010). For example, whereas conditions off southern California returned to near climatological values with the decline of La Niña and did not indicate any substantial subsequent response to El Niño, the northern CCS warmed subtantially following the decline of La Niña and was strongly affected by intense downwelling during winter 2009–10 (Bjorkstedt et al. 2010). Moreover, as the El Niño diminished rapidly in early 2010, upwelling off central and southern California resumed unusually early and strongly for a spring following an El Niño, but recovery from El Niño in early 2010 appears to have been less robust in the northern CCS (Bjorkstedt et al. 2010).

In contrast to the consistently warm conditions that dominated the CCS prior to the strong 1997–1998 El Niño, the Pacific Decadal Oscillation (PDO; Mantua et al. 1997) index suggests that the North Pacific has since been in a generally cooler state. However, the PDO has been for the past decade fluctuating at intervals of approximately two to four years between cool states marked by negative values of the PDO index and associated negative anomalies in sea surface temperature throughout the CCS (e.g., 1998–2001, 2008–09) and warmer states of positive PDO and positive SST anomalies (e.g., 2003–06) (fig. 2, and see below).This pattern appears to be continuing into spring 2011, with PDO declining to neutral values after recovering from the

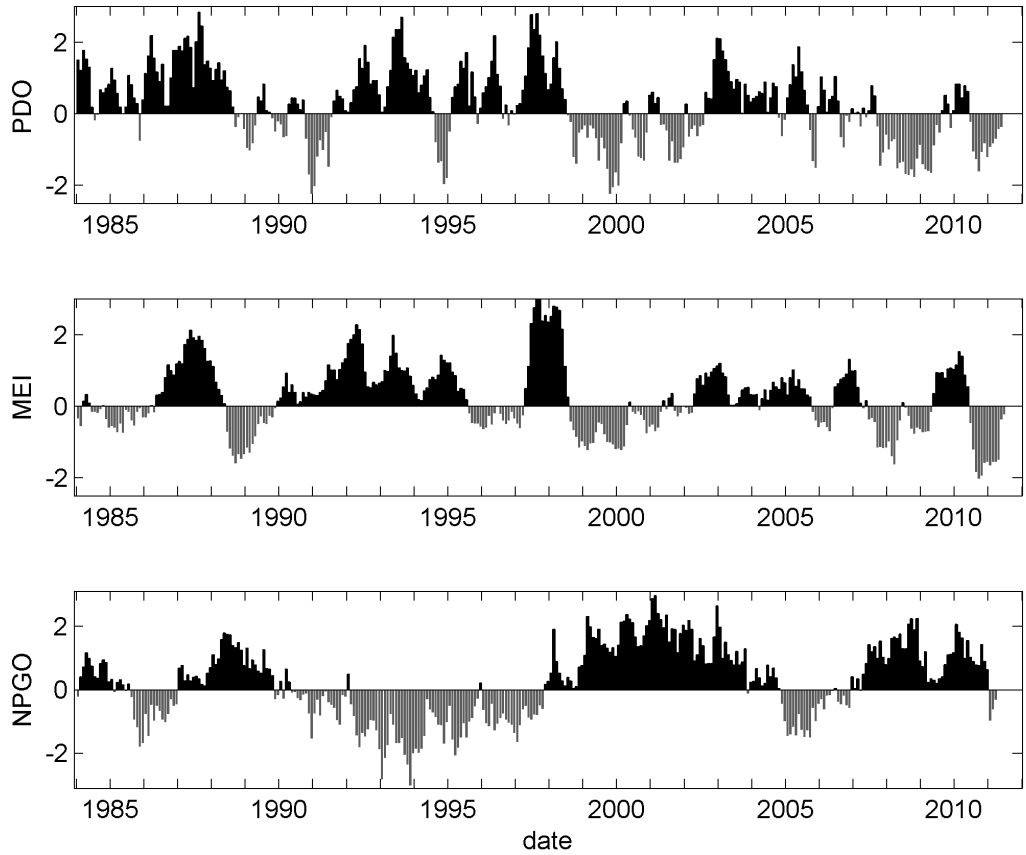

Figure 2. Time series of the Pacific Decadal Oscillation (PDO; top panel; data retrieved from http://jisao.washington.edu/pdo/PDO.latest), the Multivariate ENSO Index (MEI; middle panel; data downloaded from http://www.esrl.noaa.gov/psd/people/klaus.wolter/MEI/table.html), and the North Pacific Gyre Oscillation (NPGO; bottom panel; downloaded from http://www.o3d.org/npgo/data/NPGO.txt) for January 1984–May 2011 (March 2011 for the NPGO).

effects of the 2009–2010 El Niño. Over this period, variability in PDO exhibits a high degree of coherence with the Multivariate El Niño Southern Oscillation Index (MEI; Wolter and Timlin 1998) (fig. 2). The MEI shifted dramatically from El Niño to La Niña conditions in early 2010 and remained in a strongly La Niña state until increasing rapidly towards neutral values in early 2011. Whether a sustained "cool regime" has been in place for the CCS remains an open question. The North Pacific Gyre Oscillation (NPGO; Di Lorenzo et al. 2008), which is a measure of the strength of gyral circulation in the North Pacific, has been predominantly positive since the late 1990s indicating anomalously strong equatorward flow in the CCS (fig. 2); negative NPGO during 2005 and 2006 corresponds to the period of unusually low productivity observed through much of the CCS.

NORTH PACIFIC CLIMATE PATTERNS[1]

In the extratropical Pacific, SST anomalies in summer 2010 were generally cool (–0.5 to –1.0°C) around the North American coast and warm (>+0.5°C) in the western and central North Pacific (fig. 3a), a pattern that has persisted in recent years. This pattern also reflects a negative phase of the Pacific Decadal Oscillation (PDO), which has been predominantly in the negative phase since 2007 (fig. 2; Peterson and Schwing 2003). The tropical El Niño that developed in summer 2009 and peaked in winter 2009–10 had largely dissipated by early spring 2010. This event appears to have been an El Niño Modoki marked by anomalous warming in the central, rather than western, equatorial Pacific (Ashok et al. 2007). By July 2010, La Niña developed in the tropical Pacific, with cooler SSTs (anomalies of approximately –1.0°C) extending from the South American coast to the dateline (fig. 3a). Strong anticyclonic wind anomalies dominated the northeast Pacific at this time, resulting in cooler SSTs throughout the Gulf of Alaska and California Current. La Niña conditions strengthened through autumn 2010 and into early winter 2011, during which unusually cool SSTs (anomalies of approximately –2.0°C) occurred in parts of the equatorial Pacific (fig. 3b,c). A brief period of warm SST anomalies in the eastern North Pacific in September–October 2010 transitioned back to cool SST anomalies in early winter 2010–11 (fig. 3c). By April–May 2011, tropical

[1]Further details on month-to-month and interannual global ocean climate variability can be found at CPC's "Monthly Ocean Briefing" archive (http://www.cpc.ncep.noaa.gov/products/GODAS).

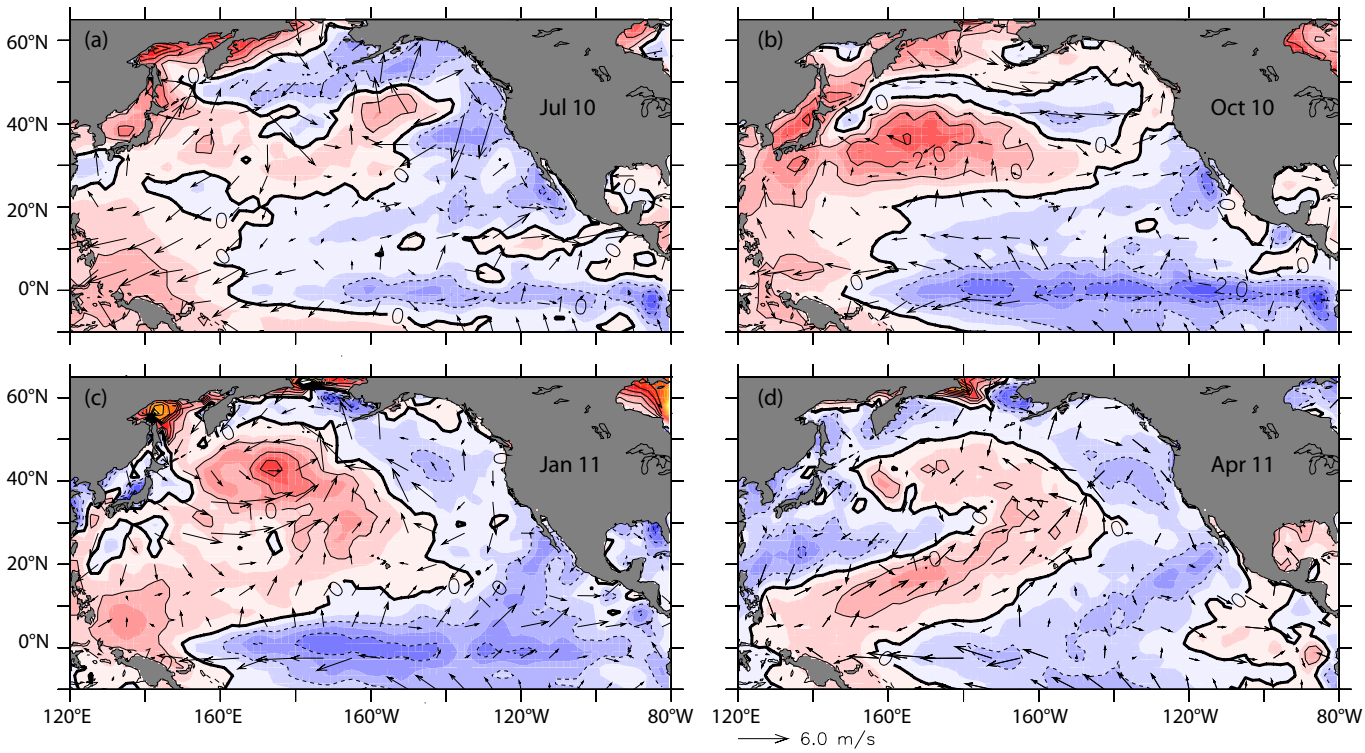

Figure 3. Anomalies of surface wind velocity and sea surface temperature (SST) in the north Pacific Ocean, for (a) July 2010, (b) October 2010, (c) January 2011, and (d) April 2011. Arrows denote magnitude and direction of wind anomaly. Contours denote SST anomaly. Contour interval is 1.0°C. Negative (cool) SST anomalies are shaded blue; positive (warm) SST anomalies are shaded red. Wind climatology period is 1968–96. SST climatology period is 1950–79. Monthly data obtained from the NOAA-CIRES Climate Diagnostics Center.

conditions had transitioned to ENSO-neutral, while the eastern North Pacific (NEP) was dominated by a strong North Pacific High (anticyclonic wind anomalies), strong upwelling in the California Current, and cooler than normal SST throughout the NEP (fig. 3d).

Recent trends and variability in major climate indices also reflect the development and decline of El Niño in the North Pacific. In spring 2010, cooling in the North Pacific is captured in the sharp transition of PDO back to strongly negative values comparable to those observed during cool conditions prior to the 2009–2010 El Niño. Following this transition, the PDO declined in magnitude more or less steadily (fig. 2). The Multivariate El Niño Southern Oscillation Index (MEI) also marked a sharp transition to strong La Niña conditions that has subsequently relaxed towards ENSO-neutral conditions (fig. 2). The North Pacific Gyre Oscillation (NPGO) index indicated a weakening of gyral circulation (i.e., a weakening of the California Current) coincident with the tropical signal of the 2009–2010 El Niño that recovered strongly in spring 2010, then gradually declined into negative anomalies in early 2011 (fig. 2). The NPGO signal associated with the 2009–2010 El Niño and its dissapation appears to lead that of the SST-based PDO (fig. 2).

CALIFORNIA CURRENT

Atmospheric Forcing, Upwelling, and Sea Surface Temperature Responses

Conditions in the North Pacific and California Current show clear responses to variability in the development and strength of seasonally dominant atmospheric pressure systems (e.g., the Aleutian Low in winter and the North Pacific High in spring and summer). Upwelling was anomalously strong throughout the California Current during midsummer 2010, reflecting persistently strong anticyclonic wind anomalies associated with a strong North Pacific High (figs. 3, 4). The rapidly changing atmospheric forcing in the northeast Pacific from autumn 2010 through winter 2011 is reflected in California Current upwelling. A strong Aleutian Low in December 2010 and March 2011 led to brief periods of anomalously strong downwelling in the northern California Current. In contrast the development of the North Pacific High in spring 2011 led to an early onset and relatively strong upwelling from Baja through central California.

Conditions at coastal NDBC buoys have reflected these large-scale patterns, with high volatility in both surface winds and SST (fig. 5). Strong event-scale vari-

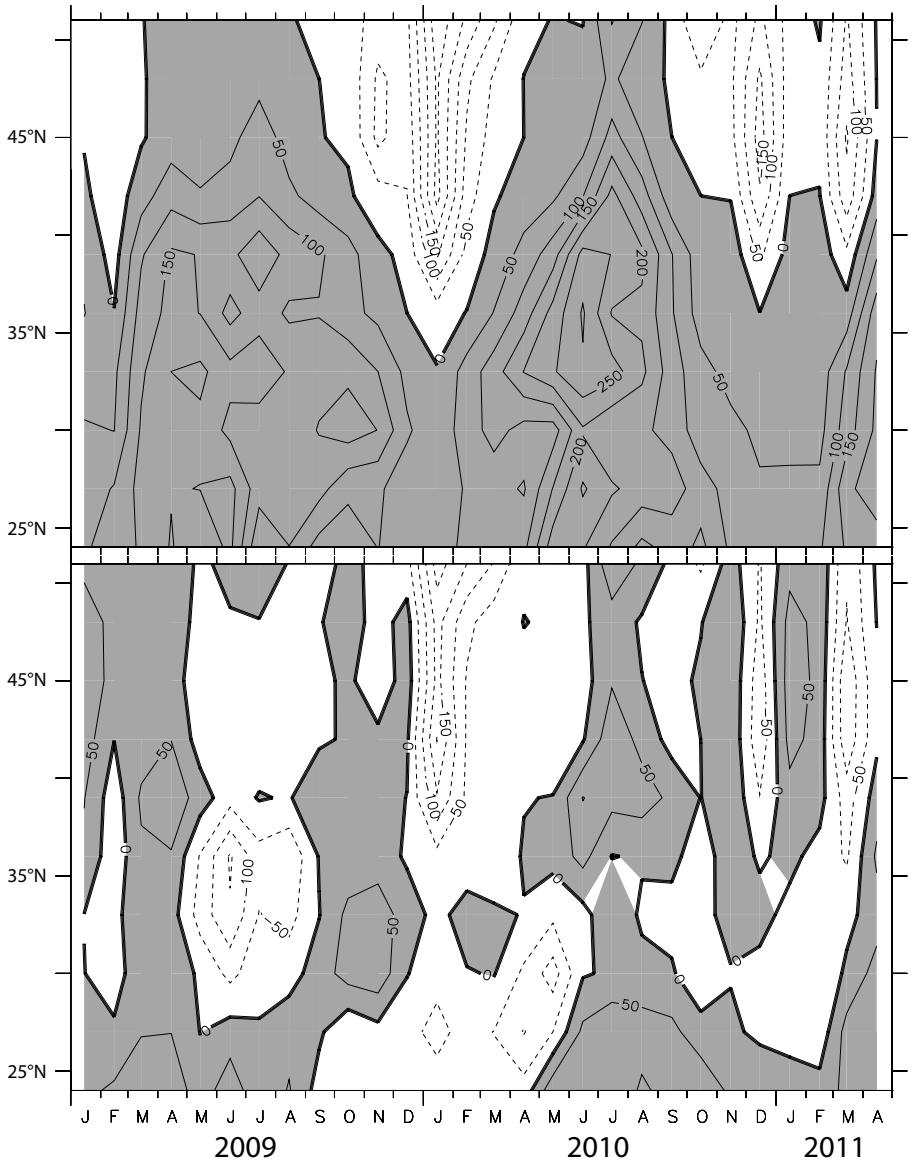

Figure 4. Monthly upwelling index (top) and upwelling index anomaly (bottom) for January 2009–April 2011. Shaded areas denote positive (upwelling-favorable) values in upper panel, and positive anomalies (generally greater than normal upwelling) in lower panel. Anomalies are relative to 1948–67 monthly means. Units are in m^3/s per 100 km of coastline.

ability (i.e., variability over time scales of several days to weeks) prevailed in the summers of 2009 and 2010, as it has since 2007, with numerous upwelling and relaxation events and corresponding variations in SST, particularly in the northern California Current. Strong event-scale variability was also evident in nearshore winds during the winters of 2009–10 and 2010–11. While SSTs in winter 2009–10 were anomalously warm—a consequence of a strong Aleutian Low and intense downwelling associated with the El Niño—SSTs in winter 2010–11 were generally cooler than normal in the California Current. Strong upwelling in the southern California Current in April 2011 led to strong negative SST anomalies at the southern buoys.

Latitudinal variation in cumulative upwelling[2] further illustrates the contrasts in recent years (fig. 6) . Off southern California, upwelling patterns have been quite similar and near average despite the transition from La Niña conditions through the 2009–2010 El Niño and back to La Niña. Moving north, however, differences between years become more apparent, to the point that off Oregon, cumulative upwelling in early 2009 was among the strongest observed, yet among the weakest in early 2010. Cumulative upwelling in 2011 showed a similar latitudinal pattern, with differences between northern and

[2]Cumulative upwelling was calculated from the 6-hourly Bakun Index obtained from the NOAA Fisheries Environmental Research Division obtained through http://www.pfeg.noaa.gov/products/PFEL/modeled/indices/PFELindices.html.

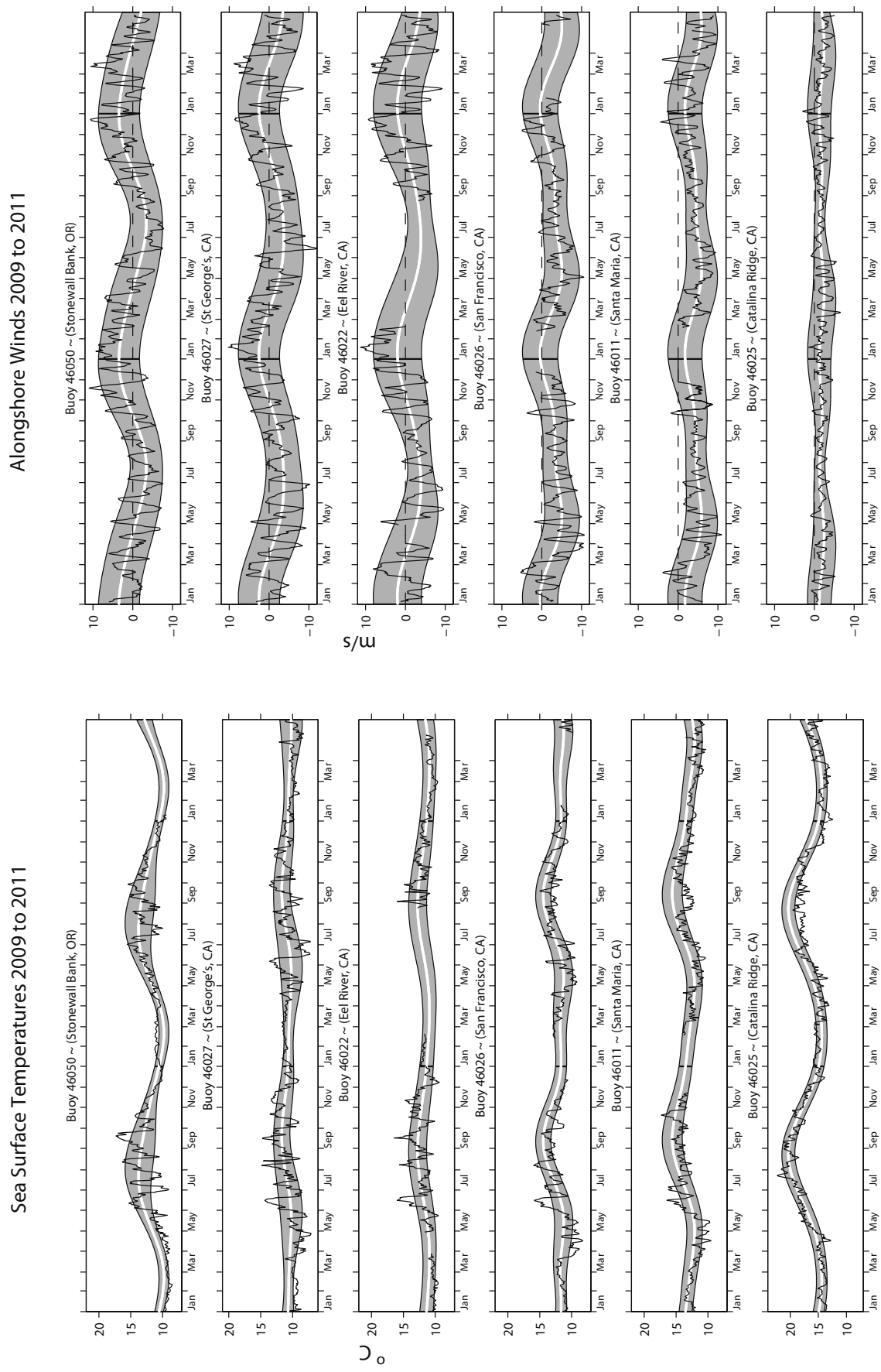

Figure 5. Time series of daily-averaged SST (left) and alongshore winds (right) for January 2009–April 2011 at selected NOAA National Data Buoy Center (NDBC) coastal buoys. Bold lines are the biharmonic annual climatological cycle at each buoy. Shaded areas are the standard errors for each Julian day. Series have been smoothed with a 7-day running mean. Data provided by NOAA NDBC. Coordinates for buoy locations are at http://www.ndbc.noaa.gov/to_station.shtml.

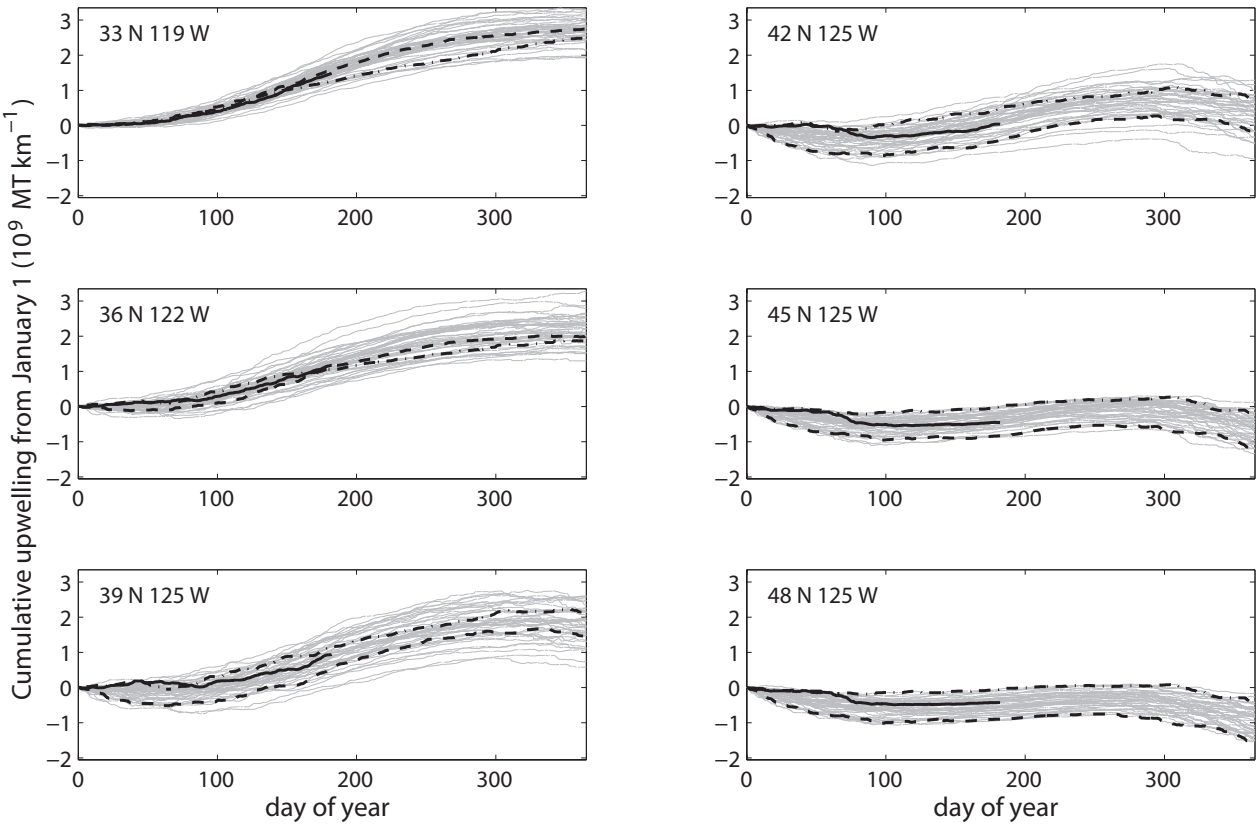

Figure 6. Cumulative upwelling from January 1 calculated from the Bakun Index at indicated locations along the West Coast of North America for 1967–2008 (grey lines), 2009 (dash-dotted line), 2010 (dashed line), and 2011 (solid line).

southern locations arising as a consequence of strong downwelling in the north in spring 2011. The prolonged sequence of downwelling events in early 2011 led to a slightly delayed spring transition[3] in the northern California Current (e.g., at 45°N; fig. 7).

HF Radar Surface Current Observations[4]

Seasonal mean surface currents observed with HF radar provide further evidence of the contrast between spring 2010 through spring 2011 and the previous year. In spring 2010 (March through May), mean currents are directed southward throughout the domain (including the Southern California Bight) and have a clear offshore component off central California (fig. 8). During the summer, a marked offshore orientation of mean flows is evident throughout the upwelling region from Point Conception to the mouth of the Columbia River. In the Southern California Bight, flow is weaker and mostly poleward in summer and fall. In fall (September through November), currents weaken in the upwelling region and consistent upwelling is not evident north of Cape Mendocino.

Persistent enhanced offshore flow is evident in the seasonal mean as upwelling jets either at or just south of major capes (e.g., Cape Blanco, Cape Mendocino, Point Arena, Point Reyes, Point Ano Nuevo, and Point Conception; fig. 8). These features varied in strength and structure between years. In contrast to 2009, during which strong features observed in spring weakened during summer (Bjorkstedt et al. 2010), these features were weaker in spring 2010, but strengthened through the summer (June through August), particularly off Cape Blanco and Point Arena. Also in contrast with observations from the previous year, the "Mendocino Eddy" (Halle et al. in review) is not evident as a closed circulation pattern in the mean flow patterns, yet mean flows do include a persistent offshore flow just north of Point Arena—most strikingly in fall, when wind forcing was relatively weak—that is consistent with the southern portion of the Mendocino Eddy (fig. 8).

[3]Spring transition date is based on the day on which cumulative upwelling reaches its most negative value immediately prior to the onset of sustained positive upwelling. Usually this corresponds to the lowest value of cumulative upwelling, but in some years the spring transition corresponds to a second-most negative value of cumulative upwelling following a weak upwelling event.

[4]High Frequency (HF) Radar currents presented herein are calculated hourly at 6-km resolution using optimal interpolation (Kim et al. 2008; Terrill et al. 2006) and further averaged to 20-km resolution prior to display. Real-time displays of HF-Radar surface currents can be viewed at the regional association Web sites: http://www.sccoos.org/data/hfrnet/ and http://www.cencoos.org/sections/conditions/Google_currents/ and at Web sites maintained by the institutions that contributed data reported here (listed in Acknowledgments).

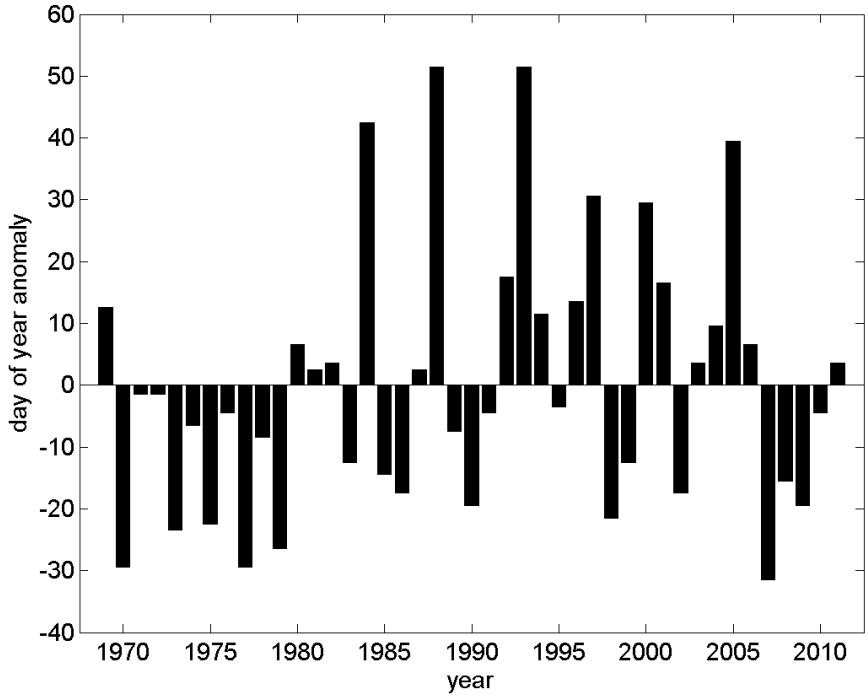

Figure 7. Variability in spring transition dates around the mean of observed transition dates calculated from the Bakun Index at 45°N 125°W. Negative anomalies indicate early spring transitions, positive anomalies indicate late transitions. Day of transition is from the most negative value of cumulative upwelling immediately prior to onset of sustained upwelling. Mean spring transition date is Day 103 (April 13).

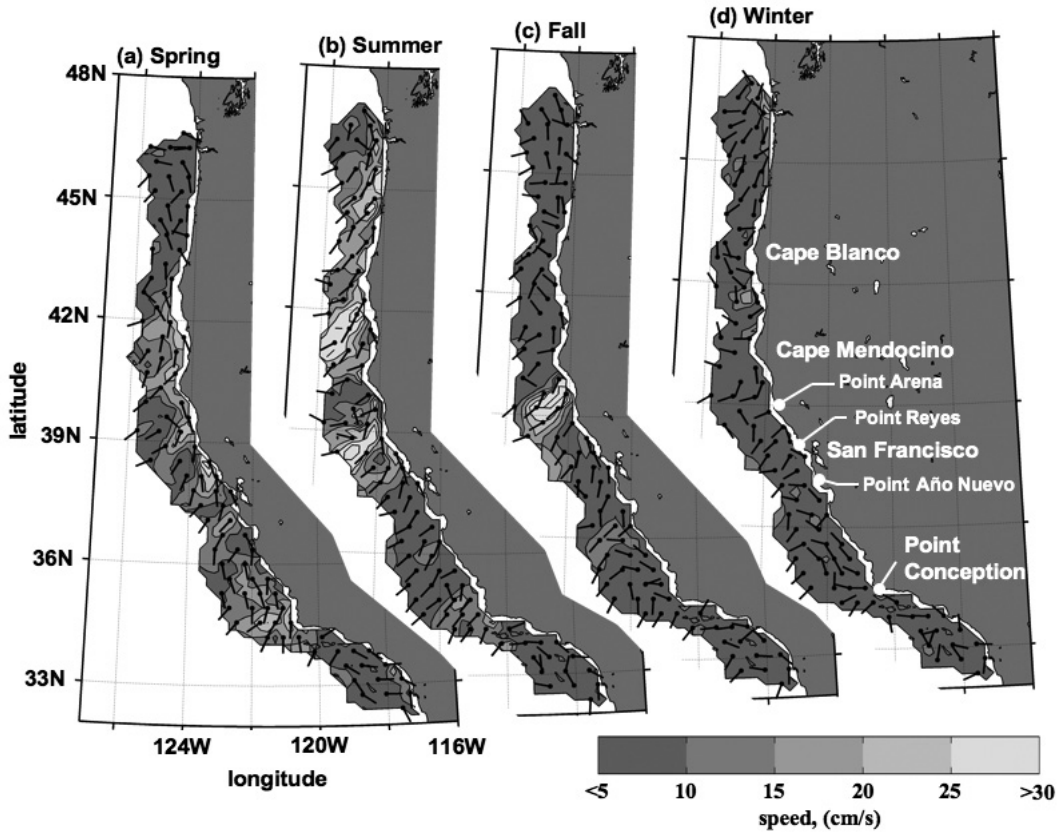

Figure 8. Mean seasonal maps of surface currents observed throughout the CCS with coastal HF radar for March 2010 through February 2011. The seasons are spring (March–May), summer (June–August), fall (September–November), and winter (December–February). Mean surface currents are calculated at 20-km resolution using hourly HF-radar observations. Current speeds are indicated by shading. Current direction is given by direction of lines extending from black dots that indicate the location of the measured currents. For clarity, roughly one-sixth of the directions associated with the gridded 20-km currents are shown.

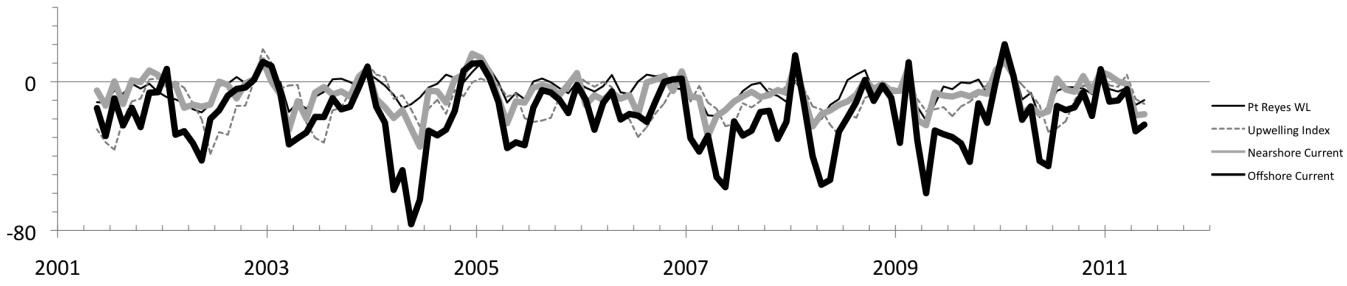

Figure 9. Monthly averages of spatially averaged surface flow past Point Reyes, CA between 30 and 60 km offshore (38°00' to 38°10'N and 123°20' to 123°40'W; thick black line) and between 0 and 15 km offshore (38°00' to 38°10'N and 123°00' to 123°10'W; thick grey line). Positive values indicate poleward flow in cm/s. Fine, grey dashed line: cross-shelf Ekman transport indexed as the negative Upwelling Index at 39°N (i.e., positive values indicate onshore Ekman transport in units of 10 m^3/s per 100 m of coastline). Fine black line: sea level at Point Reyes relative to 1 m above MLLW (units cm).

Following strong northward flows during the 2009–10 winter, southward flow off Point Reyes returned to moderate levels in 2010 and exhibited greater correlation between nearshore (0–15 km) and offshore (30–60 km) flows than was observed in 2009 (fig. 9). These flows were strongest during May and June 2010, but relatively weak earlier in the spring and later in the summer. In fact, mean flow past Point Reyes near the coast was approximately zero from July onward. Flows were variable and weak during the 2010–11 winter and continued to appear weak into early 2011 (fig. 9). As in previous years, the seasonal development of alongshore flow past Point Reyes leads that of local wind forcing as indicated by the Upwelling Index (fig. 9; see Garcia-Reyes and Largier (in review) for further discussion). Indeed, alongshore flow is better correlated with monthly mean water level at the Point Reyes tide gage, which reflects both wind forcing and forcing related to offshore eddies (e.g., Kaplan et al. 2009).

REGIONAL SURVEY OBSERVATIONS

Baja California—IMECOCAL Surveys[5]

Within the IMECOCAL study region off Baja California, temporal variability in both temperature and salinity (expressed in terms of mean 10 m anomalies) effectively capture climate events and clearly illustrate the onset and dissipation of the recent 2009–2010 El Niño event (fig. 10). In Spring 2010, colder, fresher conditions developed, eventually leading to the coldest (October 2010) and freshest (January 2011) conditions recorded in time series (fig. 10). The 2010–11 freshening event exceeds the 2002–03 event in scale, which had been the result of an anomalous intrusion of subarctic waters into the CC (Venrick et al. 2003; Gómez-Valdes and Jeronimo 2009). Subsequent observations show both temperature and salinity reverting to long-term mean values.

Temporal variability in chl *a* (expressed as anomalies of chlorophyll integrated over the upper 100 m of the water column) also capture the consequences of climate variability off Baja California at interannual to decadal scales, including El Niño-La Niña cycles (Gaxiola-Castro et al. 2008). These patterns show a positive relationship with the NPGO (North Pacific Gyre Oscillation) index, but low relation to MEI (Gaxiola-Castro et al. 2010). Positive chl *a* anomalies were present off Baja California from 2008 to 2011 (April), except for the spring 2010 survey, which is likely to have been a consequence of the 2009–2010 El Niño in the region (fig. 11). Anomalously high concentrations of chl *a* were observed off Baja California from the second half of 2010 through spring 2011, but remain lower than those observed in 2002 (Gaxiola-Castro et al. 2008).

During 2010 and into early 2011, zooplankton displacement volumes were relatively high, which is consistent with patterns observed since 2004 (fig. 12; Lavaniegos 2009). In early 2010, however, crustacean zooplankton grazers were relatively rare and high indices of zooplankton abundance reflected the high abundance of gelatinous groups (not shown). Indeed, abundance of medusae reached a record value for the IMECOCAL series (1998–2010) in early 2010. In contrast, copepods and euphausiids returned to relatively high abundance during July and October 2010 (fig. 12), presumably as a consequence of cool water and enhanced production associated with La Niña.

Southern California—CalCOFI Surveys[6]

Unusually high sea levels associated with the 2009–2010 El Niño cycle returned to normal and slightly negative values by the summer of 2010 (fig. 13a). Mixed

[5]The IMECOCAL study region spans 93 stations off Baja California, Mexico (fig. 1). IMECOCAL cruise schedules, data collection protocols, analysis methods, and additional substantiating data are fully described at http://imecocal.cicese.mx. Note that results from the present analysis based on 10 m anomalies have been corroborated and correlate well with patterns in anomalies based on analysis of mixed layer properties (Durazo 2009; Gómez-Valdes and Jeronimo 2009; Bjorkstedt et al. 2010).

[6]Results are presented here as cruise averages over all 66 stations (fig. 1c) or as anomalies with respect to the 1984–2008 time series to augment ongoing time series of observations. Detailed descriptions of the cruises and methods used to collect data and analyze samples are given in previous reports and are available at http://www.calcofi.org.

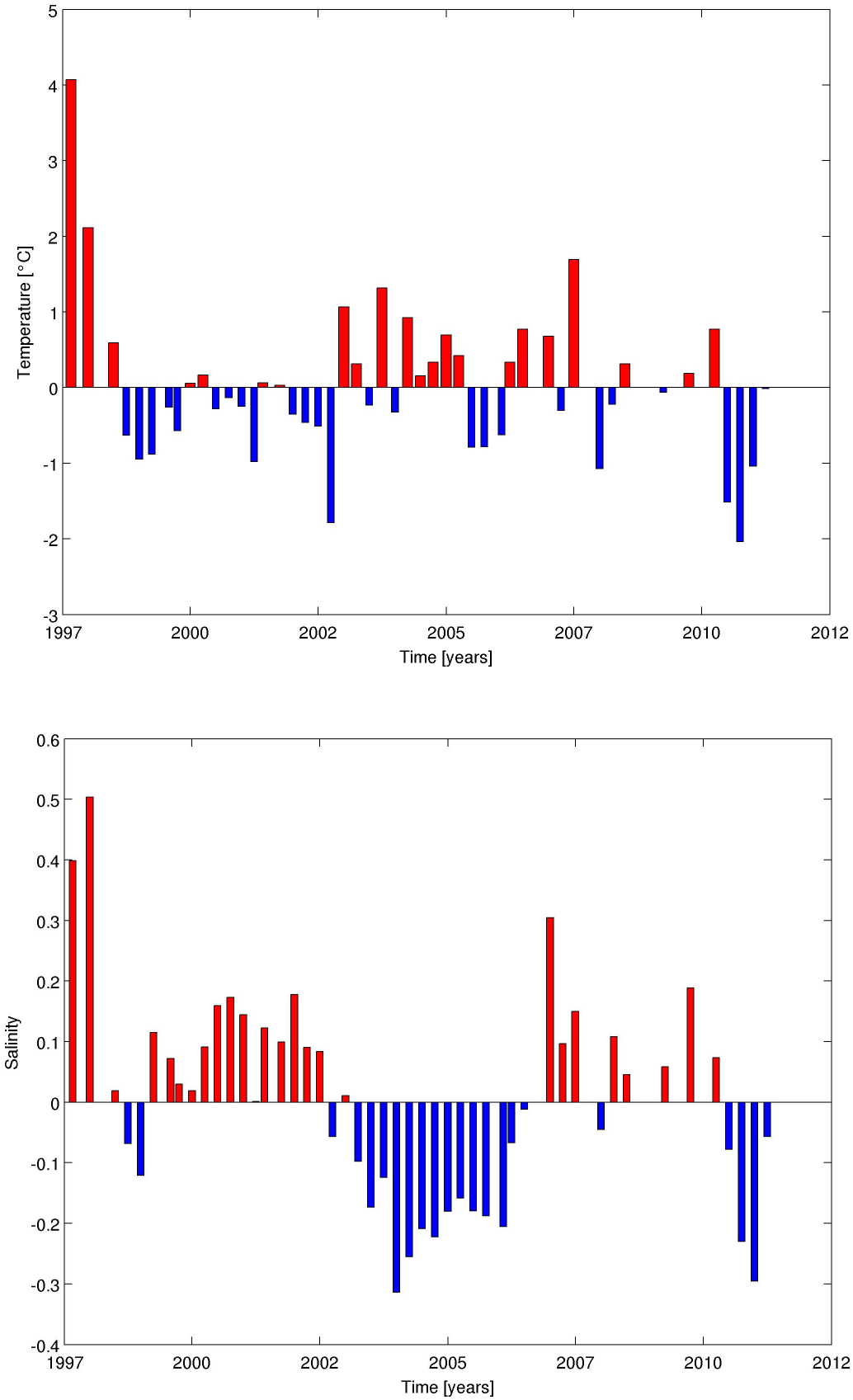

Figure 10. Mean anomalies of temperature (upper panel) and salinity (lower panel) at 10 m over the IMECOCAL study region for the period 1997–2011.

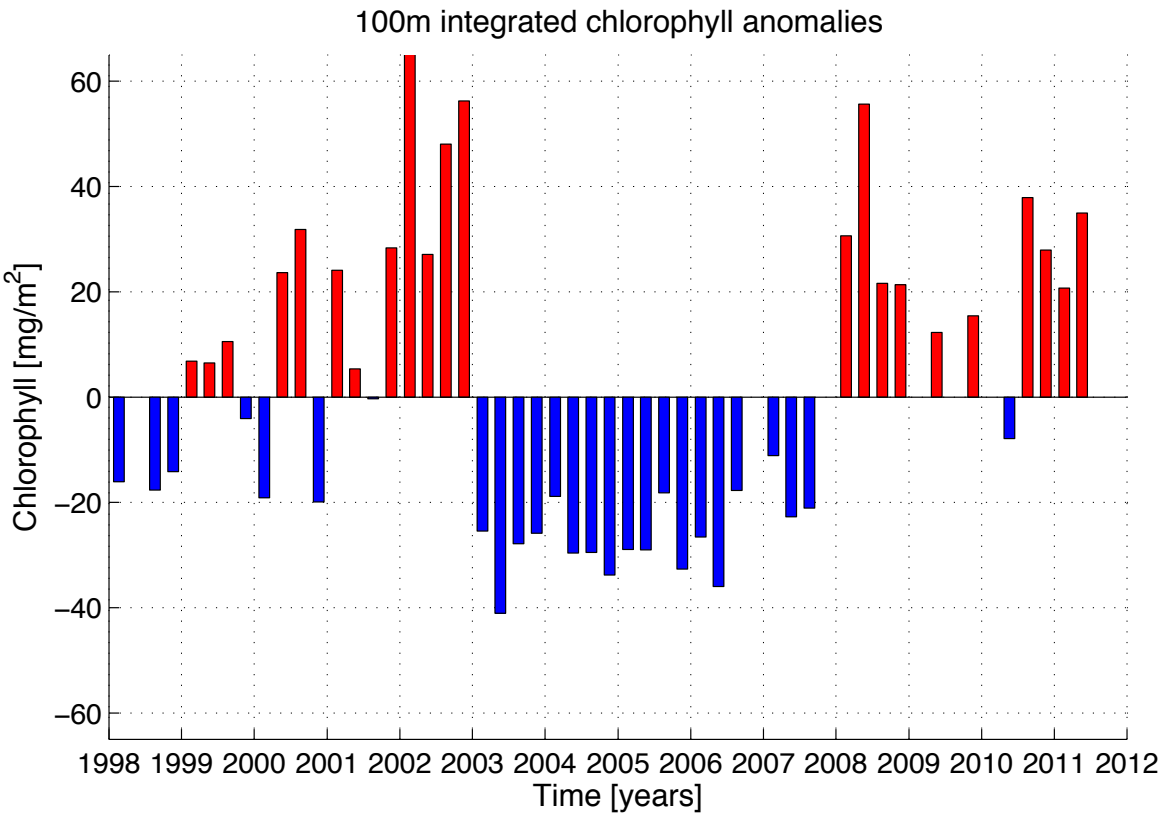

Figure 11. Anomalies of average water-column integrated chl *a* in the IMECOCAL study region off Baja California from 1998 to spring 2011.

layer temperature continued to remain slightly cooler than the long term average, continuing a trend established after the 1998–1999 El Niño. Mixer layer temperature was substantially cooler than normal during summer 2010, reflecting the strong equatorial La Niña conditions, but subsequently returned towards recent mean values (fig. 13c).

Values of mixed layer salinity, which is not expected to be affected by ENSO cycles, continued to decline through 2010 and into 2011 (fig. 13d). This pattern is reflected in many regions within the CalCOFI study area that continue to exhibit freshening of the upper water column, as has been observed over the last few years (Bjorkstedt et al. 2010). Indeed, this freshening trend either persisted or became stronger in the case of the southern California Current (fig. 14), and likely reflect a general strengthening of the California Current.

During the 2009–2010 El Niño, the σ_t 26.4 isopycnal[7] was deeper than usual (i.e., exhibiting a positive depth anomaly), but returned to depths similar to those observed over the last decade following the development of La Niña (fig. 15a). Temperature and oxygen anomalies at the σ_t 26.4 isopycnal did not change substantially over the last ENSO cycle (fig. 15), suggesting that water masses at the isopycnal did not change substantially during this time. Considering these rather subtle changes in properties, the large observed increase in nitrate concentrations over the last years is surprising (fig. 15). Although the increasing trend in nitrate concentration since 2000 coincides with a decline in oxygen concentration (to levels that have persisted into 2011), the sharp increase in nitrate over the past two years is not matched by a corresponding additional decrease in oxygen concentrations. Thus, it appears that the increase of nitrate over the last two years can not have been driven by increased local remineralization without some other mechanism present to offset the expected draw down of dissolved oxygen. The largest anomalies in nitrate concentration at the σ_t 26.4 isopycnal were observed along the offshore sections of lines in the northern (lines 77 and 80) and southern (lines 90 and 93) of the CalCOFI grid (fig. 1). This nitrate concentration anomaly also does not appear to be related to the freshening of the upper water column since analogous trends in nitrate and oxygen concentrations are not observed higher in the water column (e.g., at the σ_t 25.6 isopycnal which is located at a depth of about 90 m with a temperature of about 11°C, data not shown).

[7]The σ_t 26.4 isopycnal is located within the pycnocline, at an average depth of about 200 m off S. California, and is largely independent of processes affecting the mixed layer (i.e., local forcing).

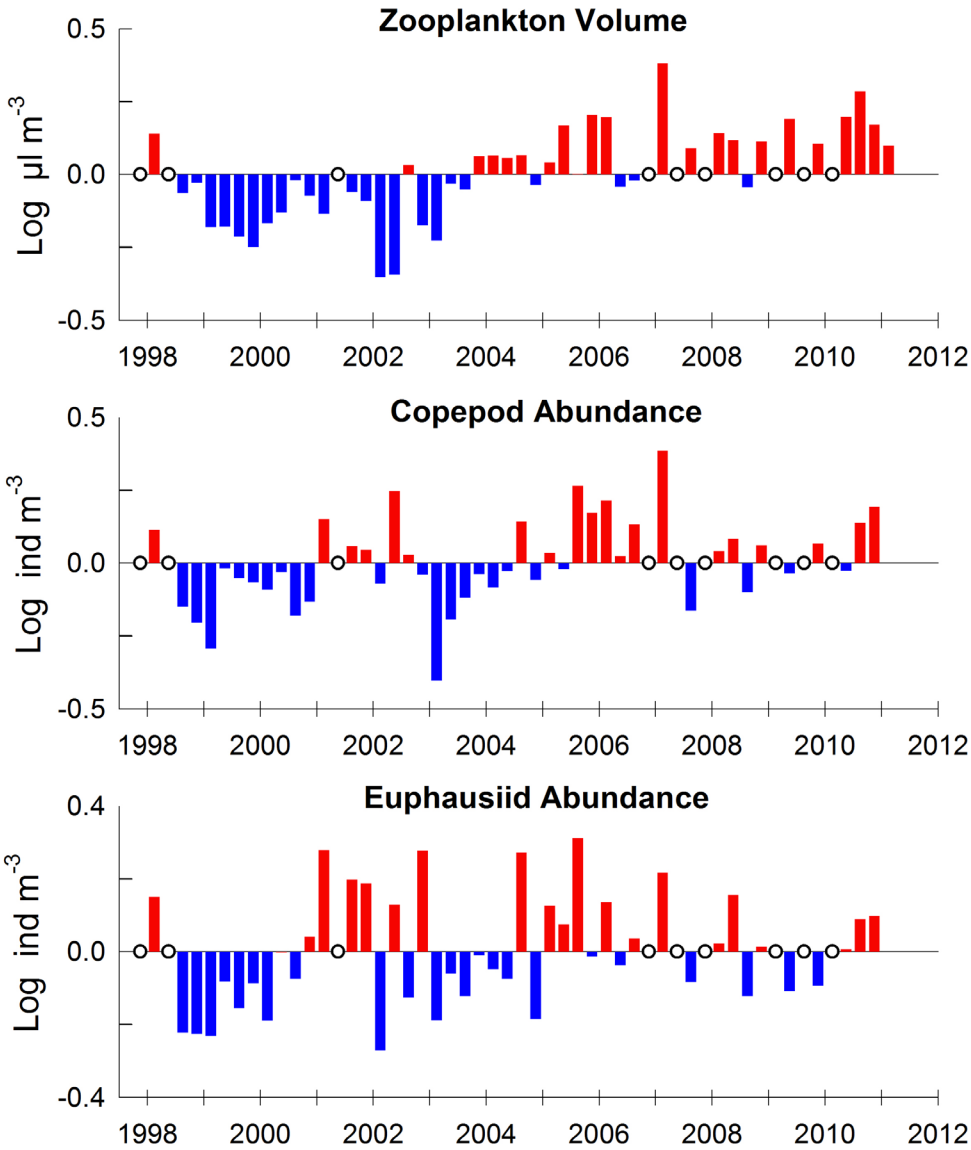

Figure 12. Anomalies of average zooplankton densities observed in the IMECOCAL study region off Baja California from 1998 to fall 2010. Top panel: Anomalies of zooplankton displacement volume. Middle panel: Anomalies in estimated copepod abundance based on nighttime samples. Bottom panel: Anomalies in estimated euphausiid abundance based on nighttime samples. Open circles indicate missing cruises or cruises with reduced area coverage that were excluded from calculation of anomalies. Zooplankton data for January 2011 are not yet available.

Nitracline depths in the CalCOFI area were similar to values observed since 1999 (fig. 13b). Whereas nitracline depth responded significantly to the La Niña conditions of 2007–2008 it did not respond strongly to the El Niño conditions of 2009–2010, as it had during previous El Niños (fig. 13b). Consistent with the observation of nitracline depth, concentrations of mixed layer nitrate were slightly above long-term averages and concentrations of silicic acid and phosphate were similar to long-term averages over the last decade (fig. 16). Concentrations of nitrate and N-P ratios have been increasing slightly over the last decades, but no such trend can be detected for concentrations of silicic acid and phosphate.

The spatially-averaged concentration of mixed layer chl *a* observed over the last year was similar to long-term averages (fig. 17a). These trends for the whole region reflect processes in specific areas as well. Concentrations of chl *a* have been higher than normal at the edge of the central gyre and in the California Current in past years and these have been lower than average in the northern coastal areas. In 2010, concentrations of chl *a* returned to average values in these areas. (fig. 18). The exception is the southern coastal region where exceptionally high concentrations of chl *a* were observed this year. Rates of primary production were slightly above long-term averages (fig. 17b), a trend possibly related to the slight increase in nitrate concentration over the last year. Zoo-

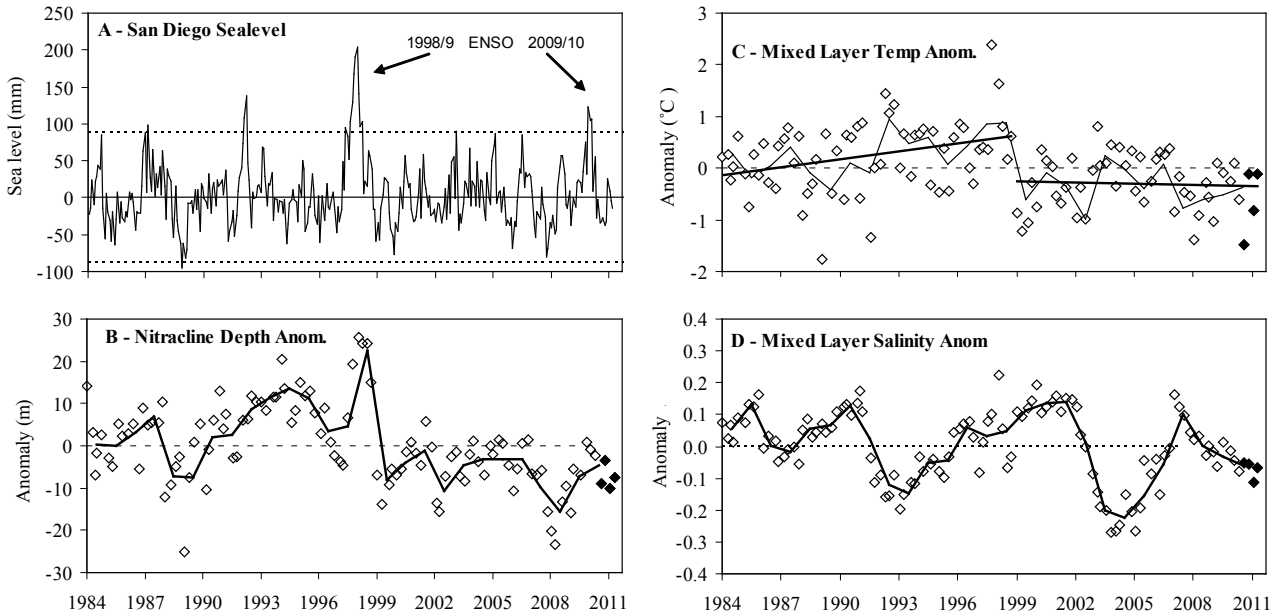

Figure 13. Anomalies of detrended San Diego sea level (A), nitracline depth (B), mixed layer (ML) temperature (C), and ML salinity (D) off southern California (CalCOFI standard grid, CalCOFI fig. 1). Data from the last four CalCOFI cruises are plotted as solid symbols, data from previous cruises are plotted as open diamonds. The thin solid lines represent the annual averages, the dotted lines the climatological mean, which in the case of anomalies is zero and the straight solid lines, when present, long-term trends.

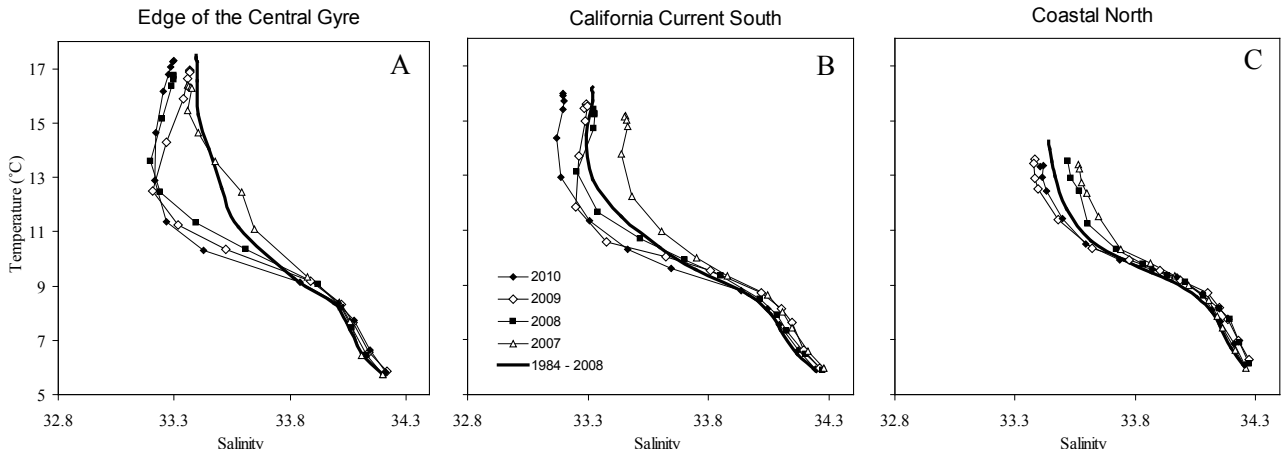

Figure 14. TS plots for three representative areas of the CalCOFI region. A. The edge of the central gyre (Lines 90–93, Stations 100–120); B. the southern California Current region (Lines 87–93, Stations 60–90); and C. the coastal areas in the north (Lines 77–80, Stations 60 and inshore). Each data point represents the average TS characteristic of one standard depth level for the specified time periods, i.e., 1984–2008, 2007, 2008, 2009 and 2010.

plankton displacement volume, a proxy for zooplankton biomass, has not been affected by the last ENSO cycle, in contrast to the 1998–99 ENSO cycle when zooplankton biomass decreased by 70%.

Central California—Monterey Bay and Line 67[8]

Observations off central California also reflected the decline of the 2009–2010 El Niño event in mid-spring 2010 and the transition to La Niña conditions which have persisted into spring 2011 (fig. 19). In the outer reaches of Monterey Bay, the upper water column was unusually warm during January 2010 (anomalies greater than 0.8°C extended from the surface to a depth of 100 m), but by November 2010, this pattern had completely reversed: the upper water column was unusually cool (anomalies of approximately –0.8°C at 100 m) and salty (salinity anomaly of 0.2 S). These changes were in part explained by changes in regional Ekman transports and were also consistent with Monterey sea level measurements (data not shown). The development and persistence of La Niña conditions was also evident in the development of anomalously high chl *a* concentrations in the upper 100 m of the water column during summer 2010. In contrast to the preceding summer, when phytoplankton were both less abundant and concentrated at depth (as is more typi-

[8]Data on temperature and salinity at the surface and 100 m for Monterey Bay are based on MBARI monthly cruises and mooring data.

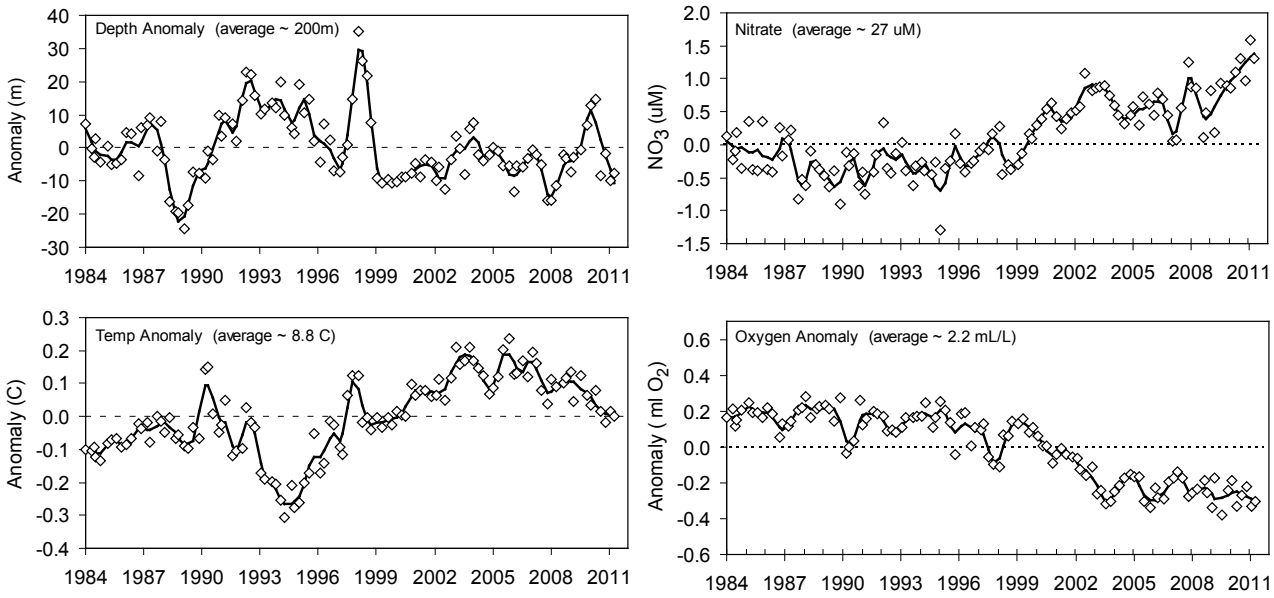

Figure 15. Property anomalies of the σ_t 26.4 isopycnal calculated and presented as described above for Figure 13. Shown are anomalies of the isopycnal depth anomaly, concentrations of nitrate, temperature and oxygen. Average values for the properties are given as well.

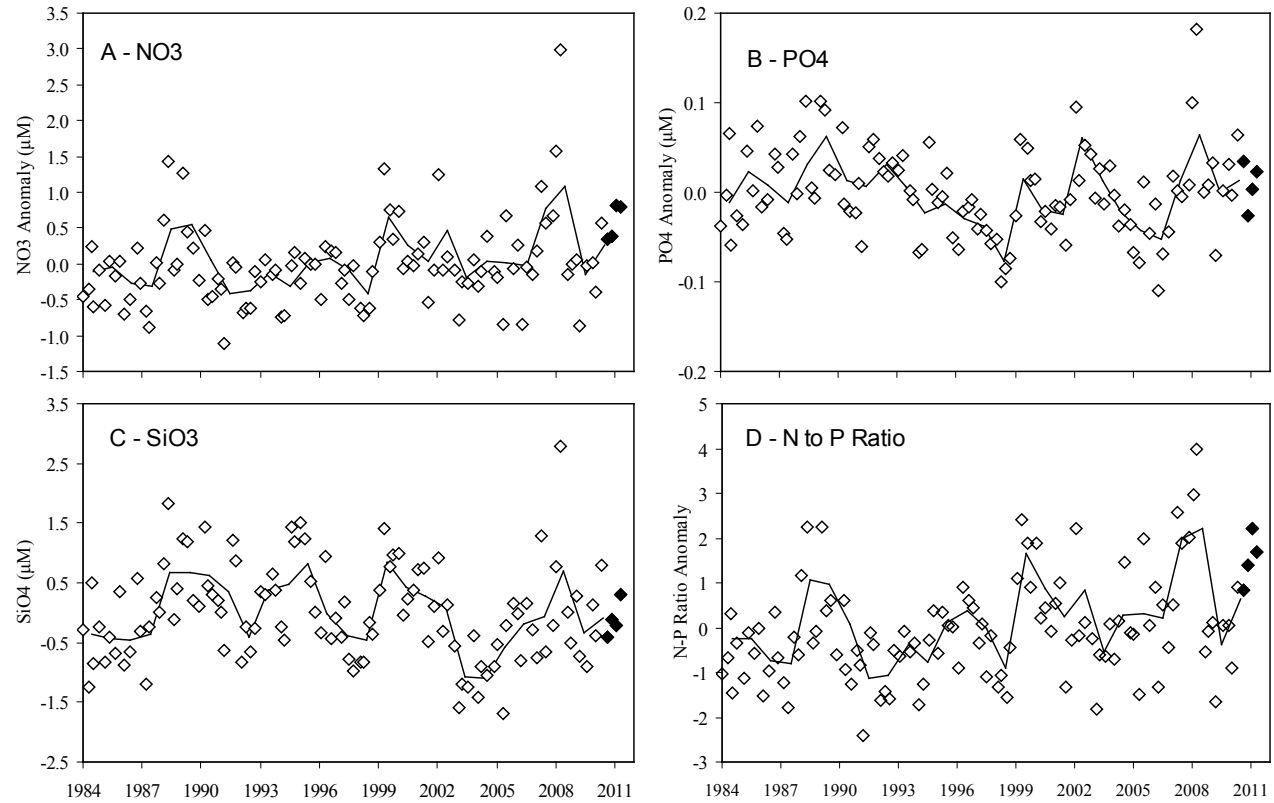

Figure 16. CalCOFI region anomalies for mixed layer concentrations of (A) nitrate, (B) phosphate, (C) silicic acid and nitrate to phosphate ratio. Data are plotted as described in Figure 13.

cal of locations far from the coast), much of the phytoplankton was concentrated towards the surface (a more typical nearshore pattern).

Observations along Line 67 during late July and early November 2010 likewise encountered cold conditions following the development of La Niña (fig. 20). Mean temperature of the halocline was the lowest observed, continuing the long-term trend since the section began in 1997 (fig. 19). In both July and November, the inshore edge of the California Current was observed between

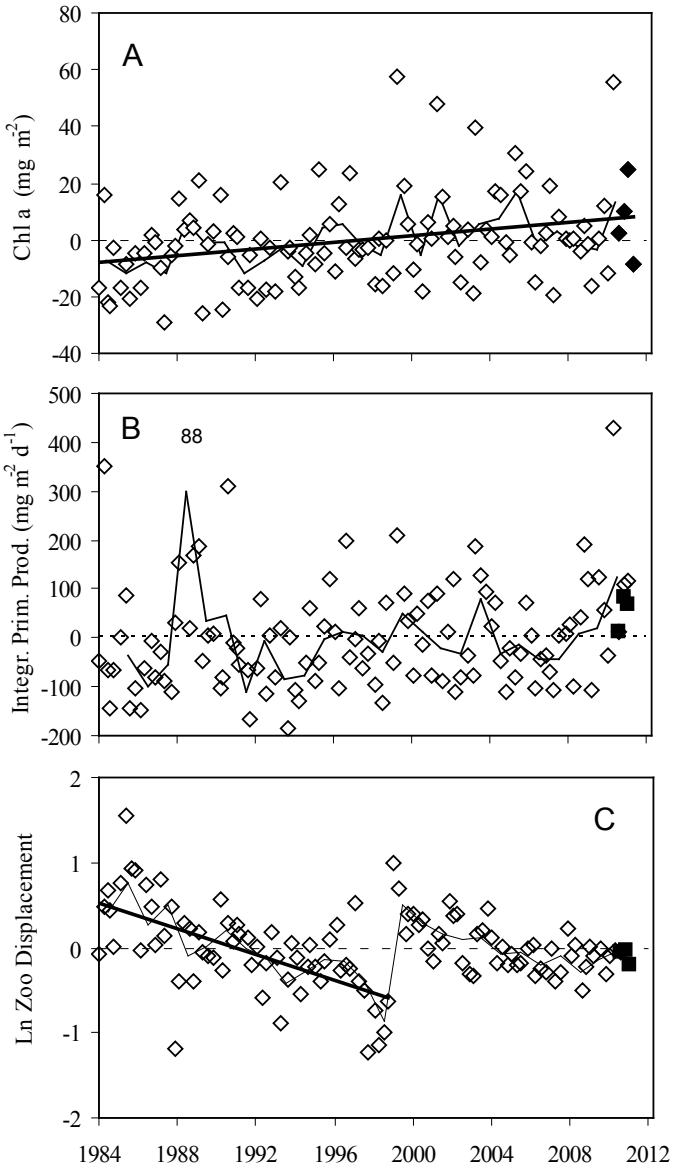

stations 67–70 and 67–65 (approximately 110-150 km nm off the mouth of Monterey Bay). Seasonal salinity anomalies in the upper 200 m on the offshore (inshore) side of the front were –0.4 (+0.4) in both July and November. The pattern of seasonal temperature anomalies associated with the salinity anomalies was complex but with generally warmer (cooler) waters on the offshore (inshore) side of the front with anomalies about ~1°C (–1°C). These patterns suggest an intensification of flow in the upper ocean along the front.

Northern California Current—Newport Hydrographic Line and Trinidad Head Line

Observations along the Newport Hydrographic Line[9] indicate a strong transition from El Niño to La Niña conditions from spring 2010 to summer 2010. Spring 2010 was marked by some of the the warmest and freshest waters observed in the time series, similar to 1997 and to other warm ocean years (1998, 2003, 2005 and 2006). In strong contrast, deep midshelf waters in summer 2010 were the coldest on record (fig. 21).

Monthly average values of copepod species richness off Oregon continue to track the PDO and SST quite closely, with cold conditions (negative PDO) dominated by a few subarctic taxa and warm conditions (pos-

[9]Regular sampling of the Newport Hydrographic (NH) line along 44.65°N continued on a biweekly basis along the inner portions of the line, at seven stations ranging from 1 to 25 nautical miles from shore. Details on sampling protcols are available in previous reports and at http://www.nwfsc.noaa.gov/research/divisions/fed/oeip/ka-hydrography-zoo-ichthyoplankton.cfm. Temperature anomalies along the Newport line are based on the Smith et al. (2001) climatology. Copepod data are based on samples collected with a 0.5 m diameter ring net of 202 μm mesh, hauled from near the bottom to the sea surface. A TSK flowmeter was used to estimate distance towed.

Figure 17. CalCOFI region averages for standing stocks of chl *a* (A) and rates of primary production (B) and zooplankton displacement volume (C). Data and symbol codes are the same as those in Figure 13.

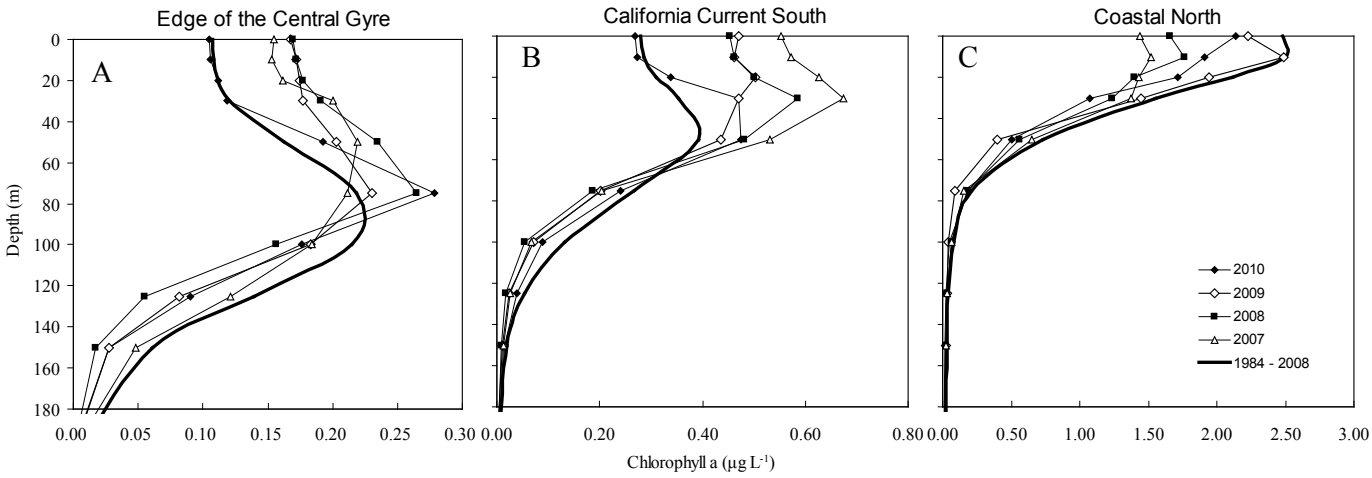

Figure 18. Average annual chl *a* profiles at standard depths for the three regions defined in Figure 14.

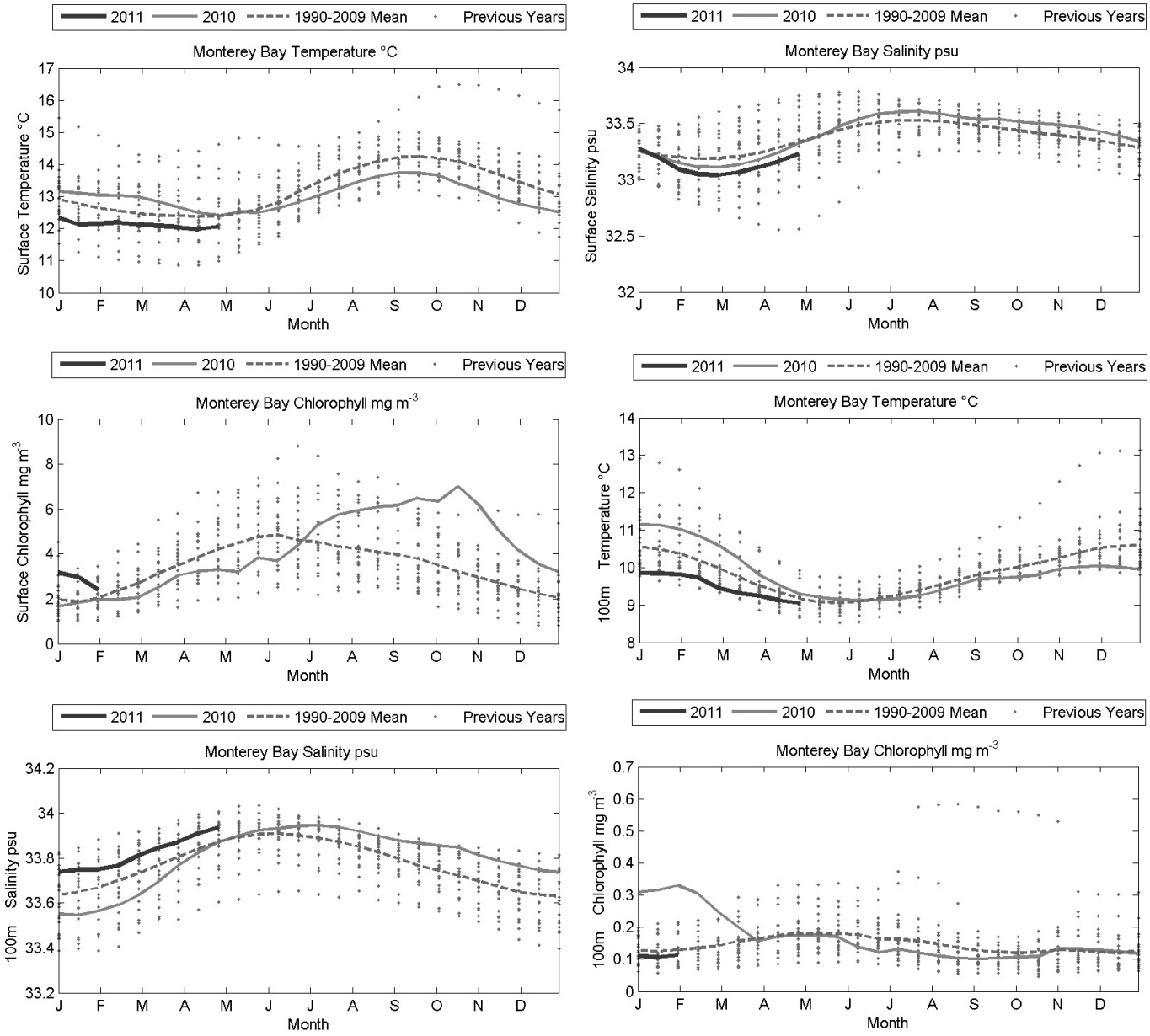

Figure 19. Temperature (top panels), salinity (middle panels) and chl *a* concentration (bottom panels) at the surface (left hand column) and at 100 m (right hand column) observed at the M1 mooring.

itive PDO) dominated by a more speciose subtropical assemblage. The copepod assemblage observed throughout much of 2009 was relatively depauperate, but species richness increased in response to the 2009–2010 El Niño event to reach anomalously high values by summer 2010 that persisted throughout the year (fig. 22). Copepod species richness reached the same magnitude as that observed during the 1998 El Niño event and the period between 2003 and 2006 marked by a consistently positive PDO. Species richess declined in early 2011, save for during March, when anomalously strong downwelling appears to have driven a temporary enrichment of the copepod assemblage over the Oregon shelf with southern and oceanic species (fig. 22).

The response of the plankton ecosystem to seasonal and climate variability is also indicated by the relative biomass of several copepod species with northern biogeographic affinities (*Pseudocalanus mimus*, *Calanus marshallae* and *Acartia longiremis*) to total copepod biomass (fig. 23). Biomass of northern copepods declined in response to the 2009–2010 El Niño, and this change in assemblage structure persisted well into summer 2010 before recovering to moderately high levels in late 2010 (fig. 23).

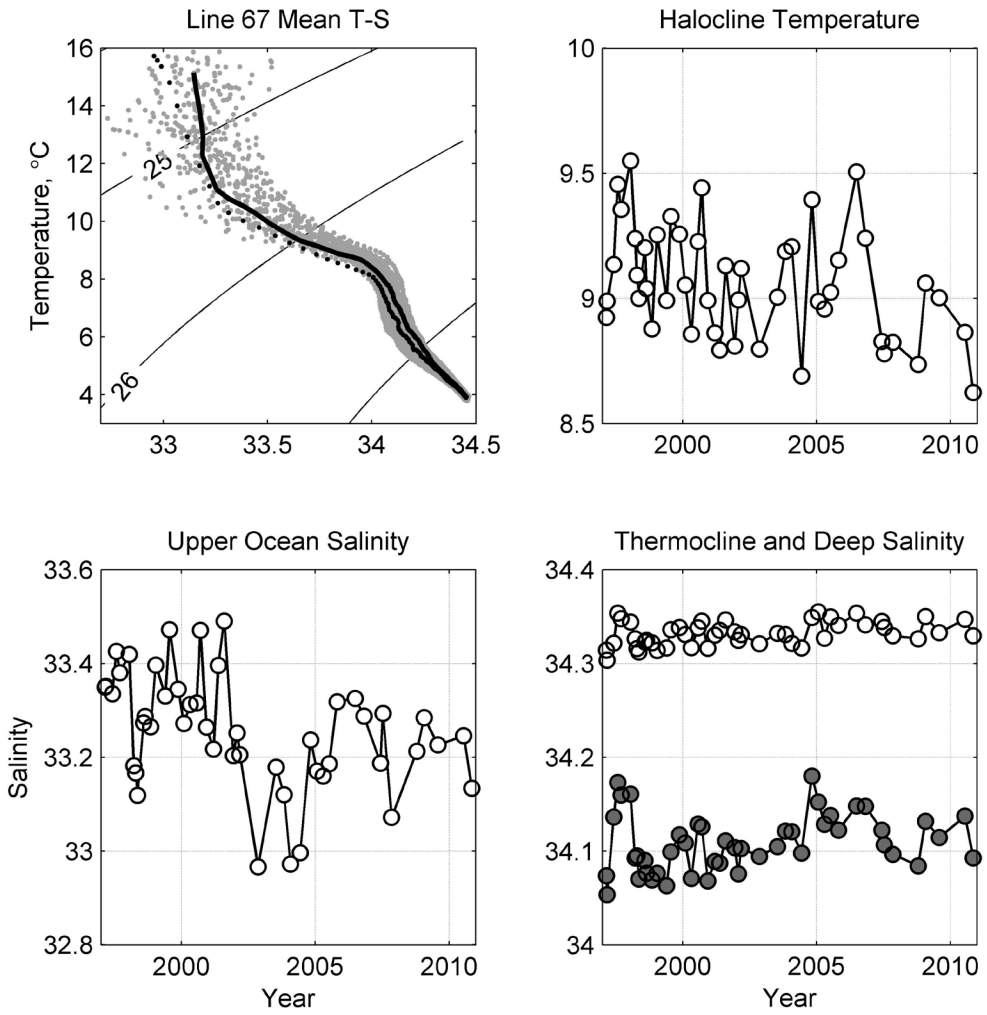

Figure 20. Hydrographic properties along Line 67 from 1997 to 2010. Each cruise included 17 stations along line 67 spaced 20 km apart from H3 (at the entrance to Monterey Bay) to station 67–90 (located 320 km offshore of H3). Data for 47 cruises are shown. (upper left) Mean T-S properties for each cruise. The July 2010 cruise is a solid black line and the November 2010 cruise is a black dotted line. Isopycnals are spaced at 1 kg/m^3 intervals. (upper right) Mean temperature of halocline waters, 33.6<S<34.0. (lower left) Mean salinity of upper ocean waters (waters whose temperature is greater than 10°C). (lower right) Mean salinity of the thermocline, 6°C<T<8°C (closed dots), and deeper waters, T<6°C.

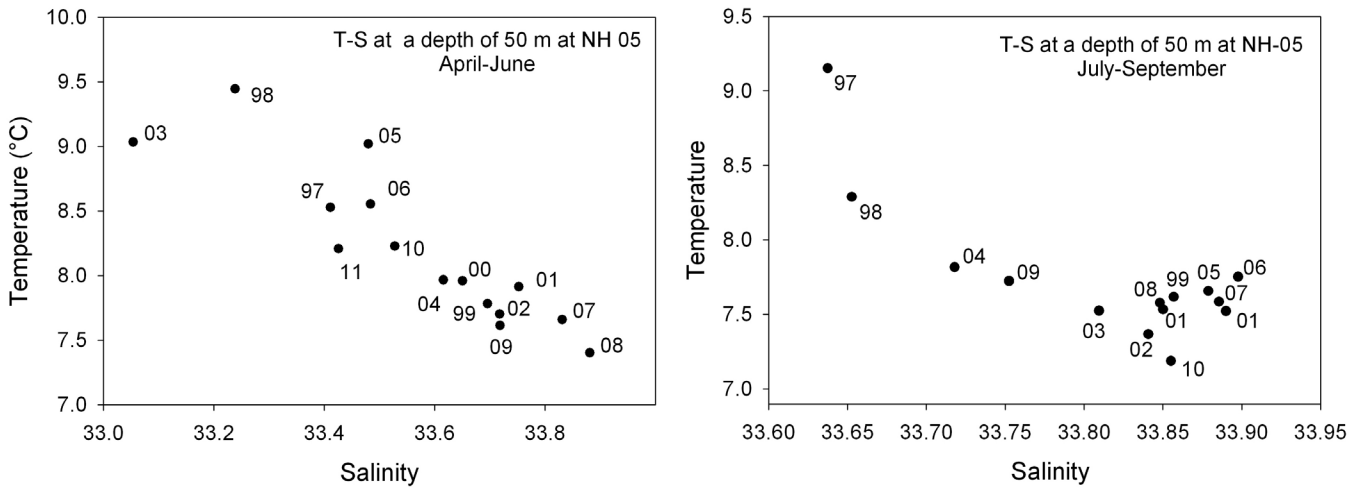

Figure 21. Seasonal mean temperature and salinity at 50 m depth at NH-05 along the Newport Hydrographic Line for spring (left panel) and summer (right panel). Note changes in scale on both temperature and salinity axes. Numbers next to points indicate year of observations.

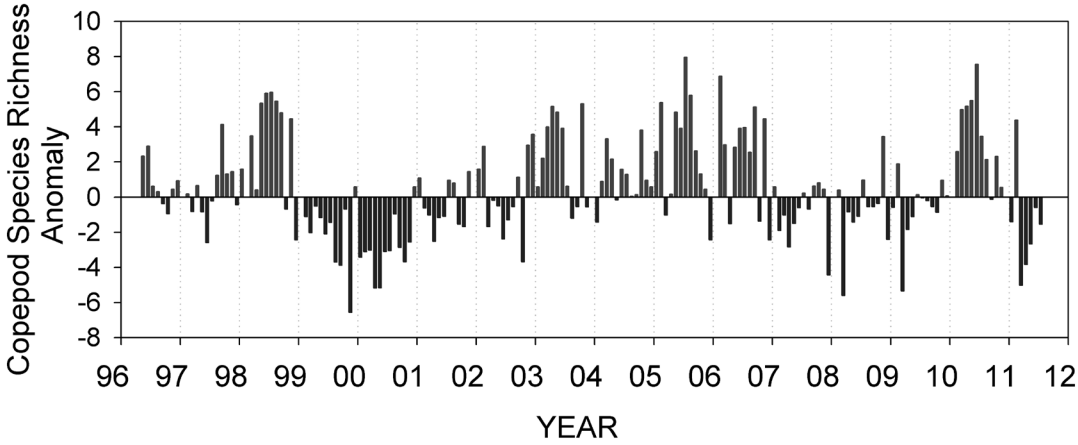

Figure 22. Monthly averaged copepod species richness anomalies at station NH 05 off Newport, Oregon.

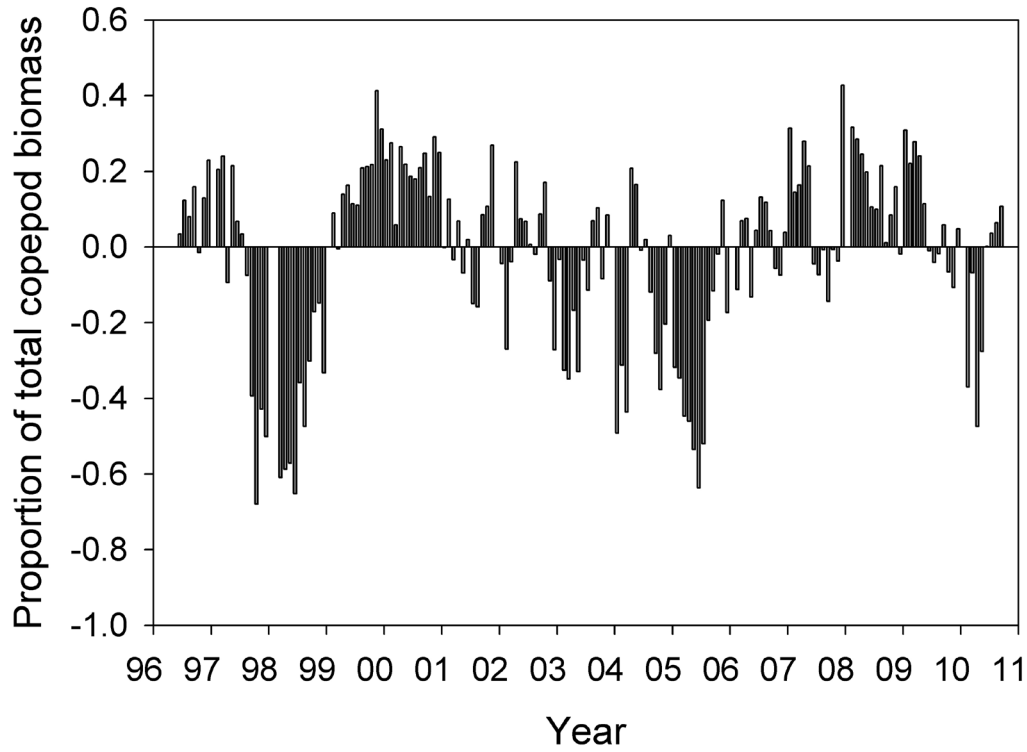

Figure 23. Monthly anomalies in proportion of copepod biomass in samples from the Newport Station 5 [NH05] biweekly time series that was made up by the three dominant northern copepod species (*Pseudocalanus mimus*, *Calanus marshallae* and *Acartia longiremis*; upper panel).

Observations along the Trinidad Head Line[10] indicate a similarly strong reversal from El Niño conditions to La Niña conditions as indicated by the properties of deep, midshelf waters, but also indicate that water properties over the narrow shelf in this region are highly dynamic and respond rapidly to short term variability in wind forcing. In winter 2010, these waters were the warmest observed and nearly the freshest observed (fig. 24). Some of the the coldest, saltiest deep midshelf water was observed during one cruise in July 2010, but this cold water was replaced by moderately cool waters within a few weeks, so that an unambiguous signal of unusually strong, sustained upwelling was not apparent in the ship-based observations (fig. 24, see also upper panels of fig. 25). Anomalously warm, fresh waters comparable to those observed in winter 2010 were observed in December 2010, but were quickly replaced by cooler, saltier water during active upwelling in early 2011 (figs. 24, 25). Concentrations and distributions of chl *a* at midshelf in summer 2010 were somewhat less than those observed in summer 2008 yet were much greater than in 2009 (data

[10]Details on sampling protocols for the Trinidad Head Line are available in previous reports and online at http://swfsc.noaa.gov/HSU-CFORT/.

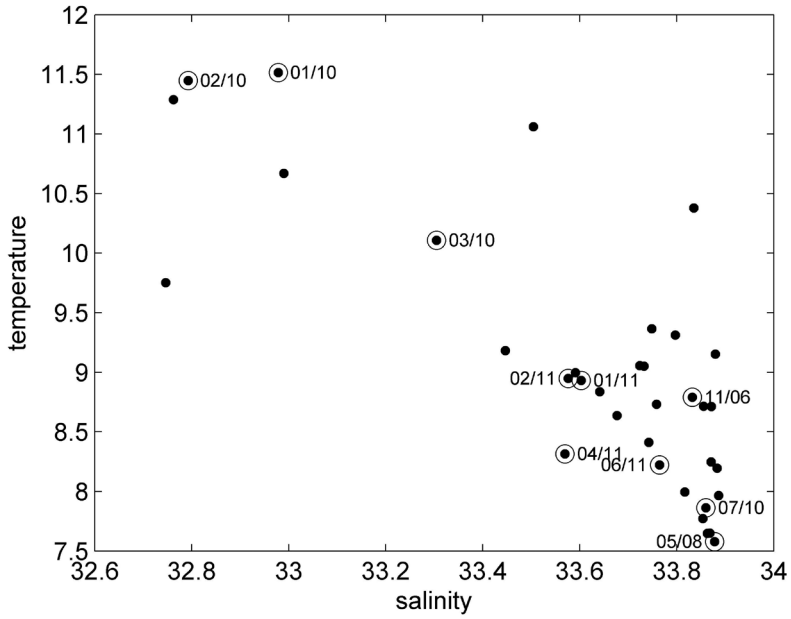

Figure 24. Temperature and salinity at 60 m depth at midshelf (station TH02) along the Trinidad Head Line. Most points represent observations from a single monthly cruise, but several represent average observations from two closely spaced cruises. Date (month/year) labels apply to circled points.

not shown). Observations in early 2011 indicate small blooms, presumably in response to upwelling events in January and February, but high concentrations of phytoplankton over the shelf had not yet been observed.

The copepod assemblage at midshelf along the Trinidad Head Lines continues to have a more southern, more oceanic composition than is observed off Newport, which is consistent with the location of the Trinidad Head Line relative to Newport and the narrow shelf off Trinidad Head (fig. 25). In contrast to the coherent seasonal signals in copepod abundance observed in previous years (Bjorkstedt et al. 2010), copepod densities were low off Trinidad in summer 2010, yet quite high off Newport (fig. 25). This may reflect differences in circulation related to the narrow shelf off Trinidad Head, which might favor (temporary) export of copepods during periods of intense upwelling and offshore Ekman transport. Off Trinidad Head, the copepod assemblage during winter 2010–11 was similar to that observed during the weak 2009–2010 El Niño, in that the assemblage was dominated by more southern taxa. Southern taxa remained common throughout 2010, despite the dissipation of El Niño. In contrast to spring 2010, northern, neritic species had returned in abundance by spring 2011.

ECOSYSTEM SURVEYS & BIOLOGICAL RESPONSES OF HIGHER TROPHIC LEVELS

Southern California Pelagic Ecosystem

Spawning of small pelagic fish, such as Pacific sardine (*Sardinops sagax*), northern anchovy (*Engraulis mordax*), and jack mackerel (*Trachurus symmetricus*), is sensitive to temperature, among other factors, with individual species responding differently to a particular suite of environmental conditions. Information on spawning distributions provides an integrated picture of the CCS from the perspective of these important fishes, and is important to the design of fisheries surveys used to estimate spawning stock biomass from daily egg production.

Comparisons of the spatial distribution of eggs[11] among years with "warm" or "cool" SSTs in April[12] showed that sardine changed their spawning distribution during warm years more than did anchovy or jack mackerel (fig. 26). Sardine moved the furthest north in the warm springs of 2006 and 2010 (fig. 26). The coordinates of the median egg density for April 2011 are also highlighted for comparison. Spawning sardine occurred 30–60 miles northwards and shoreward in warm years. Greater numbers of sardine eggs to the east (shoreward) during warm years may have been caused by movement of spawning sardine into coastal waters during warm Aprils marked by reduced upwelling (fig. 26).

[11]The distribution and density of eggs was determined from the Continuous Underway Fish Egg Sampler (CUFES) using standard methods documented for ichthyoplankton surveys. The data were restricted to latitudes between San Diego and San Francisco to avoid bias by the few surveys that sampled the entire U.S. West Coast (2006, 2008 and 2010).

[12]Monthly Sea Surface Temperature (SST) data (centered on mid-month) were obtained from the Pathfinder v.5 sensor at 5.5 km resolution for each April (approximate center of spawning for Pacific sardine) from 1997 to 2010 between 20–40°N and 116–127°W. SST anomalies at each pixel were calculated by subtracting the mean April value at that pixel for all years, thereby creating an anomaly image. Boxplots centered on the median anomaly value for each anomaly image (i.e., April 1997, April 1998, etc.) were used to create a time series of April SST anomalies which were used to characterize warm and cool years. Eight of the 14 years were warm (1997, 1998, 2000, 2003–2006, and 2010) in April whereas there were 6 cool April years (1999, 2001–2002, and 2007–2009).

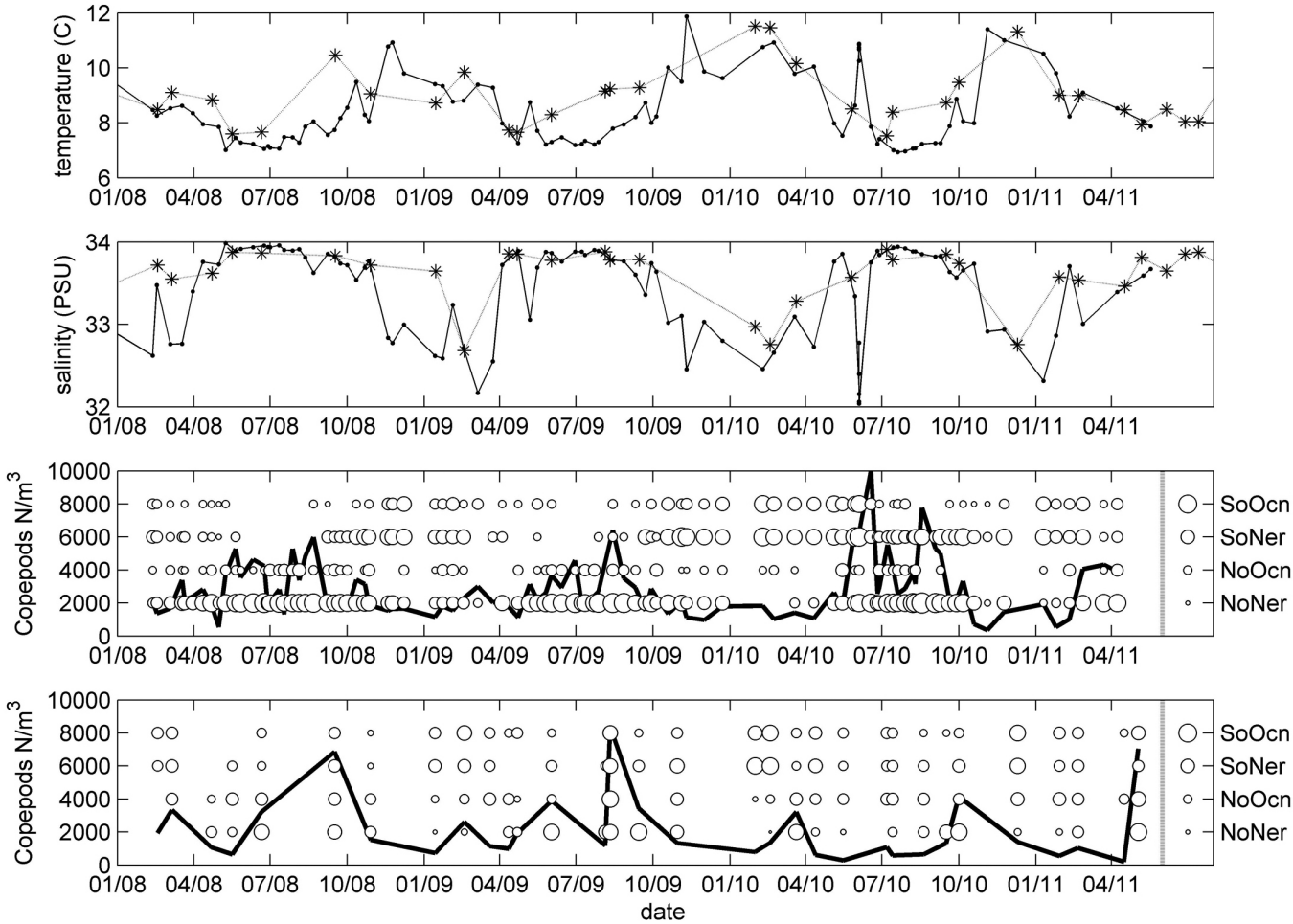

Figure 25. Top two panels: cruise-specific near-bottom temperature and salinity for stations NH05 (solid line with dots) and TH02 (dotted line with asterisks). Bottom two panels: copepod density in vertical ring-net samples collected at stations NH05 (Newport Line, 44.65°N, 124.18°W, 77 m) and TH02 (Trinidad Head Line, 41.06°N, 124.27°W, 77 m), respectively. Dark lines indicate total copepod density. Horizontal series of circles indicate pooled density of selected species from assemblages identified in Hooff and Peterson (2006): northern neritic (*Calanus marshallae*, *Acartia longiremis*, *Acartia hudsonica*, *Centropages abdominalis*), northern oceanic (*Metridia pacifica*, *Microcalanus pusillus*), southern neritic (*Acartia tonsa*, *Ctenocalanus vanus*, *Paracalanus parvus*, *Corycaeus anglicus*), southern oceanic (*Acartia danae*, *Calanus pacificus*, *Clausocalanus* spp, *Eucalanus californicus*). Density scale for assemblage data is given by symbols to the right of the grey line, which represent densities (from bottom to top) of 1, 10, 100, and 1000 copepods m^{-3}.

Spawning anchovy also moved eastward in warmer years, but the spawning range did not move toward shore. In contrast to sardine, anchovy did not show any detectable northward shift in warm years (fig. 26). Jack mackerel appear to have expanded their range of spawning northwards in warmer years, yet did not exhibit a corresponding move closer to shore (fig. 26).

It is important to note that this analysis is for an operationally defined region (San Francisco to San Diego) for which the most extensive time series data (14 years) are available. A similar analysis of data from the three coastwide surveys (2006 warm, 2008 cool and 2010 warm years) suggests that northward shifts of both sardine and anchovy are enhanced (and detected) during warm years, but change little for jack mackerel. These patterns are consistent with observations of considerable spawning of sardine off Oregon in some years, and the presence of anchovy eggs off the Columbia River mouth. We anticipate that future analysis of coastwide data sets will resolve responses of spawning distributions to ocean conditions in greater detail as the time series of coastwide surveys continues to grow.

Spawning distributions observed in spring 2011 present a mixed picture of ocean conditions. The distribution of sardine eggs resembles that of warm years, in that the position of median egg density was coincident with that observed for warm years (fig. 26). There was almost no spawning of sardine in the Southern California Bight in April 2011, and instead sardine spawned off the southern part of Central California (south of San Francisco), including areas near to shore. This pattern was similar to that observed in the warm years of 2004 and 2010, yet differs from other years (e.g., 2002–05) during which sardine spawned in the northwest portion of the survey

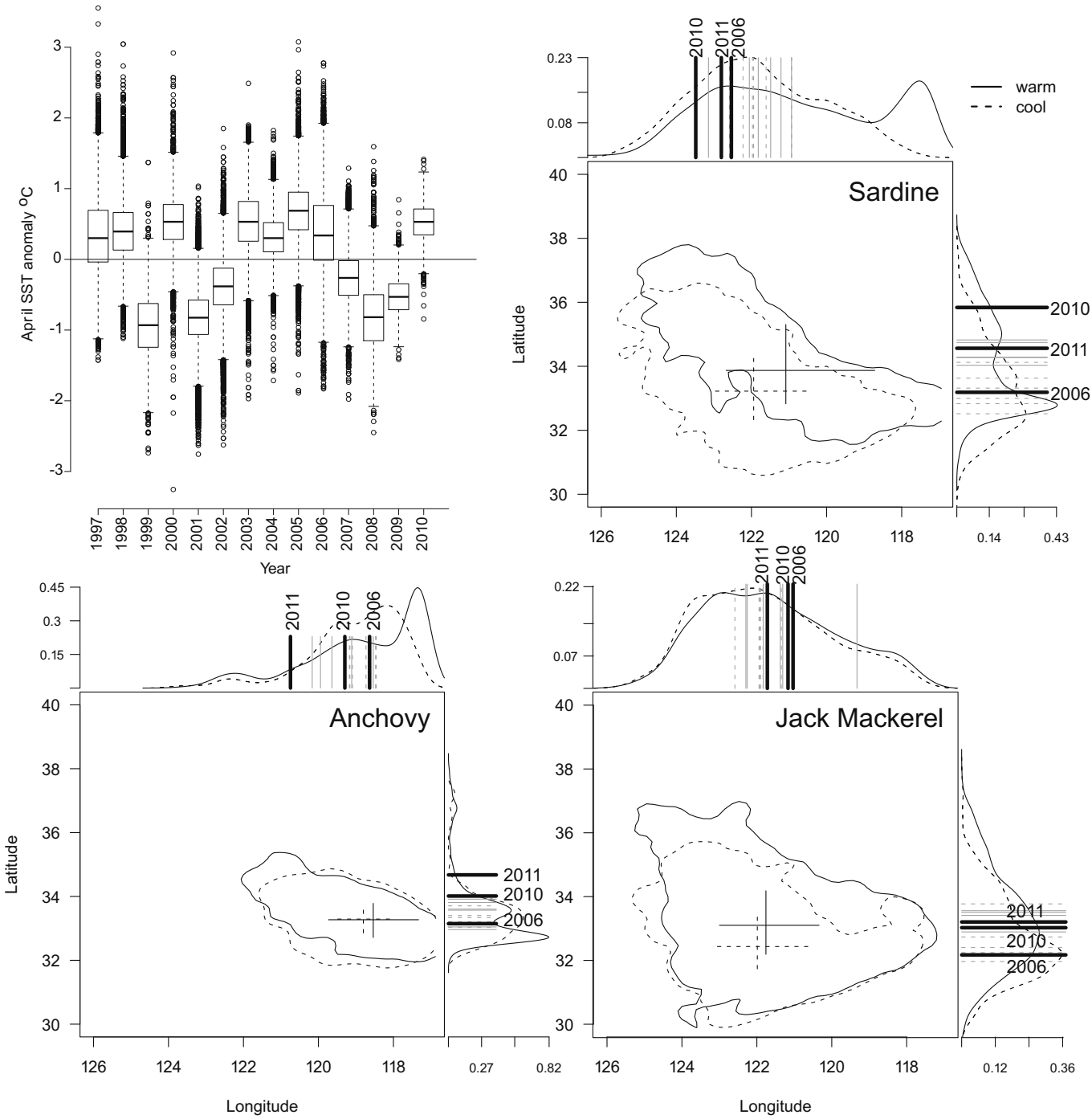

Figure 26. Upper left panel: boxplots of satellite SST anomalies used to characterize spring temperatures as either warm or cool. Distributions of sardine (upper right panel), anchovy (lower left panel) and jack mackerel (lower right panel) spawning observed between San Francisco and San Diego in anomalously warm compared to anomalously cool years (n = 14 years). Marginal plots show the density distribution of sardine eggs in relation to latitude and longitude. Heavy black lines show the position of the median density distributions in April 2006, 2010 and 2011. Cross hairs on the main plot show the location of the median density and the 25th and 75th inter-quartile range for the latitude and longitude. Ellipses show the 99% confidence interval for the bivariate density distribution of the eggs (i.e., 0.5% of the distribution at the tails of each of the marginal plot density distributions are outside the ellipse).

region. In contrast, jack mackerel spawned to the west of 122°W at 34–35°N, which is about 60 miles south of where they usually spawn in warm years. Patterns of sardine and jack mackerel spawning are consistent with intermediate April conditions (i.e., neither notably warm or cool). There was little anchovy spawning in April 2011, consistent with expected timing of anchovy spawning in late winter rather than coincident with the spring survey.

In spring 2010, sardine eggs remained far less abun-

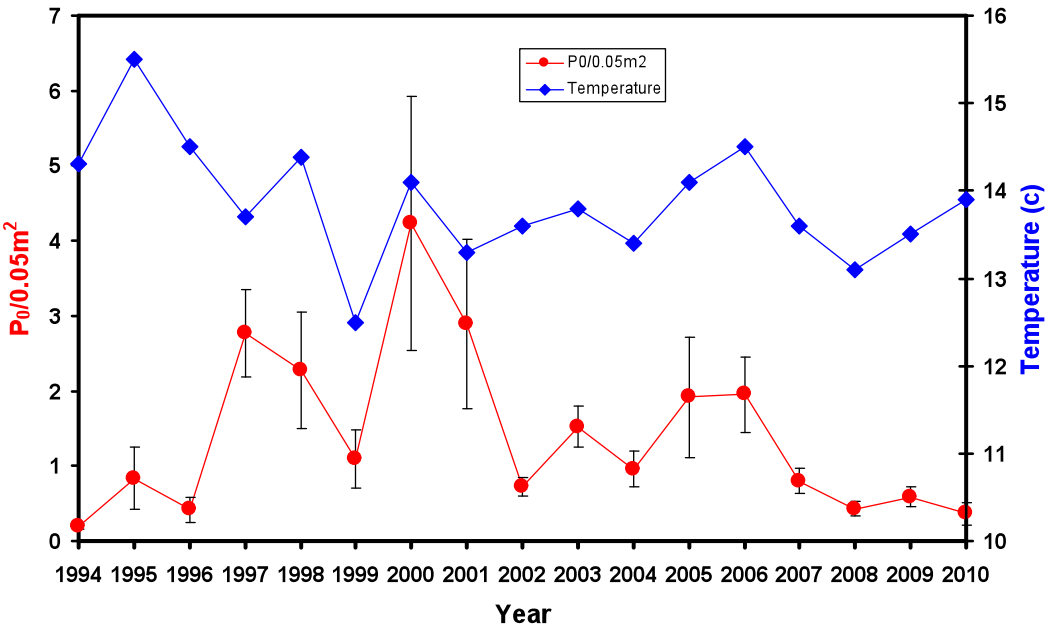

Figure 27. Daily egg production/0.05m^2 of Pacific sardine (circle) (+ and – one standard error) and average sea surface temperature (°C) (diamond) during March–April DEPM cruises from 1994–2010.

dant than in years prior to 2007. Spawning biomass Pacific sardine[13] based on analysis of these data using daily egg production methods suggests that Pacific sardine biomass remains small relative to the late 1990s and early 2000s (fig. 27). There is no evidence for an increase in daily egg production in relation to increased average sea surface temperatures observed in 2010.

Southern California Cetaceans

Visual surveys for cetaceans on quarterly CalCOFI cruises found that the relative abundance of various species of small cetaceans in 2010–11 was similar to that observed for previous years with the exception of Dall's porpoise (*Phocoenoides dalli*) which exhibited the second highest sighting rate observed for this species across the seven-year sampling period. Colder than average water temperatures in 2010–11 may have contributed to the increased relative abundance of Dall's porpoise as this species is generally restricted to cold/temperate waters. Relative abundance of baleen whales also increased from previous years for three of four common baleen whale species, fin whales (*Balaenoptera physalus*), humpback whales (*Megaptera noveangliae*) and gray whales (*Eschrichtius robustus*), all of which were sighted at rates nearly double the average, representing the second highest levels observed for the three species across the seven-year study period. The increase in sighting rates of large planktivorous whales is likely to reflect behavioral responses abundant prey resources in the region.

Despite the increase in sighting rates for several taxa, the visual surveys did not detect substantial changes in the cetacean assemblage off Southern California. While annual species richness (average number of species per km of effort) of cetaceans was similar to that observed during previous years, species richness was higher in spring 2010 and lower in summer 2010 relative to the seasonal averages since 2004, despite sighting rates were consistent with previous years' efforts (data not shown).

Central California Pelagic Ecosystem

Analysis of catch composition and abundance of key taxa from annual midwater trawl surveys[14] off Central California indicated that 2011 continues the trend observed in recent years towards increasing abundance of species and assemblages that tend to thrive under cool,

[13]The spring 2010 California Current Ecosystem (CCE) survey was conducted aboard one NOAA research vessel: *Miller Freeman* and a chartered fishing vessel: F/V *Frosti*. *Miller Freeman* (April 2–22) covered the area off California from San Diego to Monterey Bay (CalCOFI lines 95 to 66.7) and the F/V *Frosti* (March 28–April 28) covered the area from just south of Cape Flattery, Washington to just south of Monterey Bay, California (48.07°N to 34.88°N, i.e., CalCOFI line 70). During the CCE surveys, CalVET tows, bongo tows, CUFES and trawls were conducted aboard both vessels. After the CCE survey, the routine spring CalCOFI survey was carried out aboard *Miller Freeman* from April 26–May 17 to cover six lines from 93.3 to 76.6 and CalVET and bongo tows were taken. Only data from CCE survey were included in estimation of spawning biomass of Pacific sardines. Data from all spring cruises were used to examine the spatial distributions of Pacific sardine, northern anchovy and jack mackerel.

[14]Observations reported here are based on midwater trawl surveys that target small (1–20 cm) pelagic fishes and invertebrates conducted off central California (a region running from just south of Monterey Bay to just north of Point Reyes, CA, and from near the coast to about 60 km offshore) since 1990 (see Sakuma et al. 2006 for methods and details on spatial extent of survey). Cruises cruises have been conducted on the NOAA ship *David Starr Jordan* (1990–2008), the NOAA Ship *Miller Freeman* (2009), the F/V *Frosti* (2010), and the F/V *Excalibur* (2011). Data for the 2011 survey presented here are preliminary, and data collected since 2009 do not account for potential vessel-related differences in catchability. Data are reported as standardized anomalies from the log of mean catch rates. Most taxa reported are considered to be well sampled, but the survey was not designed to accurately sample krill.

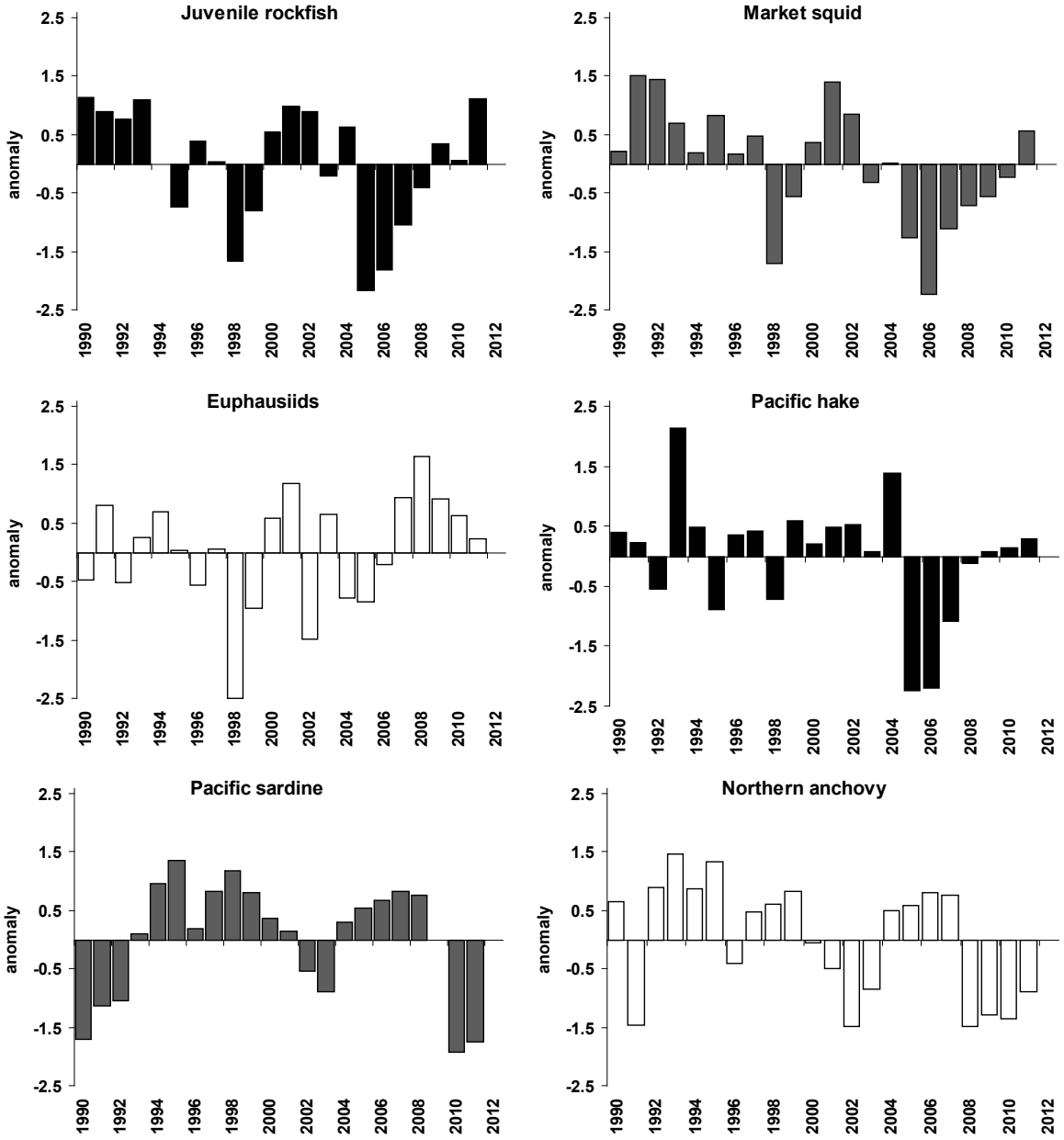

Figure 28. Long-term standardized anomalies of several of the most frequently encountered pelagic forage species from the central California rockfish recruitment survey in the core region (1990–2011 period only, not all taxa were recorded from 1983–89).

productive conditions, and a return to ecosystem characteristics similar to those seen in the early 1990s and early 2000s (fig. 28). In 2011, juvenile rockfish (*Sebastes* spp.), market squid (*Loligo opalescens*), and other groundfish (such as Pacific hake [*Merluccius productus*], shown, and Pacific sanddabs [*Citharichthys sordidus*], not shown) were at their highest levels since the early 2000s and early 1990s. By contrast, the coastal pelagic forage species (adult northern anchovy and Pacific sardine) were at low levels in 2010 and 2011, although this is likely a greater reflection of their local availability and ocean conditions rather than their coastwide or regional abundance. Euphausiids continued to be abundant, but less so than in 2008–10. For the second year in a row, no Humboldt squid were captured during the survey.

Trends observed in the six indicators shown in Figure 28 are consistent with trends across a number of other taxa within this region. Results from a Principal Components Analysis of annual catch data[15] highlight

[15]Principal Components Analysis (PCA) was applied to the covariance among fifteen of the most frequently encountered species and species groups, yielding strong loadings for various young-of-the-year groundfish taxa (rockfish, Pacific hake, rex sole and sanddabs), cephalopods, and euphausiids, with slightly weaker (and inverse) loadings for Pacific sardine, northern anchovy, and several species of mesopelagic fishes. The first and second components explain 39% and 14% of the variance in the data respectively (representing strong covariance among young-of-the-year groundfish, cephalopods and euphausiids, which in turn tend to be negatively correlated with coastal pelagic and mesopelagic fishes).

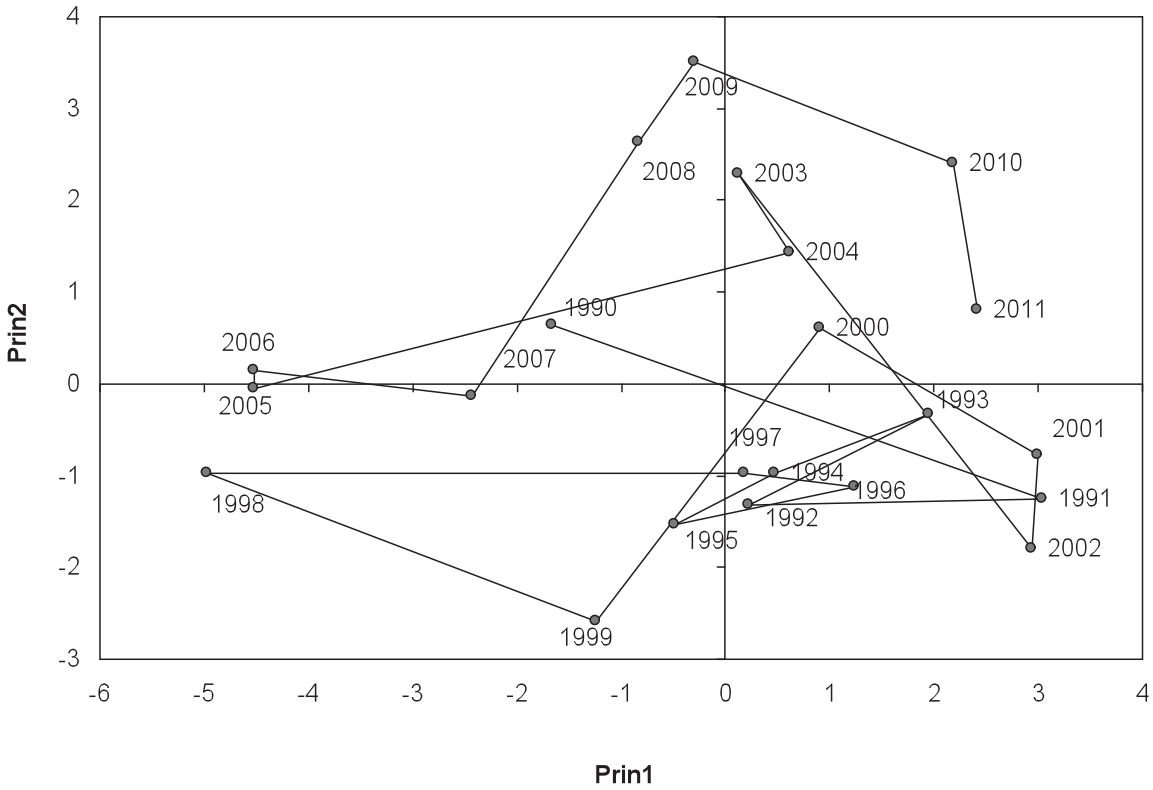

Figure 29: Temporal changes in pelagic ecosystem structure off central California based on PCA of the fourteen most frequently encountered species groups in the NMFS midwater trawl survey. Data are take from stations in the core area (Point Reyes to Monterey Bay) from 1990–2011.

changes in the midwater assemblage over time: the clupeoid-mesopelagic group was prominent during the 1998 El Niño and during the anomalously warm years 2005–07, while the groundfish group prospered during the early 1990s, the cool-phase between 1999 and 2003, and most recently from 2009 through 2011 (fig. 29). As with the 2009 and 2010 data, results from 2011 continue to represent a return towards conditions similar to the 1999 to 2003 period for many groups, while others are at moderate levels that approximate long term mean conditions.

Seabirds Off Central and Southern California

Two data sets provide observations on seabirds off the California coast: estimates of reproductive success of seabirds on the Farallon Islands[16], a major breeding colony for several seabird species, and at-sea densities of seabirds from ship surveys off southern California[17]. Observations from SE Farallon Island indicate that the 2010 breeding season was extraordinarily successful for most seabirds on the Farallon Islands, with many species having their best breeding year since 2004 (Warzybok and Bradley 2010). Productivity of Cassin's auklets (*Ptychoramphus aleuticus*) was the highest ever recorded for this species, due in part to unprecendented high rates of successful double brooding (the fledging of a second chick after a successful first attempt) (fig. 30). Among the piscivorus seabirds, common murres (*Uria aalge*) and rhinoceros auklets (*Cerorhinca monocerata*) had their highest level of breeding success in the last 20 years (fig. 30). Productivity of pigeon guillemots (*Cepphus columba*) exceeded the long term mean for the first time since 2004 (fig. 30). Pelagic cormorants (*Phalacrocorax pelagicus*) showed a second year of strong productivity after 4 years of near breeding failure (fig. 30). The high productivity of these species is likely to reflect elevated productivity in the Gulf of the Farallones during spring and summer 2010: euphausiids and juvenile rockfish were both highly abundant. In contrast, western gulls (*Larus occidentalis*) had their poorest year on record, and Brandt's cormorants (*Phalacrocorax penicillatus*) continued to suffer very low reproductive success though they did manage to fledge a small number of young this season after two years of near complete breeding failure (2008–09) (fig. 30).

Off southern California, at-sea densities of sooty shearwater (*Puffinus griseus*) showed an increase in relative abundance in 2009 and 2010, despite a long-term decline that has persisted across seasonal and multiyear

[16]See Warzybok and Bradley 2010 for a description of methods.

[17]Surveys of marine birds have been conducted in conjunction with seasonal CalCOFI/CCE-LTER cruises since May 1987 (84 surveys through July 2010). Observations are collected by experienced observers, who identify and count seabirds within a 300 m wide strip transect while the ship is underway at speeds >5 k (see Yen et al. 2006 for details). Relative abundance is expressed as density of birds at sea (birds km^{-2}).

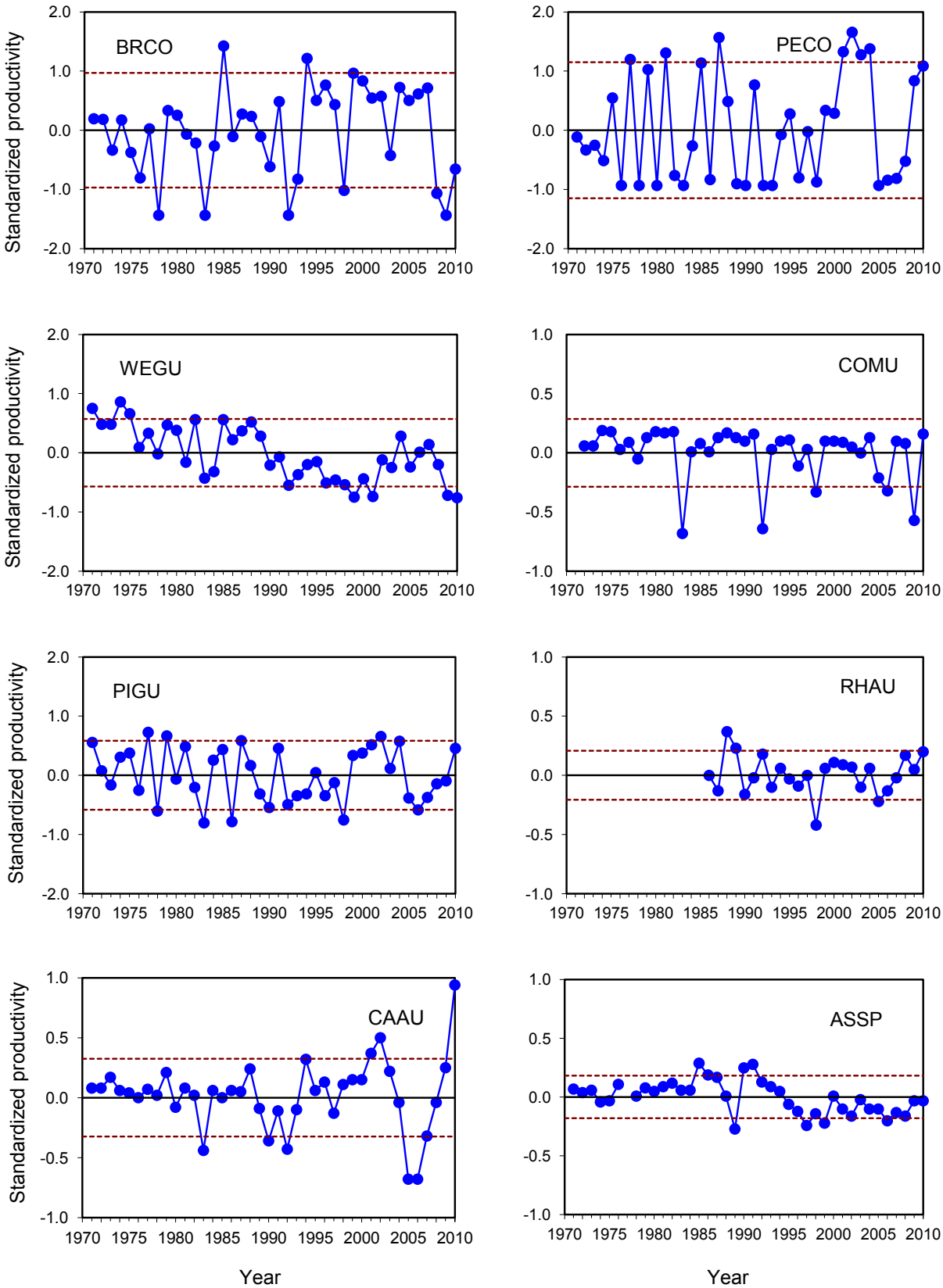

Figure 30. Anomalies of productivity (annual productivity—long-term mean) for 8 species of seabirds on SE Farallon Island, 1971–2010. Dashed lines represent 80% confidence intervals for the long-term means. Species are Brandt's cormorant (*Phalacrocorax penicillatus*; BRCO), western gull (*Larus occidentalis*; WEGU), pigeon guillemot (*Cepphus columba*; PIGU), Cassin's auklet (*Ptychoramphus aleuticus*; CAAU), pelagic cormorant (*Phalacrocorax pelagicus*; PECO), common murre (*Uria aalge*; COMU), rhinocerous auklet (*Cerorhinca monocerata*; RHAU), and ashy storm petrel (*Oceanodroma homochroa*; ASSP).

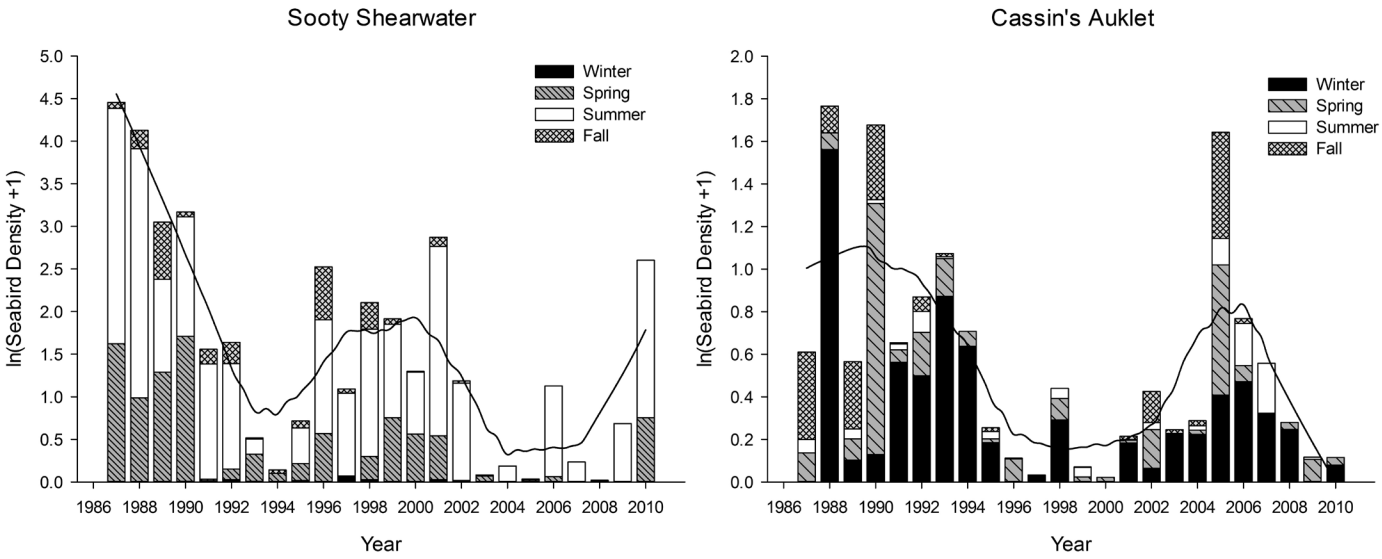

Figure 31. Changes in relative abundance (birds km^{-2}) of sooty shearwater (*Puffinus griseus*) and Cassin's auklet (*Ptychoramphus aleuticus*) observed during CalCOFI surveys, May 1987–July 2010. Bars denote summed seasonal density estimates (stacked bars), with a Lowess smoothing (bandwidth=0.3) line shown for each species.

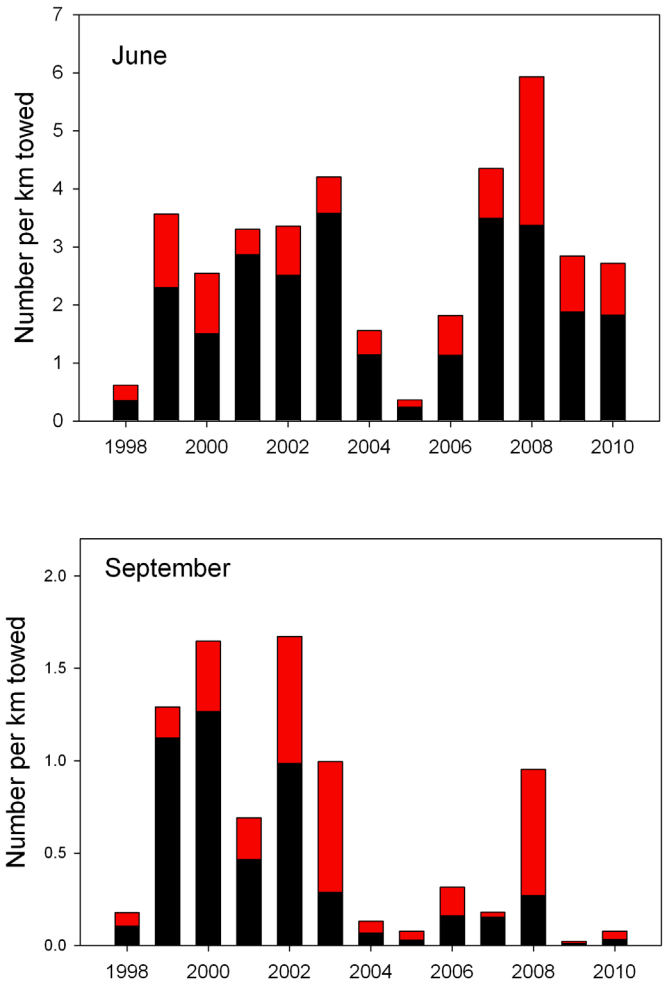

Figure 32. Catches of juvenile coho (black bars) and Spring Chinook (grey bars) salmon off the coast of Oregon and Washington in June and September, from 1998–2010.

(e.g., peak-to-peak) temporal scales (fig. 30). In contrast, at-sea densities of Cassin's auklet (*Ptychoramphus aleuticus*) off southern California were observed to decline in 2009 and 2010 (fig. 31). Although both shearwaters and auklets are species with cold-water affinities (Hyrenbach and Veit 2003) that have spatial associations with euphausiids (Santora et al. 2011), these divergent temporal patterns are consistent with differences in life history of the two species. Shearwaters are (austral) wintering migrants from southern hemisphere (Shaffer et al. 2006), and are likely to respond more directly, in terms of abundance and distribution, to the distribution and density of local prey resources. Auklets breed in the CCS (Abraham and Sydeman 2004) and thus can be expected to have a more complex response to changes in prey availability. For example, in years when auklet breeding effort was compromised by poor prey availability in the Gulf of the Farallones (e.g., 2005 and 2007), auklets abandoned their major breeding site on SE Farallon Island and may have moved south in search of prey (Sydeman et al. 2006, 2009). In contrast, the high abundance of euphausiids and other prey in the Gulf of the Farallones during 2009 and 2010 would not force such emigration.

Pelagic Fishes Off Oregon and Washington[18]

Catches of juvenile salmonids in pelagic rope trawl surveys were about average in June 2010 but very low by September 2010, including the second lowest num-

[18]For information on methods and sampling locations for the juvenile salmon surveys, see http://www.nwfsc.noaa.gov/research/divisions/fed/oeip/a-ecinhome.cfm. Data on pelagic predatory and forage fishes are from ongoing bimonthly surface trawls conducted from May to August off the Columbia River and Willapa Bay. See Phillips et al. 2009 for details on methods used for sampling larval and juvenile fishes.

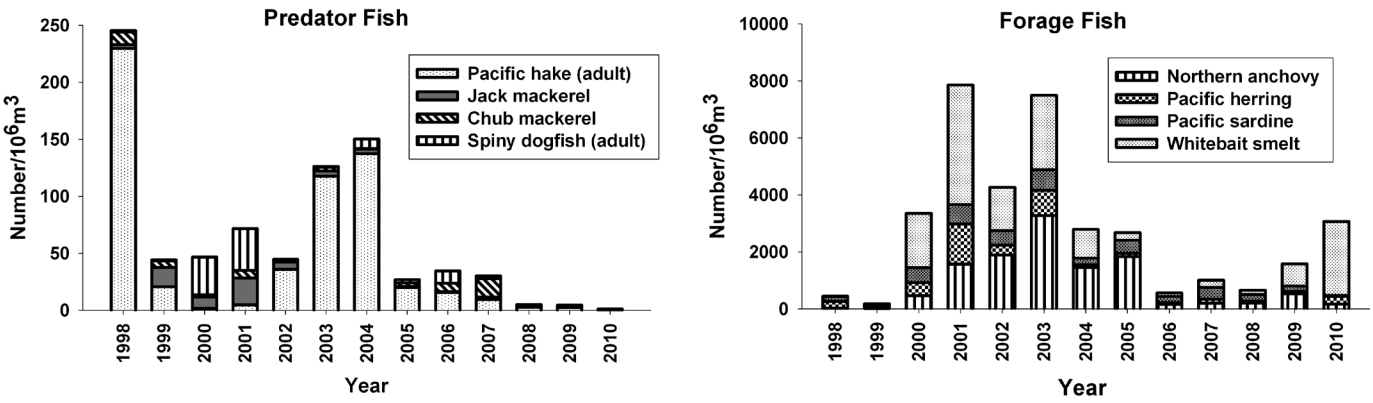

Figure 33. Annual average densities of predatory fishes (left panel) and forage fishes (right panel) captured off the Columbia River/Willapa Bay by nighttime surface trawling between May and September.

ber of coho salmon (*Oncorhynchus kisutch*) caught in the 13 year time series (fig. 32). This pattern is similar to that observed in 2009, in which moderately high abundances of juvenile salmonids in summer appear to have not carried through into the fall.

In 2010, average densities of predatory fishes[19] between May and September off Oregon and Washington were the lowest observed during the 13 year study period (fig. 33a). In contrast, average density of aggregate forage fishes off Willapa Bay (north of the Columbia River) in 2010 reached its highest value since 2003, and fourth highest overall (fig. 33b). This pattern was not consistent across species. Whitebait smelt (*Allosmerus elongatus*) and Pacific herring (*Clupea pallasi*) were both abundant. Migratory species with more southern affinities showed a different pattern: Pacific sardine (*Sardinops sagax*) catches were the lowest in the 13-year time series, and those of northern anchovy (*Engraulis mordax*) were the lowest since 2006 (the fourth lowest overall; fig. 32b).

Along the Newport Hydrographic Line, nearshore concentrations of larvae were higher in winter 2010 than in any winter since 1998 (data not shown; Auth et al., in prep.). This concentration of larval fishes near the coast during the early (El Niño) period of 2010 (including offshore taxa) was also marked by unusual onshore distributions of offshore taxa and the presence of taxa with more southern affinities, but these patterns were strongly reversed following the transition to La Niña later in spring 2010 during which low nearshore concentrations of larval fishes occurred (Auth et al., in prep.).

The transition from El Niño to La Niña also influenced the distribution and structure of the ichthyoplankton assemblage in the northern California Current. Surveys off Oregon and Washington encountered relatively low concentrations of larval fishes (primarily rockfishes *Sebastes* spp.) in June and September 2010 (fig. 34). Among the assemblage of juvenile fishes, rockfishes and flatfishes showed a marked increase from low numbers in June to the highest catches recorded, but Pacific hake were notably rare in 2010 (fig. 34). Moreover, the mean size of juvenile rockfish caught in September was the highest recorded in this survey, suggesting that growth was strong during the spring and summer. Juvenile northern anchovy were relatively abundant in June 2010 (similar to levels observed in 2005), but, in contrast to 2009, made up only a minor component of the assemblage in September 2010 (fig. 34).

Humboldt Squid

The presence of Humboldt squid (*Dosidicus gigas*) in the CCS appears to have declined to trace levels. In contrast to the record numbers encountered in 2009, no squid were captured by either of the two trawl surveys reported above, and relatively few squid were captured during fall sampling and in the hake fishery.

DISCUSSION

The state of the California Current system (CCS) since spring 2010 has evolved in response to the development of cooler La Niña following the dissipation of the relatively weak and short-lived El Niño event of 2009–2010 (Bjorkstedt et al. 2010). The 2009–2010 El Niño appears to have dissipated quite rapidly in early spring 2010, yet the transition to anomalously cool conditions followed somewhat later with the onset of anomalously strong upwelling throughout the CCS in summer 2010. Patterns in winds and sea surface temperature reported at several moorings along the coast were corroborated by remotely sensed surface current fields that captured the signature of intense upwelling throughout much of the CCS in the spring and summer of 2010. Moreover, the broad patterns discerned from coastwide observations were also reflected in the unusually cool

[19]This analysis focuses on four common species of predatory fishes: chub mackerel (*Scomber japonicus*), jack mackerel (*Trachurus symmetricus*), adult Pacific hake (*Merluccius productus*), and spiny dogfish (*Squalus acanthias*). Juvenile (yearling) Pacific hake are not yet piscivorous at the ages and sizes present in the collections, and so are not included in the estimates of predatory fish density.

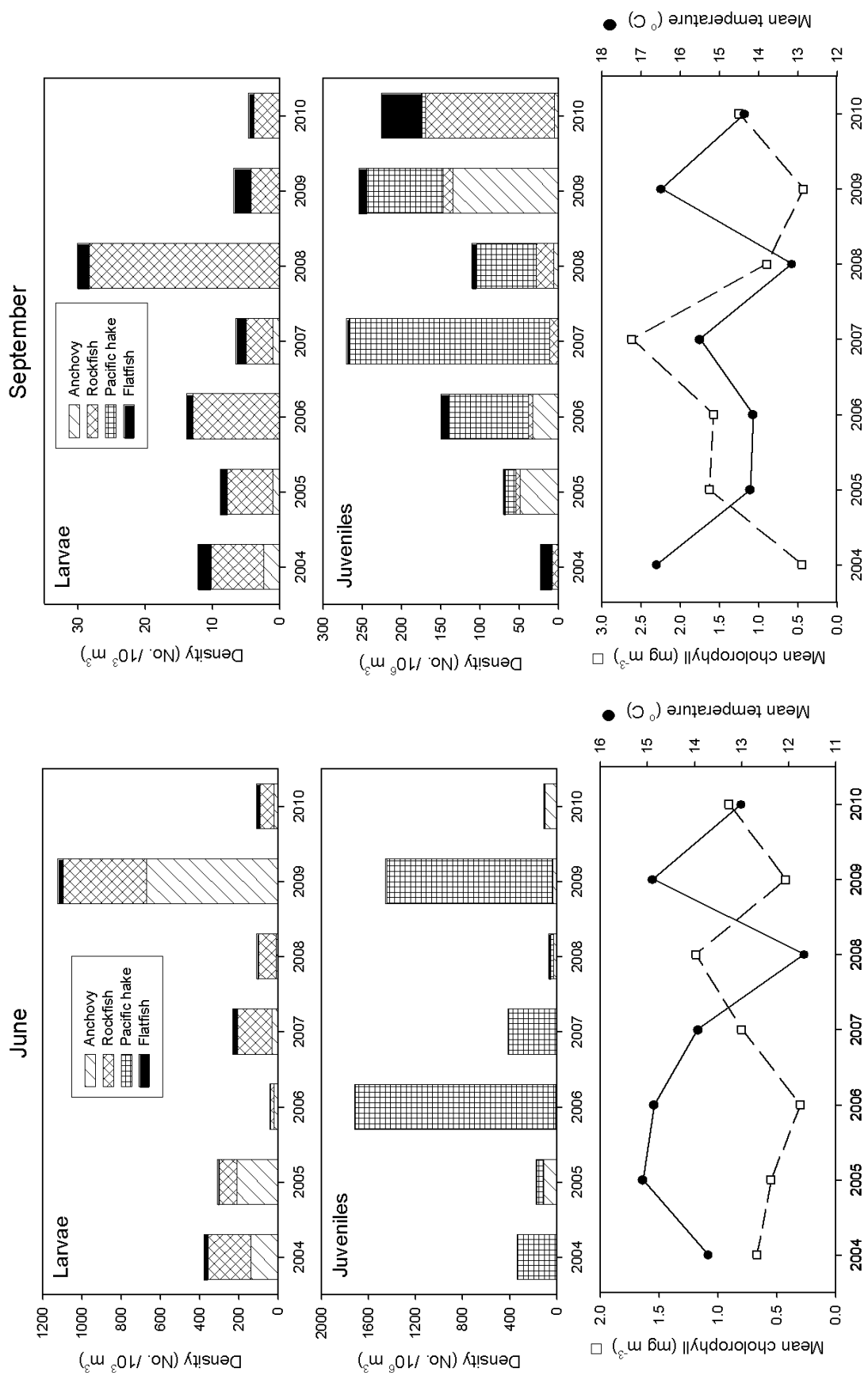

Figure 34. Mean densities of the dominant taxa for larval (top) and juvenile (middle) fish densities and mean temperature and chlorophyll concentrations (bottom) from the upper 50 m of the water column collected concurrently with the fish data for cruises conducted in June (left hand column) and September (right hand column) of each year (2004–10). See Phillips et al. 2009 for sampling details.

conditions observed during ship surveys throughout the CCS in summer 2010 (off Oregon and California) and fall 2010 (Baja California), some of which encountered the coldest (spatially averaged) conditions within the respective surveys' observational record.

Although the transition to cooler conditions was reported throughout the CCS, several factors contributed to continued regional variability in the response of the CCS to climate forcing. In particular, important differences continue to be observed between the northern and southern portions of the CCS, which appear to be related to regional differences in the timing, direction, and magnitude of climate forcing. For example, whereas the return to cooler conditions in spring and summer 2010 was fairly general across the CCS, regional variability was clearly evident in the fall when anomalously warm SST emerged briefly in the northern CCS while temperatures remained anomalously low in the southern portion of the CCS. This pattern correponds with the decline from strong positive to moderately negative anomalies in upwelling, such that upwelling persisted in the south, but effectively relaxed in the north. Regional variability was also apparent during winter 2010 and into early 2011. During this period, the northern CCS was affected by highly variable winds, including strong downwelling events associated with winter storm activity that persisted well into spring 2011 and a prolonged period of quiescent winds in midwinter 2011. In contrast, the southern CCS appears to have experienced more consistent upwelling at near normal levels throughout the year.

Ecosystem responses to the transition from El Niño to La Niña follow some predictable patterns, such as the increase in phytoplankton (as indexed by chl *a*) in several regions, particularly those areas most directly influenced by coastal upwelling. Observations of zooplankton and higher trophic levels in several regions suggest responses that are also consistent with cooler, presumably more productive, conditions. Interestingly, however, the regional variability observed in the strength and timing of the transition from El Niño to La Niña and subsequent evolution of climate forcing and responses across the CCS appears also to manifest in the several different ecosystem data sets that were considered here. For example, off central California, the nektonic assemblage continued its trend towards a "cool conditions" assemblage into 2010 and 2011, and several species of seabirds that depend on this euphausiid-groundfish rich nektonic assemblage fared exceedingly well in 2010 despite the El Niño. Likewise, the recent resurgence of crustacean zooplankton off Baja California points to increased enrichment and productivity. A similar response was not apparent in spatially averaged zooplankton data for southern California, but increased densities of migratory seabirds and planktivorous cetaceans are consistent with a more productive ecosystem. In contrast, the copepod assemblage off Oregon, which is a useful indicator for salmon productivity, did not recover rapidly and retained some characteristics of the assemblage observed during the transition from La Niña to El Niño in 2009, despite the onset of strong upwelling in early summer 2010. Juvenile salmon off Oregon also showed a sharp decline in abundance over the summer comparable to that observed during the onset of the 2009–2010 El Niño, yet, this occurred under consistently cool conditions, suggesting that prey availability and quality may have affected survival, with temperature proving less useful than prey data as an indicator of salmon productivity.

Interpretation of ecosystem responses to climate variability is likely to be confounded by inertia in ecosystem dynamics related to population dynamics and persistent effects of transport that preclude or blur "instantaneous" response to climate forcing. For example, while phytoplankton may respond rapidly to enrichment events, zooplankton and higher trophic levels may be as or more sensitive to "pre-conditioning" of the ecosystem during the winter (Black et al. 2010), to the standing stock based on productivity or transport events during the previous year, or to dynamics unfolding over longer time scales. For example, the persistence of copepod species with southern affinities in the northern CCS into 2010 may reflect lingering effects of poleward transport, and changes in distributions of pelagic fishes throughout the CCS may integrate the consequences of and responses to conditions in previous years. The potential role of unusual species interactions in the dynamics of higher trophic levels must also be considered, e.g., the potential effects of high abundances of Humboldt squid (*Dosidicus gigas*) in recent years may have contributed to reductions in pelagic fishes (Litz et al., this issue).

Several recent trends or novel observations warrant further consideration and closer examination in future reports. For example, data from the southern regions (CalCOFI and IMECOCAL surveys) have indicated a freshening trend in the upper water column. How pervasive this trend might be throughout the CCS is of interest, as it may be indicative of recent strengthening of the California Current and enhanced equatorward transport of subarctic water. Likewise, the unusual increase in nitrate concentration within the CalCOFI region requires additional consideration and, ideally, comparison to analogous data sets elsewhere along the coast. Trends in the composition of the zooplankton community (e.g., changes in the dominance of gelatinous taxa, as reported off Baja California) also bear further examination to determine the scale at which such dynamics unfold in the CCS.

To summarize, observations of the state of the CCS during 2010 and early 2011 capture the development of cooler La Niña conditions throughout the CCS, but continue to indicate substantial regional variability in how climate variability measured by basin-scale indices manifest locally. Off southern California, the effects of both the 2009–2010 El Niño and subsequent return to La Niña conditions appear to have had modest effects on the system, and the patterns that attract interest appear to be unfolding over longer time scales (e.g., freshening of upper water column and trends in nitrate and oxygen concentrations). In contrast, the northern California Current has exhibited much more dramatic short-term changes over the past two years, due in part to greater variability in environmental forcing affecting this region. At the time of writing, tropical conditions are ENSO neutral and forecast to remain so into fall 2011 and possibly into early 2012[20], yet the PDO remained strongly negative into summer 2011. It is therefore uncertain whether the return to cool conditions observed in the past year will continue to govern the state of the California Current.

Looking forward, we note that several questions are raised by the recent perception of regional structure in the way the CCS responds to climate variability, a perception supported by several data sets reviewed in this paper and in previous reports in this series (Goericke et al. 2005; Peterson et al. 2006; Goericke et al. 2007; McClatchie et al. 2008, 2009; Bjorkstedt et al. 2010). Moreover, of the several spatial and temporal modes of climate variability that influence the CCS (Mantua et al. 1997; Wolter and Timlin 1998; Ashok et al. 2007; Di Lorenzo et al. 2008), some, particularly those associated with El Niño Modoki, have been strengthening in recent decades, and exhibit spatial patterns that vary within the domain of the CCS (Messié and Chavez 2011). The possibility for emergent or enhanced regional variability in the CCS to be a consequence of climate forcing clearly warrants closer scrutiny. Ideally, these questions will be amenable to more comprehensive analysis of data sets from established research and observing programs, but are also likely to profit greatly by integrating data from the several coastwide surveys that have been established in recent years. Such efforts should yield deeper insight to the scale and magnitude of regional variability in responses to climate forcing. Just as importantly, we expect that such efforts will also provide greater opportunity for connecting to ongoing efforts to develop and enhance ecosystem assessments for the California Current.

ACKNOWLEDGEMENTS

We thank three anonymous reviewers for their comments, which improved the present paper and also provide useful guidance for development of future reports in this series. Xuemei Qiu prepared several figures for the basin- and regional-scale review. The IMECOCAL program thanks officers and crew of the CICESE RV *Francisco de Ulloa*, as well as students, technicians, and researchers participating in the surveys. Special thanks to Martin De la Cruz-Orozco for assistance in cruise coordination and chlorophyll analysis, Jose Luis Cadena for zooplankton counting, and R. Durazo for CTD data processing. IMECOCAL surveys were supported by CICESE, SEMARNAT-CONACYT 23804 and 107267, and SEP-CONACYT projects (129611, 82529). Observations along the Newport Hydrographic Line and off the OR-WA coast were supported in part by NOAA's FATE and SAIP programs and CAMEO. Trinidad Head Line surveys were supported by NOAA Fisheries Service and the California Ocean Protection Council and by the able efforts of Captain Scott Martin and the crew of the RV *Coral Sea,* Phil White, Kathryn Crane, Jose Montoya, and the many HSU students and volunteers who sailed on these cruises. Phil White assisted with analysis of CTD data from the Trinidad Head Line. Seabird surveys in recent years were supported by grants from the California Ocean Protection Council, California Sea Grant, NOAA, NSF, and NASA. Sonoma County Water Agency funds observations along the Bodega Line. HF radar mapping ocean surface currents has been sponsored by the State of California under the Coastal Ocean Currents Monitoring Program (COCMP), the National Oceanic and Atmospheric Administration (NOAA), the National Science Foundation (NSF), Office of Naval Research (ONR). HF radar data were provided by Scripps Institution of Oceanography at University of California, San Diego; University of Southern California; Marine Science Institute at University of California, Santa Barbara; California Polytechnic State University; Naval Postgraduate School; Romberg Tiburon Center at San Francisco State University; Humboldt State University; Bodega Marine Laboratory at University of California, Davis; and Oregon State University.

[20]http://www.cpc.noaa.gov/products/analysis_monitoring/enso_advisory

LITERATURE CITED

Abraham, C. L., and W. J. Sydeman. 2004. Ocean climate, euphausiids and auklet nesting: inter-annual trends and variation in phenology, diet and growth of a planktivorous seabird, *Ptychoramphus aleuticus*. Mar. Ecol. Prog. Ser. 274:235–250.

Ashok, K., S. K. Behera, S. A. Rao, H. Weng, & T. Yamagata. 2007. El Niño Modoki and its possible teleconnection. J. Geophys. Res. 112, C11007, doi:10.1029/2006JC003798.

Bjorkstedt, E.P., R. Goericke, S. McClatchie, E. Weber, W. Watson, N. Lo, B. Peterson, B. Emmett, J. Peterson, R. Durazo, G. Gaxiola-Castro, F. Chavez, J. T. Pennington, C.A. Collins, J. Field, S. Ralston, K. Sakuma, S. Bograd, F. Schwing, Y. Xue, W. Sydeman, S. A. Thompson, J. A. Santora, J. Largier, C. Halle, S. Morgan, S.Y. Kim, K. Merkens, J. Hildebrand, L. Munger. 2010. State of the California Current 2009–2010: Regional variation persists through transition from La Niña to El Niño (and back?). CalCOFI Reports 51: 39–69.

Black, B. A., I. Schroeder, W. Sydeman, S. Bograd, P. Lawson. 2010. Wintertime ocean conditions synchronize rockfish growth and seabird reproduction in the central California Current Ecosystem. Can. J. Fish. Aquatic Sci. 67:1149–1158.

Bograd, S. J., and R. J. Lynn. 2003. Anomalous subarctic influence in the southern California Current during 2002. Geophysical Research Letters 30:8020.

Bograd, S. J., P. M. DiGiacomo, R. Durazo, T. L. Hayward, K. D. Hyrenbach, R. J. Lynn, A. W. Mantyla, F. B. Schwing, W. J. Sydeman, T. Baumgartner, B. Lavaniegos, and C. S. Moore. 2000. The State of the California Current, 1999–2000: Forward to a new regime? CalCOFI Rep., 41:26–52.

Bograd, S. J., C.G. Castro, E. Di Lorenzo, D. M. Palacios, H. Bailey, W. Gilly, and F. P. Chavez. 2008. Oxygen declines and the shoaling of the hypoxic boundary in the California Current. Geophys. Res. Lett., 35: L12607.

Brinton, E., and A. Townsend. 2003. Decadal variability in abundances of the dominant euphausiid species in southern sectors of the California Current. Deep-Sea Res. II. 50:2449–2472.

Di Lorenzo E., N. Schneider, K. M. Cobb, K. Chhak, P. J. S. Franks, A. J. Miller, J. C. McWilliams, S. J. Bograd, H. Arango, E. Curchister, T. M. Powell, and P. Rivere. 2008: North Pacific Gyre Oscillation links ocean climate and ecosystem change. Geophys. Res. Lett., 35, L08607, doi:10.1029/2007GL032838.

Durazo, R. 2009. Climate and upper ocean variability off Baja California, Mexico: 1997–2008. Prog. Oceanogr., 83, 361–368, doi: 10.1016/j.pocean.2009.07.043.

Garcia-Reyes, M. and J. L. Largier 2011. Seasonality of coastal upwelling off California. J. Geophys. Res. (in review).

Gaxiola-Castro, G., R. Durazo, B. Lavaniegos, M. E. De la Cruz-Orozco, E. Millán-Nuñez, L. Soto-Mardones, J. Cepeda-Morales. 2008. Pelagic ecosystem response to interannual variability off Baja California. Cienc. Mar., 263–270.

Goericke, R., E. Venrick, T. Koslow, W. J. Sydeman, F. B. Schwing, S. J. Bograd, W. T. Peterson, R. Emmett, J. R. Lara Lara, G. Gaxiola Castro, J. Gómez Valdez, K. D. Hyrenbach, R. W. Bradley, M. J. Weise, J. T. Harvey, C. Collins, and N. C. H. Lo. 2007. The State of the California Current, 2006–2007: Regional and Local Processes Dominate, CalCOFI Rep. 48:33–66.

Goericke, R., E. Venrick, A. Mantyla, S. J. Bograd, F. B. Schwing, A. Huyer, R. L. Smith, P. A. Wheeler, R. Hooff, W. T. Peterson, G. Gaxiola-Castro, J. Gómez-Valdez, B. E. Lavaniegos, K. D. Hyrenbach, and W. J. Sydeman. 2004. The state of the California current, 2003–2004: a rare "normal" year. CalCOFI Rep., 45: 27–59.

Goericke, R., E. Venrick, A. Mantyla, S. J. Bograd, F. B. Schwing, A. Huyer, R. L. Smith, P. A. Wheeler, R. Hooff, W. T. Peterson, F. Chavez, C. Collins, B. Marinovic, N. Lo, G. Gaxiola-Castro, R. Durazo, K. D. Hyrenbach, and W. J. Sydeman, 2005. The state of the California current, 2004–2005: still cool? CalCOFI Rep., 46: 32–71.

Gómez-Valdes, J., and G. Jeronimo. 2009. Upper mixed layer temperature and salinity variability in the tropical boundary of the California Current, 1997–2007. J. Geophys. Res. 114, C03012, doi:10.1029/2008JC004793.

Halle, C. M., J. L. Largier and G. Crawford 2011. The Cape Mendocino Eddy: A persistent coast-attached mesoscale eddy in the presence of strong upwelling and the California Current. Deep-Sea Res. (in review).

Hooff, R. C., and W. T. Peterson. 2006. Recent increases in copepod biodiversity as an indicator of changes in ocean and climate conditions in the northern California current ecosystem. Limnol. Oceanogr. 51:2042–2051.

Hyrenbach, K. D., and R. R. Veit. 2003. Ocean warming and seabird assemblages of the California Current System (1987–1998): response at multiple temporal scales. Deep-Sea Res. II. 50:2537–2565.

Kaplan, D. M., C. Halle, J. Paduan and J. L. Largier. 2009. Surface currents during anomalous upwelling seasons off central California. J. Geophys. Res., 114, doi:10.1029/2009JC005382.

Kim, S. Y., E. J. Terrill, and B. D. Cornuelle. 2008, Mapping surface currents from HF radar radial velocity measurements using optimal interpolation, J. Geophys. Res. 113, C10023, doi:10.1029/2007JC004244.

Largier, J. L., B. A. Magnell and C. D. Winant. 1993. Subtidal circulation over the northern California shelf. J. Geophys. Res., 98(C10), 18147–18179.

Lindley, S. T., C. B. Grimes, M. S. Mohr, W. Peterson, J. Stein, J. T. Anderson, L. W. Botsford, D. L. Bottom, C. A. Busack, T. K. Collier, J. Ferguson, J. C. Garza, A. M. Grover, D. G. Hankin, R. G. Kope, P. W. Lawson, A. Low, R. B. MacFarlane, K. Moore, M. Palmer-Zwahlen, F. B. Schwing, J. Smith, C. Tracy, R. Webb, B. K. Wells, and T. H. Williams. 2009. What caused the Sacramento River fall Chinook stock collapse? U. S. Department of Commerce, NOAA Technical Memorandum NMFS, NOAA-TM-NMFS-SWFSC-447, 121 p.

Mantua, N. J., S. R. Hare, Y. Zhang, J. M. Wallace, R. C. Francis. 1997. A Pacific interdecadal climate oscillation with impacts on salmon production. Bull. Am. Meteorological Soc. 78: 1069–1079.

McClatchie, S., R. Goericke, J. A. Koslow, F. B. Schwing, S. J. Bograd, R. Charter, W. Watson, N. Lo, K. Hill, J. Gottschalk, M. L'Heureux, Y. Xue, W. T. Peterson, R. Emmett, C. Collins, G. Gaxiola-Castro, R. Durazo, M. Kahru, B. G. Mitchell, K. D. Hyrenbach, W. J. Sydeman, R. W. Bradley, P. Warzybok, E. Bjorkstedt. 2008. The State of the California Current, 2007–2008: La Niña conditions and their effects on the ecosystem. CalCOFI Rep., 49, 39–76.

McClatchie, S. R. Goericke, F. B. Schwing, S. J. Bograd, W. T. Peterson, R. Emmett, R. Charter ,W. Watson, N. Lo, K. Hill, C. Collins, M. Kahru, B. G. Mitchell, J. A. Koslow, J. Gómez-Valdes , B. E. Lavaniegos, G. Gaxiola-Castro, J. Gottschalk, M. L'Heureux, Y. Xue, M. Manzano-Sarabia, E. Bjorkstedt, S. Ralston, J. Field, L. Rogers-Bennett, L. Munger, G. Campbell, K. Merkens, D. Camacho, A. Havron, A. Douglas and J. Hildebrand. 2009. The state of the California Current, 2008–2009: Cold conditions drive regional difference. CalCOFI Rep., 50, 43–68.

Messié, M., Chavez, F., 2011. Global modes of sea surface temperature variability in relation to regional climate indices. J. Climate. 10.1175/2011JCLI3941.1.

Peterson, W. T., R. Emmett, R. Goericke, E. Venrick, A. Mantayla, S. J. Bograd, F. B. Schwing, R. Hewitt, N. Lo., W. Watson, J. Barlow, M. Lowry, S. Ralston, K. A. Forney, B. E. Lavaniegos, W. J. Sydeman, D. Hyrenbach, R. W. Bradley, P. Warzybok, F. Chavez, K. Hunter, S. Benson, M. Weise, J. Harvey, G. Gaxicola-Castro, R. Durazo. 2006. The State of the California Current, 2005–2006: warm in the north, cool in the south. CalCOFI Rep., 47:30–74.

Peterson, W. T. and F. B. Schwing. 2003. A new climate regime in Northeast Pacific ecosystems. Geophys. Res. Lett. 30(17), 1896. doi:10.1029/2003GL017528.

Phillips, A. J., S. Ralston, R. D. Brodeur, T. D. Auth, R. L. Emmett, C. Johnson, and V. G. Wespestad. 2007. Recent pre-recruit Pacific hake (*Merluccius productus*) occurrences in the northern California Current suggest a northward expansion of their spawning area. CalCOFI Rep. 48:215–229.

Phillips, A. J., R. D. Brodeur, and A. V. Suntsov. 2009. Micronekton community structure in the epipelagic zone of the northern California Current upwelling system. Prog. Oceanogr. 80:74–92.

Sakuma, K. M., S. Ralston, and V. G. Wespestad. 2006. Interannual and spatial variation in the distribution of young-of-the-year rockfish (*Sebastes* spp.): expanding and coordinating a survey sampling frame. CalCOFI Rep., 47:127–139.

Santora, J. A., S. Ralston, and W. J. Sydeman. 2011. Spatial organization of krill and seabirds in the central California Current. ICES J. Mar. Sci. doi:10.1093/icesjms/fsr046.

Schwing, F. B., N. A. Bond, S. J. Bograd, T. Mitchell, M. A. Alexander, and N. Mantua. 2006. Delayed coastal upwelling along the U.S. west coast in 2005: a historical perspective. Geophys. Res. Lett. 33: L22S01, doi:10.1029/2006GL026911.

Shaffer, S. A., Y. Tremblay, H. Weimerskirch, D. Scott, D. R. Thompson, P. M. Sagar, H. Moller, G. A. Taylor, D. G. Foley, B. A. Block, and D. P. Costa. 2006. Migratory shearwaters integrate oceanic resources across the Pacific Ocean in an endless summer. Proc. Natl. Acad. Sci. 103:12799–12802.

Sydeman, W. J., K. L. Mills, J. A. Santora, S. A. Thompson, D. F. Bertram, K. H. Morgan, B. K. Wells, J. M. Hipfner, and S. G. Wolf. 2009. Seabirds and climate in the California Current—A synthesis of change. CalCOFI Rep. 50:82–104.

Sydeman, W. J., R. W. Bradley, P. Warzybok, J. Jahncke, K. D. Hyrenbach, V. Kousky, M. A. Hipfner, and M. D. Ohman. 2006. Krill and Krill Predators: Responses of Planktivorous Auklets Ptychoramphus aleuticus to the Anomaly of 2005. J. Geophys. Res. 33, L22S09.

Terrill, E. J., M. Otero, L. Hazard, D. Conlee, J. Harlan, J. Kohut, P. Reuter, T. Cook, T. Harris, K. Lindquist, 2006. Data Management and Real-time Distribution in the HF-Radar National Network, OCEANS 2006, IEEE, 10.1109/OCEANS.2006.306883.

Venrick, E., S. J. Bograd, D. Checkley, R. Durazo, G. Gaxiola-Castro, J. Hunter, A. Huyer, K. D. Hyrenbach, B. E. Lavaniegos, A. Mantyla, F. B. Schwing, R. L. Smith, W. J. Sydeman, and P. A. Wheeler. 2003. The state of the California Current, 2002–2003: Tropical and Subarctic influences vie for dominance. CalCOFI Rep. 44:28–60.

Warzybok and Bradley. 2010. Status of seabirds on Southeast Farallon Island during the 2010 breeding season. PRBO Conservation Science (unpublished report available at http://www.prbo.org/cms/159).

Wheeler, P. A., A. Huyer, and J. Fleischbein. 2003. Cold halocline, increased nutrients and higher productivity off Oregon in 2002. Geophys. Res. Lett. 30:8021.

Wolter, K., and M. S. Timlin. 1998: Measuring the strength of ENSO events—how does 1997/98 rank? Weather. 53:315–324.

Yen, P. P.Y., W. J. Sydeman, S. J. Bograd, and K. D. Hyrenbach. 2006. Springtime distributions of migratory marine birds in the southern California Current: Oceanic eddy associations and coastal habitat hotspots over 17 years. Deep-Sea Res. II, 53:399–418.

PUBLICATIONS
1 January–31 December 2010

Alin, S. R., R. A. Feely, A. G. Dickson, J. M. Hernandez-Ayon, L.W. Juranek, M.D. Ohman, and R. Goericke. 2010. Predictive relationships for pH and carbonate saturation in the southern California Current System using oxygen and temperature data. American Geophysical Union, Fall Meeting 2010.

Baker, K., E. Weber, and J. A. Koslow. 2010. CalCOFI information management and data delivery. PICES Conference. Portland, OR.

Bjorkstedt, E., R. Goericke, S. McClatchie, E. Weber, W. Watson, N. Lo, B. Peterson, B. Emmett, J. Peterson, R. Durazo, G. Gaxiola-Castro, F. Chavez, J. T. Pennington, C. A. Collins, J. Field, S. Ralston, K. Sakuma, S. Bograd, F. Schwing, Y. Xue, W. Sydeman, S. A. Thompson, J. A. Santora, J. Largier, C. Halle, S. Morgan, S.Y. Kim, K. Merkens, J. Hildebrand and L. Munger. 2010. State of the California Current 2009–2010: Regional variation persists through transition from La Niña to El Niño (and back). Calif. Coop. Oceanic Fish. Invest. Rep., 51: 39–69.

Bograd, S. J., C. G. Castro, F. Chavez, C. A. Collins, V. Combes, E. Lorenzo, and M.D. Ohman. 2010. The California Undercurrent, 1949–2008. Proceedings from the 2010 AGU Ocean Sciences Meeting. Portland, OR.

Bograd, S. J., W. J. Sydeman, J. Barlow, A. Booth, R. D. Brodeur, J. Calambokidis, F. Chavez, W. R. Crawford, E. Di Lorenzo, R. Durazo, R. Emmett, J. Field, G. Gaxiola-Castro, W. Gilly, R. Goericke, J. Hildebrand, J. E. Irvine, M. Kahru, J. A. Koslow, B. Lavaniegos, M. Lowry, D. L. Mackas, M. Manzano-Sarabia, S. M. McKinnell, B. G. Mitchell, L. Munger, R. I. Perry, W. T. Peterson, S. Ralston, J. Schweigert, A. Suntsov, R. Tanasichuk, A. C. Thomas, and F. Whitney. 2010. Status and trends of the California Current region, 2003–2008, pp 106–141. In: S. M. McKinnell & M. J. Dagg (eds.) Marine Ecosystems of the North Pacific Ocean 2003–2008. PICES Special Publication Number 4.

Boyce, D. G., M. R. Lewis, and B. Worm. 2010. Global phytoplankton decline over the past century. Nature, 466, 591–596.

Bucklin, A., S. Nishida, S. B. Schnack-Schiel, P. H. Wiebe, D. Lindsay, R. J. Machida, and N. J. Copley. 2010. A Census of Zooplankton of the Global Ocean. In: E. A. D. McIntyre (ed.) Life in the Worlds Oceans: Diversity, Distribution and Abundance. Oxford: Wiley Blackwell Publ. Ltd.

Campbell, G. S., K. Merkens and J. Hildebrand. 2010. California Cooperative Fisheries Investigation (CalCOFI) Cruises 2009–2010 *in* Marine Mammal Monitoring for the U.S. Navy's Hawaii Range Complex and Southern California Range Complex. Annual Report 2010. Department of the Navy, U.S. Pacific Fleet: 569–573.

Campbell, G. S., K. Merkens and J. Hildebrand. 2010. California Cooperative Fisheries Investigation (CalCOFI) Cruises 2009–2010 *in* Marine Mammal Acoustic Monitoring and Habitat Investigation, Southern California Offshore Region 2010. Naval Postgraduate School Technical Report No. NPS-OC-10.

Cartamil, D., N. C. Wegner, D. Kacev, N. Ben-aderet, S. Kohin, and J. B. Graham. 2010. Movement patterns and nursery habitat of the juvenile thresher shark *Alopias vulpinus* in the Southern California Bight. Mar. Ecol. Prog. Ser. 404: 249–258.

Carter, M. and Z. Yin. 2010. Patterns of chlorophyll variability and phytoplankton community composition off southern California and the influence of macroscale and regional oceanographic processes. Proceedings from the 2010 AGU Ocean Sciences Meeting. Portland, OR.

Chekalyuk, A. M. and M. Hafez. 2010. Advanced Laser Fluorometry (ALF): New Technology, Field Observations and Findings. Proceedings from the 2010 AGU Ocean Sciences Meeting. Portland, OR.

Chenillat, F., P. C. Riviere, E. Lorenzo, S. J. Bograd, and M. D. Ohman. 2010. Low-frequency transport dynamics in the California Current. Proceedings from the 2010 AGU Ocean Sciences Meeting. Portland, OR.

Crone, P. R., K.T. Hill, J. D. McDaniel, and K. Lynn. 2011. Pacific mackerel (*Scomber japonicus*) stock assessment for USA management in the 2011–12 fishing year. Pacific Fishery Management Council, Pacific Fishery Management Council, 7700 NE Ambassador Place, Suite 101, Portland, Oregon 97220, USA. 100 p.

Davis, R. E. 2010. On the coastal-upwelling overturning cell. Journal of Marine Research 68: 369–385.

Davison, P., A. Lara-Lopez, and J.A. Koslow. 2010. Challenges in the application of acoustic survey methods to a complex aquatic community: the deep scattering layer of the California Current. CalCOFI Conference. La Jolla, CA.

Décima, M., M. R. Landrya, and R. R. Rykaczewski. 2010. Broad scale patterns in mesozooplankton biomass and grazing in the eastern equatorial Pacific. Deep Sea Research Part II: Topical Studies in Oceanography, 58, 387–399.

Décima, M., M. D. Ohman, and A. De Robertis. 2010. Body size dependence of euphausiid spatial patchiness. Limnology and Oceanography 55: 777–788.

Dickson, A. 2010. Ocean Acidification Impacts on Shellfish Workshop: Findings and Recommendations. Ocean Acidification Effects on Shellfish Workshop: Findings and Recommendations. Costa Mesa, CA: California Sea Grant College Program.

Dotson, R. C., D. A. Griffith, D. L. King, and R. L. Emmett. 2010. Evaluation of a Marine Mammal Excluder Device (MMED) for a Nordic 264 Midwater Rope Trawl. NOAA-TM-NMFS-SWFSC-455.

Edwards, M., G. Beaugrand, G. C. Hays, J. A. Koslow, and A. J. Richardson. 2010. Multi-decadal oceanic ecological datasets and their application in marine policy and management. Trends in Ecology & Evolution, 25, 602–610.

Feely, R. A., R. Wanninkhof, J. Stein, M. F. Sigler, E. Jewett, F. Arzayus, and D. K. Gledhill. 2010. NOAA Ocean and Great Lakes Acidification Research Plan.

Fuchs, H. L. and P. J. S. Franks. 2010. Plankton community properties determined by nutrients and size-selective feeding. Marine Ecology Progress Series, 413, 1–15.

Gangopadhyay, A., P. F. Lermusiaux, L. Rosenfeld, A. R. Robinson, L. Calado, H. S. Kim, W. G. Leslie, and J. Haley, J. (Submitted) The California Current System: A multiscale overview and the development of a Feature-Oriented Regional Modeling System (FORMS). Dynamics of Atmospheres and Oceans, 65.

Gilbert, D., N. N. Rabalais, R. J. Díaz, and J. Zhang. 2010. Evidence for greater oxygen decline rates in the coastal ocean than in the open ocean. Biogeosciences, 7, 2283–2296.

Goebel, N. L., C. A. Edwards, J. P. Zehr, and M. J. Follows. 2010. An emergent community ecosystem model applied to the California Current System. Journal of Marine Systems [J. Mar. Syst.], 83, 221–241.

Goetze, E. and M. D. Ohman. 2010. Integrated molecular and morphological biogeography of the calanoid copepod family Eucalanidae Deep Sea Research Part II: Topical Studies in Oceanography, 57, 2110–2129.

Gorsky, G., M. D. Ohman, M. Picheral, S. Gasparini, L. Stemmann, J. B. Romagnan, A. Cawood, S. Pesant, C. García-Comas, and F. Prejger. 2010. Digital zooplankton image analysis using the ZooScan integrated system. Journal of Plankton Research, 32, 285–303.

Heberer, C., S. A. Aalbers, D. Bernal, S. Kohin, B. DiFiore, and C. A. Sepulveda. 2010. Insights into catch-and-release survivorship and stress-induced blood biochemistry of common thresher sharks (*Alopias vulpinus*) captured in the southern California recreational fishery. Fish. Res. 106: 495–500.

Herguera, J. C., T. Herbert, M. Kashgarian, and C. Charles. 2010. Intermediate and deep water mass distribution in the Pacific during the Last Glacial Maximum inferred from oxygen and carbon stable isotopes. Quaternary Science Reviews 29: 1228–1245.

Hill, K. T., N. C. H. Lo, B. J. Macewicz, P. R. Crone, and R. Felix-Uraga. 2010. Assessment of the Pacific sardine resource in 2010 for U. S. management in 2011. U. S. Dep. Commer., NOAA Tech. Memo. NMFS-SWFSC-469. 137 p.

Hinger, E. N., G. M. Santos, E. R. M. Druffel, and S. Griffin. 2010. Carbon isotope measurements of surface seawater from a time-series site off southern California. Radiocarbon, 52, 69–89.

Hsieh, C., H. Kim, W. Watson, E. Lorenzo, E. and G. Sugihara. 2010. Climate-driven changes in abundance and distribution of larvae of oceanic fishes in the Southern California region. Proceedings from the 2010 AGU Western Pacific Geophysics Meeting. Taipei, Taiwan.

Jarvis, E.T., C. Linardich, and C.F. Valle. 2010. Spawning-related movements of barred sand bass, *Paralabrax nebulifer*, in southern California: Interpretations from two decades of historical tag and recapture data. So. Cal. Acad. of Sci. Bull. 109:123–143.

Jiao, Y., L. Rogers-Bennett, I. Taniguchi, J. Butler and P. Crone 2010. Incorporating temporal variation in the individual growth of red abalone (*Haliotis rufescens*) using hierarchical Bayesian growth models. Can. J. Fish. Aquat. Sci. 67:730–742.

Karl, D.M. (2010) Oceanic ecosystem time-series programs. Oceanography, 23, 104–125.

Karpov, K. A., M. Bergen, J. J. Geibel, P. M. Law, C. F. Valle, and D. Fox. 2010. Prospective (a priori) power analysis for detecting changes in density when sampling with strip transects. Cal. Fish and Game 96:69–81.

Koslow, J. A. and C. Allen. 2010. The influence of the ocean environment on the abundance of market squid (*Doryteuthis opalescens*) paralarvae in the Southern California Bight. CalCOFI Conference. La Jolla, CA.

Koslow, J. A., K. Brander, M. Fogarty, and F. Schwing. (In press). Integration of ocean observations into an ecosystem approach to resource management. In: J. Hall, Harrison, D. E. & Stammer, D., Eds. (ed.) Proceedings of OceanObs'09: Sustained Ocean Observations and Information for Society (Vol. 1). Venice, Italy: ESA Publication WPP-306.

Koslow, J. A., R. Goericke, A. Lara-Lopez, and W. Watson. 2010. Climate, the oxygen-minimum zone, and deepwater fishes of the southern California Current. CalCOFI Conference. La Jolla, CA.

Koslow, J. A., R. Goericke, S. McClatchie, R. Vetter, and L. Rogers-Bennett. (In press). The California Cooperative Oceanic Fisheries Investigations (CalCOFI): the continuing evolution and contributions of a 60-year ocean observation program. In: J. Hall, Harrison, D. E. & Stammer, D., Eds. (ed.) Proceedings of OceanObs'09: Sustained Ocean Observations and Information for Society (Vol. 1). Venice, Italy: ESA Publication WPP-306.

Koslow, J. A., R. Goericke, A. Suntsov, and W. Watson. 2010. Climate and larval fish assemblages in the southern California Current, 1951–2008. Climate and Fisheries Symposium. Sendai, Japan.

Koslow, J. A., R. Goericke, and W. Watson. 2010. Climate and fish assemblages of the southern California Current, 1951–2008. PICES Conference. Portland, OR.

Koslow, J. A., R. Goericke, W. Watson, and A. Lara-Lopez. (In press). Impact of declining intermediate-water oxygen on deepwater fishes in the California Current. Mar. Ecol. Prog. Ser.

Koslow, T., L. Rogers-Bennett, and D. Neilson. 2010. A time series for the phyllosoma of the California spiny lobster (*Panulirus interruptus*) off southern California, 1951–2008: relationships with climate and the fishery. CalCOFI Conference. La Jolla, CA.

Lara-Lopez, A., P. Davison, and J. A. Koslow. 2010. Methodological challenges to estimating abundance of mid-trophic organisms using multi-frequency acoustics and net sampling in contrasting hydrographic regimes off southern California. ICES Working Group on Fisheries Acoustics Science and Technology (FAST). San Diego, CA.

Larinto, T. (ed.) 2010. Status of the Fisheries Report: An Update through 2008. A Report to the Fish and Game Commission. 231 p. Available at: http://www.dfg.ca.gov/marine/status/index.asp.

Lavigne, M., T. M. Hill, H. J. Spero, and T.P. Guilderson. 2010. Climate, productivity, and intermediate water nutrients: new records from bamboo coral Ba/Ca. American Geophysical Union, Fall Meeting 2010.

Liu, K-K, L. Atkinson, R. Quiñones, L. Talaue-McManus, J. R. Moisan. 2010. Coupled Circulation/Biogeochemical Models to Estimate Carbon Flux. In: Carbon and Nutrient Fluxes in Continental Margins. Springer Berlin Heidelberg, p 539–558.

Lo, N. and B. Macewicz. 2010. Daily egg production method survey. Workshop on enhancing stock assessments of Pacific sardine in the California Current through cooperative surveys, La Jolla, CA.

Lo, N. C. H., E. Dorval, R. Funes-Rodríguez, M. E. Hernández-Rivas, Y. Huang, and Z. Fan. 2010. Utilities of larval densities of Pacific mackerel (*Scomber japonicus*) off California, USA and west coast of Mexico from 1951 to 2008, as spawning biomass indices. Ciencia Pesquera, 18, 59–75.

Lo, N. C. H., B. J. Macewicz, and D. A. Griffith. 2010. Spawning biomass of Pacific sardine (*Sardinops sagax*) off the U.S. in 2010. NOAA Technical Memorandum NMFS-SWFSC No. 1–35 pp.

Mackas, D. L., and G. Beaugrand. 2010. Comparisons of zooplankton time series. Journal of Marine Systems 79: 286–304.

Mason, J. (2010) Review of the use of California Commercial Fisheries Landings and Recreational Catch Data in stock assessments. Managing Data-Poor Fisheries: Case Studies, Models & Solutions. California Sea Grant College Program 2010.

McClatchie, S., R. Goericke, G. Auad, and K. Hill. 2010. Re-assessing the temperature index for Pacific sardine (*Sardinops sagax*) stock assessment. Canadian Journal of Fisheries and Aquatic Sciences 67: 1782–1790.

McClatchie, S., R. Goericke, R. Cosgrove, G. Auad, G. and R. Vetter. 2010. Oxygen in the Southern California Bight: Multidecadal trends and implications for demersal fisheries. Geophysical Research Letters, 37, L19602.1–L19602.5.

McVeigh, B. A. B., J. J. Geibel, and P.E. Kalvass. 2010. Sport clamming in Humboldt Bay, California during 2008: Comparisons with historical survey data. Cal. Fish and Game 96:245–255.

Munro, D. R. and P. Quay. 2010. Gross and net production estimates in the California Current System from oxygen triple isotopes and the O2/Ar ratio. American Geophysical Union, Fall Meeting 2010.

Neal, A. C., M. Gonsior, M. Gassel, H. Coleman, N. Argyropoulos, C. Hume, R. Mielke, D. Steuerman, K. D. Knobelspiesse, and B. Balestra. 2010. Initial analysis of marine debris accumulation in the Subtropical Convergence Zone of the North Pacific Gyre. Proceedings from the 2010 AGU Ocean Sciences Meeting. 2010 Ocean Sciences Meeting, Portland, OR (USA).

Nur, N., J. Jahncke, M. Herzog, J. Howar, J. A. Wiens, and D. Stralberg. 2010. Wildlife hotspots in the California Current System Technical Report to the Resources Legacy Fund Foundation No. 1–37 pp.

Parnell, P. E., E. F. Miller, C. E. Lennert-Cody, P. K. Dayton, M. L. Carter, M. L. and T. D. Stebbins. 2010. The response of giant kelp (*Macrocystis pyrifera*) in southern California to low-frequency climate forcing. Limnology and Oceanography 55, 2686–2702.

Powell, J. R., M. D. Ohman, and R. E. Davis. 2010. Glider-based analysis of covariability of ocean fronts and zooplankon acoustic backscatter in the California Current System. Proceedings from the 2010 AGU Ocean Sciences Meeting. Portland, OR.

Ralston, S., and B. R. MacFarlane. 2010. Population estimation of bocaccio (*Sebastes paucispinis*) based on larval production. Canadian Journal of Fisheries and Aquatic Sciences 67: 1005–1020.

Rogers-Bennett, L., R. F. Dondanville, J. D. Moore, and L. I. Vilchis. 2010. Response of red abalone reproduction to warm water, starvation and disease stressors: Implications of ocean warming. J. Shellfish Res. 29:599–611.

Santoro, A. E., K. L. Casciotti, and C.A. Francis. 2010. Activity, abundance and diversity of nitrifying archaea and bacteria in the central California Current. Environmental Microbiology, 12, 1989–2006.

Send, U., P. Burkill, N. Gruber, G. C. Johnson, A. Kortzinger, J. A. Koslow, R. O'Dor, S. Rintoul, and D. Roemmich. (In press). Towards an integrated observing system: *in-situ* observations. In: J. Hall, Harrison, D. E. & Stammer, D., Eds. (ed.) Proceedings of OceanObs'09: Sustained Ocean Observations and Information for Society (Vol. 1). Venice, Italy: ESA Publication WPP-306.

Song, H., A. J. Miller, and B. D. Cornuelle. 2010. Estimating ocean states during the LTER CCE-P0605 cruise using ocean data assimilation analysis. Proceedings from the 2010 AGU Ocean Sciences Meeting. Portland, OR.

Song, H., A. J. Miller, B.D. Cornuelle, and E. Di Lorenzo. (In press). Changes in upwelling and its water sources in the California Current System driven by different wind forcing. Dynamics of Atmospheres and Oceans.

Stramma, L., S. Schmidtko, L. A. Levin, and G. C. Johnson. 2010. Ocean oxygen minima expansions and their biological impacts. Deep-Sea Research I 57: 587–595.

Suntsov, A., J. A. Koslow, and W. Watson. (Submitted). The spatial structure of coastal ichthyoplankton assemblages off central and southern California. Estuarine, Coastal, and Shelf Science.

Suntsov, A. V. and J. A. Koslow. 2010. Nearshore ichthyoplankton communities off southern and central California. Climate and Fisheries Symposium. Sendai, Japan.

Sweetnam, D. 2010 Current management and fishery-dependent sampling of the U.S. Pacific Sardine Fishery. Workshop on enhancing stock assessments of Pacific sardine in the California Current through cooperative surveys, La Jolla, California.

Sydeman, W. J., and S. A. Thompson. 2010. The California Current Integrated Ecosystem Assessment (IEA), Module II: Trends and Variability in Climate-Ecosystem State, Farallon Institute for Advanced Ecosystem Research, Petaluma, California.

Todd, R. E., D. L. Rudnick, and R. E. Davis. 2010. Mesoscale and submesoscale thermohaline structure in the California Current System from glider observations. American Geophysical Union, Fall Meeting 2010.

Weber, E. D. and S. McClatchie. 2010. Predictive Models of Northern Anchovy *Engraulis mordax* and Pacific Sardine *Sardinops sagax* Spawning Habitat in the California Current. Mar. Ecol. Prog. Ser. 406: 251–263.

White, J. W. and L. Rogers-Bennett. 2010. Incorporating physical oceanographic proxies of recruitment into population models to improve fishery and Marine Protected Area management. Calif. Coop. Oceanic Fish. Invest. Rep 51:128–149.

Yu, H. 2010. Characterization of mysterious algal cultures from the California coast. Unpubl ms. Monterey Bay Aquarium Research Institute.

Zeigler, L. A., J. Badger, J. P. McCrow, I. Paulsen, E. E. Allen, S. J. Williamson, and A. Allen. 2010. Microbial metagenomics across a southern California Current upwelling mosaic. Proceedings from the 2010 AGU Ocean Sciences Meeting. Portland, OR.

Part II

SCIENTIFIC CONTRIBUTIONS

QUEENFISH (*SERIPHUS POLITUS*) AND WHITE CROAKER (*GENYONEMUS LINEATUS*) LARVAL GROWTH PARAMETERS

ERIC F. MILLER[1]
MBC Applied Environmental Sciences
3000 Red Hill Ave.
Costa Mesa, Ca 92626
P: 714-850-4830
F: 714-850-4840
E: emiller@mbcnet.net

JONATHAN P. WILLIAMS AND DANIEL J. PONDELLA, II
Vantuna Resarch Group, Occidental College
1600 Campus Road
Los Angeles, Ca 90041

ABSTRACT

Larval *Genyonemus lineatus* and *Seriphus politus* collected using bongo frames fitted with 0.333 mm mesh nets between December 2003 and September 2004 off Huntington Beach, California, were examined to characterize their daily growth patterns. Samples from one net were fixed in a 4% buffered formalin-seawater solution while those from the other net were preserved in 70% ethanol. All formalin-fixed samples were transferred to 70% ethanol ~72 hours after collection. Growth was best described by a linear equation for *G. lineatus* ($L = -0.833 + 0.242A$; $R^2 = 0.84$) and a power function for *S. politus* ($L = 0.825 \times A^{0.647}$; $R^2 = 0.76$). Sufficient *S. politus* were available to analyze seasonal effects on growth rate; no significant differences were detected. No significant difference in the *S. politus* growth rate between preservation media was detected for samples collected on September 1, 2004.

INTRODUCTION

Life-history parameters of nearshore marine fishes are critical both in understanding fish species, and for their proper management through stock assessment modeling (e.g., Hill et al. 2006). Typically, population estimates and power plant entrainment/impingement impact analyses are based on demographic models (e.g. Adult Equivalent Loss and Fecundity Hindcasting) incorporating multiple life history parameters, such as maximum age, size and age at maturity, fecundity (annual or total lifetime), growth rate (adult or larval), stage-specific mortality/survival rate, and spawning seasonality (Goodyear 1978; Parker 1980; Jensen et al. 1982; Saila et al. 1997; Lo et al. 2005; Newbold and Iovanna 2007). Sufficient research effort into these parameters has been generally limited to commercially important species, such as northern anchovy, *Engraulis mordax*, and Pacific sardine, *Sardinops sagax* (Hunter and Macewicz 1980; Butler et al. 1993; Lo et al. 1995; Butler et al. 1996; Lo et al. 2005). Substantially less information is available for recreational and forage species (Cailliet et al. 2000).

Recent power plant once-through-cooling impact characterizations have been hindered by the aforementioned lack of life-history information (MBC and Tenera 2005[2]). The lack of basic parameters precluded nearly all of the demographic models in these assessments, thereby limiting the analysis to proportional models (Boreman et al. 1981; McCall et al. 1983). Problems with population assessments, including power plant impact characterizations, are most glaring when insufficient data are available for either demographic or proportional models. This becomes pertinent in southern California where white croaker, *Genyonemus lineatus*, and queenfish, *Seriphus politus*, each historically ranked among the most frequently encountered species during shallow (<60 m deep) open-water intake and discharge environmental monitoring (Allen and DeMartini 1983; Love et al. 1986; Stull and Tang 1996). Furthermore, larvae of both species have been commonly taken during nearshore southern California plankton sampling (Barnett et al. 1984; Lavenberg et al. 1986; Walker et al. 1987; McGowen 1993) including the shallowest California Cooperative Oceanic Fisheries Investigations (CalCOFI) stations located near the coast (Moser et al. 2001). Limited life-history information substantially hindered their management and analysis in environmental impact assessments despite their commonality in the area and apparent recent population declines (Miller et al. 2009). Prior, unpublished studies of this topic used samples collected in 1978 and found a linear relationship between age and growth as well as significant seasonal differences in both species (Barnett and Sertic 1980[3]). Therefore, this project was designed to reexamine their larval age and growth. The effect of formalin fixation on otolith-based age estimation was also evaluated given the availability of simultaneously collected samples which were initially exposed to ethanol or formalin.

[1]Corresponding author: emiller@mbcnet.net

[2]MBC Applied Environmental Sciences and Tenera Environmental, Inc. 2005. AES Huntington Beach L.L.C. Generating Station Entrainment and Impingement Study Final Report. April 2005.

[3]Barnett, A. M. and P. D. Sertic. 1980. Growth rate of larval queenfish (*Seriphus politus*) and white croaker (*Genyonemus lineatus*) off San Onofre, California, in 1978. In summary report to W. Murdoch, Marine Review Committee, September 17, 1980.

MATERIALS AND METHODS

All larvae were collected in a sampling grid centered offshore of Huntington Beach, California (33.64°N 117.98°W) during monthly sampling from December 2003 to September 2004 inshore of the 22-m isobath. Sampling consisted of oblique bongo net tows from the seafloor to the surface with 333-µm mesh nets fitted with calibrated flowmeters conducted during four sampling events in each 24-hr sampling day (~1200, ~1800, ~0000, ~0600 hrs). The contents of one net from each deployment were fixed in a 4% buffered formalin-seawater solution while the other net was preserved in 70% ethanol. After survey completion, ethanol samples were archived and the formalin-fixed samples were washed and transferred to 70% ethanol for sorting and identification ~72 hours after collection. All formalin-fixed samples were sorted to remove, identify, and enumerate ichthyoplankton in support of MBC and Tenera (2005[2]). Preserved ethanol samples corresponding to formalin-fixed samples with comparatively high abundance of either target species were later sorted to provide samples free from formalin exposure.

Plankton shrinkage due to preservation was not quantified, so no adjustment to larval length was made. Furthermore, the technique utilized for the sample collection and processing was consistent with those used in all recent power plant once-through-cooling impact studies completed in the Los Angeles and Orange County areas (e.g. MBC and Tenera 2005[2]). Individuals of each species were measured by capturing digital images through a video stereoscope and processing them through image analysis to measure length (L) to the nearest 0.1 mm notochord length (prior to flexion) or standard length (post-flexion). Both sagittal otoliths were removed from each individual under stereoscope magnification using reflected light, mounted on a glass slide using immersion oil, and viewed under compound microscopy (400–1000× magnification) using transmitted, polarized light. Daily increments were counted from the core to the edge during two independent readings separated by a minimum of one week. Specimens lacking agreement between the two initial readings were read a third time for confirmation. If no confirmation could be made after the third reading, the sample was excluded. Based on laboratory-reared larvae and the assumption that sagittal otolith formation coincides with yolk-sac absorption, Barnett and Sertic (1980[3]) concluded otolith formation occurs at two days post-hatch in queenfish and five days post-hatch in white croaker. Final estimated ages in the current study incorporate these findings by adding the species-specific constant (2 or 5) to each increment count. Temporal differences in queenfish growth rate between June–July 2004 (n = 43) and August 2004 (n = 69) were compared using analysis of residual sum of squares (ARSS) derived by non-linear regression (Haddon 2001). This technique was also used to test differences in derived growth curves based on preservation technique for queenfish collected on September 1, 2004. Similar analyses were not completed for white croaker due to the small sample size of formalin-fixed larvae. Lastly, the linear growth curves for all individuals combined, by species, for specimens collected in 1978 and 2004 were compared using a Mann-Whitney U test and the mean absolute difference between the two growth estimates was derived. The 1978 and 2004 mean annual sea surface temperature (SST) collected at the end of the San Clemente Pier in San Clemente, California was gathered from the Scripps Shore Stations Program database (SIO 2011). San Clemente Pier is located near the San Onofre sampling sites while the Newport Pier in Newport Beach, California is located closer to the 2004 Huntington Beach sampling sites. The questionable validity of the SST recorded at the Newport Pier during the 2004 sampling excluded its use in this analysis (M. Carter personal communication[4]).

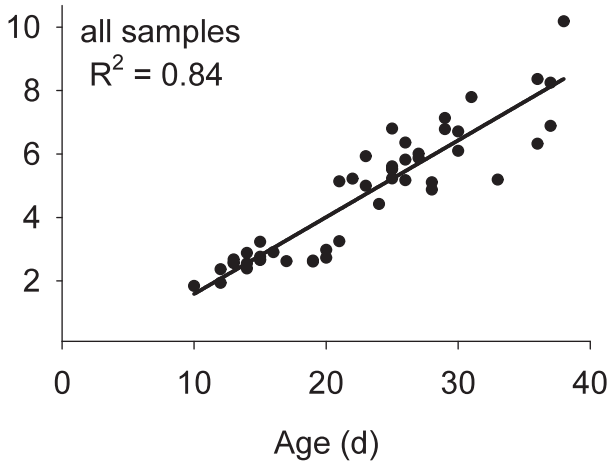

Figure 1. White croaker daily age and growth derived from increment analysis of 48 specimens collected between December 2003 and September 2004 offshore of Huntington Beach, California. The linear regression accounted for 84% of the variance (R^2 = 0.84): L = –0.833 + 0.242A.

RESULTS

White croaker (n = 48) ranged from 1.8 to 10.2 mm L and were primarily recovered from ethanol samples (n = 47), mostly taken in May and July 2004. Queenfish (n = 122) ranged from 2.5 to 10.5 mm L and were from both ethanol (n = 74) and formalin-fixed (n = 48) samples, mostly taken in July and September. White croaker specimens ranged in development from pre-flexion to post-flexion. No yolk-sac or transforming individuals were collected during the survey and therefore not available for analysis. The smallest individual was 1.84 mm L at an estimated age of 10 days while the largest speci-

[4]M. Carter, Scripps Institution of Oceanography, June 24, 2010

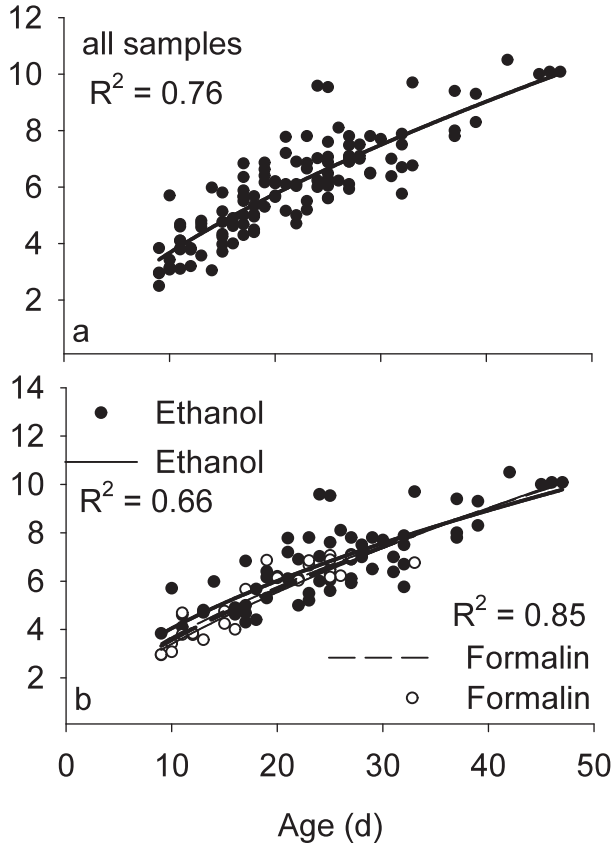

Figure 2. a) Queenfish daily age and growth derived from increment analysis of 122 specimens collected between December 2003 and September 2004 offshore of Huntington Beach, California. The non-linear regression accounted for 77% of the variance (R^2 = 0.76): L = 0.825 x $A^{0.647}$. b) Daily age and growth of a subset of queenfish collected on September 1, 2004 and initially fixed in either 70% ethanol (n = 74) or a 4% buffered formalin-seawater solution (n = 48). The linear regression captured 66% of the variance in the ethanol-preserved distribution (R^2 = 0.66) and 85% of the variance in the formalin-fixed distribution (R^2 = 0.85).

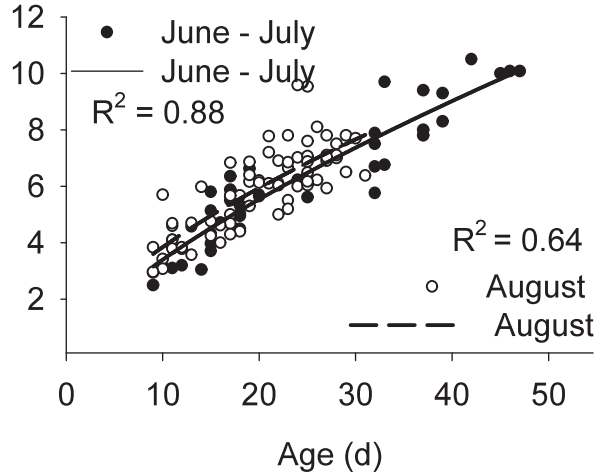

Figure 3. Queenfish age at length based on back-calculated hatch date. Non-linear regression captured 88% of the variance (R^2 = 0.88) in the distribution for those hatched in June and July (n = 43) and 64% of the variance (R^2 = 0.64) in the distribution for those hatched in August (n = 69). All samples collected offshore of Huntington Beach, California in 2004.

men was 10.18 mm L at an estimated age of 38 days. Larval white croaker daily growth was best described by the linear relationship L = –0.833 + 0.242A (R^2 = 0.84; fig. 1).

Queenfish ranged in size from 2.50 mm L at nine days old to 10.08 mm L for a 47-day-old individual. The majority of all individuals were between 3.00 mm L and 6.50 mm L. As with white croaker, no yolk-sac or transforming individuals were collected during the sampling offshore. Their growth rate gradually slowed with increasing length which resulted in it being best described by the power function: $L = 0.825 \times A^{0.647}$ (R^2 = 0.76; fig. 2a). No effect of seasonality was detected in the queenfish examined. Growth rates of queenfish hatched in June or July exhibited no significant differences in growth rate from those hatched in August (ARSS, $F_{1,114}$ = 1.82, p = 0.17; fig. 3). The growth rates of 90 queenfish taken on September 1, 2004 were analyzed for differences in their derived growth based on the initial preservative used. Twenty-five specimens were initially fixed in buffered-formalin with the remaining 65 fixed and preserved in ethanol. No significant difference in growth rates based on preservative type was detected (ARSS, $F_{1,88}$ = 2.43, p = 0.09; fig. 2b).

The queenfish growth rates derived from samples collected in 1978 and 2004 consistently differed by two days (fig. 4a). Specimens collected in 2004 were larger at each age than those taken in 1978. This difference was significant (Mann-Whitney, U = 6182.5, df = 121, p = 0.02). The two larval white croaker growth rates differed by nearly 5 days (± 0.5, standard error), on average, with the 1978 specimens older at each length in 81% of the specimens (fig. 4b). This difference was also significant (Mann-Whitney, U = 837.5, df = 47, p = 0.02). The mean annual SST at the end of the San Clemente Pier in 2004 was ~0.9°C warmer than in 1978.

DISCUSSION

The formation of daily increments on sagittal otoliths has been repeatedly confirmed in both laboratory-reared and wild-caught larvae (Victor 1982; Victor and Brothers 1982; Jones 1986; Peters and McMichael 1987; David et al. 1994). Larval daily growth patterns have been extensively studied in red drum, *Sciaenops ocellatus*, along the Gulf and Atlantic coasts (Peters and McMichael 1987; Cowan 1988; Comyns et al. 1989), but little research has been published in the primary literature on the Southern California Bight sciaenids. The current research is one of the first attempts to provide similar information on these sciaenids.

Both queenfish and white croaker exhibited steady somatic growth throughout the larval period between nine (queenfish) and 10 (white croaker) days old to 35

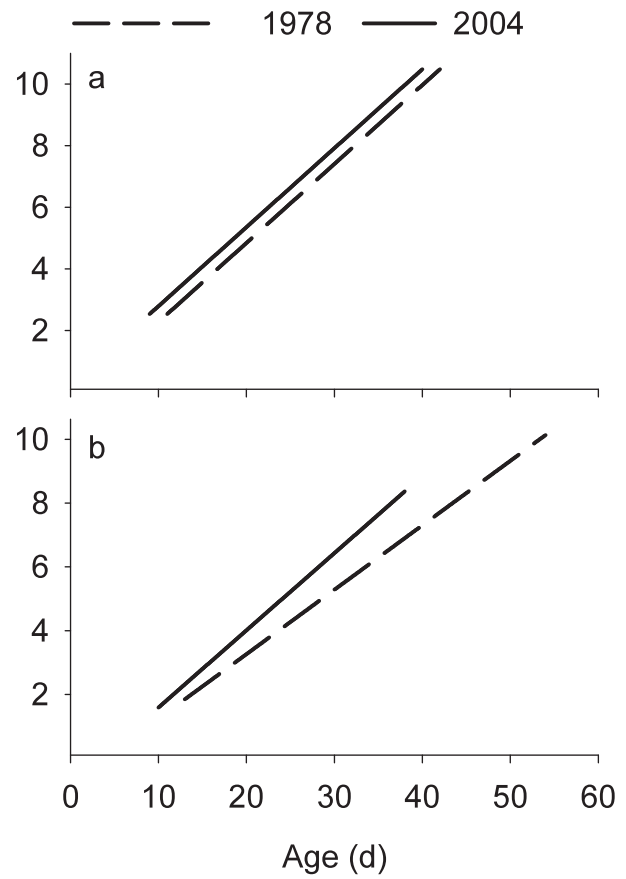

Figure 4. Linear descriptions of the larval growth rates for a) queenfish and b) white croaker based on samples collected in 1978 (Barnett and Sertic 1980[3]) offshore of San Onofre, California and in 2004 offshore of Huntington Beach, California.

days old or less. Larval growth rates in each species were well described by either linear or power functions with >75% of the variation captured by the model for each species. To date, no studies of the larval growth of wild-caught specimens of Southern California sciaenids have been published in the primary literature, thereby limiting the direct comparison of current results to other local species. A prior technical report by Barnett and Sertic (1980[3]) on this topic revealed some measured differences in the growth rates between the two sampling periods separated by over 25 years. In both studies, queenfish grew at a similar rate, but the more recent individuals were consistently two days older than was predicted by the Barnett and Sertic (1980[3]) model. This resulted in a significant difference between the two predicted ages at each length. Greater differences in growth rate were observed in the 1978- and 2004-collected white croaker (fig. 4). White croaker grew at a significantly faster rate in 2004 than the prior model predicted. Exact causes for this were outside the scope of this investigation, but the warmer SST likely contributed to this (Jones 2002). While the prior studies by Barnett and Sertic (1980[3]) identified significant differences in seasonal growth patterns, no evidence of seasonal growth patterns in queenfish was observed in the current study. This is contrary to similar studies on sciaenids, especially among Atlantic- and Gulf-coast sciaenids (Jones 2002).

Butler (1992) reviewed preservation techniques used for specimens destined for larval otolith analysis and commented that while the exclusive use of ethanol was recommended (Brothers et al. 1976; Methot and Kramer 1979), several studies had successfully used specimens fixed in up to 10% buffered formalin. Direct comparisons by Kristoffersen and Salvanes (1998) found a 4% seawater-formalin solution resulted in less weight loss in preserved larval fishes and no significant changes to their otoliths. Our results agree with both Butler (1992) and Kristoffersen and Salvanes (1998) in that no significant difference was identified in the derived growth rates of queenfish taken on the same day but exposed to different preservatives (fig. 2). In fact, more consistent results were obtained from the formalin-fixed samples. The storage medium pH was not monitored, so potential etching due to acidic effects on the otoliths cannot be verified, but increments on the formalin-fixed queenfish otoliths were noticeably more defined than their ethanol counterparts. It should be noted, however, that no larval samples remained in the 4% seawater-formalin solution for greater than 80 hrs from the time of collection before being transferred to 70% ethanol.

These results (daily growth and preservative effects) help to advance the understanding of two fishes common to the Southern California Bight. Given their frequency in monitoring surveys and potential significance to nearshore ecology, greater understanding of their basic life-history parameters is critical for their effective management. Daily growth is one of the more commonly used parameters which, until now, was not readily available for these species. While daily growth for queenfish and white croaker does not, by itself, provide for the usage of demographic models, it nevertheless fills a critical gap. Furthermore, the confirmation that specimens fixed in a formalin-seawater solution are not unusable, but rather may be more resolvable for ageing, supports the revisiting of archived collections that may hold untapped scientific value.

ACKNOWLEDGEMENTS

G. Jordan assisted with the larval identifications. We would like to thank AES Huntington Beach Generating Station for their support of the sampling program and the subsequent use of the samples for this study. K. Anthony assisted with acquiring some of the less available technical reports. Comments by S. Beck greatly improved this manuscript. This report was prepared as a result of work sponsored by the California Energy

Commission (Energy Commission). It does not necessarily represent the views of the Energy Commission, its employees, or the State of California. The Energy Commission, the State of California, its employees, contractors, and subcontractors make no warranty, express or implied, and assume no legal liability for the information in this report; nor does any party represent that the use of this information will not infringe upon privately owned rights. This report has not been approved or disapproved by the Energy Commission nor has the Energy Commission passed upon the accuracy or adequacy of the information in this report.

REFERENCES

Allen, L. G. and E. E. DeMartini. 1983. Temporal and spatial patterns of nearshore distribution and abundance of the pelagic fishes off San Onofre-Oceanside, California. United States Fish. Bull. 81:569–586.

Barnett, A. M., A. E. Jahn, P. D. Sertic, and W. Watson. 1984. Distribution of ichthyoplankton off San Onofre, California, and methods for sampling very shallow coastal waters. United States Fishery Bulletin 82:97–111.

Boreman, J., C. P. Goodyear, and S. W. Christensen. 1981. An empirical methodology for estimating entrainment losses at power plants sited on estuaries. Transactions of the American Fisheries Society 110:253–260.

Brothers, E. B., C. P. Mathews, and R. Lasker. 1976. Daily growth increments in otoliths from larval and adult fishes. United States Fishery Bulletin 74:1–8.

Butler, J. L. 1992. Collection and preservation of material for otolith analysis. In Otolith microstructural examination and analysis, eds. D. K. Stevenson and S.E. Campana, 13–17. Canadian Special Publication in Fisheries and Aquatic Sciences 117.

Butler, J. L., M. L. Granados G., J. T. Barnes, M. Yaremko, B. J. Macewicz. 1996. Age composition, growth, and maturation of the Pacific sardine (*Sardinops sagax*) during 1994. Calif. Coop. Oceanic Fish. Invest. Rep. 37:152–159.

Butler, J. L., P. E. Smith, and N. C. H. Lo. 1993. The effect of natural variability of life-history parameters on anchovy and sardine population growth. Calif. Coop. Oceanic Fish. Invest. Rep. 34:104–111.

Cailliet, G.M., E.J. Burton, J.M. Cope, L.A. Kerr, R.J. Larson, R.N. Lea, D. VanTresca, and E. Knaggs. 2000. Biological characteristics of nearshore fishes of California: a review of existing knowledge and proposed additional studies. (California Dept of Fish and Game, Sacramento). http://www.dfg.ca.gov/marine/lifehistory.asp. Accessed August 18, 2010.

Comyns, B. H., J. Lyczkowski-Schultz, C. F. Rakocinski, and J. P. Steen, Jr. 1989. Age and growth of red drum larvae in the North-Central Gulf of Mexico. Transactions of the American Fisheries Society 118:159–167.

Cowan, J. H. Jr. 1988. Age and growth of Atlantic croaker, *Micropogonias undulatus*, larvae collected in the coastal waters of the northern Gulf of Mexico as determined by increments in saccular otoliths. Bull. Mar. Sci. 42:349–357.

David, A. W., J. J. Isely, and C. B. Grimes. 1994. Differences between the sagitta, lapillus, and asteriscus in estimating age and growth in juvenile red drum, *Sciaenops ocellatus*. United States Fishery Bulletin 82:509–515.

Goodyear, C. P. 1978. Entrainment impact estimates using the equivalent adult approach. United States Fish & Wildlife Service. FWS/OBS-78/65.

Haddon, M. 2001. Modelling and quantitative methods in fisheries. Chapman and Hall/CRC. Boca Raton, FL. P 224–226.

Hill, K.T., N.C.H. Lo, B.J. Macewicz, and R. Felix-Uraga. 2006. Assessment of the Pacific sardine (*Sardinops sagax caerulea*) population for U.S. management in 2007. NOAA Technical Memorandum. NOAA-TM-NMFS-SWFSC-396.

Hunter, J. R. and B. J. Macewicz. 1980. Sexual maturity, batch fecundity, spawning frequency, and temporal pattern of spawning for the northern anchovy, *Engraulis mordax*, during the 1979 spawning season. Calif. Coop. Oceanic Fish. Invest. Rep. 21:139–149.

Jensen, A. L., S. A. Spigarelli, and M. M. Thommes. 1982. Use of conventional fishery models to assess entrainment and impingement of three Lake Michigan fish species. Transactions of the American Fisheries Society 111:21–34.

Jones, C. 1986. Determining age of larval fish with the otolith increment technique. United States Fishery Bulletin 84:91–103.

Jones, C. M. 2002. Age and growth. In Fishery science: The unique contributions of early life stages. Edited by L. A. Fuiman and R. G. Werner. Blackwell Sciences, Malden, MA. pp. 33–63.

Kristoffersen, J. B. and A. G. V. Salvanes. 1998. Effects of formaldehyde and ethanol preservation on body and otoliths of *Maurolicus muellera* and *Benthosema glaciale*. Sarsia 83:95–102.

Lavenberg, R. J., G. E. McGowen, A. E. Jahn, J. H. Petersen, and T. C. Sciarrotta. 1986. Abundance of southern California nearshore ichthyoplankton: 1978–1984. Calif. Coop. Oceanic Fish. Invest. Rep. 27:53–64.

Lo, N. C. H., B. J. Macewicz, and D. A. Griffith. 2005. Spawning biomass of Pacific sardine (*Sardinops sagax*) from 1994–2004 off California. Calif. Coop. Oceanic Fish. Invest. Rep. 46:93–112.

Lo, N. C. H., P. E. Smith, and J. L. Butler. 1995. Population growth of northern anchovy and Pacific sardine using stage-specific matrix models. Mar. Ecol. Prog. Ser. 127:15–26.

Love, M. S., J. S. Stephens, Jr., P. A. Morris, M. M. Singer, M. Sandhu, T. C. Sciarrotta. 1986. Inshore soft substrata fishes in the Southern California Bight: an overview. Calif. Coop. Oceanic Fish. Invest. Rep. 27:84–104.

MacCall, A. D., K. R. Parker, R. Leithiser, and B. Jessee. 1983. Power plant impact assessment: A simple fishery production model approach. United States Fishery Bulletin 81:613–619.

McGowen, G. E. 1993. Coastal ichthyoplankton assemblages, with emphasis on the Southern California Bight. Bull. Mar. Sci. 53:692–722.

Methot, R. D. Jr. and D. Kramer. 1979. Growth of northern anchovy, *Engraulis mordax*, larvae in the sea. United States Fishery Bulletin 77:413–423.

Miller, E. F., J. P. Williams, D. J. Pondella, II, and K. T. Herbinson. 2009. Life history, ecology, and long-term demographics of queenfish. Marine and Coastal Fisheries: Dynamics, Management, and Ecosystem Science 1:187–199.

Moser, H. G., R. L. Charter, P. E. Smith, D. A. Ambrose, W. Watson, S. R. Charter, and E. M. Sandknop. 2001. Distributional atlas of fish larvae and eggs in the Southern California Bight region, 1951–1998. Calif. Coop. Oceanic Fish. Invest. Atlas 34.

Newbold, S. C. and R. Iovanna. 2007. Population level impacts of cooling water withdrawals on harvested fish stocks. Environmental Science and Technology 47:2108–2114.

Parker, K. 1980. A direct method for estimating northern anchovy, *Engraulis mordax*, spawning biomass. United States Fishery Bulletin 78:541–544.

Peters, K. M. and R. H. McMichael, Jr. 1987. Early life history of the red drum, *Sciaenops ocellatus* (Pisces: Sciaenidae) in Tampa Bay, Florida. Estuaries 10:92–107.

Saila, S. B., E. Lorda, J. D. Miller, R. A. Sher, and W. H. Howell. 1997. Equivalent adult estimates for losses of fish eggs, larvae, and juveniles at Seabrook Station with use of fuzzy logic to represent parametric uncertainty. North American Journal of Fisheries Management 17:811–825.

SIO. 2011. Scripps Shore Stations Program. http://shorestation.ucsd.edu/active/index_active.html#sanclementestation. Accessed March 14, 2011.

Stull, J. K. and C. Tang. 1996. Demersal fish trawls off Palos Verdes, Southern California, 1973–1993. Calif. Coop. Oceanic Fish. Invest. Rep. 37:211–240.

Victor, B. C. 1982. Daily otolith increments and recruitment in two coral-reef wrasses, *Thalassoma bifasciatum* and *Halichoeres bivittatus*. Mar. Biol. 71:203–208.

Victor, B. C. and E. B. Brothers. 1982. Age and growth of the fallfish *Semotilus corporalis* with daily increments as a method of annulus verification. Canadian Journal of Zoology. 60:2543–2550.

Walker, Jr., H. J., W. Watson, and A. M. Barnett. 1987. Seasonal occurrence of larval fishes in the nearshore Southern California Bight off San Onofre, California. Estuarine and Coastal Shelf Science 25:91–109.

SPATIAL DISTRIBUTION OF SOUTHERN CALIFORNIA BIGHT DEMERSAL FISHES IN 2008

ERIC F. MILLER
MBC Applied Environmental Sciences
3000 Red Hill Ave.
Costa Mesa, CA 92626
P: 714-850-4830
F: 714-850-4840
E: emiller@mbcnet.net

KENNETH C. SCHIFF
Southern California Coastal Water Research Project
3535 Harbor Blvd., Suite 110
Costa Mesa, CA 92626

ABSTRACT

In an effort to better characterize the spatial dynamics of the assemblage, the demersal fish communities throughout the Southern California Bight (Point Conception, California to the United States-Mexico border) were sampled in 2008 utilizing standardized methods under an interagency program. Otter trawl sampling was conducted in habitats ranging from select bays and harbors out to the upper continental slope. Pacific sanddab (*Citharichthys sordidus*) was the most commonly caught species and contributed the greatest biomass. The catch compositions at each site generally segregated along depth gradients, but not latitudinal gradients except for within the bay/harbor strata. The largest catches were recorded in the central area, which includes the Santa Monica Bay and the Los Angeles–Long Beach harbors. Offshore densities peaked along the middle and outer shelf (30–200 m depth). Species diversity was comparatively stable and elevated along the deeper portions of the continental shelf relative to the inner shelf (<31 m depth) with the minimum diversity recorded in the southern portion of the inner shelf.

INTRODUCTION

The Southern California Bight (SCB) is a diverse area characterized by heterogeneous habitats (Dailey et al. 1993); the convergence of the cold southward flowing California Current and the warm poleward flowing California Countercurrent (Hickey 1992); a variable width continental shelf; and multiple, densely populated, metropolitan areas (e.g., Los Angeles, San Diego, etc.). Fishes within the SCB represent a transitional fauna indicative of the dynamic environmental conditions present, with species representative of the Oregonian and San Diegan biogeographic provinces commonly occurring in the area (Horn et al. 2006).

Environmental conditions can fluctuate widely on annual to decadal scales, often related to larger scale oceanographic phenomena affecting the California Current such as El Niño Southern Oscillation (ENSO) events (1997–98 ENSO; McGowan et al. 2003) or variability in the strength and position of the Aleutian Low (Bograd and Lynn 2003). Both low- and high-frequency variability has been linked to marked changes in the abundance and distribution of fishes, including demersal species (Mearns 1979; Stull and Tang 1996; Perry et al. 2005; Hsieh et al. 2009). Recent discoveries of an expanding oxygen minimum zone (OMZ) in the Eastern North Pacific basin, and its negative impact on demersal and benthic life raises additional concern (Levin 2003; Grantham et al. 2004; Powers et al. 2005; Bograd et al. 2008; Chan et al. 2008; Diaz and Rosenberg 2008; McClatchie et al. 2010). Within the SCB, Bograd et al. (2008) found areas with the highest rate of dissolved oxygen decline along the inner and middle shelves near the greater Los Angeles and Orange County, California, coastlines.

While fishes typically exhibit population level responses to environmental variation (Juan-Jordé et al. 2009), these oscillations can be exaggerated or masked by anthropogenic impacts such as harvesting (Brander 2007; Perry et al. 2010; Hidalgo et al. 2011), habitat alteration (Dayton et al. 1995), and ocean discharge from both point (e.g., wastewater discharge) and non-point sources (e.g., storm drain; Allen 2006a). Historically, SCB demersal fish community changes were traced to effects of wastewater discharge through either altered community demographics (composition, abundance, species diversity, etc.) or prevalence of tumors and other physical abnormalities (Perkins 1995; Stull and Tang 1996; Allen 2006a). While most wastewater discharge effects on the demersal fish community have subsided (Stull and Tang 1996; Allen 2006a,b), impacts of fishing and other anthropogenic interactions with the coastal waters can still be detected (Schroeder and Love 2002). Concerns over large, point-source ocean discharges resulted in permit-required demersal fish monitoring (Mearns 1979; Love et al. 1986; Stull and Tang 1996). Demographic indices (abundance, biomass, composition, etc.) on the demersal fish stocks of the SCB shelf are routinely monitored through this permit-required monitoring.

Despite the level of effort devoted to monitoring, however, little primary research documenting the soft-bottom demersal fish communities of the SCB beyond

site-specific programs (see Stull and Tang 1996) has been published since Love et al. (1986), which was limited to communities inshore of the 20-m isobath. Deficits in this information at a regional scale limit the detection of population responses to large scale perturbations such as OMZ intrusion. McClatchie et al. (2010) modeled the predicted effect of OMZ on cowcod (*Sebastes levis*) habitat, but abundance information will be needed to evaluate their predictions of population-level responses. As an example, Grantham et al. (2004) was able to use previously recorded demersal species abundance data collected near an oceanographic monitoring transect to report on the catastrophic effects of hypoxia on the demersal resources off the Oregon coast.

An integrated, area-wide sampling effort utilizing standardized methods can provide the necessary robust snapshot of baseline conditions to not only provide context for site-specific monitoring results but also, after repeated surveys, provide tractable evidence of community changes (Bertrand et al. 2002). The Southern California Bight 2008 Monitoring Program (Bight 2008) was conducted to provide this general overview of the SCB demersal fish community spatial dynamics. Utilizing the Bight 2008 results, this study aims to describe the spatial pattern of the SCB soft-bottom demersal fish stocks with a specific goal of characterizing the assemblage variability between discrete depth strata and latitudinal regions, for both the community as a whole but also at species-specific levels. Such information is lacking in the recently published literature and will likely benefit future evaluations of the various anthropogenic and environmental factors previously mentioned, e.g., the expanding OMZ.

MATERIALS AND METHODS

Sampling Station Description

Demersal fish on soft-bottom habitat were sampled at 143 stations by otter trawl across the SCB at stations using a probability based design (Stevens 1997) that selects sampling sites *a priori* among areas determined to be free of obstructions (able to be sampled with an otter trawl) based on reviews of bathymetric maps (fig. 1). During the Bight 2008 planning, stations were segregated into discrete shelf (depth) strata and latitudinal groups. To account for differences between expected and actual depths at each sampling site, all open coast data were reclassified after sampling into consistent shelf strata by actual sampling depth: 5–30 m = inner shelf (IS), 31–120 m = middle shelf (MS), 121–200 m = outer shelf (OS), and >200 m = upper slope (US). Sampling results from bays and harbors remained classified into the bay/harbor (BH) shelf strata. Within each stratum, latitudinal distributions were designated as: >34°N = north, 33.5–34°N = central, and <33.5°N = south. Henceforward, shelf strata-region combinations (e.g., IS-S) are referred to as blocks (e.g., IS-S block) for simplicity.

Sampling Methods

Sampling was completed during the summer (July–September, 2008) with 7.6-m head-rope semiballoon otter trawl nets fitted with 1.25-cm cod-end mesh during daylight hours. Trawls were towed along open-coast isobaths for ~10 min (~5 min in bays and harbors) at 0.8–1.0 m/sec. These tows were designed to cover an estimated distance of 300 and 600 m for 5 and 10 min trawls, respectively. The actual trawl distance was calculated from the difference between the start and stop fishing GPS coordinates recorded on the deck of the towing vessel. These acted as a proxy for the net's relative position. It was assumed the net remained on the bottom and fishing the entire time. Upon retrieval, catches were sorted, identified to species, enumerated, and batch weighed to the nearest gram (g). Each station was sampled once per survey. Catches from sampling events aborted due to equipment malfunction or protocol violations were discarded and the station was resampled, if possible.

Data Analysis

The analysis focused on the demersal communities; therefore pelagic, midwater fishes (Allen and Pondella 2006), e.g., northern anchovy (*Engraulis mordax*), were excluded as their catches likely include sampling during midwater deployment or retrieval (Biagi et al. 2002). Underwater measurements by Environmental Quality Analysts and Marine Biological Consultants (1975) determined the 7.6-m trawl net used in all four Bight surveys spread 4.9 m, on average, while under tow and fishing. The area swept in this analysis represents the distance trawled (m) × 4.9 m. Densities represent the abundance (biomass) per area swept (m^2).

Mean density (count/1000 m^2) for each species and its frequency of occurrence in individual trawl samples were derived by shelf strata. The mean density by block (e.g. inner shelf south) for the 21 most abundant species caught across the three open coast shelf strata (inner, middle, and outer shelf). Based on the probabilistic design, density by stratum was area-weighted using the ratio estimator approach following Thompson (1992):

$$m = \frac{\sum_{i=1}^{n} (p_i * w_i)}{\sum_{i=1}^{n} w_i},$$

where:
m = Area-weighted mean density for stratum j.
p_i = Parameter value (e.g. density) at station i.
w_i = Area weight for station i.
n = Number of stations in population j.

The standard error of the mean was calculated using the following equation where the 95% confidence intervals about the mean were calculated as 1.96 times the standard error.

$$\text{Standard error (SE)} = \sqrt{\frac{\sum_{i=1}^{n} ((p_i - m) * w_i)^2}{\left(\sum_{i=1}^{n} w_i\right)^2}},$$

where:
m = Area-weighted mean concentration for population j.
p_i = Parameter value (e.g. density) at station i.
w_i = Area weight for station i.
n = Number of stations in population j.

Differences in the species-specific densities between blocks were compared using a one-way ANOVA with a Bonferroni multiple comparison test after Ln (x+1) transforming the data (Sokal and Rohlf 1995). The Pacific sanddab (*Citharichthys sordidus*) and hornyhead turbot (*Pleuronichthys verticalis*) distributions were the only ones to meet the parametric assumptions after transformation. A Kruskall-Wallis ANOVA, correcting for ties, (Sokal and Rohlf 1995) was used to compare block-specific patterns in the remaining 19 species. The Shannon-Wiener species diversity index (Shannon and Weaver 1962) was derived based on the raw counts by block. Species diversity by block was compared using a Kruskall-Wallis ANOVA, correcting for ties, using station-specific values. All comparisons were executed using Number Cruncher Statistical Software (Hintze 1998). Each species' significance to the shelf stratum community was described using the rank of the index of community importance (ICI; Stephens and Zerba 1981; Love et al. 1986). Differences in assemblages between regions within each shelf stratum were subjectively examined using the species abundance distributions (SAD; McGill et al. 2007) among the ten most abundant species in each shelf stratum. The station-specific proportion of the total catch in each block and the mean across all stations in each block were derived to illustrate comparative changes in the species rank abundance with latitude. Spearman rank correlation was used to compare the means among the regions within each shelf stratum with n = 10 (species included) in all comparisons.

Similarities along the full latitudinal and depth gradients sampled were characterized using percent similarity index (PSI, Whittaker 1952; Whittaker and Fairbanks 1958) using the equation: $\text{PSI} = 100 - 0.5 * \Sigma |A_i - B_i|$ where A_i and B_i are the percentages of species i in samples A and B, respectively. Stations were segregated into 0.2° latitude bins for spatial analysis and 20-m bins for depth analysis. Each PSI distribution was evaluated to determine if the pattern fit either a linear or nonlinear regression model. Nonmetric multidimensional scaling (nMDS) was used to illustrate the station groupings within each shelf strata based on the observed assemblage after the calculation of Bray-Curtis dissimilarities of fourth-root transformed species-specific densities (Clarke and Ainsworth 1993). The bay/harbor strata was excluded from the nMDS analysis due to the lack of a northern region sampling area and the general concentration of sampling in Los Angeles and Long Beach harbors within the central region (fig. 1). A similar nMDS analysis was done to visualize the relationships between the block species diversities after calculation of the Bray-Curtis dissimilarities. These data were not transformed prior to calculation of the dissimilarities. Station-specific diversities were included in the analysis, similar to the execution of the Kruskall-Wallis ANOVA, correcting for ties. All nMDS analyses were completed using SYSTAT v. 9.0 (SYSTAT 1998).

RESULTS

Appendix A includes a master species list of all fishes caught during the 2008 sampling while appendices B1–B5 list the mean density (± standard error), frequency of occurrence, and ICI rank by shelf stratum for all fishes caught. A total of 26,546 fish weighing 932.215 kg representing 133 demersal species were caught amongst 143 stations dispersed across five shelf strata spanning three designated latitudinal regions of the SCB (tab. 1 and fig. 1). Fish were caught at all but three stations, one each in the BH-S, IS-S, and US-N blocks. Sampling stations were randomly distributed over the soft-bottom habitat although some blocks were more intensively sampled (e.g., US-N) than others (e.g., OS-C; tab. 1). Pockets of elevated densities (count/1000 m^2) were observed in the Santa Monica Bay, Los Angeles and Long Beach harbors, and offshore San Diego. Additional individual sampling sites outside these areas registered elevated densities, but their occurrence was not as clustered. The Santa Monica Bay and offshore San Diego abundance hot spots were primarily from the MS and OS strata. Relatively high density catches (>101 fish/1000 m^2) were recorded at three IS stations, with two out of the three in the northern region. Similarly high density catches were also comparatively rare in the US with sampling at two stations recording densities greater than 101 fish/1000 m^2. Bio-

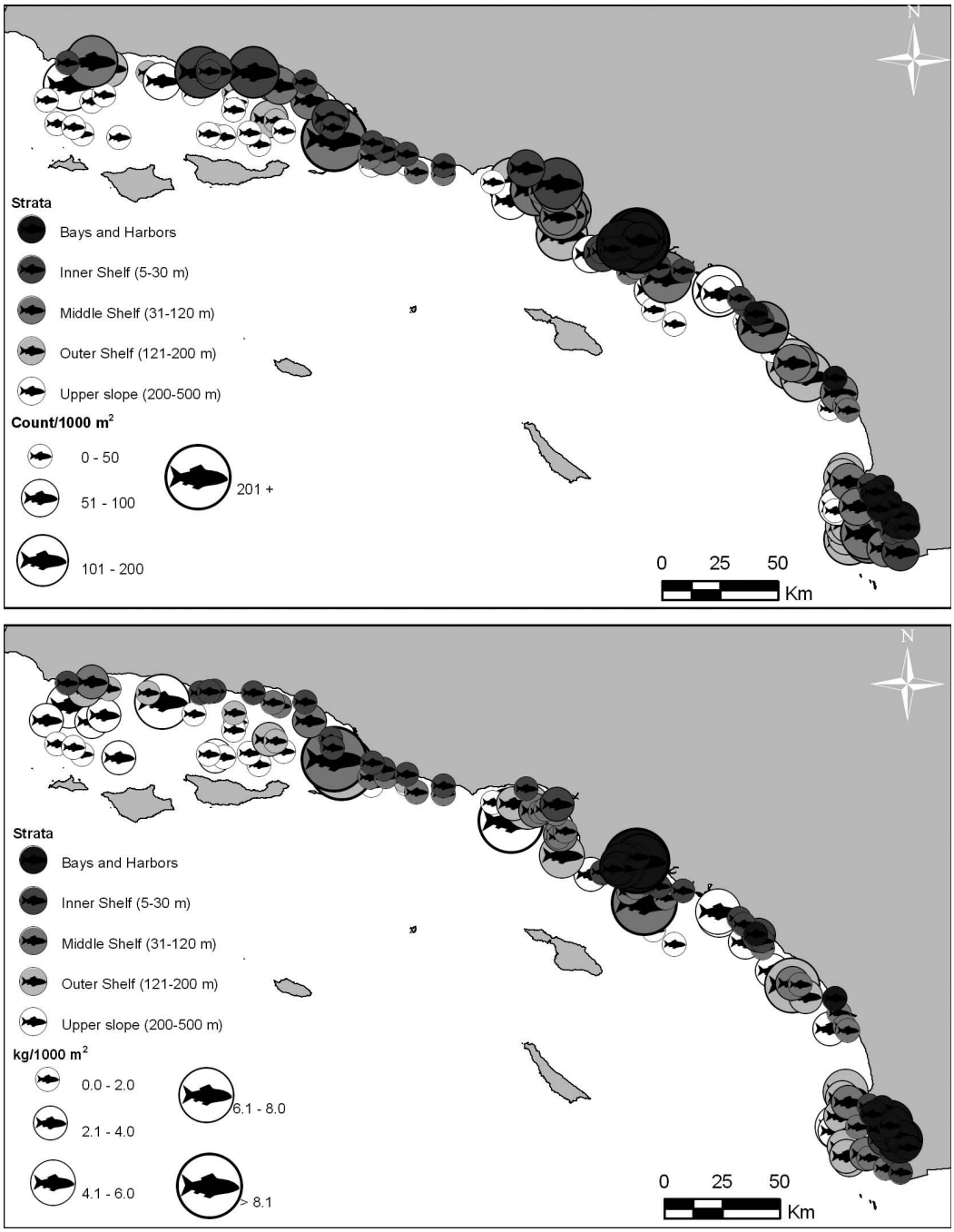

Figure 1. Demersal fish sampling stations occupied in summer 2008 distributed among the sampled shelf strata. Total sampling sites = 143. Upper panel depicts the total demersal fish abundance density (count/1000 m^2) recorded at each station per shelf strata. Lower panel depicts the total demersal fish biomass density (kg/1000 m^2) recorded at each station per shelf strata. Isobaths are depicted at 50-m intervals between the 50- and 500-m contour.

mass records (kg/1000 m^2) suggested a more dispersed pattern for the above-average catch weights, although stations in the Los Angeles and Long Beach harbor areas and offshore San Diego continued to record above average values. Species diversity ranged wildly among blocks, but was lower along the IS and BH shelf strata while relatively stable throughout the deeper sampling areas (fig. 2a). Peak diversity occurred along the MS-S with diversity at all but one station greater than 1.50 while the IS-S recorded the lowest diversity with all station-specific $H' < 1.40$. Blocks with predominately $H' < 1.50$ were segregated from the main grouping in the nMDS (fig. 2b), resulting in a significant difference between station-specific diversity (KW, $H = 37.25$, $df = 13$, $p < 0.001$).

The SADs by block revealed community variation

TABLE 1
Number of stations by shelf strata and latitudinal region sampled during the 2008 Southern California Bight monitoring survey.

Shelf Strata	Latitudinal Region	Number of Stations
Bays and Harbors	Central	6
	Southern	16
Strata Total		22
Inner Shelf (5–30 m)	Northern	12
	Central	13
	Southern	7
Strata Total		32
Middle Shelf (31–120 m)	Northern	9
	Central	13
	Southern	11
Strata Total		33
Outer Shelf (121–200 m)	Northern	11
	Central	3
	Southern	9
Strata Total		23
Upper slope (200–500 m)	Northern	20
	Central	9
	Southern	4
Strata Total		33
Total Number of Stations		143

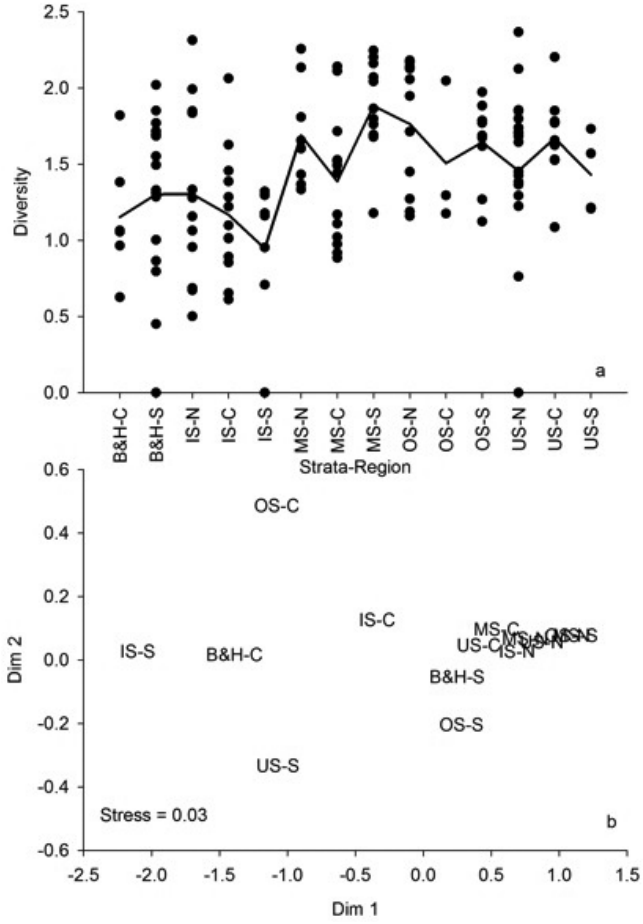

Figure 2. a) Shannon-Wiener species diversity index values for each station (dots) within each shelf strata-region block and the mean diversity for each shelf strata-region block (line). b) Nonmetric multidimensional scaling 2D distribution of the shelf strata-region blocks based on station-specific Shannon-Wiener diversity index values. Strata include: bays and harbors (BH), inner shelf (IS), middle shelf (MS), outer shelf (OS), and upper slope (US). Regions include north (N), central (C), and south (S).

along a latitudinal gradient within each shelf stratum (fig. 3). Differences between the two BH regions were the most pronounced; white croaker (*Genyonemus lineatus*) dominated the BH-C but was minimally abundant in the BH-S. This was the only shelf stratum where a negative correlation was detected between latitudinal regions ($r = -0.69$, $p < 0.02$). No significant correlations were detected for the IS between regions. This was consistent with the steady dominance of speckled sanddab (*Citharichthys stigmaeus*) throughout the stratum but variability among the lesser abundant species differentiated the regions. The same was true along the MS, except that Pacific sanddab replaced speckled sanddab as the dominant form. Along the OS and US, each region significantly correlated with the next most southerly region (OS-N:OS-C, $r = 0.89$, $p < 0.01$; OS-C:OS-S, $r = 0.62$, $p = 0.05$; US-N:US-C, $r = 0.71$, $p = 0.02$; US-C:US-S, $r = 0.76$, $p < 0.001$). No correlations, positive or negative, were detected between the northernmost and southernmost regions in any shelf stratum. Other than in the BH stratum, only the OS-C block community exhibited a substantial decline in the proportional contribution of the most abundant species across the stratum, Pacific sanddab.

Distribution of the 21 most abundant species, overall, revealed significant differences in their occurrence among the three shallowest offshore blocks (fig. 4, tab. 2). These differences were often predicated on a species complete or near-complete absence at select blocks. Four species were either entirely or largely absent outside of one stratum. Of these, splitnose rockfish (*Sebastes diploproa*) was uniquely caught in one stratum (OS), the remaining three species were represented by densities <2% of their peak block outside of their principle stratum. Only English sole (*Parophrys vetulus*) was caught in all blocks, although their peak densities were recorded in the MS-N. Pacific sanddab was the most common species (fig. 4), ranking first in abundance and the MS and OS ICI (appendices B-3 and B-4). Speckled sanddab occupied the top rank in both categories along the IS, while slender sole (*Lyopsetta exilis*) ranked first along the US in both metrics (appendix B-5). Speckled sanddab dominated the shallower IS sampling before its abundance diminished with depth where it was replaced by Pacific sanddab in the MS and OS sampling which ultimately gave way to slender sole at the greatest depths sampled.

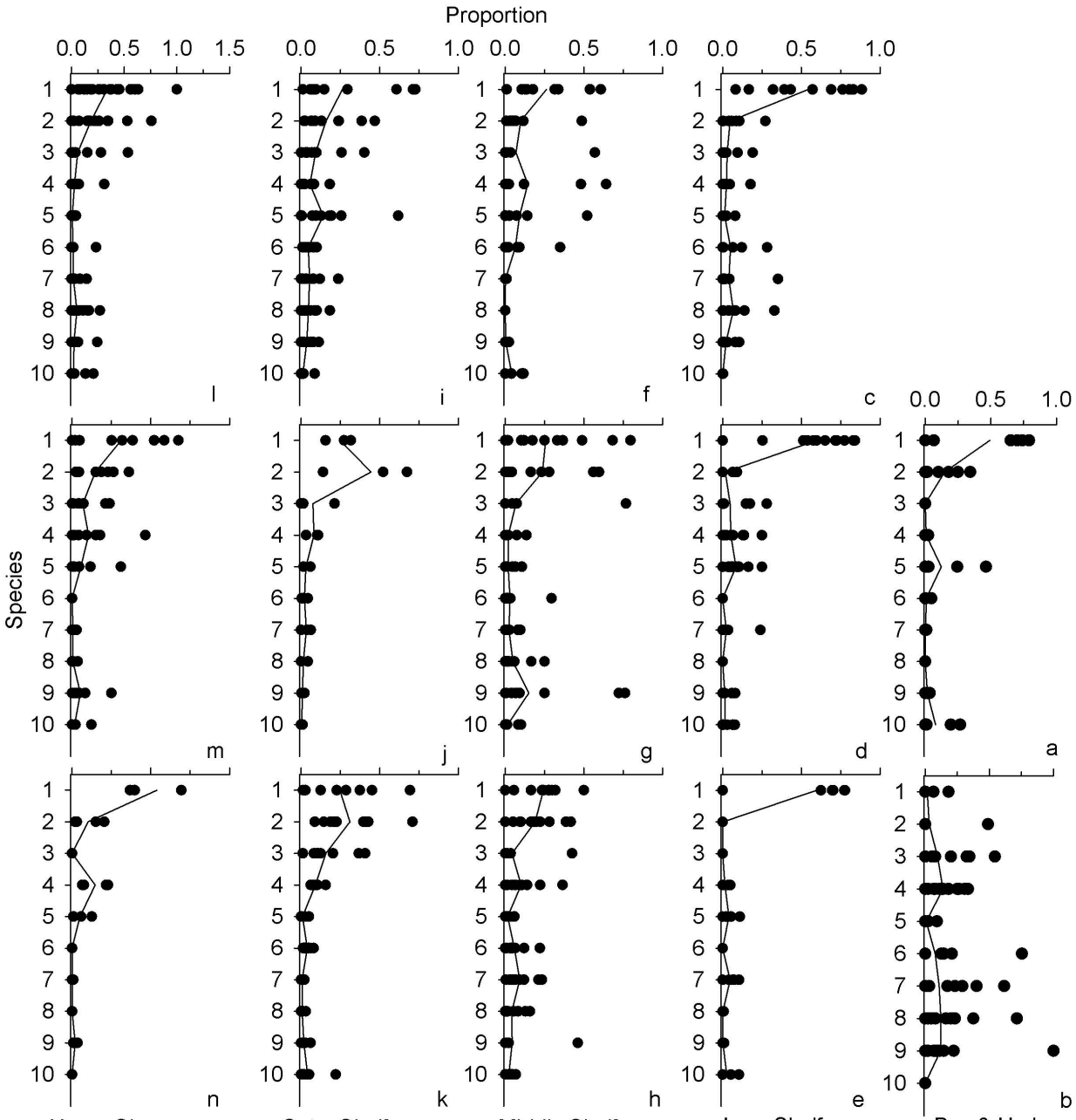

Figure 3. Demersal fish species abundance distribution as the percent of the total catch by shelf strata-region block for the ten most commonly taken species along each shelf stratum. a) Central bay & harbor, b) southern bay and harbor, c) northern inner shelf, d) central inner shelf, e) southern inner shelf, f) northern middle shelf, g) central middle shelf, h) southern middle shelf, i) northern outer shelf, j) central outer shelf, k) southern outer shelf, l) northern upper slope, m) central upper slope, n) southern upper slope. See text for bounds of strata and latitudinal ranges.

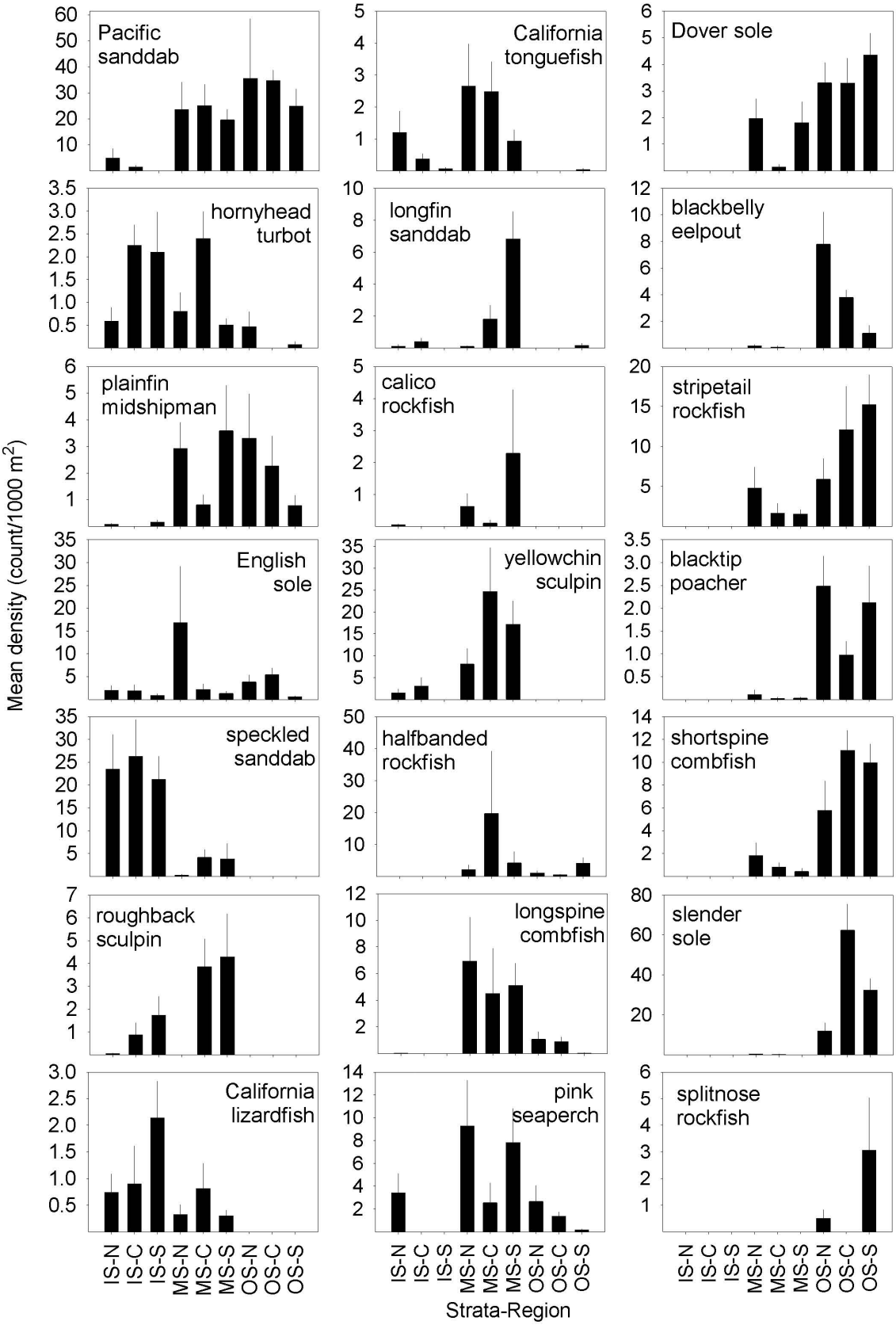

Figure 4. Area-weight adjusted mean density (fish/1000 m^2) per shelf strata-region block for the 21 most commonly occurring species in summer 2008 Southern California Bight demersal fish sampling along the inner shelf (IS), middle shelf (MS), and outer shelf (OS). Latitudinal regions are north (N), central (C), and south (S) as described in materials and methods.

TABLE 2
Results of one-way ANOVA (ANOVA) or Kruskall-Wallis (KW) test comparing the shelf strata-region trawl caught densities (count/1000 m²) for the 21 species most commoly captured during the 2008 Southern California Bight monitoring survey. Inner shelf (IS), middle shelf (MS), outer shelf (OS), north (N), central (C), and south (S). See text for depth ranges and latitudinal ranges for each shelf stratum and latitudinal region.

Species	Test	Statistic	DF	p	Significantly Differing Strata
Pacific sanddab	ANOVA	8.20	8,79	<0.001	IS: MS, OS
slender sole	KW	76.34	8	<0.001	OS: IS, MS
hornyhead turbot	ANOVA	5.71	8,79	<0.001	IS-C: MS, OS, IS-N; MS-C: OS
plainfin midshipman	KW	34.40	8	<0.001	IS-N & IS-S: MS-N, MS-S, OS-N; IS-C: MS, OS-C, OS-N
English sole	KW	8.49	8	0.39	NS
speckled sanddab	KW	54.54	8	<0.001	IS: MS, OS; MS-C: OS-N
roughback sculpin	KW	40.42	8	<0.001	MS-C: IS, OS, MS-S; MS-N: MS-C, MS-S; IS-C & IS-S: MS-S;
California lizardfish	KW	19.95	8	0.01	IS-N, IS-S, MS-C, MS-S: OS-N, OS-S
California tonguefish	KW	27.29	8	<0.001	MS-C: IS-C, IS-S, OS; MS-S: IS-S, OS-N, OS-S; OS-C & OS-N: MS
longfin sanddab	KW	46.88	8		MS-S: IS, OS, MS-N, MS-C; MS-C: IS-S, IS-N
calico rockfish	KW	19.38	8	0.01	MS-S: IS, MS-C, OS
yellowchin sculpin	KW	52.15	8	<0.001	MS: IS, OS
halfbanded rockfish	KW	21.29	8	<0.01	OS-S: IS, MS-C, MS-S
longspine combfish	KW	39.93	8	<0.01	MS: IS, MS; MS-C: OS-S; MS-N: OS-N, OS-S; MS-S: OS-N, OS-S
pink seaperch	KW	32.70	8	<0.001	IS-C: MS, IS-N, OS-N; IS-N: MS-S; IS-N: MS-C, MS-N, OS-N; MS-C: OS-S, MS-S; MS-S: OS-S
Dover sole	KW	65.58	8	<0.001	IS: OS, MS-N, MS-S; MS-C: MS-N, MS-S, OS
blackbelly eelpout	KW	47.32	8	<0.001	OS-C: IS, MS, OS-S; OS-N: IS, MS, OS-S
stripetail rockfish	KW	48.62	8	<0.001	IS: MS-N, MS-S, OS; OS-S: MS; OS-N: MS-C
blacktip poacher	KW	61.85	8	<0.001	OS: IS, MS
shortspine combfish	KW	61.81	8	<0.001	IS: OS, MS-N; MS-C:OS; MS-N: OS-S
splitnose rockfish	KW	17.92	8	<0.001	OS-N & OS-S: IS, MS

The PSI calculated across the shelf stations (IS, MS, OS) indicated limited differences along the latitudinal gradient, although a depression was observed at ~33°N, or offshore northern San Diego County (fig. 5a). Distance between stations did not result in a predictable pattern (fig. 5b). Stations along the north-south latitudinal gradient by shelf strata were generally overlapping in the nMDS analysis (fig. 6). Subtle gradients were observed in the IS and US, but stations from other regions were interspersed throughout the 2D space. Catches between ~160 and 420 m had the highest mean PSI scores (30–40%), but little similarity overall was detected with depth outside the immediately proximate depth bins (fig. 5c). Few comparisons exceeded 60% similarity, with a large proportion at <10% similarity. Similarity between depth-stratified catches declined in a linear pattern ($R^2 = 0.58$) with a negative slope ($m = -0.16$) as increasing differences in depth reduced the similarity between two catches (fig. 5d).

DISCUSSION

Demersal fish sampling in 2008 recorded a diverse and spatially distinct soft-bottom demersal community across the SCB. As expected, there was a clear difference in the species composition between the BH and offshore strata. Most species taken in BH sampling were absent or minimally present at sampling sites from the continental shelf or upper slope. Of the shelf sites, differences in species composition occurred with increasing depth. Abundance and diversity was much greater at MS and OS depths in comparison to the IS. The greatest abundance in trawl catch was observed in MS and OS depths offshore Santa Monica Bay and San Diego. In the BH straum, substantially elevated abundance was observed in the Los Angeles and Long Beach harbor. Finally, there was little difference in species composition across latitudinal gradients on the continental shelf, although shifts in species composition were observed in the BH stratum moving north to south.

The results observed during this survey were indicative of results from previous studies, such as depth stratification of the dominant flatfishes (Fager and Longhurst 1968; Biagi et al. 2002; Allen 2006b; Allen and Pondella 2006). For example, the prevalence of sanddab species, especially speckled sanddab and Pacific sanddab, has been a consistent biological feature in the SCB for over 30 years (Love et al. 1986; Stull and Tang 1996; Mearns 1979). These dominant flatfishes stratified by depth along the continental shelf in 2008; speckled sanddabs occurred shallow (<30 m), before transitioning to Pacific sanddab, and then slender sole in the deepest reaches (>200 m). This is also consistent with past survey results (Stull and Tang 1997) and Allen's (2006b) soft-bottom fish community functional structure.

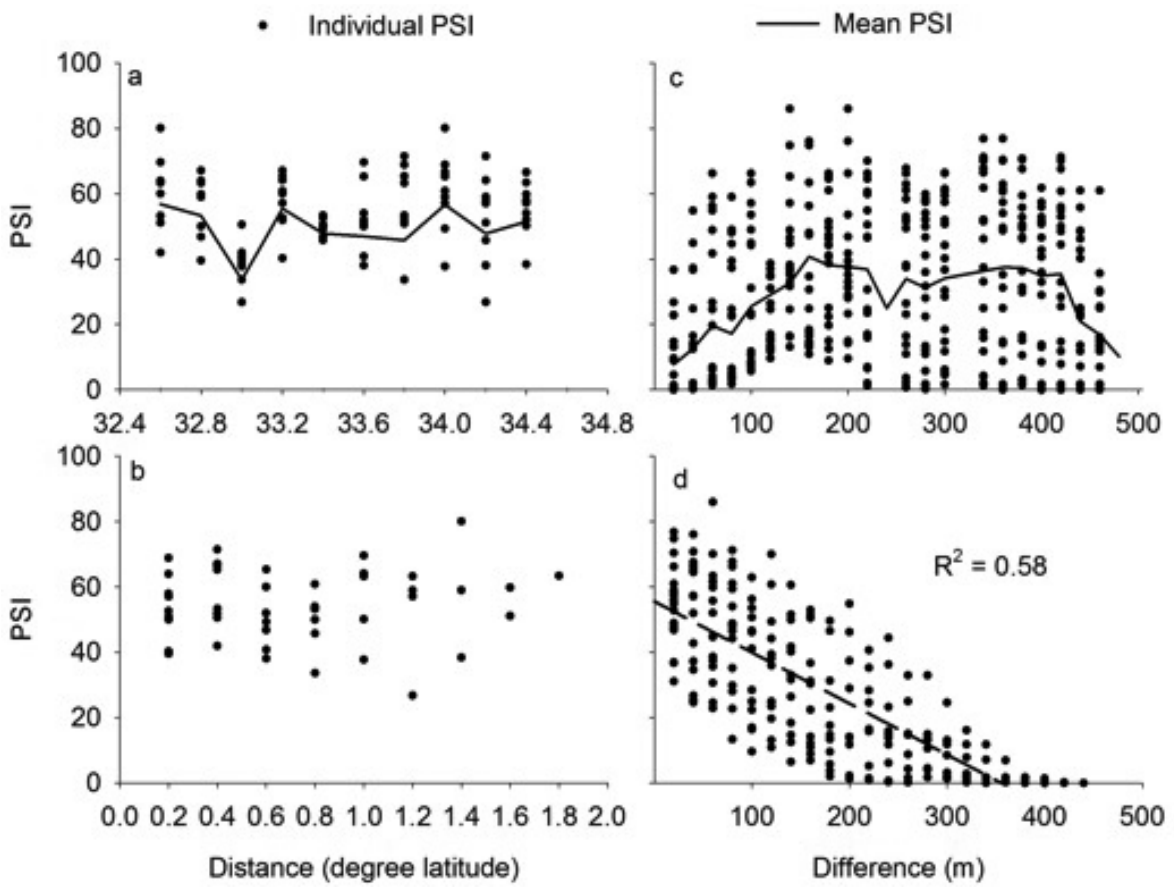

Figure 5. Percent similarity index (PSI) for the 2008 summer Southern California Bight demersal fish sampling depicting the similarity in catch composition between stations separated by a) 0.2° latitude bin, b) distance (degree latitude), c) 20-m depth bin, d) difference in depth (m). Solid lines in a and b represent the mean PSI at each x-axis value. Dashed line in d represents the best fit linear regression model (R^2 = 0.58) describing the observed pattern.

Results observed during this survey were also not indicative of previous studies. For example, the Los Angeles and Long Beach harbor areas were numerically dominated by white croaker and queenfish (*Seriphus politus*), whereas these species were caught in only 4% of the remaining SCB. The comparatively low abundances of white croaker along the open coast and in the southern BH varies dramatically from Allen (2006b) who indicated that the white croaker foraging guild occurred in >20% of all samples he examined from the IS and MS. Previously, demersal fish sampling inside of the 20-m isobaths along the SCB open coast consistently recorded both queenfish and white croaker among the most abundant species, with either one often ranking first in abundance (DeMartini and Allen 1984; Love et al. 1986). Stull and Tang (1996) first reported on the area's white croaker decline using identical techniques as the current investigation. The demise of white croaker and queenfish, especially within the central region, is consistent with the reported correlations between the planktivorous queenfish and declining nearshore zooplankton volumetric biomass beginning circa 1980 (Miller et al. 2009).

The presence of latitutinal gradients in demersal fishes has been more equivocal. For example, variations in the SADs between regional areas for each open coast shelf stratum were muted in 2008. While some community variability was detected, which may indicate some latitudinal differences within shelf stratum, it was not at a statistically significant level. However, Love et al. (1986) found significant differences with latitude, but their sampling was more intensive and focused on a limited depth range. Hence, the relatively small sample size and large spatial scale may play a role in our study, with the interaction of the two masking potential latitudinal differences.

Demonstrative conclusions regarding factors (outside of depth influences) stimulating the dispersion of soft-bottom demersal fishes in the SCB is outside the scope of one set of summer samples. These patterns, however, do provide baseline information for future comparisons. As such, these data begin to address a critical void in our ability to evaluate impacts from growing concerns, particularly at large spatial scales, such as the expanding OMZ. Given the previously documented devastating effects of nearshore hypoxia (Grantham et al. 2004), the need for baseline ecological information is becoming

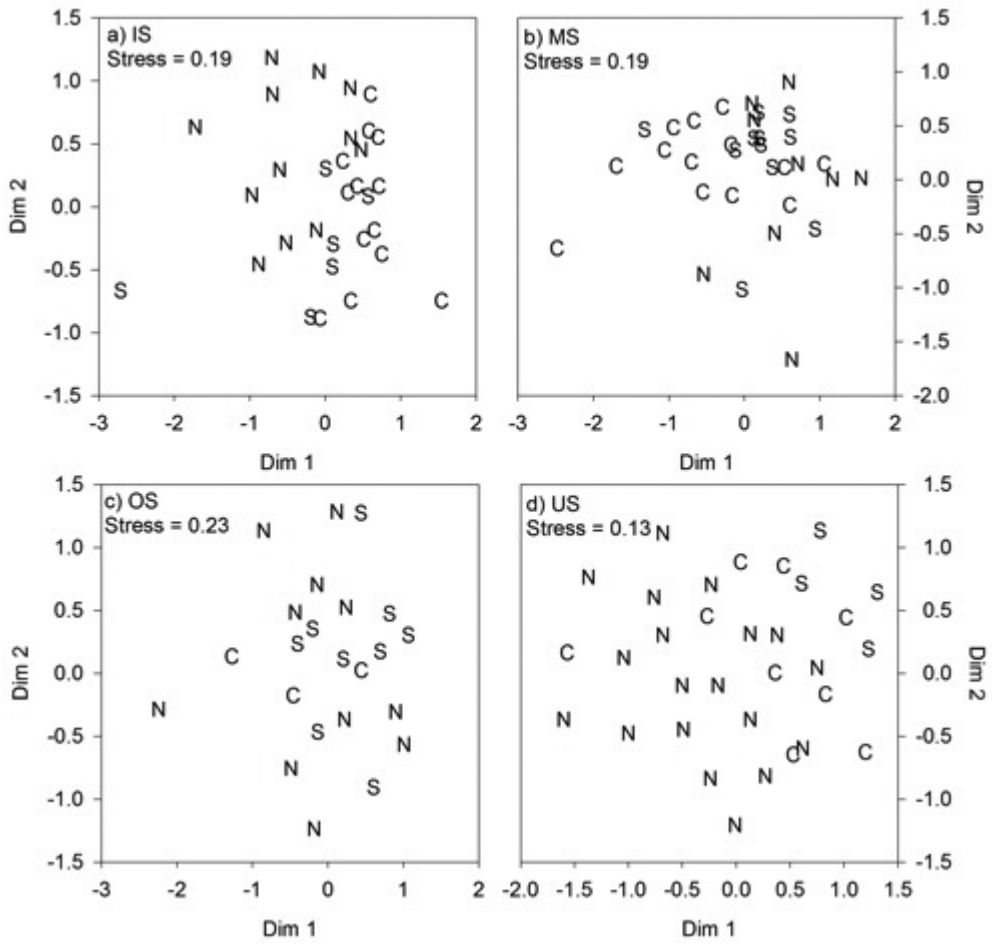

Figure 6. Nonmetric multidimensional scaling 2D distribution of stations based on sampled community density at each station segregated into latitudinal group (north = N, central = C, south = S) for the inner shelf (IS), middle shelf (MS), outer shelf (OS), and upper slope (US). Letters in each plot represent an individual station within the shelf stratum.

increasingly apparent. Programs such as the Bight 2008 demersal fish study may begin to fill this void.

Conclusions

The SCB demersal fish community was diverse and largely depth-stratified in 2008. Comparisons with previous reports indicated changes in the faunal composition have occurred, specifically the decline of the once abundant sciaenids white croaker and queenfish while various flatfish, especially sanddabs, continue to dominate the system. Bays and harbors remain unique along the SCB with several species largely limited to these areas. Likewise, the most abundant species on the upper slope were relatively uncommon along the other strata. The remaining shelf strata had a high degree of overlap amongst the species.

Acknowledgements

This report was prepared under the auspices of the Bight'08 Regional Monitoring Program and benefitted from comments and discussions with the Bight '08 Trawl Report Group. We would like to thank all the agencies participating in the regional survey. Comments by D. S. Beck and two anonymous reviewers greatly improved this manuscript. J. Rankin provided significant assistance with the preparation of the maps used. Discussions with C. Thomas significantly contributed impetus to undertake this analysis. This work was inspired by R. A. Miller.

LITERATURE CITED

Allen, M. J. 2006a. Pollution. *In*: The Ecology of Marine Fishes: California and Adjacent Waters, L. G. Allen, D. J. Pondella, II, and M. H. Horn, eds. University of California Press, Los Angeles, CA. pp. 595–610.

Allen, M. J. 2006b. Continental shelf and upper slope. *In*: The Ecology of Marine Fishes: California and Adjacent Waters, L. G. Allen, D. J. Pondella, II, and M. H. Horn, eds. University of California Press, Los Angeles, CA. pp. 167–202.

Allen, L. G. and D. J. Pondella, II. 2006. Ecological classifications. *In*: The Ecology of Marine Fishes: California and Adjacent Waters, L. G. Allen, D. J. Pondella, II, and M. H. Horn, eds. University of California Press, Los Angeles, CA. pp. 81–113.

Bertrand, J. A., L. G. De Sola, C. Papaconstantinou, G. Relini, and A. Souplet. 2002. The general specifications of the MEDITS surveys. Sci. Mar. 66:9–17.

Biagi, F., P. Sartor, G. D. Ardizzone, P. Belcari, A. Belluscio, and F. Serena. 2002. Analysis of demersal assemblages off the Tuscany and Latium coasts (northwestern Mediterranean). Sci. Mar. 66:233–242.

Bograd, S. J. and R. J. Lynn. 2003. Long-term variability in the Southern California Current system. Deep-Sea Res. II 50:2355–2370.

Bograd, S. J., C. G. Castro, E. Di Lorenzo, D. M. Palacios, H. Bailey, W. Gilly, and F. P. Chavez. 2008. Oxygen declines and the shoaling of the hypoxic boundary in the California current. Geophys. Res. Lett.35:L12607.

Brander, K. M. 2007. Global fish production and climate change. PNAS 104:19709–19714.

Chan, F., J. A. Barth, J. Lubchenco, A. Kirincich, H. Weeks, W. T. Peterson, and B. A. Menge. 2008. Emergence of anoxia in the California Current Large Marine Ecosystem. Science 319: 920.

Clarke, K. R. and M. Ainsworth. 1993. A method of linking multivariate community structure to environmental variables. Mar. Ecol. Prog. Ser. 92:205–219.

Dailey, M. D., J. W. Anderson, D. J. Reish, and D. S. Gorsline. 1993. The Southern California Bight: background and setting. *In:* Ecology of the Southern California Bight: a synthesis and interpretation, M. D. Dailey, D. J. Reish, and J. W. Anderson, eds. Los Angeles: University of California Press, pp. 1–18.

Dayton, P. K., S. F. Thrush, M. T. Agardy, and R. J. Hoffman. 1995. Environmental effects of marine fishing. Aquatic Conserv: Mar. Freshw. Ecosyst. 5:205–232.

DeMartini, E. E. and L. G. Allen. 1984. Diel variation in catch parameters for fishes sampled by a 7.6-m otter trawl in southern California coastal waters. Calif. Coop. Oceanic Fish. Invest. Rep. 25:119–134.

Diaz, R. J. and R. Rosenberg. 2008. Spreading dead zones and consequences for marine ecosystems. Science 321:926–929.

Environmental Quality Analysts and Marine Biological Consultants. 1975. Southern California Edison Company Long Beach Generating Station marine monitoring studies: 1975 annual report volume I.

Fager, E. W., A. R. Longhurst. 1968. Recurrent group analysis of species assemblages of demersal fish in the Gulf of Guinea. J. Fish. Res. Board Can. 25:1405–1421.

Grantham, B. A., F. Chan, K. J. Nielsen, D. S. Fox, J. A. Barth, A. Huyer, J. Lubchenco, and B. A. Menge. 2004. Upwelling-driven nearshore hypoxia signals ecosystem and oceanographic changes in the northeast Pacific. Nature 429:749–754.

Hickey, B. M. 1992. Circulation over the Santa Monica-San Pedro basin and shelf. Prog. Oceanog. 30:37–115.

Hidalgo, M., T. Rouyer, J. C. Molinero, E. Massuti, J. Moranta, B. Guijarro, and N. C. Stenseth. 2011. Synergistic effects of fishing-induced demographic changes and climate variation on fish population dynamics. Mar. Ecol. Prog. Ser. 426:1–12.

Hintze, J. L. 1998. Number Cruncher Statistical Systems. Kaysville, Utah.

Horn, M. H., L. G. Allen, and R. N. Lea. 2006a. Biogeography. *In*: The Ecology of Marine Fishes: California and Adjacent Waters, L. G. Allen, D. J. Pondella, II, and M. H. Horn, eds. University of California Press, Los Angeles, CA. pp. 3–25.

Hsieh, C., H. J. Kim, W. Watson, E. Di Lorenzo, and G. Sugihara. 2009. Climate-driven changes in abundance and distribution of oceanic fishes in the southern California region. Global Change Biology 15:2137–2152.

Juan-Jordá, M. J., J. A. Barth, M. E. Clarke, and W. W. Wakefield. 2009. Groundfish species associations with distinct oceanographic habitats in the Northern California Current. Fish. Ocean. 18:1–19.

Levin, L. A. 2003. Oxygen minimum zone benthos: adaptation and community response to hypoxia. Oceanogr. Mar. Biol. Ann. Rev. 41:1–45.

Love, M. S., J. S. Stephens, Jr., P. A. Morris, M. M. Singer, M. Sandhu, T. C. Sciarrotta. 1986. Inshore soft substrata fishes in the Southern California Bight: an overview. Calif. Coop. Oceanic Fish. Invest. Rep. 27:84–104.

McClatchie, S., R. Goericke, R. Cosgrove, G. Auad, and R. Vetter. 2010. Oxygen in the Southern California Bight: multidecadal trends and implications for demersal fisheries. Geophys. Res. Lett. 37:L19602.

McGill, B. J., R. S. Etienne, J. S. Gray, D. Alonso, M. J. Anderson, H. K. Benecha, M. Domelas, B. J. Enquist, J. L. Green, F. He, A. H. Hurlbert, A. E. Magurran, P. A. Maurer, A. Ostling, C.U. Soykan, K. I. Ugland, and E. P. White. 2007. Species abundance distributions: moving beyond single prediction theories to integration within an ecological framework. Ecol. Lett. 10:995–1015.

McGowan, J. A., S. J. Bograd, R. J. Lynn, and A. J. Miller. 2003. The biological response to the 1977 regime shift in the California Current. Deep-Sea Res. II 50:2567–2582.

Mearns, A. J. 1979. Abundance, composition, and recruitment of nearshore fish assemblages on the southern California mainland shelf. Calif. Coop. Oceanic Fish. Invest. Rep. 20:111–119.

Miller, E. F., J. P. Williams, D. J. Pondella, II, and K. T. Herbinson. 2009. Life history, ecology, and long-term demographics of queenfish. Marine and Coastal Fisheries: Dynamics, Management, and Ecosystem Science 4:187–199.

Perkins, E. M. 1995. An overview of hepatic neoplasms, putatively preneoplastic lesions, and associated conditions in fish sampled during the County Sanitation Districts of Orange County's 1986–1992 ocean monitoring program. Bull. South. Calif. Acad. Sci. 94:75–91.

Perry, R. I., P. Curry, K. Brander, S. Jennings, C. Möllmann, and B. Planque. 2010. Sensitivity of marine systems to climate and fishing: concepts, issues and management responses. J. Mar. Sys. 79:427–435.

Perry, A. L., P. J. Low, J. R. Ellis, J. D. Reynolds. 2005. Climate change and distribution shifts in marine fishes. Science 308:1912–1915.

Powers, S. P., C. H. Peterson, R. R. Christian, E. Sullivan, M. J. Powers, M. J. Bishop, and C. P. Buzzelli. 2005. Effects of eutrophication on bottom habitat and prey resources of demersal fishes. Mar. Eco. Prog. Ser. 302:233–243.

Schroeder, D. M. and M. S. Love. 2002. Recreational fishing and marine fish populations in California. Calif. Coop. Oceanic Fish. Invest. Rep. 43:182–190.

Shannon, C. H. and W. Weaver. 1962. The mathematical theory of communication. Urbana: University of Illinois Press. 117 pp.

Sokal, R. P. and F. J. Rohlf. 1995. Biometry: the principles and practice of statistics in biological research. 3rd ed. New York: W. H. Freeman and Co. 887 pp.

Stephens, J. S., Jr. and K. E. Zerba. 1981. Factors affecting fish diversity on a temperate reef. Env. Biol. Fish. 6:111–121.

Stevens, D. 1997. Variable density grid-based designs for continuous spatial populations. *Environmetrics* 8:167–195.

Stull, J. K. and C. Tang. 1996. Demersal fish trawls off Palos Verdes, Southern California, 1973–1993. California Calif. Coop. Oceanic Fish. Invest. Rep.37:211–240.

SYSTAT. 1998. Version 9. SPSS

Thompson, S. K. 1992. Sampling. J. Wiley and Sons. New York, NY.

Whittaker, R. H. 1952. A study of summer foliage insect communities in the Great Smokey Mountains. Eco. Mono. 22:1–44.

Whittaker, R. H. and C. W. Fairbanks. 1958. A study of plankton copepod communities in the Columbia Basin, southeaster Washington. Ecology 39:46–65.

APPENDIX A

Master species list of demersal fishes caught during 2008 Southern California Bight regional monitoring program.

Species	Common Name	Species	Common Name
Agonopsis sterletus	southern spearnose poacher	*Parophrys vetulus*	English sole
Anchoa compressa	deepbody anchovy	*Peprilus simillimus*	Pacific pompano
Anchoa delicatissima	slough anchovy	*Phanerodon furcatus*	white seaperch
Anoplopoma fimbria	sablefish	*Physiculus rastrelliger*	hundred-fathom codling
Argyropelecus affinis	slender hatchetfish	*Platyrhinoidis triseriata*	thornback
Argyropelecus lychnus	silver hachetfish	*Plectobranchus evides*	bluebarred prickleback
Argyropelecus sladeni	lowcrest hatchetfish	*Pleuronichthys decurrens*	curlfin sole
Artedius notospilotus	bonyhead sculpin	*Pleuronichthys guttulatus*	diamond turbot
Bathyagonus pentacanthus	bigeye poacher	*Pleuronichthys ritteri*	spotted turbot
Bathyraja interrupta	sandpaper skate	*Pleuronichthys verticalis*	hornyhead turbot
Careproctus melanurus	blacktail snailfish	*Porichthys myriaster*	specklefin midshipman
Ceratoscopelus townsendi	dogtooth lampfish	*Porichthys notatus*	plainfin midshipman
Cheilotrema saturnum	black croaker	*Raja inornata*	California skate
Chilara taylori	spotted cusk-eel	*Raja rhina*	longnose skate
Chitonotus pugetensis	roughback sculpin	*Rathbunella hypoplecta*	bluebanded ronquil
Citharichthys fragilis	Gulf sanddab	*Rhacochilus toxotes*	rubberlip seaperch
Citharichthys sordidus	Pacific sanddab	*Rhacochilus vacca*	pile perch
Citharichthys stigmaeus	speckled sanddab	*Rhinobatos productus*	shovelnose guitarfish
Citharichthys xanthostigma	longfin sanddab	*Rhinogobiops nicholsii*	blackeye goby
Cymatogaster aggregata	shiner perch	*Rimicola muscarum*	kelp clingfish
Embiotoca jacksoni	black perch	*Roncador stearnsii*	spotfin croaker
Enophrys taurina	bull sculpin	*Scorpaena guttata*	California scorpionfish
Eopsetta jordani	petrale sole	*Scorpaenichthys marmoratus*	cabezon
Eptatretus deani	black hagfish	*Sebastes atrovirens*	kelp rockfish
Eptatretus stoutii	Pacific hagfish	*Sebastes aurora*	aurora rockfish
Facciolella equatorialis	dogface witch eel	*Sebastes caurinus*	copper rockfish
Genyonemus lineatus	white croaker	*Sebastes chlorostictus*	greenspotted rockfish
Gibbonsia elegans	spotted kelpfish	*Sebastes crameri*	darkblotched rockfish
Gibbonsia metzi	striped kelpfish	*Sebastes dallii*	calico rockfish
Glyptocephalus zachirus	rex sole	*Sebastes diploproa*	splitnose rockfish
Gymnura marmorata	California butterfly ray	*Sebastes elongatus*	greenstriped rockfish
Heterostichus rostratus	giant kelpfish	*Sebastes eos*	pink rockfish
Hexagrammos decagrammus	kelp greenling	*Sebastes goodei*	chilipepper
Hippocampus ingens	Pacific seahorse	*Sebastes hopkinsi*	squarespot rockfish
Hippoglossina stomata	bigmouth sole	*Sebastes jordani*	shortbelly rockfish
Hydrolagus colliei	spotted ratfish	*Sebastes levis*	cowcod
Hypsurus caryi	rainbow seaperch	*Sebastes melanostomus*	blackgill rockfish
Icelinus burchami	dusky sculpin	*Sebastes miniatus*	vermilion rockfish
Icelinus cavifrons	pit-head sculpin	*Sebastes rosaceus*	rosy rockfish
Icelinus oculatus	frogmouth sculpin	*Sebastes rosenblatti*	greenblotched rockfish
Icelinus quadriseriatus	yellowchin sculpin	*Sebastes rubrivinctus*	flag rockfish
Icelinus tenuis	spotfin sculpin	*Sebastes rufus*	bank rockfish
Ilypnus gilberti	cheekspot goby	*Sebastes saxicola*	stripetail rockfish
Lepidogobius lepidus	bay goby	*Sebastes semicinctus*	halfbanded rockfish
Leptocottus armatus	Pacific staghorn sculpin	*Sebastes simulator*	pinkrose rockfish
Lestidiops ringens	slender barracudina	*Sebastes umbrosus*	honeycomb rockfish
Leuroglossus stilbius	California smoothtongue	*Sebastolobus alascanus*	shortspine thornyhead
Lycodapus fierasfer	blackmouth eelpout	*Sebastolobus altivelis*	longspine thornyhead
Lycodapus mandibularis	pallid eelpout	*Seriphus politus*	queenfish
Lycodes cortezianus	bigfin eelpout	*Squalus acanthias*	spiny dogfish
Lycodes diapterus	black eelpout	*Stenobrachius leucopsarus*	northern lampfish
Lycodes pacificus	blackbelly eelpout	*Symphurus atricaudus*	California tonguefish
Lyconema barbatum	bearded eelpout	*Syngnathus exilis*	barcheek pipefish
Lyopsetta exilis	slender sole	*Syngnathus leptorhynchus*	bay pipefish
Merluccius productus	Pacific hake	*Synodus lucioceps*	California lizardfish
Microstomus pacificus	Dover sole	*Torpedo californica*	Pacific electric ray
Mustelus henlei	brown smoothhound	*Umbrina roncador*	yellowfin croaker
Myliobatis californica	bat ray	*Urobatis halleri*	round stingray
Nezumia stelgidolepis	California grenadier	*Xeneretmus latifrons*	blacktip poacher
Odontopyxis trispinosa	pygmy poacher	*Xeneretmus leiops*	smootheye poacher
Ophiodon elongatus	lingcod	*Xeneretmus triacanthus*	bluespotted poacher
Oxylebius pictus	painted greenling	*Xenistius californiensis*	salema
Paralabrax clathratus	kelp bass	*Xystreurys liolepis*	fantail sole
Paralabrax maculatofasciatus	spotted sand bass	*Zalembius rosaceus*	pink seaperch
Paralabrax nebulifer	barred sand bass	*Zaniolepis frenata*	shortspine combfish
Paralichthys californicus	California halibut	*Zaniolepis latipinnis*	longspine combfish
Parmaturus xaniurus	filetail cat shark		

APPENDIX B-1

Area-weight adjusted mean density (count/1000 m²), standard error, frequency of occurrence (FO) and Index of Community Importance (ICI) rank for the demersal fishes caught during trawl surveys in the bay & harbor areas (n = 22) during the 2008 Southern California Bight regional monitoring survey.

Species	Mean Density (count/1000 m²)	Density Std. Err.	FO	ICI Rank
Genyonemus lineatus	22.67	9.94	7	1
Paralabrax nebulifer	1.85	0.75	15	2
Seriphus politus	7.22	2.54	6	3
Paralichthys californicus	0.79	0.16	15	4
Umbrina roncador	2.16	1.50	6	4
Paralabrax maculatofasciatus	0.75	0.26	10	6
Urobatis halleri	0.86	0.40	7	6
Cymatogaster aggregata	2.09	1.15	5	8
Anchoa delicatissima	1.65	1.31	5	9
Symphurus atricaudus	0.77	0.26	7	9
Porichthys myriaster	0.54	0.18	6	11
Cheilotrema saturnum	0.49	0.30	5	12
Citharichthys stigmaeus	0.84	0.39	3	13
Phanerodon furcatus	0.45	0.18	4	14
Heterostichus rostratus	0.08	0.13	4	15
Roncador stearnsii	0.34	0.12	3	16
Synodus lucioceps	0.30	0.15	3	16
Myliobatis californica	0.15	0.07	4	18
Embiotoca jacksoni	0.40	0.23	2	19
Hippocampus ingens	0.07	0.05	3	20
Pleuronichthys verticalis	0.11	0.05	3	20
Pleuronichthys ritteri	0.16	0.11	2	22
Pleuronichthys guttulatus	0.07	0.07	2	23
Raja inornata	0.11	0.06	2	23
Rhinobatos productus	0.09	0.06	2	23
Anchoa compressa	0.08	0.04	2	26
Icelinus quadriseriatus	0.13	—	1	26
Paralabrax clathratus	0.03	0.04	2	26
Rhinogobiops nicholsii	0.09	—	1	29
Ilypnus gilberti	0.09	—	1	30
Lepidogobius lepidus	0.07	—	1	30
Rhacochilus vacca	0.08	—	1	30
Gymnura marmorata	0.02	—	1	33
Xystreurys liolepis	0.04	—	1	33
Syngnathus leptorhynchus	0.04	—	1	33
Gibbonsia elegans	<0.01	—	1	33

APPENDIX B-2

Area-weight adjusted mean density (count/1000 m²), standard error, frequency of occurrence (FO) and Index of Community Importance (ICI) rank for the demersal fishes caught during trawl surveys in along the inner shelf (n = 32) during the 2008 Southern California Bight regional monitoring survey.

Species	Mean Density (count/1000 m²)	Density Std. Err.	FO	ICI Rank
Citharichthys stigmaeus	24.24	4.35	29	1
Pleuronichthys verticalis	1.58	0.34	21	2
Parophrys vetulus	1.74	0.67	14	3
Synodus lucioceps	1.08	0.36	17	4
Citharichthys sordidus	2.52	1.37	9	5
Icelinus quadriseriatus	1.86	0.86	9	6
Symphurus atricaudus	0.64	0.26	13	7
Cymatogaster aggregata	0.70	0.34	8	8
Paralichthys californicus	0.32	0.11	11	8
Chitonotus pugetensis	0.72	0.32	8	10
Pleuronichthys ritteri	0.28	0.10	10	11
Zalembius rosaceus	1.32	0.68	5	12
Xystreurys liolepis	0.22	0.07	11	13
Phanerodon furcatus	0.29	0.32	6	14
Citharichthys xanthostigma	0.21	0.09	7	15
Genyonemus lineatus	0.22	0.24	4	16
Leptocottus armatus	0.16	0.06	7	17
Odontopyxis trispinosa	0.23	0.15	5	17
Syngnathus exilis	0.12	0.06	6	19
Sebastes miniatus	0.23	0.13	3	20
Scorpaena guttata	0.06	0.02	6	21
Sebastes caurinus	0.23	0.13	3	21
Hypsurus caryi	0.17	0.09	4	23
Porichthys myriaster	0.09	0.04	5	23
Heterostichus rostratus	0.05	0.04	3	25
Hippoglossina stomata	0.06	0.04	3	25
Porichthys notatus	0.06	0.03	4	25
Pleuronichthys guttulatus	0.04	0.02	3	28
Rhacochilus toxotes	0.07	0.06	2	28
Platyrhinoidis triseriata	0.03	0.02	3	30
Sebastes atrovirens	0.04	0.03	2	31
Icelinus cavifrons	0.03	0.02	2	32
Paralabrax nebulifer	0.02	0.01	2	33
Raja inornata	0.02	0.01	2	33
Scorpaenichthys marmoratus	0.02	0.02	2	33
Sebastes dallii	0.02	0.01	2	33
Rhinobatos productus	0.05	—	1	37
Pleuronichthys decurrens	0.03	—	1	38
Artedius notospilotus	0.01	—	1	40
Zaniolepis latipinnis	0.01	—	1	40
Seriphus politus	0.01	—	1	40
Agonopsis sterletus	0.01	—	1	40
Rhinogobiops nicholsii	0.01	—	1	40
Gibbonsia metzi	0.01	—	1	40
Hexagrammos decagrammus	0.01	—	1	40
Oxylebius pictus	0.01	—	1	40
Embiotoca jacksoni	<0.01	—	1	40
Rimicola muscarum	<0.01	—	1	40
Roncador stearnsii	<0.01	—	1	40
Xenistius californiensis	<0.01	—	1	40

APPENDIX B-3

Area-weight adjusted mean density (count/1000 m²), standard error, frequency of occurrence (FO) and Index of Community Importance (ICI) rank for the demersal fishes caught during trawl surveys along the middle shelf (n = 33) during the 2008 Southern California Bight regional monitoring survey.

Species	Mean Density (count/1000 m²)	Density Std. Err.	FO	ICI Rank
Citharichthys sordidus	22.89	4.67	30	1
Icelinus quadriseriatus	17.68	4.45	30	2
Zalembius rosaceus	6.14	1.79	22	3
Zaniolepis latipinnis	5.37	1.70	23	3
Parophrys vetulus	5.90	3.95	21	5
Porichthys notatus	2.31	0.70	23	6
Pleuronichthys verticalis	1.34	0.30	27	7
Citharichthys xanthostigma	3.02	0.82	20	8
Symphurus atricaudus	2.02	0.56	22	9
Chitonotus pugetensis	2.96	0.84	18	10
Sebastes saxicola	2.48	0.96	16	11
Sebastes semicinctus	9.74	7.33	9	11
Microstomus pacificus	1.20	0.38	18	13
Citharichthys stigmaeus	3.00	1.34	11	14
Hippoglossina stomata	0.53	0.11	21	15
Zaniolepis frenata	0.97	0.39	12	16
Synodus lucioceps	0.51	0.19	16	17
Odontopyxis trispinosa	0.52	0.27	16	18
Sebastes dallii	0.97	0.71	8	19
Lepidogobius lepidus	0.56	0.28	7	20
Scorpaena guttata	0.21	0.07	10	21
Ophiodon elongatus	0.30	0.16	6	22
Raja inornata	0.11	0.03	11	22
Sebastes hopkinsi	0.23	0.17	4	24
Chilara taylori	0.11	0.05	7	25
Lyopsetta exilis	0.21	0.12	4	26
Xystreurys liolepis	0.12	0.06	5	26
Sebastes chlorostictus	0.18	0.14	4	28
Sebastes elongatus	0.10	0.05	5	28
Sebastes eos	0.08	0.05	4	30
Porichthys myriaster	0.06	0.03	4	31
Sebastes rosenblatti	0.06	0.03	4	31
Lycodes pacificus	0.07	0.04	3	33
Enophrys taurina	0.22	—	1	34
Sebastes miniatus	0.09	0.07	2	34
Xeneretmus latifrons	0.05	0.03	3	36
Sebastes rubrivinctus	0.06	0.05	2	37
Rathbunella hypoplecta	0.04	0.03	2	38
Genyonemus lineatus	0.03	0.02	2	39
Icelinus tenuis	0.02	0.01	2	40
Rhinogobiops nicholsii	0.02	0.01	2	40
Xeneretmus triacanthus	0.02	0.01	2	40
Cymatogaster aggregata	0.04	—	1	43
Sebastes umbrosus	0.04	—	1	44
Merluccius productus	0.01	—	1	45
Peprilus simillimus	0.01	—	1	45
Phanerodon furcatus	0.01	—	1	45
Plectobranchus evides	0.01	—	1	45
Pleuronichthys decurrens	0.01	—	1	45
Pleuronichthys ritteri	0.01	—	1	45
Sebastes jordani	0.01	—	1	45
Sebastes levis	0.01	—	1	45
Sebastes rosaceus	0.01	—	1	45
Sebastes rufus	0.01	—	1	45
Squalus acanthias	0.01	—	1	45
Torpedo californica	0.01	—	1	45

APPENDIX B-4

Area-weight adjusted mean density (count/1000 m²), standard error, frequency of occurrence (FO) and Index of Community Importance (ICI) rank for the demersal fishes caught during trawl surveys along the outer shelf (n = 23) during the 2008 Southern California Bight regional monitoring survey.

Species	Mean Density (count/1000 m²)	Density Std. Err.	FO	ICI Rank
Citharichthys sordidus	31.30	11.60	23	1
Lyopsetta exilis	26.54	5.60	23	2
Microstomus pacificus	3.71	0.57	23	3
Sebastes saxicola	10.36	2.56	20	4
Zaniolepis frenata	8.11	1.58	22	4
Lycodes pacificus	4.66	1.39	14	6
Parophrys vetulus	2.79	0.91	16	6
Xeneretmus latifrons	2.15	0.49	20	6
Porichthys notatus	2.19	0.90	14	9
Sebastes elongatus	1.00	0.30	15	10
Zalembius rosaceus	1.52	0.73	14	10
Sebastes semicinctus	2.16	0.93	12	12
Chilara taylori	0.48	0.15	12	13
Sebastes eos	0.33	0.10	12	14
Glyptocephalus zachirus	0.54	0.20	10	15
Sebastes diploproa	1.44	0.92	5	16
Zaniolepis latipinnis	0.64	0.30	6	16
Hippoglossina stomata	0.21	0.12	6	18
Sebastes rosenblatti	0.22	0.12	6	19
Merluccius productus	0.17	0.05	8	20
Sebastes chlorostictus	0.15	0.07	5	21
Pleuronichthys verticalis	0.25	0.17	4	22
Xeneretmus triacanthus	0.13	0.07	5	23
Eopsetta jordani	0.10	0.06	5	24
Hydrolagus colliei	0.09	0.04	5	24
Lycodes cortezianus	0.15	0.12	3	26
Sebastes melanostomus	0.28	—	1	27
Plectobranchus evides	0.09	0.07	3	28
Lyconema barbatum	0.04	0.03	3	29
Sebastes rubrivinctus	0.05	0.04	2	30
Citharichthys xanthostigma	0.06	—	1	31
Raja inornata	0.04	0.02	2	31
Raja rhina	0.03	0.02	2	31
Sebastes jordani	0.04	0.03	2	31
Citharichthys fragilis	0.04	—	1	36
Argyropelecus sladeni	0.01	—	1	37
Bathyraja interrupta	0.02	—	1	37
Icelinus tenuis	0.01	—	1	37
Mustelus henlei	0.02	—	1	37
Ophiodon elongatus	0.01	—	1	37
Scorpaena guttata	0.01	—	1	37
Sebastes goodei	0.01	—	1	37
Sebastes levis	0.02	—	1	37
Symphurus atricaudus	0.02	—	1	37

APPENDIX B-5

Area-weight adjusted mean density (count/1000 m²), standard error, frequency of occurrence (FO) and Index of Community Importance (ICI) rank for the demersal fishes caught during trawl surveys along the upper slope (n = 33) during the 2008 Southern California Bight regional monitoring survey.

Species	Mean Density (count/1000 m²)	Density Std. Err.	FO	ICI Rank
Lyopsetta exilis	16.18	4.12	30	1
Microstomus pacificus	5.01	1.48	30	2
Glyptocephalus zachirus	1.29	0.75	16	3
Sebastolobus alascanus	1.49	0.44	15	3
Sebastes diploproa	1.93	0.73	13	5
Merluccius productus	0.75	0.25	18	6
Lycodes pacificus	0.78	0.24	11	7
Xeneretmus latifrons	0.71	0.25	11	8
Lycodes cortezianus	0.50	0.13	14	9
Lyconema barbatum	1.02	0.80	8	9
Sebastes aurora	0.31	0.10	11	11
Facciolella equatorialis	0.42	0.17	9	12
Parophrys vetulus	0.34	0.13	8	13
Physiculus rastrelliger	0.61	0.35	6	14
Sebastes saxicola	0.77	0.55	5	15
Parmaturus xaniurus	0.19	0.07	8	16
Sebastes jordani	1.32	1.30	3	17
Nezumia stelgidolepis	0.21	0.10	7	18
Lycodes diapterus	0.28	0.12	7	19
Careproctus melanurus	0.12	0.04	10	20
Zaniolepis frenata	0.23	0.12	5	21
Sebastolobus altivelis	0.19	0.11	5	22
Stenobrachius leucopsarus	0.17	0.07	7	22
Lycodapus mandibularis	0.30	0.21	4	24
Bathyagonus pentacanthus	0.17	0.09	5	25
Raja rhina	0.08	0.03	6	26
Eptatretus stoutii	0.05	0.02	6	27
Sebastes melanostomus	0.12	0.09	3	28
Sebastes eos	0.06	0.03	4	29
Plectobranchus evides	0.03	0.01	4	30
Leuroglossus stilbius	0.07	0.05	2	31
Xeneretmus leiops	0.10	—	1	31
Icelinus burchami	0.06	—	1	33
Citharichthys sordidus	0.02	0.01	3	34
Porichthys notatus	0.02	0.02	2	34
Sebastes rosenblatti	0.04	0.03	2	34
Argyropelecus lychnus	0.07	—	1	37
Anoplopoma fimbria	0.02	0.01	2	38
Sebastes elongatus	0.02	—	1	39
Argyropelecus affinis	0.01	—	1	40
Chilara taylori	0.01	—	1	40
Argyropelecus sladeni	0.01	—	1	42
Ceratoscopelus townsendi	0.01	—	1	42
Eptatretus deani	0.01	—	1	42
Hydrolagus colliei	0.01	—	1	42
Icelinus oculatus	0.01	—	1	42
Lestidiops ringens	0.01	—	1	42
Lycodapus fierasfer	0.01	—	1	42
Sebastes crameri	0.01	—	1	42
Sebastes simulator	0.01	—	1	42

SEASONAL OCCURRENCES OF HUMBOLDT SQUID (*DOSIDICUS GIGAS*) IN THE NORTHERN CALIFORNIA CURRENT SYSTEM

MARISA N. C. LITZ AND A. JASON PHILLIPS
Cooperative Institute for Marine Resources Studies
Oregon State University
2030 Marine Science Drive
Newport, OR 97365
Tel. 541-867-0148
Fax: 541-867-0389
Email: litzm@onid.orst.edu

RICHARD D. BRODEUR AND ROBERT L. EMMETT
Estuarine and Ocean Ecology Program
NOAA Fisheries Northwest Fisheries Science Center
Newport Research Station
2032 SE OSU Drive
Newport, OR 97365

ABSTRACT

Recent visits by Humboldt squid (*Dosidicus gigas*) to the northern California Current system (CCS) were suggested to be related to larger climatic events such as El Niño, global warming, and expansion and shoaling of the oxygen minimum zone. Due to their plasticity in foraging behavior, coupled with an increased availability of prey resources, these excursions may also represent opportunistic foraging explorations. Fisheries-independent surveys initiated by the Northwest Fisheries Science Center in 1998 first encountered Humboldt squid in coastal waters off central Oregon and Washington in 2004. Squid ranging from 36–79 cm mantle length were caught during the following six years of sampling (2004–2009), with individuals generally increasing in abundance shoreward in late summer. The highest observed densities were in 2009 and measured 1,671 squid $(10^6\ m^3)^{-1}$. Physical features associated with increased squid catch included station depth, subsurface water temperature, ocean salinity, ocean density, and dissolved oxygen. In addition, the arrival of Humboldt squid onto the shelf in late summer was coincident with declines of juvenile (10–30 cm total length) Pacific hake (*Merluccius productus*), in contrast to the typical increases of hake recorded in late summer during recent years. Our results suggest that predator-prey interactions and ocean conditions in the CCS epipelagic zone lead to seasonal expansions, yet unsuccessful colonization attempts, by Humboldt squid populations. Identifying the economic and ecological impacts of this newly arrived predator should be a top research priority.

INTRODUCTION

Humboldt squid (also known as jumbo flying squid *Dosidicus gigas*) have recently visited the northern California Current system (CCS) and have been documented as far north as southeast Alaska (Pearcy 2002; Cosgrove 2005; Brodeur et al. 2006; Rodhouse et al 2006; Wing 2006; Field et al. 2007; 2008; Rodhouse 2008). They are voracious predators that can grow to 2 m and 50 kg within a year (Zeidberg and Robison 2007), and Markaida et al. (2004) found that Humboldt squid in the Gulf of California have one of the highest absolute growth rates of any squid species. In recent years off the U.S. West Coast, Humboldt squid appear to overlap in time and space with commercially important species such as Pacific hake (*Merluccius productus*), Pacific sardine (*Sardinops sagax*), and rockfish (*Sebastes* spp.), and are of major interest because of their potential ecosystem impacts (Field et al. 2007; Holmes et al. 2008).

Humboldt squid invaded waters off southern and central California in large numbers during the mid-1930s (Clark and Phillips 1936) then were virtually or totally absent until a short period in the mid-1970s, then virtually absent again until the 1990s (Field et al. 2007). Off Oregon, they were not observed until the 1997 El Niño, when Humboldt squid and other warm water species were documented over the continental shelf and slope from June through November in sea surface temperatures ranging from 13.4 to 14.3°C (Pearcy 2002). Between 2002 and 2009, Humboldt squid undertook seasonal foraging visits to the northern CCS, with many reports of summertime beach strandings/landings by commercial, scientific, and recreational fisheries off Oregon, Washington, and British Columbia (Cosgrove 2005; Brodeur et al. 2006; Trudel et al. 2006). However, little is known about the seasonal and interannual variability in the large-scale distribution of Humboldt squid in the northern CCS.

Several environmental and ecological factors have been implicated as potential drivers of the appearance of Humboldt squid in temperate waters of the northern CCS, including warming ocean temperatures, shoaling, or expansion of the oxygen minimum zone (OMZ), and overfishing of subtropical predators in the Eastern Tropical Pacific (Pearcy 2002; Gilly et al. 2006; Field et al. 2007; Zeidberg and Robison 2007; Rodhouse 2008). We hypothesize that an abundance of potential prey in the CCS, namely juvenile (10–30 cm total length [TL]) Pacific hake, Pacific sardine, northern anchovy (*Engraulis mordax*), rockfish, and myctophids, may be an equally important explanation for episodic appearances of Humboldt squid in the northern CCS. However, the biological and environmental mechanisms driving seasonal Humboldt squid visits remain poorly understood.

Here we analyze fishery and oceanographic information collected by NOAA Fisheries Northwest Fish-

eries Science Center (NWFSC) during recent surveys off Oregon and Washington (2004–2009) to examine the seasonal and interannual patterns in the occurrence of Humboldt squid. Records from these surveys represent a limited, though valuable comprehensive seasonal and annual time series of Humboldt squid catches in the Pacific Northwest to date. The objectives of this study were to explore recent catch data and find some connectivity between physical oceanographic conditions and the observed sporadic spatial and temporal occurrence of Humboldt squid in the northern California Current to provide important baseline monitoring information which will serve the research community when designing new studies. We hypothesize that changes in physical oceanographic conditions play an important role in determining ecological habitat for Humboldt squid, but also that the interactive processes of biology, prey availability, and fisheries could play a role.

METHODS

The NWFSC surveyed spring-fall marine resources off Oregon and Washington (2004–2009) by fishing at night in two separate studies: the Stock Assessment Improvement Program, or SAIP study, initiated in 2004 (see Phillips et al. 2009), and the Predator study, initiated in 1998 (see Emmett et al. 2006). Both studies fished a Nordic 264-rope trawl behind a chartered fishing vessel, but the SAIP study fished the headrope at midwater (30 m), while the Predator study fished the headrope at the surface. The SAIP study regularly sampled four transects monthly during May–September (and in November 2004 and October 2005), with stations ranging from 5–100 nautical miles (nm) offshore. A total of 412 nighttime midwater trawls were conducted between Hecata Head, OR (44°00N) and Willapa Bay, WA (46°40N; table 1a.). The Predator study sampled 535 nighttime trawls along two transects (5–30 nm from shore) off the mouth of the Columbia River, OR (46°10N) and Willapa Bay, WA (46°40N) biweekly from April–August in 2004–2009 (table 1b). While SAIP study stations spanned the shelf break and slope (station depths ranged from 55 to 3,150 m), Predator study stations were located primarily on the shelf (depths ranged from 28 to 293 m).

At each station, the trawl was towed astern of the fishing vessel for 15–30 minutes at a vessel speed averaging 3.1 kts. The deployed trawl had a mouth opening of 12 m deep by 28 m wide (336 m^2) based on previous determinations using a third-wire Simrad FS3300 backwards-looking net sounder (Emmett et al. 2004). For midwater trawls, a knotless, 6.1 m long, 3-mm mesh liner was sewn into the cod end; for surface trawls, the liner was 8-mm mesh. During both studies, all individuals caught were identified to the lowest taxon level possible and enumerated. We measured 30 randomly selected individuals of each species for length. In the event of a very large catch, we counted and weighed a subsample of each species and used the measured weight of the remaining catch to estimate the total number of individuals caught. In addition, we collected environmental information, including temperature, salinity, and water density from the surface down to 100 m (or within 5 m from the bottom at stations <100 m depth) prior to each trawl by deploying a Sea-Bird SBE SEALOGGER 25 (SAIP study) or SBE 19 SEACAT (Predator study) CTD profiler. Beginning in September 2008, the SBE 25 SEALOGGER CTD was outfitted with a dissolved oxygen (DO) sensor to measure in situ concentrations (ml L^{-1}). All CTD sensors were calibrated annually prior to the start of each cruise season.

Because of a disproportionate amount of zero catches, the relationship between environmental factors and Humboldt squid caught in our trawls was examined by a two-step or conditional modeling approach, using exploratory Generalized Additive Models (GAMs) with the mgcv-package (Wood 2006) available for R (v2.10.1) software (The R Foundation for Statistical Computing, http://www.r-project.org). GAMs were chosen for habitat analysis because the relationship between Humboldt squid and environmental variables was expected to be of a complex form, not easily fitted by standard linear or nonlinear models. GAM fitting techniques have been employed to understand and predict variations in cephalopod abundance in many systems (Bellido et al. 2001; Denis et al. 2002; Tian et al. 2009).

Both binomial and conditional Poisson GAMs were fitted to filtered data sets gathered on Humboldt squid during the SAIP Study (2004-2009). Humboldt squid presence/absence was first modeled against environmental data using (1) a binomial family fit with a logit-link function, using only stations that were repeatedly sampled over the six years where Humboldt squid were captured (n = 315 hauls). Next, Humboldt squid abundance (count), was modeled using (2) a Poisson distri-

TABLE 1
Abbreviations, descriptions, and sources of the large-scale environmental variables used in the Generalized Additive Models (GAMs).

Abbreviation	Description and source
MEI	Multivariate El Niño-Southern Oscillation Index. From the NOAA Earth System Research Laboratory Web site: http://www.cdc.noaa.gov/ENSO/enso.mei_index.html.
PDO	Pacific Decadal Oscillation Index. From the University of Washington (Nathan Mantua administrator) Web site: http://jisao.washington.edu/pdo/.
UI	Upwelling Index for 45°N, 125°W. From the NOAA Southwest Fisheries Science Center Environmental Research Division live access server Web site: http://www.pfeg.noaa.gov/products/las.html.

TABLE 2

Research cruise dates for two NOAA Fisheries Northwest Fisheries Science Center studies occurring from 2004–2009: (a) the Stock Assessment Improvement Program (SAIP) study; and (b) the Predator study. Information presented for each cruise includes survey year, dates, latitude range (°N), distance range of stations offshore (in nautical miles), total number of transects, total trawls completed (and trawls containing Humboldt squid, *Dosidicus gigas* in parentheses), total number of *D. gigas* caught, and the associated dorsal mantle length range (ML in cm).

a. Stock Assessment Improvement Program (SAIP) study nighttime cruises 2004–2009

Year	Survey Dates	Start-end latitude	Distance range offshore	Number of transects	Total number of trawls (trawls containing *D. gigas*)	Total number of *D. gigas*	Length range
2004	6/30–7/01	44°40	5–85	1	5[D]	–	–
2004	8/04–8/08	44°00–44°40	5–75	2	13	–	–
2004*	8/31–9/04	44°00–44°40	5–75	2	15 (4)	15	47–66
2004*	11/05–11/11	44°00–46°40	9–65	4	20 (8)	32	50–67
2005	6/07–6/11	44°00–46°40	10–45	4	15	–	–
2005*	7/11–7/14	44°00–46°40	10–40	3	11 (1)	1	52
2005	8/15–8/19	44°00–46°40	10–55	4	20	–	–
2005	9/19–9/23	44°40–46°40	10–55	3	14	–	–
2005*	10/19–10/24	44°00–46°40	9–65	4	21 (1)	1	62
2006	5/15–5/16	46°40	10–40	1	4	–	–
2006	6/15–6/17	46°10–46°40	10–40	2	7	–	–
2006*	8/07–8/11	44°00–46°40	10–55	4	18 (1)	70	46–63
2006*	9/24–8/28	44°00–46°40	10–55	4	20 (8)	33	51–68
2007	5/17–5/21	44°00–46°40	10–55	4	16	–	–
2007	6/16–6/20	44°00–46°40	10–55	4	16	–	–
2007	7/18–7/20	44°00–44°40	11–55	2	8	–	–
2007*	8/15–8/19	44°00–46°40	11–55	4	18 (5)	32	48–68
2007*	9/11–9/15	44°00–46°10	10–55	3	15 (3)	7	56–68
2008	5/18–5/21	44°00–46°10	20–55	3	12	–	–
2008	6/16–6/20	44°00–46°10	20–100	3	13	–	–
2008	7/15–7/19	44°00–46°40	20–55	4	15	–	–
2008	8/11–8/15	44°00–46°40	10–55	4	19	–	–
2008*	9/22–9/24	44°00–44°40	11–55	2	10 (1)	17	50–68
2009	5/16–5/20	44°00–46°40	11–55	4	17	–	–
2009	6/14–6/18	44°00–46°40	20–55	4	16	–	–
2009*	7/16–7/20	44°00–46°40	20–55	4	16 (1)	9	49–61
2009*	8/18–8/22	44°00–46°40	10–55	4	18 (6)	37	51–68
2009*	9/14–9/18	44°00–46°40	10–55	4	20 (9)	27	52–67

*Cruises with *D. gigas*
[D]Two of these trawls occurred during the daytime

bution family with over-dispersed residual errors and a log link (Ciannelli et al. 2008; 2010), using only stations with positive squid catches (n = 48 hauls). GAMs took the general form:

1) SAIP *Dosidicus gigas* Presence/Absence ~ s ("Environmental Variable")
2) SAIP *Dosidicus gigas* Count ~ Offset(ln(Volume Filtered)) + s("Environmental Variable")

The use of an offset term is necessary in Poisson-distributed models, which only accept integers as input variables (in our case squid catch). For these GAMs, the offset term was needed to standardize Humboldt squid catch by the volume filtered by the fishing net (in m^3). Humboldt squid captured in tows from the SAIP study were selected as response variables because Humboldt squid did not occur frequently enough in Predator study tows (n = 12) to allow a formal analysis. Environmental variables (covariates) considered included station depth, surface (5 m) and subsurface (20 m) temperature, salinity, density, and DO (September 2008 and May–September 2009 only). These two depth strata were chosen because they corresponded best with the mixed layer depth and maximum depth of the thermocline. Stratification in the water column was approximated by taking the difference between the surface and subsurface water properties (i.e., 5 m–20 m temperature, salinity, density, and DO). Biological covariates consisted of the five dominant potential prey densities (Field et al. 2007) including northern anchovy, juvenile Pacific hake, Pacific herring (*Clupea pallasi*), Pacific sardine, whitebait smelt (*Allosmerus elongatus*), and euphausiids (Euphausiidae). We also evaluated Humboldt squid in relation to three large scale environmental variables (MEI, UI, and PDO; table 1). Models were penalized for increased curvature or increased nodes and were evaluated based on minimizing Un-Biased Risk Estimator (UBRE) for the binomial model or Generalized Cross Validation (GCV) scores for the Poisson model (Wood 2006).

TABLE 2 (cont'd.)

Research cruise dates for two NOAA Fisheries Northwest Fisheries Science Center studies occurring from 2004–2009: (a) the Stock Assessment Improvement Program (SAIP) study; and (b) the Predator study. Information presented for each cruise includes survey year, dates, latitude range (°N), distance range of stations offshore (in nautical miles), total number of transects, total trawls completed (and trawls containing Humboldt squid, *Dosidicus gigas* in parentheses), total number of *D. gigas* caught, and the associated dorsal mantle length range (ML in cm).

b. Predator study nighttime cruises 2004–2009

Year	Survey Dates	Start-end latitude	Distance range offshore	Number of transects	Total number of trawls (trawls containing *D. gigas*)	Total number of *D. gigas*	Length range
2004	4/28–4/30	46°10–46°40	4–25	2	11	–	–
2004	5/08–5/10	46°10–46°40	4–30	2	12	–	–
2004	5/18–5/20	46°10–46°40	4–30	2	11	–	–
2004	5/29–5/31	46°10–46°40	4–30	2	12	–	–
2004	6/13–6/15	46°10–46°40	4–30	2	12	–	–
2004	6/13–6/25	46°10–46°40	4–30	2	12	–	–
2004	7/06–7/08	46°10–46°40	4–30	2	12	–	–
2004	7/17–7/19	46°10–46°40	4–30	2	12	–	–
2004	8/10–8/12	46°10–46°40	4–30	2	12	–	–
2005	4/19–4/21	46°10–46°40	4–30	2	12	–	–
2005	5/02–5/04	46°10–46°40	4–30	2	12	–	–
2005	5/12–5/14	46°10–46°40	4–30	2	12	–	–
2005	5/24–5/26	46°10–46°40	4–30	2	12	–	–
2005	6/04–6/06	46°10–46°40	4–30	2	12	–	–
2005	6/13–6/15	46°10–46°40	4–30	2	12	–	–
2005	6/26–6/28	46°10–46°40	4–30	2	12	–	–
2005	7/06–7/08	46°10–46°40	4–30	2	12	–	–
2005	7/30–8/01	46°10–46°40	4–25	2	11	–	–
2005	8/11–8/13	46°10–46°40	4–30	2	12	–	–
2006	5/11–5/13	46°10–46°40	4–30	2	12	–	–
2006	5/25–5/27	46°10–46°40	4–30	2	12	–	–
2006	6/01–6/03	46°10–46°40	4–30	2	12	–	–
2006	6/12–6/14	46°10–46°40	4–30	2	12	–	–
2006	7/05–7/07	46°10–46°40	4–30	2	12	–	–
2006	7/17–7/19	46°10–46°40	4–25	2	11	–	–
2006	8/15–8/17	46°10–46°40	4–30	2	12	–	–
2006*	8/28–8/30	46°10–46°40	4–30	2	12 (1)	2	59–63
2007	5/07–5/09	46°10–46°40	5–30	2	10	–	–
2007	5/22–5/24	46°10–46°40	5–25	2	10	–	–
2007	6/04–6/06	46°10–46°40	5–25	2	10	–	–
2007	6/21–6/23	46°10–46°40	5–25	2	9	–	–
2007	7/08–7/09	46°40	5–23	1	5	–	–
2007	7/23–7/25	46°10–46°40	5–25	2	10	–	–
2007	8/05–8/07	46°10–46°40	4–25	2	9	–	–
2007	8/21–8/23	46°10–46°40	4–25	2	10	–	–
2008	5/24–5/26	46°10–46°40	5–25	2	10	–	–
2008	6/12–6/14	46°10–46°40	5–25	2	9	–	–
2008	6/21–6/23	46°10–46°40	5–25	2	9	–	–
2008	7/01–7/03	46°10–46°40	5–25	2	10	–	–
2008	7/21–7/23	46°10–46°40	5–25	2	9	–	–
2008	8/05–8/07	46°10–46°40	4–30	2	12	–	–
2009	5/09–5/11	46°10–46°40	4–25	2	11	–	–
2009	5/23–5/25	46°10–46°40	5–25	2	10	–	–
2009	6/06–6/08	46°10–46°40	5–25	2	10	–	–
2009	6/20–6/22	46°10–46°40	5–25	2	9	–	–
2009*	7/07–7/09	46°10–46°40	5–25	2	9 (1)	5	51–56
2009	7/23–7/25	46°10–46°40	4–25	2	11	–	–
2009*	8/08–8/10	46°10–46°40	5–30	2	11 (1)	25	48–66
2009	8/23–8/25	46°10–46°40	4–30	2	12 (9)	2299	36–79

* Cruises with *D. gigas*

RESULTS

We caught Humboldt squid in 48 of 412 trawls and during every year of the SAIP study, representing a Frequency of Occurrence (FO) of 12% (table 2a). Dorsal mantle lengths (ML) for SAIP squid ranged from 46–68 cm over all years (table 2a). Length frequency histograms for SAIP study Humboldt squid catches by month and year is given in Figure 1. Comparisons of the SAIP squid lengths within each year by month found that squid significantly (t-tests, all $p < 0.05$) increased in size from

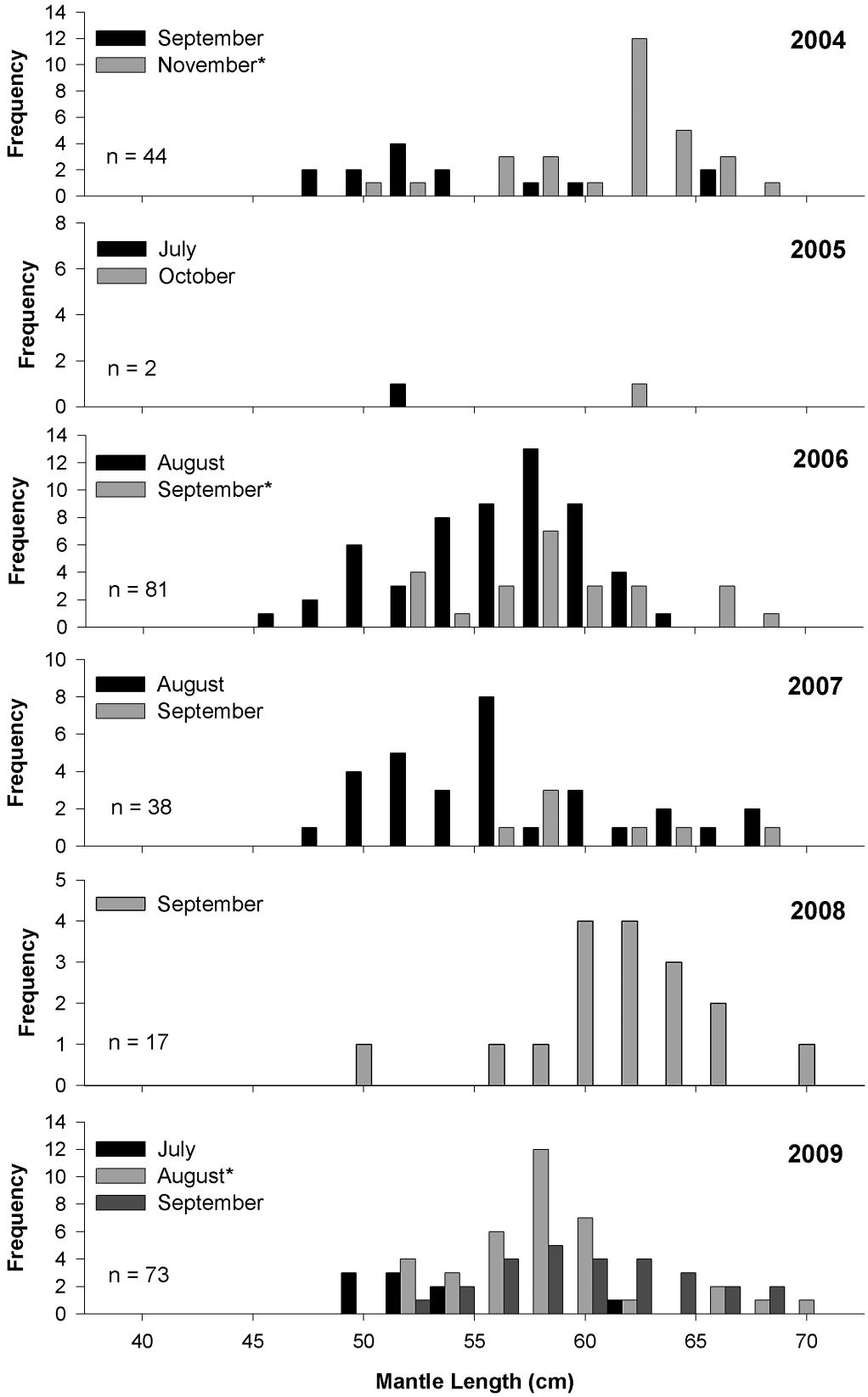

Figure 1. Length frequency histogram for dorsal mantle length (ML [cm]) measurements of Humboldt squid (*Dosidicus gigas*) caught in monthly Stock Assessment Improvement Program (SAIP) study nighttime midwater trawls shown in Figures 2 and 3 (n = 255). Only months with positive catches of *D. gigas* are presented. Months followed by a "*" represent months where lengths were significantly larger than measurements in a previous cruise. There were too few length measurements in 2005 and 2007 for statistical comparison.

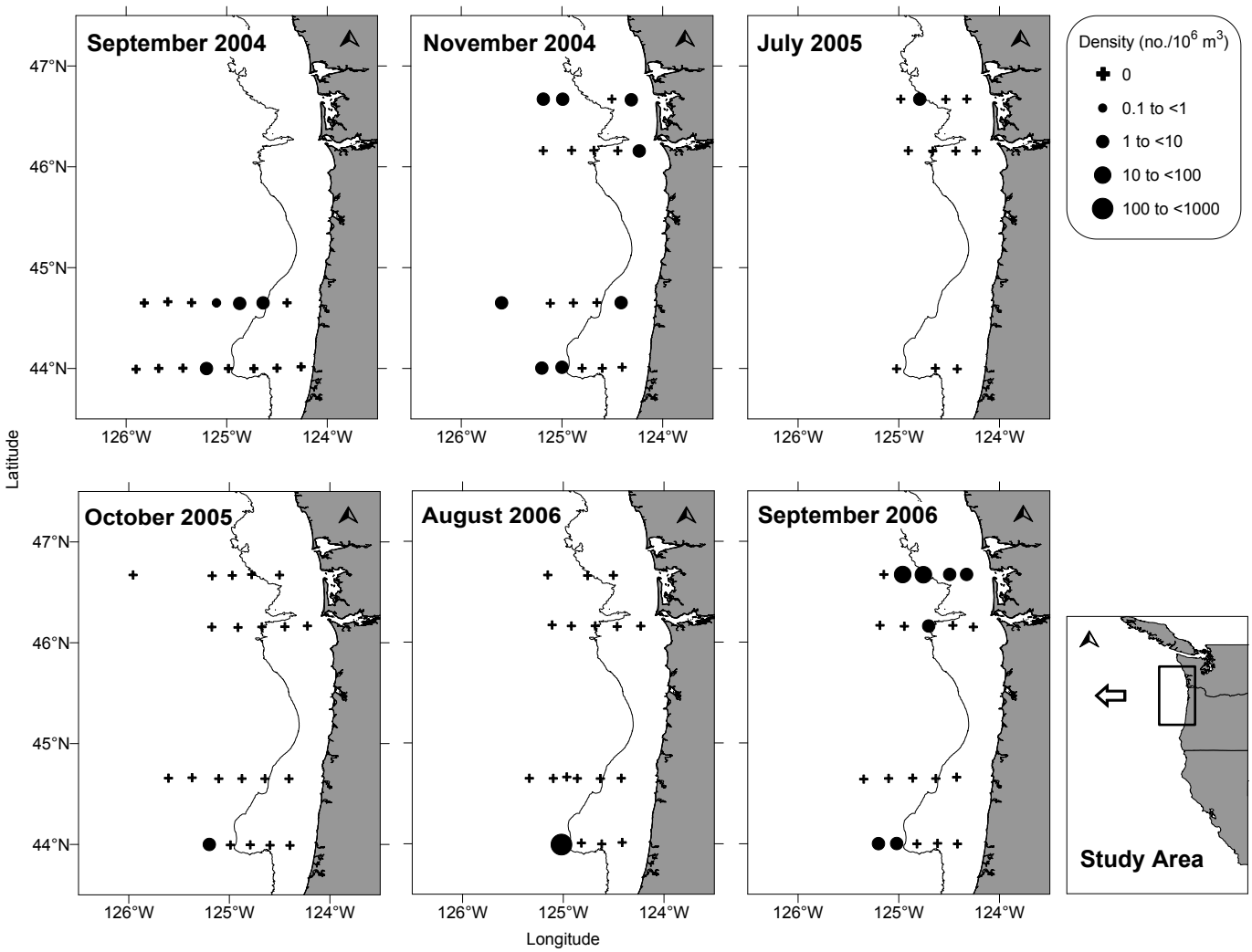

Figure 2. Maps showing the distribution and density (number $[10^6\ m^3]^{-1}$) of Humboldt squid (*Dosidicus gigas*) captured during monthly spring-fall nighttime Stock Assessment Improvement Program (SAIP) study midwater trawls between 2004 and 2006. Each map shows the shelf break isobath (200 m) and trawls with zero squid catch are represented by a "+". Despite similar sampling grids, no Humboldt squid were captured in cruises during the following months: June–August 2004, June, August–September 2005, or May–June 2006 (not shown).

September to November 2004, August to September 2006, July to August 2009, but not from August to September 2007 or 2009. Visual inspection of Humboldt squid densities and distributions for cruises with positive catches indicated that most squid were found off the shelf before August, but moved onto the shelf in later months (figs. 2 and 3).

Minimum DO concentration (ml L^{-1}) typically was observed near the bottom of each CTD cast, as expected, and at times reached levels considered hypoxic for some organisms (<1.40 ml L^{-1}). We plotted minimum DO values integrated over our entire sampling grid for cruises after 2008 in Figure 3, with Humboldt squid densities and distributions overlaid over the DO values. The highest densities of Humboldt squid occurred in August 2009 and were in hypoxic nearshore waters off the Columbia River (fig. 3).

Catches of Humboldt squid from surface trawls conducted by the Predator study in 2004–2009 were much rarer than the SAIP study. The FO for Predator study trawls was only 2% (12 of 535 trawls; table 2b). Furthermore, 11 of the 12 positive squid trawls during the Predator study were in 2009, with the only other positive trawl in July 2006. However, in August 2009, 43% of all Predator study trawls contained Humboldt squid, including one 30 minute surface trawl 20 nm off the mouth of the Columbia River at a station depth of 135 m, which contained 1,872 individuals (density of 1,671 squid $[10^6\ m^3]^{-1}$) and estimated biomass of ~25 metric tons [mt]). These individuals showed tremendous size variation, ranging from 36 to 79 cm ML (table 2b) and their density far exceeded densities (25 squid $[10^6\ m^3]^{-1}$) measured within their native range of the Gulf of California during March and April 2007 and November

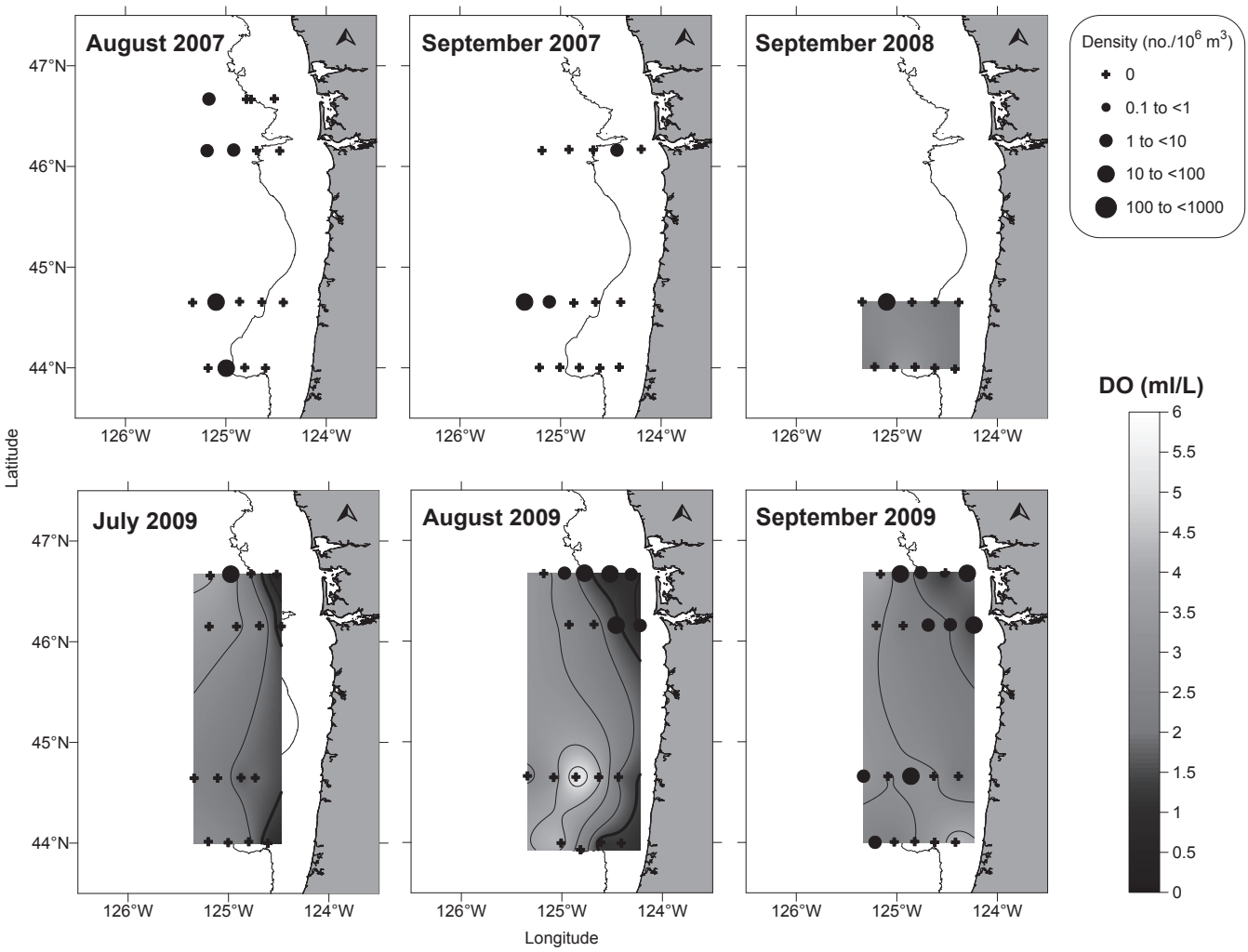

Figure 3. Maps showing the distribution and density (number [10^6 m^3]$^{-1}$) of Humboldt squid (*Dosidicus gigas*) captured during monthly spring-fall nighttime Stock Assessment Improvement Program (SAIP) study midwater trawls between 2007 and 2009. Each map shows the shelf break isobath (200 m) and trawls with zero squid catch are represented by a "+". Despite similar sampling grids, no Humboldt squid were captured in cruises during the following months: May–July 2007, May–August 2008, May–June 2006, or May–June 2009 (not shown). Beginning in 2008, we measured dissolved oxygen (DO) concentration (ml L^{-1}) from the surface to 100 m depth (or within 5 m of the bottom in stations where the depth <100 m) prior to each trawl. The last four panels show minimum DO values measured over the water column. Note the aggregation of Humboldt squid in the area of hypoxic DO conditions (>1.4 ml L^{-1}; dark black contour) during August 2009 on the shelf of the two northernmost transects (Willapa Bay and Columbia River).

2008 (Matteson and Benoit-Bird 2009). At the time of capture, large numbers of squid were observed at the surface near the vessel along with schools of adult Pacific sardine breaking the surface (personal observation).

For the SAIP study, GAMs (table 3, fig. 4) provided best-fit models and significant ($p < 0.05$) environmental variables for Humboldt squid catch data. For the binomial GAMs, salinity ranked best as an explanatory variable for Humboldt squid presence/absence (table 3, fig. 4a). For the Poisson distribution GAMs, station depth and subsurface water temperature, salinity and density at 20 m were all significantly ($p < 0.05$) associated with Humboldt squid and ranked best (lowest GCV scores without being overfit) among all models (table 3), with larger squid catches associated with a station depth of approximately 1000 m, and water at 20 m measuring 11–13°C, 32.4–32.8 psu, and 24.5–25.0 kg m^{-3}, respectively (fig. 4b). No large-scale environmental variables were reliably associated with Humboldt squid catches because of model over-fitting (fig. 4). GAMs run with a limited data set in which measurements of DO were included yielded insignificant results. Additionally, no biotic factors (prey fish) were significant variables explaining Humboldt squid catch in SAIP study tows, partially because there were too few prey measurements to allow a formal analysis.

Despite higher Humboldt squid FO in SAIP study cruises compared to Predator study cruises from 2004–2009, we observed the highest overall squid densities during Predator study cruises in 2009 (eight cruises alto-

TABLE 3

Output for Humboldt squid (*Dosidicus gigas*) two-part conditional Generalized Additive Models (GAMs), showing the association between Humboldt squid catch and environmental covariates from the Stock Assessment Improvement Program (SAIP) study. The left side (1) shows the results of GAMs from 315 tows (2004–2009) using a binomial family fit with a logit-link function on Humboldt squid presence-absence data. Individual covariates were individually explored and can be ranked by Un-Biased Risk Estimator (UBRE) score (smallest to largest). The associated p-values, fit, adjusted R-squared values, and percent deviance explained are also given. The right side (2) shows results from over-dispersed Poisson GAMs using only the 48 positive tows for squid catch fit with catch data and the log of the volume filtered. Environmental covariates for these GAMs are ranked by Generalized Cross Validation (GCV) score; associated p-values, fit, adjusted R-squared values, and percent deviance explained are also presented. The best models based on lowest UBRE/GCV scores are shown in bold. Covariates examined, but excluded from the analyses because of insufficient data or over fitting include: the large-scale environmental variables: MEI, PDO and UI; dissolved oxygen concentration, the difference between 5 and 20 m temperature, and the associated prey densities of northern anchovy (*Engraulis mordax*), juvenile (10–30 cm total length) Pacific hake (*Merluccius productus*), Pacific herring (*Clupea pallasi*), Pacific sardine (*Sardinops sagax*), whitebait smelt (*Allosmerus elongatus*), and euphausiids (Euphausiidae) from each tow.

	1. Binomial GAMs (n = 315 hauls)					2. Over-dispersed Poisson GAMs (n = 48 hauls)				
Variable	UBRE	p-value	Fit	Adjusted R-sq	Deviance Explained (%)	GCV	p-value	Fit	Adjusted R-sq	Deviance Explained (%)
Salinity 20 m	**–0.169**	*	+	**0.035**	**5.0**	**12.483**	**	+/–	**–0.348**	**39.1**
Density 20 m	–0.123	n.s.	n.s.	0.005	1.3	**12.573**	**	+/–	**–0.265**	**49.7**
Station Depth	–0.134	n.s.	n.s.	–0.003	0.1	**14.228**	***	+/–	**–0.778**	**30.7**
Salinity 5 m	**–0.163**	**	+	**0.026**	**3.5**	14.823	*	overfit	–0.853	41.8
Temperature 20 m	–0.147	n.s.	overfit	0.036	4.9	**15.566**	*	+/–	**–0.939**	**22.1**
Density 5 m	–0.126	n.s.	n.s.	0.004	1.7	16.097	*	overfit	–0.445	41.8
Salinity Difference	–0.143	n.s.	n.s.	0.005	1.1	16.171	n.s.	n.s.	–1.110	19.3
Density Difference	–0.139	n.s.	n.s.	0.023	4.3	17.608	n.s.	n.s.	–1.460	17.7
Temperature 5 m	–0.167	n.s.	overfit	0.043	6.7	18.650	n.s.	n.s.	–3.170	0.6

Significance codes: 'n.s.' p > 0.05 '*' p < 0.05 '**' p < 0.01 '***' p < 0.001

gether). We compared the time-series of squid density, sea surface temperature (SST at 3 m), and potential prey density (juvenile hake) observations from each Predator study cruise in 2009 (fig. 5). The PDO Index was in phase with SST measured at the effective sampling depth of our surface trawls (3 m; fig. 5a), and was more representative of in situ ocean conditions measured during the eight Predator study cruises of 2009 than either the MEI or UI (not shown). A clear pattern emerged between increasing SST (and PDO Index) and increasing juvenile hake density through August. However, when we began catching Humboldt squid at high densities in August 2009, juvenile hake density fell to zero (fig. 5).

DISCUSSION

Changes in ocean conditions probably contributed to northward seasonal expansions of Humboldt squid to waters off Oregon and Washington from 2004–2009. The NWFSC first captured Humboldt squid in 2004, while surveying marine resources using midwater trawls offshore of Hecata Head, OR as part of the SAIP study (fig. 2). In 2006, we recorded the first incidence of Humboldt squid in surface trawls during the Predator study (table 2b). The summer of 2006 was particularly noteworthy due to a severe expanse of hypoxic water ranging across the shelf in nearshore waters from Cape Perpetua, OR (44°17) north to La Push, WA (47°54) (Chan et al. 2008). Seasonal hypoxia has been observed in nearshore waters off Oregon and Washington in all years beginning in 2002, although the most severe event occurred in the summer of 2006 (Chan et al. 2008). The repeated hypoxic events off Oregon and Washington are considered by some to be a symptom of climate change (Grantham et al. 2004; Levin et al. 2009). Humboldt squid are extremely tolerant of low DO (Gilly et al. 2006), and on this basis we hypothesize that the low DO in shelf waters off Oregon and Washington may be suitable habitat for these aggressive predators.

During August and September 2006, we retained a subsample of Humboldt squid from the SAIP study and Field et al. (2007) conducted a dietary analysis on these specimens (n = 24; mean ML = 54 cm in August and 58 cm in September). Although net feeding may have biased results (Field et al. 2007), primary prey items in decreasing order of abundance included juvenile Pacific hake, northern lampfish (*Stenobrachius leucopsarus*), blue lanternfish (*Tarletonbeania crenularis*), Pacific sardine, euphausiids, and shortbelly rockfish (*Sebastes jordani*). Other prey items included crustaceans, pteropods, cephalopods, other unidentified coastal pelagics, mesopelagics, and flatfish. While not necessarily representative for their whole distribution range, these findings are consistent with other diet studies that found Humboldt squid prey on sardine (Ehrhardt et al. 1983; Markaida and Sosa-Nishizaki

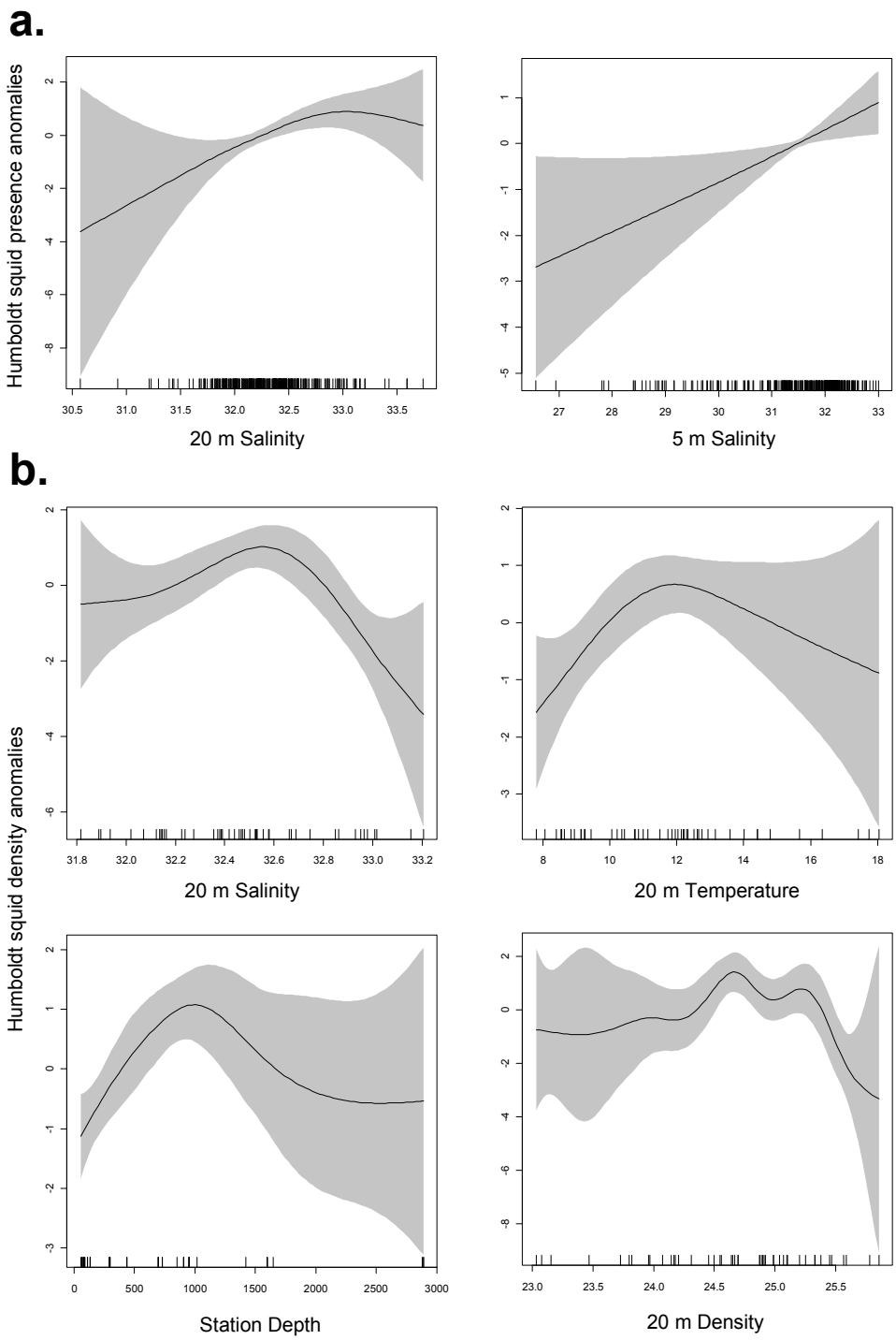

Figure 4. Significant outputs for the environmental variables used to fit the (a) binomial distribution, and (b) over-dispersed Poisson distribution Generalized Additive Models (GAMs) shown in Table 1. Variation in covariate main effects are shown along the x-axes, whereas the y-axes represent spline smoother functions for Humboldt squid (*Dosidicus gigas*). The grey area represents 95% confidence intervals surrounding the covariate main effect.

2003), hake (Markaida and Sosa-Nishizaki 2003), mackerel (Sato 1976; Ehrhardt et al. 1983), and anchovies (Sato 1976; Markaida et al. 2008), all of which are major fisheries in the CCS that could be impacted by range expansion of this predator. Furthermore, recent evidence of predatory attacks on juvenile and adult Pacific salmon (*Oncorhynchus* spp.; L. Weitkamp, NWFSC Newport and J. Field, SWFSC Santa Cruz, personal communication) suggests that salmonids may be impacted by Humboldt squid predators as well. There is clearly a need to develop alternative Humboldt squid diet sampling strategies to better understand their prey field for future work.

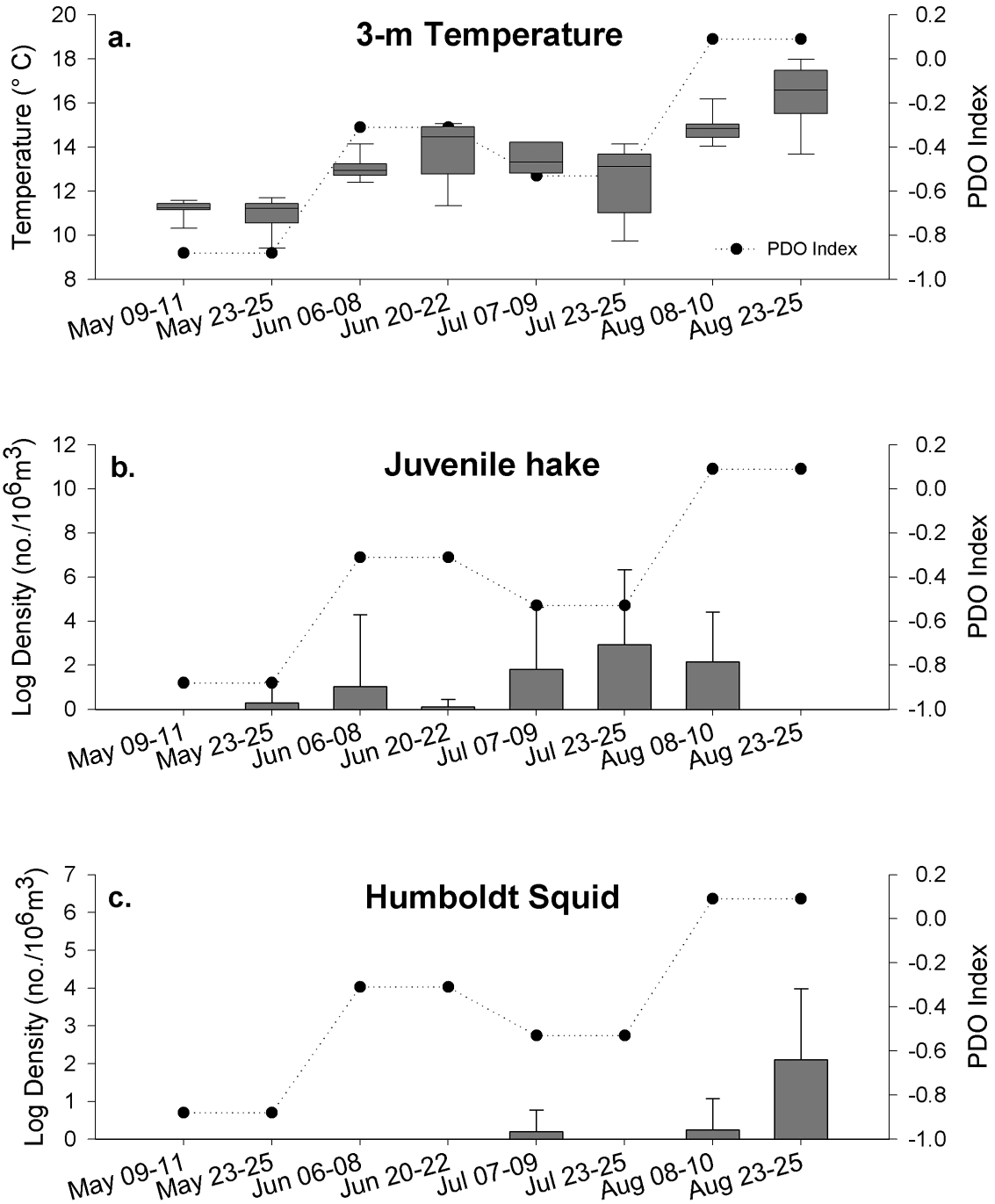

Figure 5. Plots showing (a) surface (3 m) temperature; (b) density (number [10^6 m^3]$^{-1}$) of juvenile (10–30 cm total length) Pacific hake (*Merluccius productus*); and (c) density (number [10^6 m^3]$^{-1}$) of Humboldt squid (*Dosidicus gigas*) recorded during the eight NOAA Fisheries Northwest Fisheries Science Center Predator study cruises conducted biweekly between May and August 2009 (dates on x-axis). Overlaid behind each plot is the monthly value of the Pacific Decadal Oscillation (PDO) Index during each sampling period. Note the absence of juvenile Pacific hake during the last cruise (August 23–25, 2009), coincident with high densities of Humboldt squid.

Humboldt squid have been shown to exhibit tremendous variability in their growth rates and age at maturity (Keyl et al. 2008). In both the SAIP and Predator studies, squid captured earlier in the sampling season (July–August) tended to be smaller than squid captured in later cruises (September–November), which we hypothesize is related to growth (fig. 1). However, as an aggressive and fast-growing predator, capable of migrating up to 30 km day^{-1} and making diel vertical migrations upwards of 1,000 m (Gilly et al. 2006), the physiological and energetic demands of growing so large so quickly, coupled with a semelparous reproductive strategy, make growth patterns in individuals encountered during our study difficult to estimate.

Humboldt squid are opportunistic predators, yet Pacific hake ranging from 2–42 cm TL represented the most numerically important prey item from northern CCS samples in diet studies to date (Field et al. 2007). Prior to the 1997 El Niño, juvenile Pacific hake were rarely documented in the northern CCS. Recent surveys have revealed northward expansion of hake spawning and juvenile recruitment habitat (Phillips et al. 2007; Ressler et al. 2007), which overlaps with the observed range expansion of Humboldt squid from 2004–2009. We found that juvenile hake densities were reduced coincident with Humboldt squid presence in the northern CCS in 2009 (fig. 5), which was unexpected given that juvenile hake density within our study area in recent years increased in late summer (Emmett et al. 2006; Phillips et al. 2007). However, the degree to which this was significant is unknown. Total commercial U.S. landings of Pacific hake decreased from 248 thousand mt in 2008 to 122 thousand mt in 2009, a reduction of 51% (Stewart et al. 2011), and similarly low total U.S. commercial hake landings were reported in 2010 (161 thousand mt). Holmes et al. (2008) suggested that squid predation as well as secondary effects on schooling behavior and distribution of Pacific hake was important to this fishery, but the primary reason for the decline in total U.S. hake catches in 2009 and 2010 was the decline in coastwide allowable catches (optimal yield), based on stock assessment results (Stewart et al. 2011).

While it is unlikely that the current data sources will be able to detect squid-related changes in population dynamics, our results indicate that the top-down effects of predation exerted on Pacific hake by Humboldt squid could have a negative effect on recruitment of this important species. Currently, Pacific hake represent the largest fishery along the U.S West Coast. There is evidence from the Chilean hake fishery that squid may have a large and adverse impact on abundance due to direct predation of individuals of all sizes (Alarcón-Muñoz et al. 2008). Ongoing research at the NWFSC includes developing an index of hake recruitment in the northern California Current, quantifying the bioenergetic effects of the Humboldt squid on prey resources in this region (e.g., Field et al. 2007), and modeling the potential ecosystem impacts of Humboldt squid on extant fish populations.

Our GAM analyses confirmed that Humboldt squid was most likely to occur in warmer (12–14°C) water temperatures in water at approximately 1000 m depth. Subsurface salinity was also a significant covariant with Humboldt squid density, revealing the importance of understanding the physical and biological dynamics of the epipelagic region as an area of opportunistic predation. Follow-up work should include more detailed and broader scale distribution information and include data from daytime trawling and/or acoustics. Unfortunately, there were too few DO measurements to provide meaningful results in our GAMs, although we still consider DO a reasonable explanatory abiotic variable for future consideration, particularly given the observed association between squid and DO in August 2009 (fig. 3). Our GAM findings are consistent with observations from recent tagging (Gilly et al. 2006) and diet (Field et al. 2007; Markaida et al. 2008) studies implicating that the dynamics of the upper boundary of the OMZ is important to Humboldt squid foraging ecology. We conclude that the physical properties (including the OMZ) and source water (from basin-wide phenomenon such as El Niño) of the epipelagic region determines community structure within the northern CCS, and is critical in determining seasonal Humboldt squid foraging visits.

The fact that no biotic factors (prey fish density) ranked as significant covariates with Humboldt squid in SAIP tows in any of our GAMs was related to differences in catchability of the prey sampled at 30 m in SAIP study midwater tows, patchy distribution both temporally and spatially for the prey field and Humboldt squid, and perhaps predator avoidance (table 3, fig. 4). The reliance on midwater trawl caught data from night efforts is too limiting to draw strong conclusions owing to the highly variable catchability of the different species, variability of diurnal behavior among the different prey species and the highly variable day-night depth distributions among all species. Many prey fish in the northern CCS are at the surface at night (Emmett et al. 2004; 2006), and therefore sampling the density and distribution of prey fishes is best accomplished by fishing at the surface at night. The effect of surface-caught prey (from Predator study catches) on Humboldt squid density is not represented in the biotic variables presented in our GAM analysis, and should be addressed in future studies.

Despite similar sampling efforts by the NWFSC in 2010, no Humboldt squid were caught off Oregon and Washington from May–September (Litz unpublished data). Based on these results, we conclude that ocean conditions were not favorable in 2010 to support a northerly shift of Humboldt squid and/or that available prey resources were not as abundant in 2010 as in other years. In addition, the lack of any known occurrences of larval or juvenile specimens in the northern CCS implies there was no Humboldt squid spawning or recruitment off Oregon and Washington during 2008–2009, and that the seasonal visits of Humboldt squid to the northern CCS during the period from 2004 to 2009 were opportunistic and probably related to feeding and not reproduction. However, ongoing research efforts in waters off Oregon and Washington will continue to monitor future Humboldt squid foraging visits, habitat associations, and predator-prey relationships within the northern California Current.

ACKNOWLEDGEMENTS

The authors would like to thank the captains and crew of the F/V *Piky* and the R/V *Miller Freeman* for their expertise in conducting all research trawls used for this study. We are grateful to T. Britt for managing the SAIP database. T. Auth generously provided all SAIP study CTD data and provided valuable comments on an earlier draft of this manuscript, along with P. Bentley and A. Claiborne, to whom we are also indebted for their tireless efforts in the field. We would also like to thank M. Hunsicker, J. Holmes, and two anonymous reviewers for their helpful comments and constructive criticism. We are grateful to L. Ciannelli and J. Ruzicka for providing insight on statistical methods and ecosystem modeling techniques we consider important for future endeavors. Conversations with J. Field and W. Gilly about Humboldt squid feeding habits and physiology were invaluable. Funding for the collection and analysis of these data comes from the Bonneville Power Administration and the NWFSC Stock Assessment Improvement Program.

LITERATURE CITED

Alarcón-Muñoz, R., L. Cubillos, and C. Gatica. 2008. Jumbo squid (*Dosidicus gigas*) biomass off central Chile: Effects on Chilean hake (*Merluccius gayi*). Calif. Coop. Oceanic Fish. Invest. Rep. 49: 157–166.

Bellido, J. M., G. J. Pierce, and J. Wang. 2001. Modeling intra-annual variation in abundance of squid *Loligo forbesi* in Scottish waters using generalized additive models. Fish Res. 52(1-2):23–39.

Brodeur, R. D., S. Ralston, R. L. Emmett, M. Trudel, T. D. Auth, and A. J. Phillips. 2006. Anomalous pelagic nekton abundance, distribution, and apparent recruitment in the northern California Current in 2004 and 2005. Geophys. Res. Lett. 33 doi:10.1029/2006GL026614.

Chan, F., J. A. Barth, J. Lubchenco, A. Kirincich, H. Weeks, W. T. Peterson, and B. A. Menge. 2008. Emergence of anoxia in the California Current Large Marine Ecosystem. Science. 319:920.

Ciannelli, L., P. Fauchald, K. S. Chan, V. N. Agostini, and G. E. Dingsør. 2008. Spatial fisheries ecology: Recent progress and future prospects. J. Mar. Syst. 71:223–236.

Ciannelli, L., H. Knutsen, E. M. Olsen, S. H. Espeland, L. Asplin, A. Jelmert, J. A. Knutsen, and N. C. Stenseth. 2010. Small-scale genetic structure in a marine population in relation to water circulation and egg characteristics. Ecology. 91(10):2918–2930.

Clarke, F. N. and J. B. Phillips. 1936. Commercial use of the jumbo squid, *Dosidicus gigas*. Calif. Fish Game. 22:143–144.

Cosgrove, J. A. 2005. The first specimens of Humboldt squid in British Columbia. PICES Press 13(2):30–31.

Denis, V., J. Lejeune, and J. P. Robin. 2002. Spatio-temporal analysis of commercial trawler data using General Additive models: patterns of Loliginid squid abundance in the north-east Atlantic. ICES J. Mar. Sci. 59:633–648.

Emmett, R. L., R. D. Brodeur, and P. M. Orton. 2004. The vertical distribution of juvenile salmon (*Onchorhynchus* spp.) and associated fishes in the Columbia River plume. Fish. Oceanogr. 13:392–402.

Emmett, R. L., G. K. Krutzikowsky, and P. J. Bentley. 2006. Abundance and distribution of pelagic piscivorous fishes in the Columbia River plume during spring/early summer 1998–2003: Relationship to oceanographic conditions, forage fishes and juvenile salmonids. Prog. Oceanogr. 68(1):1–26.

Ehrhardt, N. M., P. S. Jacquemin, F. García B., G. González D., J. M. López B., J. Ortiz C., and A. Solís N. 1983. On the fishery and biology of the giant squid *Dosidicus gigas* in the Gulf of California, Mexico. *In*: Advances in assessment of world cephalopod resources, J. F. Caddy, ed. FAO Fish. Tech. Pap. 231:306–339.

Field, J. C., K. Baltz, A. J. Phillips, and W. A. Walker. 2007. Range expansion and trophic interactions of the jumbo squid, *Dosidicus gigas*, in the California Current. Calif. Coop. Oceanic Fish. Invest. Rep. 48:131–146.

Field, J. C. 2008. Jumbo squid (*Dosidicus gigas*) invasions in the Eastern Pacific Ocean. Calif. Coop. Oceanic Fish. Invest. Rep. 49:79–81.

Gilly, W. F., U. Markaida, C. H. Baxter, B. A. Block, A. Boustany, L. Zeidberg, K. Reisenbichler, B. Robison, G. Bazzino, and C. Salinas. 2006. Vertical and horizontal migrations by jumbo squid *Dosidicus gigas* revealed by electronic tagging. Mar. Ecol. Prog. Ser.324:1–17.

Grantham, B. A., F. Chan, K. J. Nielsen, D. S. Fox, J. A. Barth, A. Huyer, J. Lubchenco, and B. A. Menge, 2004. Upwelling-driven nearshore hypoxia signals ecosystem and oceanographic changes in the northeast Pacific. Nature 429:749–754.

Holmes, J., K. Cooke, and G. Cronkite. 2008. Interactions between jumbo squid (*Dosidicus gigas*) and Pacific hake (*Merluccius productus*) in the northern California Current in 2007. Calif. Coop. Oceanic Fish. Invest. Rep. 49:129–141.

Keyl, F., J. Argüelles, L. Mariátegui, R. Tafur, M. Wolff, and C. Yamashiro. 2008. A hypothesis on range expansion and spatio-temporal shifts in size-at-maturity of jumbo squid (*Dosidicus gigas*) in the Eastern Pacific Ocean. Calif. Coop. Oceanic Fish. Invest. Rep. 49:119–128.

Levin, L. A., W. Ekau, A. J. Gooday, F. Jorissen, J. J. Middleburg, W. Nagvi, C. Neira, N. N. Rabalais, and J. Zhang. 2009. Effects of natural and human-induced hypoxia on coastal benthos. Biogeosci. Disc. 6(2):3563–3654.

Markaida, U. and O. Sosa-Nishizaki. 2003. Food and feeding habits of jumbo squid *Dosidicus gigas* (Cephalopoda: Ommastrephidae) from the Gulf of California, Mexico. J. Mar. Bio. Assn. U.K. 83:507–522.

Markaida, U., C. Quiñonez-Velasquez, and O. Sosa-Nishizaki. 2004. Age, growth and maturation of jumbo squid *Dosidicus gigas* (Cephalopoda: Ommastrephidae) from the Gulf of California, Mexico. Fish. Res. 66:31–47.

Markaida, U., W. F. Gilly, C. A. Salinas-Zavala, R. Rosas-Luis, and J. A. T. Booth. 2008. Food and feeding of jumbo squid *Dosidicus gigas* in the central Gulf of California during 2005–2007. Calif. Coop. Oceanic Fish. Invest. Rep. 49:90–103.

Matteson, R. S. and K. J. Benoit-Bird. 2009. Humboldt squid distribution in three-dimensional space as measured by acoustics in the Gulf of California. J. Acoustic. Soc. Am. 125(4):2550.

Pearcy, W. G. 2002. Marine nekton off Oregon and the 1997–98 El Niño. Prog. Oceanogr. 54:399–403.

Phillips A. J., S. Ralston, R. D. Brodeur, T. D. Auth, R. L. Emmett, C. Johnson, and V. G. Wespestad. 2007. Recent pre-recruit Pacific hake (*Merluccius productus*) occurrences in the northern California Current suggest a northward expansion of their spawning area. Calif. Coop. Ocean Fish. Invest. Rep. 48:215–229.

Phillips A. J., R. D. Brodeur, and A. V. Suntsov. 2009. Micronekton community structure in the epipelagic zone of the northern California Current upwelling system. Prog. Oceanogr. 80:74–92.

Ressler, P. H., J. A. Holmes, G. W. Fleischer, R. E. Thomas, and K. D. Cooke. 2007. Pacific hake (*Merluccius productus*) autecology: A timely review. Mar. Fish. Rev. 69:1–24.

Rodhouse, P. G. with C. M. Waluda, E. Morales-Bojórquez, and A. Hernández-Herrera 2006. Fishery biology of the Humboldt squid, *Dosidicus gigas*, in the Eastern Pacific Ocean. Fish. Res. 79:13–15.

Rodhouse, P. G. 2008. Large-scale range expansion and variability in ommastrephid squid populations: a short review. Calif. Coop. Ocean Fish. Invest. Rep. 49:83–89.

Sato, T. 1976. Results of exploratory fishing for *Dosidicus gigas* (D'Orbigny) off California and Mexico. FAO Fish Rep. 170(Supl. 1):61–67.

Stewart, I. J., R. E. Forrest, C. Grandin, O. S. Hamel, A. C. Hicks, S. J. D. Martell, and I. G. Taylor. 2011. Status of the Pacific hake (Whiting) stock in U.S. and Canadian Waters in 2011. Joint U.S. and Canadian *Hake* Technical Working Group. Final SAFE document. 217 pp.

Tian, S., X. Chen, Y. Chen, L. Xu, and X. Dai. 2009. Standardizing CPUE of *Ommastrephes bartramii* for Chinese squid-jigging fishery in Northwest Pacific Ocean. Chin. J. Oceanogr. Limnol. 27(4):729–739.

Trudel, M., G. Gillespie, J. Cosgrove, and B. Wing. 2006. Warm water species in British Columbia and Alaska. p. 53. *In*: DFO. State of the Pacific Ocean 2005. DFO Sci. Ocean Status Report. 2006/001.

Wood, S. M. 2006. Generalized Additive Models, An Introduciton with R. London: Chapman and Hall, 392 pp.

Wing, B. L. 2006. Unusual invertebrates and fish observed in the Gulf of Alaska, 2004–2005. PICES Press. 14(2):26–28.

Zeidberg, L. D. and B. H. Robison. 2007. Invasive range expansion by the Humboldt squid, *Dosidicus gigas*, in the eastern North Pacific. Proc. Nat. Acad. Sci. 104:12948–12950.

A NOTE ON THE DETECTION OF THE NEUROTOXIN DOMOIC ACID IN BEACH-STRANDED *DOSIDICUS GIGAS* IN THE SOUTHERN CALIFORNIA BIGHT

FERNANDA F. M. MAZZILLO
Department of Ocean Sciences
University of California at Santa Cruz
1156 High Street
Santa Cruz, California 95064, USA
mazzillo@gmail.com
1-831-459-2948

DANNA J. STAAF
Hopkins Marine Station
Stanford University
Oceanview Boulevard
Pacific Grove, California 93950, USA

JOHN C. FIELD
Fisheries Ecology Division
Southwest Fisheries Science Center
National Marine Fisheries Service
110 Shaffer Road
Santa Cruz, California 95060, USA

MELISSA L. CARTER, MARK D. OHMAN
Scripps Institution of Oceanography
University of California at San Diego
9500 Gilman Drive
La Jolla, California 92093-0218, USA

ABSTRACT

The first occurrence of the neurotoxin domoic acid (DA) in Humboldt squid (*Dosidicus gigas*) during a toxic *Pseudo-nitzschia* bloom in the Southern California Bight is reported. Bloom levels of cells within the *Pseudo-nitzschia delicatissima* group were detected on 6 July 2009 at 4 nearshore collection sites in the Southern California Bight (Scripps Pier, Newport Pier, Goleta Pier and Sterns Wharf). Particulate DA was detected in all of these locations, except for Newport Pier. Stranded Humboldt squid were found south of the Scripps pier 5 days after the toxic bloom was detected. DA was measured using ELISA and low DA concentrations were detected in the stomach or mantle tissue of the stranded specimens. Stomach content analysis indicated that possible DA vectors to Humboldt squid included both pelagic (Pacific hake, *Merluccius productus*, and Pacific sardine, *Sardinops sagax*) and nearshore (pile surfperch, *Damalichthys vacca*, and shiner surfperch, *Cymatogaster aggregata*) fish species. Although low DA levels were detected in stranded squid specimens, neurological symptoms of DA toxicity were not observed and low DA concentrations alone may not have been the cause of the strandings. Further studies should focus on DA toxic effects in *D. gigas* to verify whether this pelagic predator can be affected by a toxin frequently detected in pelagic ecosystems influenced by the California Current System.

INTRODUCTION

The Humboldt squid *Dosidicus gigas* is a large neritic-oceanic squid and an important link between lower trophic levels and apex predators in the pelagic food web. *D. gigas* is an opportunistic predator of small mesopelagic, pelagic and demersal fish, crustaceans and squid (Markaida and Sosa-Nishizaki 2003; Field et al. 2007) and common prey for billfish, sharks, pinnipeds, and toothed whales (Olson and Watters 2003; Ruiz-Cooley et al. 2004; Vetter et al. 2008). *D. gigas* is endemic to the eastern Pacific Ocean between 30°N and 20–25°S and 140°W (Nigmatullim et al. 2001) and can cover great horizontal distances within this range at speeds up to 30 km d^{-1} (Gilly et al. 2006). Poleward excursions have been reported in both hemispheres, with significant range expansions taking place over the past decade (Zeidberg and Robison 2007; Field et al. 2007; Alarcón-Muñoz et al. 2008).

Large-scale (ranging from dozens to thousands of individuals) beach stranding events of *D. gigas* have taken place both historically and recently along the Eastern Pacific rim, particularly in the fringes of the squid's range and during periods of episodic high abundance (Mearns 1988; Alarcón-Muñoz et al. 2008). Beach strandings frequently result in flurries of short-term media attention and speculation into the causes of mortality, often with minimal scientific consultation. The frequency and range of reporting on these events has spiked over the past five to ten years along the west coast of the USA and Canada (fig. 1). Among the most significant strandings in recent years include events in July 2002 in La Jolla, CA; October 2003 in Carmel, CA; October 2004 in Westport, WA; January 2005 in Los Angeles and Newport Beach, CA; March 2005 in Oceanside, CA; October 2008 in Westport, WA; July 2009 in La Jolla, CA (samples reported in this manuscript); September 2009 in Westport, WA, Seaside, OR and Vancouver Island, British Columbia (J. Field, unpublished data). The reasons for *D. gigas* mortality and strandings remain unknown.

The primary focus of this paper is to explore the hypothesis that *D. gigas* can be exposed to domoic acid (DA) during toxic *Pseudo-nitzschia* algal blooms. Investigation of this hypothesis may help understand whether or not domoic acid poisoning (DAP) can be considered a contributing factor to *D. gigas* mortality and strandings. DA is a neurotoxin produced by several species of the diatom *Pseudo-nitzschia* (Moestrup and Lundholm 2007) and has caused mass mortality of marine mammals and

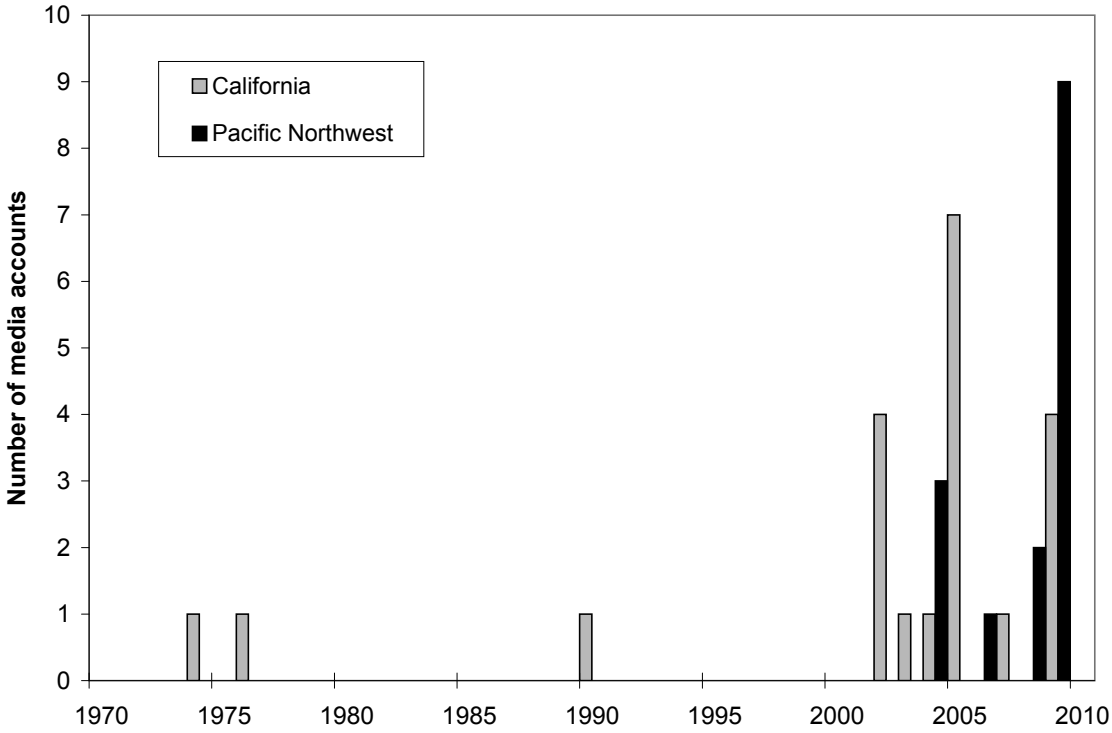

Figure 1. Frequency of media reports of stranding events in California and the Pacific Northwest over the past forty years.

birds (Work et al. 1993; Scholin et al. 2000). However, determining that DAP is the cause of death in marine animal strandings is difficult. Studies that have come to that conclusion used a combination of observations such as (1) DA detection in hundreds of specimens in question and/or in their prey items; (2) DA detection in the water along with high concentration ($<10^4$ cells L^{-1}) of DA-producing cells; and (3) observations of typical DA neurological symptoms (i.e., seizures, ataxia, head weaving, and stereotypic scratching) and (4) histopathology to show lesion in hippocampus brain region characteristic of DA poisoning (Work et al. 1993; Scholin et al. 2000; Gulland et al. 2002).

Accordingly, pelagic predators have been detected with DA, but DA toxicity effects and whether or not DA could cause the death of these animals have not been verified. For example, North Atlantic right whales (*Eubalaena glacialis*), pygmy sperm whales (*Kogia breviceps*) and dwarf sperm whales (*Kogia sima*) found stranded along the U.S. Atlantic coast were tested positive with low DA levels (Fire et al. 2009; Leandro et al. 2010), but DA toxicity symptoms were not determined in these studies and thus DA could not be related to the cause of stranding. However, Leandro et al. (2010) hypothesized that the observed long-term exposure of North Atlantic right whales to DA may perhaps enhance mortality due to other well-documented factors in their populations since it has been found that chronic DA exposure can impair navigational abilities of other marine mammals such as sea lions (Goldstein et al. 2007). Furthermore, high DA levels have been found in feces and prey of blue whales (*Balaenoptera musculus*) and humpback whales (*Megaptera novaeangliae*) during a toxic *Pseudo-nitzschia* bloom in Monterey Bay (California, USA) (Lefebvre et al. 2002). Although DA toxicity was not observed, the high DA doses that these whales were exposed to could lead to DA neurotoxicity effects (Lefebvre et al. 2002).

Additionally, DA has been detected in cephalopods such as market squid (*Loligo opalescens*), cuttlefish (*Sepia officinalis*) and common octopus (*Octopus vulgaris*) after feeding on DA-contaminated prey items (Costa et al. 2004; 2005; Bargu et al. 2008). *D. gigas* could be exposed to DA through a variety of vectors. Humboldt squid are active predators of small pelagic fish such as northern anchovies (*Engraulis mordax*) and Pacific mackerel (*Scomber japonicus*) (Markaida and Sosa-Nishizaki 2003; Markaida 2006; Field et al. 2007), which have been previously identified as DA vectors to marine mammals and birds (Sierra-Beltran et al. 1998; Lefebvre et al. 1999). Krill are also a potential vector of DA, as they are a prey item of *D. gigas* (Field et al. 2007) and have been found to acquire DA (Bargu et al. 2003). Furthermore, Pacific hake consume both krill and northern anchovies (Buckley and Livingston 1997; Mackas et al. 1997), and are a key prey item of *D. gigas* in California waters (Field et al. 2007).

DA effects in cephalopods have not been confirmed. Only a few studies focused on the DA effects in invertebrates, mostly shellfish, and the results are conflict-

ing (Maeda et al. 1987; Jones et al. 1995a; b; Dizer et al. 2001; Blanco et al. 2006; Liu et al. 2007a, b, 2008). However, *D. gigas* might be susceptible to DA neurotoxicity effects. DA is structurally similar to glutamic acid, a neurotransmitter in central nervous systems (CNS) of mammals (Nakajima et al. 1985). Such a similarity allows DA to bind to the same receptors of glutamic acid and trigger a cascade of molecular reactions inducing neuronal degradation, and consequently, DA neurotoxicity effects (Pulido 2008). Evidence indicates that DA binds with high affinity to 2 glutamate receptor subtypes: kainic acid and AMPA receptors (Hampson et al. 1992); a third receptor subtype, NMDA, is a co-participant in inducing DA neurotoxicity effects (Pulido 2008). These receptors are concentrated in the hippocampus of mammals (Foster et al. 1981; Debonel et al. 1989; Scallet et al. 1993), a brain region responsible for memory and spatial navigation and thus, hippocampus lesions are common in mammals and humans after exposure to specific DA doses (Teitelbauum et al. 1990; Gulland et al. 2002). Cephalopods have the largest brains of any invertebrate with a complexity analogous to those of vertebrates (Messenger 1996), and it has been suggested that the arrangement of neurons in the vertical lobe of octopus is involved in memory and it has structural similarities to the vertebrate hippocampus (Boycott and Young, 1950; Young, 1965). Moreover, glutamic acid also serves as a neurotransmitter in invertebrates (Messenger, 1996) and all 3 subtypes of glutamate receptors (i.e., kainic acid, NMDA and AMPA receptors) have been detected in central and peripheral nervous systems of cephalopods (Evans et al. 1992; Messenger, 1996, Garcia 2002; Lima et al. 2003; Di Cosmos et al. 2004). The fact that cephalopods have highly developed CNS and similar glutamate receptors as mammals potentially indicate that Humboldt squid may be susceptible to DA neurotoxicity effects.

The goal of this study was to ascertain whether beach stranded *D. gigas* found in two different locations in San Diego (California, USA) were exposed to DA during the summer of 2009. Our approach was to (1) measure DA in stomach content and lining as well as in mantle tissue of 5 stranded *D. gigas*, (2) analyze surface water particulate DA in locations within 300 km of the stranding site, and (3) examine the stomach contents of the stranded individuals to identify possible DA vectors.

METHODS

Water Sample Collection

Surface (~1 m) seawater samples were collected weekly from five pier sampling stations as part of the Southern California Coastal Ocean Observing (SCCOOS) Harmful Algal Bloom Monitoring Program (fig. 2). Samples were collected with surface bucket and provided subsamples for DA analysis and *Pseudo-nitzschia* identification and quantification. Cross-contamination of samples was avoided by acid washing the sampling gear and bucket with dH_2O 3 times after sample collections and 3 times with seawater before sample collections.

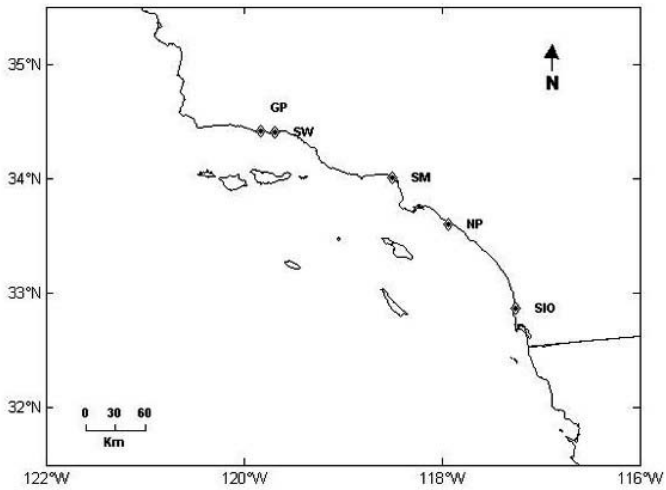

Figure 2. Locations of samples collected for DA analysis and *Pseudo-nitzschia* identification and quantification: Scripps Institution of Oceanography Pier (SIO), Newport Pier (NP), Santa Monica Pier (SM), Stearns Wharf (SW), Goleta Pier (GP). Stranded squid were found between 3km and 6km south of the SIO pier.

DA in Seawater

Particulate DA concentrations were measured by filtering 200 mL of seawater onto GF/F Whatman filters. Filters were stored frozen at –80°C until shipped in dry ice and analyzed within 1 week to 5 months of sample collection, using Rapid Enzyme-Linked Immunosorbent Assay (ELISA) obtained from Mercury Science, Inc. (Durham, NC27713) at the University of Southern California following Schnetzer et al. (2007). The detection limit for the ELISA assay on water samples was 0.02 ng mL^{-1} (ppb).

Toxic *Pseudo-nitzschia* Identification and Quantification

Abundances of two size class categories of the genus *Pseudo-nitzschia*, *seriata* group (frustule width > 3 μm) and *delicatissima* group (frustule width < 3 μm), were determined from settling 10–50 mL of seawater preserved with 4% formaldehyde (Uthermöhl 1958). Cells were categorized under an inverted light microscope. DA-producing *Pseudo-nitzschia* species are found in both of these groups (Hasle and Syvertsen 1997; Moestrup and Lundholm 2007).

Humboldt Squid Sample Collection

Stranded *D. gigas* were collected on 11 July 2009 at La Jolla Shores beach and on 12 July 2009 at La Jolla

TABLE 1
Domoic acid content (μg g^{-1} or ppm) of *Dosidicus gigas* specimens collected in La Jolla, CA, on 11–12 July 2009.

Tissues analyzed for domoic acid (DA)	Mean	SD	Median	Range	Number of replicates	Date Collected	Individual Size (cm)	Sex
Stomachs	0.27	0.05	0.3	0.2–0.3	3	11-Jul-09	na	na
	nd	nd	nd	nd	3	11-Jul-09	na	na
	nd	nd	nd	nd	3	11-Jul-09	na	na
	nd	nd	nd	nd	3	12-Jul-09	63	Female
	nd	nd	nd	nd	3	12-Jul-09	63	Female
Mantle tissue	0.43	0.05	0.4	0.4–0.5	3	11-Jul-09	na	na
	nd	nd	nd	nd	3	11-Jul-09	na	na
	nd	nd	nd	nd	3	11-Jul-09	na	na
	nd	nd	nd	nd	3	11-Jul-09	na	na

Cove. The stranding event was relatively small; only five animals were found in sufficiently good condition to be sampled. Based on media reports and conversations with beachgoers, we concluded that the animals stranded in the early morning of 11 July, and that they were alive at the time of stranding. At the time of dissection, they were dead, most likely through a combination of asphyxiation and partial predation by seagulls. We estimate that the animals dissected on 11 July had been dead for 6–8 hrs, while those dissected on 12 July had been dead for 24–30 hrs. The mantles were in sufficiently good condition that dorsal mantle length (DML) could be measured. Stomachs and samples of mantle tissue (approximately 2×2×2 cm) were removed and frozen at –20°C, then moved to –80°C within 48 hrs. All samples were kept frozen for 3–4 months until stomach content observations and DA analysis could be performed.

Stomach Content and DA Analysis of Humboldt Squid

The stomach contents of the five squid sampled for DA were evaluated as described in Field et al. (2007). Following these observations, DA was analyzed in stomach contents and lining (hereafter referred to as stomach) and mantle tissue using ELISA obtained from Mercury Science, Inc. (Durham, NC27713). Stomach and mantle tissue samples were weighed and each sample was homogenized with a hand-held tissue homogenizer (Tissue Mixer, model PNF2110, Fisher Scientific). Aliquots of 4 g were removed from the homogenized samples and 16 mL of 50:50 MeOH:Nanopure was added. Samples were then sonicated with a Sonifier cell disruptor (Model W185D, Branson Sonic Power) and centrifuged for 20 min at 3800 rpm (1698 × *g*). The supernatant were filtered through a 3 μm polycarbonate filter. The filtrate was diluted at 1:100 and 1:1000 in the buffer solution provided in the ELISA kit and aliquoted in 3 replicates for each sample (table 1). Samples diluted at 1:1000 were below the detection limit of 0.1 ng mL^{-1} (ppb) in the ELISA kit, but samples in the 1:100 dilution were within the detection limit. The diluted samples were used in the ELISA plates following the protocol accompanying the kit. An EMax Precision Microplate Reader (Model E10968, Molecular Devices) was used to measure absorbance at 450 nm. Final concentrations of DA in squid samples are expressed as μg DA g^{-1} wet tissue mass.

RESULTS & DISCUSSION

DA was detected in the stomach of one *D. gigas* specimen and in the mantle tissue of one specimen found stranded in La Jolla beach (table 1). Mantles and stomachs were not labeled individually, so it is unknown whether the specimen with DA in its mantle tissue also had DA in its stomach. Low particulate DA concentration, just above the detection limit, was recorded in surface waters at Scripps Pier 5 days before the stranding occurred (fig. 3A). Scripps Pier is located 3 to 5 km north of the stranding locations, well within documented swimming speeds for *D. gigas* of 30 km day^{-1} (Gilly et al. 2006). Particulate DA was also detected on Goleta Pier and Stearns Wharf, but those are located >30 km north of the stranding location (fig. 2 and 3A). DA levels at these three sites peaked on 6 July 2009 and tapered off to below detection levels within one to three weeks. Peak DA concentrations for July occurred at the same time as an increase in the abundance of cells within the *Pseudo-nitzschia delicatissima* group was observed (fig. 3C). At these 3 locations, *P. delicatissima* group densities ranged from 5.6×10^4 to 5.4×10^5 cells L^{-1}, which are typical bloom levels (i.e. $>10^3$ cells L^{-1}). Moreover, the abundance of cells within the *Pseudo-nitzschia seriata* group never exceeded 9.1×10^2 cells L^{-1} at the Scripps Pier. This suggests that *Pseudo-nitzschia* species from the *delicatissima* group were probably responsible for the DA production at that time.

Squid stomach analyses indicated the presence of Pacific sardine, shiner surfperch (*Cymatogaster aggregata*), and pile surfperch (*Damalichthys vacca*). DA has been detected in Pacific sardine and other surfperch species (i.e. rainbow surfperch) within 7 days of the detection of DA in surface waters (Mazzillo et al. 2010), suggesting that these fish found in the stomachs of *D. gigas* could

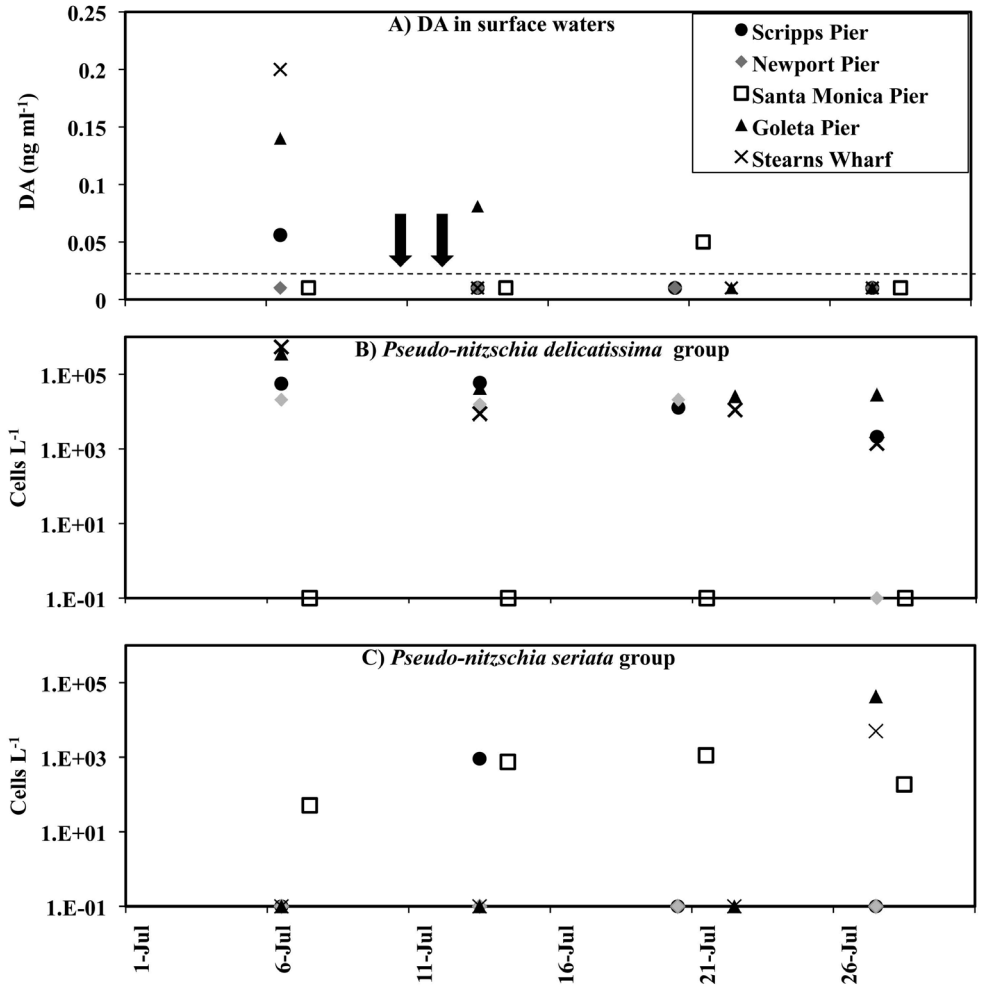

Figure 3. Particulate domoic acid (DA) levels (a), and cell density of *Pseudo-nitzschia delicatissima* group (b) and *Pseudo-nitzschia seriata* group (c) for 1–30 July 2009 from surface waters (1m) at five sites along southern the California coastline: Scripps Pier (●), Newport Pier (♦), Santa Monica Pier (□), Goleta Pier (▲), and Sterns Wharf Pier (×). Arrows in panel (a) indicate collection dates for squid analyzed here: horizontal dashed line indicates analytical detection limit.

have been the DA vectors. Other prey items and potential DA sources included Pacific hake, topsmelt silversides (*Atherinops affinis*) and an unidentified species of *Gonatus* squid, future work should include the examination of these species during periods of algal blooms. Macroalgae and sand were also observed in all stomachs, suggesting other behaviors that are not typical of the class cephalopoda.

Here we showed that *D. gigas* can be exposed to DA by preying on pelagic and nearshore species when toxic *Pseudo-nitzschia* blooms are detected. However, linking the Humboldt squid strandings themselves to domoic acid poisoning (DAP) is difficult. First, DA was not detected in all stranded individuals, indicating that there could be other reasons for their death. Most of the observed prey items are frequently, if not exclusively, found in shallow water, and the nearshore species are unusual targets for *D. gigas*, further demonstrating the opportunistic feeding strategy of this species. The presence of sand and algae in the stomachs also supports the hypothesis that these animals were actively foraging in shallow waters. If this is an atypical habitat for them to exploit, they may have become disoriented and accidentally swam onshore.

Second, we cannot determine from this study whether DA was absorbed from the stomach into the bloodstream and interacted with the squid nervous system via blood causing DAP, although we have evidence that DA was transferred to the mantle tissue. We measured low DA values in the squid stomach (table 1) and DA absorption from the gastrointestinal tract to the bloodstream is known to be minimal in vertebrates (Iverson et al. 1989; Truelove et al. 1997; Lefebvre et al. 2001). The range of DA values detected in the stomach and mantle tissue of stranded squid is within the lower limit range of DA detected in body fluids of DAP stranded California sea lions. Urine and serum of California sea lions were found to contain 0.03–3.72 μg DA mL^{-1} and 0.17–0.20

μg DA mL^{-1}, respectively (Scholin et al. 2000). However, Scholin et al. (2000) also measured DA levels >6,000 times higher in fecal material, and observed common DAP neurological symptoms in addition to the detection of DA, making the DAP diagnosis in these marine mammals more certain.

Although DAP was implicated in mass mortality of marine birds and sea lions (Work et al. 1993; Scholin et al. 2000), the causes of other marine mammal strandings remain largely unknown (Bogomolni et al. 2010), and the same appears to be true of Humboldt squid strandings. Even though we report for the first time *D. gigas* exposure to DA, our results cannot be implicated as the cause of death of the stranded squid since we do not know whether the low DA concentrations measured were absorbed from the squid gastrointestinal tract into the blood and interacted with squid CNS at enough concentrations to cause neurotoxicity effects. Nevertheless, it is quite possible that *D. gigas* could be exposed to higher DA levels than those observed here, since higher DA levels have been previously detected in the waters off the coast of California and in the prey of *D. gigas* (Trainer et al. 2000; Busse et al. 2006; Anderson et al. 2009; Mazzillo et al. 2010). Additionally, cephalopods have the similar glutamate receptor sites as mammals, and as DA binds to these sites it triggers toxicity which indicates that *D. gigas* can potentially be susceptible to DA neurotoxicity effects. However, juvenile leopard sharks (*Triakis semifasciata*) appear not to be affected by DA even though it possesses kainic acid-type glutamate receptors (Schaffer et al. 2006). Thus, *D. gigas* susceptibility to DA toxicity is possible, but remains an unanswered question. Laboratory studies designed to verify DA toxicity in squids could be performed using the California market squid (*Doryteuthis opalescens*) or Atlantic longfin squid (*Doryteuthis pealei*) as models since *D. gigas* cannot be kept in captivity for more than 10 days. Laboratory experiments should include observations of squid behavioral response to DA doses, measurements of DA uptake, as well as quantification of DA in brain tissue to evaluate whether or not DA toxicity occurs in squids and thus could responsible for *D. gigas* mass strandings. Sampling larger *D. gigas* stranding events would also be desirable, as our sample size for this study was limited by the small number of stranded individuals.

ACKNOWLEDGEMENTS

We thank M. Silver for valuable comments on this manuscript; E. Seubert for analyzing particulate DA samples and water sample collection; M. Hilbern, R. Shipe, and J. Goodman for sample collection and cell counts; C. Shadle, A. Lemke, and J. Webb for assistance with sampling stranded squids; A. Townsend for shipping samples; B. Matsubu for help compiling the media accounts of strandings; W. Walker for help with otolith identification; and E. Hubach for assistance with squid toxin extractions; and the three anonymous reviewers. We also thank the Pelagic Invertebrates Collection of the Scripps Institution of Oceanography for the use of facilities, the NSF for funding the California Current Ecosystem LTER site, NOAA for supporting travel to La Jolla and the pier-based harmful algal bloom monitoring funded by NOAA IOOS through the SCCOOS, Grant No. UCSD 20081362.

LITERATURE CITED

Anderson, C. R., D. A. Siegel, R. M. Kudela, and M. A. Brzezinski. 2009. Empirical models of toxigenic *Pseudo-nitzschia* blooms: Potential use as a remote detection tool in the Santa Barbara Channel. Harmful Algae. 8:478–492.

Alarcón-Muñoz, R., L. Cubillos, and C. Gatica. 2008. Jumbo Squid (*Dosidicus gigas*) Biomass off Central Chile: Effects on Chilean Hake (*Merluccius gayi*) Calif. Coop. Oceanic Fish. Invest. Rep. 48:157–166.

Bargu, S., B. Marinovic, S. Mansergh, and M. W. Silver. 2003. Feeding responses of krill to the toxin-producing diatom *Pseudo-nitzschia*. J. Exp. Mar. Biol. Ecol. 284:87–104.

Bargu, S., C. P. Powell, Z. Wang, G. J. Doucette, and M. W. Silver. 2008. Note on the occurrence of *Pseudo-nitzschia australis* and domoic acid in squid from Monterey Bay, CA (USA). Harmful algae. 7:45–51.

Blanco, J., J. Cano, M. D. C. Marino, and M. J. Campos. 2006. Effect of phytoplankton containing paralytic shellfish and amnesic shellfish toxins on the culture of the king scallop *Pecten maximus* in Malaga (SE Spain). Aquat. Living Resour. 19 (3):267–273.

Bogomolni, A. L., K. R. Pugliares, S. M. Sharp, K. Patchett, C. T. Harry, J. M. LaRoque, K. M. Touhey, and M. Moore. 2010. Mortality trends of stranded marine mammals on Cape Cod and southeastern Massachussetts, USA, 2000–2006. Dis. Aquat. Organ. 88:143–155.

Boycott, B. B. and J. Z. Young. 1950. A memory system in *Octopus vulgaris* Lamarck. Proc. R. Soc. Lond. 143:449–480.

Buckley, T. W. and P. A. Livingston. 1997. Geographic variation in the diet of Pacific hake, with a note on cannibalism. Calif. Coop. Oceanic Fish. Invest. Rep. 38:53–62.

Busse, L. B., E. L. Venrick, R. Antrobus, P. E. Miller, and others. 2006. Domoic acid in phytoplankton and fish in San Diego, CA, USA. Harmful Algae. 5:91–101.

Costa, P. R., E. R. Rosa, and M. A. M. Sampayo. 2004. Tissue distribution of the amnesic shellfish toxin, domoic acid, in *Octopus vulgaris* from the Portuguese coast. Mar. Biol. 144:971–976.

Costa, P. R., E. R. Rosa, A. Duarte-Silva, V. Brotas, and M. A. M. Sampayo. 2005. Accumulation, transformation and tissue distribution of domoic acid, the amnesic shellfish poisoning toxin, in the common cuttlefish, *Sepia officinalis*. Aquat. Toxicol. 74:82–91.

Debonel, G., M. Weiss, and C. Montigny. 1989. Reduced neuroexcitatory effect of domoic acid following mossy fiber denervation of the rat dorsal hippocampus: further evidence that toxicity of domoic acid involves kainate receptor activation. Can. J. Physiol. Pharmacol. 67:904–908.

Dizer, H., B. Fischer, A. S. A. Harabawy , M. C. Hennion, and P. D. Hansen. 2001 Toxicity of domoic acid in the marine mussel *Mytilus edulis.* Aquat. Toxicol. 55:149–156.

Di Cosmos, A., M. Paolucci, and C. D. Cristo. 2004. N-methyl-d-aspartate receptor-like immunoreactivity in the brain of *Sepia* and *Octopus*. J. Comp. Neurol. 477:202–219.

Evans, P. D., V. Reale, R. M. Merzon, and J. Villegas. 1992. N-methyl-d-aspartate (NMDA) and non-NMDA (metabotropic) type glutamate receptors modulate the membrane potential of the Schwann cell of the squid giant nerve fibre. J. Exp. Biol. 17:229–249.

Field, J. C., K. Baltz, A. J. Phillips, and W. A. Walker. 2007. Range expansion and trophic interactions of the jumbo squid, *Dosidicus gigas*, in the California Current. Calif. Coop. Oceanic Fish. Invest. Rep. 48:131–146.

Fire, S. P., Z. Wang, T. A. Leighfield, S. L. Morton, W. E. McFee, W. A. McLellan, R. W. Litaker, P. A. Tester, A. A. Hohn, G. Lovewell, C. Harms, D. S. Rotstein, S. G. Barco, A. Costidis, B. Sheppard, G. D. Bossart, M. Stolen,

W. K. Durden, and F. M. Van Dolah. 2009. Domoic acid exposure in pygmy and dwarf sperm whales (*Kogia* spp.) from southeastern and mid-Atlantic U.S. waters. Harmful Algae. 8:658–664.

Foster, A. C., Mena, E. E., Monaghan, D. T., Cotman, C. W. 1981. Synaptic localization of kainic acid binding sites. Nature, 289:73–75.

Garcia, R. A. G. 2002. Glutamate Uptake by Squid Nerve Fiber Sheaths. J. Neurochem. 67:787–794.

Gilly, W. F., U. Markaida, C. H. Baxter, B. A. Block, A. Boustany, L. Zeidberg, K. Reisenbichler, B. Robison, G. Bazzino, and C. Salinas. 2006. Vertical and horizontal migrations by the jumbo squid *Dosidicus gigas* revealed by electronic tagging. Mar. Ecol. Prog. Ser. 324:1–17.

Goldstein, T., J. A. K. Mazet, T. S. Zabka, G. Langlois, K. M. Colegrove, M. Silver, S. Bargu, F. Van Dolah, T. Leighfield, P. A. Conrad, J. Barakos, D. C. Williams, S. Dennison, M. A. Haulena, and F. M. D. Gulland. 2007. Novel symptomatology and changing epidemiology of domoic acid toxicosis in California sea lions (*Zalophus californianus*): an increasing risk to marine mammal health. Proc. R. Soc. B. 275 (1632):267–276.

Gulland, F. M. D., M. Haulena, D. Fauquier, G. Langlois, M. E. Lander, T. Zabka, and R. Duerr. 2002. Domoic acid toxicity in Californian sea lions (*Zalophus californianus*): clinical signs, treatment and survival. Vet. Rec. 150:475–480.

Hampson, D. R., X. P. Huang, J. W. Wells, J. A. Water, and J. L. C. Wright. 1992. Interaction of domoic acid and several derivatives with kainic acid and AMPA binding sites in rat brain. Eur. J. of Pharmacol. 218:1–8.

Hasle, G. R., E. E. Syvertsen. 1997. Marine Diatoms. *In* Identifying Marine Phytoplankton, T. R. Carmelo, ed. San Diego: Academic Press, pp. 5–361.

Iverson, F., J. Truelove, E. Nera, L. Tryphonas, J. Campbell, and E. Lok. 1989. Domoic acid poisoning and mussel-associated intoxication: preliminary investigations into the response of mice and rats to toxic mussel extract. Food Chem. Toxicol. 27:377–384.

Lefebvre, K. A., C. L. Powell, M. Busman, G. J. Doucette, and others. 1999. Detection of domoic acid in northern anchovies and California sea lions associated with an unusual mortality event. Nat. Toxins. 7:85–92.

Lefebvre, K. A., S. L. Dovel, and M. W. Silver. 2001. Tissue distribution and neurotoxic effects of domoic acid in a prominent vector species, the northern anchovy *Engraulis mordax*. Mar. Biol. 138:693–700.

Lefebvre, K. A., S. Bargu, T. Kieckhefer, and M. W. Silver. 2002. From sanddabs to blue whales: the pervasiveness of domoic acid. Toxicon. 40:971–977.

Leandro, L. F., R. M. Rolland, and P. B. Roth. 2010. Exposure of the North Atlantic right whale *Eubalaena glacialis* to the marine algal biotoxin, domoic acid. Mar. Ecol. Prog. Ser. 398:287–303.

Jones, T. O., J. N. C. Whyte, L. D. Townsend, N. G. Ginther, and G. K. Iwama. 1995a. Effects of domoic acid on haemolymph pH, PCO_2 and PO_2 in the Pacific oyster, *Crassostrea gigas* and the California mussel, *Mytilus californianus*. Aquat. Toxicol. 31:43–55.

Jones, T. O., J. N. C. Whyte, J. N. C. Ginther, N. G., Townsend, L. D., and G. K. Iwama. 1995b. Haemocyte changes in the Pacific oyster, *Crassostrea gigas*, caused by exposure to domoic acid in the diatom *Pseudonitzschia pungens* f. *multiseries*. Toxicon 33:347–353.

Lima, P. A., G. Nardi, E.R. Brown. 2003. AMPA/kainate and NMDA-like glutamate receptors at the chromatophore neuromuscular junction of the squid: role in synaptic transmission and skin patterning. Eur. J. Neurosci. 17:507–516.

Liu, H., M. S. Kelly, D. A. Campbell, S. L. Dong, J. X. Zhu, J. G. Fang, and S. F. Wang. 2007a. Exposure to domoic acid affects larval development of king scallop *Pecten maximus* (Linnaeus, 1758). Aquat. Toxicol. 81:152–158.

Liu, H., M. S. Kelly, D. A. Campbell, S. L. Dong, J. X. Zhu, and S. F. Wang. 2007b. Ingestion of domoic acid and its impact on king scallop *Pecten maximus* (Linnaeus, 1758). J. Ocean Univ. China. 6:175–181.

Liu, H., M. S. Kelly, D. A. Campbell, J. Fang, and J. Zhu. 2008. Accumulation of domoic acid and its effect on juvenile king scallop *Pecten maximus* (Linnaeus, 1758). Aquaculture 284: 224–230.

Mackas, D. L., R. Kieser, M. Saunders, D. R. Yelland, R. M. Brown, and D. F. Moore. 1997. Aggregation of euphausiids and Pacific hake (*Merluccius productus*) along the outer continental shelf off Vancouver Island. Can. J. Fish Aquat. Sci. 54:2080–2096.

Maeda, M. T., T. Kodama, T. Tanaka, Y. Ohfune, K. Nomoto, K. Nishimura, and T. Fujita. 1987. Insecticidal and neuromuscular activities of domoic acid and its related compounds. J. Pestic. Sci. 9: 27.

Markaida, U. and Sosa Nishizaki, O. 2003. Food and feeding habits of jumbo squid *Dosidicus gigas* (Cephalopoda:Ommastrephidae) from the Gulf of California, Mexico. J. Mar. Biol. Ass. U. K. 83 (3): 507–522.

Markaida, U. 2006. Food and feeding of jumbo squid *Dosidicus gigas* in the Gulf of California and adjacent waters after the 1997–98 El Niño event. Fish. Res. 79:16–27.

Mazzillo, F. M. M., C. Pomeroy, J. Kuo, P. Ramondi, R. Prado, and M. W. Silver. 2010. Domoic acid uptake in anglers via contaminated fishes. Aquat. Biol. 9:1–12.

Mearns, A. J., 1988. The "odd fish": unusual occurrences of marine life as indicators of changing ocean conditions. *In* Marine Organisms as Indicators, D. F. Soule and G. S. Kleppel, eds. New York: Springer-Verlag., pp. 137–176.

Messenger, J. B. 1996. Neurotransmitters of cephalopods. Invertebr. Neurosci. 2: 95–114.

Moestrup, Ø., and N. Lundholm. 2007. http://www.bi.ku.dk/ioc/group1.asp. Accessed on 7 July 2010.

Nakajima, T., K. Nomot, Y. Ohfune, Y Shiratori, T. Takemoto, H. Takeuchi, and K. Watanabe. 1985. Effects of glutamic acid analogues on identifiable giant neurons, sensitive to β-hydroxy-L-glutamic acid, of an African giant snail (*Achatine fulica* Ferussac). Br. J. Pharmacol. 86:645–654.

Nigmatullin, Ch.M., K. N. Nesis, and A. I. Arkhipkin. 2001. A review of the biology of the jumbo squid *Dosidicus gigas* (Cephalopoda: Ommastrephidae). Fish. Res. 54: 9–19.

Olson, R. J. and G. M. Watters. 2003. A model of the pelagic ecosystem in the Eastern Tropical Pacific Ocean. Inter-Amer. Trop. Tuna Com. Bull. 22 (3):135–218.

Pulido, O., 2008. Domoic acid toxicologic pathology: a review. Mar. Drugs. 6:180–219.

Ruiz-Cooley, R. I., D. Gendron, S. Aguíñiga, S. Mesnick, and J. D. Carriquiry, 2004. Trophic relationships between sperm whales and jumbo squid using stable isotopes of C and N. Mar. Ecol. Prog. Ser. 277: 275–283.

Scallet, A. C., Z. Blnlenda, F. A. Caputo, S. Hall, M. G. Paule, R. L. Rountree, L. Schmued, T. Sobotka, and W. Shkker Jr. 1993. Domoic acid-treated cynomolgus monkeys (*M. fascicularis*) effects of dose on hippocampal neuronal and terminal degeneration. Brain Res. 627:307–313.

Schaffer, P., C. Reeves, D. R. Casper, and C. R. Davis. 2006. Absence of neurotoxic effects in leopard sharks, *Triakis semifasciata*, following domoic acid exposure. Toxicon. 47 (7):747–752.

Schnetzer, A., P. E. Miller, R. A. Schaffner, Stauffer, B. A., Jones, B. H., S. B. Weisberg, P. M. DiGiacomo, W. M. Berelson, D.A. Caron. 2007. Blooms of *Pseudo-nitzschia* and domoic acid in the San Pedro Channel and Los Angeles harbor areas of the Southern California Bight, 2003–2004. Harmful Algae 6:372–387.

Scholin, C.A., F. Gulland, G. J. Doucette, S. Benson, and others. 2000. Mortality of sea lions along the central California coast linked to a toxic diatom bloom. Nature 403: 80–84.

Sierra-Beltran, A.P., A. Cruz, E. Nunez, L. M. Del Villar, J. Cerecero, and J. L. Ochoa. 1998. An overview of the marine food poisoning in Mexico. Toxicon. 36: 1493–1502.

Teitelbaum, S., R. J. Zatorre, S. Carpenter, D. Gendron, A. C. Evans, A. Gjedde, N. R. Cashman. 1990. Neurologic sequelae of domoic acid intoxication due to the ingestion of contaminated mussels. N. Engl. J. Med. 322:1781–1787.

Trainer, V. L., N. G. Adams, B. D. Bill, C. M. Stehr, J. C. Wekell, P. Moeller, M. Busman, and D. Woodruff. 2000. Domoic acid production near California coastal upwelling zones, June 1998. Limnol. Oceanogr. 45 (8):1818–1833.

Truelove, J., R. Mueller, O. Pulido, and F. Iverson. 1996. Subchronic toxicity study of domoic acid in the rat. Food Chem. Toxicol. 34:525–529.

Vetter, R., S. Kohin, A. Preti, S. McClatchie, and H. Dewar. 2008. Predatory interactions and niche overlap between mako shark, *Isurus oxyrinchus*, and jumbo squid, *Dosidicus gigas*, in the California Current. Calif. Coop. Oceanic Fish. Invest. Rep. 49:142–156.

Work, T. M., B. Barr, A. M. Beale, L. Fritz, M. A. Quilliam, and J. L. C. Wright. 1993. Epidemiology of domoic acid poisoning in brown pelicans (*Pelecanus occidentalis*) and Brandt cormorants (*Phalacrocorax penicillatus*) in California. J Zoo. Wildl. Med. 24:54–62.

Young, J. Z. 1965. The organization of a memory system. Proc. R. Soc. Lord. B Biol. Sci. 163:285–320.

Zeidberg, L. D. and B. H. Robison. 2007. Invasive range expansion by the Humboldt squid, *Dosidicus gigas*, in the eastern North Pacific. Proc. Natl. Acad. Sci. 104:12948–12950.

DAILY EGG PRODUCTION, SPAWNING BIOMASS AND RECRUITMENT FOR THE CENTRAL SUBPOPULATION OF NORTHERN ANCHOVY 1981–2009

BENJAMIN E. FISSEL
NOAA, Alaska Fisheries Science Center
Economics and Social Sciences Research Program
7600 Sand Point Way NE
Seattle, WA 98115
Email: Ben.Fissel@noaa.gov

NANCY C. H. LO
Fisheries Resources Division
Southwest Fisheries Science Center
8604 La Jolla Shores Drive
La Jolla, CA 92037
Email: Nancy.Lo@noaa.gov

SAMUEL F. HERRICK JR.
Fisheries Resources Division
Southwest Fisheries Science Center
8604 La Jolla Shores Drive
La Jolla, CA 92037
Email: Sam.Herrick@noaa.gov

ABSTRACT

This paper updates estimates of critical stock assessment parameters for the central subpopulation of northern anchovy (*Engraulis mordax*). Ichthyoplankton data from the CalCOFI database were used to implement the historical egg production method and estimate annual mortality curves, from which daily egg production, and egg and larval mortality parameters were derived. Spawning biomass was estimated using historical data under the assumption of a constant daily specific fecundity. A Ricker recruitment model, augmented with environmental factors, was estimated based on historical data and used to predict recruitment using the new spawning biomass data. We found that egg densities were highly variable while larval densities have been persistently low since 1989. Recruitment estimation suggests that poor environmental conditions have potentially contributed to the low productivity. Mortality estimation reveals through an increasing egg mortality rate that low larval densities were primarily the result of high mortality during the pre-yolk-sac period.

1 INTRODUCTION

This paper updates the egg production statistics, spawning stock biomass, and recruitment time series from 1981–2009 for the central subpopulation of northern anchovy (*Engraulis mordax*) which occupies the California Current Ecosystem from San Francisco, California south to Punta Baja, Baja California, Mexico. It is the largest of the North Pacific subpopulations, and supported a significant U.S. fishery throughout the 1970s and 1980s. In 1978 the fishery came under federal management through the Pacific Fisheries Management Council's (PFMC) Northern Anchovy Fishery Management Plan (FMP) (PFMC 1978). In 1983 the FMP was amended (Amendment 5) in recognition that harvest should be adjusted annually to reflect the current status of the stock (PFMC 1983) and annual stock assessments were conducted to inform the annual U.S. anchovy harvest quota.

During the 1980s anchovy abundance started to decline as environmental conditions in the California Current ecosystem became less favorable for anchovy productivity. Concurrently, the conditions were favorable for the recovery of the Pacific sardine (*Sardinops sagax caerulea*) population and fishing effort began to shift from anchovy to sardine. With the shift in fishing effort from anchovy to sardine, conservation and management resources were redirected toward managing the expanding sardine fishery, and since 1995 no stock assessments have been conducted for the central subpopulation of northern anchovy (Jacobson et al. 1995). Our updated stock statistics are intended to provide valuable information about the anchovy's abundance trajectory over the past 15 years.

The core range of the bulk of the central subpopulation lies within the California Bight. Portions of the central subpopulation, thought to be smaller, exist north off the coast of San Francisco and Monterey, as well as south in Mexico (PFMC 2010). The bight has been regularly sampled by research cruises since 1949 and cataloged in the California Cooperative Oceanogrpahic and Fisheries Investigation (CalCOFI) database. The cruises conducted ichthyoplankton surveys at regular intervals, known as CalCOFI stations (Eber and Hewitt 1979). Anchovy ichthyoplankton from the surveys is preserved and later larvae are counted and lengths recorded, while eggs are only counted. The perserved lengths allow for the binning of larvae counts and aging, known as staging (Lo 1985a).

Numerous methods have been developed to analyze anchovy ichthyoplankton data (Hewitt 1981; Zweifel and Smith 1981; Hewitt and Methot 1982; Lasker 1985). The historical egg production method (HEPM) of Lo (1985a) is the method most amenable to the available CalCOFI data and is the closest to the daily egg production method (DEPM) (Lasker 1985) currently used for sardine (Lo et al. 2008). The HEPM is a method for estimating daily egg production (P_0) and other early life history mortality parameters of archived ichthyoplankton data. The HEPM was designed to provide indices of abundance for anchovy dating back to 1951 when no staging data for anchovy eggs were available. The DEPM was designed to estimate the spawning biomass for fish populations with indeterminate fecundity like anchovy and sardine (Hunter and Macewicz 1985) but requires

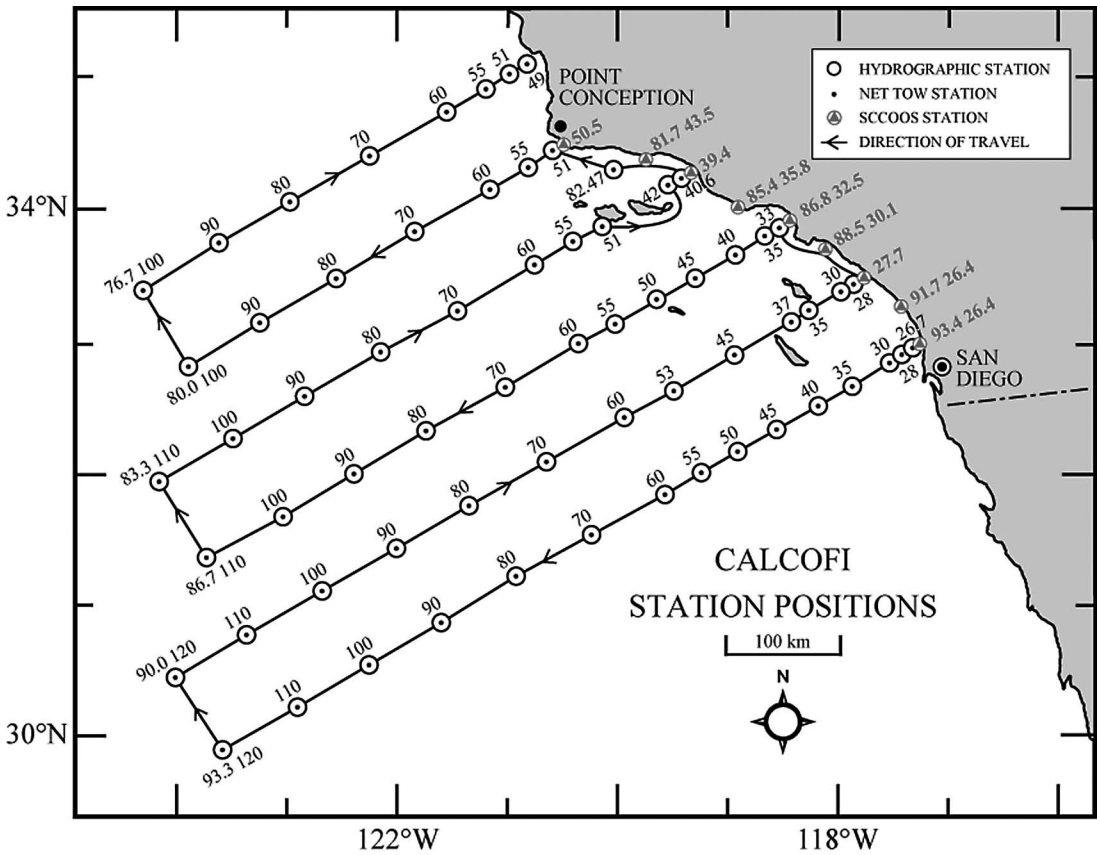

Figure 1. CalCOFI Stations in the core range. From: http://www.calcofi.org/cruises/stapos-depth/75stapattern.html accessed 08/23/10

staged eggs. While the more data intensive DEPM is preferred, HEPM provides an unbiased index of the daily egg production (Lo 1985a). The spawning stock biomass can then be estimated using daily egg production and daily specific fecundity of the stock (Parker 1980; Hewitt 1985).

The Ricker stock-recruitment model (Ricker 1954) can in turn be used to estimate recruitment from spawning biomass. The stock-recruitment relationships are typically highly variable as it spans the development phases of growth which are subject to a variety of influence. Theories explaining the dynamics of fishes often cite sensitivity in recruitment linked to environmental factors (Aydin 2005) as being a major driver. Previous research shows that anchovy recruitment success is influenced by wind stress driven upwelling (Husby and Nelson 1982; Peterman and Bradford 1987; Rykaczewski and Checkley 2008) and temperatures in the upper strata of the ocean (Butler 1989; Zweifel et al. 1976; Fiedler et al. 1986). We augment the Ricker model with wind stress and temperature to produce an environmental Ricker stock-recruitment model.

In this paper, daily egg production and mortality parameters were estimated using the HEPM. Spawning biomass was estimated using a model that regressed daily egg production on historical spawning biomass data (Jacobson et al. 1995) thereby assuming constant daily specific fecundity over time. Historical stock and environmental data was used to estimate the environmental Ricker stock-recruitment model and statistical validity of the model was explored. Bootstrapping was used to characterize variation in mortality.

2 DATA AND METHODS

2.1 Data

Data for the analysis was obtained from the CalCOFI database. Data were constrained to the central subpopulation's core range of the 75 CalCOFI stations (fig. 1) south of CalCOFI line 76.7 and north of line 93.3. Ichthyoplankton surveys over the core range from 1981–2009 were used. Our analysis was constrained to data collected during the peak anchovy spawning season between January and April (Hewitt and Methot 1982; Hewitt and Brewer 1983). We verified in our data that the peak spawning season has remained in this interval. The 75 stations analyzed had a median sampling frequency of 2.03 samples per year between Jan–April. Each cruise was weighted equally in our analysis.

Three different types of nets were used for ichthy-

oplankton surveys over 1981–2009. The CalBOBL or Bongo net (*CB*), the CalVET (*CVT*) and two connected CalVET nets called the PairOVET (*PV*) (*CVT* and *PV* are referred to collectively as *CVT/PV*)[1]. Our analysis utilizes ichthyoplankton samples from *CB* and *CVT* nets for 1981–1984 and *CB* and *PV* nets for 1985–2009.

2.2 Daily egg production

Egg production methods estimate the production of eggs at age zero, the time of spawning. Estimation of age-zero egg production per 10 m^2 (P_0) from the counts of eggs and larvae was carried out in a series of steps. Procedures for correcting raw ichthyoplankton counts and aging have followed the literature closely and incorporate previously derived parameters. Appendix A provides details on the methods used for egg and larval density construction and aging, and they are summarized in the following paragraph.

First, larvae were sorted into size classes based on preserved larval size. The size classes were 2.5 mm, 3.25 mm, 4.25 mm,…, 9.25 mm[2]. Extrusion and avoidance corrections were applied and standard haul factors were used to rescale egg and larval counts to a 10 m^2 area-density (appendix A1). The time it takes eggs to reach the developed stage, incubation time (t^I), was calculated using a temperature-dependent relationship (Lo 1983). A live larval length correction was made to preserved samples, and live lengths were used in a temperature and month-dependent two-stage Gompertz growth curve (GGC) (Lo 1983; Hewitt and Methot 1980) to estimate larval age (t) (appendix A2). The first stage of the GGC spans the first three larval classes (2.5 mm, 3.25 mm, 4.25 mm) and is designed to model growth over the period of yolk-sac consumption. The second stage of the GGC covers post-yolk-sac consumption growth (5.25 mm,…, 9.25 mm) when larvae must seek out food in their environment. Aggregation of the samples over cruises and stations yielded annual age and density statistics for the region. The daily larval production (*DLP*) is the daily production of larvae in a size class per 10 m^2 area-density, and was constructed as the standing stock of larvae in a size class over the number of days that larvae spend in that size class as determined by the growth curve.

Methods for the estimation of the mortality curves are presented in the following subsection 2.2.1. However, it is useful to first summarize the approach. Figure 2 displays a conceptual graph of the HEPM estimation process. First, daily larval production and corresponding size

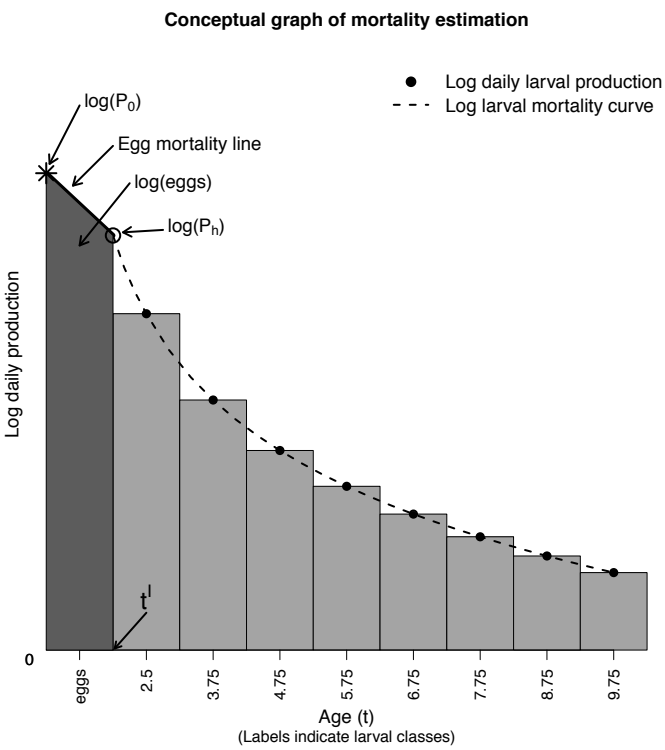

Figure 2. Conceptual graph of HEP mortality estimation, on log-linear axes.

class ages were used to construct larval mortality curves (Lo 1985c). The mortality curve was parameterized such that the fitted *DLP* at the age of incubation time, $t = t^I$, gives the production at the time of hatching (P_h). Under the assumption that the egg instantaneous mortality rate (IMR) is constant across egg stages[3], the egg IMR can be found as the value that is consistent with the observed standing stock of (unstaged) eggs (the dark shaded region in fig. 2). Having obtained the egg IMR over the time of incubation, production of eggs at age 0 (P_0), can be estimated using the egg mortality curve from P_h back to the time of spawning.

Residual bootstrapping (MacKinnon 2006) of the annual mortality curves was used to provide annual estimates of variability for larval and egg mortality parameters (appendix B). Bootstrap based variation is reported as 95% confidence intervals (CIs) which were constructed by taking the 0.025 and 0.975 quantiles of the relevant bootstrapped distribution. Details on the bootstrap procedure are provided in appendix B.

2.2.1 Mortality curves and daily egg production. An annual Pareto type mortality curve was used to model the mortality of larvae from the time of hatching. The variables of daily larval production, $dlp_{c,s}$, average age of larvae ($t_{c,s}$) and incubation time t^I_s for larval class c in year s (see appendix A) are used to identify the parameters

[1]Further details on sampling procedures and nets are available from the Southwest Fisheries Science Center (SWFSC), CalCOFI, Smith and Richardson (1977).

[2]Larval class sizes greater than 9.25 mm were discarded because mature larvae are more adept at avoiding nets thereby introducing significant bias into production calculations (appendix A3).

[3]This assumption was verified in Lo (1985a) for select years.

in the model. Each year was estimated independently using the equation:

$$dlp_{c,s} = P_{h,s}\left(t_{c,s}/t^{I}_{s}\right)^{-\beta_s} + \varepsilon_{c,s} \quad (1)$$

where the mortality curve parameterization was chosen by Lo (1985a) so that $P_{h,s}$ is the production at the time of hatching ($t = t^{I}_{s}$), and β_s is the coefficient of the larval instantaneous mortality rate. The larval instantaneous mortality rate decreases as larvae age, and at age t is β/t (Hewitt and Brewer 1983). We assume the error term, $\varepsilon_{c,s}$, is distributed with a mean-zero, however, we allow for heteroskedasticity across ages through our bootstrap methods (appendix B). Equation 1 was fit using nonlinear least squares (NLS). A grid search over initial conditions was performed and the parameters that minimized the sum-of-squared errors were used. A residual bootstrap of equation 1 was used to construct 95% CIs for β_s and $P_{h,s}$ (appendix B).

An exponential curve, which applied a constant instantaneous mortality rate (IMR), α, was used to model egg mortality to $P_{h,s}$: $\log(P_0) - \alpha^* t = \log(\text{egg production at age } t)$, for $t \in (0, t^I)$, where $\log(P_0) - \alpha^* t^I = \log(P_h)$[4]. Manipulation of the definition for the observed standing stock of eggs and the production at the time of hatching (Lo 1985a) yields a definition that was used to calculate the egg IMR:

$$\frac{m_s}{P_{h,s}} = \frac{e^{\alpha_s * t^I_s} - 1}{\alpha_s} \quad (2)$$

where m_s is the observed corrected standing stock of eggs, and the egg IMR, α_s, was estimated by iterative method. Daily egg production can now be estimated as the production at time zero, $P_{0,s}$, necessary to produce the estimated $P_{h,s}$ give the egg mortality rate α_s, and the time it takes to incubate t^I:

$$P_{0,s} = P_{h,s}\, e^{\alpha_s * t^I_s} \quad (3)$$

Ninety-five percent CIs for α_t and $P_{0,s}$ were derived by re-estimating equations 2 and 3 at each iteration of the larval bootstrap (appendix B).

2.3 Spawning stock biomass estimation

To obtain estimates of *SSB* overlapping, historical data from Jacobson et al. (1995) was used and daily specific fecundity, D_s, was assumed constant over time so that the SSB_s is proportional to $P_{0,s}$. With this assumption a simple linear regression without a constant is estimated:

$$SSB_s = \gamma\, P_{0,s} 10^5 \Lambda + \eta D1_s + \epsilon_s \quad (4)$$

where $P_{0,s}10^5$ is the daily egg production per km^2 Λ is the area of the core CalCOFI region (approx. 200,500 km^2). From 1981–1986 data from south of the Mexican border was used by *National Marine Fisheries Service's Southwest Fisheries Science Center* (SWFSC) to calculate SSB_s and other stock statistics, D1 is a categorical variable accounting for this: 1981–1986 ($D1$=1) and 1987-2009 ($D1$=0). The model was fit using the estimated $\widehat{P_{0,s}}$ (equation 3) and SSB_s from Jacobson et al. (1995) over the years 1981–1995. The fitted model was used to estimate the SSB_s from 1981–2009. The standard estimate of prediction error associated with ordinary least squares is reported.

2.4 Recruitment

Estimates of spawning stock biomass were used in conjunction with a Ricker curve to provide recruitment estimates and explore the impact of environmental conditions. The last anchovy stock assessment (Jacobson et al. 1995) provided estimates of both spawning stock biomass and recruitment for the years 1964–1995. Consistent with Jacobson et al. (1995) we refer to recruits as age-0 anchovy on July 1.

Two environmental factors were incorporated into our recruitment model, north-south (N-S) wind stress and sea surface temperature[5]. The Ricker stock-recruitment model was augmented with these variables in the exponential, which yields an environmental Ricker model:

$$R_s = A^* SSB_s * e^{B^* SSB_s + \rho_1 * NSWind5_s + \rho_2 * tanom_s} + \varepsilon_s \quad (5)$$

where R_s is recruitment in year s, $tanom_s$ is the mean annual sea surface temperature (SST) anomay at Scripps pier and $NSWind5_s$ is the 5% quantile of the annual north-south wind stress anomaly distribution. Wind stress and sea surface temperature anomalies were computed as deviations from the monthly means across all available years. Recruitment and spawning biomass were normalized by their standard deviation, then fit using NLS over the stock and environmental data from 1964–1995. The standard Ricker curve ($\rho_1 = \rho_2 = 0$) was used as the null model, M^0, to evaluate the benefit of added

[4]Lo (1985a) provided two separate mortality estimates: first under the assumption of constant IMR to yolk-sac larval stage, and second constant through the first yolk-sac larval stage. Constant mortality through the first larval stage was a helpful assumption for the historical data used because *CVT/PV* samples were not present. The use of the *CVT/PV* nets in our data gives us sufficiently accurate sampling from from smaller larvae classes.

[5]North-south (N-S) wind stress data were obtained from the Environmental Research Division of the SWFSC through their Live Access Server http://www.pfeg.noaa.gov/products/las.html. The wind stress vectors are National Center for Environmental Predictions derived monthly wind stresses from the location 32.5 degrees north and 117.5 degrees west, and span 1948–2009. Data on Scripps pier SST data were obtained from the ocean informatics datazoo http://oceaninformatics.ucsd.edu/datazoo/data/ hosted by Scripps Institution of Oceanography.

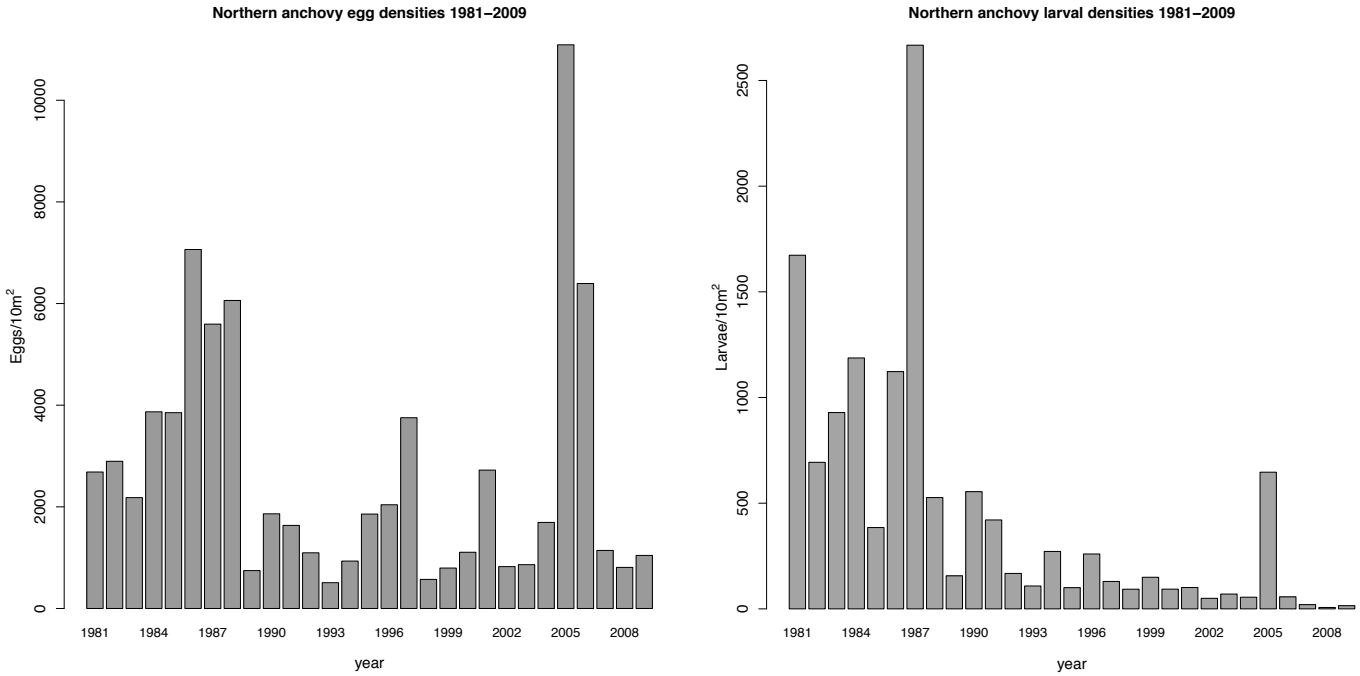

Figure 3. Annual egg and larval densities per 10 m² in the core CalCOFI region 1981–2009.

information from the full environmental Ricker model, M^{WT} (ρ_1, ρ_2 unconstrained). The Akaike information criterion (AIC) was used to compare the models. The ratio of likelihoods was formed as $^{L(M^0)}/_{L(M^{WT})} = \exp((AIC^{WT} - AIC^0)/2)$, which is the likelihood that the constrained null model minimizes the information loss relative to the unconstrained model that uses the environmental factors (Burnham, K. P. and D. R. Anderson (2002)), which we denote by $I(M^{WT}) \leq I(M^0)$. Similar AIC probability calculations were carried out on different model specification to assess the relative contribution of the individual environmental factors. *SSB* estimates obtained from equation 4 were used with the fitted environmental Ricker model to estimate recruitment from 1981–2009.

3 RESULTS

Annual density plots for the core CalCOFI stations show the temporal variation of eggs and larvae (fig. 3, table 1). Since approximately 1989, egg densities in general, have been lower although more highly variable than the years preceding. Prior to 1989 densities ranged from 2182/10 m² to 7063/10 m² with a mean of 4276/10 m², while later densities showed a range of 508/10 m² to 11091/10 m² and a mean of 2070/10 m² with pronounced episodes of high density particularly in 2005–2006 (table 1). In contrast, larvae densities have declined fairly steadily since 1989 except for 2005 when an increase in larval density was associated with the correspondingly high egg density (fig. 3 right panel). Larval densities ranged from 394.1/10 m² to 2870.2/10 m² with a mean of 1177.9/10 m² prior to 1989, and after had a range of 6.3/10 m² to 648.8/10 m² and a mean of 166.3/10 m² with pronounced episodes of high density particularly in 2005–2006 (table 1). Larvae densities do not track the dynamics of egg densities closely and are considerably smaller than densities observed through the mid to late 1980s; similar to patterns in 1951–1982 (Lo 1985a).

Egg density closely mirrors P_0 (figs. 3 and 4, table 1). P_0 displays high post-1989 production around 1997, 2001 and a pronounced episode of high density in 2005. In the early '80s *DEP* appears comparatively low in contrast to the relative egg density owing to the low egg IMR (α) during that period (fig. 4 upper-right panel, table 1). The larval mortality coefficient (β) has been variable but has maintained an average value of approximately –1.89 (fig. 4 lower right panel). In contrast, the egg IMR has been increasing from low levels in the early '80s to over 2 in the late 2000s. A linear time trend has been superimposed on the egg IMR time series and shows that the egg IMR has been increasing by approximately 0.06 per year. Bootstrap CIs indicate that estimation of the egg IMR is more precise than the coefficient of larval mortality (fig. 4 right panel). The imprecision in the estimation of β is largely due to higher residual variance in the pre-yolk-sac-consumption larval phases (fig. B1). CIs for *DEP* indicate that the random variation in larval mortality does not significantly contribute to the observed pattern of *DEP*.

The spawning stock has shown periods of low biomass since 1989, but has been highly variable (fig. 5, table 2) with high post-1990 biomass around 1997, 2001

TABLE 1
Annual egg, larval and mortality statistics

Year	Egg dens. 10 m²	Larvae dens. 10 m²	β	P_h	α	P_0
1981	2685.26	1673.18	–1.96	1015.49	–0.04	912.35
			[–2.05,–1.84]	[866.5,987.3]	[–0.05,0.04]	[862,983]
1982	2896.23	693.44	–1.56	255.62	0.7	2279.5
			[–1.74,–1.23]	[186.4,280.1]	[0.61,0.8]	[2052,2495]
1983	2181.7	928.23	–2.02	616.87	0.24	1139.14
			[–2.17,–1.85]	[504.4,616.2]	[0.2,0.34]	[1061,1242]
1984	3869.8	1189.92	–1.82	598.47	0.56	2770.29
			[–1.92,–1.68]	[497,572.3]	[0.52,0.6]	[2601,2826]
1985	3853.01	394.07	–2.67	263.97	0.76	3177.28
			[–2.93,–2.06]	[191,282.3]	[0.71,0.88]	[3022,3578]
1986	7063.25	1144.54	–2.54	1196.2	0.43	4239.8
			[–2.69,–2.41]	[1129.7,1322.1]	[0.38,0.47]	[3993,4434]
1987	5595.11	2870.22	–2.2	1719.78	0.05	2021.12
			[–2.24,–2.15]	[1647.7,1714.2]	[0.05,0.08]	[1994,2069]
1988	6060.64	529.37	–2.22	282.93	0.82	5254.26
			[–2.48,–1.85]	[234.7,346]	[0.77,0.93]	[5011,5846]
1989	745.66	155.23	–2.06	80.66	0.62	542.7
			[–2.46,–1.2]	[43,87]	[0.5,0.82]	[464,656]
1990	1862.97	534.85	–1.96	313.13	0.5	1239.04
			[–2.18,–1.69]	[191.5,255.6]	[0.47,0.61]	[1133,1336]
1991	1634.47	421.06	–1.28	114.16	0.94	1658.65
			[–1.47,–0.91]	[80.1,129.2]	[0.82,1.05]	[1467,1791]
1992	1095.67	167.43	–1.89	85.94	0.98	1165.09
			[–2.35,–1.28]	[54.9,105.3]	[0.83,1.16]	[1011,1331]
1993	507.68	108.98	–1.52	37.55	0.87	476.87
			[–2.01,–0.68]	[18.7,56.5]	[0.68,1.23]	[403,642]
1994	932.9	271.69	–2.15	125.74	0.52	609.87
			[–2.5,–1.83]	[123.2,165.1]	[0.44,0.6]	[571,684]
1995	1857.66	99.84	–2.1	33.36	1.2	2270.21
			[–2.63,–1.26]	[28.8,59.5]	[1.24,1.56]	[2370,2927]
1996	2041.04	259.41	–2.65	156.04	0.86	1912.72
			[–2.93,–2.1]	[142.5,201.6]	[0.8,0.98]	[1836,2151]
1997	3753.55	130.25	–1.41	39.92	1.82	6884.84
			[–1.88,–0.83]	[22.8,56.1]	[1.57,1.94]	[5952,7319]
1998	572.02	85.71	–1.73	36.36	1.23	740.98
			[–2.08,–1.07]	[22.3,39.3]	[1.09,1.39]	[662,816]
1999	795.65	140.46	–1.97	71.66	0.64	581.51
			[–2.33,–1.5]	[45.3,77.2]	[0.53,0.75]	[499,646]
2000	1106.24	93.36	–2.47	55.3	1.06	1226.33
			[–2.85,–1.6]	[28.9,56.2]	[0.97,1.26]	[1127,1420]
2001	2722.55	101.16	–2.49	63.22	1.33	3689.34
			[–2.86,–1.65]	[31,57.7]	[1.22,1.46]	[3391,4010]
2002	823.98	49.78	–0.9	7.39	1.45	1200.32
			[–1.57,–0.28]	[4,14.3]	[1.24,1.7]	[1038,1401]
2003	862.19	70.08	–1.58	21.63	1.31	1150.54
			[–1.93,–1.05]	[14.3,27.5]	[1.22,1.5]	[1078,1307]
2004	1693.4	55.18	–2.61	33.95	1.51	2592.44
			[–2.99,–1.7]	[15.9,40]	[1.32,1.7]	[2274,2892]
2005	11091.12	648.81	–1.27	143.84	1.53	17161.25
			[–1.39,–1.12]	[137.3,171.6]	[1.57,1.67]	[17617,18637]
2006	6394.01	57.13	–1	9.41	2.34	14972.47
			[–1.8,0]	[3.5,26.3]	[1.99,2.73]	[12610,17272]
2007	1142.23	19.76	–1.13	3.41	2.03	2320.7
			[–1.87,–0.36]	[1.7,5.8]	[1.77,2.21]	[2023,2524]
2008	808.21	6.3	–1.92	1.89	2.02	1633.54
			[–2.46,–0.13]	[0.6,2.5]	[1.79,2.27]	[1447,1836]
2009	1044.16	14.8	–1.6	3.42	1.92	2012.21
			[–1.9,–0.32]	[2,4.5]	[1.86,2.15]	[1945,2249]

Egg and larval densities, the coefficient of the larval instantaneous mortality rate (IMR) (β), larval production at the time of hatching (P_h), egg IMR (α), and egg production at age at age zero per 10 m² (P_0). 95% bootstrap larval mortality confidence intervals are in brackets below the estimates.

and a pronounced episode of high biomass in 2005–2006. *SSB* has been comparatively lower in recent years. For the overlapping years of Jacobson et al. (1995) *SSB*, and our *SSB* estimates (fig. 5 left panel) there is some discrepancy but the respective trends are nearly identical ($R^2 = 0.825$) (table 3). The high biomass in 2005 is not without precedent; similar levels were seen around 1976. The parameter on *SSB*, γ, was significant at the

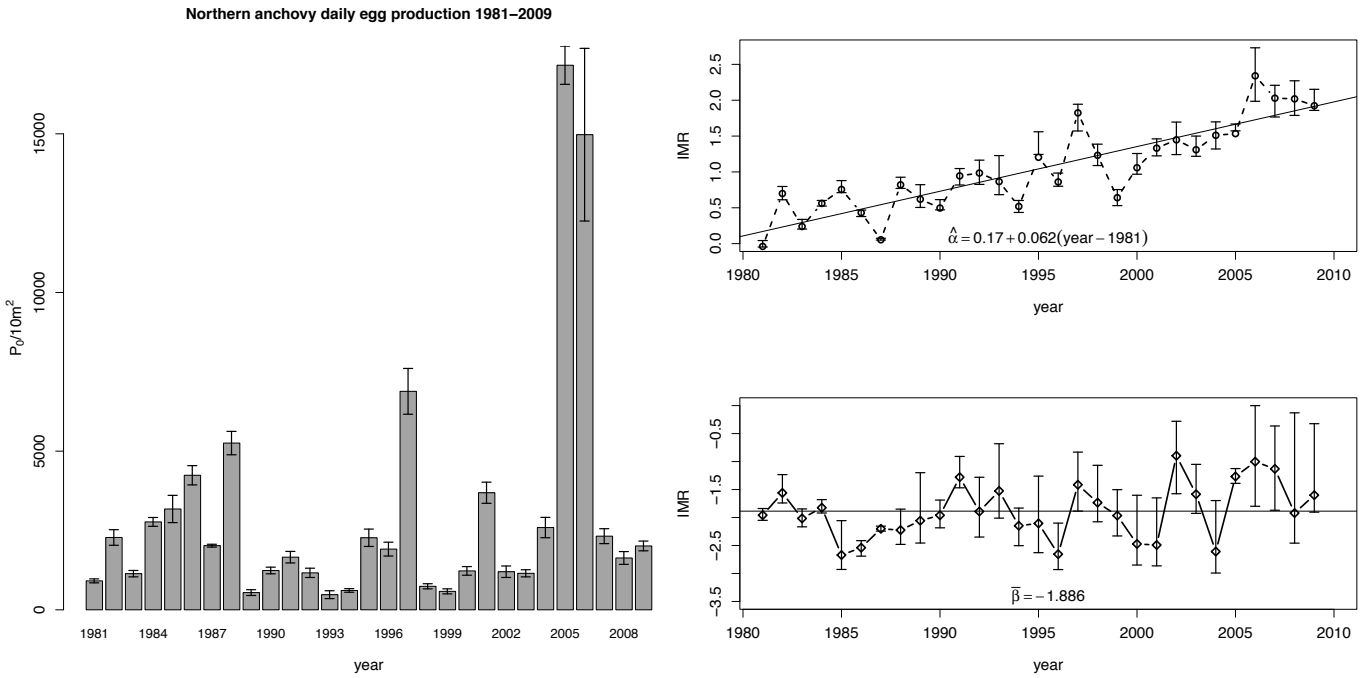

Figure 4. Annual daily egg production (P_0) (left panel) and egg IMR and coefficient of larval IMR (right panel). IMR regression coefficients displayed have a p-value ≤ 0.01. Error bars represent 95% bootstrapped larval mortality confidence intervals.

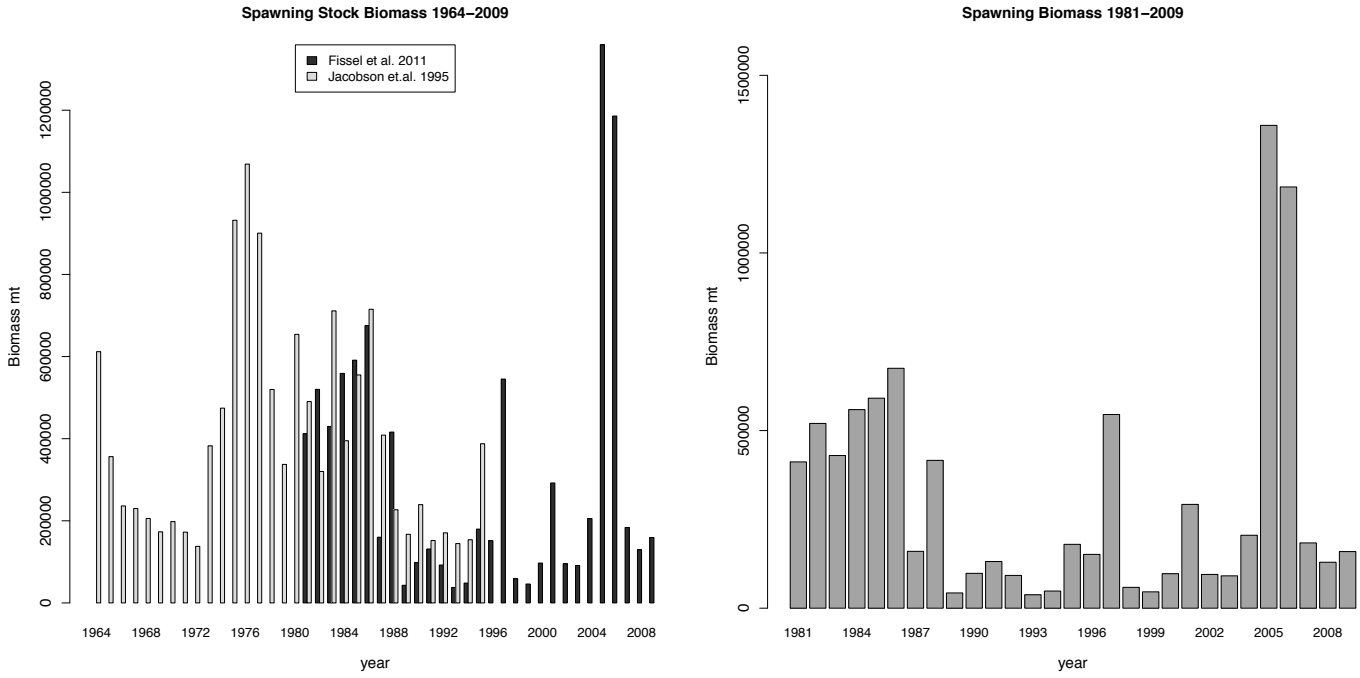

Figure 5. Comparison of historical and new annual spawning stock biomass (SSB_s) 1964–2009 (left panel). Annual spawning stock biomass 1981–2009 (right panel).

0.1% level (table 3) and can be roughly interpreted as the inverse of the daily specific fecundity per metric ton of *SSB*[6]. However, because of the assumptions and the reduced form nature of the regression γ may be capturing some latent changes over time. The implied daily specific fecundity (number of eggs produced per day per unit fish weight) per metric ton of biomass was $1/\gamma = 2.532$ E+08. Aggregate specific fecundity can be obtained by multiplying this by the *SSB*.

[6]The fecundity parameters of the stock relate *SSB* to P_0 (Parker 1980; Hewitt 1985). The stocks sex-ratio (Q), the proportion of mature females spawning (F), and the average batch fecundity (E) relative to the mature female weight (W) give the daily specific fecundity, $1/\gamma = Q^*F^*(E/W)$. The daily specific fecundity and daily egg production can be related to the spawning biomass by: $P_0 = SSB^*(1/\gamma)$.

TABLE 2
Annual spawning biomass and recruitment statistics

Year	Spawning biomass	SSB Predic. Error	Recruitment	Wind S. .05 quant	Temp. mean
1981	411825.77	76469.05	670506.17	–0.848	0.512
1982	520106.22	68050.61	2292236.85	–1.728	0.022
1983	429787.65	74202.51	557112.61	–0.850	0.855
1984	558977.70	68459.06	1058457.90	–1.633	1.199
1985	591212.10	70215.62	482741.42	–0.320	0.109
1986	675365.57	80059.39	282065.59	–0.115	0.612
1987	160075.84	46971.72	393716.32	–0.732	0.451
1988	416146.22	122111.51	851826.18	–0.739	–0.113
1989	42983.16	12612.73	193872.87	–0.886	0.081
1990	98134.15	28795.91	240347.47	–0.790	0.786
1991	131368.04	38547.87	331156.59	–0.384	–0.144
1992	92276.93	27077.20	102489.76	–0.221	1.137
1993	37769.26	11082.79	38983.16	–0.056	1.149
1994	48302.66	14173.65	56698.02	–0.070	0.910
1995	179804.42	52760.76	594143.98	–1.170	0.681
1996	151490.66	44452.53	261865.36	–0.600	0.858
1997	545291.08	160007.02	352430.96	–1.067	2.084
1998	58686.52	17220.63	71883.07	–0.218	1.077
1999	46056.91	13514.67	311754.70	–0.906	–0.609
2000	97127.44	28500.51	154578.31	–0.273	0.582
2001	292202.02	85742.05	389139.87	–0.308	0.276
2002	95067.77	27896.13	224820.84	–0.487	0.290
2003	91125.05	26739.20	180510.05	–0.443	0.536
2004	205325.91	60249.63	195895.29	–0.344	1.237
2005	1359200.63	398835.88	117862.60	–0.214	1.166
2006	1185845.47	347967.55	190403.04	–0.378	0.996
2007	183803.71	53934.28	212452.88	–0.132	0.576
2008	129379.08	37964.24	175467.13	–0.100	0.427
2009	159370.30	46764.69	590413.16	–0.965	0.167

Spawning biomass (SSB) (mt) with prediction error and recruitment (mt). Mean sea surface temperature anomaly (Temp.) and the 0.05 quantile of the north-south wind stress anomaly distribution (Wind S.).

TABLE 3
Spawning Stock Biomass Regression

Coefficients	Estimate	Std. Error	t value	Pr(>|t|)
γ	3.950E-09	1.159E-09	3.408	0.00467**
η	3.396E+05	8.822E+04	3.849	0.00201**

Signif. codes: 0 '***' 0.001 '**' 0.01 '*' 0.05 '.' 0.1 ' ' >0.1
Residual standard error: 166500 on 13 deg. of freedom
Multiple R^2: 0.848, Adjusted R^2: 0.825
F-statistic: 36.34 on 2 and 13 DF, p-value: 4.749E-06

Coefficients of the regression are the inverse of the daily specific fecundity per metric ton of *SSB* (γ) and a categorical variable for the inclusion of Mexican data, 1981–1986 (η).

TABLE 4
Standard and environmental Ricker regressions

Standard Ricker M^0			Environmental Ricker M^{WT}		
Coefficient	Estimate	Std. Error	Coefficient	Estimate	Std.Error
A	1.3991*	0.5437	A	0.5659	0.2959
B	–0.5074*	0.1384	B	–0.5074**	0.1384
			ρ_1	–106.171**	36.359
			ρ_2	–0.5663*	0.2145
Resid std. error: 0.9815			Resid std error: 0.8026		
df = 3; AIC = 93.5538			df = 5; AIC = 82.4666		

Signif. codes: 0 '***' 0.001 '**' 0.01 '*' 0.05 '.' 0.1 ' ' >0.1

Comparison of the standard and environmental Ricker recruitment models with coefficient estimates for Ricker model parameters, the 0.05 quantile of the N-S wind stress anomaly (ρ_1) and mean sea surface temperature anomaly (ρ_2).

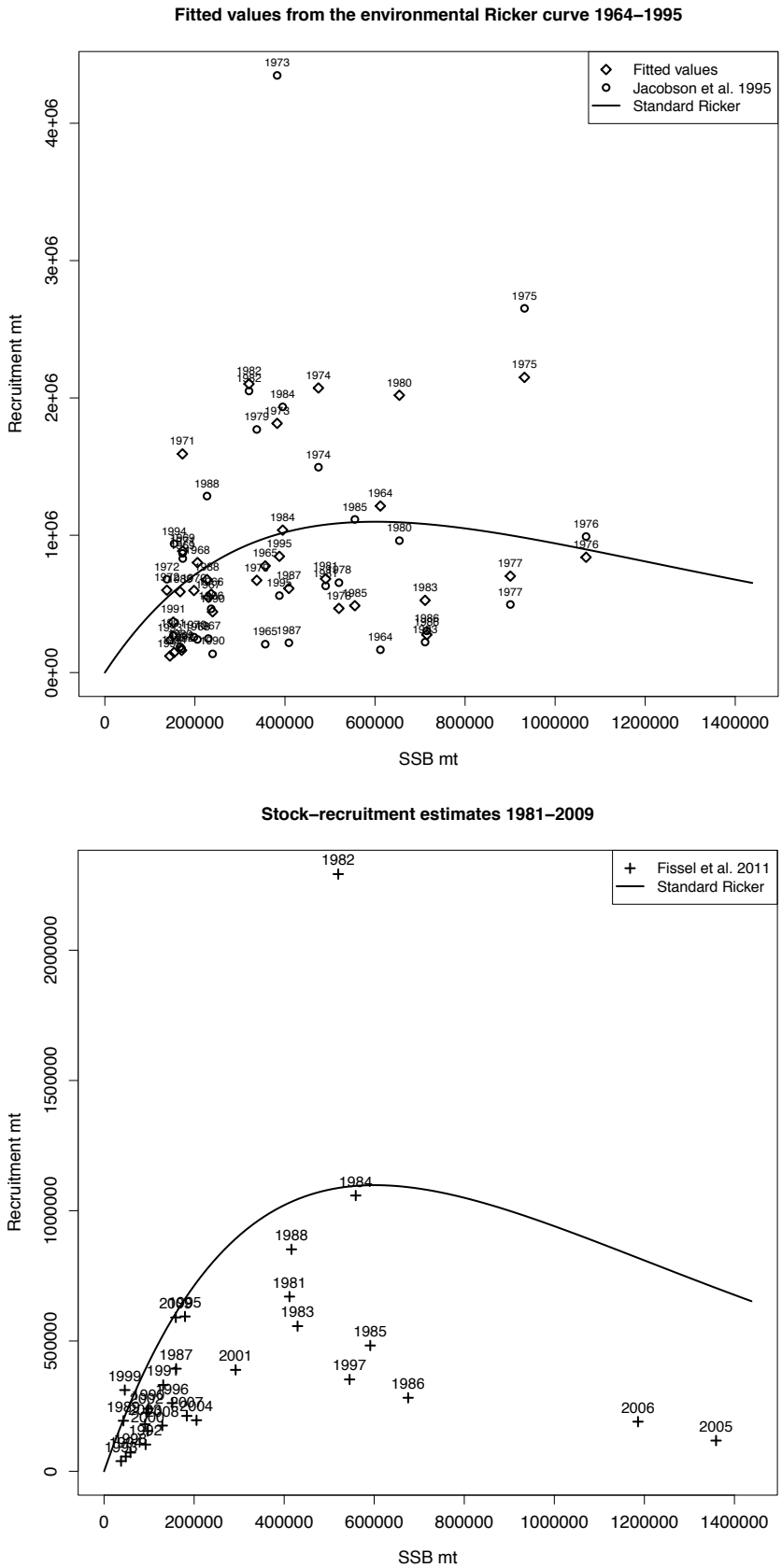

Figure 6. Fitted values of environmental Ricker model 1964–1995 (left panel) and predicted recruitment from the environmental Ricker curve 1981–2009 based on our $\widehat{SSB}_s$ (right panel).

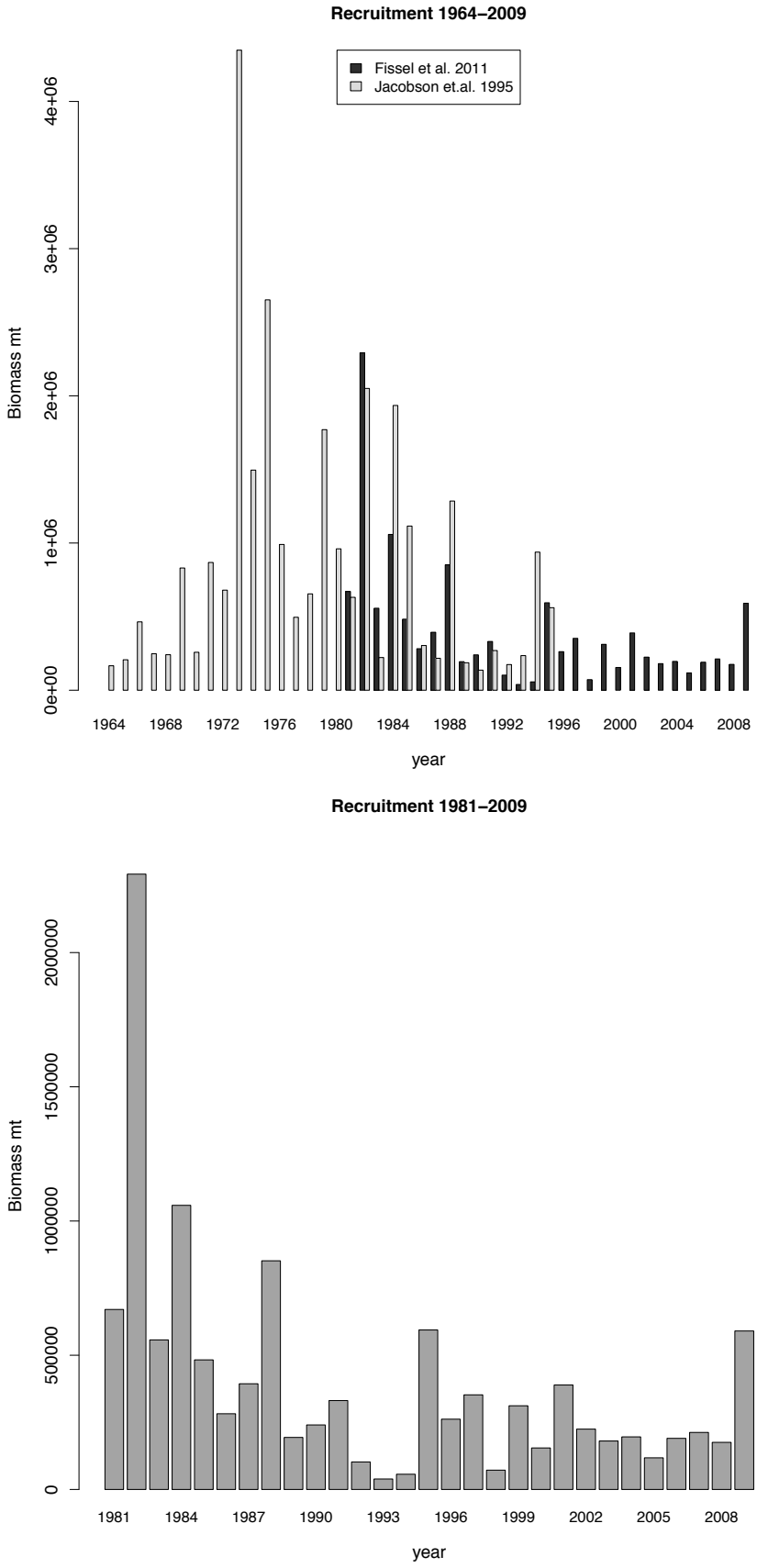

Figure 7. Comparison of historical and new annual recruitment (R_s) 1964–2009 (left panel). Annual recruitment 1981–2009 (right panel).

TABLE 5
AIC comparisons of the Ricker model specifications

AIC statistics				
Model	M^0 ($\rho_1 = \rho_2 = 0$)	M^T ($\rho_1 = 0, \rho_2 uc$)	M^W ($\rho_1 uc, \rho_2 = 0$)	M^{WT} ($\rho_1 uc, \rho_2 uc$)
AIC	93.5538	88.5827	87.5796	82.4666
Relative information likelihood statistics				
Model Comp.	$I(M^{WT}) \leq I(M^0)$	$I(M^T) \leq I(M^0)$	$I(M^W) \leq I(M^0)$	$I(M^{WT}) \leq I(M^w)$
Likelihood	0.0039	0.0833	0.0504	0.0776

Model M^0 is the standard Ricker null model, M^{WT} is the full environmental Ricker model, and M^W and M^T are models with only wind and temperature respectively. Likelihood ratios show relative information ($I(*)$) content. (*uc* means the coefficient was unconstrained).

The environmental factors were significant in the Ricker stock-recruitment model (fig. 6, table 4). The .05 quantile of the north-south wind stress anomaly was significant at the 0.1% level, and mean sea surface temperature anomaly at the 1% level. The contribution of the variables to explaining recruitment was further explored through an analysis of the AIC statisitics from different models (table 5). The unconstrained model M^{WT} had the lowest AIC. Models with only temperature (M^T) and only wind stress (M^W) were compared to the null model (M^0), the standard Ricker curve (section 2.4). The likelihood ratio statistic shows the contribution of the incorporating environmental information (table 5). The information gain in predicting recruitment provided by both environmental factors relative to the null model $I(M^{WT}) \leq I(M^0)$ is 0.004, below a 1% significance threshold. Temperature alone provides some improvement relative to the null model $I(M^T) \leq I(M^0)$ with a likelihood statistic of 0.08 which is below a 10% significance threshold, while a model with only wind stress $I(M^T) \leq I(M^0)$ is marginally above a 5% significance threshold with statistic of 0.05. The full model was compared to the model with only wind stress $I(M^{WT}) \leq I(M^w)$ and had a likelihood ratio statistic of 0.08 which is below a 10% level of significance. Both wind stress and temperature are significant in explaining recruitment, however wind stress has a comparatively larger influence. Both environmental variables were used in reported recruitment estimation (table 2). Graphical comparison of the standard Ricker and the environmental Ricker (fig. 6 left panel) shows that the temperture and wind stress produce improved fits for many years (e.g. 1975, 1977, 1982, and others), although this is not uniformly true for all years (e.g. 1976, 1980, and others).

The difference between the recruitment estimates and the standard Ricker curve shows the estimated influence of the environmental factors for 1981–2009 (fig. 6 right panel). Recruitment estimates above the standard Ricker line indicate favorable environmental conditions, while estimates below indicate the opposite. Many recent years, even when spawning biomass is high, fall below the standard Ricker curve. Comparison of Jacobson's historical data to ours show that the low recruitment levels are not without precedent and were observed in the mid to late '60s (fig. 7 left panel).

4 DISCUSSION

The anchovy ichthyoplankton data are not without their shortcomings. Previous anchovy assessments (Jacobson et al. 1995) used the *CB*, *CVT* and *PV* surveys with targeted adult and juvenile trawl surveys, and aerial spotter plane data. The latter two surveys are no longer conducted, hindering the calculation of a time-varying daily specific fecundity. Previous assessments also had staged eggs allowing the implementation of the DEPM and fundamental growth parameters had been recently estimated. While the precision of available parameters (Lo 1983) should be sufficiently accurate for HEPM estimation, parameters could hypothetically be time-varying and require updating to reflect the current environmental regime. Updated and extended sampling and research could provide further accuracy in future studies, but would not affect the trend in our estimates as these are driven by observed egg and larval densities.

The episodes of high egg densities, *SSB* and P_0 around 1997 and particularly in 2005 are prominent features of the data (fig. 3). Despite the periodic surges in spawning productivity we observed comparatively low larval densities (fig. 3). The low larval counts result in low corresponding estimates of the production at the time of hatching (P_h) which by the estimation procedure then translates into a high egg IMR. However, P_h is not directly observed and is estimated. Thus, the hatching transition itself has the potential to be a source of mortality, and one potentially susceptible to a variety of influences. Mortality at, or very shortly after, the time of hatching could confound egg IMR estimates. Regression discontinuity could be used to test this but would require staged eggs and thorough sampling to ensure accurate densities estimates around the hatching threshold.

Interpreted within the context of the modeling approach, the steady increase in the egg IMR is the primary cause of the low larval densities as opposed to the comparatively more stable coefficient of larval mortality (fig. 4). High mortality during the larval post-

yolk-sac consumption period, or critical period, would come through in mortality estimation as a lower (more negative) coefficient of larval mortality which does not appear in the data. Residual analysis does, however, show a slight negative residual bias in the later size classes that can be viewed as indicative of a critical period. The first feeding for anchovy larvae typically occurs at approximately 5mm (fig. B1 left panel). However, the magnitude of the residuals and the high egg IMR suggest post-yolk-sac stages are not the dominant source of mortality in anchovy ELH.

The assumption of a constant specific fecundity over time, used to estimate *SSB* (section 2.3), could bias estimates of *SSB*. Because anchovy are indeterminant spawners they will adjust their daily specific fecundity according to the environmental conditions: in high productivity years they will have a higher daily specific fecundity. The likely effect of our inability to capture this is overestimation of the spawning biomass in high egg productivity years (e.g. 2005–2006, fig. 5)[7]. Lacking data on spawning parameters it is unclear how to adjust the daily specific fecundity to account for temporal variation. Time trends and environmental factors in the specification of the daily specific fecundity were not significant. Despite our simplifying assumptions and inferior data, our estimates *SSB* fit the Jacobson et al. (1995) data quite well.

The failure of strong *SSB* to translate into strong *R* is analogous to the observation that high egg densities failed to translate into high larval densities. We observe higher pre-1989 larval densities and estimate strong pre-1989 recruitment classes. Larval densities after 1989 appear markedly smaller and correspondingly the environmental conditions estimate a lower recruitment through the environmental Ricker (fig. 6 right panel). The inclusion of environmental factors in the recruitment estimation was intended to provide insight into the potential sources of larval mortality by estimating a reduced form relationship between *SSB* and *R*. The time between spawning and recruitment spans the egg and larval phases of development. These phases of development are thought to be when pre-recruitment mortality is greatest. Motivated by Peterman and Bradford (1987), who examined the impact of wind speed exceeding a threshold on larval survival and hence recruitment, we use the 5% quantile of the north-south wind stress anomaly to capture this. Cooler temperatures are thought to allow for the fuller development of anchovy larvae; as such we use the mean temperature anomaly. The environmental variables are incorporated into the regression in a straightforward fashion as exponential terms.

The reduced form approach to examining environmental influences employed in this paper does not identify the point during the development process that these factors (or factors for which they're proxying) are influencing mortality. Nonetheless, one can interpret environmental Ricker as a linear model for the growth rate and carrying capacity. Equation 5 can be algebraically manipulated to express the growth rate as $\log(A) + \rho^* x$ where x is vector of environmental factors[8]. If one interprets the growth rate as an aggregate index of potential, then survival/mortality is a component of this index and the environmental Ricker serves as a model for the influence of environmental factors on ELH mortality. Stock-recruitment modeling, in general, cannot single out specific ELH stage(s) that the environmental factors influence, nor can it provide the direct linkage to the physiological mechanism impacting mortality. However, these mechanisms may be complex, nonlinear and difficult to model parametrically on a small scale. The environmental Ricker can be viewed as testing the association between the aggregate ELH mortality impact on growth rates and the environment. The utility of this interpretation clearly depends on one's perspective regarding stock-recruitment growth rates and ELH mortality. The significance of wind stress in particular (table 4) coupled with the biological research of Peterman and Bradford (1987) on larval survival support the straight forward incorporation of environmental factors in Ricker model as useful method for potentially capturing some environmental influences on ELH mortality.

Recruitment estimates indicated that the strong years of productivity (e.g. 1997 and 2005, 2006) did not translate into large recruitment classes due to poor environmental conditions. Warmer than normal sea surface temperatures and unfavorable wind patterns have contributed to poor recruitment. However, the vast majority of changes in mortality for the egg through 9.25 mm larval class appears to have occurred during the egg phase. Temperature is a potential cause of the increasing egg IMR; however, were temperature a significant contributor one would think it should be a stronger predictor of recruitment. Other potential explanations for the increasing egg IMR could be conceived, such as an increased abundance of euphausiids that can prey on the stationary eggs more easily than the mobile mature larvae. Exploration of hypotheses such as this are left for future research. Also, stock-recruitment modeling may not be ideal for identifying factors influencing the egg IMR, as large variation in the late larval and juvenile phases may leave a strong signature on recruitment, masking the straightforward identification of environmental influences on egg mortality. Ultimately, we are

[7]Daily specfic fecundity is $1/\gamma$, so underestimating fecundity results in overestimation of *SSB*, $SSB = P_0{}^*\gamma$.

[8]The Ricker model $R = SSB^* e^{r(1+SSB/K)}$ has growth rate r and carrying capacity K. Let x be a vector of environmental factors. Rewrite Equation 5 as $A^* SSB^* e^{B^* SSB + \rho^* x} = SSB^* e^{(\log(A)+\rho^* x)(1+(B/(\log(A)+\rho^* x))SSB)}$. By analogy, the environmental Ricker has growth rate $r = \log(A) + \rho^* x$ and capacity $K = (\log(A) + \rho^* x)/B$.

currently unable to explain through biological or environmental reasons the increases in the egg IMR.

While this paper does not give an overall estimate of the stock size, prolonged regimes of low productivity and recruitment combined with the short life spans of anchovy will eventually translate into a lower overall stock size. Given that the regime of low productivity has persisted for fifteen plus years, there is reason to believe that the northern anchovy stock as a whole is not as large and strong as it once was in its heyday of the '80s or even the mid '90s, and impacts on the stock and potentially the ecosystem may be at risk if a large fishery for anchovy develops. Recognizing the global demand for small pelagic fish is strong and that U.S. landings in the anchovy fishery have been on the increase (PFMC 2010), additional attention, sampling, and research into the anchovy fishery would be prudent.

5 IMPROVING FUTURE ANALYSIS

Our analysis was based on the best available data and well-established methods for estimating key population parameter. However, there are shortcomings which are not defects in the analysis, but rather directions for future research and data collection. We highlight these issues so that they may be considered for improving future anchovy stock assessments.

- Unstaged eggs preclude the use of the more accurate DEPM. The staging of anchovy eggs would provide data on egg production-at-age which could be used to model the egg mortality curve and provide more precise estimates of egg production and the IMR (Lo 1985b).
- Parameter estimates obtained from the literature (e.g. aging, see appendix A2), were estimated around 1985 and may require updating. It's possible that parameter values could have changed over time.
- Because no trawl surveys were undertaken, we had to assume constant stock parameters to infer spawning stock biomass. Targeted trawl sampling of the anchovy stock would enable the estimation of a time-varying daily specific fecundity.
- The methods used here were developed twenty years ago. More complex Bayesian hierarchical models (BHM) might be considered, enabling one to utilize data from other years (Clark 2007). Research into developing up-to-date statistical methods for anchovy that explicitly account for the various stages of estimation could improve estimation precision.

A sampling scheme tailored for the range of northern anchovy and updated parameters and methods would improve the accuracy of estimation but would not substantially affect the trends in the data or the conclusions. Despite these areas where improvements are needed, the results provided in this paper accurately reflect trends in the status of the central subpopulation of northern anchovy.

6 ACKNOWLEDGMENTS

We thank Ed Weber for providing the data; participants at the CalCOFI conference 2010 for their many helpful comments; Kevin Hill; John Field; and reviewers for insightful comments on earlier versions of this paper. The findings and conclusions in the paper are those of the authors and do not necessarily represent the views of the National Marine Fisheries Service.

LITERATURE CITED

Aydin, K. 2005. Fisheries and the Environment: Ecosystem Indicators for the North Pacific and Their Implications for Stock Assessment. NMFS AFSC Proceeds of the First Annual Meeting of the National Marine Fisheries Service's Ecological Indicators Research Program.

Butler, J. 1989. Growth during the larval and juvenile stages of the northern anchovy in the California Current during 1980–84. Fishery Bulletin. 87:645–652.

Burnham, K. P. and D. R. Anderson. 2002. Model Selection and Multimodel Inference: A Practical Information-Theoretic Approach. Springer Verlag.

CalCOFI Net Descriptions. 2010. Description of Nets Cal1MOBL (C1), CalBOBL (CB), CalVET (CVT), PairOVET (PV). http://swfsc.noaa.gov/textblock.aspx?Division=FRD&ParentMenuId=213&id=1376. Accessed 08–23–2010.

Clark. J. S. 2007. Models for Ecological data, an Introduction. Princeton University Press. 817pp.

Eber, L. E. and R. P. Hewitt. 1979. Conversion Algorithms of the CalCOFI Station Grid. Calif. Coop. Oceanic Fish Invest. Rep. 20:135–137.

Fiedler, P., R. D. Methot, and R. P. Hewitt. 1986. Effects of California El Niño 1982–1984 on the northern anchovy. Journal of Marine Research. 44:317–338.

Hewitt, R. P. 1981. The Value of Pattern in the Distribution of Young Fish. Rapp. P.-v. Reun. Cons. Int. Explorer. Mer. 178:229–245.

Hewitt, R. P. and R. D. Methot. 1982. Distribution and Mortality of Northern Anchovy Larvae in 1978 and 1979. Calif. Coop. Oceanic Fish Invest. Rep. 23:226–137.

Hewitt, R. P. and G. D. Brewer. 1983. Nearshore Production of Young Anchovy. Calif. Coop. Oceanic Fish Invest. Rep. 24:235–244.

Hewitt, R. P. 1985. Comparison between Egg Production Methods and Larval Census Method for Fish Biomass Assessment. An egg production method for estimating spawning biomass of pelagic fish: application to the northern anchovy, *Engraulis mordax*. US Dep. Commer., NOAA Tech. Rep. NMFS. 36:95–99.

Hushby, D. and C. Nelson. 1982. Turbulence and vertical stability in the California Current. Calif. Coop. Oceanic Fish Invest. Rep. 23:113–129.

Hunter, J. R. and B. J. Macewicz. 1985. Measurement of spawning frequency in multiple spawning fishes. Lakser ed. NOAA Technical Report NMFS. 36(iii):79–94.

Jacobson, L. D., N. C. H. Lo, S. F. Jr. Herrick, and T. Bishop. 1995. Spawning Stock Biomass of the Northern Anchovy in 1995 and Status of the Coastal Pelagic Fishery During 1994. Administrative Report LJ-95-11. NMFS.

Jacobson, L. D., N. C. H. Lo, and J. T. Barnes. 1994. A biomass-based assessment model for northern anchovy, *Engraulis mordax*. Fishery Bulletin. 92(4):711–724.

Lasker, R. 1981. Factors contributing to variable recruitment of the northern anchovy in the California current: contrasting years, 1975–1978. Rapp. P.-v. Reun. Cons. Int. Explorer. Mer. 178:375–388.

Lasker, R. 1985. An egg production method for estimating spawning biomass of pelagic fish: application to the Northern Anchovy, *Engraulis mordax*. NOAA Technical Report NMFS. 36(iii):1–99.

Lo, N. C. H. 1983. Re-estimation of three parameters associated with anchovy egg and larval abundance: temperature dependent incubation time, yolk-sac growth rate and egg and larval retention in mesh nets. NOAA Technical Memorandum NMFS. NOAA-TM-NMFS-SWFC-33:1–33.

Lo, N. C. H. 1985a. Egg production of the central stock of northern anchovy, *Engraulis mordax*, 1951–1982. Fishery Bulletin, 83:137–150.

Lo, N. C. H. 1985b. A model for temperature-dependent northern anchovy egg development and an automated procedure for the assignment of age to staged eggs. An egg production method for estimating spawning biomass of pelagic fish: application to the northern anchovy, *Engraulis mordax*. US Dep. Commer., NOAA Tech. Rep. NMFS. 36:43–50.

Lo, N. C. H. 1985c. Modeling life-stage-specific instantaneous mortality rates, an application to northern anchovy, *Engraulis mordax*, eggs and larvae. Fishery Bulletin. 84:395–407.

Lo, N. C. H., B.J. Macewicz, D.A. Griffith, and R.L. Charter. 2008. Spawning biomass of Pacific sardine (*Sardinops sagax*) off U.S. in 2008. NOAA Technical Memorandum NMFS. 430:1–33.

MacKinnon, J. G. 2006. Bootstrapping methods in econometrics. The Economic Record. 82:S2–S18.

Methot, R. D. and R. P. Hewitt. 1980. A Generalized Growth Curve For Young Anchovy Larvae: Derivation and Tabular Example. Administrative Report LJ-80-17, NMFS.

PFMC. 1978. 1983. Northern anchovy fishery management plan. PFMC, Portland, OR. Federal Register 43(141):31655–31783. PFMC Amendment 5 to the Northern anchovy fishery management plan: Incorporating the final supplementary EIS/DRIR/IRFA. PFMC, Portland, OR.

PFMC 2010. Status of the Pacific Coast Coastal Pelagic Species Fishery and Recommended Acceptable Biological Catches: Stock Assessment and Fishery Evaluation. PFMC, Portland, OR.

Peterman, R. and M. Bradford. 1987. Wind speed and mortality rate of marine fish: northern anchovy. Science. 235:354–365.

Ricker, W. E. 1954. Stock and Recruitment. Fisheries Research Board of Canada.

Rykaczewski, R. and D. Checkley. 2008. Influence of ocean winds on the pelagic ecosystem in upwelling regions. Proceedings of the National Academy of Sciences. 105:1965–1970.

Smith, P. E. and S. L. Richardson. 1977. Standard techniques for pelagic fish eggs and larval survey. FAO Fisheries Techniques Paper. 175:27–73.

Weber, E. and S. McClatchie. 2009. rcalcofi: Analysis and Visualization of CalCOFI Data in R. Calif. Coop. Oceanic Fish Invest. Rep. 50:178–185.

Zweifel, J. and R. Lasker. 1976. Prehatch and posthatch growth of fishes: a general model. Fisheries Bulletin. 74:609–621.

Zweifel, J. and P. E. Smith. 1981. Estimates of Abundance and Mortality of Larval Anchovies (1951–75): Application of a New Method. Rapp. P.-v. Reun. Cons. Int. Explorer. Mer. 178:284–259.

APPENDIX A: METHODS FOR DENSITY CALCULATIONS AND AGING

A1 EGG AND LARVAE DENSITY CORRECTIONS

Assignment into larval size classes was necessary prior to adjusting for extrusion and avoidance as the likelihood of extrusion decreases with length but avoidance increases with age (which is an increasing function of length). Sorting is based on preserved larval size which is recorded at the time of staging. Length thresholds for the larval size classes (Lo 1985a) are listed in table A1. Because of differences in mesh sizes of the nets, *CVT/PV* and *CB* nets differ in their sampling efficiency. Smaller larvae and eggs are more likely to extrude through the *CB* net, but are retained more efficiently in the finer mesh size of the *CVT/PV*. However, *CB* is more efficient at catching larger larvae. Extrusion factors (table A1), calculated by Lo (1983) to compensate for these differences, were applied to the size classes to obtain extrusion free counts (0.075 mm mesh was treated as extrusion free (Lo 1983)).

Avoidance corrections were made to *CB* samples to correct for the propensity for older developed larvae to avoid the net. No avoidance corrections are necessary for *CVT/PV* because the net is pulled vertically through the water column. The avoidance equation from Lo et al. (1989) was used for the correction:

$$avd_c = \frac{1 + DNl_c}{2} + \frac{1 - DNl_c}{2} * cos(2\pi * hr/24) \quad (1)$$

where *hr* is the time of day on a 24 hour clock the tow was taken, and DNl_c represents the day/night catch ratio for larval size class *c*. The DNl_c used here differs from the one used in Lo et al. (1989). In contrast to Lo et al. (1989) we calclated DNl_c as $DNl_c = e^{-0.229*c}$ because it is more up-to-date and logically consistent.

Raw egg and larval counts were standardized to an area-density using standard haul factors (*SHF*) (Kramer et al. 1972); where *SHF* = 10*(tow depth/volume of water filtered) which represents abundance beneath an area of 10 m^2 integrated over the depth of the tow. This 10 m^2 area-density will be refered to simply as a 10 m^2 density. A second adjustment was made for the percentage of total plankton volume sorted from the samples. The overall adjustment can be represented as $rct_k * shf_k / prst_k$ where rct_k is the raw count (egg or larval), $prst_k$ is the percentage sorted and shf_k is the *SHF* for sample k[1].

TABLE A1
Larval size classes and length ranges, extrusion correction factors for bongo (CB), calvet and pairovet (CVT/PV) and growth curve coefficients.

Size Class	Range [a]	*CB*[b]	*CVT/PV*[c]	Month	a^{mn} [d]
eggs	N/A	12.76	1.10	Jan.	0.046
2.5	[2,3.25]	6.08	1.46	Feb.	0.048
3.75	[3.25,4.25]	2.58	1.37	March	0.05
4.75	[4.25,5.25]	1.62	1.30	April	0.052
5.75	[5.25,6.25]	1.24	1.25		
6.75	[6.25,7.25]	1.10	1.21		
7.75	[7.25,8.25]	1.00	1.00		
8.75	[8.25,9.25]	1.00	1.00		
9.75	[9.25,10.25]	1.00	1.00		

[a]Assignment to classes is based on preserved larval lengths (section 2.2.2). All larval sizes are measured in mm.
[b]Extrusion factors for *CB* computed directly from the logistic model of Lo (1983) equation (6), table 4.
[c]Extrusion factors for *CVT* and *PV* are fitted values of a logistic regression on the raw estimates from Lo (1983).
[d]Gompertz growth second stage parameter (Methot and Hewitt 1980).

A2 EGG INCUBATION TIME AND AGING OF LARVAE

Unstaged egg data precluded us from aging individual or even groups of eggs, however, the incubation time has a known temperature dependent functional from Lo (1983). Missing temperature data from the surveys were rare; occurances were interpolated using an inverse distance spatially weighted average of other observed temperatures during that cruise. Temperature measurements at each sample, *k*, were used in the relationship specified by Lo (1983) to calculate incubation times:

$$t_k^I = 18.726 * e^{-0.125 * tmp_k} \quad (2)$$

where t_k^I is the incubation time and tmp_k is the temperature measured in degrees Celsius.

The calculation of larvae age requires the live larval length. Preserving agents used at the time of sampling and tow time can shrink larvae. Therefore adjustments for these factors were made before aging using the correction function specified in Theilaker (1980):

$$l_k = \log(ff * pls_k) + 0.289 * \exp(-0.434 * ff * pls_k * q^{-0.68}) \quad (3)$$

where l_k is the estimated length of live larvae in millimeters (mm) from sample *k* with a preserved larval length of pls_k mm, a tow time of *q* minutes, and *ff* is a paramter base on the preserving agent. Formalin was the preserving agent so *ff* = 1.03 (Theilaker 1980). Tow time was not included in our data set and was assumed to be 15.5 minutes based on CalCOFI sampling guidelines (Cal-

[1]Sample indices *k* are specific to a year, cruise, and station. Furthermore, occasionally multiple samples were observed at a station on a cruise, each would have its own index *k*. Without loss of generality, a single index is used here, and later, as explicitly specifying all dimensions of the indices would provide no further insight.

COFI 2010). The remaining numeric values were taken from Theilaker (1980). No rounding of *pls* by grouping into size classes was carried out prior to estimation of *l* and *pls* was recorded up to the precision of 0.1 mm in our data set.

Larvae were aged using a two-stage Gompertz growth curve (GGC). This approach was first proposed for the use on anchovy larvae by Methot and Hewitt (1980) and later with updated first-stage parameter estimates by Lo (1983). The first stage of the GGC accounts for growth through yolk-sac consumption, which is approximately the first two size classes 2.5 mm and 3.75 mm. Aging during the first stage of the GGC is temperature dependent while aging during the second stage is month-of-sampling dependent. Because of this, it is necessary to compute ages as sample specific. The first stage of the GGC is specified as:

$$T1(l_k) = \left(\frac{-1}{a_k^{tmp}}\right) * \log\left(\frac{\log(l_k/4.25)}{\log(0.32/4.25)}\right) \text{ for } l_k \le 4.1 \text{ mm}$$

$$a_k^{temp} = 0.1108 * e^{0.1173 * tmp_k} \quad (4)$$

where $T1(l_k)$ is the estimated age of larvae with length l_k (equation A3). The value 4.25 controls the upper bound of the growth curve (mm) during the first stage of growth while the value 0.32 is the hypothetical minimum larval size. The temperature dependent parameter a_k^{tmp} was specified by Lo (1983). The second stage of the GGC is meant to capture the post yolk-sac consumption period of larval growth, and is specified as:

$$T2(l_k) = \left(\frac{-1}{a^{mn}}\right) * \log\left(\frac{\log(l_k/27)}{\log(4.1/27)}\right) \text{ for } 4.1 \text{ mm} < l_k < 27 \text{ mm} \quad (5)$$

where $T2(l_k)$ is the age of larvae length l_k (from equation A3) since the first stage. The value 27 controls the upper bound of the second-stage GGC and 4.1 is the length at which larvae transition into the second stage of growth. The monthly parameter α^{mn} was estimated by Methot and Hewitt (1980) and its values are listed in table A1. The total age of the larvae is $t(l_k) = T1(l_k)$ for yolk-sac larvae which haven't entered the second stage of growth ($l_k \le 4.1$ mm) and $t(l_k) = T1(4.1) + T2(l_k)$ for larvae beyond the yolk-sac stage ($l_k > 4.1$ mm)[2].

A3 DAILY LARVAL PRODUCTION

Even with regularly scheduled ichtyoplankton surveys the number of eggs or larvae from a single sample on a given cruise at a station is too few to accurately characterize densities. To minimize small sample biases, aggregation over cruises was necessary prior to the calculation of production statistics and mortality estimation. Each sample tow was assigned to a CalCOFI station (Weber and McClatchie 2009; Eber and Hewitt 1979) and multiple samples observed at a station on a cruise were averaged. No weighting of cruises was used and all data were averaged across cruises occuring during January through April of a year to obtain annual station specific data. A final average over stations was needed to obtain accurate annual mortality curve estimates for the region as a whole.

The production of larvae in a size class per day per unit area, *DLP*, is estimated as standing stock of larvae in a size class over the days that larvae spend in that class, or duration. Duration is the difference between the ages (equations 4 and 5) at the size class break points (table A1). Let $n_{c,s}$ be the standing stock of larvae[3] and $d_{c,s}$ be the duration of size class *c* in year *s*. *DLP* is then calculated as $dlp_{c,s} = n_{c,s} / d_{c,s}$. Avoidance by larvae older than twenty days (Lo 1985a) biases estimates of *DLP*. Larvae were found to have reached an age of twenty days towards the end or just after the 9.75 mm size class. To mitigate these biases we omitted class sizes larger than 9.75 mm from the analysis.

[2]Frequently, age will be referred to simply as *t*, and the functional dependence of age on length $t(l_k)$ being explicit only where needed.

[3]The standing stock of larvae is the total corrected count of all larvae in a size class and can be viewed as the integral over ages in that size class, e.g. $n_{c=3.75\text{ mm}} = P_h \int_{t(l=3.25\text{ mm})}^{t(l=4.25\text{ mm})} \left(x/t^l\right)^{-\beta} dx$.

APPENDIX A LITERATURE CITED

Eber, L. E. and R. P. Hewitt. 1979. Conversion Algorithms of the CalCOFI Station Grid. Calif. Coop. Oceanic Fish Invest. Rep. 20:135–137.

Kramer, D., M. Kalin, G. Stevens, J. R. Thrailkill, J. R. Zweifel. 1972. Collecting and processing data on fish eggs and larve in the California Current Region. NOAA Tech. Rep. NMFS Circ.370:38.

Lo, N. C. H. 1983. Re-estimation of three parameters associated with anchovy egg and larval abundance : temperature dependent incubation time, yolk-sac growth rate and egg and larval retention in mesh nets. NOAA Technical Memorandum National Marine Fisheries Services. NOAA-TM-NMFS-SWFC-33:1–33.

Lo, N. C. H. 1985a. Egg production of the central stock of northern anchovy, *Engraulis mordax,* 1951–1982. Fishery Bulletin, 83:137–150.

Lo, N. C. H., J. R. Hunter, and R. P. Hewitt. 1989. Precision and bias of estimates of larval mortality. Fishery Bulletin, 87(3):399-416.

Methot, R. and R. P. Hewitt. 1980. A Generalized Growth Curve For Young Anchovy Larvae: Derivation and Tabular Example. Administrative Report LJ-80-17, National Marine Fisheries Services.

Theilacker, G. H. 1980. Changes in body measurements of larval northern anchovy, *Engraulis mordax*, and other fishes due to handling and preservation. Fishery Bulletin. 78(3):685–692.

APPENDIX B: BOOTSTRAPPING MORTALITY PARAMETERS

B1 INTRODUCTION

This appendix explains the bootstrapping methods used to estimate the annual variability of the early life-history parameters: production at the time of hatching (P_h), the coefficient of larval mortality (β), egg instantaneous mortality (IMR) (α) and the daily egg production (P_0). Mortality curves estimated in the main manuscript (section 2.2.1), used a Pareto type mortality curve (this regression will be referred to as MC^0). The iterative procedure used to identify the egg IMR (α) (equation 2) and the calculation of P_0 (equation 3) yields only point estimates for α and P_0. Lo (1985a) approached the problem of estimating variability for these point estimates using an approximation based on the delta method. When applied to our data the standard errors produced were too large to be meaningful, frequently displaying a coefficient of variation greater than 1.

The bootstrap is used to provide more precise estimates of the variability using confidence intervals of the bootstrapped distributions. An advantage of this approach is that it characterizes confidence intervals for a general class of true underlying distributions, in particular accurate interval construction is more robust to fat tails and extreme tail events. The residual bootstrap method (MacKinnon 2006) is used, which samples from the residual empirical cumulative distribution function (cdf) of MC^0 and applies the resampled residuals to the fitted daily larval production estimates $\widehat{dlp}$ to for bootstrapped $\widehat{dlp}^*$, on which new mortality curves with new parameters were estimated. Normalization is required to stabilize the heteroskedasticity in the residual distribution. When applied to equations 1–3 annual bootstrap distribution of β, P_h, α, and P_0 are created from which we take the 0.025 and 0.975 quantiles as the 95% confidence interval of the associated statistics.

The results of methods used in this appendix are 95% confidence intervals for β, P_h, α, and P_0. In addition, the residual analysis necessary for the heteroskedasticity stabilization is discussed in the results and discussion section.

The next section describes the bootstrapping methods in detail. Section three reports some of the intermediate estimation results and section four discusses the methods used and the residual distribution. Confidence intervals were referenced in the text of the main manuscript and can be found in table 1, and figure 4.

B2 METHODS

The residual bootstrap uses the empirical cdf of the residuals from the initial estimation of the mortality curve MC^0 (section 2.2.1) as a measure of the true error term associated with larval mortality estimation. Residuals are given by

$$\widehat{\varepsilon_{c,s}} = dlp_{c,s} - \widehat{dlp_{c,s}}, \text{ where } \widehat{dlp_{c,s}} = \widehat{P_{h,s}} \left({t_{c,s}}/{t_s^I} \right)^{\widehat{-\beta_s}} \quad \text{(B1)}$$

and $\widehat{\beta_s}$ and $\widehat{P_{h,s}}$ are the annual (s = 1981, 1982, …, 2009) estimated parameter values relating daily larval production ($dlp_{c,s}$) to larval ages ($t_{c,s}$) over the incubation time (t_s^I) for larval size class ($c \in \{$*larval class* 2.5 mm, 3.75 mm, …, 9.75 mm$\}$) (appendix A1 and table A1).

There were eight larval size classes in a year and simply resampling from the eight residuals on that year would not provide a sufficiently rich set of residuals to characterize the true residual distribution. Furthermore, size class dependent heteroskedasticity precluded resampling from this small set of residual. To overcome this residuals from all 29 years of mortality estimation normalized by exploiting the longitudinal structure were of the residual data. Linear approaches to bootstrap normalization are not applicable for nonlinear regression (MacKinnon 2006)[1]. We use a linear regression with ages and years as independent variables to model the heteroskedasticity and purge the residuals of class and temporal dependence. Higher-order polynomial terms and other categorical variables were tried, and a first-order linear regression minimized the AIC criterion. The heteroskedasticity stabilizing regression is:

$$\omega_{c,s} = |\widehat{\varepsilon_{c,s}}|, \quad \gamma_s = \frac{s - mean(s)}{stdev(s)}$$

$$\omega_{c,s} = \theta_0 + \theta_1 t_{c,s} + \theta_2 \gamma_s + \theta_3 D2_s + \nu_{c,s} \quad \text{(B2)}$$

where $\omega_{c,s}$ is the absolute deviation of the residual, γ_s is the normalized year, $t_{c,s}$ is the larval size class age, $D2_s$ is a categorical 0–1 variable capturing the anomalous years 2005 and 2006 ($D2_s$ = 1) (section 2.3) and $\nu_{c,s}$ is the error term. Outliers exerted excessive leverage and led to a poor fit. Outliers were determined from a preliminary regression of B2 as observations associated with a preliminary residual z-score greater than six, $6 \leq {\widehat{\nu}_{c,s} - mean_{0.01}(\widehat{\nu})}/{stdev_{0.01}(\widehat{\nu})}$ (where the 0.01 subscript indicates a trimmed mean/standard deviation). This identified three observations as outliers. Equation B2 was then fit with outliers removed to determine the final fit. The fitted root-squared residuals were then used to normalize the residuals distribution.

[1] E.g. using the diagonal element of the hat data matrix $X(X'X)X'$ where X is the data matrix used in liear regression.

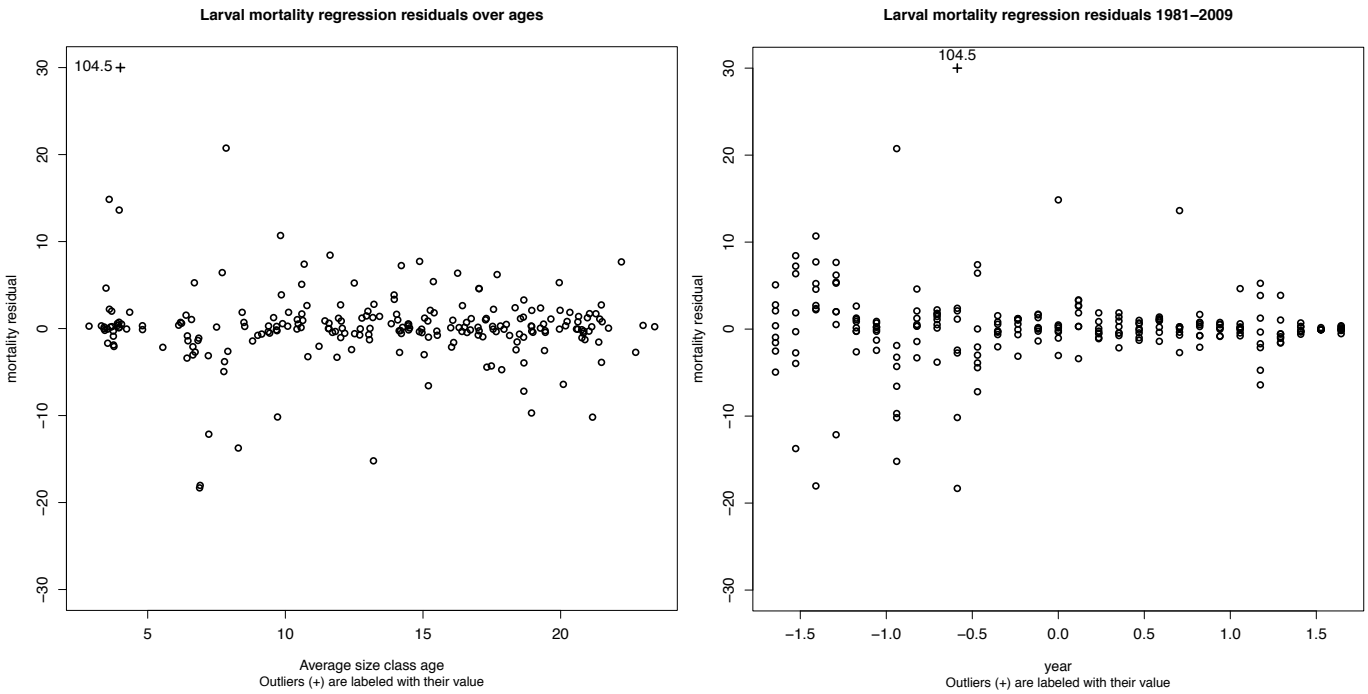

Figure B1. Larval mortality residuals (from equation 1) over the average size-class ages ($t_{c,s}$) (left panel), and normalized years (y_s) (right panel) 1981–2009.

$$\widetilde{\varepsilon}_{c,s} = \varepsilon_{c,s} \Big/ |\widehat{\omega}_{c,s}| \tag{B3}$$

where

$$\widehat{\omega}_{c,s} = \hat{\theta}_0 + \hat{\theta}_1 t_{c,s} + \hat{\theta}_2 \gamma_s + \hat{\theta}_3 D2_s \tag{B4}$$

This procedure produces a set (29 years x 8 classes = 232) of temporally and class "independent" residuals forming a distribution that was used to perform the bootstrapped. For each year s, eight residuals (one for each size class) were randomly sampled with replacement from the set of residual, $\varepsilon^{BS} \in \{\widetilde{\varepsilon}_{c,s}\}$. Residuals were centered and rescaled to the have the size class and temporal variance as determined by equation B4. The new resampled residuals were added to the fitted daily larval production from the initial estimation stage (equation 1 and B1) to obtain bootstrapped *DLP* estimates.

$$\varepsilon^{BS'} = \varepsilon^{BS} - \frac{1}{8}\sum_{i=1}^{8} \varepsilon_i^{BS}, \; \varepsilon^*_{c,s} = \varepsilon^{BS'} * |\widehat{\omega}_{c,s}|,$$

$$\text{and } dlp^*_{c,s} = \widehat{dlp}_{c,s} + \varepsilon^*_{c,s} \tag{B5}$$

The bootstrapped *DLP* $dlp^*_{c,s}$ estimates were then used to fit a new mortality curve.

$$dlp_{c,s}{}^* = \widehat{P_{h,s}}^* \left(t_{c,s} \Big/ t_s^I \right)^{\widehat{-\beta}_s^*} \tag{B6}$$

The estimated production at the time of hatching $\widehat{P}_{h,s}{}^*$ was then used with the standing stock of eggs (m_s) and the incubation time (t_s^I) to determine the egg IMR ($\hat{\alpha}_s^*$) by iterative method (section 2.2.1, equation 2).

$$\hat{\alpha}_s^* \text{ is the } \alpha_s \text{ such that } \frac{m_s}{\widehat{P}_{h,s}{}^*} = \frac{e^{\alpha_s * t_s^I} - 1}{\alpha_s} \tag{B7}$$

Bootstrapped $\widehat{P}_{0,s}{}^*$ was obtained by the calculation (section 2.2.1, equation 3):

$$\widehat{P}_{0,s}{}^* = \widehat{P}_{h,s}{}^* e^{\widehat{\alpha}_s^* * t^I} \tag{B8}$$

The preceding bootstrap algorithm (equations B1–B6) was repeated 1000 times. On occasion, some of the bootstrap residuals ($\varepsilon^*_{c,s}$) would be sufficiently negative to produce a daily larval production value less than zero ($dlp^*_{c,s} < 0$) which was treated as if no larvae were observed for that class. If this happened for more than two size classes during an iteration then that iteration was discarded and repeated. If NLS failed to converge or β_s was estimated to be positive (illogical curvature of the mortality curve) or $\beta_s < -3$ (suggesting convergence in a bad area of the parameter space) then a log linearization was performed and parameters were estimated using OLS. Final estimates of $P_{h,s}$ were then calculated assuming normality of $\log(P_{h,s})$ (i.e. $P_{h,s}$ is log normally distributed).

This algorithm produced bootstrap distributions ($\{\widehat{\beta}_s^*\}$, $\{\widehat{P}_{h,s}{}^*\}$, $\{\widehat{\alpha}_s^*\}$, $\{\widehat{P}_{0,s}{}^*\}$) each with 1000 observations. The 0.025 and 0.975 quantiles of these distri-

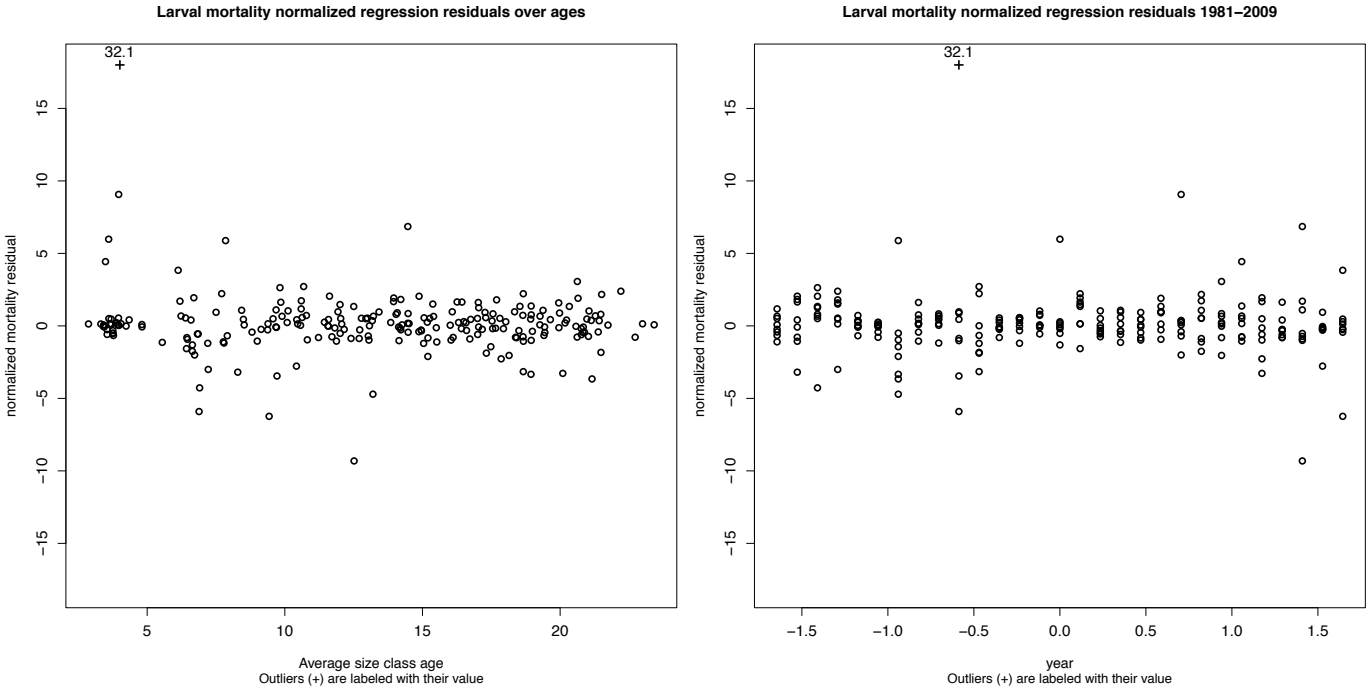

Figure B2. Larval mortality residuals over average size-class ages from hatching ($t_{c,s}$) (left panel), and normalized years (y_s) (right panel) after normalization.

butions were taken as a nonparametric estimate of their respective 95% confidence intervals.

B3 RESULTS

The residuals from MC^0 (section 2.2.1, equation 1) displayed heteroskedasticity across both ages and years (fig. B1). Coefficient estimates for the heteroskedasticity stabilizing regression support the visual observation of a decreasing volatility with both age and time (table B1).

Based on the observed heteroskedasticity in the residuals, failing to stabilize the class and temporally dependent variation would introduce spurious nonstationarity into the residuals upon resampling for the bootstrap. The heteroskedasticity stabilizing regression (equation B2) does an acceptable job of modeling the heteroskedasticity in MC^0 (table B1). Graphical analysis shows that dispersion around the mean is more evenly distributed (fig. B2) after the variance stabilization. Outliers are still outliers in the normalized residuals as they were intentionally removed during the regression. The normalized residual distribution is still highly leptokurtotic even with the outliers removed with a kurtosis of 12.08 (a standard normal distribution has a kurtosis of 3). Thus, heavy tails and extreme tail events are still a feature of the residual distribution used for resampling.

The grid search algorithm over initial condition during the NLS estimation (section 2.23) made more iterations computationally prohibitive in R. Furthermore, it was verified through histograms of 1000 iterations per-year that the number of iterations was sufficient. Marginal increases in the number of iterations to 1500 and 2000 iteration failed to noticeably change the distribution or confidence intervals from it.

Bootstrapped confidence intervals were referenced in the text of the main manuscript and can be found in table 1, and figure 4.

B4 DISCUSSION

Residual bootstrapping treats the empirical distribution formed by the set of residuals as sufficient for the true distribution. Resampling randomly reassigns residual from other classes and times to the fitted *dlp* estimates. Failing to account for the class and temporal differences in the residual distribution would introduce spurious variation into the residuals upon resampling for the bootstrap. The linear model for the heteroskedasticity is based on a Breusch-Pagan test for heteroskedasticity (Breusch-Pagan 1979), except it uses the absolute deviation. The normalization is identical to the normalization performed in a feasible weighted least squares heteroskedasticity correction (Cameron and Trivedi 2005). The heteroskedasticity stabilizing regression appears to have stabilized the variation as indicated by the more homogeneous variance (fig. B2). The heavy tails or extreme tail events of the normalized residual distribution is quite likely a feature of the true mortality error distribution which should be retained during resampling.

An implied assumption in this approach of the estimation variability for P_0 and α is that all variability comes from random error at the larval stage, $\varepsilon_{c,s}$ (equation 1).

Other potential sources of variation in P_0 and α were explored. The calculation of P_0 and the iterative method for α are simple definitional relationships and any error in the methods for the point estimates calculated after mortality estimation is negligible. The standing stock of eggs (m) and incubation time (t^I) are also used in HEP estimation and can potentially have a stochastic component. Reduced form attempts to model this stochasticity, that attempted to exploit the spatial variation over station within a year, were explored. A residual bootstrap method was again used with residual taken as deviation from a reduced form spatial model such as a spatial moving average process, spatial autoregressive process or a spatial distributed lag process. The results were that some additional variation was introduced but did not widen the confidence intervals for the parameters of interest significantly. The ad-hoc nature of this approach coupled within its marginal contribution led us to abandon this approach. Furthermore, aggregation over samples, cruises, and stations is likely to smooth the stochasitic components of m and t^I. Thus, we assume that the calculated values of m and t^I are accurate annual statistics for the region in the sense that randomness in sampling or other sources is minimized by the aggregation. Alternatively, our bootstrapped distributions can be interpreted as conditional on the observed m and t^I.

Calculations of higher order moments (such as the variance) of the data can be particularly sensitive to extreme tail events. Thus, confidence intervals for parameter estimates can have poor coverage when constructed using standard errors based on a distribution prone to extreme tail events. The large standard error estimates for α_s and P_0 based on the delta method were likely the result of the heavy-tailed distributions. Furthermore, extreme events can also result in uncentered distributions. We obtain accurate coverage for parameter confidence intervals by reporting bootstrapped confidence intervals in place of the regression standard errors for the NLS estimation of MC^0 (equation 1).

APPENDIX B LITERATURE CITED

Breusch, T. and A. Pagan. 1979. A Simple Test for Heteroscedasticity and Random Coefficient Variation. Econometrica. 47:1287–1294.

Cameron, A. C. and P. K. Trivedi. 2005. Microeconometrics: methods and applications. Cambridge University Press.

Lo, N. C. H. 1985a. Egg production of the central stock of northern anchovy, *Engraulis mordax*, 1951–1982. Fishery Bulletin, 83:137–150.

MacKinnon, J. G. 2006. Bootstrapping methods in econometrics. The Economic Record. 82:S2–S18.

STOCK ASSESSMENT OF THE WARTY SEA CUCUMBER FISHERY (*PARASTICHOPUS PARVIMENSIS*) OF NW BAJA CALIFORNIA

ERNESTO A. CHÁVEZ
Centro Interdisciplinario de Ciencias Marinas
IPN La Paz, B.C.S. 23096, México
echavez@ipn.mx

MA. DE LOURDES SALGADO-ROGEL
Instituto Nacional de Pesca (INAPESCA)
Centro Regional de Investigación
Pesquera Ensenada (CRIP) Ensenada
Baja California 22760, México
lusaro_mx@yahoo.com

JULIO PALLEIRO-NAYAR
Instituto Nacional de Pesca (INAPESCA)
Centro Regional de Investigación
Pesquera Ensenada (CRIP) Ensenada
Baja California 22760, México
juliopalleiro@yahoo.com.mx

ABSTRACT

The catch of the warty sea cucumber *Parastichopus parvimensis* off northwestern Baja California declined since 1997 from 622 metric tons to almost one third through the last thirteen years, in a relatively stable harvest. The fishery employs 294 fishermen, with annual profits of $243,000 USD. The goal of the study was to assess the stock biomass, the socioeconomic performance of the fishery, and to evaluate harvesting scenarios. A relative constancy of fishing mortality (F) and the stock biomass were observed the last thirteen years. Current profits per fisher are near the maximum the fishery can produce, which is profitable under a narrow combination of age of first catch and F. Fishermen seem to avoid unprofitable activity when fishing intensity increases, so there is an apparent tendency to reduce economic risk by exerting a low effort. Immature animals are exploited, but under the low F applied, the stock can withstand it without showing signs of depletion.

INTRODUCTION

Holothurian fisheries are generally small scale and based on a few deposit-feeding species belonging to two families and five genera (Conan and Byrne 1993). *Parastichopus parvimensis* (Clark) is common from Baja California, Mexico, to Monterey Bay, California, USA, although only scattered individuals were reported to occur north of Point Conception, California. *Parastichopus parvimensis* is found mainly in low energy environments from the intertidal down to 30 m and can reach a maximum length of 30–40 cm (Bruckner 2006). These animals are an important component of benthic communities of the subtidal zone, recycling nutrients and cleaning the environment (Yingst 1982), being more commonly found on rocky and stony grounds from the low-tide level to >60-m depth (Woodby et al. 2000). They are dioecious and the gender ratio is 1:1 during the reproductive stage. Breeding season varies latitudinally along the west coast of Baja California, as in the stocks of Todos Santos Bay and El Rosario located in the northern peninsula, where it occurs in the spring-summer period, whereas in Isla Natividad and Bahia Tortugas, located off the center of the peninsula, it occurs in winter-spring (Fajardo-León et al. 2008). Fully developed gonads were observed in individuals whose body weight ranges from 120 to 160 g (Pérez-Plascencia 1995, Espinoza-Montes 2000; Fajardo-Leon et al. 2008) and they begin reproducing when they are about two years old (Pérez-Plascencia 1995).

There is little information on the population dynamics of the warty sea cucumber. Muscat (1982) mentioned that recruitment is sporadic and that natural mortality is very high. Schroeter et al. (2001) found seasonal variations in the density of this species in California, USA, recording the highest values in spring and the lowest in autumn. Toral-Granda and Martínez (2007) describe the reproductive biology and population structure of the sea cucumber of the Galapagos Islands. The fishery of the warty sea cucumber in Baja California, Mexico, started formally in 1989, and is done mainly by the red sea urchin fishermen, who obtained fishing permits for its commercial exploitation, making this activity complementary and alternative to that of the sea urchin fishery. This activity takes place mainly when the red sea urchin fishery is closed from March to June each year. Currently, stakeholders are mostly red and purple sea urchin fishermen, who use the same fishing grounds, equipment, and capture system (hookah diving). Each team consists of a fishing boat with three crew members: the captain, the air provider, and a diver (Salgado-Rogel and Palleiro-Nayar, 2008). Fishing takes place along the Pacific coast of Baja California, from Ensenada, Baja California close to the US border, to Bahia Asuncion, southern Baja California, in the middle of the peninsula. In the the state of Baja California Sur, the fishermen require special permits, whereas in Baja California (northern Baja) it is entirely commercial. In Mexico, *P. parvimensis* is exempt from the NOM-059-ECOL-2001, which includes species under special protection (DOF 2002); however the National Fisheries Chart (DOF 2004), the Mexican regulatory legal instrument, states that the sea cucumber fishery is deteriorating and that management guidelines should be based on the assignment of catch quotas, with the removal of 10% of the exploitable biomass. The warty sea cucumber fishery in Baja California is based on the catch of nearly 250 metric tons (mt)

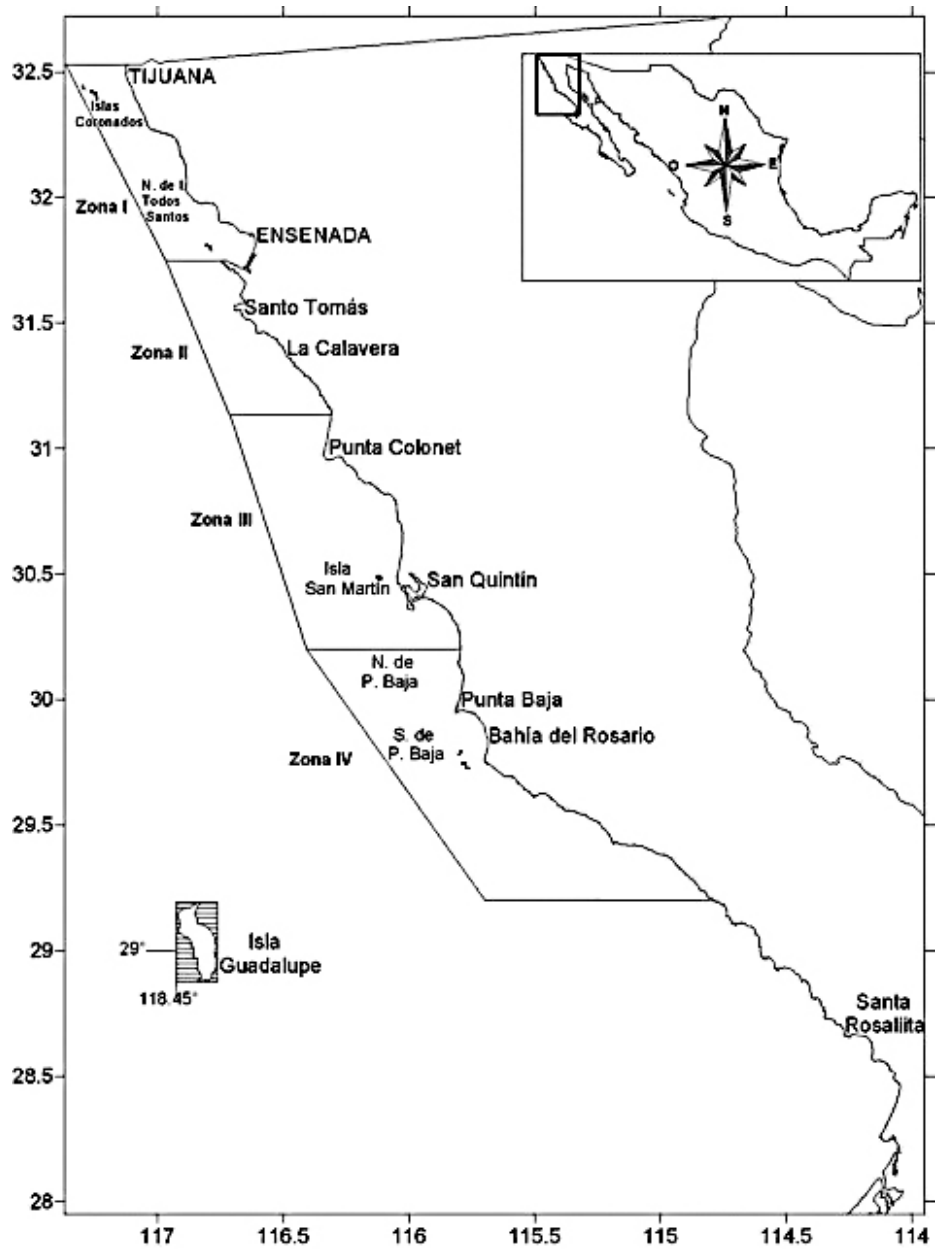

Figure 1. Fishing zones of the warty sea cucumber along the northwestern coast of Baja California, Mexico.

by 270 fishermen in 90 fishing boats allocated to four fishing zones (fig. 1), during a 55-day fishing season, and made at depths no deeper than 20 m.

The fishery takes place along the northern half of the western Baja California peninsula, between 29°2' and 32.5°N latitude. There is a high demand by the Asian market for the warty sea cucumber. This and the apparent scarcity of the product led to the assumption that the stock is overexploited and the need to assess this fishery with a socioeconomic diagnosis. For this reason, this paper provides some management options that are not considered in Mexican fishery regulations. The stock is exploited in four fishing zones. The fishing zone I goes from the USA border to Punta Banda, zone II ranges from Punta Banda to Punta Colonet, zone III from Punta Colonet to El Socorro, and zone IV from El Socorro to El Rosario (figs. 1, 2).

Exploitation of the sea cucumber has become a productive activity for exporter countries to Asian markets, where the demand for this product seems to be constantly increasing. In consequence, some tropical producers, such as Mexico and Ecuador, have responded to this demand by exploiting their sea cucumber stocks to the point of depleting some populations, which are not

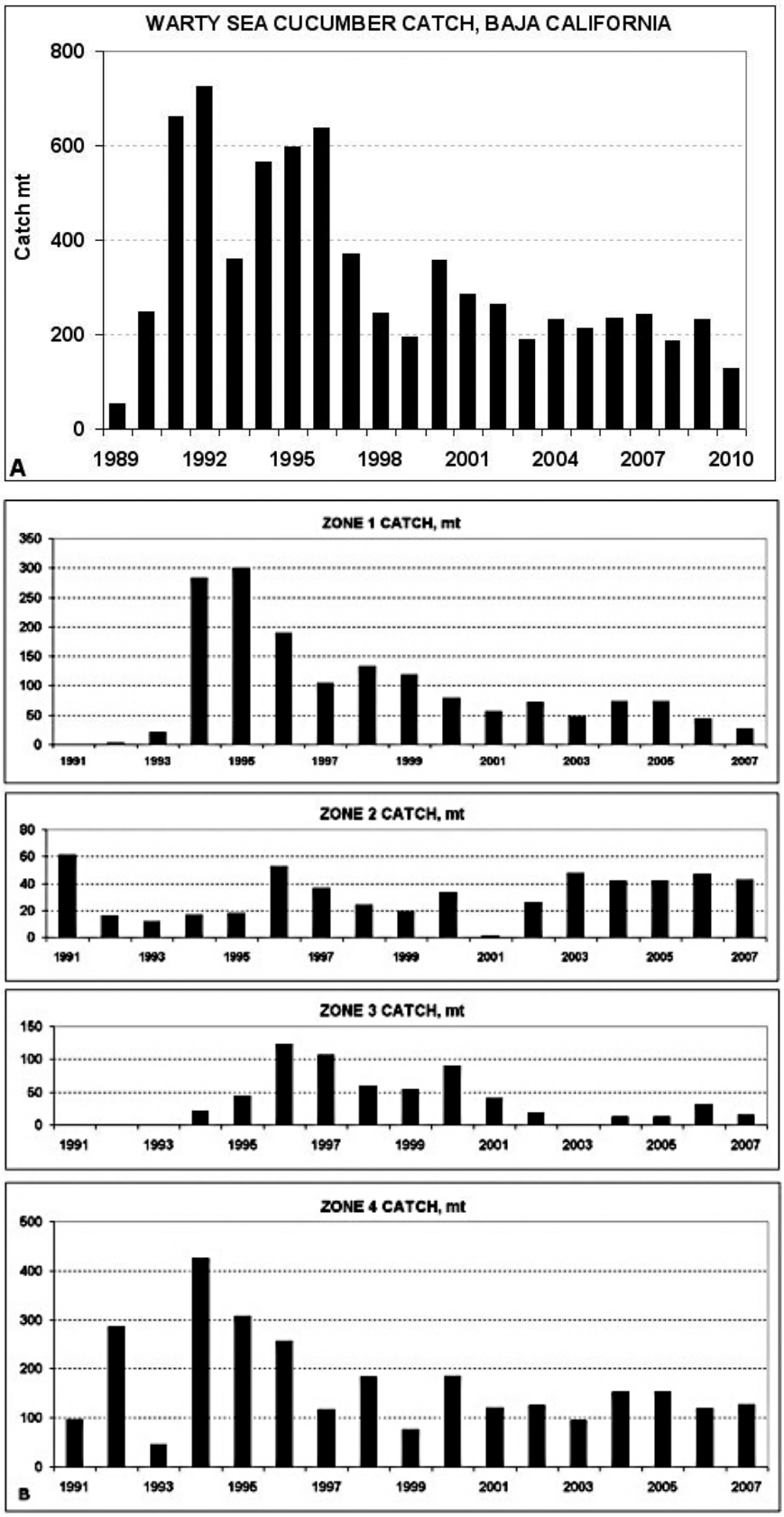

Figure 2. Catch records (t) of the warty sea cucumber exploited in all fishing zones (A) and in each of the four fishing zones (B) off the northwestern coast of Baja California, Mexico.

abundant and whose dynamics are characterized by being density-dependent, with a low recruitment rate, long lives, and consequently easily overexploited (Anonymous 2004; Toral-Granda and Vasconcellos 2008; Friedman and Gisawa 2010). Examples of this have been shown by the *Isostichopus fuscus* fisheries in the lower Gulf of California (Herrero-Pérezrul and Chávez 2005), Ecuador and the Galapagos Islands (Carranza and Andrade 1996; Anonymous 2000a), which were depleted, led the Mexican authorities to close the fishery during the late 1990s (Anonymous 1994; Anonymous 2000b; Sonnenholzner 1997) and reopen it in 2002 under strict control of the access to the fishing grounds.

The maximum catch of the warty sea cucumber was recorded in 1992, with 723 mt, but landings decreased to around 240 mt in recent years (fig. 2; Salgado-Rogel et al. 2009).

METHODS

Monthly samplings were made on sea cucumber landings from all fishing grounds during the season. At each sampling, twenty kilos from each of two boats were taken and each sea cucumber was put in a plastic bag and weighed without water.

Age and growth rate

A requirement for stock assessment is the knowledge of the age and growth rate of exploited stocks. This condition imposed the need of trying to evaluate the growth rate of the warty sea cucumber with sampling data and establishing the correspondence between length and weight. The lack of hard structures where growth rings are usually read led to the use of the analysis of this process by means of methods based on the indirect estimation of age based in the modal-progression analysis of size. First, the data from Pérez-Plascencia (1995) were reworked to obtain the parameters *a* and *b* of the exponential length-weight regression to transform the weight data into their corresponding lengths, because the software analyzing growth uses only length data. The power regression is

$$W = a \cdot L^b$$

The assessment of the stock was made using catch data for the last fifteen years. Changes in abundance over time were determined by using the catch data as a reference for estimating the population size. Population parameter values were determined by the use of the ELEFAN and Bhattacharya methods in the FISAT software package (Gayanilo et al. 1996). Before using these methods, it was necessary to transform weight data into their corresponding lengths. Weight-frequency values were obtained from samplings made on the catch (figures 3a, b).

Once the catch data and growth rate were known, with the aid of the FISAT software package, estimates of the age composition of the catch were made and further analysis, including scenarios of feasible harvesting strategies, were evaluated with the aid of the simulation model FISMO (Chávez 2005). With these partial results the total mortality (Z_t) could be determined with the exponential decay model as

$$N_{a+1} = N_a \cdot e^{(-z_t)} \quad (1)$$

where N_{a+1} is the number of warty sea cucumbers of age a+1 and N_a is the number of warty sea cucumbers of age *a* in reconstructed age groups. With the numbers per age known, the use of the von Bertalanffy growth equation allowed the determination of their corresponding lengths at age. Time units are years.

In the virtual population reconstructed, the age structure for each year was estimated assuming a constant, natural mortality (M). In the exploited age groups, the fishing mortality (F) was added to M and so the total mortality was known, Z = M + F. For setting the variables of the initial state, the abundance per age-class ($N_{a,y}$) was set using the age-specific abundance $N_a/\Sigma N_a$ obtained from equation (1). In subsequent years, the age structure was defined after the estimation of the number of one-year-old recruits. These values were used to calculate catch-at-age as proposed by Sparre and Venema (1992) and were integrated into the simulation model as

$$Y_{a,y} = N_{a,y} \cdot W_{a,y} \frac{F_t}{(F_t + M)} \left(1 - e^{(-F_t - M)}\right)$$

where $Y_{a,y}$ is the catch-at-age *a* of each year y, $N_{a,y}$ is the number of warty sea cucumbers at age *a* in year y, $W_{a,y}$ is the warty sea cucumber weight equivalent to $N_{a,y}$, F_t and M are as described. Given the initial conditions, the values of $Y_{a,y}$ were adjusted by varying the initial number of recruits and linked to the equations described above until the condition of the following equation was fulfilled,

$$\sum_{a}^{\lambda} Y_{a,y} = Y_{y(REC)}$$

where $Y_{y(REC)}$ is the yield recorded during the year y, *a* = 2 years, and t_λ = 3/K or longevity, where K is the growth constant of the von Bertalanffy growth equation and t_λ = 5 years. The value of *a* was found by assuming that a reasonable life expectancy (L_{max}) is when 95% of the population reaches 95% of L∞, the asymptotic length. Thus, by making $L_{max} = 0.95L\infty$ in the von Bertalanffy growth equation and finding the respective value of t, the longevity value was found. However, in the simulation, the model considers up to 20 age groups. Use of the catch equation was made for each year in the time-series analyzed.

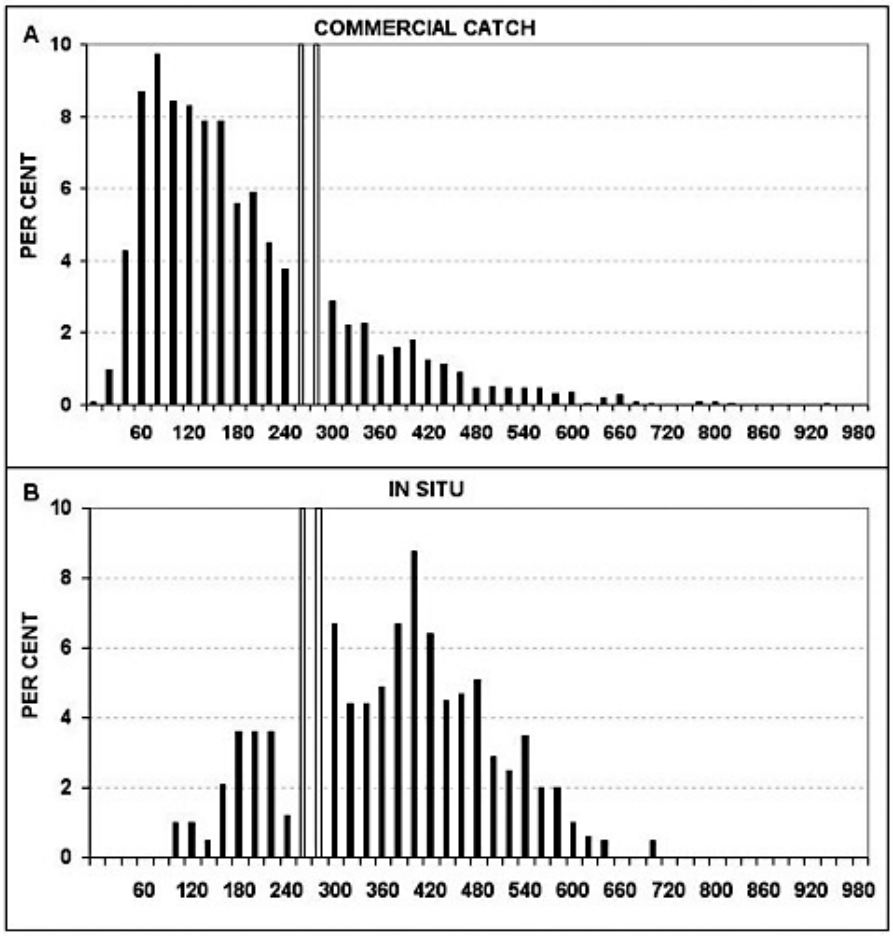

Figure 3. Weight-frequency distribution of the warty sea cucumber stock after samplings made in A, sampling of landings, and B, fishery-independent samplings. The weight at first catch is about 280 g, shown as two white bars, which also is the weight at first maturity.

Mortality

For the estimation of the natural mortality (M), the criterion proposed by Jensen (1996, 1997) was adopted, where M = 1.5K. For purposes of comparison, other M values were estimated by using methods proposed by other authors and are presented in Table 1. Estimations of the stock biomass and the exploitation rate E = [F/(M+F)] were made for each age-class in every fishing year analyzed by the model. These values were compared to the E value at the maximum sustainable yield level (F_{MSY}), a special case, which is the maximum exploitation rate that a fishery should attain before the stock is overexploited. A diagnosis of which years of the series the stock was under- or overexploited was then made, providing a way to diagnose the status of the stock and to recommend either a further increase or decrease in F at the fishery.

The annual cohort abundance ($N_{a,y}$) coming from ages older than age-at-maturity (t_m = 2 years) was used to estimate the annual abundance of adults (S_y) over the years, whereas the abundance of the one-year-old group was used as the number of recruits (R_y). The stock-recruitment relationship was evaluated by using a slightly modified version of the Beverton and Holt (1957) model in the form

$$R_{y+1} = \frac{a'S_oS_y}{S_y + b'S_o} \quad ,$$

where R_{y+1} is the number of one-year-old recruits in year y+1, S_y is the number of adults in year y, S_o is the maximum number of adults in the population, and *a*' and *b*' are parameters modified from the original model where a' is the maximum number of recruits and *b*' is the initial slope of the recruitment line, which was constant through the simulation. The intensity of recruitment depends to a great extent on the stock size, as part of an ecological mechanism related to density dependence and carrying capacity.

Model Simulation

The population parameters plus the catch and socioeconomic data were analyzed with the aid of the simu-

TABLE 1
Population parameter values obtained after the analysis of the length-frequency data used for the evaluation of the warty sea cucumber fishery. M values obtained after three other methods used for estimating M apart from M = 1.5K are also shown.

Parameter	Value	Units-Model	Source
K	0.6	Bertalanffy	This paper (ELEFAN)
L∞	50	mm, Bertalanffy	This paper (ELEFAN)
W∞ (g)	514	Live weight, Bertalanffy	This paper
to	–0.10	Years, Bertalanffy	This paper
a	0.4	Length–weight	This paper
b	1.83	Length–weight	This paper
Age of 1st catch	2	Years, both sexes	This paper
Maturity age	2	Years	Tapia et al. 1996
Longevity	5	Years	As 3/K, this paper
a'	0.29	Beverton & Holt S-R	After age structure
b'	3.16	Beverton & Holt S-R	After age structure
M	0.83	Instantaneous rate	Pauly (1980); Rikhter & Efanov (1976)
M	0.85	Instantaneous rate	Hoenig (1983)
M	0.9	Instantaneous rate	As I.5K (Jensen 1996, 1997)
E_{max}	0.25	$F_{MSY}/(M+ F_{MSY})$	Exploit. rate at MSY, this paper
Phi'	3.2	Log K + 2Log L∞	Growth performance, this paper

lation model FISMO (Chávez 2005). The weight at first maturity has been estimated to be at about 75 g eviscerated weight (Tapia-Vásquez et al. 1996) and after the analysis of weight-frequency of the landed catch and the estimation of growth rate, we found that the age of first capture is 2 years, which was maintained constant in the analysis of the catch records.

The model reconstructs the age structure over time and exploitation scenarios were simulated under different combinations of fishing intensities and the age-at-first catch to maximize the biomass, the profits, and the social benefits, as the number of fishermen in the fishery and the maximum profit per fisherman. For this purpose, analytical procedures adopting the concepts and views of Chávez (1996; 2005) and Grafton et al. (2007) were used.

The approach to the socioeconomics of the fishery was made through the explicit consideration of the costs of fishing per boat per fishing day ($41.30), the number of boats (98), the number of fishermen per boat (3), and the number of fishing days during the fishing season (55). The catch value ($2.00) is the price at the dock of the warty sea cucumber landed before adding value. The difference between the costs of fishing (C) and the catch value (the benefit, B) is known, so the value divided by the cost is the B/C ratio. In the simulation, the costs of fishing per day-boat and catch value were assumed constant over time. The information of the 2009 fishing season allowed us to reconstruct the economic trend of this fishery for the last fifteen years with the aid of the simulation model, using the estimates of fishing mortality over time as a reference and its correspondence to the economic variables. The changes in the population abundance using the number of survivors in each cohort were estimated. The initial condition is set by assigning a seed value to F, usually choosing F_{MSY}, which at $t_c = 2$ years, is $F_{MSY} = 0.3$, allowing an estimation of an initial recruitment number and then estimations of abundance for each cohort during each year.

Model Validation

The model was developed with 15 years of catch data. In the validation process, the 15th year was left out of the direct evaluation and its value was simulated as if it were unknown. Then the model was fitted to the whole series of 15 years. The difference between the recorded and simulated values of this 15th year provided a way to evaluate the uncertainty in the assessment made for 2009, the last year of the catch records analyzed. The catch was displayed by the model, where the stock biomass and the fishing mortality for each year of the series were estimated.

RESULTS

Evidence of overexploitation of recruits is shown in the weight-frequency bar graphs (figs. 3a, b) showing a remarkable bias towards the exploitation of juvenile sea cucumbers by the fishermen from samplings made of the catch landed, as compared to the weight-frequencies recorded from fishery-independent samplings. This is what is known in fishery biology as recruitment overfishing (Hilborn and Walters 1992).

For transforming weight (g) data into their corresponding lengths (cm), the parameters of the length-weight regression found are $a = 0.4$ and $b = 1.83$. Then the Fisat software package by Gayanilo et al. (1996) was used, where the Battacharya method for extracting normal components from length-frequency data was used intially. Next, the routine named as Elefan method was used for the estimation of the growth parameter values. These and the other population parameter values found and used as input of the model are shown in Table 1.

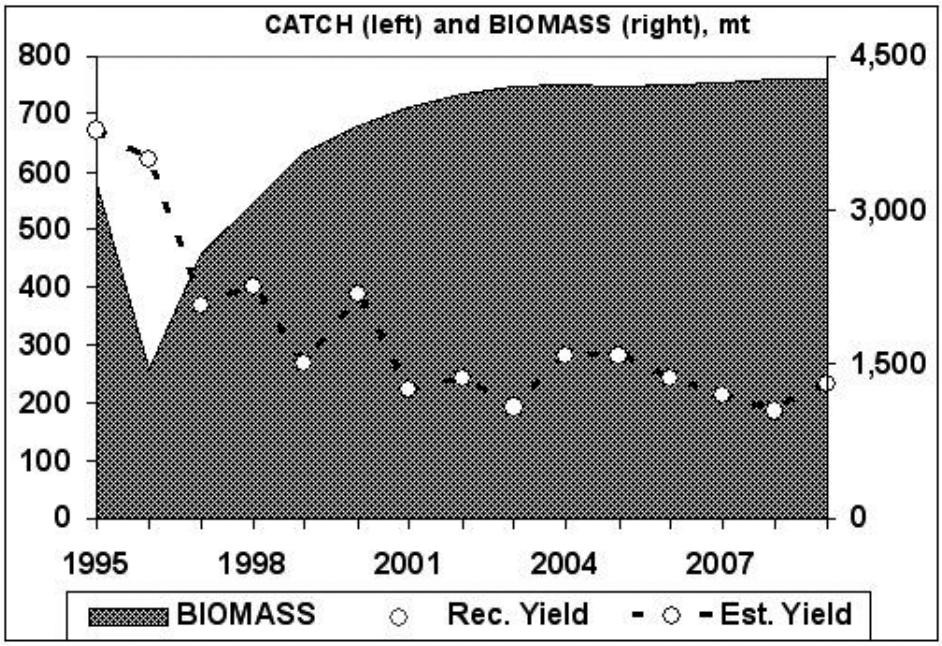

Figure 4. Stock biomass (left) and catch (right) in mt of the warty sea cucumber fishery off the northwestern Baja California peninsula.

Condition of the Fishery

Stock biomass. The results show that the stock biomass had a declining trend since the beginning of the fishery and during the period of analysis since the first year (1995), when the catch was 671 mt. Through the 2000s, the catch has been low and relatively stable at low levels, probably caused by the low profits obtained during the years of high fishing intensity leading to a reduction of fishing effort. The maximum stock biomass of the years of analysis also is about 4,300 mt (fig. 4). The difference between direct estimations of catch and those obtained by simulation ranged between –5.9% and +3.3%, with a coefficient of variation of CV = 0.46.

The intensity of exploitation indicates that the fishery had a very high exploitation intensity during the second year. In an apparent consequence of this, the exploitation rate E in 1996 was almost twice the level of E_{MSY}, with a decrease in biomass, when the model output suggests that there were no profits. In an apparent response to this condition, the fishing effort was considerably reduced afterward and the catch decreased by nearly 50% for 1995 and 1996. Further reductions of catch took place thereafter ranging between 186 mt and 282 mt since 2001 (fig. 4). At first sight, this trend and the overexploitation of juveniles shown in Figure 3, led us to assume that the catch was reduced because the stock was over-exploited. However, after an initial decline in 1996, the analysis indicates that the biomass has been quite stable since 2000 and therefore a decline in the catch must have been generated by a different cause, not overfishing.

Fishing intensity and exploitation rate. After the estimation of the stock biomass, part of the diagnosis consisted in the estimation of F and E over time. For F, results show that excepting 1996, when the stock was clearly overexploited, in all other years the F values suggest that the fishery was underexploited and in ten of the fifteen years examined, the F values are below 0.1, indicating a condition of underexploitation, as compared to the F at the MSY level that is 0.3, as shown in Figure 5. The performance of the E values is consistent with those of F in 1996, when a strong overexploitation is evident. The exploitation rate suggests a condition of underexploitation, in particular through the last eleven years, when values range below 0.1, with the threshold or MSY level at E = 0.25 (fig. 5; table 2).

Bioeconomic Analysis

In 2009, the fishery provided jobs to 270 fishermen on 90 boats, each boat working 55 days per fishing season. The cost of each fishing-day per boat was $41.30 USD and the total fishing effort was 5,390 days. The catch obtained was 233 mt with a value of $466,000, producing profits of $243,000 with a benefit/cost ratio of 2.1, which is twice the cost of fishing operations (fig. 6). These results indicate that with exception of 1996 and 1997, when apparently there were no profits, the fishery has been a profitable activity and stable economically.

To examine the stock response and its economic condition as a function of the fishing intensity, the simulation describes a series of curves, of which four were selected to display the potential socioeconomics of the

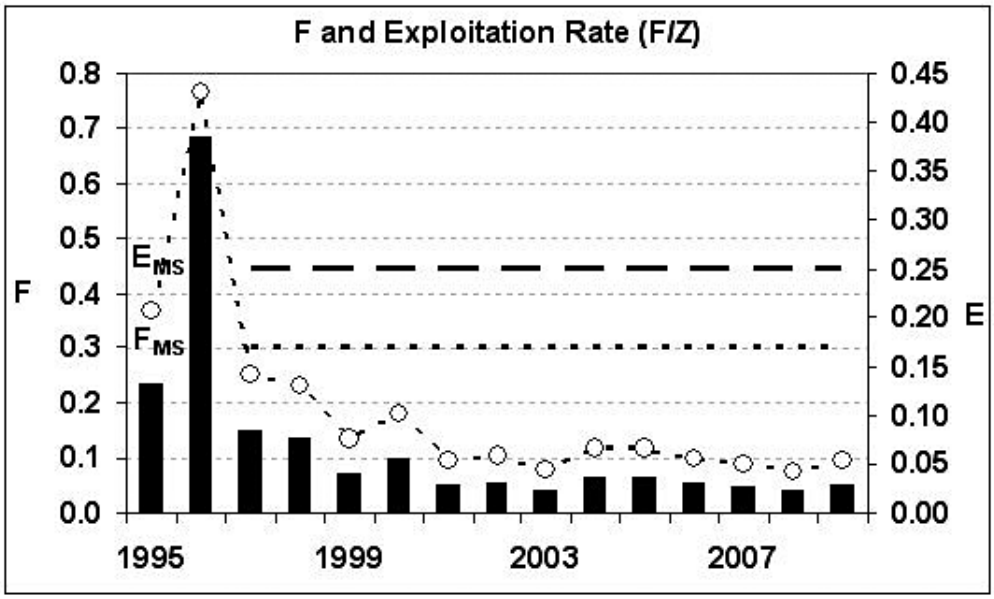

Figure 5. Exploitation rate (E) and fishing mortality (F) values of the warty sea cucumber stock, also showing the values of E and F at the MSY level (horizontal broken lines) over the fifteen years of analysis.

TABLE 2

Management scenarios for the warty sea cucumber fishery off Baja California. The condition for the 2009 fishing season is used as reference. The management options are F_{MSY} = F at the MSY level; F_{MEY} = F at the MEY level, both with a t_c = 1 year. Costs and value are in USD. Yields are those to be obtained in the long term after the stock is restored. The fishing effort per boat was maintained constant in the 55 days per season, as recorded from the year 2009. Daily cost per boat is also constant at $41.30, which per fishing season is $9,587.00. C.V. is the coefficient of variation of recorded catch, 46.4%. Catch value is expressed in thousand USD. M$/Fisher is the condition of the fishery where profits per fisher are a maximum. EE = Economic equilibrium, when catch value is equal to the cost of fishing.

INDICATORS	2009	F_{MSY}	F_{MEY}	M$/Fisher	EE	Units
F (/y)	0.05	0.5	0.028	0.03	0.32	Rate
t_c	2	1	1	2	2	Years
E	5	36	3	3	26	Percent
CATCH	233	1,479	219	143	681	mt
VALUE	466	2,958	437	286	1,362	1,000 USD
FISHING DAYS	5,405	51,975	2,911	2,911	32,998	Per year
FISHERS	294	11,842	259	98	2,510	3/Boat
BOATS	98	3,947	86	33	837	
FLEET CAP.	49	1,973	43	18	419	mt
TOTAL COSTS	223	2,146	120	120	1,362	1,000 USD
B/C	2.1	1.4	3.6	2.2	1.0	
PROFITS	243	813	317	148	328	1,000 USD
PROFITS/BOAT	2	0.2	4	4	0	1,000 USD
PROFITS/FISHER	827	69	1,225	1,521	0	USD

fishery. These are the yield, the profits, the number of fishermen, and the profits per fisher. In two of them (yield and fishermen), the maximum F value (F_{MSY}) is at F = 0.35 (fig. 7). At this fishing intensity, the maximum potential yield would be 685 mt, the number of boats required would be 846, providing employment to 2,538 fishermen. However, under this fishing intensity, the fishery is no longer profitable, because the B/C = 1 is attained at F = 0.32. Therefore, the performance of the output variables imposes the need that F < 0.32 for the existence of an economic activity. It is interesting to mention that if t_c is reduced to t_c = 1, then the potential yield at F_{MSY} would be 1,486 mt with a profitable activity, but if t_c = 2, the B/C value at the equilibrium would be atained at F = 0.317 and the catch at F_{MSY} would be reduced to only 685 mt but the fishery would be not profitable. The F necessary for maximum profits is found at F_{MEY} = 0.028 with t_c = 1, and the profits would be about $317 million (M). However, to get to this condition, the fishing effort should be reduced from the current 5,405 fishing days to 2,911 (fig. 7; table 2), implying a reduction of the number of fishermen from 294 in the current condition to 259.

The F_{MSY} was used here as a reference point to evalu-

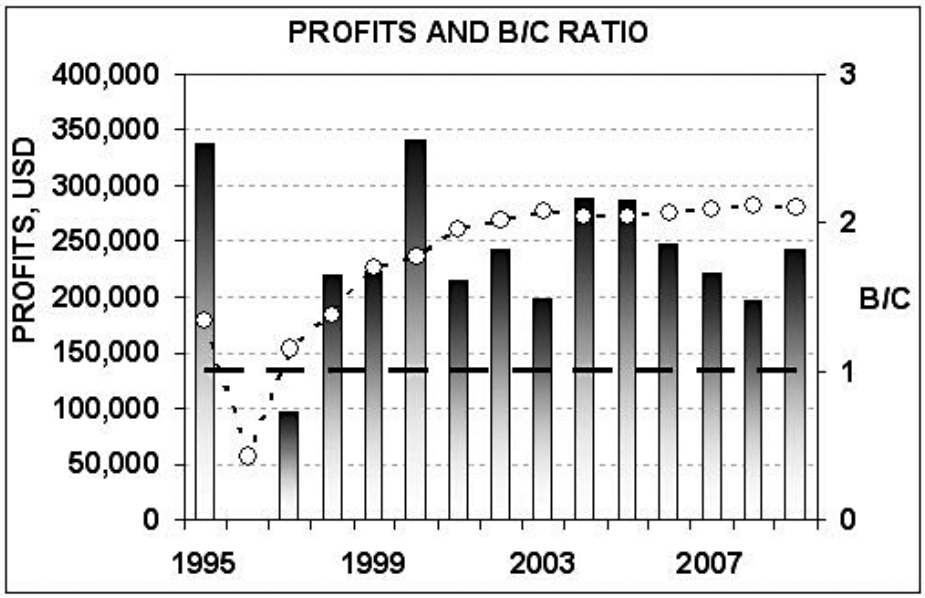

Figure 6. Reconstruction of total profits (bars, left scale) and the benefit/cost ratio (right scale) over fifteen years of the warty sea cucumber fishery off the northwestern coast of the Baja California peninsula. The horizontal broken line is the B/C ratio at the equilibrium level (B/C = 1). When B = C the economic condition of the fishery is at equilibrium, meaning that the exploitation is not profitable, and when this ocurrs it means the begining of a socioeconomic crisis.

ate the biological, economic, and social consequences of using the current fishing effort or other possible options, as shown in Table 2, where three different scenarios are compared to the current condition. The values of all other variables depend on F and t_c, so these should be considered as the reference or independent variables, and indicators in the ouput are the consequences of any strategy chosen. The maximum social benefit is derived from the number of boats fishing, so their maximum number is multiplied by the number of fishermen per boat and this is how the maximum social benefit is known. The economic-equilibrium level indicates the F value at the limit, where the fishing intensity cannot be increased because beyond that level it becomes unprofitable.

MANAGEMENT OPTIONS

Trends in the fishing mortality (F) over time and the estimates of the total stock biomass were examined. The criteria for evaluation of fishing scenarios were based on the F and the age of first catch at the maximum sustainable yield (F_{MSY}) and at maximum economic yield (F_{MEY}), and are shown in Table 2. If the fishing authorities decide to adopt any of these options, it would be convenient to examine in detail the best way to apply the chosen one in such a way that the fishery is sustained in the long term and the social problems are minimized.

With the aid of the simulation model, four possible options of F and t_c were explored and the most likely consequences of each one were evaluated: the condition under the F_{MSY}, the condition under F_{MEY}, the F producing the maximum profits per fisherman, and the state of variables at the economic equilibrium (B/C = 1). When the F_{MSY} is chosen as target of the fishery, at F = 0.5, the age of first catch must be reduced to t_c = 1. Here the catch would increase to more than six times the current value, but this is not a good option because it would not be profitable. After a review and evaluation of the current and other possible harvesting strategies, we concluded that as consequence of the narrow range of profitable F and t_c values, the current one is close to the most convenient option. In Table 2 the most likely results of the application of these management strategies are shown.

DISCUSSION

World capture of sea cucumbers reached a peak of 23,400 mt in 2000, decreasing to about 18,900 mt in 2001 (Vannuccini 2004). The high economic value of the sea cucumber fisheries in the international market and their low biomass and low turnover rate are factors contributing to their vulnerability, making these stocks easily overexploited. However, apart from the belief of a depleted condition of the stock before this analysis, we concluded that the fishery is currently exploited very near to the level of maximum profit per fisher, which we believe is intuitively adopted by the fishermen. A possible explanation to this is that the fishery is profitable under a very narrow range of t_c and F values and therefore it is suspected that after an empirical knowledge of this from the fishermen's viewpoint, they may find it easier to exploit the stock under less risky conditions, leading to harvesting the warty sea cucumber within the

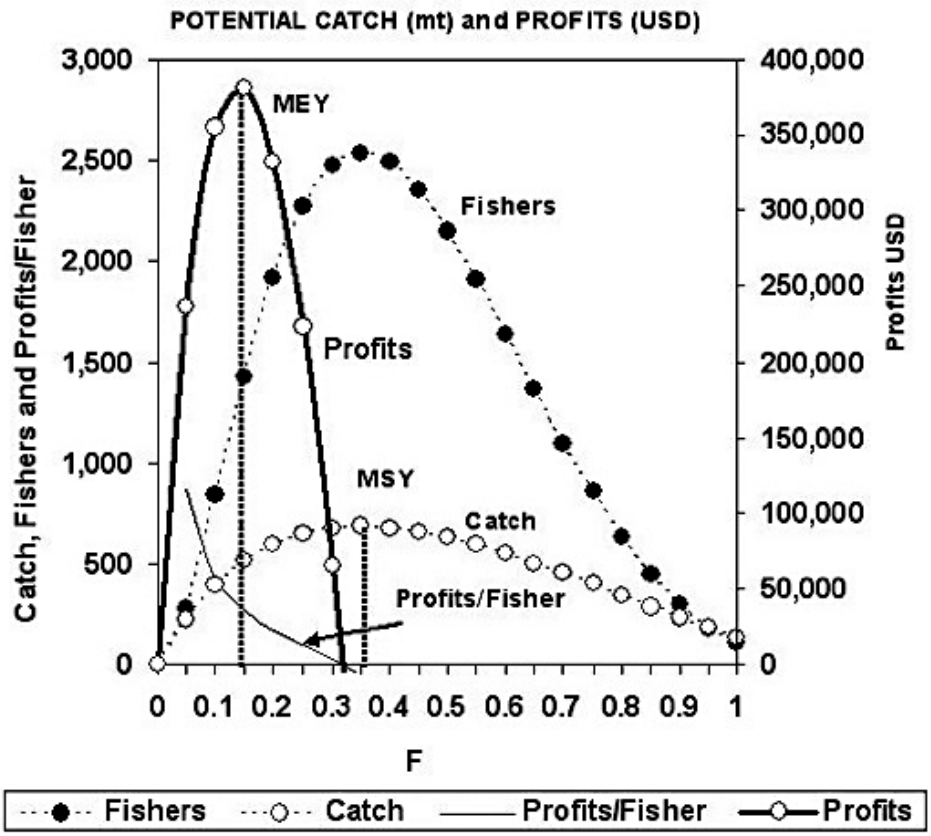

Figure 7. Bioeconomic stock response of the warty sea cucumber fishery off the northwestern Baja California peninsula, showing the trend of the potential yield, potential profits, the number of fishermen, and the potential profits/fisher, as a function of the fishing mortality, tc=2 years. The maximum profits (MEY) are attained at an F level lower than the one required for the MSY. The line describing the numbers of fishermen reaches its maximum at the same F_{MSY} value. The profits/fisher are positive at values F < 0.32.

most profitable range of age of first catch and fishing intensity such that it is exploited sustainably.

The dynamics of the sea cucumber fisheries are characterized by overfishing and depletion worldwide, and although the solution to restore the stocks seems to be a problem far from being solved, action is often taken after the stocks have been driven to low levels (Rosenberg 2003). Unfortunately, most of these stocks lack evaluation and rarely are under effective control and supervision, as stated in papers documenting overexploitation, overcapitalization, and threats to food security in general (Beddington and Kirkwood 2005; Bruckner 2005) and with the sea cucumber in particular (Conand and Byrne 1993; Lovatelli et al. 2004; Toral-Granda et al. 2008). The issues raised include whether restocking and stock enhancement should be used to manage the sea cucumber fisheries (Lovatelli et al. 2004). Unfortunately, most sea cucumber fisheries confirm the statement that they have rarely been "sustainable" (Pauly et al. 2002). The warty sea cucumber stock is under recruitment overfishing, which given the low intensity of its exploitation, it does not have a negative impact on the stock biomass nor on the stock recruitment process. Results presented in this paper indicate that the exploitation of the warty sea cucumber stock in Baja California seems to be an exception to the most frequent condition seen in sea cucumber fisheries.

The lack of ability to gather the basic information needed for management plans, weak enforcement, the high demand from international markets, and the pressure exerted from resource-dependent communities are identified as the important factors responsible for the critical status of the sea cucumber fisheries worldwide (Carranza and Andrade 1996; Sonnenholzner 1997; Anonymous 2000a; 2004; Herrero-Pérezrul and Chávez 2005; Hearn and Pinillos 2006; Toral-Granda et al. 2008; Friedman and Gisawa 2010), leading to an increased concern for their management (Anonymous 1994; Richmond 1996; Salgado-Rogel et al. 2006; Rogers-Bennett and Ono 2001; Kaly et al. 2007; Friedman et al. 2008).

When a fishery is in a condition of severe exploitation, which is not the case of the warty sea cucumber, the obvious recommendation is to close it, because the conservation of the resource becomes a priority as compared to social or economic considerations and then rights-based management is probably not appropriate

for all fisheries (Hilborn et al. 2005). Under these circumstances, and if the depletion is not as severe, the key point is to find a way to constrain the access to the fishing grounds by minimizing the social impact, the number of jobs. This is not an easy task because the stock effect is a nonlinear function of yield and difficult to estimate with a high level of precision (Hannesson 2007). In overexploited fisheries, choosing the F_{MSY} or F_{MEY} as the target of the fishery, evidently would be a convenient option and any of these should be adopted once the stock is restored.

In many instances, a sustainable management of a fishery depends on reliable assessments of the stock. However, this is a necessary but not sufficient condition because an effective control of the access to fishing grounds and a sound and strict application of regulations are also indispensable conditions to guarantee a long-term exploitation.

Ecological extinction caused by overfishing precedes all the other pervasive human disturbances to the coastal ecosystems, but data also demonstrate achievable goals for restoration and management (Jackson et al. 2001). Unsuccessful systems have generally evolved from open access, attempts at a top-down control with a poor ability to monitor and implement regulations, or reliance on consensus (Hilborn et al. 2005). New definitions of sustainability will attempt to incorporate the economic and social aspects of the fisheries (Quinn and Collie 2005) and our work is an example of such an approach.

The profits of any fishery depend upon the cost of fishing operations and the catch value, such that even under the same fleet size, changes in catchability caused by seasonal changes in behavior or physiological condition, and accessibility of the stock to fishers may lead to a different catch per unit of effort even if the effort is relatively constant. These changes imply differences in costs and profits. In a well-managed fishery it is usually more convenient to adopt the F_{MEY} value as the target rather than the F_{MSY} because it implies a lower risk of overexploitation (Chávez and Gorostieta 2010). Appropriate control regulations are required to control the exploitation to maintain the warty sea cucumber fishery sustainable over time and space. The conversion of scientific advice into policy, through a participatory and transparent process, is at the core of achieving fishery sustainability (Mora et al. 2009) and it is hoped that the results given here can be used for a sustainable exploitation of the warty sea cucumber fishery off the Baja California peninsula.

ACKNOWLEDGEMENTS

Dinorah Herrero-Pérezrul read the manuscript and made valuable suggestions. Thanks to Dr. Ellis Glazier for editing this English-language text. The senior author received a partial support from EDI and COFAA-IPN.

LITERATURE CITED

Anonymous. 1994. Determinación de las especies y subespecies sujetas a protección especial y especificaciones para su protección. NOM-059-ECOL-1994. Diario Oficial de la Federación. Mayo, 16. México:2–59.

Anonymous. 2000a. Evaluation of the trade of sea cucumber *Isostichopus fuscus* (Echinodermata: Holothuroidea) in the Galapagos Islands during 1999. TRAFFIC South America, Quito, Ecuador. 19 pp.

Anonymous. 2000b. Modificación de la NOM-059-ECOL-1994 para el pepino de mar *Isostichopus fuscus*. Diario Oficial de la Federación. Marzo 22. México: 9–10.

Anonymous. 2004. Managing Marine and Coastal Protected Areas: A TOOLKIT for South Asia SHEET I6, Spiny lobster and sea cucumber fisheries:191–192.

Beddington, J. and G. Kirkwood. 2005. Introduction: fisheries, past, present and future. Phil. Trans. R. Soc. B 360:3–4.

Beverton, R. J. H. and S. J. Holt. 1957. On the dynamics of exploited fish populations. Fishery Investigations, London, Series 2, 19, 533 p.

Bruckner A. W. 2005. The recent status of sea cucumber fisheries in the continental United States of America. SPC Beche-de-mer Information Bulletin 22:39–46.

Bruckner A. W. 2006. Sea cucumber population status fisheries and trade in the United satates. *In*: Proceedings of the CITES workshop on the conservation of the sea cucumber in the families Holoturidae and Stichopodidae. A. W. Brucker (Ed), NOAA Thecnical Memorandum NFS-OPR-34, USA, pp. 192–202.

Carranza, C. and M. Andrade. 1996. Retrospectiva de la pesca de pepino de mar a nivel continental. Fundación Charles Darwin. Para Islas Galápagos. ORSTOM, Quito 54 pp.

Chávez, E. A. 1996. Simulating fisheries for the assessment of optimum harvesting strategies. Naga ICLARM, 19(2):33–35.

Chávez, E. A. 2005. FISMO: A Generalized Fisheries Simulation Model. *In*: Kruse, G. H., V. F. Gallucci, D. E. Hay, R. I. Perry, R. M. Peterman, T. C. Shirley, P. D. Spencer, B. Wilson, and D. Woodby (eds.), Fisheries assessment and management in data-limited situations. Alaska Sea Grant College Program, University of Alaska Fairbanks. pp:659–681.

Chávez, E. A. and M. Gorostieta. 2010. Bioeconomic assessment of the spiny lobster fisheries of Baja California, Mexico. CALCOFI Rep. 51:153–161.

Conand, C. and M. Byrne. 1993. A review of recent developments in the world sea cucumber fisheries. Marine Fisheries Review 55(4):1–13.

DOF. 2002. Norma Oficial Mexicana 059-ECOL-2001, Protección ambiental-especies nativas de México de flora y fauna silvestres-Categoría de riesgo y especificaciones para su inclusión o cambio-Lista de especies en riesgo. Diario Oficial de la Federación. México, March 6, 2002.

DOF. 2004. Carta Nacional Pesquera y su anexo. Diario Oficial de la Federación. México. March 15, 2004.

Espinoza-Montes, A. 2000. Ciclo reproductivo del pepino de mar *Parastichopus parvimensis* (H. L. Clark, 1913) (Echinodermata, Holothuroidea) en Isla Natividad, Baja California Sur, Mexico. B Sc. Thesis University of Guadalajara. Mexico. 60p.

Fajardo-León, M. C., M. C. L. Suárez-Higuera, A. del Valle Manríquez y A. Hernández-López. 2008. Biología reproductiva del pepino de mar *Parastichopus parvimensis* (Echinodermata: Holothuroidea) de Isla Natividad y Bahía Tortugas, Baja California Sur, México. Ciencias Marinas, 23(2):165–177.

Friedman K., S., Purcell, J. Bell, and C. Hair. 2008. Sea cucumber fisheries: a manager's toolbox. ACIAR Monograph No. 135, 32 pp.

Friedman, K. and L. Gisawa. 2010. Fisheries: sea cucumbers—early retirement or renewal? Surge in demand puts pressure on resource. Islands Business Web Page, 2010.

Gayanilo, F., P. Sparre, and D. Pauly. 1996. The FAO-ICLARM stock assessment tools (FISAT) user's guide. FAO Computerized Information Series (Fisheries) 7.

Grafton, R. Q., T. Kompas, and R. Hilborn. 2007. Economics of Overexploitation Revisited. Science 7(318):1601–1635.

Hannesson, R. 2007. A Note on the "Stock Effect". Marine Resource Economics, Vol. 22:69–75.

Hearn, A. and F. Pinillos. 2006. Baseline information on the warty sea cucumber *Stichopus horrens* in Santa Cruz, Galápagos, prior to the commencement of an illegal fishery. SPC Beche-de-mer Information Bulletin 24:1–10.

Herrero-Pérezrul, M. D. and E. A. Chávez. 2005. Optimum fishing strategies for *Isostichopus fuscus* (Echinodermata: Holothuroidea) in the Gulf of California, Mexico. Rev. Biol. Trop. (Int. J. Trop. Biol. ISSN-0034-7744) Vol. 53 (Suppl. 3): 357–366.

Hilborn R. J. and C. J. Walters. 1992. Quantitative Fisheries Stock Assessment. Chapman & Hall.

Hilborn, R., J. K. Parrish, and K. Litle. 2005. Fishing rights or fishing wrongs? Reviews in Fish Biology and Fisheries 15:191–199.

Hoenig, J. M. 1983. Empirical use of longevity data to estimate mortality rates. Fish. Bull. NOAA/NMFS 81(4):898–903.

Jackson, J. B. C., M. X. Kirby, W. H. Berger, K. A. Bjorndal, L. W. Botsford, B. J. Bourque, R. H. Bradbury, R. Cooke, J. Erlandson, J. A. Estes, T. P. Hughes, S. Kidwell, C. B. Lange, H. S. Lenihan, J. M. Pandolfi, C. H. Peterson, R. S. Steneck, M. J. Tegner, and R. R. W. Arner. 2001. Historical Overfshing and the Recent Collapse of Coastal Ecosystems. Science 293: 629–638.

Jensen, A. L. 1996. Beverton and Holt life history invariants result from optimal trade off of reproduction and survival. Canadian Journal Fisheries and Aquatic Sciences 53:820–822.

Jensen, A. L. 1997. Origin of the relation between K and Linf and synthesis of relations among life history parameters. Canadian Journal of Fisheries and Aquatic Sciences 54: 987–989.

Kaly, U., G. Preston, J. Opnai, and J. Ain. 2007. Sea cucumber survey, New Ireland Province—[Kavieng]: National Fisheries Authority and Coastal Fisheries Management and Development Project, 37 p.

Lovatelli, A., C. Conand, S. Purcell, S. Uthicke, A. Hamel, and J. F. Mercier (eds.). 2004. Advances in sea cucumber aquaculture and management. FAO Fisheries Technical Paper. No. 463. FAO, Rome 425 pp.

Mora C., R. A. Myers, M. Coll, S. Libralato, T.J. Pitcher, R.U. Sumaila, D. Zeller, R. Watson, K.J. Gaston, and B. Worm. 2009. Management Effectiveness of the World's Marine Fisheries. PLoS Biol 7(6): e1000131.

Muscat, A. M. 1982.The fishery biology and market preparation of sea cucumbers. Washington Department of Fisheries Technical Report No. 22. 43 pp.

Muse, B. 1998. Management of the British Columbia Sea Cucumber Fishery. CFEC 98-4N.

Pauly, D. 1980. On the interrelationship between natural mortality, growth parameters, and mean environmental temperature in 175 fish stocks. J. Cons. CIEM 39(2):175–192.

Pauly D., V. Christensen, S. Guénette, T. J. Pitcher, U.R. Sumaila, C. J. Walters, R. Watson and D. Zeller. 2002. Towards sustainability in world fisheries. Nature (418): 689–695.

Pérez-Plascencia, G. 1995. Crecimiento y reproducción del pepino de mar en la Bahía de Todos Santos, Baja California, México. M. Sc. Thesis, University of Baja California (UABC), Mexico 67 pp.

Quinn, T. J. II, and J. S. Collie. 2005. Sustainability in single-species population models. Phil. Trans. R. Soc. *B* 360:147–162.

Richmond, R. 1996. Regional Management Plan for Sea Cucumber in Micronesia. University of Guam Marine Laboratory. National Marine Fisheries Service, Southwest Regional Office.

Rikhter, V. A. and V. N. Efanov. 1976. On one of the approaches to estimation of natural mortality of fish populations. ICNAF Res. Doc., 76/VI/8: 12 p.

Rogers-Bennett, L. and D.S. Ono. 2001. Sea cucumbers. California living marine resources: A status report. California Department of Fish and Game:131–134.

Rosenberg, A. 2003. Managing to the margins: the overexploitation of fisheries. Front. Ecol. Environ. 1(2):102–106.

Salgado-Rogel, M.L. and J. Palleiro-Nayar. 2008. Disminución de la abundancia del erizo rojo y propuestas para su manejo en Baja California, México. Ciencia Pesquera 16:37–45.

Salgado-Rogel, M.L., J. Palleiro-Nayar, E. Vázquez-Solórzano, F. Uribe-Osorio, and D. Aguilar. 2006. Densidad y estructura poblacional del pepino de mar *Parastichopus parvimensis* en la porción suroeste de El Rosario, Baja California III Foro Científico de Pesca Ribereña. Puerto Vallarta, México: 159–160.

Salgado-Rogel, M. L., J. S. Palleiro Nayar, J. L. Rivera Ulloa, D. Aguilar, E. Vázquez, and M. C. Jiménez. 2009. La pesquería y propuestas de manejo del pepino de mar *Parastichopus parvimensis* en Baja California, México. Ciencia Pesquera 17(1):17–26.

Schroeter, S. C., D. C. Reed, D.J. Kushner, J. A. Estes, and D. S. Ono. 2001. The use of marine reserves in evaluating the dive fishery for the warty sea cucumber (*Parastichopus parvimensis*) in California, USA. Canadian Journal of Fisheries and Aquatic Sciences 58:1773–1781.

Sonnenholzner, J. 1997. A brief survey of the commercial sea cucumber *Isostichopus fuscus* (Ludwig, 1875) in the Galapagos Islands. SPC Bêche de Mer. Inf. Bull. 9:11–15.

Sparre, P. and S.C. Venema. 1992. Introduction to tropical fish stock assessment. Part 1. Manual FAO Fisheries Technical paper, 306 (1), 376 p.

Tapia-Vázquez, O., J. J. Castro, and H. Valles. 1996. Madurez gonádica del pepino de mar *Parastichopus parvimensis* en la costa occidental de Baja California, México en 1994. Ciencia Pesquera 12:5–12.

Toral-Granda, M. V. and P.C. Martínez. 2007. Reproductive biology and population structure of the sea cucumber *Isostichopus fuscus* (Ludwig 1875) (Holothuroidea) in Caamaño, Galápagos Islands, Ecuador. Marine Biology, 151(6): 2091–2098.

Toral-Granda, V. Lovatelli, and A. Vasconcellos. (eds). 2008. Sea cucumbers. A global review of fisheries and trade. FAO Fisheries and Aquaculture Technical Paper. No. 516. FAO, Rome 317 pp.

Vannuccini, S. 2004. Sea cucumbers: a compendium of fishery statistics. *In*: Lovatelli, A. (comp./ed.); Conand, C.; Purcell, S.; Uthicke, S.; Hamel, J.-F.; Mercier, A. (eds.) Advances in sea cucumber aquaculture and management. FAO Fisheries Technical Paper. No. 463. Rome, FAO. 2004. 425 p.

Woodby, D., S. Smiley, and R. Larson. 2000. Depth and habitat distribution of *Parastichopus californicus* near Sitka, Alaska. Alaska Fishery Research Bulletin 7:22–32.

Yingst, J.Y. 1982. Factors influencing rates of sediment ingestion by *Parastichopus parvimensis* (Clark), an epibenthic deposit-feeding Holothurian. Estuarine, Coastal and Shelf Science, 141:119–134.

ANALYSIS OF THE SPRING-FALL EPIPELAGIC ICHTHYOPLANKTON COMMUNITY IN THE NORTHERN CALIFORNIA CURRENT IN 2004–2009 AND ITS RELATION TO ENVIRONMENTAL FACTORS

TOBY D. AUTH
Cooperative Institute for Marine Resources Studies
Oregon State University
Hatfield Marine Science Center
2030 Marine Science Drive
Newport, OR 97365, USA

e-mail: toby.auth@noaa.gov phone: 541-867-0350 fax: 541-867-0389

ABSTRACT

The taxonomic composition, distribution, concentration, and community structure of ichthyoplankton off the Oregon and Washington coasts were examined in 2004–2009 to investigate annual, seasonal, latitudinal, and cross-shelf variability. Larval concentrations and community structure were also analyzed in relation to several local and larger-scale environmental variables. The dominant taxa, comprising 94% of the total larvae collected, were *Engraulis mordax*, *Sebastes* spp., *Stenobrachius leucopsarus*, *Tarletonbeania crenularis*, and *Lyopsetta exilis*. Larval concentrations and diversity generally varied across the temporal and spatial scales. Several seasonal and cross-shelf assemblages were identified, and annual, seasonal, latitudinal, and cross-shelf gradients of taxonomic associations with significant indicator taxa were found. Distance from shore, salinity, and temperature were the local environmental factors that explained the most variability in larval fish concentrations, while Columbia River outflow and sea-surface temperature were the larger-scale factors that explained the most variability in 2–4 month lagged larval fish concentrations and diversity.

INTRODUCTION

The northern California Current (NCC) is a highly dynamic and productive upwelling environment similar to other eastern boundary current regions around the world (Bakun 1993; Fréon et al. 2009). Like these other regions, the NCC supports a wide array of ecologically and commercially important forage and predatory taxa such as anchovy, lanternfish, flatfish, and rockfish (Brodeur et al. 2006; Checkley and Barth 2009). A key component to understanding the processes that influence the spawning, trophic dynamics, recruitment, and survival of these important fish stocks is an understanding of the ichthyoplankton communities, and the environmental factors that influence them, within these upwelling regions (Brodeur et al. 2008; Auth et al. 2011).

Many ichthyoplankton studies have been conducted in the NCC region over the past 40 years, but these have been generally limited with respect to spatial and temporal coverage. Past studies have incorporated only coastal (<50 km from shore) stations (Mundy 1984; Boehlert et al. 1985; Brodeur et al. 1985; Brodeur et al. 2008; Parnel et al. 2008), or were based on sampling efforts limited to one year (Waldron 1972; Richardson 1973), one transect (Richardson and Pearcy 1977; Auth and Brodeur 2006; Auth et al. 2007; Auth 2009 [although a second transect was sampled one time]), or one season (Richardson et al. 1980; Auth 2008). During 1980–1987, Doyle (1992) collected ichthyoplankton in conjunction with temperature and salinity data from multiple cross-shelf transects during multiple seasons along the northern and central California Current, but did not conduct any formal statistical analyses of the observed spatial and temporal patterns. Subsequently, several studies have suggested that local and larger-scale environmental variables can influence larval fish communities in the NCC (Doyle 1995; Brodeur et al. 2008), Gulf of Alaska (Doyle et al. 2009), Humboldt Current off Peru (Suntsov 2000), the North Sea (Beaugrand et al. 2003), and elsewhere (Hsieh et al. 2007).

The present study is the first to incorporate such a large data set of ichthyoplankton samples collected from multiple cross-shelf stations, latitudinal transects, seasons, and years into a comprehensive analysis of the ichthyoplankton community structure in relation to both local and larger-scale environmental factors within the NCC ecosystem. The objectives of this study are to (1) identify and describe the variability within the taxonomic, annual, seasonal, latitudinal, and cross-shelf ichthyoplankton assemblages within the NCC, (2) identify larval taxa indicative of each temporal and spatial assemblage, and (3) identify the local and larger-scale environmental factors that may influence changes in ichthyoplankton concentrations. The results of this study establish basic information on the distribution, composition, and variability of NCC ichthyoplankton assemblages and their dominant taxa with respect to dynamic environmental factors that influence them. This information should be of great use to fisheries researchers and managers in assessing the impact of environmental processes on early-life histories and subsequent recruitment of important forage and commercial stocks.

METHODS

Sampling Procedures

A total of 489 ichthyoplankton samples were collected from 28 monthly cruises between May and October/November 2004–2009. Samples were collected primarily at five stations extending ~20–100 km offshore at ~20 km intervals along each of four transects (i.e., Willapa Bay [WB: 46.67°N], Columbia River [CR: 46.16°N], Newport Hydrographic [NH: 45.65°N], and Heceta Head [HH: 44.00°N]) for a total of ~20 stations per monthly cruise off the southern Washington and central Oregon coasts from May to September. Additional stations extending as far inshore as 9 km and as far offshore as 238 km were sampled occasionally (fig. 1). The 9 km inshore station along the NH transect was only sampled in June and September 2004 and May 2006, the 116 km far-offshore station along the CR transect was only sampled in May 2006, the far-offshore stations along the HH transect were only sampled in August 2004, and the far-offshore stations along the NH transect were only sampled as follows: 120 km station in June, August, September, and November 2004, October 2005, May 2006, and June 2008; 139 km station in August 2004; 157 km station in June and September 2004, May 2006, and June 2008; 208 and 238 km stations in June 2008. No sampling was conducted in May and July 2004, May 2005, or July 2006. However, additional samples were collected in November 2004 and October 2005. Not all stations were sampled during all cruises due to inclement weather or equipment malfunctions. Sampling was done primarily at night (n = 372), although some samples were collected during crepuscular periods (n = 117) due to the lack of sufficient night hours during the summer months. Since no diel pattern of variability in larval concentrations (no. 1000 m^{-3}) was found through ordination analysis or ANOVA ($p > 0.34$), all samples were used in subsequent analyses regardless of time of sampling.

Samples were collected using a bongo net with a 60-cm (70-cm in June, September, and November 2004, October 2005, and May 2006) diameter mouth opening and fitted with 335-μm mesh. The bongo was fished as a continuous oblique tow from ~100 m (or within 5 m of the bottom at stations <100 m) to the surface at a retrieval rate of 33 m min^{-1} and ship speed of 1.0–1.5 m s^{-1}. A depth recorder and flowmeter placed in the net during each tow allowed determination of tow depth and volume of water filtered. The mean water volume filtered was 161.6 m^3 (standard error, SE = 2.6). Temperature (°C), salinity, density (sigma theta, kg m^{-3}), fluorescence (mg m^{-3}, an indicator of chlorophyll), and turbidity (mg m^{-3}) were measured throughout the water column during most cruises using a Seabird SBE 25 CTD (Sea-Bird Electronics Inc., Bellevue, WA, USA). Seabird model SBE 911 was used in November 2004, October 2005, and May 2006. During 2008 and 2009, dissolved oxygen concentration (DO, ml L^{-1}), and DO saturation (%) were also measured. Not all environmental parameters were measured at all stations due to periodic instrumentation malfunctions.

Ichthyoplankton samples collected in 2004–2008 were preserved at sea in a 10% buffered-formalin seawater solution. Samples collected in 2009 were preserved at sea in 95% ethanol for ~72 hours, then filtered and re-preserved in fresh 95% ethanol. Larval fish from each sample were completely sorted, counted, and identified to the lowest taxonomic level possible in the laboratory using a dissecting microscope. Most *Citharichthys* spp., *Cyclothone* spp., osmerids, *Pholis* spp., *Scopelosaurus* spp., *Sebastes* spp., and *Sebastolobus* spp. larvae were not identifiable below the generic or family level based on meristics and pigmentation patterns, so no species-specific inferences are intended for these taxa in this study. However, the majority of individuals classified as *Citharichthys* spp. are either *C. sordidus* or *C. stigmaeus* based on the larger, identifiable individuals collected and dominance of these paralichthyid species in the NCC ichthyoplankton (Matarese et al. 1989). All larvae of rare taxa or a random subsample of 30 individuals of abundant taxa in each sample were measured to the nearest 0.1 mm standard length (SL), or notochord length (NL) for preflexion larvae, using UTHSCSA Image Tool Version 3.0 image processing and analysis software (http://ddsdx.uthscsa.edu/dig/itdesc.html 2010).

Data Analyses

Hierarchical cluster analyses in conjunction with nonmetric multidimensional scaling (MDS) ordinations were used to identify potential larval fish taxonomic, annual, seasonal, latitudinal, and cross-shelf assemblages (Field et al. 1982). For analyses of taxonomic assemblages, only those larval taxa (n = 13) found in >5% of the samples were included, while all identifiable taxa (n = 60) were included in the other assemblage analyses. Samples lacking larval fish were not included in the cluster and MDS analyses.

Taxonomic, annual, seasonal, latitudinal, and cross-shelf dendrograms were created using hierarchical, group-averaged clustering from Bray-Curtis similarities on fourth root-transformed larval fish concentrations (Clarke and Warwick 2001). Larval concentrations for each taxon were averaged for each cruise (n = 28) and station (n = 30), which constituted the sampling units in the respective multivariate matrices. In order to verify dendrograms interpretations, nonmetric MDS ordinations were preformed using similarity matrices from the cluster analyses with 20 random restarts each to minimize stress levels. A two-dimensional ordination

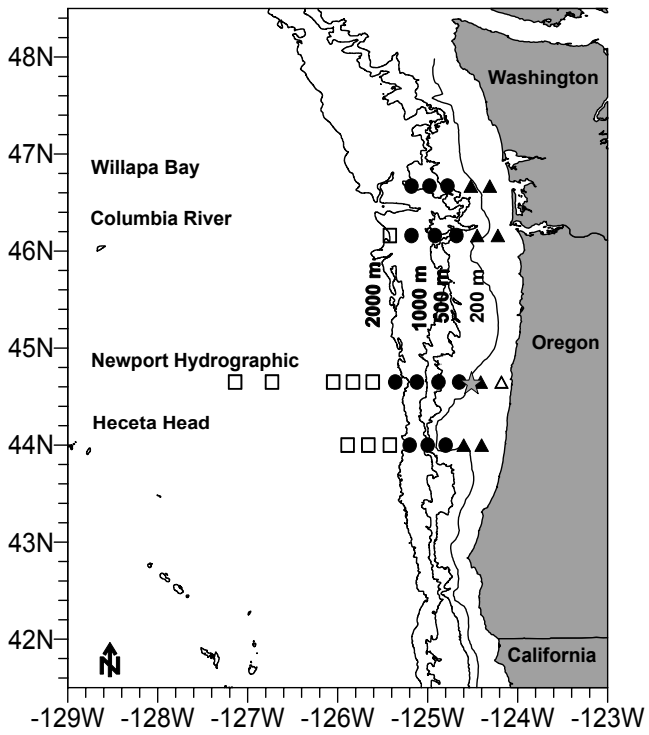

Figure 1. Locations and classifications (coastal [triangles], offshore [circles], and far-offshore [squares]) of stations sampled during this study off the Oregon and Washington coasts in 2004–2009. Contour lines representing the 200-, 500-, 1000-, and 2000-m isobaths are shown. Filled symbols depict normally-sampled stations, and open symbols depict irregularly-sampled stations. The filled star symbol represents the location of the National Oceanic and Atmospheric Administration's (NOAA) Stonewall Banks buoy.

approach was adopted because stress levels were sufficiently low (≤0.16) in all cases and results were sufficiently interpretable ecologically in two-dimensional space (Clarke and Warwick 2001).

For the cross-shelf distributional analyses, stations were classified as coastal (<~50 km from shore), offshore (~50–100 km), and far-offshore (>~100 km) (fig. 1) based on the results of the MDS and cluster analyses. The Shannon-Wiener diversity index (*H'*) was used to measure larval diversity, where higher *H'* values denote greater diversity (Shannon and Weaver 1949). Taxa evenness was assessed using Pielou's evenness index (*J'*), although evenness was not included in the analyses because it was highly negatively correlated with diversity ($p < 0.0001$). Analysis of variance (ANOVA) and Tukey's multiple range tests were applied to the $\log_e(n + 0.1)$-transformed larval station concentrations and diversity measures to test for significant differences ($p < 0.05$) between annual, seasonal, latitudinal, and cross-shelf scales. Weighted mean (based on concentration) larval lengths of dominant taxa were also calculated for each sample, and were similarly tested for significant differences between annual, seasonal, latitudinal, and cross-shelf scales.

A non-parametric multi-response permutation procedure (MRPP) was used to test for between-group differences in larval concentrations within several factors by calculating an A-statistic ranging from 0 to 1, with the maximum value indicating complete agreement between groups (McCune and Mefford 1999). Factors and groups within those factors were defined as: (1) year (2004, 2005, 2006, 2007, 2008, and 2009), (2) month (May, June, July, August, September, October/November), and (3) latitude (WB, CR, NH, and HH transects) and (4) cross-shelf (coastal, offshore, and far-offshore). Statistical significance was determined at the $\alpha = 0.001$ level. Indicator species analysis (ISA) was also performed on the fourth root-transformed larval fish concentrations using 5000 random restarts for each Monte Carlo simulation to test taxonomic fidelity within each group (Dufrêne and Legendre 1997). Statistical significance for this test was determined at the $\alpha = 0.05$ level. All MRPP and ISA analyses were performed using PC-Ord Version 5 statistical software (McCune and Mefford 2006).

Because sampling during October (2005) and November (2004) only occurred in one year, the samples were combined into a single seasonal unit (October/November) and only included in between-month cluster, MDS, ANOVA, MRPP, and ISA analyses. Also, because far-offshore stations were only sampled periodically, the data were only included in similar cross-shelf analyses. Unidentified larvae were excluded from all analyses except for ANOVA tests involving total larvae.

A non-parametric multivariate procedure (BIO-ENV) was used to analyze the relationship between select local environmental variables and larval fish community structures. The details of the BIO-ENV algorithm and its suitability for use in analyzing biological/environmental data interactions are described by Clarke and Warwick (2001) and Clarke and Gorley (2006). Sample concentration by taxonomic similarity matrices were analyzed in association with several environmental variables: latitude, station depth (m), station distance from shore (km), and water temperature, salinity, density, fluorescence, and turbidity all measured at 20-m depth. Since DO and DO saturation data were only collected in 2008 and 2009, two separate analyses were performed: one using the sample by taxonomic similarity matrix in association with only latitude, station depth, station distance from shore, temperature, salinity, density, fluorescence, and turbidity (336 samples × 60 taxa), and the other incorporating samples with all environmental data available including DO and DO saturation (151 samples × 60 taxa). Samples containing either no larvae or coincidental environmental data were excluded from analyses. Both BIO-ENV analyses were performed using the Spearman rank correlation method on normalized Euclidean distance similarity matrices of

$\log_e(n + 1)$-transformed, non-standardized environmental variables by fourth root-transformed larval sample concentrations (Clarke and Gorley 2006). All cluster, MDS, and BIO-ENV analyses were performed using PRIMER Version 6.1.7 statistical software (Clarke and Gorley 2006).

Pair-wise correlation analyses were conducted to assess the relationship between concentrations of the most abundant taxa (i.e., *Engraulis mordax*, *Lyopsetta exilis*, *Sebastes* spp., *Stenobrachius leucopsarus*, and *Tarletonbeania crenularis*) and total fish larvae, larval diversity, and both local and larger-scale environmental variables. As noted above, local environmental variables are water temperature, salinity, density, fluorescence, and turbidity for all years, and DO and DO saturation for 2008 and 2009. Larger-scale environmental variables that were easily available and may influence the distribution, concentration, and transport of coastal pelagic fish larvae in the NCC region included: Multivariate El Niño-Southern Oscillation Index (MEI; http://www.esrl.noaa.gov/psd/people/klaus.wolter/MEI/ 2011), Pacific Decadal Oscillation (PDO; http://jisao.washington.edu/pdo/ 2011), Northern Oscillation Index (NOI; http://www.pfeg.noaa.gov/products/PFEL/modeled/indices/NOIx/noix.html 2011), sea-surface temperature (SST, °C; http://www.ndbc.noaa.gov/ 2011) recorded from NOAA's Stonewall Banks buoy located 20 nm west of Newport, Oregon (44.64°N, 124.50°W), and eastward Ekman transport (EET, kg m^{-1}; http://www.pfeg.noaa.gov/products/las.html 2011), northward Ekman transport (NET, kg m^{-1}; http://www.pfeg.noaa.gov/products/las.html 2011), and Upwelling Index (UPW; http://www.pfeg.noaa.gov/products/PFEL/modeled/indices/PFELindices.html 2011) each for 45°N, 125°W, and Columbia River outflow (COL, 1000 ft s^{-1}; http://www.cbr.washington.edu/dart/river.html 2011) measured at Bonneville Dam located 235 km upriver from the mouth of the Columbia River. SST recorded from NOAA's Stonewall Banks buoy was used as a consistent, general indicator of SST in the study region as a whole (Brodeur et al. 2008; Auth et al. 2011), and thus is referred to as a larger-scale variable. Missing values in the SST data set were due to equipment failure on the buoy. Values for the local environmental variables used in analyses were taken from different depths in the water column at each station corresponding to the mean depth for each taxon as reported by Auth and Brodeur (2006) and Auth et al. (2007): *E. mordax*, 10–m depth; *Sebastes* spp., total larvae, and larval diversity, 20–m depth; *L. exilis* and *S. leucopsarus*, 40–m depth; *T. crenularis*, 50–m depth. Monthly-averaged larval concentrations and diversity were lagged 0–5 months behind the larger-scale environmental variables to account for delayed effects of changes in basin-wide atmospheric-oceanic processes on regional hydrography affecting larval concentrations and diversity. Due to the large amount of zero values in the data set, samples with no larvae were excluded from the local environmental analysis. Similarly, since *E. mordax* and *L. exilis* larvae were highly seasonal and therefore not collected during several cruises in the study ($n = 9$ and 8, respectively), those cruises were excluded from the larger-scale environmental analyses for these species. Prior to inclusion in the analyses, larval concentrations were $\log_e(n + 0.1)$-transformed. Statistical significance was determined at the $\alpha = 0.0l$ level. All ANOVA and correlation analyses were performed using the statistical software JMP Version 7.0 (SAS Institute Inc. 2007).

Non-parametric multiplicative regression (NPMR) analysis was similarly conducted to further assess the relationship between concentrations of dominant taxa and total larvae, larval diversity, and local and larger-scale environmental variables, and to test for interactions between these variables. Details of the NPMR algorithm and its suitability for use in analyzing biological/environmental data interactions are described by McCune (2006). Best-fit models were developed using a local mean estimator with a Guassian weighting function, a predictor ratio minimum of 10, 5% improvement criterion, a minimum average neighborhood size of n (samples) × 0.05, a step size equal to 5% of the range, with 10% maximum allowable missing estimates, a minimal backtracking search method, and leave-one-out cross validation. Prior to inclusion in the analyses, larval concentrations were $\log_e(n + 0.1)$-transformed. Statistical significance for each selected model was evaluated after 1000 random runs. All NPMR analyses were performed using the statistical software HyperNiche Version 2.0 (McCune and Mefford 2009).

RESULTS

Environmental Factors

Larger-scale (i.e., MEI, PDO, NOI, SST, EET, NET, UPW, COL) environmental factors varied annually and seasonally throughout the study (fig. 2). Weak El Niño conditions were prevalent during the 2004 sampling season, while 2005 was marked by highly anomalous late upwelling (mid-July) unrelated to the El Niño-Southern Oscillation (ENSO) (Brodeur et al. 2006; Schwing et al. 2006) followed by a sudden negative shift in the MEI that persisted through mid-2006. La Niña conditions were prevalent during most of the 2007 and 2008 sampling seasons, followed by a switch to El Niño conditions in mid-2009. Monthly-averaged MEI, PDO, and SST values were positively correlated with each other but negatively correlated with NOI values, while SST values were positively correlated with UPW but negatively correlated with EET values ($p < 0.01$).

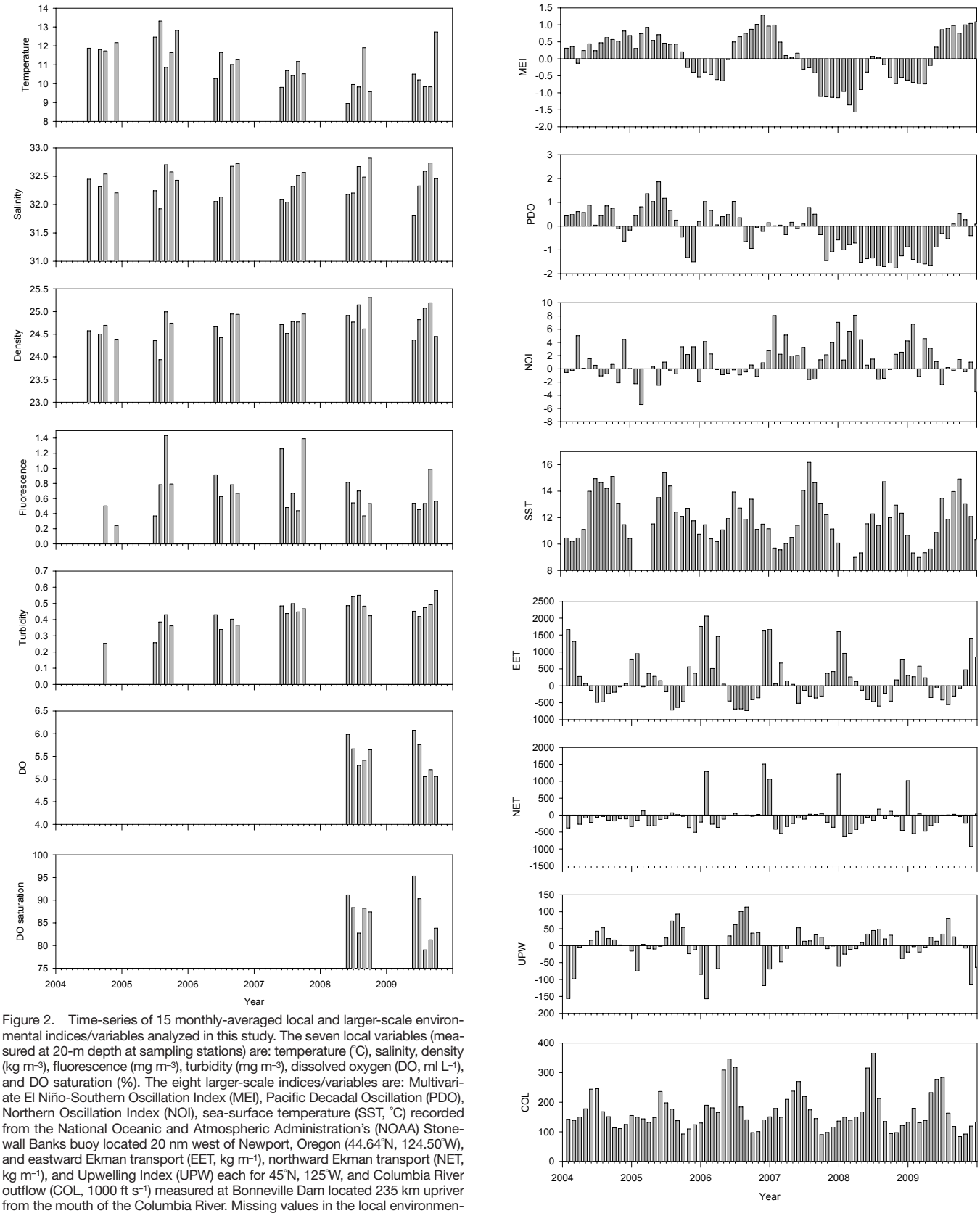

Figure 2. Time-series of 15 monthly-averaged local and larger-scale environmental indices/variables analyzed in this study. The seven local variables (measured at 20-m depth at sampling stations) are: temperature (°C), salinity, density (kg m^{-3}), fluorescence (mg m^{-3}), turbidity (mg m^{-3}), dissolved oxygen (DO, ml L^{-1}), and DO saturation (%). The eight larger-scale indices/variables are: Multivariate El Niño-Southern Oscillation Index (MEI), Pacific Decadal Oscillation (PDO), Northern Oscillation Index (NOI), sea-surface temperature (SST, °C) recorded from the National Oceanic and Atmospheric Administration's (NOAA) Stonewall Banks buoy located 20 nm west of Newport, Oregon (44.64°N, 124.50°W), and eastward Ekman transport (EET, kg m^{-1}), northward Ekman transport (NET, kg m^{-1}), and Upwelling Index (UPW) each for 45°N, 125°W, and Columbia River outflow (COL, 1000 ft s^{-1}) measured at Bonneville Dam located 235 km upriver from the mouth of the Columbia River. Missing values in the local environmental variable data sets are due to either equipment failure on the CTD or lack of sampling due to inclement weather or other equipment malfunctions, while missing values in the SST data set are due to equipment failure on the buoy.

TABLE 1

Taxon composition, frequency of occurrence, mean concentration (no. 1000 m^{-3}), percent of total concentration, month (May [M], June [Jn], July [Jy], August [A], September [S], October [O], November [N]), latitudinal transect (north-south: Willapa Bay [WB], Columbia River [CR], Newport Hydrographic [NH], and Heceta Head [HH]), and cross-shelf region (C = coastal, O = offshore, F = far offshore) for all larval fish collected during this study off the Oregon and Washington coasts in 2004–2009. ⋆ = larvae collected during months outside their seasonal spawning period for this region as reported in Matarese et al. (1989).

Taxon	Common name	Frequency occurrence	Mean concentration	Total concentration	Month	Transect	Cross-shelf region
Clupeidae							
Sardinops sagax	Pacific sardine	0.01	0.22	0.11	M, Jy	WB, NH	C, O, F
Engraulidae							
Engraulis mordax	Northern anchovy	0.23	75.94	36.92	M-O⋆	All	C, O, F
Bathylagidae							
Bathylagus pacificus	Pacific blacksmelt	0.01	0.06	0.03	M-Jy⋆	CR, NH, HH	C, O, F
Lipolagus ochotensis	Eared blacksmelt	0.07	0.80	0.39	M-S, N⋆	All	C, O, F
Osmeridae							
Undetermined spp.	Smelts	0.01	0.09	0.04	M-Jn	WB, CR	C
Phosichthyidae							
Cyclothone spp.	Bristlemouths	<0.01	0.01	0.01	O	CR	O
Stomiidae							
Chauliodus macouni	Pacific viperfish	0.04	0.29	0.14	M-O	All	C, O
Tactostoma macropus	Longfin dragonfish	<0.01	0.01	0.01	A	CR	O
Notosudidae							
Scopelosaurus spp.	Paperbones/Waryfish	<0.01	0.01	<0.01	M	NH	F
Paralepididae							
Lestidiops ringens	Slender barracudina	0.01	0.05	0.02	M, A, N	NH, HH	O, F
Myctophidae							
Protomyctophum crockeri	California flashlightfish	0.03	0.24	0.12	M-Jn, A-N	All	C, O, F
Protomyctophum thompsoni	Bigeye lanternfish	0.05	0.41	0.20	M-N	All	O, F
Tarletonbeania crenularis	Blue lanternfish	0.36	6.49	3.16	M-N⋆	All	C, O, F
Nannobrachium regale	Pinpoint lampfish	0.17	2.07	1.01	M-O	All	C, O, F
Nannobrachium ritteri	Broadfin lampfish	<0.01	0.01	0.01	O	CR	O
Stenobrachius leucopsarus	Northern lampfish	0.47	39.55	19.23	M-N⋆	All	C, O, F
Diaphus theta	California headlightfish	0.03	0.70	0.34	M-S	All	O, F
Undetermined spp.		<0.01	0.01	0.01	Jn	WB	O
Merlucciidae							
Merluccius productus	Pacific hake	0.02	0.26	0.13	M-Jn	All	O, F
Gadidae							
Microgadus proximus	Pacific tomcod	<0.01	0.02	0.01	M	WB	C
Ophidiidae							
Spectrunculus grandis	Pudgy cuskeel	<0.01	0.01	<0.01	M	NH	O
Bythitidae							
Cataetyx rubrirostris	Rubynose brotula	<0.01	0.01	0.01	Jn	NH	O
Trachipteridae							
Trachipterus altivelis	King-of-the-salmon	0.01	0.03	0.02	Jn, A-S	CR, NH	O, F
Melamphaidae							
Melamphaes lugubris	Highsnout bigscale	<0.01	0.02	0.01	M, S	WB, NH	O, F
Scorpaenidae							
Sebastes spp.	Rockfishes	0.64	66.48	32.32	M-N	All	C, O, F
Sebastolobus spp.	Thornyheads	0.05	0.77	0.37	M-Jy, O⋆	CR, NH, HH	C, O, F
Hexagrammidae							
Hexagrammos octogrammus	Masked greenling	<0.01	0.03	0.01	M-Jn	WB, HH	O
Cottidae							
Scorpaenichthys marmoratus	Cabezon	<0.01	0.01	0.01	M	WB	O
Chitonotus pugetensis	Roughback sculpin	<0.01	0.01	0.01	Jy⋆	HH	O
Paricelinus hopliticus	Thornback sculpin	0.01	0.11	0.05	M, A-S	NH, HH	C, O
Radulinus asprellus	Slim sculpin	0.01	0.13	0.06	M, Jy	All	C
Ruscarius meanyi	Puget Sound sculpin	0.01	0.03	0.02	M	CR, NH, HH	C
Artedius harringtoni	Scalyhead sculpin	0.03	0.23	0.11	M-Jn, A-S	All	C, O
Cottus asper	Prickly sculpin	<0.01	0.01	0.01	M	CR	C
Undetermined spp.	Sculpins	<0.01	0.01	0.01	A	CR	O
Agonidae							
Xeneretmus latifrons	Blacktip poacher	<0.01	0.03	0.01	M, A⋆	CR, NH	C, O
Bathyagonus pentacanthus	Bigeye poacher	<0.01	0.06	0.03	Jn	NH	F
Psychrolutidae							
Malacocottus zonurus	Darkfin sculpin	<0.01	0.01	0.01	Jn	HH	O

TABLE 1 (CONT'D.)

Taxon composition, frequency of occurrence, mean concentration (no. 1000 m^{-3}), percent of total concentration, month (May [M], June [Jn], July [Jy], August [A], September [S], October [O], November [N]), latitudinal transect (north-south: Willapa Bay [WB], Columbia River [CR], Newport Hydrographic [NH], and Heceta Head [HH]), and cross-shelf region (C = coastal, O = offshore, F = far offshore) for all larval fish collected during this study off the Oregon and Washington coasts in 2004–2009. ⋆ = larvae collected during months outside their seasonal spawning period for this region as reported in Matarese et al. (1989).

Taxon	Common name	Frequency occurrence	Mean concentration	Total concentration	Month	Transect	Cross-shelf region
Liparidae							
Liparis fucensis	Slipskin snailfish	0.13	1.11	0.54	M-S, N⋆	All	C, O, F
Liparis pulchellus	Showy snailfish	<0.01	0.04	0.02	Jn-Jy	WB, CR	C
Liparis spp.	Snailfishes	<0.01	0.03	0.01	M, Jy	NH, HH	C, O
Carangidae							
Trachurus symmetricus	Jack mackerel	<0.01	0.01	<0.01	A	WB	O
Bathymasteridae							
Ronquilus jordani	Northern ronquil	<0.01	0.04	0.02	M	CR, NH	C
Stichaeidae							
Poroclinus rothrocki	Whitebarred prickleback	<0.01	0.01	<0.01	M	CR	C
Plectobranchus evides	Bluebarred prickleback	0.01	0.08	0.04	M, A	NH, HH	C, O
Pholidae							
Pholis spp.	Gunnels	<0.01	0.02	0.01	M	WB	C
Icosteidae							
Icosteus aenigmaticus	Ragfish	0.01	0.09	0.04	M	WB, CR, NH	C, O, F
Gobiidae							
Rhinogobiops nicholsii	Blackeye goby	<0.01	0.02	0.01	A	NH	O
Centrolophidae							
Icichthys lockingtoni	Medusafish	0.01	0.08	0.04	M-Jn	CR, NH, HH	O, F
Paralichthyidae							
Citharichthys sordidus and *stigmaeus*	Pacific and speckled sanddab	0.15	1.81	0.88	M-N⋆	All	C, O, F
Pleuronectidae							
Atheresthes stomias	Arrowtooth flounder	<0.01	0.02	0.01	M	CR, HH	O
Embassichthys bathybius	Deepsea sole	<0.01	0.01	<0.01	Jn	WB	O
Eopsetta jordani	Petrale sole	<0.01	0.01	<0.01	M	NH	O
Glyptocephalus zachirus	Rex sole	0.09	0.85	0.41	M-S⋆	All	C, O, F
Isopsetta isolepis	Butter sole	0.03	0.24	0.12	M-Jn⋆	WB, CR, HH	C, O
Lyopsetta exilis	Slender sole	0.25	5.20	2.53	M-S⋆	All	C, O, F
Microstomus pacificus	Dover sole	0.06	0.55	0.27	M-S⋆	All	O, F
Parophrys vetulus	English sole	0.01	0.02	0.01	M-Jn⋆	NH, HH	C, O
Platichthys stellatus	Starry flounder	<0.01	0.02	0.01	M⋆	CR	C
Psettichthys melanostictus	Sand sole	0.01	0.07	0.03	M-Jy	All	C, O
Undetermined		0.02	0.14	0.07	M-A	WB, CR, NH	C, O

Taxonomic Composition

A total of 16,524 fish larvae were collected and represented 60 taxa and 30 families (table 1). Five families accounted for 98% of the total standardized larval concentration: Engraulidae (37%), Scorpaenidae (33%), Myctophidae (24%), Pleuronectidae (3%), and Paralichthyidae (1%). Within these families, five taxa were dominant based on total mean concentration (94% of the total standardized larval concentration) and frequency of occurrence from all samples: *E. mordax*, *Sebastes* spp., *S. leucopsarus*, *T. crenularis*, and *L. exilis*. Several other taxa were collected at relatively high frequencies but with lower mean concentrations: *Nannobrachium regale*, *Citharichthys* spp., *Liparis fucensis*, *Glyptocephalus zachirus*, *Lipolagus ochotensis*, *Microstomus pacificus*, *Protomyctophum thompsoni*, *Sebastolobus* spp., *Chauliodus macouni*, *Diaphus theta*, *Artedius harringtoni*, *Isopsetta isolepis*, and *Protomyctophum crockeri* (listed in order of highest to lowest mean concentration).

Cluster and Multidimensional Scaling (MDS) Analyses

Several taxonomic, seasonal, and cross-shelf assemblages were identified, although no annual or latitudinal assemblages were apparent (figs. 3a–c, 4a–b). Taxonomic assemblages could not be explained by differences in a single factor (e.g., cross-shelf affiliation), but rather seem to be the result of an association between certain taxa based on the interaction between multiple factors (e.g., annual, seasonal, latitudinal, and cross-shelf). Larvae clustered as four seasonal assemblages along a continuous temporal gradient: spring (May), early summer (June–July), late summer (August–September), and fall (September–October/November). Cluster and MDS analyses indicated the presence of three cross-shelf assemblages: coastal (<~50 km from shore), offshore (~50–100 km), and far-offshore (>~100 km). Although there appears to be a continuous spatial gradient between these assemblages, the offshore

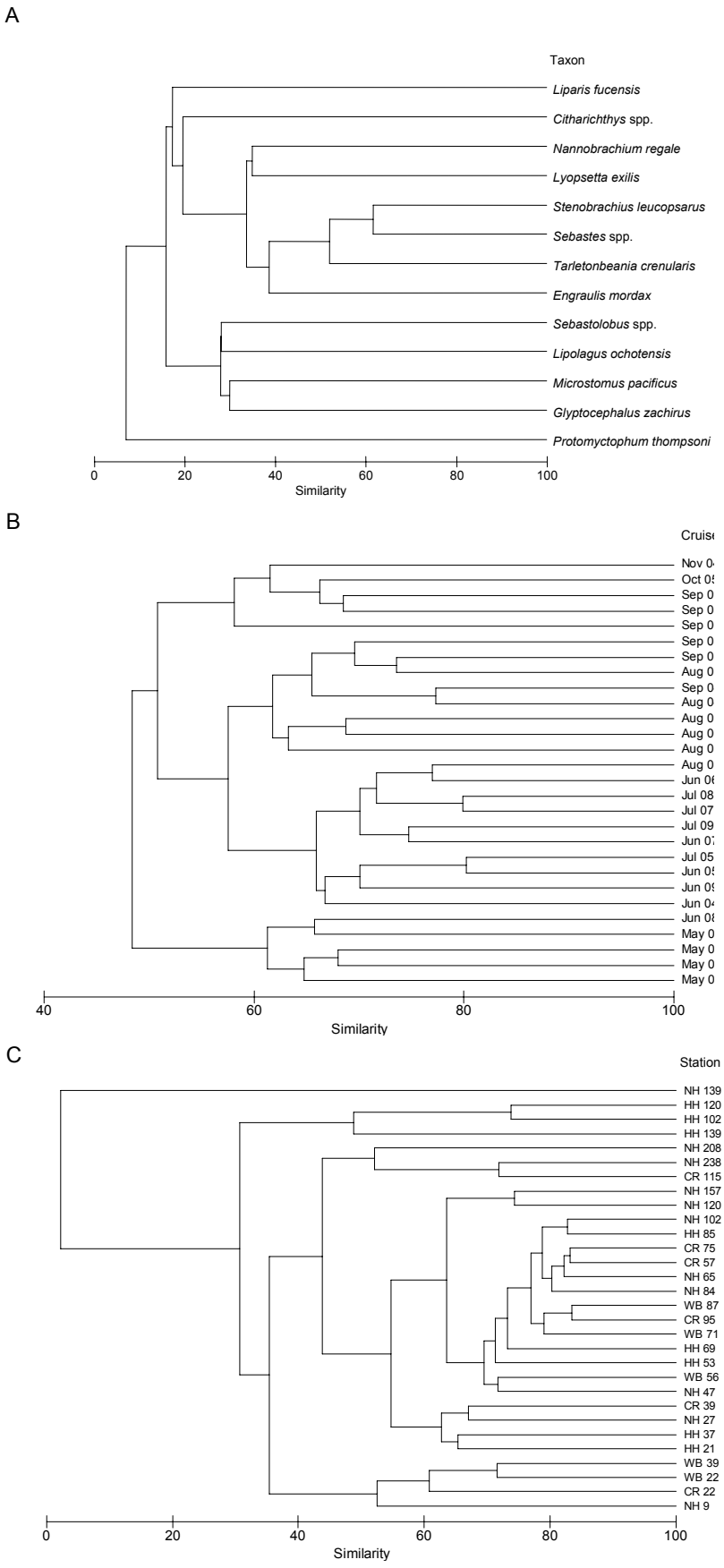

Figure 3. Dendrograms resulting from cluster analysis performed on larval fishes collected during this study off the Oregon and Washington coasts in 2004–2009: (A) taxon, (B) cruise (month and year), and (C) station (transect [north-south: Willapa Bay (WB), Columbia River (CR), Newport Hydrographic (NH), and Heceta Head (HH)] and distance from shore [km]).

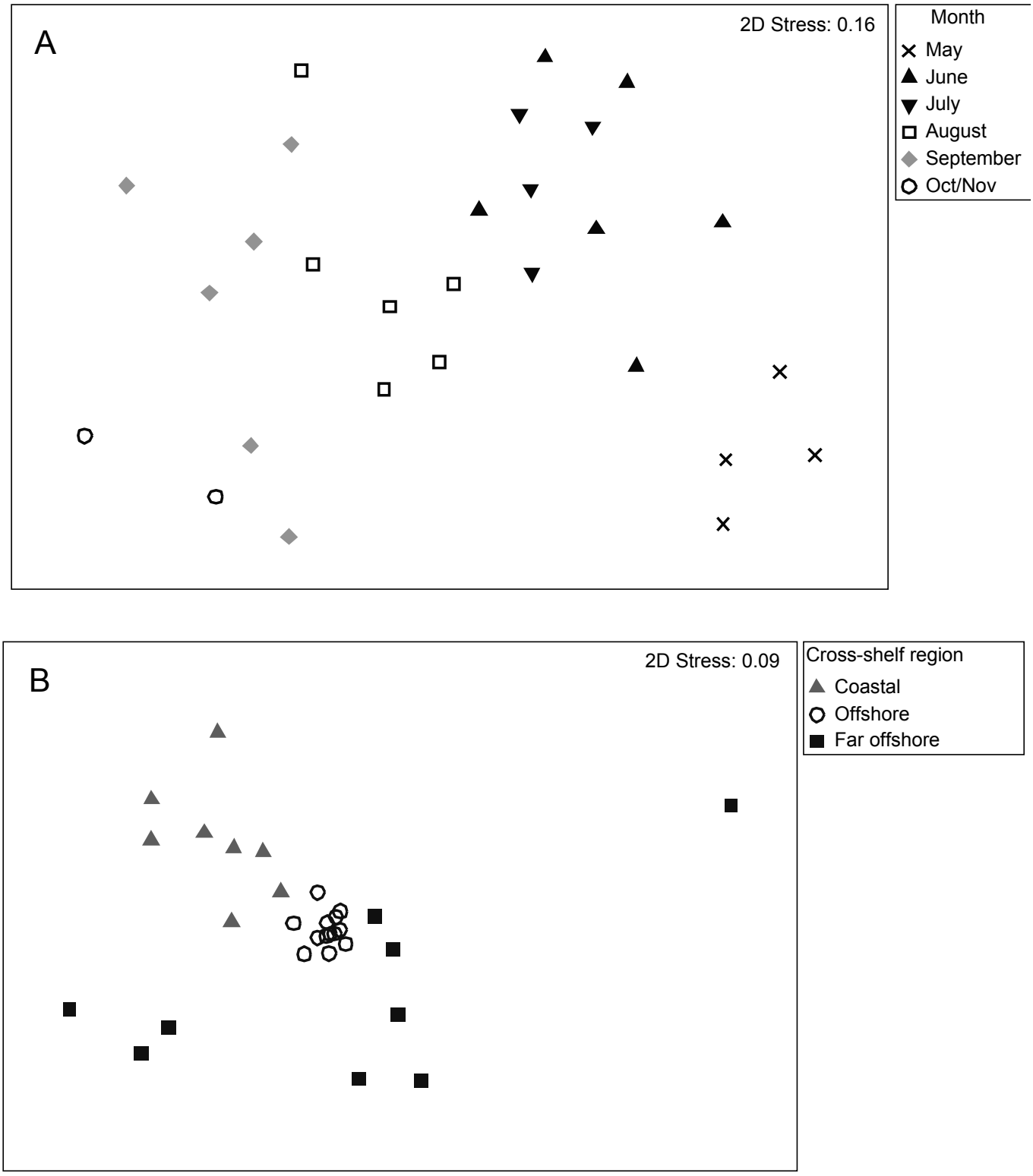

Figure 4. Plots resulting from multidimensional scaling analysis performed on larval fishes collected during this study off the Oregon and Washington coasts in 2004–2009: (A) month and (B) cross-shelf region.

TABLE 2
Annual mean concentrations (no. 1000 m^{-3}) and diversity (H') of fish larvae collected during this study off the Oregon and Washington coasts in 2004–2009 (1 SE in parentheses). For between-year comparisons of each taxon and larval diversity, different superscripts indicate significant differences (ANOVA $p < 0.05$).

	2004	2005	2006	2007	2008	2009
Engraulis mordax	20.6 (9.5)^{ab}	215.3 (78.1)^{a}	4.2 (1.7)^{b}	13.0 (4.9)^{b}	62.3 (56.9)^{b}	141.2 (106.2)^{b}
Lyopsetta exilis	4.0 (1.8)^{ab}	1.3 (0.4)^{b}	3.6 (1.1)^{ab}	10.1 (2.2)^{a}	3.6 (1.2)^{ab}	8.5 (1.7)^{a}
Sebastes spp.	89.2 (28.6)	52.7 (13.6)	22.9 (4.6)	60.5 (18.3)	68.3 (13.7)	129.6 (49.2)
Stenobrachius leucopsarus	4.0 (1.6)^{b}	37.1 (10.7)^{ab}	44.1 (10.9)^{ab}	48.2 (9.6)^{a}	45.3 (9.6)^{a}	36.3 (7.9)^{ab}
Tarletonbeania crenularis	2.6 (1.1)	9.0 (2.2)	5.1 (1.3)	4.9 (0.9)	6.3 (1.4)	7.2 (1.4)
Total larvae	126.5 (40.3)	328.0 (82.4)	92.0 (15.5)	149.5 (26.1)	194.2 (61.0)	337.4 (126.0)
Diversity	0.76 (0.05)	0.68 (0.04)	0.72 (0.03)	0.77 (0.03)	0.69 (0.03)	0.74 (0.03)

TABLE 3
Monthly mean concentrations (no. 1000 m^{-3}) and diversity (H') of fish larvae collected during this study off the Oregon and Washington coasts in 2004–2009 (1 SE in parentheses). For between-month comparisons of each taxon and larval diversity, different superscripts indicate significant differences (ANOVA $p < 0.05$).

	May	June	July	August	September	Oct/Nov
Engraulis mordax	0.2 (0.2)^{b}	206.4 (114.8)^{a}	257.6 (110.9)^{a}	5.6 (1.8)^{b}	0.6 (0.3)^{b}	0 (0)^{b}
Lyopsetta exilis	14.1 (2.0)^{a}	12.5 (2.3)^{a}	2.0 (0.8)^{b}	0.6 (0.2)^{b}	0.1 (0.1)^{b}	0 (0)^{b}
Sebastes spp.	64.6 (17.4)^{ab}	187.2 (53.3)^{a}	85.5 (20.4)^{a}	25.0 (3.6)^{bc}	9.7 (2.3)^{d}	24.7 (18.3)^{cd}
Stenobrachius leucopsarus	72.2 (12.1)^{a}	71.0 (11.0)^{a}	41.6 (10.5)^{ab}	21.2 (5.9)^{b}	1.8 (0.7)^{c}	0.9 (0.5)^{c}
Tarletonbeania crenularis	4.7 (1.1)	9.6 (1.9)	7.5 (1.8)	5.6 (1.0)	4.2 (0.8)	2.5 (0.8)
Total larvae	179.3 (23.6)^{a}	505.4 (134.5)^{a}	400.7 (114.3)^{a}	65.3 (9.4)^{b}	20.1 (2.6)^{c}	30.9 (18.6)^{c}
Diversity	0.74 (0.02)^{b}	0.62 (0.03)^{c}	0.60 (0.04)^{c}	0.82 (0.02)^{ab}	0.87 (0.03)^{a}	0.81 (0.08)^{ab}

TABLE 4
Latitudinal (north-south: Willapa Bay [WB], Columbia River [CR], Newport Hydrographic [NH], and Heceta Head [HH] transects) mean concentrations (no. 1000 m^{-3}), diversity (H'), and weighted (by concentration) mean lengths (mm) of fish larvae collected during this study off the Oregon and Washington coasts in 2004–2009 (1 SE in parentheses). For between-transect comparisons of each taxon and larval diversity, different superscripts indicate significant differences (ANOVA $p < 0.05$).

	Mean concentration				Mean length			
	WB	CR	NH	HH	WB	CR	NH	HH
Engraulis mordax	203.7 (119.4)	36.8 (11.4)	24.3 (8.7)	85.3 (46.5)	7.4 (0.2)^{b}	10.0 (0.3)^{ab}	7.4 (0.3)^{ab}	10.7 (0.3)^{a}
Lyopsetta exilis	2.0 (0.5)^{c}	2.2 (0.6)^{bc}	7.0 (1.5)^{ab}	10.5 (1.8)^{a}	7.9 (0.6)	9.4 (0.6)	8.3 (0.3)	8.8 (0.3)
Sebastes spp.	37.0 (8.4)^{b}	27.1 (6.0)^{b}	77.1 (18.4)^{ab}	138.5 (42.0)^{a}	5.0 (0.1)^{ab}	5.9 (0.1)^{a}	4.4 (0.1)^{b}	4.5 (0.1)^{b}
Stenobrachius leucopsarus	43.2 (9.3)^{ab}	56.6 (10.4)^{a}	39.2 (7.4)^{a}	22.9 (4.9)^{b}	8.3 (0.1)	7.5 (0.1)	7.4 (0.1)	7.7 (0.1)
Tarletonbeania crenularis	4.1 (0.8)	7.8 (1.4)	7.7 (1.3)	5.2 (1.2)	9.6 (0.6)	9.0 (0.4)	7.1 (0.3)	8.5 (0.4)
Total larvae	300.9 (129.1)	142.7 (21.1)	168.5 (26.7)	272.9 (64.1)				
Diversity	0.71 (0.03)	0.75 (0.02)	0.74 (0.02)	0.68 (0.03)				

assemblage is far more tightly clustered and distinct than the coastal and far-offshore groups.

Concentrations and Distributions

Annual Total mean larval concentration decreased from 328 1000 m^{-3} in 2005 to 92 1000 m^{-3} in 2006, and subsequently increased each year to a high of 337 1000 m^{-3} in 2009 (table 2). Larval *E. mordax* concentration in 2005 was >50 times higher than 2006, and was significantly higher than in subsequent years (2006–2009). In contrast, peak concentrations of *L. exilis* in 2007 and 2009 were significantly higher than in 2005, while *S. leucopsarus* concentrations in 2007 and 2008 were significantly higher than in 2004. *Sebastes* spp. and *T. crenularis* larvae exhibited no significant interannual concentration differences.

Monthly Seasonally, total larval concentrations were highest in May–July, decreased significantly in August, and declined further in September–October/November (table 3). Larval *L. exilis* were found predominantly in May–June, while *S. leucopsarus* concentrations peaked in May and decreased steadily to October/November. Larval *E. mordax* were found almost exclusively in June–July, while *Sebastes* spp. larvae were also found in significantly higher concentrations in June–July than in August–October/November. There were no significant

TABLE 5
Cross-shelf (coastal, offshore, far-offshore) mean concentrations (no. 1000 m^{-3}), diversity (H'), and weighted (by concentration) mean lengths (mm) of fish larvae collected during this study off the Oregon and Washington coasts in 2004–2009 (1 SE in parentheses). For between-zonal comparisons of each taxon and larval diversity, different superscripts indicate significant differences (ANOVA $p < 0.05$).

	Mean concentration			Mean length		
	Coastal	Offshore	Far-offshore	Coastal	Offshore	Far-offshore
Engraulis mordax	24.0 (12.5)^{b}	116.3 (45.5)^{a}	65.3 (39.8)^{ab}	9.9 (0.3)	8.5 (0.2)	6.0 (0.4)
Lyopsetta exilis	4.7 (0.9)	6.2 (0.9)	6.6 (2.3)	9.1 (0.4)	8.4 (0.2)	10.6 (0.8)
Sebastes spp.	15.8 (3.9)^{b}	103.6 (19.1)^{a}	13.2 (4.1)^{ab}	4.0 (0.05)^{b}	4.9 (0.04)^{a}	6.5 (0.5)^{a}
Stenobrachius leucopsarus	1.8 (0.6)^{b}	61.0 (5.9)^{a}	134.6 (44.4)^{a}	7.1 (0.3)	7.7 (0.1)	6.7 (0.1)
Tarletonbeania crenularis	0.3 (0.2)^{c}	9.5 (0.9)^{b}	24.1 (6.3)^{a}	7.7 (1.2)	8.4 (0.2)	6.5 (0.3)
Total larvae	53.1 (13.2)^{b}	311.4 (52.5)^{a}	285.7 (71.2)^{a}			
Diversity	0.82 (0.03)^{a}	0.69 (0.01)^{b}	0.68 (0.06)^{ab}			

TABLE 6
Monthly weighted (by concentration) mean lengths (mm) of fish larvae collected during this study off the Oregon and Washington coasts in 2004–2009 (1 SE in parentheses). For between-month comparisons of each taxon, different superscripts indicate significant differences (ANOVA $p < 0.05$).

	May	June	July	August	September	Oct/Nov
Engraulis mordax	2.2 (0)^{b}	5.0 (0.1)^{b}	12.4 (0.2)^{a}	15.3 (0.7)^{a}	16.3 (3.3)^{a}	—
Lyopsetta exilis	7.7 (0.2)^{b}	8.5 (0.3)^{b}	14.2 (1.0)^{a}	16.2 (1.8)^{a}	14.1 (4.5)^{ab}	—
Sebastes spp.	4.1 (0.1)^{cd}	4.2 (0)^{d}	5.0 (0.1)^{bc}	7.1 (0.2)^{a}	5.0 (0.3)^{b}	4.6 (0.2)^{bcd}
Stenobrachius leucopsarus	7.0 (0.1)^{d}	6.6 (0.1)^{d}	8.7 (0.1)^{c}	10.9 (0.2)^{b}	13.5 (0.6)^{a}	6.2 (2.1)^{d}
Tarletonbeania crenularis	6.9 (0.5)^{b}	6.4 (0.2)^{b}	10.4 (0.5)^{a}	10.5 (0.5)^{a}	8.4 (0.5)^{ab}	6.3 (0.6)^{b}

monthly differences in mean concentration for *T. crenularis* larvae. These seasonal patterns in larval concentrations persisted within each sampled year.

Latitudinal Concentrations of *Sebastes* spp. and *L. exilis* larvae were significantly greater along the southernmost than northern transects, while concentrations of *S. leucopsarus* larvae were significantly higher along the central than southernmost transects (table 4). Concentrations of total larvae and *E. mordax* were highest along the northern- and southernmost transects, while *T. crenularis* larvae showed the opposite pattern. However, despite these regional differences, the distribution patterns of the three groups did not exhibit a significant north to south concentration pattern. These latitudinal patterns were also similar within most sampled months and years.

Cross-shelf Concentrations of the five dominant taxa and total larvae were higher in the offshore and far-offshore regions than in the coastal region (table 5); a pattern that persisted within each sampled month and year. Larval *E. mordax* and *Sebastes* spp. concentrations were significantly higher in the offshore than coastal region, while *S. leucopsarus* and total larval concentrations were significantly higher in both the offshore and far-offshore regions than in the coastal region. Larval *T. crenularis* concentration increased steadily and significantly from onshore to far-offshore direction; a similar sequential increase in *L. exilis* concentration was not significant.

Lengths

Weighted mean length differences of most taxa examined generally exhibited patterns opposite to their concentration differences across monthly, latitudinal, and cross-shelf scales (i.e., largest sizes were in regions with lowest concentrations; table 3–6), and generally within months and years. However, both concentration and length of *Sebastes* spp. larvae were significantly larger offshore than in coastal waters and, on average, the largest larvae occurred far-offshore.

Diversity

Larval diversity varied significantly between months and cross-shelf regions, but not between years or latitudinal transects (table 2–5). Diversity was generally inversely proportional to larval concentration. It was highest in September and lowest in June and July, and decreased with distance from shore. These patterns were generally consistent within months and years.

Multi-response Permutation Procedure (MRPP) and Indicator Species Analysis (ISA)

The results of MRPP analyses revealed significant between-group differences in larval concentrations within each of the annual, monthly, latitudinal, and cross-shelf factors (table 7). A-statistic values indicated that taxonomic association was strongest for the monthly and cross-shelf factors. Significant indicator taxa were also

TABLE 7

Results of the multi-response permutation procedure (MRPP) and indicator species analysis (ISA) for annual (2004–2009), monthly (May–October/November), latitudinal (north-south: Willapa Bay [WB], Columbia River [CR], Newport Hydrographic [NH], and Heceta Head [HH] transects), and cross-shelf (coastal, offshore, far-offshore) differences in composition of fish larvae collected during this study off the Oregon and Washington coasts. Significant indicator taxa ($p < 0.05$) are listed with the factor category with which each taxon is associated in parentheses. Full taxon names are listed in Table 1.

Factor	MRPP A-statistic	*p*-value	Indicator taxa
Year	0.021	<0.001	*Sebastes* spp. (2004); *Citharichthys* spp. and *E. mordax* (2005); *L. ochotensis*, *M. productus*, and *P. crockeri* (2006); *G. zachirus* (2008)
Month	0.076	<0.001	*G. zachirus*, *I. aenigmaticus*, *I. isolepis*, *L. fucensis*, *L. ochotensis*, *L. exilis, M. productus*, *M. pacificus*, *P. evides*, *R. asprellus*, *R. meanyi*, *S. leucopsarus* (May); *N. regale* (June); *E. mordax* and *Sebastes* spp. (July)
Latitude	0.014	<0.001	*L. fucensis,* Osmeridae, *S. sagax* (WB); *P. crockeri* (CR); *L. exilis*, *P. evides*, and *Sebastes* spp. (HH)
Cross-shelf	0.049	<0.001	*A. harringtoni* and *R. asprellus* (coastal); *Sebastes* spp. (offshore); *B. pentacanthus*, *D. theta*, *I. lockingtoni, I. aenigmaticus*, *L. ochotensis, M. productus*, *M. pacificus*, *N. regale*, *S. sagax*, *Scopelosaurus* spp., *Sebastolobus* spp., *S. leucopsarus*, *T. crenularis*, and *T. altivelis* (far-offshore)

TABLE 8

Correlation coefficients for 15 variables collected during this study: station distance from shore (km, Dist. shore), temperature (°C), salinity, density (sigma theta, kg m^{-3}), fluorescence (mg m^{-3}), turbidity (mg m^{-3}), dissolved oxygen concentration (DO, ml L^{-1}), DO saturation (%), $\log_e(n + 0.1)$-transformed concentrations (no. 1000 m^{-3}) of *Engraulis mordax*, *Lyopsetta exilis*, *Sebastes* spp., *Stenobrachius leucopsarus*, *Tarletonbeania crenularis*, and total larvae, and larval diversity (*H'*). Samples containing no larvae were excluded. Values for the environmental variables used in the analysis were taken from different depths in the water column at each station corresponding to either near the surface or the weighted mean depth for each taxon as reported in previous studies: environmental inter-variable comparisons: 1-m depth; *E. mordax*: 10-m depth; *Sebastes* spp., total larvae, and larval diversity: 20-m depth; *L. exilis* and *S. leucopsarus*: 40-m depth; *T. crenularis*: 50-m depth. Sample size (*n*) in parentheses. ⋆ = $p < 0.01$.

	Dist. shore	Temperature	Salinity	Density	Fluorescence	Turbidity	DO	DO saturation
Temperature	0.24⋆ (478)		-0.12 (464)	-0.35⋆ (445)	-0.40⋆ (401)	-0.12 (386)	-0.46 (169)	–0.09 (169)
Salinity	0.18⋆ (464)			0.97⋆ (445)	-0.009 (401)	-0.34⋆ (386)	-0.16⋆ (169)	-0.06 (169)
Density	0.11 (445)				0.08 (396)	–0.29⋆ (386)	–0.06 (169)	–0.04 (169)
Fluorescence	–0.36⋆ (401)					0.33⋆ (386)	0.59⋆ (169)	0.46⋆ (169)
Turbidity	–0.32⋆ (386)						0.38⋆ (169)	0.30⋆ (169)
DO	–0.21⋆ (169)							0.91⋆ (169)
DO Saturation	–0.14 (169)							
Engraulis mordax		0.10 (107)	–0.25⋆ (107)	–0.23 (107)	–0.29⋆ (100)	–0.25 (100)	–0.26 (37)	–0.34 (37)
Lyopsetta exilis		–0.16 (112)	–0.10 (101)	–0.03 (101)	–0.14 (98)	0.24 (98)	0.002 (48)	–0.003 (48)
Sebastes spp.		0.001 (295)	–0.29⋆ (283)	–0.16⋆ (272)	–0.17⋆ (254)	–0.03 (252)	0.25⋆ (114)	0.24⋆ (114)
Stenobrachius leucopsarus		0.28⋆ (214)	–0.38⋆ (202)	–0.38⋆ (199)	0.21⋆ (194)	0.03 (194)	0.53⋆ (91)	0.54⋆ (91)
Tarletonbeania crenularis		0.04 (168)	–0.19 (158)	–0.17 (152)	0.19 (145)	0.04 (144)	0.35⋆ (66)	0.36⋆ (66)
Total larvae		0.17⋆ (389)	–0.45⋆ (374)	–0.36⋆ (360)	–0.12 (338)	–0.13 (336)	0.45⋆ (151)	0.47⋆ (151)
Diversity		0.02 (315)	0.22⋆ (300)	0.10 (290)	–0.02 (276)	0.03 (275)	–0.26⋆ (127)	–0.22 (127)

identified for most years, months, transects, and cross-shelf regions (table 1). Results from the ISA support those from MRPP analyses, since far more significant indicator taxa were found for the monthly and cross-shelf factors than for annual and latitudinal factors.

Environmental Relationships

BIO-ENV A BIO-ENV analysis, which included local environmental variables (i.e., latitude, station depth, station distance from shore, temperature, salinity, density, fluorescence, and turbidity), revealed that the combination of distance from shore and water temperature at 20-m depth explained the most variability (36%) in larval fish concentrations in 2004–2009. The second BIO-ENV analysis, done with the addition of DO and DO saturation in 2008 and 2009, showed that the combination of distance from shore and DO saturation at 20-m depth explained the most concentration variability (42%) during those years.

Correlations Larval concentrations were generally positively correlated with temperature and dissolved oxygen and negatively correlated with salinity, density, and fluorescence, while diversity generally followed the opposite pattern (table 8). However, concentrations of *S. leucopsarus* larvae were significantly positively correlated with fluorescence, while those of *E. mordax* larvae were negatively (although not significantly) correlated with DO and DO saturation. Among the local environmental variables, distance from shore was significantly positively correlated with near-surface temperature and

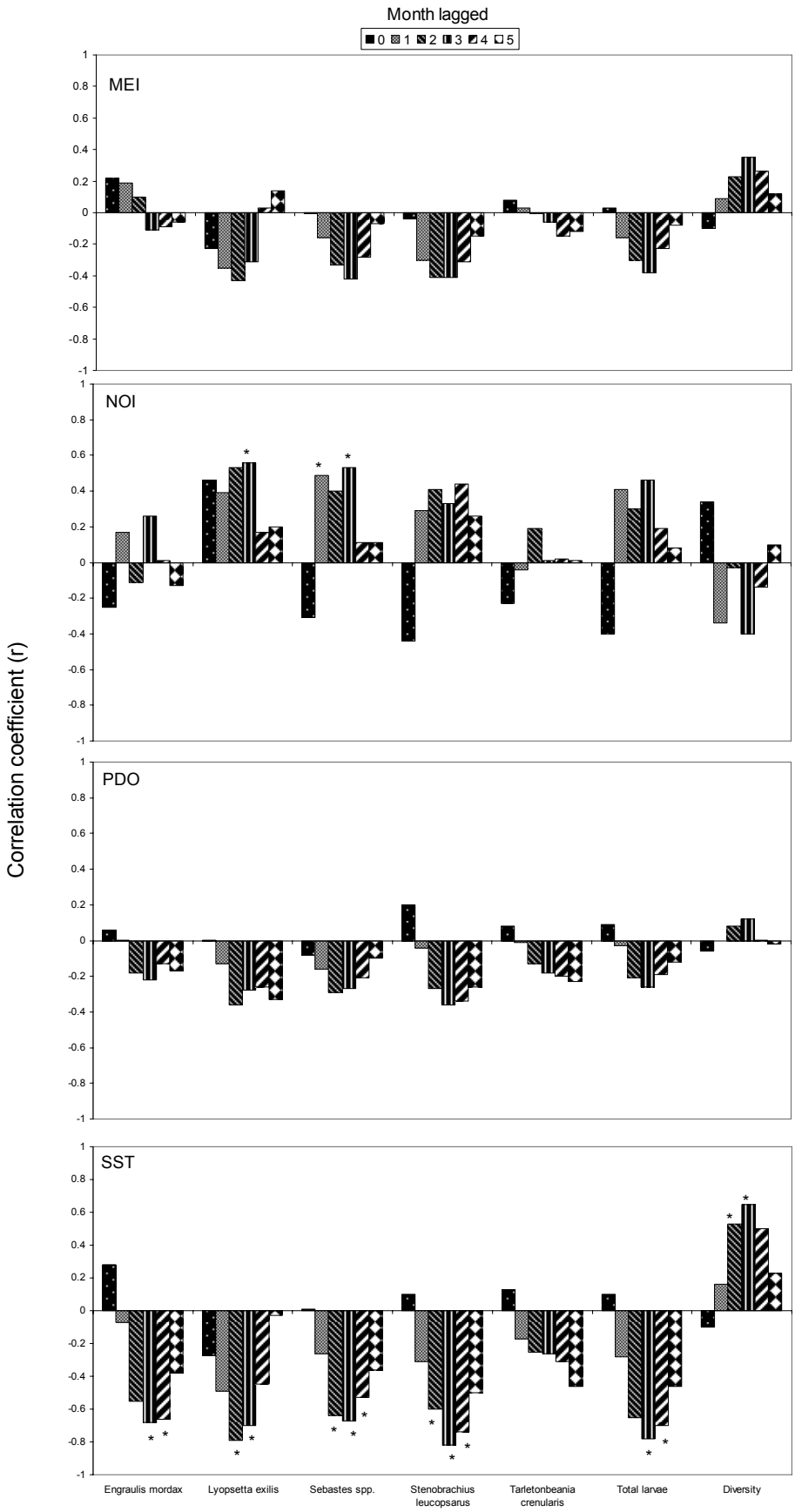

Figure 5. Correlation coefficients for the 0-, 1-, 2-, 3-, 4-, and 5-month lagged $\log_e(n + 0.1)$-transformed concentrations (no. 1000 m^{-3}) of five dominant larval fish taxa and total larvae, and larval diversity, in relation to eight monthly-averaged environmental indices/variables analyzed in this study: Multivariate El Niño-Southern Oscillation Index (MEI), Pacific Decadal Oscillation (PDO), Northern Oscillation Index (NOI), sea-surface temperature (SST, °C) recorded from the National Oceanic and Atmospheric Administration's (NOAA) Stonewall Banks buoy located 20 nm west of Newport, Oregon (44.64°N, 124.50°W), and eastward Ekman transport (EET, kg m^{-1}), northward Ekman transport (NET, kg m^{-1}), and Upwelling Index (UPW) each for 45°N, 125°W, and Columbia River outflow (COL, 1000 ft s^{-1}) measured at Bonneville Dam located 235 km upriver from the mouth of the Columbia River. * = $p < 0.01$.

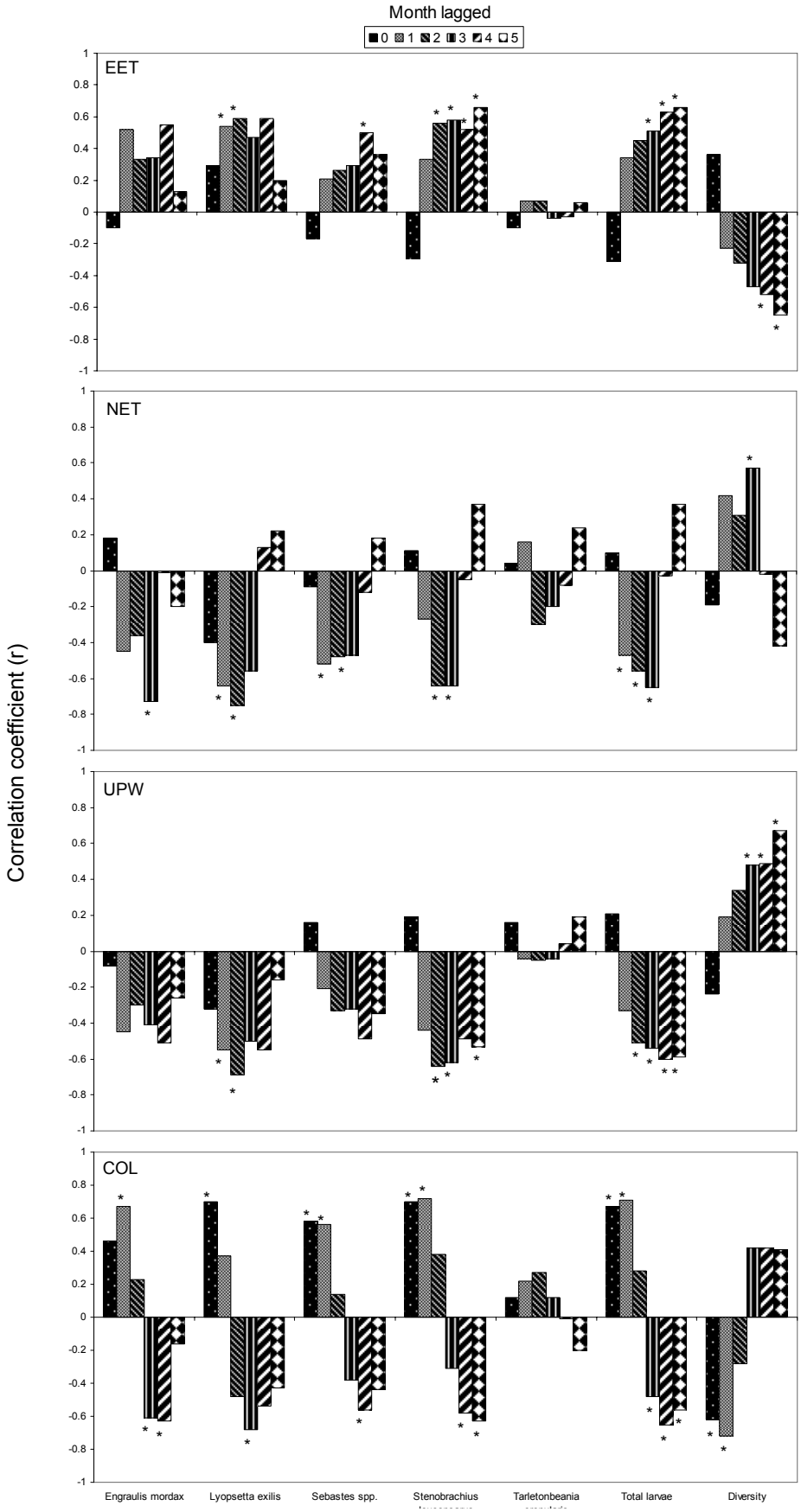

Figure 5. Correlation coefficients for the 0-, 1-, 2-, 3-, 4-, and 5-month lagged $\log_e(n + 0.1)$-transformed concentrations (no. 1000 m^{-3}) of five dominant larval fish taxa and total larvae, and larval diversity, in relation to eight monthly-averaged environmental indices/variables analyzed in this study: Multivariate El Niño-Southern Oscillation Index (MEI), Pacific Decadal Oscillation (PDO), Northern Oscillation Index (NOI), sea-surface temperature (SST, °C) recorded from the National Oceanic and Atmospheric Administration's (NOAA) Stonewall Banks buoy located 20 nm west of Newport, Oregon (44.64°N, 124.50°W), and eastward Ekman transport (EET, kg m^{-1}), northward Ekman transport (NET, kg m^{-1}), and Upwelling Index (UPW) each for 45°N, 125°W, and Columbia River outflow (COL, 1000 ft s^{-1}) measured at Bonneville Dam located 235 km upriver from the mouth of the Columbia River. * = $p < 0.01$.

TABLE 9

Best-fit non-parametric multiplicative regression (NPMR) model statistics for the analysis of the $\log_e(n + 0.1)$-transformed dominant larval fish taxa and total larval concentrations (no. 1000 m^{-3}) and larval diversity (H') in relation to five in situ environmental variables: temperature (Temp, °C), salinity (Sal), density (Den, sigma theta, kg m^{-3}), fluorescence (Fluor, mg m^{-3}), and turbidity (Turb, mg m^{-3}). Samples containing no larvae were excluded. Values for the environmental variables used in the analysis were taken from different depths in the water column at each station corresponding to the weighted mean depth for each taxon as reported in previous studies: *Engraulis mordax*: 10-m depth; *Sebastes* spp., total larvae, and larval diversity: 20-m depth; *Lyopsetta exilis* and *Stenobrachius leucopsarus*: 40-m depth; *Tarletonbeania crenularis*: 50-m depth.

Taxon/Group	Best-fit model variables	Cross-validated R^2	*p*-value	*n*
Engraulis mordax	Sal, Temp, Fluor	0.18	0.003	100
Lyopsetta exilis	Temp, Turb	0.17	0.003	98
Sebastes spp.	Sal, Fluor	0.10	<0.001	252
Stenobrachius leucopsarus	Den, Turb	0.23	<0.001	194
Tarletonbeania crenularis	Sal	0.09	0.002	144
Total larvae	Sal	0.22	<0.001	336
Diversity	Sal, Temp	0.07	0.004	275

TABLE 10

Best-fit non-parametric multiplicative regression (NPMR) model statistics for the analysis of the monthly-averaged $\log_e(n + 0.1)$-transformed dominant larval fish taxa and total larval concentrations (no. 1000 m^{-3}) and larval diversity (H') in relation to eight larger-scale environmental variables: Multivariate El Niño-Southern Oscillation Index (MEI), Pacific Decadal Oscillation (PDO), Northern Oscillation Index (NOI), sea-surface temperature (SST, °C) recorded from the National Oceanic and Atmospheric Administration's (NOAA) Stonewall Banks buoy located 20 nm west of Newport, Oregon (44.64°N, 124.50°W), and eastward Ekman transport (EET, kg m^{-1}), northward Ekman transport (NET, kg m^{-1}), and Upwelling Index (UPW) each for 45°N, 125°W, and Columbia River outflow (COL, 1000 ft s^{-1}) measured at Bonneville Dam located 235 km upriver from the mouth of the Columbia River. Months in which no larvae were collected were excluded.

Taxon/Group	Time lag (months)	Best-fit model variables	Cross-validated R^2	*p*-value	*n*
Engraulis mordax	3	COL, SST	0.59	0.13	19
Lyopsetta exilis	2	COL, SST	0.65	0.09	20
Sebastes spp.	4	COL, EET	0.50	0.04	28
Stenobrachius leucopsarus	4	SST, NET	0.64	0.01	28
Tarletonbeania crenularis	4	NOI, UPW	0.20	0.39	28
Total larvae	4	COL, SST	0.67	0.005	28
Diversity	3	COL, NET	0.65	0.002	28

salinity, and negatively correlated with near-surface fluorescence, turbidity, and DO. Descriptive statistics (mean, SE, median, upper and lower 95% confidence intervals [CIs], range [minimum-maximum values], and sample size [*n*]) for the seven local environmental variables for each of the five dominant larval fish taxa and total larvae (weighted based on concentration) collected during this study are presented in the Appendix.

Lagged monthly-averaged larval concentrations were generally positively correlated with the larger-scale environmental variables NOI and EET and negatively correlated with MEI, PDO, SST, NET, and UPW, while diversity generally followed the opposite pattern (fig. 5). The distributions of the 0–5 month lagged correlation coefficients for most of the larger-scale environmental variables were fairly normal in shape, with a mode at ~3 months for most of the dominant taxa, total larvae, and larval diversity. However, 0–2 month lagged larval concentrations were generally positively correlated with COL, while those lagged 3–5 months followed the opposite pattern. Larval *T. crenularis* showed no correlation pattern or significance when compared to any of the larger-scale environmental variables across all time lags, and no significant correlations were found between any of the 0–5 month lagged larval concentrations or diversity and MEI or PDO.

Non-parametric multiplicative regressions (NPMR) NPMR analyses revealed significant best-fit models for the multiplicative effects of both local and larger-scale environmental variables on larval concentrations and diversity. Salinity was the single most important local variable associated with concentrations of total larvae and most of the dominant taxa as well as diversity, often interacting multiplicatively with temperature and/or fluorescence (table 9). COL and SST were the most important larger-scale variables associated with 2–4 month lagged larval concentrations and diversity (table 10). However, NET was also one of two best-fit model variables explaining 3 and 4 month lagged *S. leucopsarus* concentrations and larval diversity, respectively, while EET was one of two best-fit model variable explaining 4 month lagged *Sebastes* spp. concentrations.

DISCUSSION

Taxonomic Composition

The overall composition of the NCC spring–fall epipelagic larval fish community and dominant taxa in 2004–2009 was similar to that reported in previous studies conducted here over the last 40 years (Waldron 1972; Richardson 1973; Richardson and Pearcy 1977; Doyle 1992; Auth and Brodeur 2006; Auth 2009). However, several anomalies were observed during this study period. Larval *Merluccius productus* and *Sardinops sagax* were collected in concentrations as high as 62 and 82 1000 m^{-3}, respectively, only during June/July 2005 and May 2006. These were periods corresponding to unusual late upwelling (2005) and relatively high positive PDO index values (2005 and 2006). *M. productus* generally spawn in southern California waters. Until recently, their larvae have been rarely sampled in the study area, and those encounters have exclusively been during El Niño events or periods corresponding to positive MEI values (Phillips et al. 2007). *S. sagax* have been spawning in the NCC region since the mid-1990s after an absence of nearly 40 years (Emmett et al. 2005). In addition, larvae of several (n = 16; table 1) taxa were collected during months outside of their spawning seasons as previously reported for this region (Matarese et al. 1989).

Concentrations, Distributions, and Assemblages

Annual The dramatic ichthyoplankton concentration decrease between 2005 and 2006 may have been a delayed response resulting from the adverse effects on spawning stocks of the anomalously late upwelling that occurred in the NCC during the summer of 2005 (Brodeur et al. 2006; Barth et al. 2007). The impact appears to have been especially evident in taxa that spawn farther up in the water column (e.g., *E. mordax*), that were more affected by the increased temperatures, north- and shoreward transport, and decreased productivity in the upper water column resulting from the El Niño-like conditions than more deepwater species (e.g., *L. exilis, S. leucopsarus, T. crenularis*). In fact, the three species that were identified through ISA as indicative of 2006 (i.e., larvae of *L. ochotensis*, *M. productus*, and *P. crockeri*; table 7) were all deepwater and/or more southern spawning species. The gradual increase in concentrations of *E. mordax*, *Sebastes* spp., and total larvae between 2006 and 2009 could be the result of the increasingly beneficial conditions supporting reproductive effort following the deleterious conditions resulting from the anomalous 2005 summer.

Seasonal The seasons of peak larval concentrations for dominant taxa (May/June: *L. exilis* and *S. leucopsarus*; June/July: *E. mordax* and *Sebastes* spp.), and lack of a peak season for *T. crenularis*, have previously been reported (Richardson 1973; Brodeur et al. 1985; Doyle et al. 1993; Auth and Brodeur 2006). The seasonal cycle of larval diversity observed across all six years (i.e., highest levels during the spring–summer and summer–fall transitional periods) is similar to that reported by Auth and Brodeur (2006). The significant concentration reduction of all dominant taxa and total larvae in August–November compared to May–July, along with the lack of any significant indicator taxa for the later period, suggests that the late summer–fall season is not as important as the spring–early summer season in characterizing the ichthyoplankton community in the NCC. In fact, Brodeur et al. (2008) and Auth et al. (2011) both found significantly higher concentrations of larvae in the nearshore region (9–18 km along the NH line) during the winter/spring (January–May) than summer/fall (June–December) periods, most likely resulting from the same increase in food availability during the spring that is characteristic of the NCC ecosystem.

Latitudinal Although three of the dominant larval taxa (i.e., *L. exilis*, *Sebastes* spp., and *S. leucopsarus*) had significantly elevated concentrations along specific transects during some cruises, these differences were not consistently significant between months or years. The southernmost (i.e., HH) transect was generally characterized by highest concentrations of larval *L. exilis* and *Sebastes* spp., an observation supported by the results of the ISA (table 7). Three of the five stations along this transect extend across Heceta Bank ~55 km from shore, an area that includes depths as shallow as 60 m rising from surrounding depths of 100–1000 m, which forms a major nursery area for juvenile *L. exilis* and *Sebastes* spp. (Pearcy et al. 1989; Stein et al. 1992). In contrast, the NH line just north of the HH transect appears to be more of a transitional region between Heceta Bank and transects to the north, as is evident by the lack of significant latitudinal differences between the CR, NH, and HH transects for all larval concentrations (except *S. leucopsarus*) and diversity. This is further supported by the lack of any significant indicator taxa for the NH line.

Cross-shelf The cross-shelf distribution of fish larvae, with consistently higher concentrations of all dominant taxa and total larvae in the offshore and far-offshore regions than nearshore, was similar to recent reports of ichthyoplankton distributions in the NCC (Auth and Brodeur 2006; Auth 2008; Auth 2009). However, larval diversity exhibited the opposite pattern, being significantly higher in the coastal than offshore region. Auth and Brodeur (2006) reported little cross-shelf variation in larval diversity along the NH line in 2000 and 2002, with the exception of a spike of low diversity at a single station 46 km from shore. Larval diversity may be inversely related to zooplankton community structure. Gómez-Gutiérrez et al. (2005) observed that diversity in the euphausiid community was higher in more off-

shore than inshore stations off the central Oregon coast in 1970–1972, as did Keister and Peterson (2003) for the zooplankton community in the same area in 1998–2000. Brodeur et al. (2008) found that ichthyoplankton diversity was related to zooplankton biomass and the Pacific Decadal Oscillation (PDO) index in a study conducted from 1997–2005 off the central Oregon coast. However, samples for that study were collected exclusively at very nearshore (9 and 18 km from shore) stations along the NH line, and were comprised of a different ichthyoplankton community than the one sampled in the current study. Larval diversity in this study largely reflects the number of species that are spawned in a given location and have pelagic larvae. Nearshore regions have more diverse physical structure and therefore provide many more niches for coastal species. Except for pelagic larval stages of benthic organisms, zooplankton are holoplankton, experiencing their entire life as plankton. Therefore, it is not surprising that zooplankton are more diverse offshore, while ichthyoplankton are more diverse nearshore. It should be noted that larval diversity may be underrepresented due to the difficulty in identifying some larvae to species based on meristics and pigmentation patterns (e.g., Osmeridae, *Sebastes* spp., *Sebastolobus* spp., *Citharichthys* spp.) (Matarese et al. 1989).

Length Distributions

The inverse relationship between weighted mean lengths and larval concentrations may be the result of larval dispersal and growth. Larvae resulting from the late spring/early summer spawning peak (e.g., *E. mordax*, *L. exilis*, *Sebastes* spp., *S. leucopsarus*) should, in conjunction with reduced spawning activity, demonstrate increased mean length as the season progresses. As a consequence, weighted mean length of species with a temporally limited spawning season such as *E. mordax* will progressively increase up to transformation when the early-life stages are no longer planktonic. In contrast, for taxa with more protracted spawning seasons (e.g., *L. exilis*, *Sebastes* spp., *S. leucopsarus*, *T. crenularis*), weighted mean larval lengths will initially increase during the months immediately after the spawning peak then decrease gradually as the older individuals are replaced by fewer, newly spawned larvae. In this respect, a late spring/early summer spawning peak for *T. crenularis* would explain the significant increase in weighted mean length of larvae from a low in June to a high in July/August back to a low in Oct/Nov despite the lack of significant monthly concentration differences (table 6).

The inverse relationship between cross-shelf larval concentrations and weighted mean lengths could result from cross-shelf dispersal during larval growth and development for species with inshore spawning areas. For larval *Sebastes* spp. however, both concentration and weighted mean length were significantly higher in the offshore than coastal region. The occurrence of ~45 different species of the *Sebastes* genus within the NCC (Love et al. 2002), many with different life-history parameters, may contribute to the pattern of variability in cross-shelf concentration and weighted mean length as described by Auth (2009).

Environmental Factors

Local Salinity, temperature, DO saturation, and, to a lesser degree, fluorescence, were the in situ environmental variables with strongest linkage to the distributions and concentrations of the dominant taxa and total larvae in this study. The generally positive relationships between larvae and temperature and DO saturation, and generally negative relationships with salinity and fluorescence, have previously been documented for the NCC (Auth and Brodeur 2006; Auth et al. 2007; Auth 2008; Auth 2009). However, concentrations of *S. leucopsarus* and *T. crenularis* larvae, the only two myctophids represented in the dominant taxa, were also the only taxa positively correlated with fluorescence at 40- and 50-m depth (their respective weighted mean depths), while larval *L. exilis*, a pleuronectid, was negatively (although not significantly) correlated with fluorescence at 40 m. Fluorescence at these depths was on average only 13% and 6%, respectively, of the maximum fluorescence levels recorded at a given station. Although speculative at best, this could be an early environmental cue to the ontogenetic development of the myctophids' bioluminescent photophores in low light, low fluorescence environments within the water column.

The effect of DO concentration and saturation on the distribution, growth, and survival of larval fish is well documented (Breitburg et al. 1999). Most larval taxa are positively related to DO as found in the present study. However, larval *E. mordax* were found to be negatively, although not significantly, related to DO concentration and saturation. This is not surprising since *E. mordax* larvae primarily inhabit the upper 10 m of the water column where DO limitation is not an issue. The significant negative correlation that was found between larval diversity and DO concentration could reflect the increased diversity that was found nearshore, where DO levels may be reduced through organic decomposition or other coastal processes.

Larger-scale The control that water temperature has over the early-life processes of marine fishes is well documented (Houde 2008), as is the influence that the timing and intensity of Columbia River outflow (COL) has on the ichthyoplankton community in the NCC (Parnel et al. 2008). In the present study, COL measured at Bonneville Dam located 235 km upriver from the mouth of the Columbia River and SST measured

from a buoy located 20 nm off the central Oregon coast were the most important larger-scale environmental factors affecting the spring–fall epipelagic ichthyoplankton community in the NCC. The dominance of these factors was fairly consistent for all dominant taxa, total larvae, and larval diversity as shown through both correlation and NPMR analyses (fig. 5, table 10). However, *T. crenularis* larvae were not significantly related to COL, SST, or any other single, or combination of several, larger-scale variables. This is not surprising since this species is distributed farther down in the water column than the other dominant taxa, and is thus less likely to be affected by environmental changes to the surface layer. A particularly interesting finding from this study was that 0–2 month lagged larval concentrations (except for *T. crenularis*) were significantly positively correlated with COL, while those lagged 3–5 months were significantly negatively correlated with COL. This could reflect the positive influence that increased COL—and the increased SST and decreased salinity that accompany higher river outflows—may have on larval survival and the negative influence that COL may have on conditions necessary to maintain healthy gonadal growth in the spawning stock biomass during the months preceding spawning. This is supported by the finding that larvae were generally negatively correlated with in situ salinity and positively correlated with in situ temperature, while negatively correlated when lagged 2–4 behind SST.

Implications for Sampling, Management, and Future Research

The similarity between the taxonomic composition and distribution of the dominant taxa found in this inclusive study to those found in previous studies with varying degrees of temporal and spatial definition suggests that the ichthyoplankton community in the NCC can be adequately described by the current sampling regime. In fact, this study demonstrates that sampling could be reduced to four seasonal collections (i.e., May, June–July, August–September, September–November) and fewer stations within each of three cross-shelf regions (i.e., coastal [<~50 km from shore], offshore [~50–100 km], far-offshore [>~100 km]), and still adequately describe the spring–fall ichthyoplankton community in this area. In addition, the finding that the ichthyoplankton varied similarly in composition, distribution, length, community structure, and relation to environmental variables within years and seasons reflects the robust nature of the larval community within the NCC region. This study has demonstrated that this larval community is influenced by, and can be indicative of, variable local and larger-scale environmental conditions. In particular, fisheries managers may be able to use easily-available indices such as Columbia River outflow and SST measured from a buoy located 20 nm off the central Oregon coast to help predict the spawning success of several dominant taxa 2–4 months in advance. Also, fisheries researchers and managers may be able to incorporate the annual, seasonal, latitudinal, and cross-shelf larval distributions and concentrations, along with the in situ environmental statistics, into fisheries models. Finally, this study will provide a base of information in an attempt to relate the environment and ichthyoplankton to the recruitment of important forage and commercial stocks in the NCC ecosystem in a forthcoming publication.

ACKNOWLEDGMENTS

I thank the captains and crews of the R/V *McArthur II*, R/V *Miller Freeman*, and especially F/V *Piky* for their cooperation and assistance in the sampling. I am indebted to P. Bentley, T. Britt, A. Claiborne, R. Emmett, M. Litz, P. Peterson, A. J. Phillips, and many other scientists and volunteers for their efforts in organizing cruises and collecting data at sea. I also thank the three anonymous reviewers whose critical reviews were instrumental in improving the manuscript. A special thank you goes out to R. Brodeur for his intellectual and material support, and to G. "Tommy Boy" Auth III for always being my light home. Funding was provided by NOAA's Stock Assessment Improvement Program (SAIP), Fisheries and the Environment Initiative (FATE), and Northeast Pacific GLOBEC Program. This is contribution number 705 of the U.S. GLOBEC Program.

LITERATURE CITED

Auth, T. D., and R. D. Brodeur. 2006. Distribution and community structure of ichthyoplankton off the Oregon coast, USA, in 2000 and 2002. Mar. Ecol. Prog. Ser. 319:199–213.

Auth, T. D., R. D. Brodeur, and K. M. Fisher. 2007. Diel variation in vertical distribution of an offshore ichthyoplankton community off the Oregon coast. Fish. Bull. 105:313–326.

Auth, T. D. 2008. Distribution and community structure of ichthyoplankton from the northern and central California Current in May 2004–06. Fish. Oceanogr. 17(4):316–331.

Auth, T. D. 2009. Importance of far-offshore sampling in evaluating the ichthyoplankton community in the northern California Current. Calif. Coop. Oceanic. Fish. Invest. Rep. 50:107–117.

Auth, T. D., R. D. Brodeur, H. L. Soulen, L. Ciannelli, and W. T. Peterson. 2011. The response of fish larvae to decadal changes in environmental forcing factors off the Oregon coast. Fish. Oceanogr. 20(4):314–328.

Bakun, A. 1993. The California Current, Benguela Current, and Southwestern Atlantic Shelf Ecosystems: A Comparative Approach to Identifying Factors Regulating Biomass Yields. *In* Large Marine Ecosystems, Stress, Mitigation and Sustainability, K. Sherman, L. M. Alexander, and B. D. Gold, ed. Washington, DC: American association for the advancement of science, pp. 199–221.

Barth, J. A., B. A. Menge, J. Lubchenco, F. Chan, J. M. Bane, A. R. Kirincich, M. A. McManus, K. J. Nielsen, S. D. Pierce, and L. Washburn. 2007. Delayed upwelling alters nearshore coastal ocean ecosystems in the northern California current. Proc. Natl. Acad. Sci. 104:3719–3724.

Beaugrand, G., K. M. Brander, J. A. Lindley, S. Souissi, and P. C. Reid. 2003. Plankton effect on cod recruitment in the North Sea. Nature. 426:661–664.

Boehlert, G. W., D. M. Gadomski, and B. C. Mundy. 1985. Vertical distribution of ichthyoplankton off the Oregon coast in spring and summer months. Fish. Bull. 83:611–621.

Breitburg, D. L., K. A. Rose, and J. H. Cowan, Jr. 1999. Linking water quality to larval survival: predation mortality of fish larvae in an oxygen-stratified water column. Mar. Ecol. Prog. Ser. 178:39–54.

Brodeur, R. D., D. M. Gadomski, W. G. Pearcy, H. P. Batchelder, and C. B. Miller. 1985. Abundance and distribution of ichthyoplankton in the upwelling zone off Oregon during anomalous El Niño conditions. Est. Coast. Shelf Sci. 21:365–378.

Brodeur, R. D., S. Ralston, R. L. Emmett, M. Trudel, T. D. Auth, and A. J. Phillips. 2006. Anomalous pelagic nekton abundance, distribution, and apparent recruitment in the northern California Current in 2004 and 2005. Geophys. Res. Lett. 33:L22S08. doi:10.1029/2006GL026614.

Brodeur, R. D., W. T. Peterson, T. D. Auth, H. L. Soulen, M. M. Parnel, and A. A. Emerson. 2008. Abundance and diversity of coastal fish larvae as indicators of recent changes in ocean and climate conditions in the Oregon upwelling zone. Mar. Ecol. Prog. Ser. 366:187–202.

Checkley, D. M. Jr., and J. A. Barth. 2009. Patterns and processes in the California Current system. Prog. Oceanogr. 83:49–64.

Clarke, K. R., and R. M. Warwick. 2001. Change in Marine Communities: An Approach to Statistical Analysis and Interpretation. 2nd ed. Plymouth, UK: PRIMER-E. 172 pp.

Clarke, K. R., and R. N. Gorley. 2006. PRIMER, Version 6.1.7, User Manual/Tutorial. Plymouth, UK: PRIMER-E. 91 pp.

Doyle, M. J. 1992. Patterns in distribution and abundance of ichthyoplankton off Washington, Oregon, and northern California (1980–1987). Alaska Fisheries Science Center Processed Report. 92-14:1–344.

Doyle, M. J., W. W. Morse, and A. W. Kendall, Jr. 1993. A comparison of larval fish assemblages in the temperate zone of the northeast Pacific and northwest Atlantic oceans. Bull. Mar. Sci. 53:588–644.

Doyle, M. J. 1995. The El Niño of 1983 as reflected in the ichthyoplankton off Washington, Oregon, and northern California. Can. Spec. Publ. Fish. Aquat. Sci. 121:161–180.

Doyle, M. J., S. J. Picquelle, K. L. Mier, M. C. Spillane, and N. C. Bond. 2009. Larval fish abundance and physical forcing in the Gulf of Alaska, 1981–2003. Prog. Oceanogr. 80:163–187.

Dufrêne, M., and P. Legendre. 1997. Species assemblages and indicator species: the need for a flexible asymmetrical approach. Ecol. Monogr. 67:345–366.

Emmett, R. L., R. D. Brodeur, T. W. Miller, S. S. Pool, P. J. Bentley, G. K. Krutzikowsky, and J. McCrae. 2005. Pacific sardine (*Sardinops sagax*) abundance, distribution and ecological relationships in the Pacific Northwest. Calif. Coop. Oceanic. Fish. Invest. Rep. 46:122–143.

Field, J. G., K. R. Clarke, and R. M. Warwick. 1982. A practical strategy for analyzing multispecies distribution patterns. Mar. Ecol. Prog. Ser. 8:37–52.

Fréon, P., J. Arístegui, A. Bertrand, R. J. M. Crawford, J. C. Field, M. J. Gibbons, J. Tam, L. Hutchings, H. Masski, C. Mullon, M. Ramdani, B. Seret, and M. Simier. 2009. Functional group biodiversity in eastern boundary upwelling ecosystems questions the wasp-waist trophic structure. Prog. Oceanogr. 83:97–106.

Gómez-Gutiérrez, J., W. T. Peterson, and C. B. Miller. 2005. Cross-shelf life-stage segregation of the euphausiids off central Oregon (1970–1972). Deep-Sea Res. Part II. 52:289–315.

Houde, E. D. 2008. Emerging from Hjort's shadow. J. Northwest Atl. Fish. Sci. 41:53–70.

Hsieh, H.-Y., W.-T. Lo, D.-C. Liu, P.-K. Hsu, and W.-C. Su. 2007. Winter spatial distribution of fish larvae assemblages relative to the hydrography of the waters surrounding Taiwan. Environ. Biol. Fish. 78:333–346.

Keister, J. E., and W. T. Peterson. 2003. Zonal and seasonal variations in zooplankton community structure off the central Oregon coast, 1998–2000. Prog. Oceanogr. 57:341–361.

Love, M. S., M. Yoklavich, and L. Thorsteinson. 2002. The rockfishes of the northeast Pacific. Los Angeles, California: University of California Press. 404 pp.

Matarese, A. C., A. W. Kendall, Jr., and B. M. Vinter. 1989. Laboratory guide to early life history stages of northeastern Pacific fishes. NOAA Tech. Rep. 80:1–625.

McCune, B., and M. J. Mefford. 1999. PC-Ord, Multivariate Analysis of Ecological Data, Users Guide. Gleneden Beach, Oregon: MjM Software. 237 pp.

McCune, B. 2006. Non-parametric habitat models with automatic interactions. J. Veget. Sci. 17:819–830.

McCune, B., and M. J. Mefford. 2006. PC-Ord, Multivariate Analysis of Ecological Data, Version 5. Gleneden Beach, Oregon: MjM Software.

McCune, B., and M. J. Mefford. 2009. HyperNiche, Version 2.0. Gleneden Beach, Oregon: MjM Software.

Mundy, B. C. 1984. Yearly variation in the abundance and distribution of fish larvae in the coastal upwelling zone off Yaquina Head, OR, from June 1969–August 1972. M.S. Thesis, Oregon State University, Corvallis, Oregon. 158 pp.

Parnel, M. M., R. L. Emmett, and R. D. Brodeur. 2008. Ichthyoplankton community in the Columbia River plume off Oregon: effects of fluctuating oceanographic conditions. Fish. Bull. 106:161–173.

Pearcy, W. G., D. L. Stein, M. A. Hixon, E. K. Pikitch, W. H. Barss, and R. M. Starr. 1989. Submersible observations of deep-reef fishes of Heceta Bank, Oregon. Fish. Bull. 87:955–965.

Phillips, A. J., S. Ralston, R. D. Brodeur, T. D. Auth, C. Johnson, R. L. Emmett, and V. G. Wespestad. 2007. Recent pre-recruit Pacific hake (*Merluccius productus*) occurrences in the northern California Current suggest a northward expansion of their spawning area. Calif. Coop. Oceanic. Fish. Invest. Rep. 48:215–229.

Richardson, S. L. 1973. Abundance and distribution of larval fishes in waters off Oregon, May–October 1969, with special emphasis on the northern anchovy, *Engraulis mordax*. Fish. Bull. 71:697–711.

Richardson, S. L., and W. G. Pearcy. 1977. Coastal and oceanic larvae in an area of upwelling off Yaquina Bay, Oregon. Fish. Bull. 75:125–145.

Richardson, S. L., J. L. Laroche, and M. D. Richardson. 1980. Larval fish assemblages and associations in the north-east Pacific Ocean along the Oregon coast, winter–spring 1972–1975. Est. Coast. Mar. Sci. 11:671–699.

SAS Institute, Inc. 2007. JMP, User Guide, Release 7. Cary, North Carolina: SAS Institute, Inc. 487 pp.

Schwing, F. B., N. A. Bond, S. J. Bograd, T. Mitchell, M. A. Alexander, and N. Mantua. 2006. Delayed coastal upwelling along the U.S. West Coast in 2005: An historical perspective. Geophys. Res. Lett. 33:doi:10.1029/2006GL026911.

Shannon, C. E., and W. Weaver. 1949. The Mathematical Theory of Communication. Urbana, Illinois: University of Illinois Press. 117 pp.

Stein, D. L., B. N. Tissot, M. A. Hixon, and W. Barss. 1992. Fish-habitat associations on a deep reef at the edge of the Oregon continental shelf. Fish. Bull. 90:540–551.

Suntsov, A. V. 2000. Ichthyoplankton assemblages off the coast of Peru during the initial stage of El Niño 1987. J. Ichthyol. 40 (suppl.1):139–151.

Waldron, K. D. 1972. Fish larvae collected from the northeastern Pacific Ocean and Puget Sound during April and May 1967. NOAA Tech. Rep. SSRF-663:1–16.

APPENDIX

Descriptive statistics (mean, standard error [SE], median, upper and lower 95% confidence intervals [CIs], range [minimum-maximum values], and sample size [*n*]) for seven environmental variables for each of the five dominant larval fish taxa and total larvae (weighted based on concentration) collected during this study: temperature (°C), salinity, density (sigma theta, kg m^{-3}), fluorescence (mg m^{-3}), turbidity (mg m^{-3}), dissolved oxygen concentration (DO, ml L^{-1}), and DO saturation (%). Samples containing no larvae were excluded. Values for the environmental variables used in the analysis were taken from different depths in the water column at each station corresponding to the weighted mean depth for each taxon as reported in previous studies: *E. mordax*: 10-m depth; *Sebastes* spp. and total larvae: 20-m depth; *L. exilis* and *S. leucopsarus*: 40-m depth; *T. crenularis*: 50-m depth.

	Temperature	Salinity	Density	Fluorescence	Turbidity	DO	DO saturation
Engraulis mordax							
Mean	15.0	31.4	23.2	0.24	0.40	5.6	94.9
SE	0.1	0.07	0.07	0.02	0.009	0.03	0.4
Median	14.8	31.6	23.4	0.15	0.38	5.5	95.6
Upper 95% CI	15.2	31.5	23.3	0.28	0.41	5.6	95.8
Lower 95% CI	14.8	31.2	23.0	0.20	0.38	5.5	94.1
Range	8.3-18.5	28.9-33.3	20.9-25.9	0.004-2.73	0.20-1.48	5.2-6.6	90.2-109.6
n	107	107	107	100	100	37	37
Lyopsetta exilis							
Mean	8.8	32.7	25.3	0.25	0.37	5.0	74.6
SE	0.09	0.04	0.04	0.03	0.006	0.2	2.7
Median	8.7	32.5	25.2	0.16	0.36	5.5	82.2
Upper 95% CI	8.9	32.7	25.4	0.30	0.38	5.3	80.0
Lower 95% CI	8.6	32.6	25.3	0.20	0.36	4.6	69.2
Range	7.3-11.8	32.2-33.9	24.7-26.5	0-1.73	0.18-0.54	2.1-6.3	31.1-98.1
n	112	101	101	98	98	48	48
Sebastes spp.							
Mean	11.0	32.1	24.5	0.47	0.42	6.0	94.3
SE	0.1	0.02	0.03	0.03	0.006	0.05	0.9
Median	10.9	32.3	24.6	0.46	0.42	5.9	94.2
Upper 95% CI	11.2	32.1	24.6	0.52	0.43	6.1	96.0
Lower 95% CI	10.8	32.0	24.2	0.42	0.41	5.9	92.6
Range	7.4-18.0	30.6-33.7	22.3-26.3	0.01-6.25	0.19-1.21	1.6-6.9	24.2-109.7
n	295	283	272	254	252	114	114
Stenobrachius leucopsarus							
Mean	9.6	32.5	25.1	0.39	0.35	5.9	90.1
SE	0.07	0.008	0.01	0.02	0.005	0.04	0.7
Median	9.3	32.5	25.1	0.21	0.36	5.9	88.7
Upper 95% CI	9.7	32.5	25.1	0.44	0.36	6.0	91.5
Lower 95% CI	9.5	32.5	25.0	0.34	0.34	5.8	88.8
Range	7.3-11.8	32.2-33.6	24.6-26.1	0-1.91	0.19-0.61	3.5-6.6	52.1-101.7
n	214	202	199	194	194	91	91
Tarletonbeania crenularis							
Mean	9.1	32.6	25.2	0.27	0.33	5.6	84.7
SE	0.07	0.02	0.02	0.03	0.006	0.08	1.2
Median	9.0	32.6	25.2	0.12	0.33	5.7	85.2
Upper 95% CI	9.3	32.6	25.3	0.33	0.35	5.8	87.2
Lower 95% CI	9.0	32.6	25.2	0.21	0.32	5.5	82.2
Range	7.3-12.9	32.3-33.8	24.4-26.4	0-2.19	0.18-0.59	1.6-6.4	23.5-96.6
n	168	158	152	145	144	66	66
Total larvae							
Mean	11.7	32.1	24.3	0.52	0.42	6.0	96.6
SE	0.1	0.03	0.03	0.03	0.005	0.04	0.6
Median	10.8	32.3	24.7	0.46	0.42	5.8	93.5
Upper 95% CI	11.9	32.1	24.4	0.59	0.43	6.1	97.5
Lower 95% CI	11.5	32.0	24.3	0.45	0.40	6.0	95.2
Range	7.4-18.0	30.6-33.7	22.3-26.3	0-6.91	0.19-1.21	1.6-7.2	24.2-111.4
n	389	374	360	338	336	151	151

THE FISH ASSEMBLAGES FROM THE NEARSHORE AREA OF PUNTA BAJA, B.C., MÉXICO, THE SOUTHERN LIMIT OF THE SOUTHERN CALIFORNIA BIGHT

JORGE A. ROSALES-CASIÁN
Departamento de Ecología Marina
Centro de Investigación Científica y de Educación Superior de Ensenada, B.C.
(CICESE)
Carretera Ensenada-Tijuana #3918, Zona Playitas, C.P. 22860, Ensenada, B.C., México
Phone: (646) 175-0500
Fax: (646) 175-0545
jrosales@cicese.mx

ABSTRACT

The area off Punta Baja, Baja California, Mexico, is an important coastal fishing ground. The nearshore fishes were sampled on a seasonal basis over a period of three years, from spring 2000 to winter 2003. Beam-trawl and otter trawl were towed along 5 m and 10 m depth contours; a gill net was placed between the 5–10 m depth. Low temperatures were registered from 10.8 to 15.4°C (mean = 13.5°C ± 0.2 SE). A total of 3,509 fish individuals were collected belonging to 62 fish species. The most abundant and important fish species (ICI: index of community importance composite) by the contribution of the three sampling gears was the white croaker (*Genyonemus lineatus*). Separately, the most important species varied with sampling gears, depths, years, and were the bay pipefish (*Syngnathus leptorhynchus*), the walleye surfperch (*Hyperprosopon argenteum*), the Pacific sanddab (*Citharichthys sordidus*), and *G. lineatus.* Fish abundances showed differences between seasons in all sampling gears and depths. Positive correlations between fish abundances collected with otter trawl (5 and 10 m depth) and temperature were found. The fish community of the Punta Baja area was characterized by species associated with *Macrocystis* sp. beds, sandy bottom, and deeper species like scorpaenids, all typical species from the Southern California Bight. This data represents a baseline against which any future development affecting local ecosystems can be measured.

INTRODUCTION

Temperate waters vary more seasonally than tropical waters. Upwellings along the coast of California and the Pacific Northwest are areas often with extremely cool surface waters (DeMartini and Sikkel 2006). These cold water regions are produced by the effects of ocean circulation and local wind patterns (Álvarez- Borrego 2004).

The coastal waters of Baja California are also characterized by upwellings, often associated with rocky points. These appear to be seasonally strongest in the southern region (Punta Baja to Punta Eugenia) from March to June (Bakun and Nelson 1977). Within these areas of local upwelling, there exist disjunct distributions for certain marine forms, including fishes, which are characteristic of more northern, cool temperate waters (Hubbs 1948; Emerson 1956).

Many fish species are shared between the coastal waters of California and Baja California. California's inshore fishes are separated into two faunal provinces: the northern cool temperate (Oregonian) which extends well into British Columbia to the north and terminates near Point Conception to the south; and the San Diegan warm temperate province to the south which extends south to Bahía Magdalena, Baja California Sur, México (Horn et al. 2006). Some of the latter species have their principle spawning areas off Baja California and these centers may serve as a source of eggs, larvae or YOY for California waters (Moser et al. 1993). The larvae of nearshore fish species may experience southward flow during upwelling and northward flow during relaxation events (Shanks and Eckert 2005). Presently, however, there is little available information on the coastal fish assemblages between Bahía de San Quintín, Baja California and Bahía Magdalena, Baja California Sur, México (Rosales-Casián 2004).

Punta Baja, located 390 km south of the U.S.-Mexico border, and 61 km south of San Quintín, is an important area within this little documented region. Punta Baja is a rocky headland that protects Bahía El Rosario from the wind-generated high waves. Strong upwelling is present the entire year, and the cold upwelled water generated by these winds is transported southwards into the interior of the bay (Amador-Buenrostro et al. 1995). Punta Baja is a departure site for coastal commercial fishing on the northwestern coast of Baja California, which ranks second after San Quintín, and the fishery includes ocean whitefish (*Caulolatilus princeps*), the California sheephead (*Semicossyphus pulcher*), kelp bass (*Paralabrax clathratus*), California halibut (*Paralichthys californicus*), and the rockfish species of the genus *Sebastes* (Rosales-Casián and Gonzalez-Camacho 2003).

Upwelling regions with their burgeoning planktonic resource base are sites of major fisheries worldwide. Bays and lagoons are important fish habitats which often support spawning and nursery sites as well as abundant adult populations (Allen et al. 2006). Commonly, there are major fisheries associated with upwelling regions that

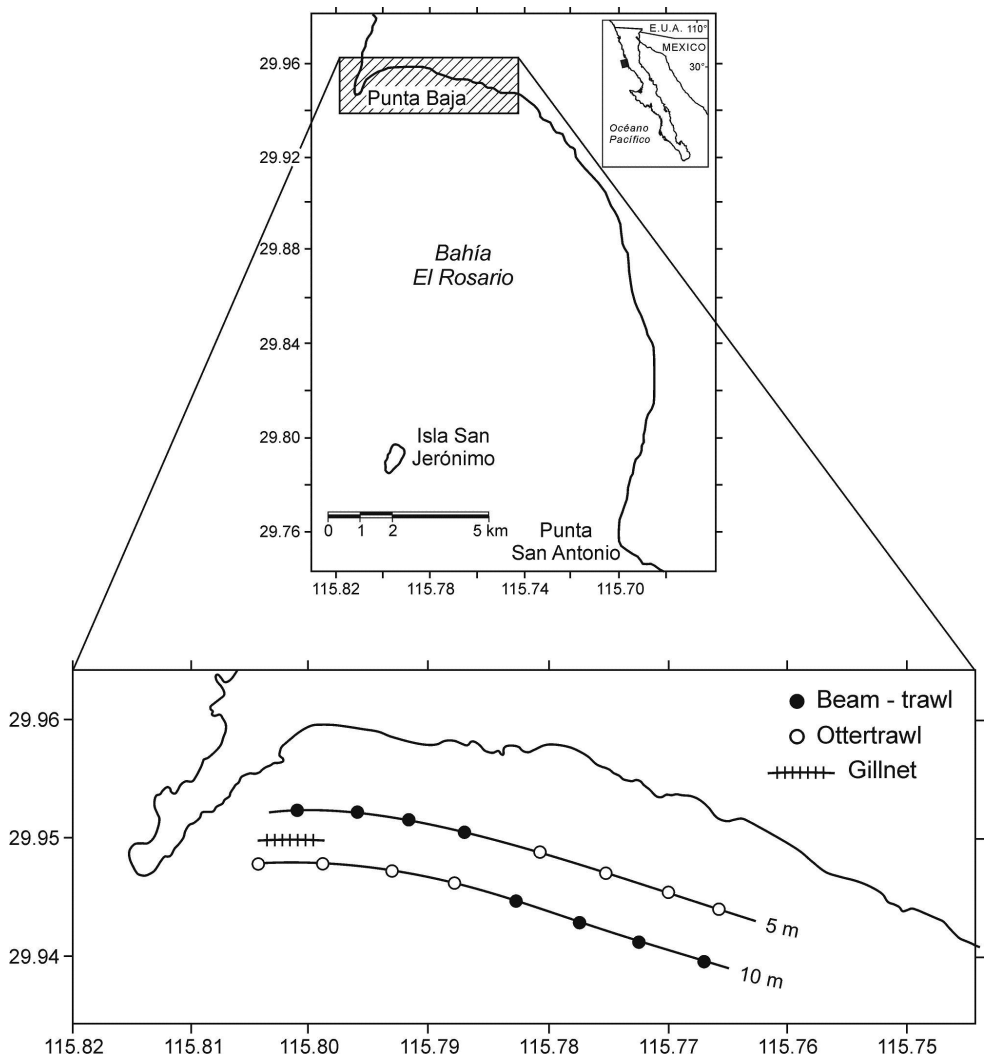

Figure 1. Localization of the study site and sampling stations in the area of Punta Baja, Baja California, México.

thrive on abundant resources. The community structure in these ecosystems is sensitive to climate variability and change, whose fluctuations in fish numbers impact both higher and lower trophic levels (Anderson and Lucas 2008). The area around Punta Baja today is an almost pristine and underdeveloped coastal region, though the threat of development in such a coastal site persists. The purpose of this study was to prepare a baseline of the area's fish assemblage and its relationship to those of adjacent and better understood sites to the north. Such a baseline is important prior to possible development or other environmental changes such as those related to global warming.

METHODS

Study Area

Punta Baja, Baja California (29°57.28'N, 115°48.09'W) is situated at 390 km south of the Baja California (México)-California (USA) border, accessed by 16 km of dirt road southwest from the town of El Rosario (fig. 1). Punta Baja is the north limit of Bahía El Rosario and Punta San Antonio the south limit (24.5 km); toward the middle of the bay is Agua Blanca fish camp (8 km south), and other important sites are Isla San Jerónimo and the Sacramento Reef at the south part of the bay (fig. 1).

Sampling Methods

The semiprotected area was sampled on a seasonal basis from spring 2000 (April 1, 2000) to winter 2003 (March 7, 2003). For the samplings, a 5 or 6 m boat with outboard motor was used. The beam trawl and otter trawl were used to capture small or slow moving fishes, and a gill net was used to capture relatively bigger and faster swimming fishes (Kramer 1990; Rosales-Casián 2004).

A variable mesh monofilament gill net (30 × 2.5 m) was placed close to a *Macrocystis* sp. bed (5–10 m depth) at the beginning of sampling and recovered at the end,

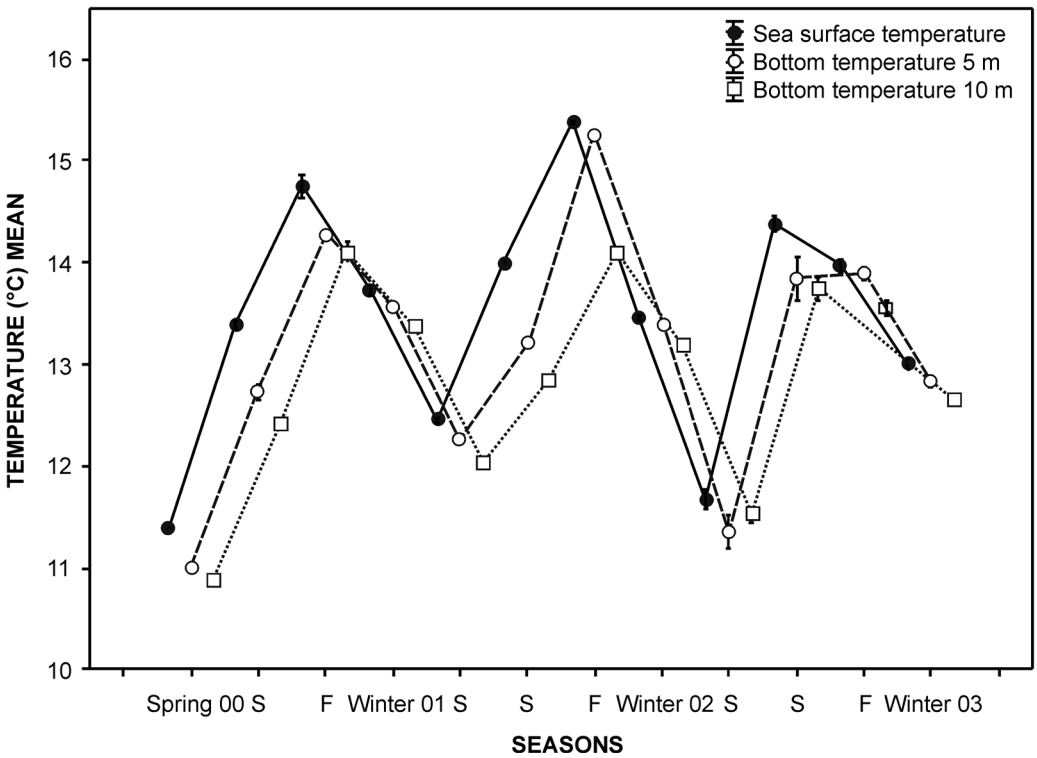

Figure 2. Temperature (°C) means distribution in the area of Punta Baja, Baja California, México (2000–2003).

for a time of six hours (07:30–13:30 hr). Four replicated 5 min tows with a 1.6 m beam trawl (horizontal 1.6 m, vertical 0.343 m opening, and 3 mm mesh size), and a 7.5 m otter trawl (10 m length with 19 mm mesh in body and 5 mm in bag end) were made at a speed of approximately 1.5 and 2.0 knots, respectively; the sampling was carried out along the 5 and 10 m depth contours, and parallel to shore. At each trawl, seawater temperature (°C) was measured at the surface and near-bottom.

Fish Identification and Measurements

All collected fishes were identified, counted, measured (standard and total length) to nearest millimeter, and weighed. Biomass was recorded to ±0.1 g for fishes weighing up to 150 g, and to ±1.0 g for those with greater weights. Identification of most species was based on Miller and Lea (1972). Rays were identified, measured, weighed, and released alive in situ.

Data Analysis

The annual total abundance (all species combined), total numbers per species, relative abundances, and frequencies of occurrence were computed by depth, sampling gear, and seasons. The gill net catch was grouped on a three-month basis to configure with the four seasons.

The data of fish abundance collected with beam trawl at 5 m depth, and with otter trawl at 5 and 10 m depths were not found to be distributed normally (Kolmogorov-Smirnoff test; KS = 0.1849, 0.1427 and 0.1695, p = 0.100, 0.200, and 0.150, respectively). Therefore, seasonal means of abundance were adjusted using a log(x+1) transformation to ensure that values were or approximated a normal distribution. To determine changes in abundances with time, a one-way ANOVA was performed on the log(x+1) transformed abundance data. To measure the degree of association between temperature (bottom and surface) and fish abundance, the Spearman correlation was used (Zar 1984).

To estimate the community contribution of each species, the Index of Community Importance (ICI) was used (Stephens and Zerba 1981; Love et al. 1986; Rosales-Casián 1997; Rosales-Casián 2004). The species were ranked by percentage of abundance as well as in percentage of frequency of occurrence, and the sum of the two ranks were the respective value of ICI for each species.

RESULTS

The overall mean of sea surface temperature at Bahía El Rosario during 2000–2003 was 13.5°C (± 0.2 SE: standard error). At 5 m and 10 m depths the mean temperatures were 13.1°C (± 0.2 SE), and 12.9°C (± 0.1 SE), respectively. Low temperatures were present in all spring seasons (fig. 2), the lowest (10.8°C) in spring 2000 and at all depths: surface (mean = 11.4°C ± 0.0 SE), 5 m

TABLE 1
Composition of trawl catches ranked by numerical, relative and cumulative abundances in the area of Punta Baja, Baja California, México, from April 2000 to March 2004.

Fish species	No	% Rel	% Cum
Genyonemus lineatus	658	18.75	18.75
Hyperprosopon argenteum	433	12.34	31.09
Engraulis mordax	301	8.58	39.67
Micrometrus minimus	250	7.12	46.79
Seriphus politus	247	7.04	53.83
Citharichthys sordidus	228	6.50	60.33
Syngnathus leptorhynchus	225	6.41	66.74
Embiotoca jacksoni	143	4.08	70.82
Citharichthys stigmaeus	128	3.65	74.47
Phanerodon furcatus	125	3.56	78.03
Amphistichus argenteus	113	3.22	81.25
Gibbonsia elegans	90	2.56	83.81
Cymatogaster aggregata	78	2.22	86.04
Sardinops sagax	67	1.91	87.95
Aulorhynchus flavidus	56	1.60	89.54
Synodus lucioceps	54	1.54	91.08
Heterostichus rostratus	45	1.28	92.36
Syngnathus californiensis	39	1.11	93.47
Scomber japonicus	32	0.91	94.39
Atherinops californiensis	25	0.71	95.10
Umbrina roncador	23	0.66	95.75
Gibbonsia metzi	18	0.51	96.27
Paralichthys californicus	13	0.37	96.64
Rhacochilus toxotes	10	0.28	96.92
Oxyjulis californica	8	0.23	97.15
Rhacochilus vacca	8	0.23	97.38
Sebastes rastrelliger	7	0.20	97.58
Sebastes sp.	6	0.17	97.75
Sebastes auriculatus	6	0.17	97.92
Pleuronichthys guttulatus	6	0.17	98.09
Sebastes paucispinis	5	0.14	98.23
Scorpaenichthys marmoratus	5	0.14	98.38
Cheilotrema saturnum	5	0.14	98.52
Hexagrammos superciliosus	4	0.11	98.63
Platyrhinoidis triseriata	4	0.11	98.75
Pleuronichthys verticalis	3	0.09	98.83
Paralabrax nebulifer	3	0.09	98.92
Artedius lateralis	2	0.06	98.97
Amphistichus rhodoterus	2	0.06	99.03
Strongylura exilis	2	0.06	99.09
Amphistichus koelzi	2	0.06	99.15
Apodichthys flavidus	2	0.06	99.20
Brachyistius frenatus	2	0.06	99.26
Ulvicola sanctaerosae	2	0.06	99.32
Ophidion scrippsae	2	0.06	99.37
Xystreurys liolepis	2	0.06	99.43
Scorpaena guttata	2	0.06	99.49
Girella nigricans	2	0.06	99.54
Leuresthes tenuis	2	0.06	99.60
Gibbonsia montereyensis	2	0.06	99.66
Paralabrax maculatofasciatus	1	0.03	99.66
Odontopyxis trispinosa	1	0.03	99.72
Chirolophis nugator	1	0.03	99.74
Peprilus semillimus	1	0.03	99.77
Raja binoculata	1	0.03	99.80
Heterodontus francisci	1	0.03	99.83
Trachurus symmetricus	1	0.03	99.86
Menticirrhus undulatus	1	0.03	99.89
Sebastes carnatus	1	0.03	99.91
Paralabrax clathratus	1	0.03	99.94
Leptocottus armatus	1	0.03	99.97
Atherinops affinis	1	0.03	100.00
Total	3509	100.0	

depth (11.0°C ± 0.0 SE), and 10 m depth (10.9°C ± 0.05 SE). High temperatures were present in fall 2000, 2001, and summer 2002 (fig. 2). The highest mean temperatures were recorded during fall 2001 at all depths: surface: 15.4°C (± 0.03 SE), 5 m-depth: 15.3°C (± 0.03 SE), and 10 m depth: 14.1°C (± 0.0 SE) (fig. 2).

A total of 3,509 individuals were collected belonging to 62 fish species (table 1). The most abundant species were the white croaker, *Genyonemus lineatus* (18.8%), the walleye surfperch, *Hyperprosopon argenteum* (12.3%), the northern anchovy, *Engraulis mordax* (8.6%), the dwarf surfperch, *Micrometrus minimus* (7.1%), and the bay pipefish, *Syngnathus leptorhynchus* (7%). Sixteen fish species accounted for 91% of the total abundance, and the other species contributed 1.3% per species or less (table 1).

At 5 m depth, a total of 458 fishes were collected with beam-trawl tows, with an overall mean of 9.2 fish/tow (± 1.2 SE: standard error). The highest mean catch was 21.8 fish/tow (± 3.1 SE) during winter 2001, and the lowest was 2.3 fish/tow (± 0.8 SE) during spring 2002 (fig. 3). At 10 m depth, the total number of fish collected was 531 individuals, and with an overall mean abundance of 11.1 fish/tow (± 1.9 SE); the highest mean abundance (46.5 fish/tow ± 3.9 SE) was seen in spring 2000, with the lowest of 2.8 fish/tow (± 0.8 SE) in spring 2002 (fig. 3). Significant differences in the mean abundances between seasons at 5 m depth (ANOVA, $F = 3.775$, $p = 0.001$), and 10 m depth (ANOVA, $F = 13.684$, $p = 0.000$) were found.

No correlations were found between the fish abundance collected by beam-trawl tows at 5 m, with temperature from surface, 5 m and 10 m bottom ($R = 0.0645, 0.1677, 0.1579$; $p = 0.662, 0.254$, and 0.283, respectively). Fish abundance at 10 m depth was also not correlated with temperature (Spearman $R = –0.154, –0.077, –0.161$; $p = 0.299, 0.605$ and 0.273, respectively).

With otter-trawl tows (5 m depth), the total catch was 1,013 fishes with an overall mean catch of 21.1 fish/tow (± 2.5 SE). The highest mean was present in summer 2002 with 42.3 fish/tow (± 17.1 SE), and the lowest in spring 2002 (4.3 fish/tow, ± 0.5 SE) in June (fig. 4). The total catch of the otter trawl at 10 m depth was 820 fishes, with an overall mean catch of 16.3 fish/tow (± 2.2 SE); the highest mean catch was in winter 2002 (35.3 fish/tow, ± 14.2 SE), and the lowest (2.8 fish/tow, ± 0.5 SE) in summer 2000 (fig. 4). Significant differences in the mean abundances at 5 m depth between seasons (ANOVA, $F = 4.200$, $p = 0.001$), and at 10 m depth (ANOVA, $F = 4.726$, $p = 0.000$) were found.

Significant correlations of the otter trawl fish abundances (5 m depth) with the surface temperature, 5 m bottom and 10 m bottom temperatures (Spearman $R = 0.492$, $p = 0.004$; $R = 0.530$, $p = 0.000$; $R = 0.536$, $p =$

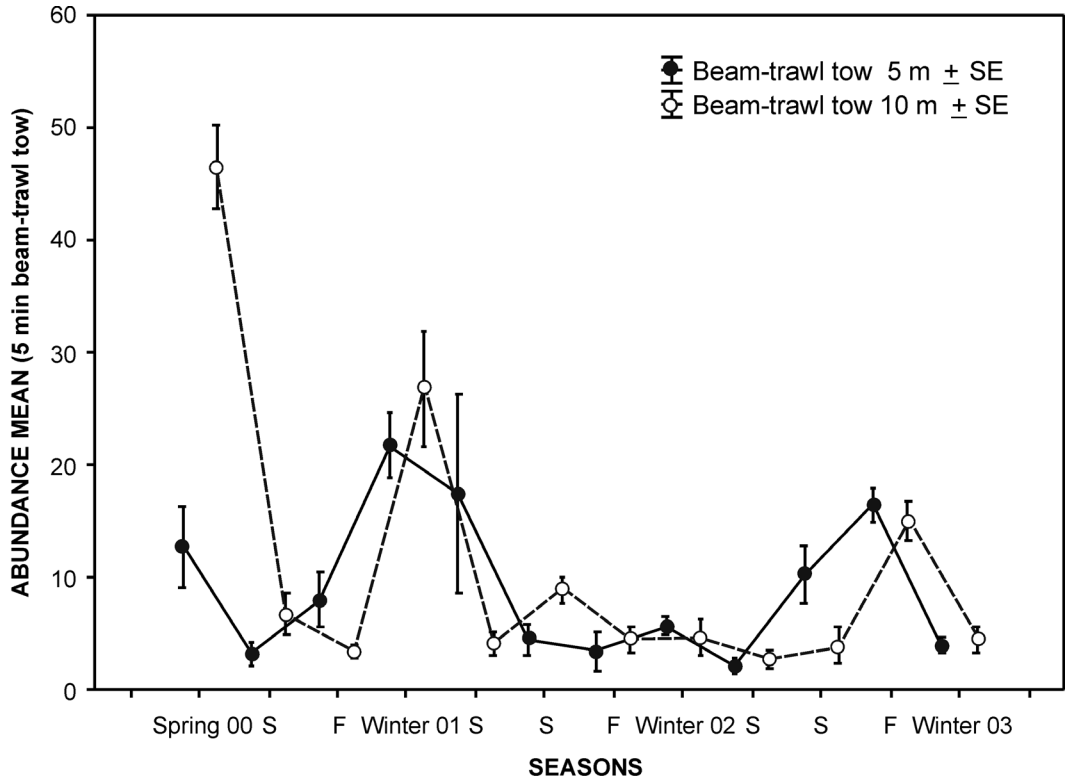

Figure 3. Abundance means of beam-trawl tows (5 and 10 m depth) in the area of Punta Baja, Baja California, México.

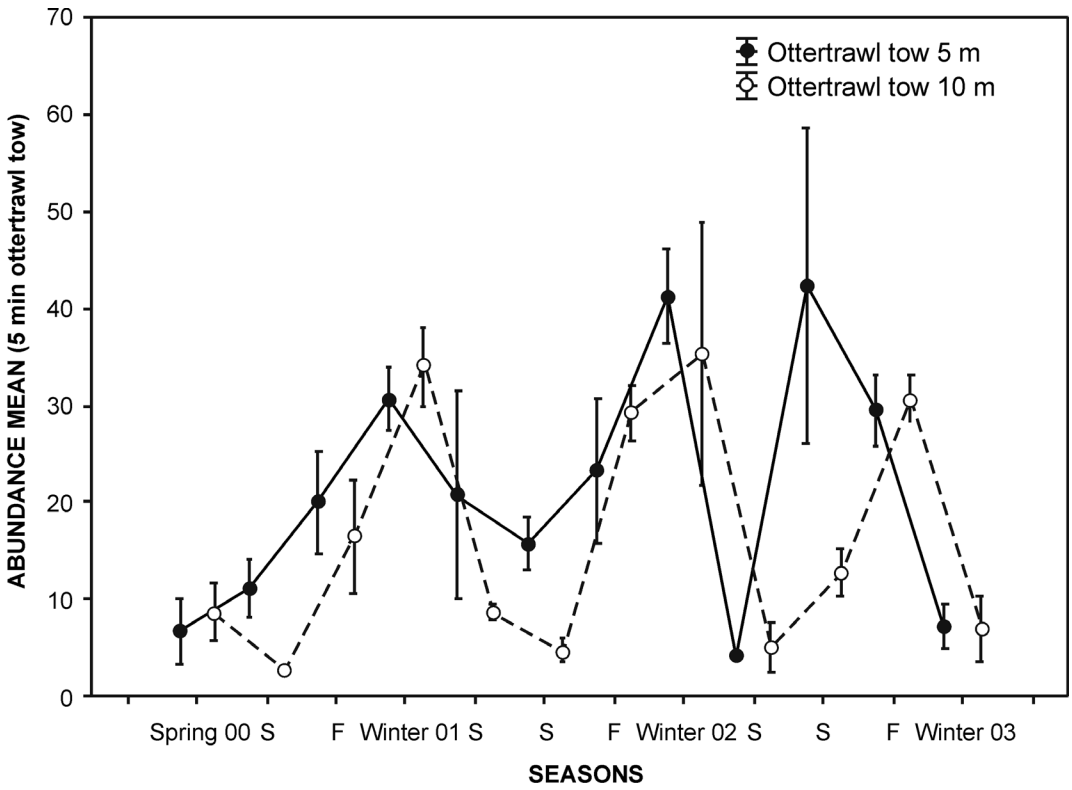

Figure 4. Abundance means of otter-trawl tows (5 and 10 m depth) in the area of Punta Baja, Baja California, México.

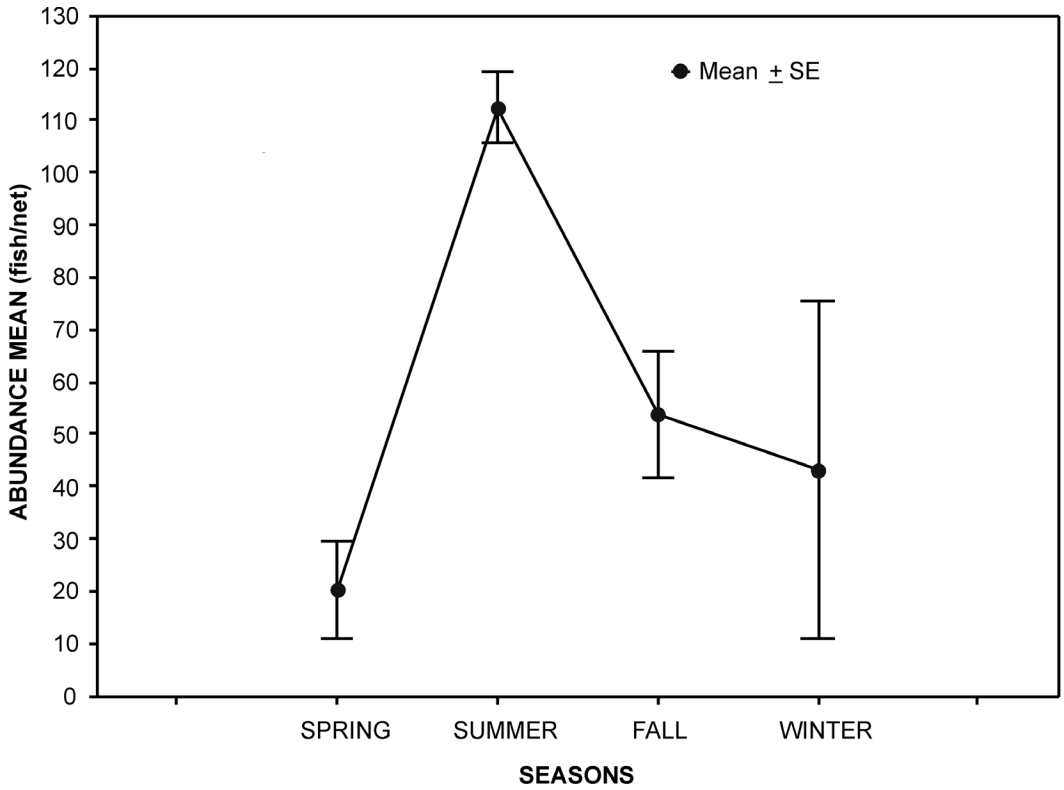

Figure 5. Abundance means of gill net catch in the area of Punta Baja, Baja California, México.

0.000, respectively) were found. At 10 m depth, the fish abundances in otter trawls were also significantly correlated with the surface temperature, and with 5 m depth and 10 m depth temperatures (Spearman R = 0.414, p = 0.003; R = 0.558, p = 0.000; R = 0.537, p = 0.000, respectively).

An interannual (2000–2001, 2001–2002, and 2002–2003) comparison of the abundances collected with beam trawl at 5 m depth, and otter trawl at 5 m and 10 m depths were not significant (ANOVA, F = 1.146, p = 0.326: F = 1.161, p = 322; F = 0.278, p = 0.758, respectively); the three-year abundances for the beam trawl at 5 m depth and the otter trawl (5 m and 10 m depths) were grouped together. The interannual comparison of abundances detected differences in the beam trawl abundances only at 10 m depth (ANOVA, F = 6.080, p = 0.004), and the Index of Community Importance (ICI) was determined separately by year.

The overall mean of the gill net catch was 57.3 fish/net (± 13.1 SE). The seasonal abundance of the gill net catch showed that the lowest mean abundance was present during spring (20 fish/net ± 20.8 SE), followed by the greatest increase in summer (112.3 fish/net ± 7.2 SE), and the number declined in fall and winter (fig. 5). The analysis of variance detected significant differences between the seasonal mean abundances (ANOVA, F = 172.086, p = 0.000). The fish abundance collected by gill net was not correlated with temperatures from surface, 5 m bottom, or 10 m bottom (Spearman R = –0.1049, –0.1049, –0.1156, p > 0.05, respectively).

A total of 458 individuals belonging to 24 fish species were collected with beam-trawl tows at 5 m depth (table 2). The most abundant species were the white croaker (*G. lineatus*, 26.4 %), the bay pipefish (*S. leptorhynchus*, 14.2 %), and the walleye surfperch (*H. argenteum*, 12.9 %). In frequency, the bay pipefish occurred in 66.7 % of the tows, followed by the dwarf surfperch (*M. minimus*, 41.7 %), and the spotted kelpfish (*Gibbonsia elegans*, 37.5 %). The order of most important fish species by the ICI were the bay pipefish, the white croaker, the dwarf surfperch, the walleye surfperch, and the spotted kelpfish (table 2).

With respect to the otter-trawl tows at 5 m depth during the complete study, the total number captured was 1,013 fishes belonging to 37 species (table 3). The walleye surfperch, *H. argenteum*, contributed the highest abundance (17.5%), the northern anchovy, *E. mordax* in second place with 10.4%, and the queenfish, *S. politus* in third (9.4%). The fish species with the highest frequency of occurrence was *E. jacksoni* that was present in 54.2% of the samples, followed by *S. leptorhynchus* (52.1%), and *H. argenteum* with 47.9% (table 3). The order in species importance (ICI rank) was the walleye surfperch (*H. argenteum*), the bay pipefish (*S. leptorhynchus*), the dwarf

TABLE 2
Fish species composition and Index of Community Importance (ICI) by the beam-trawl tows (5 m depth) in the area of Punta Baja, B.C., México (2000–2003).

Fish Species	Number	% Relative	Rank 1	% FO	Rank 2	ICI
Syngnathus leptorhynchus	65	14.2	2	66.7	1	3
Genyonemus lineatus	121	26.4	1	29.2	4.5	5.5
Micrometrus minimus	45	9.8	4	41.7	2	6
Hyperprosopon argenteum	59	12.9	3	29.2	4.5	7.5
Gibbonsia elegans	28	6.1	6	37.5	3	9
Citharichthys sordidus	25	5.5	7	27.1	6	13
Engraulis mordax	29	6.3	5	12.5	8.5	13.5
Heterostichus rostratus	9	2.0	10	14.6	7	17
Cymatogaster aggregata	15	3.3	9	12.5	8.5	17.5
Phanerodon furcatus	19	4.1	8	10.4	11	19
Embiotoca jacksoni	8	1.7	11.5	10.4	11	22.5
Citharichthys stigmaeus	8	1.7	11.5	8.3	13	24.5
Gibbonsia metzi	5	1.1	14	10.4	11	25
Seriphus politus	5	1.1	14	4.2	15	29
Syngnathus californiensis	5	1.1	14	4.2	15	29
Oxyjulis californica	3	0.7	16	4.2	15	31
Aulorhynchus flavidus	2	0.4	17	2.1	20	37
Pleuronichthys verticalis	1	0.2	20	2.1	20	40
Synodus lucioceps	1	0.2	20	2.1	20	40
Gibbonsia montereyensis	1	0.2	20	2.1	20	40
Artedius lateralis	1	0.2	20	2.1	20	40
Paralichthys californicus	1	0.2	20	2.1	20	40
Hexagrammos superciliosus	1	0.2	20	2.1	20	40
Sebastes rastrelliger	1	0.2	20	2.1	20	40
Total	458	100.0				

surfperch (*M. minimus*), the black surfperch (*E. jacksoni*), and the Pacific sanddab, *C. sordidus* (table 3).

The beam-trawl tows at 10 m depth during 2000–2001 captured a total of 334 fishes belonging to 20 fish species (table 4a). The most abundant species were the white croaker (*G. lineatus*, 31.7%), the queenfish (*Seriphus politus*, 11.7%), and the Pacific sanddab (*C. sordidus*, 10.5%). The species with greatest occurrence were the spotted kelpfish (*G. elegans*) and the black perch, *Embiotoca jacksoni* (43.8%, both), and the white croaker and the speckled sanddab, *Citharichthys stigmaeus* (37.5%, both). The most important species (ICI rank) were *G. lineatus*, *C. stigmaeus*, *C. sordidus*, *G. elegans*, and *H. argenteum* (table 4a).

In 2001–2002, the beam-trawl tows at 10 m depth collected 92 individuals from 17 fish species (table 4b). The most abundant fish species were *S. leptorhynchus* (16.3%), *Phanerodon furcatus* (13.0%), and *G. elegans* (12.0%), while the species with the highest frequency of occurrence were *S. leptorhynchus*, *M. minimus*, and *C. sordidus* (43.8%, each). The order for the five most important fish species according to Index of Community Importance (ICI) were the bay pipefish, the dwarf surfperch, the Pacific sanddab, the spotted kelpfish, and the white seaperch (table 4b).

In 2002–2003, the beam-trawl tows at 10 m depth collected 105 individuals belonging to 17 fish species (table 4c). The northern anchovy (*E. mordax*) was the most abundant (20.0%), followed by the white croaker, *G. lineatus* (16.2%), and the bay pipefish, *S. leptorhynchus* (11.4%). The species that occurred most frequently in the samples were the Pacific sanddab, *C. sordidus* (43.8%), the bay pipefish *S. leptorhynchus* (37.5%), and the dwarf surfperch, *M. minimus* (31.3%). The order of the most important fish species (ICI rank) was *C. sordidus*, *S. leptorhynchus*, *E. mordax*, *G. lineatus*, and *M. minimus* (table 4c).

At 10 m depth, the otter trawl collected a total number of 820 fishes belonging to 32 fish species, during the three years (table 5). The most abundant fish species were *G. lineatus* (14.9%), *E. mordax*, and *S. politus* that contributed with 13.2 and 10.7%, respectively. The species that occurred with highest frequency in the samples were *G. lineatus* (52.1%), *C. sordidus* (50%), and *M. minimus* (41.7%). The most important fish species (ICI rank) for the otter-trawl catch (10 m depth) were the white croaker (*G. lineatus*), the Pacific sanddab (*C. sordidus*), the dwarf surfperch (*M. minimus*), the speckled sanddab (*C. stigmaeus*), and the northern anchovy (*E. mordax*) (table 5).

The total gill net catch was 687 fishes belonging to 32 species, and eleven of those species accounted for 90% of total abundance (table 6). The most abundant species were *G. lineatus* (32.4%), *H. argenteum* (17%), the barred surfperch, *Amphistichus argenteus* (13.7%), the Pacific sardine, *Sardinops sagax* (4.8%), and the Pacific mackerel, *Scomber japonicus* (4.7%). The fish species with greatest %

TABLE 3
Fish species composition and Index of Community Importance (ICI) by otter-trawl tows (5 m depth) in the area of Punta Baja, B.C., México (2000–2003).

Fish Species	Number	% Relative	Rank 1	% FO	Rank 2	ICI
Hyperprosopon argenteum	177	17.5	1	47.9	3	4
Syngnathus leptorhynchus	78	7.7	5.5	52.1	2	7.5
Micrometrus minimus	86	8.5	4	43.8	4.5	8.5
Embiotoca jacksoni	63	6.2	8	54.2	1	9
Citharichthys sordidus	64	6.3	7	43.8	4.5	11.5
Seriphus politus	95	9.4	3	33.3	8.5	11.5
Genyonemus lineatus	78	7.7	5.5	35.4	7	12.5
Engraulis mordax	105	10.4	2	20.8	12	14
Phanerodon furcatus	50	4.9	9	41.7	6	15
Gibbonsia elegans	24	2.4	11	27.1	10	21
Heterostichus rostratus	21	2.1	13.5	33.3	8.5	22
Cymatogaster aggregata	22	2.2	12	22.9	11	23
Aulorhynchus flavidus	43	4.2	10	12.5	15	25
Citharichthys stigmaeus	21	2.1	13.5	18.8	13	26.5
Amphistichus argenteus	9	0.9	15	12.5	15	30
Gibbonsia metzi	7	0.7	16	12.5	15	31
Syngnathus californiensis	14	1.4	15	10.4	17	32
Sebastes sp.	6	0.6	17	8.3	18.5	35.5
Sebastes rastreliger	5	0.5	18	8.3	18.5	36.5
Synodus lucioceps	4	0.4	21	6.3	21.5	42.5
Paralichthys californicus	4	0.4	21	6.3	21.5	42.5
Pleuronichthys guttulatus	4	0.4	21	6.3	21.5	42.5
Sebastes paucispinis	5	0.5	18	4.2	25.5	43.5
Scorpaenichthys marmoratus	3	0.3	23	6.3	21.5	44.5
Sardinops sagax	5	0.5	18	2.1	31.5	49.5
Oxyjulis californica	2	0.2	27.5	4.2	25.5	53
Amphistichus rhodoterus	2	0.2	27.5	4.2	25.5	53
Strongylura exilis	2	0.2	27.5	4.2	25.5	53
Amphistichus koelzi	2	0.2	27.5	2.1	31.5	59
Platyrhinoidis triseriata	2	0.2	27.5	2.1	31.5	59
Umbrina roncador	2	0.2	27.5	2.1	31.5	59
Apodichthys flavidus	2	0.2	27.5	2.1	31.5	59
Brachyistius frenatus	2	0.2	27.5	2.1	31.5	59
Ulvicola sanctaerosae	1	0.1	33.5	2.1	31.5	65
Sebastes auriculatus	1	0.1	33.5	2.1	31.5	65
Paralabrax maculatofasciatus	1	0.1	33.5	2.1	31.5	65
Artedius lateralis	1	0.1	33.5	2.1	31.5	65
Total	1,013	100.0				

occurrence in samplings coincided with the most important species (ICI): *G. lineatus*, *A. argenteus, A. californiensis*, *H. argenteum*, and *S. japonicus* (table 6).

The ICI composite by the contribution of the three sampling gears showed that the most important fish species was the white croaker, *G. lineatus* (table 7), followed by two species (*S. japonicus* and *Atherinopsis californiensis*) that were present in the gill net only. In fourth and fifth place were *M. minimus* and *S. leptorhynchus* that were recollected with beam trawl and otter trawl, and sixth place was occupied by the walleye surfperch *H. argenteum* captured with three gears (table 7).

DISCUSSION

Low temperatures were registered at the study site (10.8–15.4°C) of Punta Baja. Temperatures at Punta Baja were lower than those measured at Punta Entrada off Bahía de San Quintín which is characterized by upwelling, and which showed an annual range of 11.2–18.6°C (Rosales-Casián 1997). The presence of intense upwelling was the result of the Punta Baja effect at the study site, and this wind-induced upwelling is generated almost the entire year, which likely causes cold water to be transported southwards to the interior of Bahía El Rosario (Amador-Buenrostro et al. 1995).

In the present study of Punta Baja, a total of 62 fish species was identified. The site closest to Punta Baja with published fish research is the Bay and Coast of San Quintín (Rosales-Casián 2004). In the Coast of San Quintín, a total of 71 fish species belonging to 33 families was identified and showed 24.7 % higher fish abundance (Rosales-Casián 1996; 2004) than Punta Baja. In the present study, however, the beach seine gear was discarded in Punta Baja because of high waves and rocks on bottom at nearshore.

A total of 40 species were shared between the sites of Punta Baja and the coast of San Quintín. Sixteen fish species were recorded at Punta Baja but not at the

TABLE 4
Fish species composition and Index of Community Importance (ICI) by the beam-trawl tows (10 m depth) in the area of Punta Baja, B.C., México, during (a) 2000–01, (b) 2001–02, and (b) 2002–03.

a

Species 00-01	No.	% Rel	R 1	% FO	R 2	ICI
G. lineatus	106	31.7	1	37.5	3.5	4.5
C. stigmaeus	20	6.0	5	37.5	3.5	8.5
C. sordidus	35	10.5	3	31.3	6	9
G. elegans	10	3.0	10	43.8	1.5	11.5
H. argenteum	21	6.3	4	25.0	8	12
M. minimus	19	5.7	6	31.3	6	12
E. jacksoni	9	2.7	11	43.8	1.5	12.5
S. leptorhynchus	17	5.1	7	31.3	6	13
S. politus	39	11.7	2	12.5	15.5	17.5
E. mordax	15	4.5	8	18.8	10.5	18.5
S. sagax	7	2.1	12	18.8	10.5	22.5
S. lucioceps	13	3.9	9	12.5	15.5	24.5
S. californiensis	4	1.2	14.5	18.8	10.5	25
A. flavidus	3	0.9	16.5	18.8	10.5	27
C. aggregata	5	1.5	13	12.5	15.5	28.5
P. furcatus	4	1.2	14.5	12.5	15.5	30
H. superciliosus	3	0.9	16.5	12.5	15.5	32
H. rostratus	2	0.6	18	12.5	15.5	33.5
A. argenteus	1	0.3	19.5	6.3	19.5	39
P. guttulatus	1	0.3	19.5	6.3	19.5	39
Total	334	100.0				

b

Species 01-02	No.	%Rel	R 1	% FO	R 2	ICI
S. leptorhynchus	15	16.3	1	43.8	2	3
M. minimus	10	10.9	4.5	43.8	2	6.5
C. sordidus	10	10.9	4.5	43.8	2	6.5
G. elegans	11	12.0	3	37.5	4	7
P. furcatus	12	13.0	2	18.8	7	9
H. rostratus	6	6.5	7	25.0	5	12
E. mordax	9	9.8	6	18.8	7	13
C. aggregata	3	3.3	9	18.8	7	16
G. lineatus	5	5.4	8	12.5	10	18
S. lucioceps	2	2.2	11	12.5	10	21
S. californiensis	2	2.2	11	12.5	10	21
G. metzi	2	2.2	11	6.3	14.5	25.5
H. argenteum	1	1.1	15	6.3	14.5	29.5
P. triseriata	1	1.1	15	6.3	14.5	29.5
G. montereyensis	1	1.1	15	6.3	14.5	29.5
U. sanctaerosae	1	1.1	15	6.3	14.5	29.5
S. sagax	1	1.1	15	6.3	14.5	29.5
Total	92	100.0				

c

Species 02-03	No.	% Rel	R 1	% FO	R2	ICI
C. sordidus	11	10.5	4	43.8	1	5
S. leptorhynchus	12	11.4	3	37.5	2	5
E. mordax	21	20.0	1	25.0	5.5	6.5
G. lineatus	17	16.2	2	25.0	5.5	7.5
M. minimus	6	5.7	6	31.3	3	9
G. elegans	7	6.7	5	25.0	5.5	10.5
C. stigmaeus	5	4.8	7.5	25.0	5.5	13
C. aggregata	5	4.8	7.5	12.5	10	17.5
E. jacksoni	4	3.8	10	18.8	8	18
A. argenteus	4	3.8	10	12.5	10	20
P. furcatus	3	2.9	12	12.5	10	22
H. argenteum	4	3.8	10	6.3	15	24.5
S. sagax	2	1.9	13	6.3	15	27.5
S. lucioceps	1	1.0	15.5	6.3	15	30
O. trispinosa	1	1.0	15.5	6.3	15	30
C. nugator	1	1.0	15.5	6.3	15	30
A. flavidus	1	1.0	15.5	6.3	15	30
Total	105	100.0				

TABLE 5
Fish species composition and Index of Community Importance (ICI) by otter trawl tows (10 m depth) in the area of Punta Baja, B.C., México (2000–2003).

	Number	% Rel	Rank 1	% FO	Rank 2	ICI
Genyonemus lineatus	122	14.9	1	52.1	1	2
Citharichthys sordidus	82	10.0	5	50.0	2	7
Micrometrus minimus	84	10.2	4	41.7	3	7
Citharichthys stigmaeus	67	8.2	6	35.4	4	10
Engraulis mordax	108	13.2	2	29.2	8	10
Seriphus politus	88	10.7	3	20.8	9.5	12.5
Hyperprosopon argenteum	54	6.6	7	31.3	6	13
Syngnathus leptorhynchus	38	4.6	8	31.3	6	14
Embiotoca jacksoni	34	4.1	9	31.3	6	15
Cymatogaster aggregata	28	3.4	10	20.8	9.5	19.5
Synodus lucioceps	15	1.8	11	14.6	12	23
Phanerodon furcatus	11	1.3	13	14.6	12	25
Gibbonsia elegans	9	1.1	14	14.6	12	26
Sardinops sagax	19	2.3	10	8.3	17.5	27.5
Heterostichus rostratus	7	0.9	15.5	12.5	14.5	30
Aulorhynchus flavidus	7	0.9	15.5	12.5	14.5	30
Amphistichus argenteus	5	0.6	17	8.3	17.5	34.5
Sebastes auriculatus	4	0.5	18.5	8.3	17.5	36
Gibbonsia metzi	4	0.5	18.5	8.3	17.5	36
Syngnathus californiensis	14	1.7	12	4.2	24.5	36.5
Paralichthys californicus	3	0.4	20.5	6.3	21	41.5
Oxyjulis californica	3	0.4	20.5	6.3	21	41.5
Ophidion scrippsae	2	0.2	23.5	6.3	21	44.5
Scorpaenichthys marmoratus	2	0.2	23.5	4.2	24.5	48
Xystreurys liolepis	2	0.2	23.5	4.2	24.5	48
Pleuronichthys verticalis	2	0.2	23.5	4.2	24.5	48
Sebastes rastrelliger	1	0.2	28.5	2.1	29.5	58
Peprilus simillimus	1	0.2	28.5	2.1	29.5	58
Raja binoculata	1	0.1	28.5	2.1	29.5	58
Pleuronichthys guttulatus	1	0.1	28.5	2.1	29.5	58
Paralabrax nebulifer	1	0.1	28.5	2.1	29.5	58
Scorpaena guttata	1	0.1	28.5	2.1	29.5	58
Total	820	100.0				

San Quintín coast: *M. minimus, G. elegans, G. metzi, G. montereyensis, Aulorhynchus flavidus, Sebastes paucispinis, Strongylura exilis, Ulvicola sanctaerosae, Artedius lateralis, Apodichthys flavidus, Brachyistius frenatus, Ophidium scrippsae, Leuresthes tenuis, Paralabrax maculatofasciatus, Raja binoculata*, and *Chirolophis nugator.* However 27 species found at the Coast of San Quintín (Rosales-Casián 1997) were not common with Punta Baja.

The fish community of Punta Baja was characterized by species associated with small patches of *Macrocystis* sp. beds, mainly, from the sandy bottom areas (*G. lineatus*, *S. politus*, *C. sordidus*), and also deeper species like scorpaenids. The most abundant species belong to Embiotocidae, Scorpaenidae, Sciaenidae, and Clinidae families (eleven, five, four, and four species, respectively), accounting for 65% of total abundance.

In San Diego Bay, California (388 km north of Punta Baja), a total of 78 fish species was identified (Allen et al. 2002), however 38% of the species registered at Punta Baja were not present at San Diego Bay, and vice versa: 58% of the species registered at San Diego were not common with Punta Baja. This variation can be due to the environmental differences between the semiprotected area of Punta Baja and the coastal lagoon of San Diego, and the long sampling period (1994–1999) in San Diego Bay which preceded the current study period of 2000–2003. In a study at the marine reserve of Cabrillo National Monument localized at the protected southwestern side of Point Loma at the mouth of San Diego Bay (Craig and Pondella 2006), a total of 47 fish species was identified, and shared 23 species with Punta Baja, but the gill net was the only common sampling gear. In another gill net study at Santa Catalina Island, 67 species were registered, however there was a stronger representation of rocky-reef fishes with *Heterodontus franciscanus* as the most abundant (Pondella and Allen 2000), while at Punta Baja the first species was a sandy-bottom habitant (*G. lineatus*), which at Santa Catalina Island was positioned at number 64.

The collection of two species at Punta Baja, the penpoint gunnel (*Apodichthys flavidus*), and the mosshead warbonnet (*Chirolophis nugator*), is interesting because their southern distributions are established at Santa Barbara Island and San Miguel Island, respectively, in

TABLE 6
Fish species composition and Index of Community Importance (ICI) by the gill net (5–10 m depth) in the area of Punta Baja, B.C., México (2000–2003).

Species	Number	% Rel	Rank 1	% FO	Rank 2	ICI
Genyonemus lineatus	209	30.42	1	66.67	1.5	2.5
Amphistichus argenteus	94	13.68	3	66.67	1.5	4.5
Hyperprosopon argenteum	117	17.03	2	41.67	5	7
Scomber japonicus	32	4.66	5	41.67	5	10
Atherinops californiensis	25	3.64	7.5	50.00	3	10.5
Phanerodon furcatus	26	3.78	6	33.33	7.5	13.5
Sardinops sagax	33	4.80	4	25.00	9.5	13.5
Seriphus politus	20	2.91	10	41.67	5	15
Embiotoca jacksoni	25	3.64	7.5	33.33	7.5	15
Synodus lucioceps	18	2.62	11	25.00	9.5	20.5
Umbrina roncador	21	3.06	9	16.67	13	22
Rhacochilus toxotes	10	1.46	13	16.67	13	26
Rhacochilus vacca	8	1.16	14	16.67	13	27
Citharichthys stigmaeus	7	1.02	15	16.67	13	28
Paralichthys californicus	5	0.73	16.5	16.67	13	29.5
Engraulis mordax	14	2.04	12	8.33	24	36
Cheilotrema saturnum	5	0.73	16.5	8.33	24	40.5
Girella nigricans	2	0.29	19	8.33	24	43
Paralabrax nebulifer	2	0.29	19	8.33	24	43
Leuresthes tenuis	2	0.29	19	8.33	24	43
Scorpaena guttata	1	0.15	26.5	8.33	24	50.5
Heterodontus francisci	1	0.15	26.5	8.33	24	50.5
Gibbonsia elegans	1	0.15	26.5	8.33	24	50.5
Platyrhinoidis triseriata	1	0.15	26.5	8.33	24	50.5
Trachurus symmetricus	1	0.15	26.5	8.33	24	50.5
M. undulatus	1	0.15	26.5	8.33	24	50.5
S. carnatus	1	0.15	26.5	8.33	24	50.5
Citharichthys sordidus	1	0.15	26.5	8.33	24	50.5
Sebastes auriculatus	1	0.15	26.5	8.33	24	50.5
Paralabrax clathratus	1	0.15	26.5	8.33	24	50.5
Leptocottus armatus	1	0.15	26.5	8.33	24	50.5
Atherinops affinis	1	0.15	26.5	8.33	24	50.5
Total	687	100.0				

Southern California (Love et al. 2005). The presence of a continuous upwelling at Punta Baja may provide a "cold oasis" for opportunistic northern species, whose eggs are dispersed by different ways, and which use these local disturbances for survival of later developmental stages (DeMartini and Sikkel 2006). In an analysis of the oceanographic conditions, nutrient and phytoplankton dynamics in the San Quintín area, it was found that low salinity water parcels arrive to the area, and it is suggested that they originate at the subarctic or at the Columbia River, implicating a genetic flux by spores, eggs, etc. (Alvarez-Borrego 2004). As evidence, at El Socorro coast, a site between Punta Baja and Coast of San Quintín, in December 2008 a green sturgeon (*Acipenser medirostris*) was captured 200 km south of the southern limit of known distribution (Bahía de Todos Santos), and may it be using these water parcels during La Niña conditions (Rosales-Casián and Almeda-Jauregui 2009).

The California halibut (*Paralichthys californicus*), an important component in fish species assemblages in the Southern California Bight (Kramer 1990), was ranked 23rd (0.37% relative abundance) at Punta Baja. In the Coast of San Quintín, influenced as well by upwelling, the California halibut occupied the 9th place with also a low relative abundance (2.7%) and that compared with Bahía de Todos Santos (232 km north) where this flatfish contributed a greater relative abundance (13.0%) and was ranked 2nd place (Rosales-Casián 1997). Juvenile California halibut appear to succeed better in bays and estuaries and prefer a range of temperatures between 15–23°C (Innis 1990), the benefit being a faster growth because of high food production and warm waters (Kramer 1990), and therefore, the low temperatures registered at Punta Baja do not suggest it is a prime habitat for this species.

The gill net overall mean abundance on a seasonal basis at Punta Baja (CPUE 57.3 fish/net) was higher than the 16.9 fish/net found at the Coast of San Quintín (Rosales-Casián 1997) and the 27.5 fish/net found at Cabrillo National Monument, San Diego, California (Craig and Pondella 2006), but was lower than the mean CPUE of 193.3 fish/net found at the Scripps Coastal Reserve (Craig et al 2004). Sampling with a gill net is

TABLE 7
Composite ICI for the fish species assemblage at Punta Baja, B.C., México (2000–2003).

Fish species	ICI composite	Beam-trawl	Otter trawl contributions	Gill net	Sum
Genyonemus lineatus	1	2	1	1	4
Scomber japonicus	1			4	4
Atherinopsis californiensis	3			5	5
Micrometrus minimus	4	3	4		7
Syngnathus leptorhynchus	5	1	6.5		7.5
Hyperprosopon argenteum	6	5	2.5	3	10.5
Hexagrammos superciliosus	7	20			20
Cymatogaster aggregata	8	11	11		22
Embiotoca jacksoni	9	9	5	8.5	22.5
Rhacochilus toxotes	10			23	23
Sebastes sp.	11		23.5		23.5
Scorpaenichthys marmoratus	11		23.5		23.5
Rhacochilus vacca	13			24	24
Phanerodon furcatus	14	10	9	6.5	25.5
Heterostichus rostratus	15	12	14		26
Gibbonsia montereyensis	16	27			27
Odontopyxis trispinosa	16	27			27
Chirolophis nugator	16	27			27
Sebastes paucispinis	16		27		27
Cheilotrema saturnum	20			28	28
Ophidion scrippsae	20		28		28
Seriphus politus	22	13	8	8.5	29.5
Syngnathus californiensis	22	14.5	15		29.5
Girella nigricans	24			30	30
Leuresthes tenuis	24			30	30
Aulorhynchus flavidus	24	18	12		30
Amphistichus rhodoterus	27		30.5		30.5
Strongylura exilis	27		30.5		30.5
Xystreurys liolepis	27		30.5		30.5
Gibbonsia metzi	30	16	18		34
Amphistichus koelzi	31		35		35
Apodichthys flavidus	31		35		35
Brachyistius frenatus	31		35		35
Heterodontus francisci	34			36.5	36.5
Trachurus symmetricus	34			36.5	36.5
Menticirrhus undulatus	34			36.5	36.5
Sebastes carnatus	34			36.5	36.5
Paralabrax clathratus	34			36.5	36.5
Leptocottus armatus	34			36.5	36.5
Atherinops affinis	34			36.5	36.5
Amphistichus argenteus	41	19	17	2	38
Engraulis mordax	42	7	6.5	27	40.5
Synodus lucioceps	42	14.5	16	10	40.5
Paralabrax maculatofasciatus	44		41		41
Peprilus simillimus	44		41		41
Raja binoculata	44		41		41
Sardinops sagax	47	17	19	6.5	42.5
Citharichthys stigmaeus	48	8	10	25	43
Citharichthys sordidus	48	4	2.5	36.5	43
Oxyjulis californica	50	21	23.5		44.5
Umbrina roncador	51		35	11	46
Sebastes rastrelliger	52	27	21		48
Pleuronichthys guttulatus	53	27	26		53
Gibbonsia elegans	54	6	13	36.5	55.5
Pleuronichthys verticalis	55	27	30.5		57.5
Sebastes auriculatus	56		23.5	36.5	60
Artedius lateralis	57	27	41		68
Ulvicola sanctaerosae	57	27	41		68
Paralabrax nebulifer	59		41	30	71
Paralichthys californicus	60	27	20	26	73
Scorpaena guttata	61		41	36.5	77.5
Platyrhinoidis triseriata	62	27	35	36.5	98.5

an effective method of taking fish species in sites with rocky and sandy bottoms, the otter trawl is most effective on sandy bottoms (Craig et al. 2004; Craig and Pondella 2006).

Comparison of the coastal fishes from Punta Baja with northern sites in California is difficult because of the differences in sampling methods. The fish species richness registered at Punta Baja was similar to the Scripps Coastal Reserve at La Jolla (San Diego, California), where a total of 59 fish species was found using otter-trawl tows and gill nets, but scuba surveys and ichthyocide in tidepools were also used (Craig et al. 2004).

Like many sites of coastal Baja California, Punta Baja has been under pressure for development, which has now mostly been suspended. Only at Bahía de Santa Rosalillita, 210 km south of Punta Baja (the Nautical Stairway, Okolodkov et al. 2007) were facilities to launch boats and two rocky stone jetties recently constructed to receive boats from California and to move the vessels overland to Bahía de Los Ángeles, another proposed site for a large marina. Future development may still occur, however.

The 62 fish species identified at the Punta Baja area belong to a typical temperate community (Allen et al. 2006) of the Southern California Bight. The present study constitutes a baseline reference for possible future developments, and major anthropogenic impacts.

ACKNOWLEDGEMENTS

This study was supported with funds from CICESE, mainly. Thanks to the many people that helped in the seasonal samplings during the complete study. Boat operators: Martín Díaz, Juan Sidón, Luis Demetrio Arce. Students: Silvia Avilés, Oscar González, Julio Hernández, Clara Hereu, Jorge Isaac Rosales, Laura Rosales, Sussane Adam, Alejandra Hernández, Rubí Ruz, Filiberta Lucena, Zullete Andrade, Guillermo Ortuño, Alejandro Medina. Special thanks to my father Zenaido Rosales († February 28, 2011) who repaired the nets after every trip, and my brothers David and Humberto Rosales for helping me with three of the samplings. Thanks to Dan Pondella (Occidental College, Los Angeles) and Augie Vogel (USC, Los Angeles), who made the trip to Punta Baja to participate in the samplings of February 16 and May 31, 2002, respectively. The drawing of Punta Baja was realized by Jose Maria Dominguez and Francisco Ponce. Thanks to Karen Englander (Facultad de Idiomas, Universidad Autónoma de Baja California) for her English review of this manuscript. Thanks to two anonymous reviewers for making helpful comments on this manuscript.

LITERATURE CITED

Allen, L. G., A. M. Findlay, and C. M. Phalen. 2002. Structure and standing stock of the fish assemblages of San Diego Bay, California from 1994 to 1999. Bull. Southern California Acad Sci. 10(2):49–85.

Allen, L. G., M. M. Yoklavich, G. M. Cailliet, and M. H. Horn. 2006. Bays and estuaries, pp. 119–148. *In*: The ecology of Marine Fishes: California and adjacent waters. Allen, L.G., D.J. Pondella II, and M.H. Horn (eds.). University of California Press, Berkeley and Los Angeles, California, USA.

Álvarez-Borrego, S. 2004. Nutrient and phytoplankton dynamics in a coastal lagoon strongly affected by coastal upwelling. Cienc. Marinas 30:1–19.

Amador-Buenrostro, A., M. L. Argote-Espinoza, M. Mancilla-Peraza, and M. Figueroa-Rodríguez. 1995. Short term variations in the anticyclonic circulation in Bahía Sebastian Vizcaíno, BC. Cienc. Marinas 21(2):201–223.

Anderson, T. R., and M. I. Lucas. Upwelling ecosystems, pp. 3651–3661. *In*: Encyclopedia of Ecology. Jorgensen, S. E. and B. Fath (eds.). Elsevier B.V. Amsterdam, The Netherlands.

Bakun, A. and C. S. Nelson. 1977. Climatology of upwelling related processes off Baja California. Calif. Coop. Oceanic Fish. Invest. Rep. 19:107–127.

Butler, J. L., L. D. Jacobson, J. T. Barnes, and H. G. Moser. 2003. Biology and population dynamics of cowcod (*Sebastes levis*) in the Southern California Bight. Fish. Bull. 101:260–280.

Commission on Engineering and Technical Systems, CETS. (1990). Monitoring Southern California's coastal waters. National Academy Press. Washington, D.C. USA. pp. 154.

Craig, M. T., F. J. Fodrie, and P.A. Hastings. 2004. The nearshore fish assemblage of the Scripps Coastal Reserve, San Diego, California. Coastal Management, 32:341–351.

Craig, M.T. and D. J. Pondella. 2006. A survey of the fishes of the Cabrillo National Monument, San Diego, California. Cal. Fish and Game 92(4): 172–183.

DeMartini, E. D., and P. C. Sikkel. 2006. Reproduction, p. 483–523. *In*: The ecology of Marine Fishes: California and adjacent waters. Allen, L. G., D. J. Pondella II, and M.H. Horn (eds.). University of California Press, Berkeley and Los Angeles, California, USA.

Emerson, W. 1956. Upwelling and associated marine life along Pacific Baja California, México. J. Paleontology. 30(2):393–397.

Horn, M. H., L. G. Allen, and R. Lea. 2006. Biogeography, pp. 3–25. *In*: The ecology of Marine Fishes: California and adjacent waters. Allen, L. G., D. J. Pondella II, and M.H. Horn (eds.). University of California Press, Berkeley and Los Angeles, California, USA.

Hubbs, C. L. 1948. Changes in the fish fauna of western North America correlated with changes in ocean temperature. J. Mar. Res. 7: 459–482.

Innis, D. B. 1990. Juvenile California halibut, *Paralichthys californicus*, growth in relation to thermal effluent, pp. 153–165. *In*: The California halibut, *Paralichthys californicus*, resource and fisheries. Haugen C. W. (ed.). Calif. Dept. Fish and Game, Fish Bull. 174.

Kramer, S. H. 1990. Habitat specificity and ontogenetic movements of juvenile California halibut, *Paralichthys californicus,* and other flatfishes in shallow waters of Southern California. NOAA-SFSC, Administrative Report LJ-90-22, pp. 157.

Love, M. S., J. S. Stephens, Jr., P. A. Morris, M. M. Singer, M. Sandhu and T. C. Sciarrotta. 1986. Inshore soft substrata fishes in the Southern California Bight: an overview. Calif. Coop. Oceanic Fish. Invest. Rep. 27:84–104.

Miller, D. J. and R. N. Lea. 1972. Guide to coastal marine fishes of California. Bull. Calif. Dept. Fish and Game. No. 157. 235 pp.

Moser, H. G., R. L. Charter, P. E. Smith, D. A. Ambrose, S. R. Charter, C. A. Meyer, E. M. Sandknop, and W. Watson. 1993. Distributional atlas of fish larvae and eggs in the California current region: Taxa with 1000 or more total, larvae 1951 through 1984. CalCOFI Atlas 31. 233 pp.

Okolodkov, Y. B., R. Bastida-Zavala, A. L. Ibáñez, E. Suárez-Morales, F. Pedroche, and F.J. Gutierrez-Mendieta. 2007. Especies acuáticas no indígenas de México. Ciencia y Mar, XI (32): 29–67.

Pondella, D. J., II, and L. G. Allen. 2000. The nearshore fish assemblage of Santa Catalina Island. *In*: The Proceedings of the Fifth California Islands Symposium, David R. Browne, Kathryn L. Mitchell and Henry W. Chaney editors. Santa Barbara Museum of Natural History, Santa Barbara, California: 394–400.

Rosales-Casián, J. A. 1996. Ichthyofauna of Bahía de San Quintín, Baja California, México and its adjacent coast. Cienc. Marinas 22:443–458.

Rosales-Casián, J. A. 1997. Estructura de la comunidad de peces y el uso de los ambientes de bahías, lagunas y costa abierta en el Pacífico Norte de Baja California. PHD thesis, Ecología Marina, CICESE. 201 p.

Rosales-Casián, J. A. 2004. Composition, importance and movement of fishes from San Quintín Bay, Baja California, México. Cienc. Marinas 30:119–132.

Rosales-Casián, J. A. and C. Almeda-Jauregui. 2009. Unusual occurrence of a green sturgeon *Acipenser medirostris*, at El Socorro, Baja California, México. Calif. Coop. Oceanic Fish. Invest. Rep. 50:169–171.

Rosales-Casián, J. A., and J. R. Gonzalez-Camacho. 2003. Abundance and Importance of fish species from the artisanal fishery on the Pacific coast of Northern Baja California. Bull. South. Calif. Acad. Sci. 102(2):51–65.

Sanford, E. 1999. Regulation of keystone predation by small changes in ocean temperature. Science 283(5410):2095–2097.

Shanks, A. L. and G. L. Eckert. 2005. Population persistence of California current fishes and benthic crustaceans: a marine drift paradox. Ecological Monographs, 75(4):505–524.

Stephens, J. S., Jr. and K. E. Zerba, 1981. Factor affecting fish diversity on a temperate reef. Environ. Biol. Fishes. 6:111–121.

U.S. Globec (1994). Eastern boundary current program: A science plan for the California current. University of California, Berkeley CA. Report No. 11. 123 pp.

Zar, J. H. 1984. Biostatistical analysis. 2a ed. Englewood Cliffs N.J.: Prentice Hall. 718 pp.

THE STRUCTURE OF MARINE PHYTOPLANKTON COMMUNITIES— PATTERNS, RULES AND MECHANISMS

RALF GOERICKE
Scripps Institution of Oceanography
University of California, San Diego
9500 Gilman Drive
La Jolla, CA 92093-0205

ABSTRACT

The taxonomic structure of marine phytoplankton communities was studied in nearshore, coastal and offshore environments of the Atlantic, Pacific and Indian Ocean to search for common distributional patterns that might suggest mechanisms controlling these. Contributions of different taxa to total phytoplankton pigment-biomass (TChl *a*) were calculated from concentrations of taxon-specific pigments. In most environments studied, variability of phytoplankton biomass was dominated by diatoms or dinoflagellates, the bloom taxa. The pigment biomass of non-bloom-forming taxa varied as an asymptotic function of TChl *a*. Observed patterns for any taxon were often strikingly similar in different environments but differed significantly between taxa in any one environment. Simple functions were used to describe these patterns, which can be used to predict phytoplankton community structure from TChl *a*. The observed patterns are consistent with predictions derived from a simple conceptual model that suggests that total phytoplankton biomass is generally limited by the availability of a critical nutrient, i.e., by bottom-up forces, but that the biomass of some taxa, particularly picoautotrophs, is controlled by grazers under mesotrophic to eutrophic conditions, i.e., top-down forces. The distribution of cyanobacteria suggests that their population dynamics, unlike those of other taxa, is not tightly lined to the dynamics of their grazers, likely because the latter are grazing concurrently on heterotrophic bacteria.

INTRODUCTION

The taxonomic structure of the phytoplankton community is an important determinant of ecosystem function with far-reaching implications for the cycling of energy and matter in the marine environment. For example, blooms of coccolithophorids or diatoms differ significantly in their impacts on the export of inorganic carbon or silica, respectively (Smetacek 1999; Tyrrell et al. 1999). Similarly, differences in grazer communities are expected to affect rates of carbon export (Michaels and Silver 1988). However, our realization of the importance of phytoplankton or zooplankton community structure in the marine environment is not complemented by a good understanding of its controls (Verity and Smetacek 1996). In the case of phytoplankton communities our understanding is limited to a more or less qualitative understanding (e.g., Margalef 1978). Most models of phytoplankton communities attempting to elucidate the coexistence of multiple species of algae in the same parcel of water are still at the level of two to four taxa or functional groups (e.g., Anderies and Beisner 2000; Litchman et al. 2006; Friedrichs et al. 2007), even though phytoplankton communities of the open ocean are known to consist of tens to hundreds of species (e.g., Venrick 1982; Venrick 2002). On the other hand, attempts to model the community using multiple groups of phytoplankters (e.g., Bissett et al. 1999; Moore et al. 2002) encounter the problem that the number of parameters that must be parameterized increases approximately with the square of the number of the model's taxa (Denman 2003). Clearly, we are far removed from a solid, mechanistic understanding that would allow us to understand and predict the taxonomic structure of phytoplankton communities.

An alternative approach to the problem is to ask if there are consistent patterns characterizing the distribution and abundance of phytoplankton taxa, i.e., rules that can be used to predict phytoplankton community structure. Indeed, some rules have been known for a long time. The seasonal succession of temperate phytoplankton has often been described as progressing from diatoms to flagellates, i.e., from non-motile to motile species (Smayda 1980) or from sinkers to floaters (Macintyre et al. 1997). Similarly, the variability of phytoplankton biomass in the ocean has often been attributed to larger autotrophs; picoautotrophs are viewed as ever-present, contributing to the background biomass (Chisholm 1992; Li 2002). Goericke (2011) recently tested a set of rules implied by Chisholm's (1992) description of variations of phytoplankton size structure with total phytoplankton biomass and found that these did not hold in the California Current system.

Very detailed studies can be carried out using microscopy; however, this wealth of information on species distributions is rarely complemented by physiological information on all these species. Chemotaxonomy, based on compounds that are specific or even unique for different taxa of microalgae, can alternatively be used to

determine the contributions of those taxa to total phytoplankton biomass. Compounds of choice are carotenoids and chlorophylls (Jeffrey et al. 1997). Some of these groups and their associated pigments are diatoms (fucoxanthin), dinoflagellates (peridinin), some groups of oceanic prymnesiophytes (19'-hexanoyloxyfucoxanthin), cryptophytes (alloxanthin), pelagophytes (19'-butanoyloxyfucoxanthin), chlorophytes (chlorophyll *b*, i.e., Chl b_1, and neoxanthin), cyanobacteria (zeaxanthin), and *Prochlorococcus* sp. (divinyl-chlorophyll *a*; i.e., Chl a_2). Contributions of different microalgal taxa to pigment biomass, often expressed as total chlorophyll a (TChl *a*, the sum of chlorophyll *a*, i.e., Chl a_1, and Chl a_2), can in principle be determined from concentrations of these biomarkers (Letelier et al. 1993; Mackey et al. 1996; Goericke and Montoya 1998).

This pigment-based approach was applied to data from the monsoonal Arabian Sea (Goericke 2002) to determine contributions of different photoautotrophs to phytoplankton pigment biomass (henceforth "biomass" for brevity). While these distributions were only weakly related to parameters such as temperature and inorganic nutrients, coherent patterns were observed when the biomass of different taxa was plotted against TChl *a*. Diatoms were the bloom species in this system, dominating phytoplankton biomass at high concentrations of TChl *a*. An abundance threshold also existed for diatoms, i.e., these contributed negligibly to phytoplankton biomass when TChl *a* was less than ~0.25 μg L^{-1}. Abundance thresholds were also observed for taxa not forming blooms. Once TChl *a* increased above 1 to 2 μg L^{-1} upper limits were observed for the biomass of most taxa, ranging from 0.05 to 0.5 μg Chl L^{-1}. The one exception to those patterns was *Prochlorococcus*, which contributed significantly to total biomass at low levels of TChl *a*, but whose biomass declined when TChl *a* reached high values. These results suggest that, at least in the Arabian Sea, phytoplankton community structure is a predictable function of TChl *a*. Similar patterns were observed for concentrations of taxon-specific pigments in the North Atlantic and Mediterranean Sea (Claustre 1994).

The patterns observed in the Arabian Sea for different microalgal taxa are very similar to those described by Raimbault et al. (1988) for the contribution of different size classes of autotrophs to total autotroph biomass in the Mediterranean (see also Chisholm 1992). Thingstad (1998) presented a simple conceptual model predicting exactly such patterns. The essence of the model is nutrient limitation of total phytoplankton biomass and grazer control of the abundance of all groups, except those forming blooms, once total biomass reaches a critical level. Thus, distributional patterns observed in the Arabian Sea provide empirical support for the model of Thingstad. In order to test the generality of these patterns and the conceptual model of Thingstad, variations of phytoplankton taxon-specific biomass with TChl *a* were analyzed in four other environments: a nearshore environment off San Diego, U.S.A.; the coastal/offshore North Pacific off Southern California; the southern sector of the Indian Ocean; and the Sargasso Sea off Bermuda. Distributional patterns observed in these environments were very similar to those of the Arabian Sea (Goericke 2002), suggesting that phytoplankton community structure in the world's oceans varies predictably as a function of TChl *a* and that community structure is controlled by a balance between bottom-up forces, i.e., the availability of resources, and top-down control, i.e., grazers.

METHODS

Sampling and Chromatography. Seawater was collected at the pier of the Scripps Institution of Oceanography (Scripps Pier) with Niskin bottles from the top meter of the water column (bottom depth 4 to 7 m) between August 1997 and July 2000 at least twice a week. Samples (1L) were stored in amber bottles and filtered in the laboratory within 3 hours onto a Whatman GF/F filter (Goericke et al. 2000). The filters were stored in liquid nitrogen until analysis on a C8-column based high-pressure liquid-chromatography (HPLC) system (Goericke et al. 2000). In the California Current system (CalCOFI cruises during April and October 1995 and October 1996, Scripps Institution of Oceanography 1997) 2.2 to 4.4 L samples were collected from 2 to 3 depths within the mixed layer. The seawater was filtered and processed as described above. Pigment data from previously published studies were used as well: from the Sargasso Sea (U.S. JGOFS BATS program off Bermuda covering the years 1989 until 1998; data retrieved from the U.S. JGOFS Web site), the temperate, subpolar and polar Southern Indian Ocean between 40 and 60°S and 45 and 65°E (Francois et al. 1993), and the Arabian Sea (U.S. JGOFS Arabian Sea program during the NE and early SW monsoons, i.e., cruises TN43, 49, 54; Goericke, 2002).

Nutrient Enrichment Experiments. During the October 1996 CalCOFI cruise seawater was collected before sunrise by CTD rosette from the mixed layer at CalCOFI stations 93.40, 93.120, 90.53, 87.100, 83.55 and 80.90 and was filled into a carboy and distributed into 2.8 L polycarbonate bottles that had been acid washed and Milli-Q water rinsed. Enrichments were made using 2 μM NH_4Cl, 2 μM $NaNO_3$ and 0.4 μM K_2HPO_4 as initial enrichments, and untreated samples as a control. Treatments and controls were done in duplicate. Bottles were incubated at 60% ambient light in a Plexiglas incubator, cooled with surface-seawater. Samples for pigment analysis were taken every 24 hours for 3 to 4 days and stored as described above.

Calculation of taxon-specific biomass. The pigment biomass of different taxa was determined from concentrations of taxon-specific pigments as previously described (Goericke and Montoya 1998; Goericke 2002). For the optimization procedure pigment ratios were only constrained to be larger than zero. The independence of derived pigment ratios from initial conditions was tested in each case by using different sets of initial parameters. For the Scripps Pier and the California Current system contributions to TChl *a* by dinoflagellates, diatoms, haptophytes, pelagophytes, "green" algae (i.e., chlorophytes, prasinophytes, etc.), cryptophytes, *Synechococcus* and *Prochlorococcus* were calculated. Contributions of *Prochlorococcus*, dinoflagellates and cryptophytes were estimated directly from concentrations of Chl a_2, peridinin and alloxanthin, respectively. Contributions of haptophytes, pelagophytes, diatoms and *Synechococcus* were estimated, respectively, from concentrations of 19'-hexanoyloxyfucoxanthin, 19'-butanoyloxyfucoxanthin, fucoxanthin and zeaxanthin, corrected for contribution by pelagophytes, haptophytes, haptophytes and *Prochlorococcus*, respectively.

Contributions of "chlorophytes" and "prasinophytes" were also determined by including prasinoxanthin in the algorithm. However, prasinophytes did not contribute significantly to phytoplankton biomass in the California Current system as evidenced by very low or zero concentrations of prasinoxanthin. Off the Scripps Pier different groups of "green" algae were present and differentiated as follows: The characteristic pigments of chlorophyta are violaxanthin, neoxanthin and Chl b_1; only neoxanthin was used to estimate the contribution of chlorophytes to pigment biomass. Prasinophycean biomass was estimated from prasinoxanthin. Larger, transient contributions of euglenophyceae would be evident from changes in the ratio of Chl *b* and neoxanthin. This ratio however, did not vary systematically with the seasons, nor did it display large transients (data not shown), suggesting that euglenophyceae did not contribute significantly to pigment biomass. Eustigmatophyceae (chromophyta) are characterized by high concentrations of violaxanthin relative to other accessory pigments. Thus their presence can be gauged from high violaxanthin-neoxanthin ratios (V:N-ratio). Indeed, the V:N-ratio reached a value of 35 g g^{-1} during September '97, suggesting that eustigmatophyceae were present during this time. The estimated abundance is shown in Figure 1C (bold line). The eustigmatophycean violaxanthin-Chl *a* ratio was estimated as 0.67 g g^{-1}. During the rest of the time series the V:N-ratio varied with the seasons; during February and August average values were 1.7 and 3.4 g g^{-1}, respectively (data not shown). Statistical analysis and nonlinear curve fitting were carried out in MS Excel.

RESULTS

Scripps Pier. Off the Scripps Pier total chlorophyll *a* (TChl *a*, i.e. the sum of Chl a_1 and Chl a_2) ranged from 0.4 to 11 μg L^{-1} with an average value of 2.2 μg L^{-1} for the study period, August 1997 to August 2000 (fig. 1A). A strong seasonal pattern was not evident from monthly averages of TChl *a*, except for elevated concentrations of TChl *a* during the spring. Differences between months were significant (ANOVA, df = 11, F = 8.5, P < 0.01) and were driven by the months of March and April (data not shown).

Concentrations of taxon-specific pigments indicate that the phytoplankton community off the Scripps Pier consisted primarily of dinoflagellates, diatoms, prymnesiophyceae, "green" algae (predominantly prasinophyceae in the case of this study), pelagophyceae, cryptophyceae, eustigmatophyceae (only observed during September 1997), and the two cyanobacterial groups *Synechococcus* and *Prochlorococcus*. Dramatic differences in the abundance of the different taxonomic groups are evident (fig. 1 B-D). Dinoflagellates were responsible for the major blooms; their pigment biomass ranged from less than 0.01 μg Chl *a* L^{-1} to ~10 μg Chl *a* L^{-1} (fig. 1B). The biomass of other groups either varied with the seasons (e.g., chlorophyta, fig. 1C) or without distinct seasonal pattern (e.g., prymnesiophytes, fig. 1D). TChl *a* can also be partitioned into "larger autotrophs" (diatoms and dinoflagellates; fig. 1E) and "picoautotrophs" (prymnesiophytes, pelagophytes, cryptophytes, chlorophyta, eustigmatophyceae and cyanobacteria; fig. 1F). Temporal variability of TChl *a* was dominated by the larger autotrophs; these were responsible for 81% of the observed variability. The variability of picoautotroph abundance was small compared to that of the larger autotrophs. The pigment biomass of larger autotrophs differed significantly between months (ANOVA, df = 11, F = 9.6, P < 0.01), with monthly averages differing by a factor of 5. Blooms of larger autotrophs occurred primarily during March–June and during November. Picoautotroph pigment biomass also differed significantly between months (ANOVA, df = 11, F = 6.3, P < 0.01); however, monthly averages differed by only a factor of 2; results driven primarily by low values during June.

It is evident from the time series (fig. 1) that phytoplankton community structure varied with TChl *a*. To analyze this relationship in detail, the pigment biomass of different taxonomic groups was plotted against TChl *a* (fig. 2, see also Goericke 2002). Different types of patterns emerged: Variations of dinoflagellate biomass with TChl *a* were biphasic, as is evident from differences in slopes of point-clusters between 0.4 to 1.6 and 1.6 to 4 μg-TChl *a* L^{-1}. Dinoflagellates were the bloom taxon in this system, accounting for most of the phytoplankton biomass when TChl *a* was >2 μg L^{-1} (fig. 2, left-hand

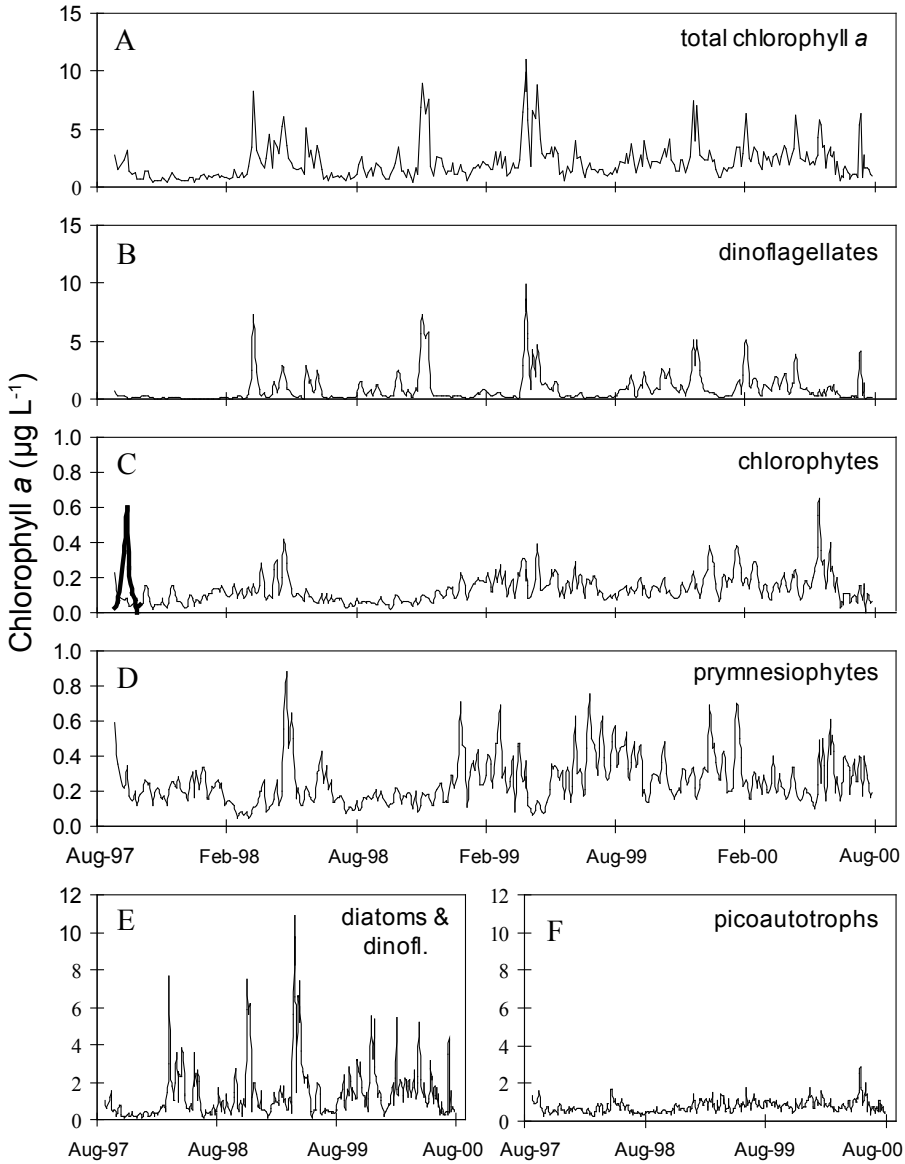

Figure 1. TChl *a* (A) and pigment biomass (Chl *a*) of dinoflagellates (B), chlorophyta (C), prymnesiophyceae (D), diatoms & dinoflagellates (E) and picoautotrophs (F) off the pier of the Scripps Institution of Oceanography (Scripps Pier). More pronounced dinoflagellate blooms or aggregations (TChl *a* > 100 µg L^{-1}) were observed in 1995, 1996 and 2001. The bold line in panel C likely represents eustigmatophyceae.

panel). The contribution of diatoms to TChl *a* increased linearly with TChl *a* and saturated at values of 1 to 1.5 µg Chl *a* L^{-1} for TChl *a* of 4 to 10 µg L^{-1}. The pigment biomass of prymnesiophytes, pelagophytes, chlorophytes, and cryptophytes initially increased with TChl *a* and eventually leveled off at higher TChl *a*, reaching maximum values of 0.2 to 0.5 µg Chl *a* L^{-1} (fig. 2). The biomass of *Synechococcus* increased only slightly with TChl *a*, saturating at concentrations of 0.15 to 0.2 µg L^{-1}, with possibly decreasing values when TChl *a* was larger than 4 µg L^{-1}. The biomass of *Prochlorococcus* appeared to decline with increasing TChl *a*; note, however, that measurements of Chl a_2 are unreliable when TChl *a* is larger than 4 µg L^{-1} due to the interference of the large Chl a_1 peak with the more than 100 times smaller Chl a_2 peak. Overall, these data suggest that the biomass of the different groups of autotrophs, when plotted against TChl *a*, follows distinct and predictable patterns. Analyses carried out on one-year data batches yielded very similar results (data not shown), demonstrating that patterns were consistent from year to year.

To quantify these patterns, exponential functions were fit to the data. The functions used (table 1) took the following into account: 1. the potential presence of abundance thresholds (i.e., negligible contributions to total phytoplankton biomass below certain values of TChl *a*), 2. the asymptotic value reached when TChl *a* is large, 3. the biphasic patterns for dinoflagellates and 4. decreas-

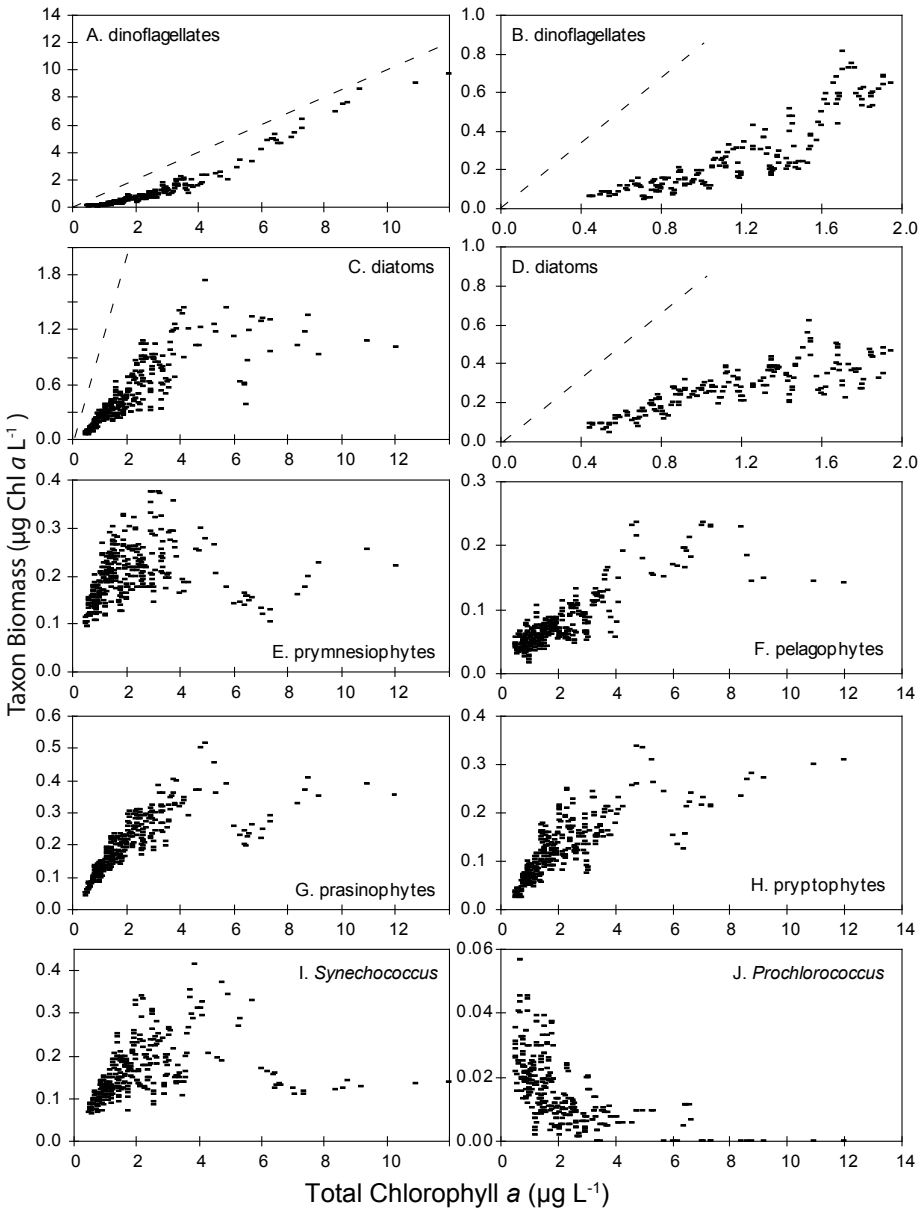

Figure 2. The pigment biomass of different groups of autotrophs off the Scripps Pier plotted against TChl *a*. The abundance of dinoflagellates and diatoms was plotted on entire TChl *a* scale (A, C) and on a reduced TChl *a* scale (B, D) to show variations of abundance at low TChl *a*. The dotted lines represent the 1:1 relationship. All data were subjected to 7-point smoothing to emphasize trends. Examples of unsmoothed data are shown in Figure 3 and 7.

ing pigment biomass for high values of TChl *a* in the case of *Synechococcus* and *Prochlorococcus*. The equations used are assumed to be descriptions of the data; no type of mechanism is implied by the use of any of these functions. These functions were fit to the raw data for the Scripps Pier and other environments (see below). Examples of curve fits are shown in Figure 3. The percent variance explained by these regressions (table 1) was high in most cases; up to 95% for some bloom taxa and on the average 42% for the other groups, with values of up to 75%. However, variance explained by the regressions was low for some groups, particularly *Synechococcus*; reflecting, for the most part, small variations of pigment biomass with TChl *a*. The three-parameter fits for diatoms and cryptophytes off the Scripps Pier suggest that abundance thresholds exist for these taxa, which is confirmed by data from other environments (see below). In the case of dinoflagellates the "threshold" parameter can not be interpreted as such due to the more complicated function used to describe biphasic abundance changes in the 0.4 to 2.0 µg L^{-1} TChl *a* range. Asymptotic values of pigment biomass for the different taxonomic groups differed dramatically at the Scripps Pier, ranging from 0.8 µg Chl L^{-1} for diatoms to 0.06 µg-Chl L^{-1} for *Synechococcus*.

TABLE 1

Parameter estimates for fits of exponential equations to plots of taxon-specific biomass vs. TChl *a* for the five environments studied. For *Prochlorococcus* the equation Biomass = B_{max} (1-EXP(-K_1 (TChl *a* - Threshold)))-K_2 (TChl *a* - Threshold) EXP(-K_3 (TChl *a* - Threshold)^2)) was used. For all other groups Biomass = B_{max} (1-EXP(-K_1 (TChl *a* - Threshold)))-K_2 (1-EXP (-K_3 (TChl *a* - Threshold))) was used. When threshold values for 3-parameter fits were less than 25% of the lowest value of TChl *a*, the threshold value was forced to be zero, which is indicated by 0 values in the table. r^2 designates the variance explained by the regressions. For 5-parameter fits values of "Threshold" are no longer interpretable as a threshold.

Scripps Pier (0.4 - 11.0 µg Chl *a* L^{-1})

	dinoflagel.	diatoms	prymnesiop.	pelagop.	chlorop.	cryptop.	*Synechoc.*	*Prochloro.*
Threshold	–0.030	0.292	0	0	0.128	0	0.050	0.103
B_{max}	90.76	0.802	0.262	0.173	0.195	0.242	0.204	0.015
K_1	0.017	0.455	1.585	0.286	0.673	0.337	1.257	8.380
K_2	6.412	0	0	0	0	0	0.131	–0.090
K_3	0.257	0	0	0	0	0	0.008	5.037
r^2 (%)	86	28	10	39	36	36	9	6

California Current System (0.03 - 10.6 µg Chl *a* L^{-1})

	dinoflagel.	diatoms	prymnesiop.	pelagop.	chlorop.	cryptop.	*Synechoc.*	*Prochloro.*
Threshold	0.090	0.518	0.006	0.061	0.107	0.176	0	0.167
B_{max1}	0.165	78.26	0.133	0.029	0.074	0.365	0.105	0.007
K_1	0.555	0.013	2.587	7.062	1.314	0.274	3.149	6.508
B_{max2}	0	0	0	0	0	0	0.089	–0.324
K_2	0	0	0	0	0	0	1.562	25.29
r^2 (%)	26	95	46	21	64	75	26	51

Southern Indian Ocean (0.02 - 1.44 µg Chl *a* L^{-1})

	dinoflagel.	diatoms	prymnesiop.	pelagop.	chlorop.	cryptop.	cyanobac.	*Prochloro.*
Threshold	0.041	0.027	0	0.015	0.063	0	n.d.	0
B_{max1}	1.389	54.44	0.17	0.180	0.307	0.222	n.d.	1.302
K_1	0.068	0.008	1.070	0.189	1.879	0.172	n.d.	7.408
B_{max2}	0	0	0	0	0	0	n.d.	1.298
K_2	0	0	0	0	0	0	n.d.	6.140
r^2 (%)	73	69	66	73	84	—	—	—

Arabian Sea (0.14 - 1.88 µg Chl *a* L^{-1})

	dinoflagel.	diatoms	prymnesiop.	pelagop.	chlorop.	cryptop.	*Synechoc.*	*Prochloro.*
Threshold	0	0.296	0.025	0.071	0.084	0.187	0	0.010
B_{max1}	0.034	54.07	0.368	0.048	0.104	0.622	0.034	1.289
K_1	1.451	0.009	2.29	5.694	1.399	0.115	109	12.63
B_{max2}	0	0	0	0	0	0	0	1.286
K_2	0	0	0	0	0	0	0	9.533
r^2 (%)	39	68	57	23	25	55	0	45

Sargasso Sea - (0.01 - 0.54 µg Chl *a* L^{-1})

	dinoflagel.	diatoms	prymnesiop.	pelagop.	chlorop.	cryptop.	cyanobac.	*Prochloro.*
Threshold	0.026	0	0	0.016	0.146	n.d.	0	n.d.
B_{max1}	0.004	0.016	2.288	0.659	0.066	n.d.	0.042	n.d.
K_1	144.4	5.121	0.255	0.456	1.444	n.d.	2.356	n.d.
r^2 (%)	54	29	96	90	62	—	19	—

California Current System. To test the generality of these patterns, similar analyses were carried out on pigment data from the mixed layer of the California Current system at stations 5 to ~700 km off the coast of Southern California. Concentrations of TChl *a* usually declined from values of up to 10 µg L^{-1} in eutrophic coastal regions to values of <0.1 µg L^{-1} in oligotrophic offshore regions. The biomass of diatoms, dinoflagellates, cryptophytes and chlorophytes (fig. 4) was negligible when TChl *a* fell below threshold values that ranged from 0.1 to 0.5 µg L^{-1}. No such thresholds were observed for prymnesiophytes, pelagophytes, *Synechococcus* and *Prochlorococcus*. Diatoms were the bloom taxon in this system and dominated phytoplankton biomass when TChl *a* was high (fig. 4). Dinoflagellate biomass in the CCS reached maxium values of less than 1 µg Chl *a* L^{-1}. Chlorophyte and cryptophyte biomass (fig. 4) reached maxium values of ~0.1 and 0.2 µg Chl a L^{-1},

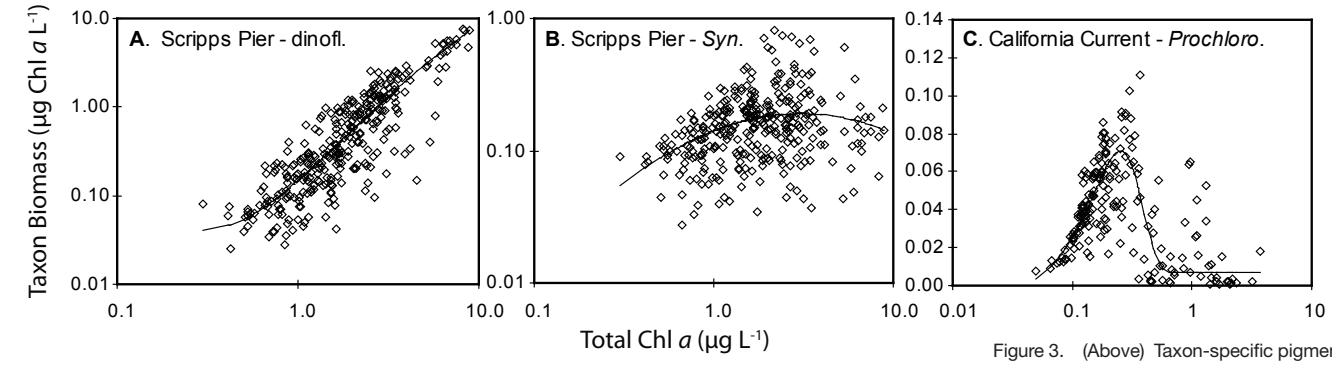

Figure 3. (Above) Taxon-specific pigment biomass plotted against TChl *a* (discrete symbols) and fits of exponential functions (solid lines) to these data for dinoflagellates (A) and *Synechococcus* (B) off the Scripps Pier and *Prochlorococcus* in the California Current system (C). Parameter values for the curves are given in Table 1.

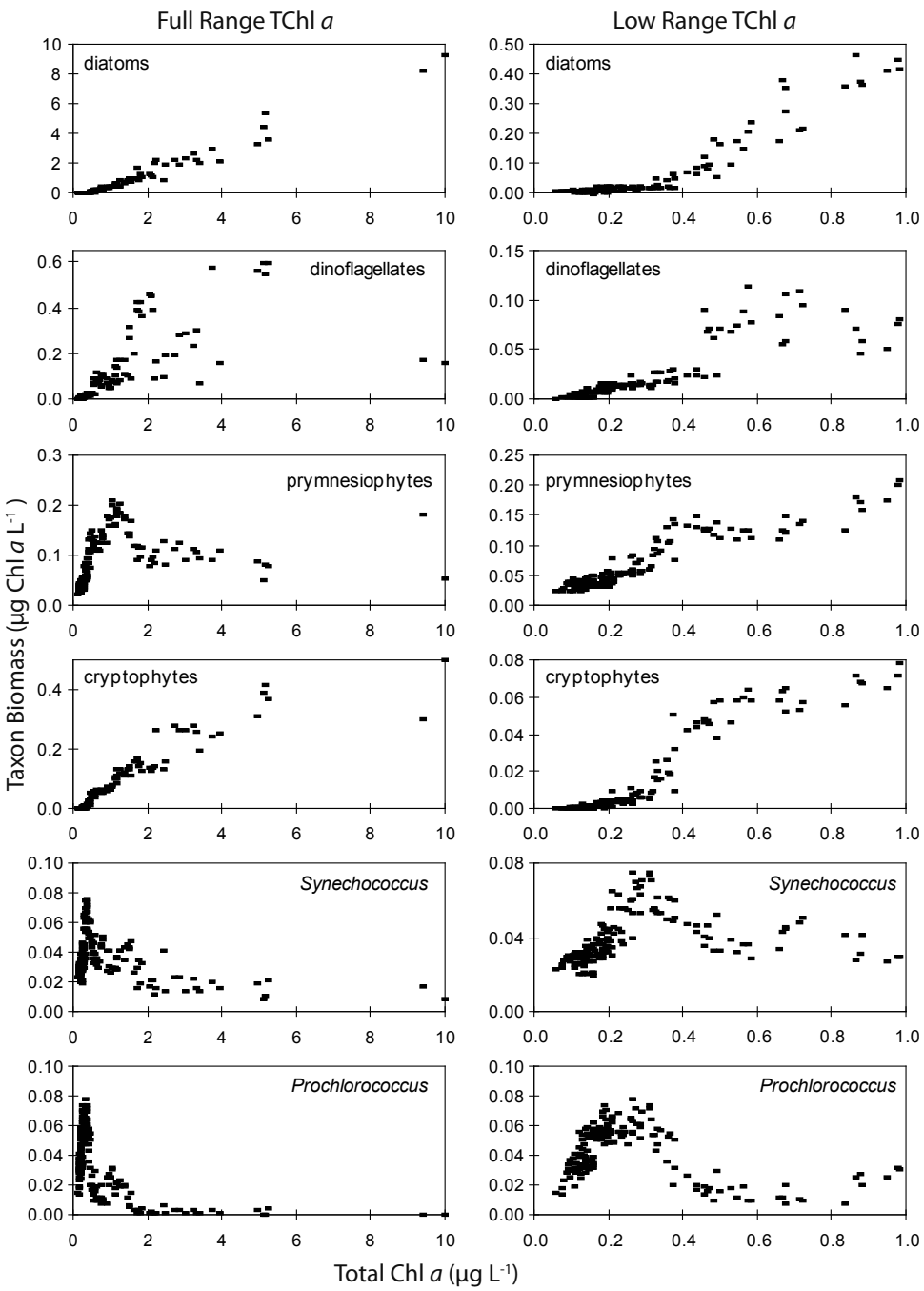

Figure 4. The pigment biomass of selected algal taxa plotted against TChl *a* for the California Current system. All data were subjected to 7-point smoothing. Unsmoothed data for *Prochlorococcus* are shown in Figure 3C. Plots in the left-hand column are for the whole range of TChl *a* values and plots in the right-hand column are for TChl *a* < 1 µg L^{-1}. Note the different scales of the abscissae in the left- and right-hand columns.

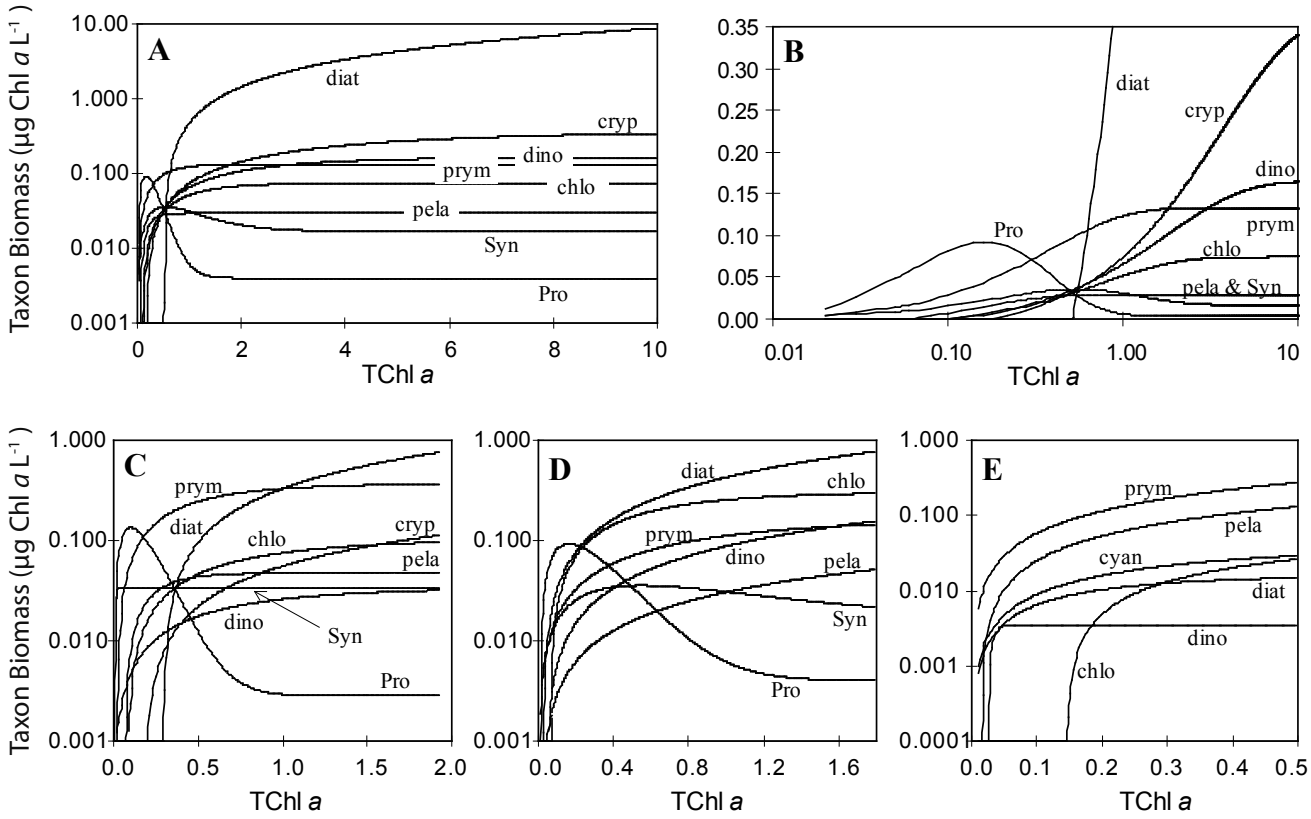

Figure 5. Regressions of pigment biomass of different taxa against TChl *a* for the California Current system (A, B), the Arabian Sea (C), the Southern Indian Ocean (D), and the Sargasso Sea (E). Taxa are diatoms (diat), *Prochlorococcus* (Pro), cryptophytes (cryp), dinoflagellates (dino), prymnesiophytes (prym), chlorophytes (chlo), pelagophytes (pela), *Synechococcus* (Syn) and cyanobacteria (cyan, in case it was not possible to differentiate between Syn and Pro). Note the change of scales of axes between Figure 5A and B. Equations and parameter values for these regressions are given in Table 1.

respectively, when TChl *a* reached values of 3–5 µg L^{-1}. The contributions of *Synechococcus* to TChl *a* increased linearly with TChl *a* up to values of 0.3 µg L^{-1} and decreased above this value (fig. 4). Variations of *Prochlorococcus* biomass with TChl *a* were very similar to variations of *Synechococcus* biomass (fig. 4). Nonlinear regressions of taxon-pigment biomass against TChl *a* accounted for a large fraction of the total variability for most groups (fig. 5A, B; table 1). The predicted abundance of different taxa as a function of TChl *a* is shown in Figure 5 A and B for the California Current system, which illustrate changes of the phytoplankton community as TChl *a* increases. The implication of the plots is that the changes are driven by increasing nutrient loading or nutrient content, sensu Thingstad (1998), of the system. However, observed changes could also be due to geographical differences within the study domain.

Enrichment Experiments. To differentiate between these two possible explanations of the field data, the response of phytoplankton community structure to nutrient enrichments was studied. In October 1996 six experiments were performed in the California Current system with water collected from the mixed layer in regions with undetectable and detectable levels of macronutrients. Moderate phytoplankton blooms were always observed in incubation bottles enriched with ammonium and nitrate, or in samples naturally enriched with nutrients. No blooms were observed in low-nutrient controls or in phosphate enrichments (data to be presented elsewhere). Blooms in incubation bottles were dominated in all cases by diatoms; the biomass of other groups of algae also increased in response to nutrient enrichments but never as rapidly as observed for diatoms. Diatoms did not contribute significantly to TChl *a* when TChl *a* was less than 0.5 µg L^{-1} (fig. 6). This threshold value is similar to values observed in situ (cf. fig. 4). The biomass of all other groups of algae reached maximum values as TChl *a* increased, ranging from 0.03 µg Chl *a* L^{-1} for dinoflagellates to 0.3 µg Chl L^{-1} for prymnesiophytes. In most cases there was a good correspondence, qualitatively, between variations of taxon-specific pigment biomass with TChl *a* for experiments (discrete symbols in fig. 6) and those observed in situ (lines in fig. 6 derived from fits to data shown in fig. 4). The exceptions were cyanobacteria, whose biomass did not decrease as TChl *a* increased, unlike pattern observed in situ (fig. 4).

Other Environments. To explore if biomass distribu-

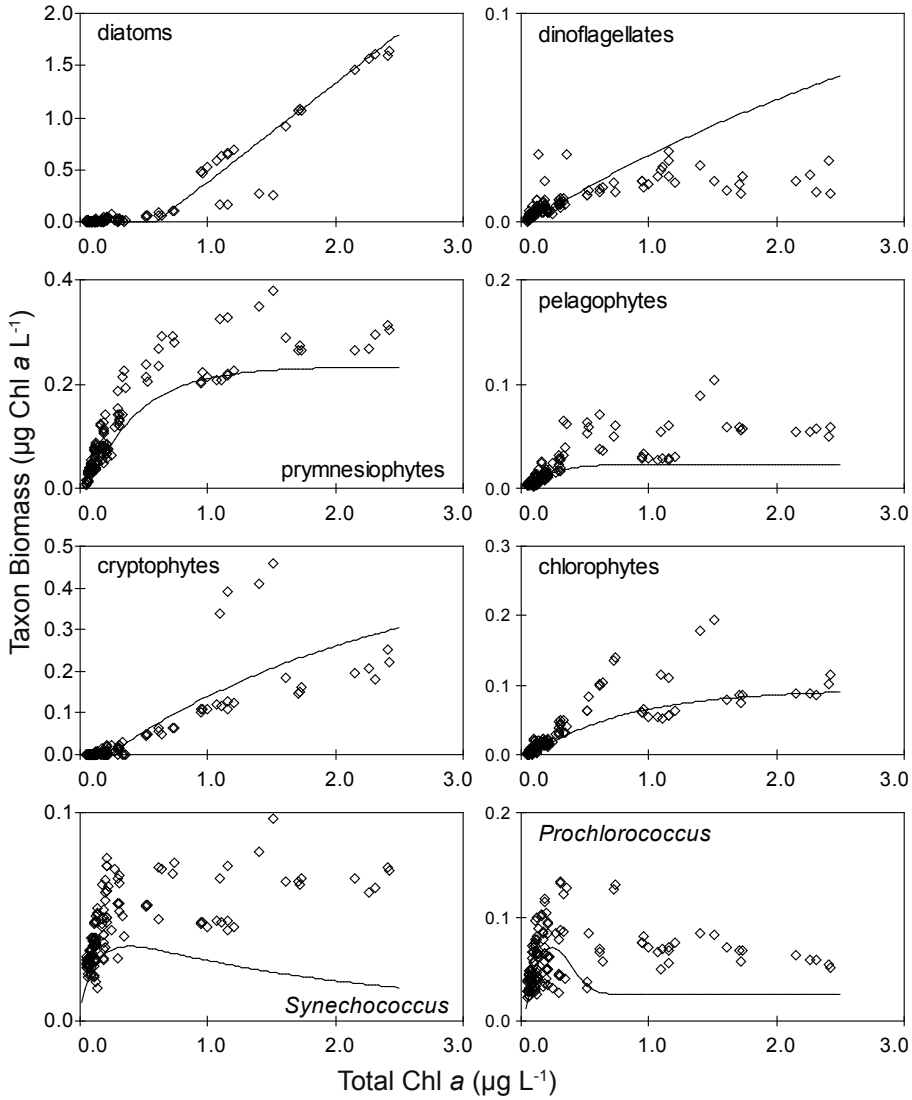

Figure 6. The pigment biomass of selected algal taxa plotted against TChl *a* for nutrient enrichment experiments performed in October 1996 in the California Current system (open diamonds). All experimental time points, i.e., t=0 to t=72 hours, were plotted. Lines are regressions of in situ data from the same time period (samples from the mixed layer collected during CalCOFI cruise 9610); i.e., these are not regressions derived from data points shown here. TChl *a* at time zero ranged from 0.08 to 0.85 µg L^{-1}.

tions in other environments are similar to those found off Southern California, mixed-layer-pigment data sets from the Southern Indian Ocean, the Sargasso Sea and the monsoonal Arabian Sea were analyzed. The pigment biomass of different taxa was determined for these environments (for the Arabian Sea see fig. 8 of Goericke 2002) and data were regressed against TChl *a* (table 1). The observed patterns were qualitatively similar among the different environments, as illustrated in Figure 5 for the complete data sets and in Figure 7 for prymnesiophytes and chlorophytes from different environments. This similarity is also reflected in the parameter values derived from the regressions (table 1). For example, asymptotic values of pelagophyte biomass (B_{max}) ranged from about 0.05 to 0.2 µg Chl L^{-1}, in those environments where it could be estimated accurately; a very narrow range considering that maximal values of TChl *a* ranged from 0.5 to 10 µg L^{-1}. Similarly, values of chlorophyte abundance thresholds and B_{max} (fig. 7) were 0.11 $\pm$ 0.03 and 0.15 $\pm$ 0.10 µg Chl L^{-1}, respectively, in five different environments. In some cases parameter values differ dramatically between environments for any one group. Examples are parameters describing diatom and dinoflagellate distributions.

DISCUSSION

Describing Phytoplankton Community Structure. The structure of the phytoplankton community was explored using taxonomic units as defined by taxon-specific pigments. The data presented here and physiological data

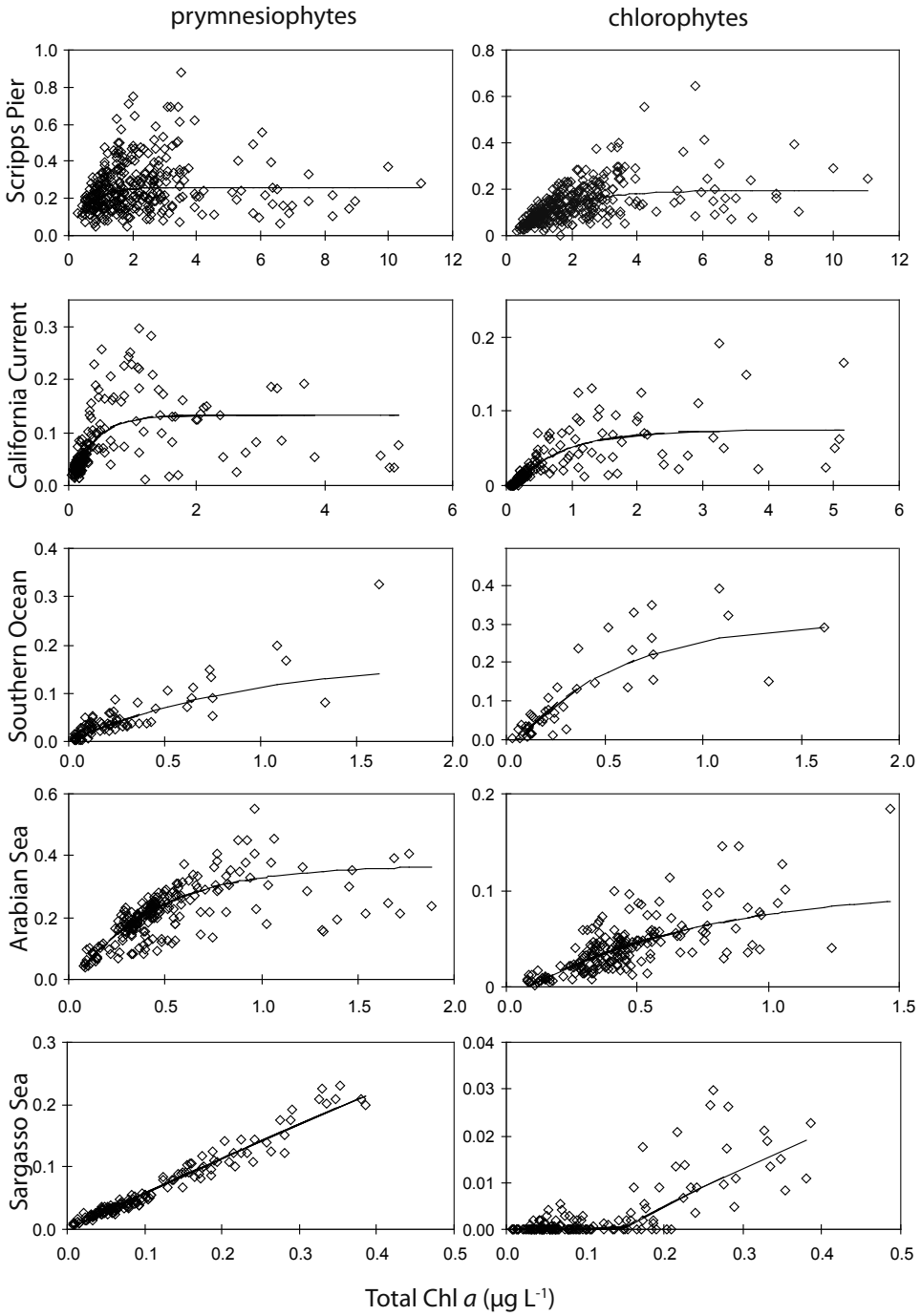

Figure 7. Prymnesiophyte and chlorophyte pigment biomass plotted against TChl *a* for the Scripps Pier, the California Current system, the Southern Indian Ocean, the monsoonal Arabian Sea (open ocean stations only) and the Sargasso Sea (BATS Station). Data were not smoothed.

presented by others (e.g., Claustre 1994; Latasa et al. 1997; Goericke 1998; Brown et al. 2002; Goericke 2002) demonstrate that these broad pigment-defined taxonomic categories are functionally and ecologically distinct units. The abundance of these groups off the Scripps Pier, in the California Current system, the Arabian Sea, the Sargasso Sea and the Southern Indian Ocean (Goericke 2002, this study) varied predictably as a function of TChl *a* and varied coherently along transects more than 1000 km long. Distributional patterns differed significantly among groups. In the Arabian Sea growth rates of these groups, measured using the pigment labeling method, varied predictably as a function of a proxy for the availability of inorganic nitrogen and also differed significantly among groups (Goericke 2002). Indeed, these data show that categories delineated by

taxon-specific pigments are one solution to the aggregation problem (O'neill et al. 1986) which has baffled phytoplankton ecologists for the last century; i.e., How can a phytoplankton community be partitioned into functionally relevant aggregates that are more amenable to study than the 100s of species it consist of?

The interpretation of patterns observed in the field is not straightforward since TChl *a* varied in many environments as a function of latitude and/or distance from shore and, associated with that, temperature. The observed distributions could simply reflect the presence of different phytoplankton communities in different regions of the study domain or the advection of different water masses with differing phytoplankton communities into specific regions. However, an underlying assumption of the approach is that observed changes within any study domain are similar to changes that would occur if an enrichment of the system occurred at that point. The enrichment experiments that were performed in the California Current system and the grow-out experiments performed in the Arabian Sea (Goericke 2002) are tests of this assumption. Indeed, changes of phytoplankton community structure with TChl *a* observed over the course of these experiments in the California Current system (fig. 6) and the Arabian Sea (fig. 10 of Goericke 2002) were qualitatively and, for the most part, quantitatively very similar to observations in the field. Thus, results from these experiments demonstrate that differences in phytoplankton community structure observed over the whole study domain can also occur at any one point of the study domain when an enrichment of the system occurs.

What are the Patterns—Are there Rules? The variability of autotroph biomass off the Scripps Pier was primarily due to blooms of dinoflagellates and to some extent diatoms, i.e., the larger autotrophs that contributed 81% to the variability of TChl *a* over time (fig. 1E). Their contributions to TChl *a* ranged from 0.04 to 10 μg L^{-1}, in strong contrast to the contributions of prymnesiophytes, pelagophytes, chlorophytes, cryptophytes and cyanobacteria, i.e., the "picoplankters" (fig. 1F), whose contributions ranged from 0.2 to 1.8 μg Chl a L^{-1}. Seasonal variability off the Scripps Pier is similarly dominated by larger autotrophs; while seasonal variation of picoautotroph biomass is small. A striking aspect of the data from the Scripps Pier is the absence of any obvious correlation between the bloom periods of the larger autotrophs and the abundance of picoautotrophs. Indeed, the abundance of picoautotrophs is not significantly related to the abundance of larger autotrophs for TChl *a* > 1 μg L^{-1}. These results do not imply that some picoautotrophs do not go through bloom periods. At times *Synechococcus* biomass increased more than 5-fold over average values; eustigmatophyceae (fig. 1C, Sept. 1997) are another good example. However, these blooms of picoautotrophs were not large contributors to the variability of total biomass.

Results from the California Current system, the Arabian Sea and the Southern Indian Ocean are strikingly similar: The variability of phytoplankton biomass in these oceanic regions was dominated by diatoms while the biomass of all other groups saturated at specific levels, often significantly lower than values of TChl *a*. Malone (1971), Mullin (1998; 2000) and Anderson et al. (2008) similarly noted that variations of pigment biomass in the California Current were primarily driven by larger size classes. Claustre (1994), based on the analysis of pigment samples from the North Atlantic and the Mediterranean Sea, also found that the variability of pigment biomass was dominated by diatoms and dinoflagellates. These results support the rule that picoautotrophs are the ever-present lawn of the ocean, on which the occasional, large tree, the diatom or dinoflagellate bloom, is found that supports orders of magnitude higher levels of autotroph biomass (Chisholm 1992; Li 2002; Goericke 2011). This rule implies that the variability of autotroph biomass in the ocean is dominated by larger autotrophs, diatoms in most cases. It is likely that this rule also applies to other environments that are similar to the ones studied. But this rule is clearly not universally valid. For example, blooms of the picoautotroph *Chrysochromolina* sp. have been observed off the west coast of Sweden and blooms of the prymnesiophytes *Pheocystis pouchetii* and *Emiliania huxleyi* are known to occur in many regions of the world's ocean. These exceptions do not invalidate the proposed rules, as rules are only persistent patterns with possible or known exceptions; rules without possible exceptions are laws. The existence of such rules is important for our understanding of the ocean, as their existence implies that the mechanisms that control or generate these patterns are the same, or at least similar, in different environments.

Detailed size-fractionation experiments performed in the Mediterranean Sea suggested that the amount of TChl *a* in the <1, <3, and <10 μm size fractions have upper bounds of 0.5, 1, and 2 μg L^{-1}, and that Chl *a* is added to the system by first completing the "quotas" of the smallest size class before filling the next one (Raimbault et al. 1988). Thus, contributions of different size classes to TChl *a* are thought to display saturation patterns with differing maximum contributions to TChl *a*. Since specific phytoplankton taxa are often associated with distinct size classes (Chisholm 1992), similar saturation patterns were expected for plots of the abundance of different taxa against TChl *a*, which was indeed observed (fig. 2, 4 and Goericke 2002). Common to all environments studied so far is the presence of a bloom taxon—dinoflagellates off the Scripps Pier

and diatoms in the California Current system, the Arabian Sea and the Southern Indian Ocean. The Arabian Sea was unusual since blooms did not occur offshore in spite of high growth rates and replete nutrients. However, diatom blooms were observed in incubation bottles and close to the coast, suggesting that diatom abundance offshore was controlled by grazers, i.e., top-down forces (Goericke 2002). The abundance of other taxa in all these environments covaried with TChl *a* at low values, but leveled off to constant values as TChl *a* increased to values larger than 1 to 4 μg L^{-1}. The average maximum biomass reached by some of the taxa, e.g., cryptophytes, pelagophytes, and chlorophytes, was surprisingly similar in most environments (table 1). Similarly, some of the taxa consistently had abundance thresholds, which also were similar in the different environments; examples are chlorophytes and cryptophytes (table 1).

Whereas distributions of eukaryotes were, for the most part, characterized by simple saturating functions with or without abundance thresholds, variations of *Synechococcus*, and in particular *Prochlorococcus* biomass with TChl *a* were characterized by initial increases, maximum biomass at low levels of TChl *a*, followed by decreases as TChl *a* reached high values. In the Arabian Sea this decrease was only in part related to temperature, since a similar decrease was observed during grow-out experiments at constant temperature (Goericke 2002). High levels of TChl *a* in the California Current system were also related to low temperatures, likely accounting for some of the observed decrease of *Prochlorococcus* biomass. However, such a decrease, albeit not as strong, was observed as TChl *a* increased during nutrient enrichment experiments, suggesting that it is also driven by community processes. The decrease of *Synechococcus* biomass for high values of TChl *a* was less pronounced, but still evident, off the Scripps Pier and in the California Current system. Claustre (1994) observed similar patterns for pigments likely derived from cyanobacteria in the North Atlantic and the Mediterranean.

Predicting the Patterns. Time series of taxon-specific pigment biomass (e.g., fig. 1) reflect the short-term variability of phytoplankton biomass, which is likely driven by varying rates of nutrient-autotroph and autotroph-heterotroph interactions. Understanding such patterns is possible in principle; however, making predictions of these over large spatial or temporal scales is virtually impossible. The problem is quite similar to that faced by meteorologists: Weather can only be predicted over short temporal scales. However, climate, which is weather expected on the average, can accurately be specified for particular times of the year or for specific conditions, such as an El Niño, as long as historical weather records are available. The approach proposed here is quite similar: It is suggested that relationships between taxon-specific biomass and TChl *a* are used to predict the composition of the community for any value of TChl *a*. Or rephrased, it is proposed that such relationships be used to characterize the "ecological climate", realizing that such relationships can not be used to predict the "ecological weather".

The quantitative relationships derived here (e.g., fig. 6) will allow us more accurate descriptions, predictions and explanations. For example, studies off Bermuda noted that spring phytoplankton blooms were not dominated by diatoms (Goericke 1998; Steinberg et al. 2001), even though this was the case during the late 1950s (Hulburt et al. 1960; Menzel and Ryther 1960). This could be interpreted as a change of the phytoplankton community over the last few decades. However, when diatom blooms were observed during the late 1950s, surface layer Chl *a* was at least 1 μg L^{-1}; recently only values of up to 0.5 μg Chl *a* L^{-1} were observed (Goericke 1998; Steinberg et al. 2001). A comparison of the Sargasso Sea biomass plot (fig. 5E) with those from other regions (e.g., fig. 5A) suggests that values of TChl *a* in the Sargasso Sea never reached likely threshold levels for diatoms (~0.5 μg Chl *a* L^{-1}) to contribute significantly to TChl *a*. Observations made in eddies off Bermuda (Ewart et al. 2008) and in other oligotrophic environments (Brown et al. 2002) corroborate this interpretation.

Some of the observed distributions of non-bloom taxa are strongly related to TChl *a*; regressions of pigment biomass for some taxa against TChl *a* explain up to 70% of the variance in the data sets. It is straightforward using these relationships to predict the abundance of those groups of autotrophs to TChl *a* with a high degree of confidence. Variance explained by the regressions is very low for other taxa though, particularly *Synechococcus*. This result, however, does not imply that the biomass of these groups cannot be predicted; it only implies that the abundance of these groups is relatively invariant in these environments. Powerful predictions can still be derived from such relationships, as is the case for the monsoonal Arabian Sea were the expected pigment biomass of *Synechococcus* is 0.04 μg Chl L^{-1} with a standard error of 0.02 μg Chl L^{-1} for TChl *a* ranging from 0.1 to 1.8 μg L^{-1}.

The data presented here constitute a very simple means to predict phytoplankton community structure from TChl *a*. The relationships between taxon-specific biomass and TChl *a* can be described using functions with 2 to 5 free parameters. Considering that TChl *a* can be remotely sensed, or is a standard product of coupled biological-physical models, such relationships may be the simplest means to incorporate phytoplankton community structure into biophysical models that cannot be burdened with detailed descriptions of the interactions between different taxa of autotrophs and different classes

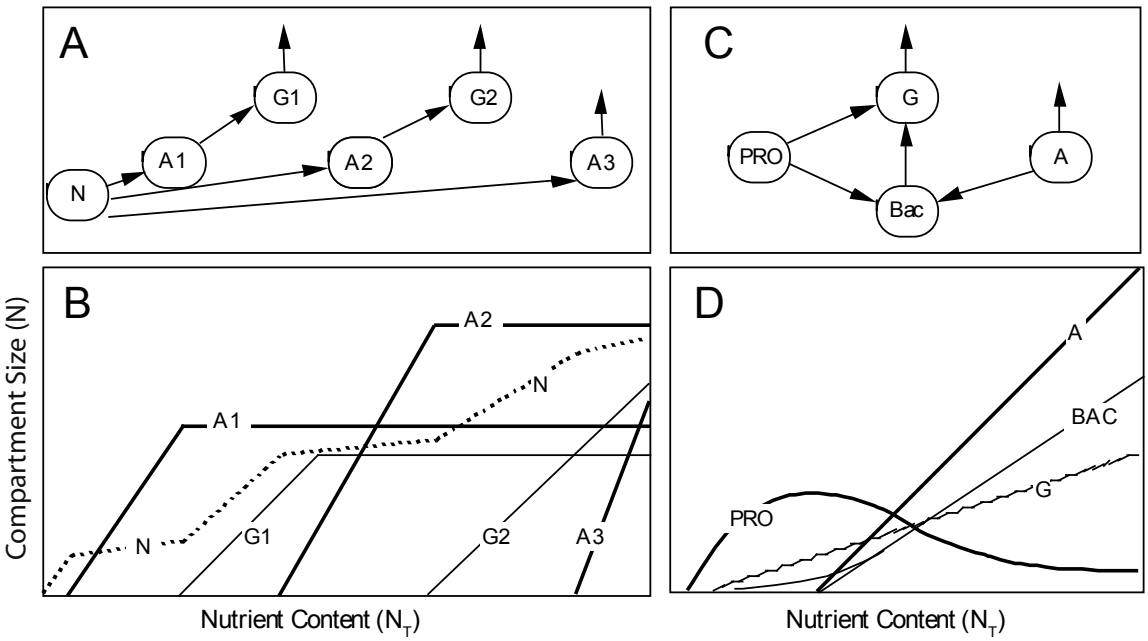

Figure 8. Food web diagrams and predicted biomass variations as a function of a system's nutrient content (N_T). A. Food web consisting of one nutrient pool (N), three autotrophs (A1, A2, A3) and two grazers (G1, G2). B. Variations of predicted nutrient concentrations and autotroph and grazer biomass as a function of N_T for the system shown in A (adapted from Thingstad, 1998). C. A food web showing interactions between *Prochlorococcus* (PRO), one grazer (G), heterotrophic bacteria (BAC) and other autotrophs (A). D. Biomass variations of autotrophs (PRO, A), heterotrophic bacteria (BAC) and a grazer (G) as a function of nutrient content for the system shown in C.

of grazers. Clearly, such models would not contribute to our understanding of the controls of phytoplankton community structure, but these models could contribute to our understanding of the effects of phytoplankton community structure on carbon cycling. Critical to such approaches to modeling is a good understanding of the limitations of such data sets. For example, the different distributions observed off Southern California in the nearshore and the California Current system suggest that nearshore communities differ fundamentally from coastal oceanic communities (see also Goericke 2002). Clearly, it is necessary to characterize nearshore, coastal and oceanic phytoplankton communities in greater detail. A second example is distributions for cyanobacteria that suggest that temperature may exert important secondary effects on phytoplankton community structure. Taking this into account might allow us to better describe and predict of variations of phytoplankton community structure in the ocean. Unfortunately, the data in hand do not allow us to do this since temperature and phytoplankton biomass are too strongly related (data not shown).

What are the Mechanisms? Marine pelagic communities are likely never at steady state, due to continuously varying physical forcing. Thus it is practically impossible to predict the state of the community accurately at any point of time or space. Instead one can attempt to understand and predict the average state of pelagic communities. Plotting the abundance of different taxa against TChl *a* and calculating the average distributions (fig. 5) conveys such an average state of the system. A conceptual model that allows us to understand the average state of pelagic communities has been proposed by Thingstad (1998). Thingstad's models are centered on the control that the "nutrient content" of the photic zone exerts on the size structure of the phytoplankton community. In this context "nutrient" refers to that element that limits total biomass in the system, or at least the biomass of most compartments of the system. The nutrient content (N_T) of the system is the sum of the concentrations of this element in all compartments of the system. Increasing the flux of this *critical* nutrient into the photic zone is expected to increase total standing stock of the organisms.

For this study, TChl *a* is used as an index of phytoplankton biomass. Relationships between TChl *a* and phytoplankton biomass are variable but predictable (Geider et al. 1996; Goericke and Montoya 1998). Phytoplankton biomass can be assumed to covary roughly within any one environment with the biomass of other trophic levels (Sheldon et al. 1977; Sprules and Munawar 1986). Thus, it is possible to view TChl *a* in this context as a proxy for N_T and to interpret varying TChl *a*, at least on the average, as varying fluxes of the critical nutrient into the system. Even though it can and should not be assumed that the relationship between TChl *a* and N_T is linear, it is quite likely that the relationship between the two parameters is governed by a monotonically increasing function.

Thingstad's conceptual model (1998) predicts biomass variations of different size classes of autotrophs with increasing N_T that are strikingly similar to biomass variations of different taxa with TChl *a* (cf. fig. 5). Thingstad assumes that the system is at steady state and discusses changes of the community as N_T increases. Thus, the focus of Thingstad's analysis is not the transients that result when fluxes of a nutrient into a system are increased; rather it is how the steady state of an ideal system changes as a function of N_T. When N_T is zero, organisms, by definition, do not exist. When N_T increases, the first organism capable of growing must be that autotroph (A1) that has the highest affinity for the critical nutrient (N). This will be the smallest autotroph capable of living in the system (fig. 8A, B). Data presented here and those discussed by others (e.g., Campbell et al. 1994) support this prediction since *Prochlorococcus*, the smallest known photoautotroph (Chisholm et al. 1992), dominates phytoplankton abundance when TChl *a* is extremely low (fig. 5). Further increasing N_T increases the biomass of the autotroph A1.

The presence of A1 opens a niche for a grazer (G1) capable of feeding on A1. As N_T increases the biomass of A1 and G1 will increase as well. Thingstad postulated that the dynamics of the predator-prey pair will increasingly be decoupled from the availability of N; i.e., eventually reaching a stable equilibrium or exhibiting stable limit cycles (e.g., May 1981). At this point the biomass of A1 and G1 will be independent of N_T and will remain constant, at least when averaged over appropriate time periods. Thus, the predicted dependence of A1 on N_T is linear for low values of N_T, but eventually levels off and reaches a constant value at high values of N_T. The predicted patterns (fig. 8B) are similar to variations of observed taxon-specific biomass with TChl *a* (fig. 5). A corollary of the conceptual model is that autotroph division rates will be maximal, i.e. unconstrained by the availability of inorganic nutrients, once the biomass no longer increases with N_T. This implies that plots of biomass variations (e.g., fig. 2) could be used to determine when groups of autotrophs are expected to grow at rates close to their physiological maxima; a hypothesis that still has to be tested.

As the biomass of A1 and G1 becomes increasingly independent of N_T, further increases of N_T opens a niche for a second, larger autotroph (A2). The abundance of A2, when plotted against N_T, will display a threshold similar to those observed for chlorophytes, cryptophytes and diatoms in the California Current system (fig. 4). The increase of A2 opens a niche for a second grazer G2. As N_T further increases the biomass of A2 and G2, they will reach constant levels when their rates of growth and loss are, on the average, balanced. Further increases of N_T will open a niche for a third, yet larger, autotroph A3, etc. The predicted variations of A1, A2 and A3 abundance with N_T (fig. 8B) are very similar to field data presented above (fig. 5). The progressive waves of autotrophs and grazers will come to an end once a mismatch arises between the response time scales of the autotrophs to increasing levels of nutrients and the response time scales of the grazers to increasing biomass of larger autotrophs (e.g., Franks 2001). This state is usually reached once the grazers are crustaceans. Whereas maximum growth rates of protozoa overlap those of their prey (e.g., Fenchel and Finlay 1983), maximum growth rates of crustacean grazers are roughly one order of magnitude less than that of their prey (Banse 1982). Thus, blooms of large autotrophs are expected once a mismatch has been established between the response time scales of the prey and predator.

The characteristic feature of the model is, as noted by Thingstad (1998), that strong top-down forces limit the biomass of smaller autotrophs and open up niches for larger autotrophs. Even though total phytoplankton biomass may be limited by the availability of a critical nutrient, i.e., by bottom-up effects, the biomass of most individual taxa is controlled by grazers, i.e., top-down forces, except for the largest taxon that form blooms. Clearly, there are differences between the predictions of the idealized model of Thingstad (1998) and the field data. The field data do not show a staggered succession of autotrophs; rather, new taxa of autotrophs appear before the biomass of those taxa, that are already present, has saturated. This is no surprise; the above predictions were only based on the presence of a single nutrient and no interactions between herbivores or grazing of herbivores on multiple autotroph taxa were considered. It is quite conceivable that other environmental factors and additional biological interactions exert secondary effects, which open up niches for other autotrophs. Even though these differences exist between the predicted and observed patterns, the predictive capabilities of the conceptual model are surprising once the similarities of patterns shown in Figure 5 and Figure 8B are considered.

The only pattern that is not predicted by the model is the decline of the biomass of *Prochlorococcus* for large values of TChl *a*. It was discussed above that temperature effects could have been partially responsible for this phenomenon. However, since such a decline was also observed at constant temperatures during grow-out experiments in the Arabian Sea, it is worth analysis in this context. The observed simple saturation patterns for other autotrophs can be attributed to the establishment of a balance between a predator and a prey: At high TChl *a* the predator's carrying capacity is set by prey biomass which no longer increases as TChl *a* increases. However, the cell size of *Prochlorococcus* is similar to the size of marine heterotrophic bacteria and it is likely that

some herbivores that graze on *Prochlorococcus*, e.g., heterotrophic or mixotrophic flagellates or ciliates (Christaki et al. 1999; Guillou et al. 2001; Frias-Lopez et al. 2009), also graze on heterotrophic bacteria (fig. 8C). The biomass of bacteria is expected to increase as total autotroph biomass increases, since all autotrophs directly or indirectly produce dissolved organic carbon on which bacteria depend for growth (fig. 8D). Thus, the biomass of bacterial grazers is expected to increase with TChl *a* as well. Since it is likely that these also graze on *Prochlorococcus*, grazing pressure on *Prochlorococcus* is expected to increase with increasing autotroph biomass, even if *Prochlorococcus* biomass has leveled off. A consequence of the increasing grazing pressure and constant division rates will be a decline of the biomass of *Prochlorococcus* at high TChl *a*, as observed in the field data (fig. 5). Thus, the decline in the abundance of *Prochlorococcus* with larger values of TChl *a* is likely due to a decoupling of predator-prey dynamics between *Prochlorococcus* and its grazers due to the availability of other prey for these.

To conclude, this study has both important practical and theoretical implications. The observed patterns allow us to predict the response of phytoplankton communities to changes in ocean climate, for example those associated with global climate change. Those predictions are more akin to predictions of ecological climate rather than forecasts of ecological dynamics. An important theoretical implication is the empirical confirmation of Thingstad's (1998) model at the level of taxonomic groups. These results suggest that forcing of phytoplankton community structure by either bottom-up or top-down forces does not occur. Phytoplankton community structure is controlled by a balance between those, and likely other, forces. The results also imply that the microbial loop in places covered by this study is mostly at a steady state that varies in a predictable manner with rates of nutrient input to the system. Data based on rate measurements, not only standing stocks of biomass, that support these arguments were also presented by Goericke & Welschmeyer (1998) and Goericke (2002). These conclusions support the arguments of Banse (1992; 1995) and Verity and Smetacek (1996), who have argued that predation is a powerful, and often neglected, force in the marine environment.

ACKNOWLEDGMENTS

I am grateful to the crews of the R/V *Revelle* and *New Horizon* for support at sea, Amy Shankle, Maria Mendez and Connie Fey for pier sampling, and to Jason Pearl for help in the lab. K. Banse, M. Roadman, B. Palenik, E. Venrick and three anonymous reviewers are thanked for their critical and helpful comments on the manuscript. The research was supported by a grant from ONR (N00014-98-1-005) and NSF (OCE-01018038).

LITERATURE CITED

Anderies, J. M., and B. E. Beisner. 2000. Fluctuating environments and phytoplankton community structure: A stochastic model. Am. Nat. 155:556–569.

Anderson, C. R., D. A. Siegel, M. A. Brzezinski, and N. Guillocheau. 2008. Controls on temporal patterns in phytoplankton community structure in the Santa Barbara Channel, California. J. Geophys. Res.-Oceans 113:16.

Banse, K. 1982. Mass-scaled rates of respiration and intrinsic growth in very small invertebrates. Mar. Ecol. Prog. Ser. 9:281–297.

Banse, K. 1992. Grazing, temporal changes in phytoplankton concentrations, and the microbial loop in the open sea, p. 409–440. *In* P. G. Falkowski and A.D. Woodhead [eds.], Primary productivity in the sea. Plenum.

Banse, K. 1995. Zooplankton: Pivotal role in the control of ocean production. ICES J. mar. Sci. 52:265–277.

Bissett, W. P., J. J. Walsh, D. A. Dieterle, and K. L. Carder. 1999. Carbon cycling in the upper waters of the Sargasso Sea: I. Numerical simulation of differential carbon and nitrogen fluxes. Deep-Sea Res. I 46:205–269.

Brown, S. L. and others 2002. Microbial community dynamics and taxon-specific phytoplankton production in the Arabian Sea during the 1995 monsoon seasons. Deep-Sea Res. II 49:2345–2376.

Campbell, L., H. A. Nolla, and D. Vaulot. 1994. The importance of *Prochlorococcus* to community structure in the central North Pacific Ocean. Limnol. Oceanogr. 39:954–961.

Chisholm, S. W. 1992. Phytoplankton size, p. 213–237. *In* P. G. Falkowski and A. D. Woodhead [eds.], Primary productivity and biogeochemical cycles in the sea. Plenum.

Chisholm, S. W. and others. 1992. *Prochlorococcus marinus* nov. gen. nov. sp.: an oxyphototrophic marine prokaryote containing divinyl chlorophyll *a* and *b*. Arch. Microbiol. 157:297–300.

Christaki, U. and others. 1999. Growth and grazing on *Prochlorococcus* and *Synechococcus Limnol Oceanogr* 44:52–61.

Claustre, H. 1994. The trophic status of various oceanic provinces as revealed by phytoplankton pigment signatures. Limnol. Oceanogr. 39:1206–1210.

Denman, K. L. 2003. Modelling planktonic ecosystems: parameterizing complexity. Prog. Oceanogr. 57:429–452.

Ewart, C. S. and others. 2008. Microbial dynamics in cyclonic and anticyclonic mode-water eddies in the northwestern Sargasso Sea. Deep-Sea Research Part Ii-Topical Studies in Oceanography 55:1334–1347.

Fenchel, T., and B. J. Finlay. 1983. Respiration rates in heterotrophic, free-living protozoa. Microb. Ecology 9:99–122.

Francois, R. and others. 1993. Changes in the $\delta^{13}C$ of surface water particulate organic matter across the subtropical convergence in the S. W. Indian Ocean. Global Biogeochem. Cycles 7:627–644.

Franks, P. J. S. 2001. Phytoplankton booms in a fluctuating environment: the roles of plankton response time scales and grazing. J. Plank. Res. 23:1433–1441.

Frias-Lopez, J., A. Thompson, J. Waldbauer, and S. W. Chisholm. 2009. Use of stable isotope-labelled cells to identify active grazers of picocyanobacteria in ocean surface waters. Environ. Microbiol. 11:512–525.

Friedrichs, M. A. M. and others. 2007. Assessment of skill and portability in regional marine biogeochemical models: Role of multiple planktonic groups. J. Geophys. Res.-Oceans 112:22.

Geider, R. J., H. L. Mcintyre, and T. M. Kana. 1996. Dynamic model of phytoplankton growth and acclimation: Responses of the balanced growth rate and the chlorophyll *a* : carbon ratio to light, nutrient-limitation and temperature. Mar. Ecol. Prog. Ser. 148:187–200.

Goericke, R. 1998. Response of phytoplankton community structure and taxon-specific growth rates to seasonally varying physical forcing at a station in the Sargasso Sea off Bermuda. Limnol. Oceanogr. 43:921–935.

Goericke, R. 2002. Top-down control of phytoplankton biomass and community structure in the monsoonal Arabian Sea. Limnol. Oceanogr. 47:1307–1323.

Goericke, R. 2011. The size structure of marine phytoplankton communities—What are the rules? CalCOFI Reports in press.

Goericke, R., and J. Montoya. 1998. Estimating the contribution of microalgal taxa to chlorophyll *a* in the field–variations of pigment ratios under nutrient- and light-limited growth. Mar. Ecol. Prog. Ser. 169:97–112.

Goericke, R., R. J. Olson, and A. Shalapyouok. 2000. A novel niche for *Prochlorococcus* sp. in low-light suboxic environments in the Arabian Sea and the Eastern Tropical North Pacific. Deep-Sea Res. I 47:1183–1205.

Goericke, R., and N. A. Welschmeyer. 1998. Response of Sargasso Sea phytoplankton biomass, growth rates, and primary production to seasonally varying physical forcing. J. Plankton Res. 20:2223–2249.

Guillou, L., S. Jacquet, M. J. Chretiennot-Dinet, and D. Vaulot. 2001. Grazing impact of two small heterotrophic flagellates on *Prochlorococcus* and *Synechococcus*. Aquat. Microb. Ecol. 26:201–207.

Hulburt, E. M., J. M. Ryther, and R. R. L. Guillard. 1960. The phytoplankton of the Sargasso Sea off Bermuda. J. Con. Int. Explor. Mer. 25:115–128.

Jeffrey, S. W., R. F. C. Mantoura, and S. W. Wright. 1997. Phytoplankton pigments in oceanography. UNESCO Publishing.

Latasa, M., M. R. Landry, L. Schlüter, and R. R. Bidigare. 1997. Pigment-specific growth and grazing rates of phytoplankton in the equatorial Pacific. Limnol. Oceanogr. 42:289–298.

Letelier, R. M. and others. 1993. Temporal variability of phytoplankton community structure based on pigment analysis. Limnol. Oceanogr. 38:1420–1437.

Li, W. K. W. 2002. Macroecological patterns of phytoplankton in the northwestern North Atlantic Ocean. Nature 419:154–157.

Litchman, E. and others. 2006. Multi-nutrient, multi-group model of present and future oceanic phytoplankton communities. Biogeosciences 3:585–606.

Macintyre, J. G., J. J. Cullen, and A. D. Cembella. 1997. Vertical migration, nutrition and toxicity in the dinoflagellate *Alexandrium tamarense*. Mar. Ecol. Prog. Ser. 148:201–216.

Mackey, M. D., D. J. Mackey, H. W. Higgins, and S. W. Wright. 1996. CHEMTAX—a program for estimating class abundances from chemical markers: application to HPLC measurements of phytoplankton. Mar. Ecol. Prog. Ser. 144:265–283.

Malone, T. C. 1971. The relative importance of nanoplankton and netplankton as primary producers in tropical oceanic and neritic phytoplankton communities. Limnol. Oceanogr. 16:633–639.

Margalef, R. 1978. Life-forms of phytoplankton as survival alternatives in an unstable environment. Oceanol. Acta 1:493–509.

May, R. M. 1981. Models for two interacting populations, p. 78–104. *In* R. M. May [ed.], Theoretical Ecology. Sinauer Assoc.

Menzel, D. W., and J. H. Ryther. 1960. The annual cycle of primary production in the Sargasso Sea off Bermuda. Deep-Sea Res. 6:351–367.

Michaels, A. F., and M. W. Silver. 1988. Primary production, sinking fluxes and the microbial food web. Deep-Sea Res. 35:473–490.

Moore, J. K. and others. 2002. An intermediate complexity marine ecosystem model for the global domain. Deep Sea Research II 403–462.

Mullin, M. M. 1998. Biomasses of large-celled phytoplankton and their relation to the nitricline and grazing in the California Current system off Southern California, 1994–1996. CalCOFI Reports 39:117–123.

Mullin, M. M. 2000. Large-celled phytoplankton, the nitricline, and grazing during the California 1997–98 El Niño. CalCOFI Reports 41:161–166.

O'neill, R. V., D. L. Deangelis, J. B. Waide, and T. F. H. Allen. 1986. A hierarchical concept of ecosystems. Princeton Univ. Press.

Raimbault, P., M. Rodier, and I. Taupier-Letage. 1988. Size fraction of phytoplankton in the Ligurian Sea and the Algerian Basin (Mediterranean Sea): Size distribution versus total concentration. Mar. Microb. Food Webs 3:1–7.

Scripps Institution of Oceanography. 1997. Physical, Chemical and Biological Data, CalCOFI cruises 9607 and 9610.

Sheldon, R. W., W. H. Sutcliffe, Jr., and M. A. Paranjape. 1977. Structure of pelagic food chain and relationship between plankton and fish production. J. Fish. Res. Board Can. 34:2344–2353.

Smayda, T. J. 1980. Phytoplankton species succession, p. 493–570. *In* I. Morris [ed.], The physiological ecology of phytoplankton. Blackwell.

Smetacek, V. 1999. Diatoms and the ocean carbon cycle. Protist 150:25–32.

Sprules, W. G., and M. Munawar. 1986. Plankton size spectra in relation to ecosystem productivity, size, and perturbation. Can. J. Fish. Aquat. Sci. 43:1789–1794.

Steinberg, D. K. and others. 2001. Overview of the US JFOFS Bermuda Atlantic Time-series Study (BATS): a decade-scale look at ocean biology and biogeochemistry. Deep-Sea Res. II 48:1405–1447.

Thingstad, T. F. 1998. A theoretical approach to structuring mechanisms in the pelagic food web. Hydrobiologia 363:59–72.

Tyrrell, T., P. Holligan, and C. Mobley. 1999. Optical impacts of oceanic coccolithophore blooms. J. Geophys. Res. 104:3223–3242.

Venrick, E. L. 1982. Phytoplankton in an oligotrophic ocean: observations and questions. Ecol. Monogr. 52:129–154.

Venrick, E. L. 2002. Floral patterns in the California Current System off southern California: 1990–1996. J. Mar. Research 60:171–189.

Verity, P. G., and V. Smetacek. 1996. Organism life cycles, predation, and the structure of marine pelagic ecosystems. Mar. Ecol. Prog. Ser. 130:277–293.

THE SIZE STRUCTURE OF MARINE PHYTOPLANKTON—WHAT ARE THE RULES?

RALF GOERICKE
Scripps Institution of Oceanography
University of California, San Diego
9500 Gilman Drive
La Jolla, CA 92093-0205

(Accepted, CalCOFI Reports, 2011)

ABSTRACT

It has been suggested that the size structure of marine phytoplankton communities varies with concentrations of chlorophyll *a* (Chl *a*): When total biomass is low, biomass is added only to the smallest size class until an upper limit to Chl *a* in this size class—its biomass quota—has been reached. At this point biomass can only be added to the community by adding Chl *a* to the next larger size class until its quota too is reached, whereupon the next largest size class is filled up, etc. These rules predict a maximum biomass for all size classes, except for the largest one whose maximum biomass is set by the availability of inorganic nutrients, and abundance thresholds for all size classes except for the smallest one. Here these predictions were tested in a variety of environments, the California Current system, the Eastern Tropical North Pacific, and the Sargasso Sea. Even though the smallest and largest size classes followed the above rules, i.e., these had an upper biomass limit and an abundance threshold, respectively, biomass distributions of intermediate size classes did not support the simple set of rules. These results question the general validity of these rules.

INTRODUCTION

Marine phytoplankton communities often consist of hundreds of species. Describing and understanding these communities in terms of these species is either impractical due to the large number of species present or impossible due to the small size of many, which precludes their identification. Instead other parameters, such as size, gross taxonomic affiliation or functional group can be used to describe phytoplankton communities. Using size to describe these has many advantages. Size is easily determined (Malone 1980; Chisholm 1992) and rates of metabolic processes can often be estimated for different size classes using simple allometric relationships (Banse 1982; Peters 1983; Moloney and Field 1989; Finkel et al. 2010, hallo). These advantages have lead to the development of models of phytoplankton communities based on size (Moloney and Field 1991; Armstrong 1996; Thingstad 1998; Armstrong 1999; Irwin et al. 2006).

After reviewing field data, Chisholm (1992) suggested simple size-based rules for the assembly of marine phytoplankton communities; Thingstad (1998) presented a simple conceptual model that explains these rules. The rules are: 1. Phytoplankton communities are dominated by the smallest cells when total phytoplankton biomass is low, a rule for which ample empirical evidence exists (Chisholm 1992; Agawin et al. 2000). 2. As biomass increases it is added only to the smallest size class until an upper limit to total Chl *a* in this size class is reached, which will be called its biomass quota. For example, the quota for the <1 μm size fraction is about 0.5 μg- Chl *a* L^{-1} (Chisholm 1992). 3. Once this quota has been reached, biomass can be added to a system only by adding a larger size class of cells until its quota has been reached as well. This cycle continues, only limited by the maximum biomass that a system can attain (Thingstad 1998). This implies that for all size classes, except for the smallest one, there are thresholds of total phytoplankton biomass that have to be met before cells of these size classes are found in the system. Thus, phytoplankton pigment biomass of different size classes, when plotted against total Chl *a* (TChl *a*), are predicted to show successive waves of size classes, all eventually leveling out once they reached their biomass quota (fig. 1A). For example, Raimbauld et al. (1988) observed that phytoplankton biomass in the <1, <3, and <10 μm size classes had upper limits of 0.5, 1 and 2 Chl *a* L^{-1} in the Adriatic Sea. The following testable hypotheses are predicted by these rules: 1. The biomass of smaller size classes attains a constant value for large values of TChl *a*. 2. There exists an abundance threshold for all size classes except the smallest one, i.e., a threshold below which cells of any particular size class do not contribute significantly to phytoplankton biomass. 3. Relative contributions of intermediate size classes to TChl *a* will follow a characteristic sawtooth pattern when plotted against TChl *a* (fig. 1B).

The empirical rules above only refer to the average state of a system. In the case of Thingstad's (1998) model these refer to a system at steady state with a given level of total nutrients, which, when nitrogen is limiting phytoplankton biomass, would be the total nitrogen content of the system. Thingstad's (1998) model is based on the dependence of nutrient uptake rates on size and sim-

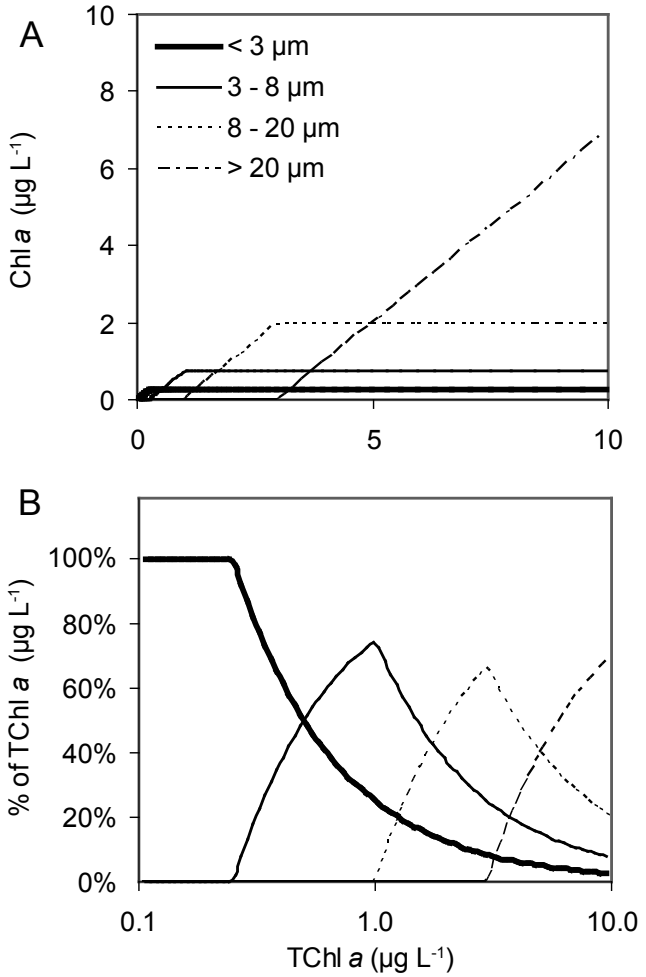

Figure 1. A graphical representation of the rules governing the contributions of different size classes to total phytoplankton biomass (TChl *a*). These graphs were derived from concepts in Thingstad (1998). A. The cumulative biomass of all size classes is plotted against TChl *a*. Note abundance thresholds for all size classes except for the smallest one and the attainment of class-characteristic upper biomass limits, i.e., quota, when TChl *a* is high. B. Using the data shown in panel A, the relative contribution of the size classes (% of total) was calculated and plotted against to log of TChl *a*.

ple predator-prey interactions that predict variations of phytoplankton size structure with total system biomass. The model implies that total phytoplankton biomass is controlled by the availability of resources but that community size-structure is controlled by grazers; i.e., by a balance of bottom-up and top-down forces.

The observations discussed above and Thingstad's model imply that simple rules exist that describe variations of phytoplankton size structure with total phytoplankton biomass. Their existence would suggest that phytoplankton community size structure can be predicted using simple rules and that phytoplankton community structure is primarily determined by size-dependent factors. However, these are only rules and we should expect that there are exceptions to these rules. For example, blooms of very small flagellates that are at times observed in nearshore and coastal environments impacted by eutrophication (Gieskes and Krey 1983; Dahl et al. 1989) demonstrate that the patterns described above are not universally followed, i.e., these do not constitute laws. But are these patterns generally found in the marine environment, i.e., do these rules hold generally and has this been demonstrated? Demonstrating that these rules are generally valid would also lend further empirical support to Thingstad's model. The first step to test these rules will be made here using data from the California Current system as well as data from the Sargasso Sea and the Eastern Tropical North Pacific. The distributional patterns observed in these environments did not follow predicted patterns, suggesting that the rules described above may not be generally true.

METHODS

For this study size classes are operationally defined by the pore size of the filters used in the size fractionation experiment. Size fractionation experiments were carried out in the Southern California Bight and the California Current system during the April and July 2003 California Cooperative Oceanic Fisheries Investigations (CalCOFI) cruises (CC0304 and CC0307, respectively). Additional experiments, carried out as part of other studies, were carried out during two cruises to the Eastern Tropical North Pacific south and southwest of Baja California in February and November 2003 (MEX0302 and MEX0311) and during cruises to the Sargasso Sea off Bermuda during 1985 and 1986 (Goericke 1998). Water from the mixed layer, collected with hydrowire- or rosette-mounted Niskin bottles from a depth of 1 or 10 m, was used in all cases. The sum of chlorophyll *a* (Chl a_1) and divinyl-chlorophyll a (Chl a_2), was used as a proxy for total phytoplankton biomass and will be referred to as Chl *a* or TChl *a*. Samples were analyzed either using the fluorometric method (Holm-Hansen et al. 1965) to determine Chl *a* and "pheopigments" or by high-pressure liquid-chromatography (HPLC) to determine concentrations of chlorophylls and carotenoids. For fluorometric analysis, 250 or 500 ml seawater were filtered on 25 mm Whatman GF/F filters, 3 and 8 µm Nuclepore filters and 20 µm Nitex circles. Filtrations were carried in parallel. Each treatment was carried out in triplicate. During cruises CC0307 and MEX0311 1-µm filters were used as well. The filters were extracted for 24 hours in 90% acetone at –18°C. Concentrations of Chl *a* were determined on a Turner Designs 10AU fluorometer. For pigment analysis by HPLC, three samples, each from cruises CC0307 and MEX0311 were filtered onto 25 mm Whatman GF/F and 47 mm 3 and 8 µm Nuclepore filters. These filters were stored in liquid nitrogen for at least 24 hours and extracted in 100% acetone. Extracts were analyzed on a

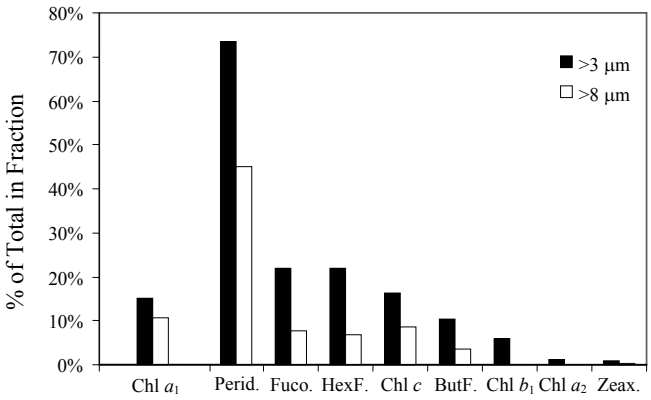

Figure 2. Size fractionation experiments in the California Current system (CalCOFI stations 93.100, 93.90, 90.80; i.e., n=3). For each pigment the contributions of the 3 to 8 and > 8µm size classes to the total concentration of that pigment are plotted. These pigments are representative of different groups of autotrophs, i.e., *Prochlorococcus* (Chl a_1; stdev = 1%), dinoflagellates (peridinin, Perid.; stdev = 31%), diatoms & haptophytes (fucoxanthin, Fucox.; stdev = 9%), haptophytes (19'-hexanoyloxyfucoxanthin, HexF.; stdev = 1%), chromophytes (chlorophyll $c_{1,2}$, Chl *c*; stdev = 2%), pelagophytes (19'-butanoyloxyfucoxanthin, ButF.; stdev = 3%), chlorophytes & *Prochlorococcus* (Chl *b*; stdev = 5%), *Prochlorococcus* (Chl a_2; stdev = 1%) and zeaxanthin (cyanobacteria, Zeax.; stdev = 0.6%).

C8-column based reverse-phase HPLC system as previously described (Goericke and Repeta 1993). Contributions of size fractions were calculated by subtraction, e.g., pigment biomass of the 3 to 8 µm size class was calculated by subtracting Chl *a* in the >8 µm treatment from Chl *a* in the >3 µm treatment. Chl *a* collected on Whatman GF/F filters was assumed to represent total Chl *a* present in the system and will be referred to as TChl *a*. In the California Current system the TChl *a* retention efficiency of these filters, relative to that of 0.2 µm Nuclepore filters, is 98 ± 2 % (n=24) (Goericke 2002). Statistical analysis of the data was carried out in Microsoft Excel.

RESULTS

In the California Current system size fractionation experiments were carried out in environments ranging from eutrophic coastal with TChl *a* larger than 10 µg L^{-1} to oligotrophic offshore, located at the edge of the central gyre of the North Pacific, with TChl *a* less than 0.1 µg L^{-1}. The Eastern Tropical North Pacific and the Sargasso Sea were typical of tropical and subtropical oligotrophic environments. Thus stations sampled for this study can be assumed to be representative of large areas of the world's ocean.

The effectiveness of filtration protocols used for size fractionation experiments was tested in the California Current system (CC0304) and the Eastern Tropical North Pacific (MEX0311) by combining size fractionations with the analysis of taxon-specific pigments by HPLC in samples from oligotrophic areas. In the California Current system, 17 and 9% of the chlorophyll *a* was retained by 3 and 8 µm Nuclepore filters, respectively (fig. 2). In contrast only 0 and 1% of divinylchlorophyll *a* and zeaxanthin were retained by these filters, respectively, i.e., pigments which in the open ocean are characteristic of the cyanobacteria *Prochlorococcus* sp. and *Synechococcus* sp. (Guillard et al. 1985; Goericke and Repeta 1992), the smallest known photoautotrophs. As expected, retention efficiencies of pigments associated with eukaryotes were higher. Highest values were observed for peridinin, the pigment characteristic of dinoflagellates. The relatively low retention efficiency of fucoxanthin by large pore-size filters (fig. 2) reflects the fact that fucoxanthin in these samples was primarily associated with haptophytes where it is a minor pigment (Jeffrey et al. 1997). Very similar results were obtained in the Eastern Tropical North Pacific where Chl a_2 and zeaxanthin in the >3 and >8 µm size fractions were only 0 to 1 % of the total (n = 3). These results show that the filtration procedures used effectively separated very small cells, such as Prochlorococcus, from larger cells and that small photoautotrophs were not significantly associated with larger particles or adhered to particles during sampling and filtration.

A large range of TChl *a* values was encountered in the California Current system. Thus results from that

TABLE 1

Size distribution of TChl *a* for open ocean stations where TChl *a* was less than 0.3 µg L^{-1}. Data are from cruises in April and July of 2003 in the California Current system (CC0304 and CC0307), the Sargasso Sea (Sargasso) during 1985 and 1986 (Goericke 1998) and the Eastern Tropical North Pacific (ETNP) during February and November 2003. Given are the average TChl *a* concentration (Average TChl *a*), the percent contribution of each size class to TChl *a*, and the number of samples used for the analysis (N). Significant regressions (type I, 95% significance level) of relative biomass (%) against TChl *a* (µg Chl *a* L^{-1}) are indicated with a '*'. The number of samples from each cruise or environment is given by 'N'.

	California Current system		Sargasso	ETNP	
	CC0304	CC0307	—	MEX0302	MEX0311
Average TChl *a*	0.16	0.16	0.11	0.17	0.17
<3 µm	75 ± 5 *	75 ± 5 *[1]	79 ± 4 *	86 ± 7 *	91 ± 6 *[1]
3 to 8 µm	16 ± 4 *	15 ± 5 *	12 ± 3 *	7 ± 1 *	4 ± 2
8 to 20 µm	6 ± 4	6 ± 2 *	5 ± 2 *	4 ± 2	3 ± 2
>20 µm	3 ± 1	4 ± 2	4 ± 2	3 ± 4	2 ± 1
N	20	12	7	9	18

[1]Biomass in the 1 to 3 µm size class was determined as well and varied significantly with TChl *a*.

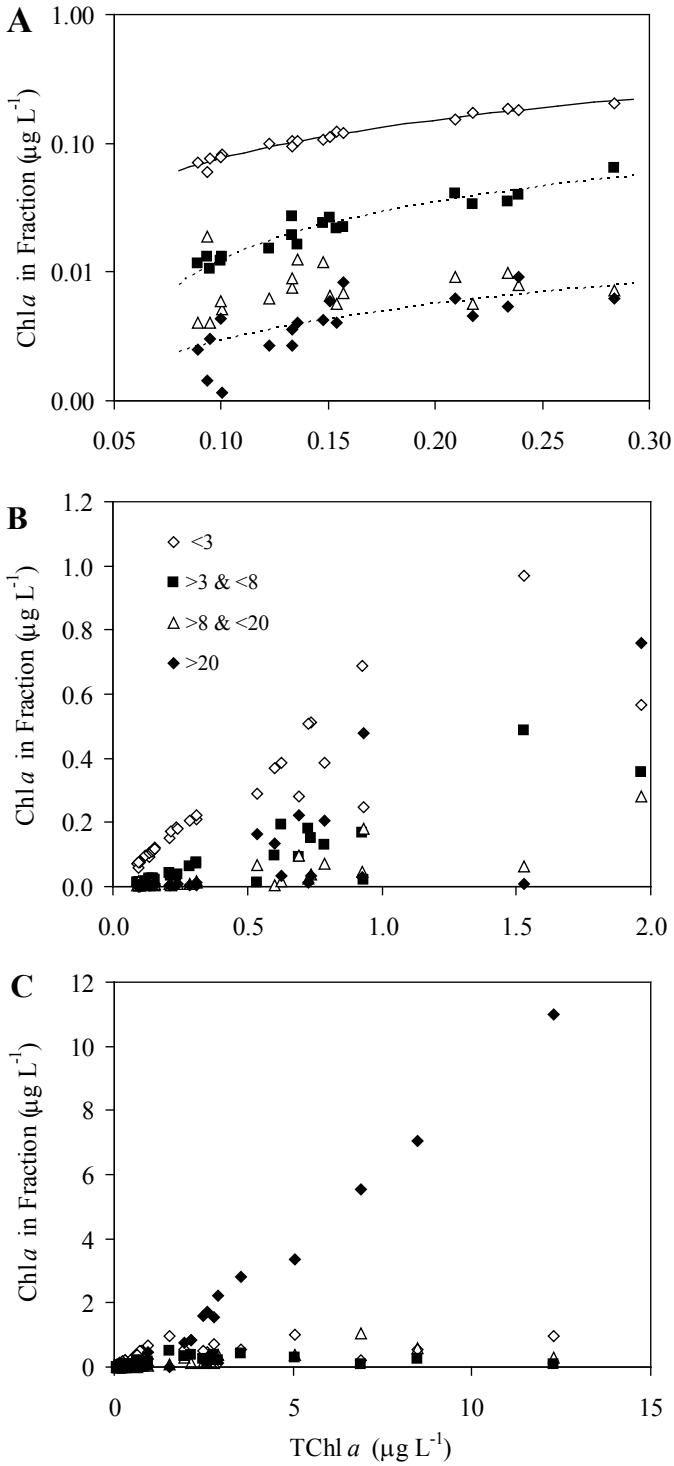

Figure 3. The pigment biomass (µg Chl *a* L^{-1}) of the <3, 3 to 8, 8 to 20 and >20 µm size classes plotted against TChl *a* for data collected on cruise CC0304 in the California Current system. A) the log of the size class pigment biomass is plotted against TChl *a* for values of TChl *a* ranging from 0 to 0.3 µg Chl *a* L^{-1}. B) The data plotted on a linear scale with TChl *a* ranging from 0 to 2 µg Chl *a* L^{-1}. C) The data plotted on a linear scale with TChl *a* ranging from 0 to 14 µg Chl *a* L^{-1}; the latter represents the largest TChl *a* concentration sampled for these experiments.

environment will be presented in detail. During April 2003 the <3 µm size class dominated total pigment biomass (TChl *a*) in the California Current system when TChl *a* was low (i.e., TChl *a* < 0.3 µg L^{-1}). The <3 µm size class contributed on the average 75% to TChl *a* (fig. 3a, table 1). The 3 to 8 µm, 8 to 20 µm and >20 µm size classes contributed on the average 16, 6 and 3% to TChl *a*, respectively (table 1, fig. 3a) in these sample. Biomass in the <3 and the 3 to 8 µm size class varied significantly with TChl *a* (<3 µm: $r^2 = 0.90$, p(slope = 0) < 0.01; 3 to 8 µm: $r^2 = 0.99$, p(slope = 0) < 0.01). This observation implies that the <3 µm and 3 to 8 µm size classes are "filled" simultaneously. Virtually identical results were obtained during July 2003 for low TChl *a* samples (CC0307, table 1) in regards to contributions to TChl *a* and variations of biomass in different size classes with TChl *a* (<1 µm: $r^2 = 0.92$, p(slope = 0) < 0.01; 1 to 3 µm: $r^2 = 0.62$, p(slope = 0) < 0.01; 3 to 8 µm: $r^2 = 0.28$, p(slope = 0) < 0.05). Data for TChl *a* values of up to 0.3 µg L^{-1}, collected in other subtropical environments showed similar patterns (table 1); biomass in the 3 to 8 µm size class was a linear function of TChl *a* in both environments (Sargasso: $r^2 = 0.92$, p(slope = 0) < 0.001; ETNP: $r^2 = 0.68$, p(slope = 0) < 0.05). These patterns clearly do not follow the rule that stipulate that larger size classes are only filled up once smaller size classes have reached their biomass quota.

As TChl *a* increased above 0.3 µg L^{-1}, contributions of different size classes to TChl *a* were much more variable (fig. 3b). In the California Current System the biomass of the <3 and 3 to 8 µm size classes reached apparent saturation values only once TChl *a* was larger than 1 to 2 µg L^{-1} (fig. 3c). However, the variability of the data and the absence of large numbers of data points in that range of TChl *a* precludes us to reach a firm conclusion. In contrast, biomass of the >20 µm size classes did not reach saturation values (fig. 3c). Plots of relative contributions of different size classes to TChl *a* illustrate these patterns in more detail and allow a comparison of the field data from the cruises CC0304 and CC0307 in the California Current system (fig. 4) with predicted patterns (fig. 1b). Only the <3 µm and >20 µm size classes displayed the predicted patterns (fig. 4 a, d): the <3 µm fraction had a constant relative biomass of about 75% when TChl *a* was low and started declining dramatically once TChl *a* was larger than 0.5 µg L^{-1}. The >20 µm fraction had, as predicted, an abundance threshold at about 0.5 µg-Chl L^{-1}; below this threshold its relative biomass was constant and very low; once TChl *a* reached values larger than 0.5 µg L^{-1} its relative biomass increased dramatically, until it dominated TChl *a* for large values thereof. In contrast, the 3 to 8 µm fraction failed to attain small values of relative biomass for small values of TChl *a* as is predicted. The relative contribution of the 8 to 20 µm

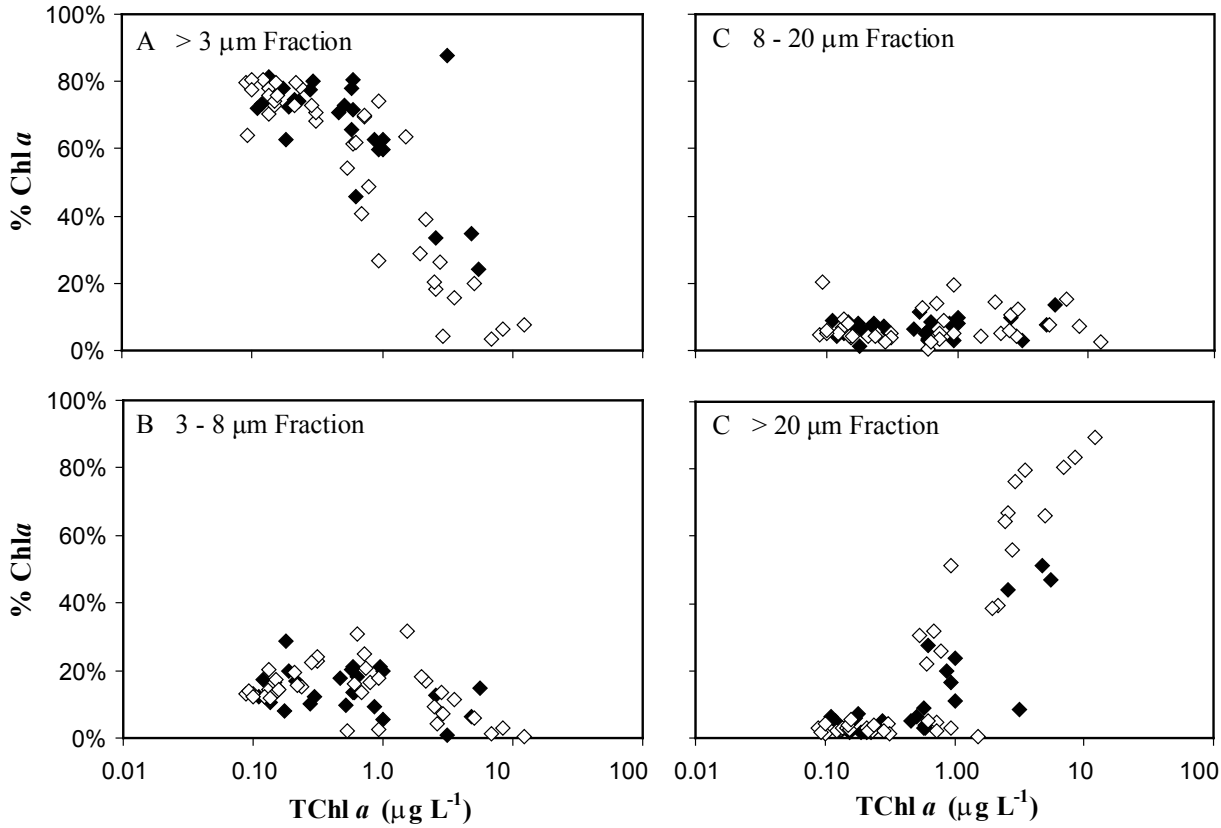

Figure 4. The relative pigment biomass (% of TChl *a*) of the <3 (A), 3 to 8 (B), 8 to 20 (C) and >20 (D) µm size classes plotted against log TChl *a* for data collected on cruises CC0304 (open symbols) and CC0307 (solid symbols) in the California Current system. Note that TChl *a* is plotted on a logarithmic scale for comparison with Figure 1b.

size class to TChl *a* varied from less than 5 % to 15% of the total but did not vary systematically with TChl *a* (fig. 4c) as is predicted (fig. 1 a,b). Overall the distributions of the 3 to 8 and 8 to 20 µm size classes do not display the expected sawtooth pattern (c.f. fig. 1b), i.e., do not follow the predicted patterns.

DISCUSSION

The objective of this study was to test a simple set of rules governing the size structure of phytoplankton communities (fig. 1), using data from the California Current system and other marine environments. Chl *a* was used as a proxy for phytoplankton carbon biomass in this study. Even though carbon to Chl *a* ratios are quite variable in algae (Geider 1987), ratios of Chl *a* in different size classes of algae reflect the corresponding carbon ratios well (Tremblay and Legendre 1994). This suggests that Chl *a* is an appropriate proxy for phytoplankton biomass for this study.

Results presented here suggest that the rules outlined in the introduction do not adequately describe contributions of different size classes to TChl *a*. In the California Current system small phytoplankters dominated phytoplankton biomass when TChl *a* was low, as predicted and as expected based on empirical data from many studies (Chisholm 1992; Agawin et al. 2000). When phytoplankton biomass was high picoautotrophs were still present as predicted, contributing on the average 0.5 µg Chl *a* L^{-1} to the total. Or, put differently, in the ocean there is a constant background of planktonic autotrophs, regardless of the waning and waxing of larger phytoplankters, such as diatoms or dinoflagellates (Chisholm 1992). The biomass of some size classes also attains maximum values, as predicted, even though these values were quite variable. For example, even though the <3 µm size class in the California Current system had an average biomass of ~0.5 µg Chl *a* L^{-1} for TChl *a* larger than 1 to 2 µg Chl *a* L^{-1}, values as high as 2.7 µg Chl *a* L^{-1} were observed for the <3 µm size class during cruise CC0307. Nonetheless, this study illustrates, similar to many others (see reviews by Malone 1980 and Chisholm 1992), that the variability of phytoplankton biomass in the ocean is generally due to the larger phytoplankters.

The most significant deviation of observed distributional patterns from those predicted is the absence of discrete abundance thresholds for some size classes. For example, it was not possible to unambiguously identify an abundance threshold for the 3 to 8 µm and 8 to 20

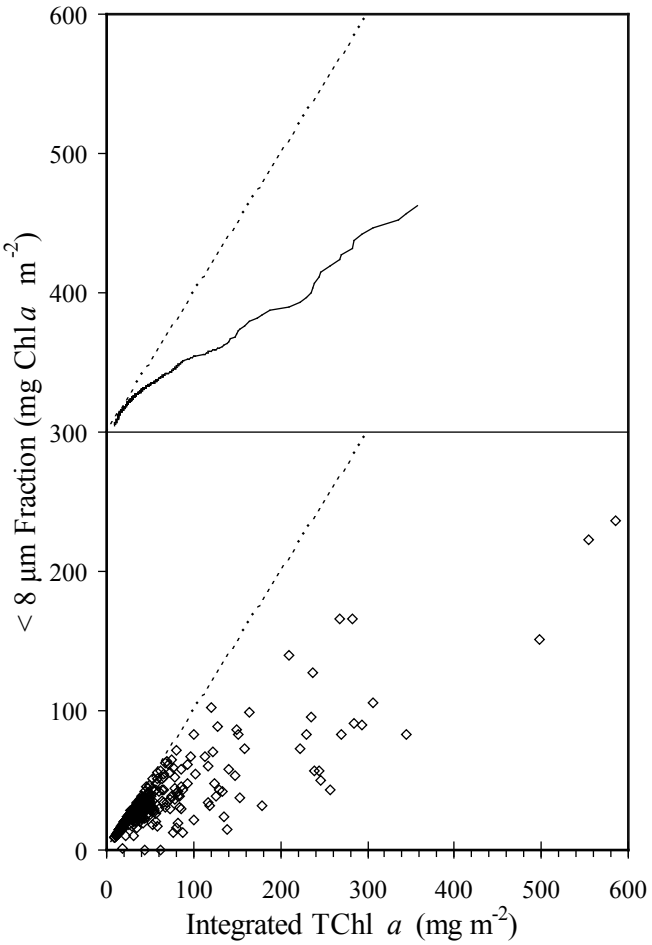

Figure 5. The contribution of the <8 μm size class to euphotic zone integrated TChl *a* (mg Chl *a* m^{-2}) in the California Current system from Mullin (1998). The data, n = 557, were collected by the CalCOFI technical group on cruises between 1994 and 1996. The lower panel shows the individual data points, the upper one shows the data smoothed using a loess function. The dotted line represents a 1:1 line for the data. In the California Current system stations with integrated TChl *a* > 100 mg m^{-2} have typically surface TChl *a* concentrations larger than 5 μg L^{-1}.

μm size classes in data from three different environments, the California Current system, the Sargasso Sea and the Eastern Tropical North Pacific. It also appears that the biomass of the 8 to 20 μm size class does not reach an upper limit, i.e., its relative contribution to TChl *a* is constant, even when TChl *a* is large (fig. 3c). This point is also well illustrated by data published by Mullin (1998; 2000) that show convincingly (n = 557) that the biomass of the <8 μm size class in the California Current system does not saturate as TChl *a* increases, even when TChl *a* reaches values larger than 10 μg L^{-1} (fig. 5, replotted from data in Mullin 1998 and 2000). Li (2002), using flow-cytometry data, observed patterns very similar to those described here. Whereas a decrease of the cellular abundance of picoautotrophs (<2 μm) with increasing Chl *a* standing stocks was mirrored by an increase in the cellular abundance of larger nanoautotrophs (10 to 20 μm), the cellular abundance of smaller nanoautotrophs did not vary with Chl *a* standing stock within the range of 10 to 1000 mg-Chl m^{-2}. The latter result confirms our observations for the intermediate size classes.

The data presented here illustrates that the variability of autotroph biomass in the California Current system is dominated by larger autotrophs. In contrast Marañón et al. (2001) reported that in the open North and South Atlantic variability of phytoplankton biomass was due to picoautotrophs only (<2 μm). It is interesting to note that Marañón et al. (2001) confined their analysis to stations with standing stocks of less than 40 mg TChl *a* m^{-2}, i.e., stations where TChl *a* concentrations were mostly below ~0.4 μg L^{-1} (Marañón et al. 2000). An analysis of the California Current system with stations confined to those with mixed layer TChl *a* less than 0.4 μg L^{-1} would result in a conclusion similar to that of Marañón et al. (c.f. fig. 3a), since larger taxa, such as diatoms, which are responsible for blooms in the California Current system (Venrick 2002; Goericke 2011), are virtually absent from the system when TChl *a* is less than 0.4 μg L^{-1}. These results imply that the answer to the question "What dominates the variability of autotroph biomass in the ocean?" scales with the range of pigment concentrations observed in the study.

These results show that the rules that were suggested by Chisholm (1992) and given a theoretical justification by Thingstad (1998) cannot be applied without modifications to the California Current system. Some aspects of these rules—implied abundance thresholds for intermediate size classes and the postulated upper limits to total Chl *a* in some size classes—fail to adequately describe the size structure of phytoplankton communities in the California Current system and in other environments as well. Considering that the California Current system is a very heterogeneous system, likely representative of other temperate/subtropical marine systems (c.f. table 1), these results should caution us to use simple sets of rules to describe the size structure of phytoplankton communities in any marine environment without first testing these.

These results imply that size is just one of many important dimensions of phytoplankton community structure. These data suggest that size-based trophic interactions are insufficient to explain the different size distributions observed in the various environments, particularly distributions for intermediate-sized phytoplankters. For example, Irvin et al. (2006) have shown theoretically that phytoplankton size structure, among other factors, also depends on the maximum growth rate of the different groups of phytoplankters. This implies more consistent distributional patterns could emerge when taxon-specific biomass is used for such a study instead of size-class specific biomass since maximum

growth rates vary significantly among taxa, often independent of size (Chisholm 1992; Finkel et al. 2010). An analysis of taxon-specific biomass distributions from the California Current system confirms this (Goericke 2011); the biomass of different phytoplankton taxa followed patterns such as those shown in Figure 1.

ACKNOWLEDGEMENTS

I am grateful to the crews of the R/V *Revelle* and *New Horizon* for support at sea and to R. Elliot, J. Gorga and J. Clermont for help at sea and in the lab. The late Mike Mullin provided the data for Figure 6. Karl Banse and 2 anonymous reviewers are thanked for their critical and helpful comments on the manuscript. The research was supported by a grant from NSF (OCE-01018038).

LITERATURE CITED

Agawin, N. S. R., C. M. Duarte, and S. Agusti. 2000. Nutrient and temperature control of the contribution of picoplankton to phytoplankton biomass and production. Limnol. Oceanogr. 45:591–600.

Armstrong, R. A. 1996. Grazing limitation and nutrient limitation in marine ecosystems: Steady state solutions of an ecosystem model with multiple food chains. Limnol. Oceanogr. 39:597–608.

Armstrong, R. A. 1999. Stable model structures for representing biogeochemical diversity and size spectra in plankton communities. J. Plank. Res. 21:445-465.

Banse, K. 1982. Mass-scaled rates of respiration and intrinsic growth in very small invertebrates. Mar. Ecol. Prog. Ser. 9:281–297.

Chisholm, S. W. 1992. Phytoplankton size, p. 213–237. *In* P. G. Falkowski and A. D. Woodhead [eds.], Primary productivity and biogeochemical cycles in the sea. Plenum.

Dahl, E., O. Lindahl, E. Paasche, and J. Throndsen. 1989. The *Chrysochromulina polylepis* bloom in Scandinavian waters during spring 1988. *In* E. M. Cosper, V. M. Bricelj and E. J. Carpenter [eds.], Novel Phytoplankton Blooms. Springer Verlag.

Finkel, Z. V. and others 2010. Phytoplankton in a changing world: cell size and elemental stoichiometry. J. Plankton Res. 32:119-137.

Geider, R. J. 1987. Light and temperature dependence of the carbon to chlorophyll *a* ratio in microalgae and cyanobacteria: implications for physiology and growth of phytoplankton. New Phytol. 106:1–34.

Gieskes, W. W. C., and G. W. Krey. 1983. Dominance of cryptophyceae during the phytoplankton spring bloom in the central North Sea detected by HPLC analysis of pigments. Mar. Biol. 75:179–185.

Goericke, R. 1998. Response of phytoplankton community structure and taxon-specific growth rates to seasonally varying physical forcing at a station in the Sargasso Sea off Bermuda. Limnol. Oceanogr. 43:921–935.

Goericke, R. 2002. Bacteriochlorophyll *a* in the ocean: Is anoxygenic bacterial photosynthesis important? Limnol. Oceanogr. 47:290–295.

Goericke, R. 2011. The structure of marine phytoplankton communities—Patterns, rules and mechanisms. CalCOFI Reports in press.

Goericke, R., and D. J. Repeta. 1992. The pigments of *Prochlorococcus marinus*: the presence of divinyl chlorophyll *a* and *b* in a marine prochlorophyte. Limnol. Oceanogr. 37:425–433.

Goericke, R., and D. J. Repeta. 1993. Chlorophylls *a* and *b* and divinylchlorophylls *a* and *b* in the open subtropical North Atlantic Ocean. Mar. Ecol. Prog. Ser. 101:307–313.

Guillard, R. R. L., L. S. Murphy, P. Foss, and S. Liaaen-Jensen. 1985. *Synechococcus spp.* as likely zeaxanthin-dominant ultraphytoplankton in the North Atlantic. Limnol. Oceanogr. 30:412–414.

Holm-Hansen, O., C. J. Lorenzen, R. W. Holmes, and J. D. H. Strickland. 1965. Fluorometric determination of chlorophyll. J. Cons. perm. int. Explor. Mer 30:3-15.

Irwin, A. J., Z. V. Finkel, O. M. E. Schofield, and P. G. Falkowski. 2006. Scaling-up from nutrient physiology to the size-structure of phytoplankton communities. J. Plankton Res. 28:1–13.

Jeffrey, S. W., R. F. C. Mantoura, and S. W. Wright. 1997. Phytoplankton pigments in oceanography. UNESCO Publishing.

Malone, T. C. 1980. Algal Size, p. 433–464. *In* I. Morris [ed.], The Physiological Ecology of Phytoplankton. Univ. Calif. Press.

Marañón, E. and others. 2001. Patterns of phytoplankton size structure and productivity in contrasting open-ocean environments. Mar. Ecol. Prog. Ser. 216:43-56.

Marañón, E. and others. 2000. Basin-scale variability of phytoplankton biomass, production and growth in the Atlantic Ocean. Deep-Sea Res. I 47:825–857.

Moloney, C. L., and J. G. Field. 1989. General allometric equations for rates of nutrient uptake, ingestion, and respiration in plankton organisms. Limnol. Oceanogr. 35:1290–1299.

Moloney, C. L., and J. G. Field. 1991. The size-based dynamics of plankton food webs. I. A simulation model of carbon and nitrogen flows. J. Plankton Res. 13:1003–1038.

Mullin, M. M. 1998. Biomasses of large-celled phytoplankton and their relation to the nitricline and grazing in the California Current system off Southern California, 1994–1996. CalCOFI Reports 39:117–123.

Mullin, M. M. 2000. Large-celled phytoplankton, the nitricline, and grazing during the California 1997-98 El Niño. CalCOFI Reports 41:161–166.

Peters, R. H. 1983. The ecological implication of body size. Cambridge Univ. Press.

Raimbault, P., M. Rodier, and I. Taupier-Letage. 1988. Size fraction of phytoplankton in the Ligurian Sea and the Algerian Basin (Mediterranean Sea): Size distribution versus total concentration. Mar. Microb. Food Webs 3:1–7.

Thingstad, T. F. 1998. A theoretical approach to structuring mechanisms in the pelagic food web. Hydrobiologia 363:59–72.

Tremblay, J. E., and L. Legendre. 1994. A model for the size-fractionated biomass and production of marine phytoplankton. Limnol. Oceanogr. 39:2004–2014.

Venrick, E. L. 2002. Floral patterns in the California Current system off southern California: 1990–1996. J. Mar. Research 60:171–189.

THE INFLUENCE OF THE OCEAN ENVIRONMENT ON THE ABUNDANCE OF MARKET SQUID, *DORYTEUTHIS (LOLIGO) OPALESCENS*, PARALARVAE IN THE SOUTHERN CALIFORNIA BIGHT

J. ANTHONY KOSLOW[1] AND CAITLIN ALLEN
Scripps Institution of Oceanography
University of California, San Diego
La Jolla, CA 92093-0218
[1](858) 534-7284
email: jkoslow@ucsd.edu.

ABSTRACT

Using data from January–May CalCOFI surveys from 1981 to 2008, we investigated how the abundance of market squid paralarvae in the southern California Current varied in relation to local and large-scale environmental variables. Market squid paralarval abundance was significantly correlated with both near-surface temperature, nutrient and chlorophyll concentrations; and the El Niño–Southern Oscillation (ENSO) index. Stepwise regression analysis indicated a significant relationship primarily with ENSO and secondarily with the Pacific Decadal Oscillation, with local variables not entering significantly due to their high collinearity with ENSO. Paralarval abundance provides a fishery-independent index of stock biomass, and these statistical relationships suggest that the ENSO and PDO indices can be used for adaptive management of the market squid fishery. CPUE seems to have deficiencies as an index of stock biomass because the fishery is carried out on spawning aggregations.

INTRODUCTION

Doryteuthis (Loligo) opalescens (market squid) have been fished in California since the mid-1800s, when Chinese fishermen used small rowboats and torches to catch adult squid (Fields 1950; Porzio and Brady 2007; Vojkovich 1998). The fishery was of relatively limited value and importance, with landings generally on the order of 10,000 t or less, until the mid-1980s. The fishery then shifted from brail and lampara nets to purse seines (and later, drum seines), and landings increased markedly. In the mid-1990s, market squid became the largest California fishery in terms of both landings and revenue. In 2009, squid fishermen landed over 92,000 metric tons of squid, with an ex-vessel value of about $56.5 million (Sweetnam 2010).

Despite the regional importance of the fishery, the fishery is "monitored," without a formal stock assessment to guide management. The squid fishery is regulated with restrictions on gear, weekend closure dates, a seasonal 118,000 ton catch limit, and permit limits (California Department of Fish and Game 2005). The catch limit is based on the approximate maximum landings obtained in three seasons since 1998–2000, but landings over the past decade have been mostly about half the total allowable catch. Catch per unit effort (CPUE) has been relatively steady, but CPUE is generally unreliable as a proxy for stock biomass, particularly for a fishery with evolving gear technology and that targets spawning aggregations (Hilborn and Walters 2001).

The market squid lives to only 6–9 months (Butler et al. 1999), and the population fluctuates markedly from year to year, largely in apparent response to environmental factors. During El Niño events, the fishery has declined precipitously by an order of magnitude and more. However, it recovers typically within a few years, particularly in response to La Niña events (Zeidberg et al. 2006). The preponderance of evidence indicates that these dramatic fluctuations are more likely due to changes in abundance than mere shifts in availability to the fishery (Reiss et al. 2004). However, the impact of the fishery on the population is not understood, and there are concerns about overexploitation during the periodic downturns of the population (Zeidberg et al. 2006). Improved proxies for stock biomass, as well as a better understanding of the species' response to environmental conditions may contribute to the sustainable management of the fishery.

The role of squid in the food web of the California Current has not been quantified. However, as juveniles they feed predominantly on pelagic crustaceans, such as copepods and euphausiids, shifting to larger prey, such as fish, as they mature (Fields 1965; Karpov and Caillet 1978). They are consumed in turn by a variety of predatory fishes, seabirds, and marine mammals (Fields 1965; Morejohn et al. 1978). In view of their apparently high abundance and rapid turnover, they presumably play a key role in the transfer of production from the plankton to higher trophic levels within the California Current.

To examine changes over time in market squid abundance, we used data from California Cooperative Oceanic Fisheries Investigations (CalCOFI) research cruises. These cruises, carried out quarterly since 1984,

Keywords: market squid, *Doryteuthis opalescens*, paralarvae, El Niño, ENSO, Pacific Decadal Oscillation, catch per unit effort.

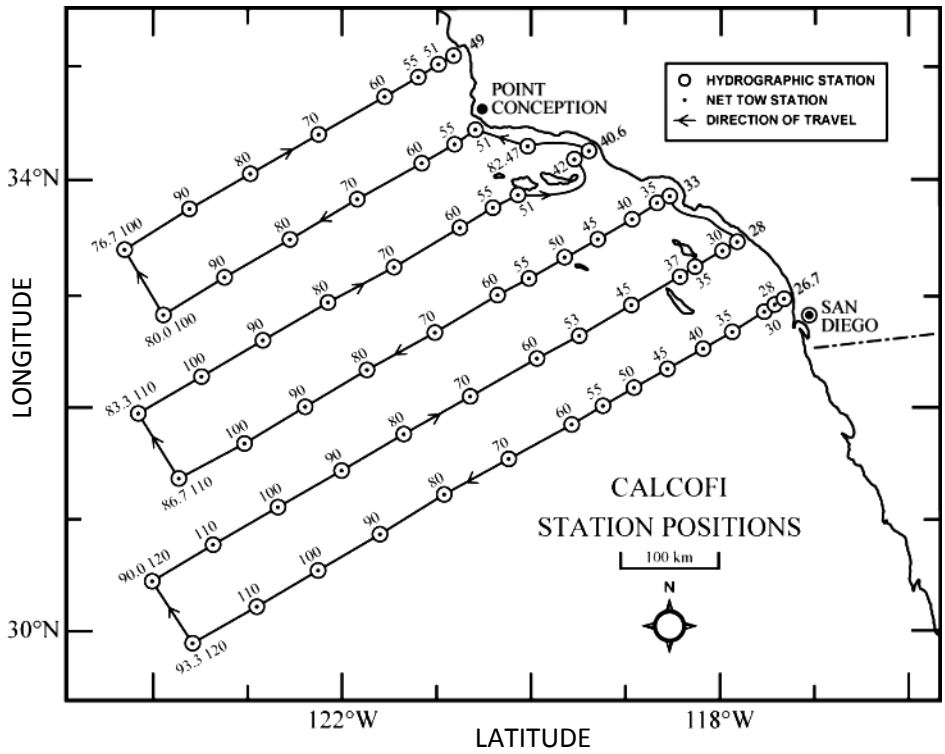

Figure 1. CalCOFI station map showing the core CalCOFI transects and stations. Market squid paralarvae were examined from station lines 76.7 to 93.3 and station numbers 26.7 to 70.

collect data on the physical, chemical and biological oceanography of the southern California Current, including plankton samples from a regular grid of stations (fig. 1). Larval squid, known as paralarvae, are regularly sampled and enumerated from the plankton tows. Although formal stock assessments based on egg and larval data make use of ancillary data on fecundity and other factors (Lasker 1985), ichthyoplankton abundance alone has been shown to be significantly correlated with more formal stock assessments for a variety of taxa (Moser and Watson 1990; Moser et al. 2000, 2001; Koslow et al. in press). Most of the ichthyoplankton obtained on CalCOFI cruises are at very early (preflexion) stages of development, due to net avoidance by better developed larval and juvenile fish. The ichthyoplankton data therefore primarily reflect spawning effort, a function of adult spawning biomass, rather than subsequent recruitment. Market squid largely spawn nearshore, so the paralarval distribution is only partially sampled by CalCOFI (Zeidberg and Hamner 2002). However, CalCOFI presumably samples a reasonably constant proportion of the market squid population during its early life history. Given the length of the CalCOFI data set, its consistency and broad spatial coverage, we believe it may provide insight into the factors affecting market squid population dynamics if examined in relation to environmental variables.

MATERIALS AND METHODS

Several plankton net tows are carried out at each station on CalCOFI cruises: double oblique tows with a bongo net, neuston tows with a manta net, and vertical tows. However, market squid paralarvae were only obtained in sufficient quantities for time-series analysis in the manta tows, which sample 8 cm below the air-sea interface for 15 minutes at about 1.5 knots. Previous studies have also observed a low abundance and low incidence of *Doryteuthis opalescens* from oblique plankton tows (Okutani and McGowan 1969; Recksiek and Kashiwada 1979). The manta data for market squid paralarvae begin in January 1981 and continue through January 2008 and can be found in the NOAA/Scripps Institution of Oceanography Ichthyoplankton Database (IchthyoDB: http://oceaninformatics.ucsd.edu/ichthyoplankton). More detailed descriptions of tow protocol can be found on www.calcofi.org/cruises/stationwork.html. Because the paralarvae are predominantly found in coastal waters (fig. 2) (Zeidberg and Hamner 2002), we used CalCOFI's standard 66 station grid and examined station lines 76.7 to 93.3 and station numbers 26.7 to 70 (fig. 1). Our index of paralarvae abundance in the study area was based on data from January through May, when they were most abundant (see Results). This period corresponds, with appropri-

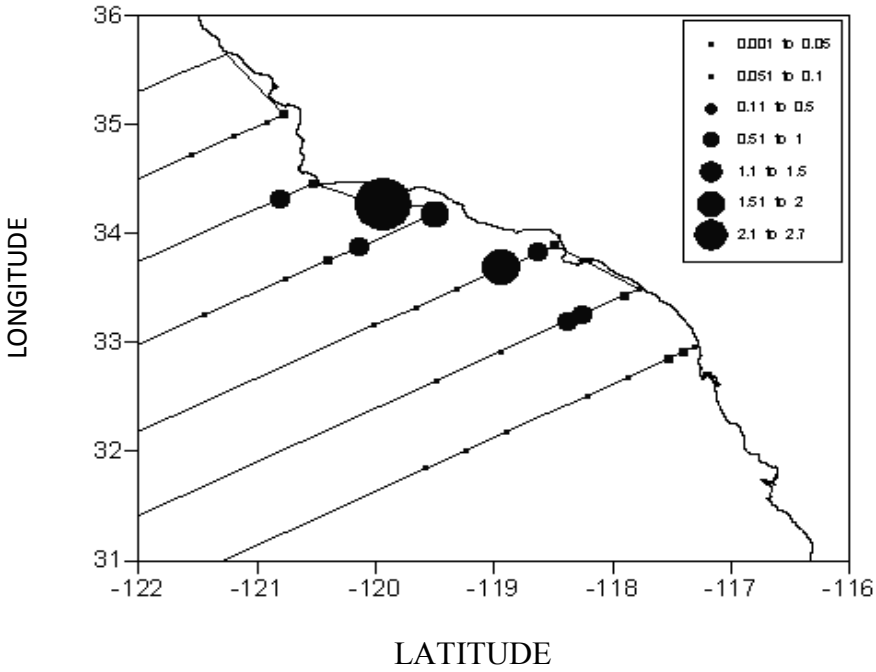

Figure 2. The average abundance (numbers/m^3) of market squid paralarvae at CalCOFI stations, showing their predominantly coastal distribution.

ate lag for the 1–2 month incubation period for the squid eggs (Zeidberg et al. 2011), with the December–April period of peak fishing on spawning aggregations of market squid in southern California waters. Only data from the night tows were used in the time-series analysis because of their far greater abundance at night (see Results). "Night" was defined as an hour after sunset to an hour before sunrise, based on the average sunrise and sunset times for each month sampled. The paralarval data were quantified as numbers per 1000 m^3. To obtain the annual mean abundance index, market squid paralarval abundance from all night manta tows within the grid of interest from January to May were averaged. One anomalous data point was removed from our paralarval data set: station 83.3, 51 on the April 1992 cruise, at which 1,563 paralarvae were obtained, the highest value by a factor of about five for any station in the time series. For the remainder of the cruise, only 6 market squid were caught at a single other station. The anomalous station was likely the result of sampling recently hatched paralarvae above an egg mass.

We examined the relationship between annual mean paralarval abundance and environmental variables sampled on the CalCOFI cruise and indices for several large-scale environmental features: the El Niño–Southern Oscillation (ENSO) (National Oceanic and Atmospheric Administration (NOAA) Climate Prediction Center: http://www.cpc.noaa.gov/data/indices); the Pacific Decadal Oscillation (PDO) (University of Washington: http://jisao.washington.edu/pdo/PDO); the North Pacific Gyre Oscillation (NPGO) (Di Lorenzo: http://www.o3d.org/npgo/data/NPGO.txt); and upwelling based on offshore Ekman transport at 33°N and 119°W (Pacific Fisheries Environmental Laboratory: http://las.pfeg.noaa.gov/las6_5/servlets/dataset). All environmental variable values were averaged between January and May based on monthly mean data.

Physical and biological data were obtained from the same CalCOFI cruises as the paralarvae for temperature (°C), salinity, oxygen (O_2), phosphate (PO_4), silicate (SiO_3), nitrate (NO_3), and chlorophyll *a* (chl *a*) from a depth of 10 m, and zooplankton displacement volume (DV) integrated over the water column (0–200 m) from double oblique bongo tows, from which zooplankton > 5 mL DV (i.e., large gelatinous plankton, such as medusae, salps, and doliolids) were removed. These local oceanographic variables were averaged between January and May to obtain annual means corresponding to conditions over the spawning period and early life history. These data were obtained from the CalCOFI database: http://oceaninformatics.ucsd.edu/datazoo/data/calcofi-sio/datasets?action=summary&id=78.

Market squid catch and effort data were obtained from California Department of Fish and Game for the southern California sector of the fishery, the area covered by the CalCOFI grid (D. Sweetnam and B. Brady, California Department of Fish and Game, pers. commn.). We estimated catch per unit effort (CPUE) as average catch per landing for the peak months of the southern California fishery from December through April: the

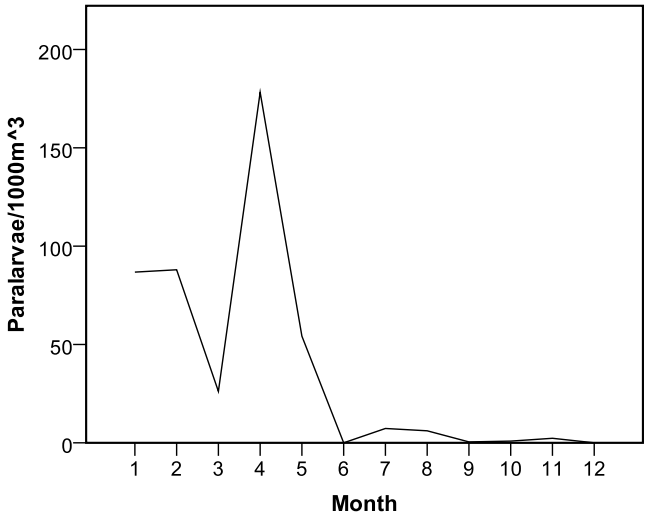

Figure 3. The mean monthly abundance of *Doryteuthis opalescens* paralarvae (1981–2008) (#/1000 m^3) at the core CalCOFI stations.

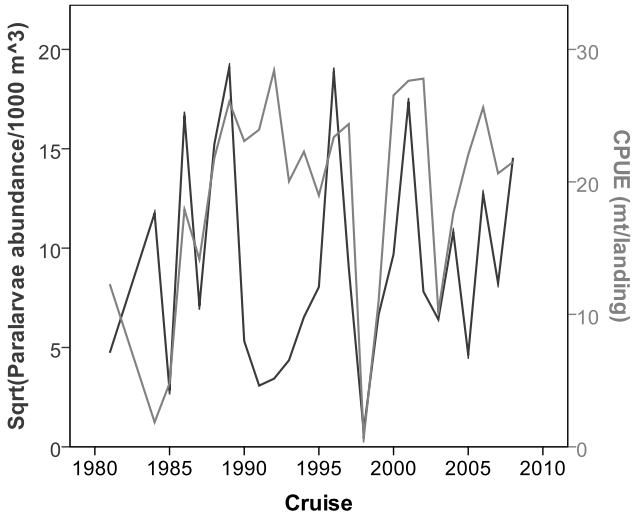

Figure 4. Time series of *Doryteuthis opalescens* paralarval abundance ((#/1000 m^3)^{½}) and CPUE for the southern California commercial fishery (mt/landing).

total squid catch for those months divided by the number of vessel landings.

Significant deviations from normality were assessed based on visual inspection of the probability distributions combined with the Kolmogorov-Smirnov test. The paralarval abundance and zooplankton data departed significantly from normality and were square-root transformed, which better achieved normality than log-transformation.

We initially carried out an exploratory analysis in which we examined for the presence of significant correlations among the time series. Where there were nominally significant correlations, we examined first for the presence of significant trends among the time series, which can be a source of spurious correlations. Where present, trends were removed by replacing the original time series with the residuals from the regression of the original time series with YEAR. Correlation analysis was rerun on the residual time series, and where the correlation remained significant based on the nominal degrees of freedom, we examined the time series correlograms for autocorrelation of the time series at successive lags. Autocorrelation reduces the effective number of independent data points (or degrees of freedom), leading to inflated estimates of significance, if uncorrected (Pyper and Peterman 1998). Autocorrelation was not detected as a significant source of bias in our analysis.

Because many local environmental variables were intercorrelated, we applied a principal component analysis (PCA) to reduce the dimensionality of the variable set (Legendre and Legendre 1983). The PCA was based on the correlation matrix for the following variables: upwelling, temperature, salinity, O_2, NO_3, chl *a*, and zooplankton DV. Several nutrient variables were removed from the PCA due to their high collinearity with NO_3 (see Results). Stepwise regression analysis was used to assess the contribution of environmental variables and indices to explaining the variability of the paralarval data set.

RESULTS

Doryteuthis opalescens paralarvae were 26-fold more abundant from January to May than during the latter part of the year (fig. 3). During this period of peak abundance, the larvae were 520 times more abundant in the night than the daytime manta tows, indicating a strong tendency to migrate into near-surface waters at night. There was no significant difference in the size composition of *D. opalescens* paralarvae from the manta and oblique bongo tows (William Watson, pers. commn., SWFSC), indicating that diel vertical migrations are carried out through the paralarval period of the life history.

The paralarvae were most abundant around the coastal islands and inshore regions of the Southern California Bight (fig. 2). They were infrequently present in deeper waters out to station 70, less than 300 km from shore, but were rarely observed farther out to sea. This is consistent with other studies of their distribution based on other sampling methods, such as with oblique bongo tows (Okutani and McGowan 1969; Zeidberg and Hamner 2002).

Paralarval Abundance as an Index of Spawning Stock Biomass

We examined the market squid paralarval abundance in relation to the catch per unit effort (CPUE) data for the commercial fishery to assess their suitability as indices of *D. opalescens* spawning stock biomass (fig. 4). The

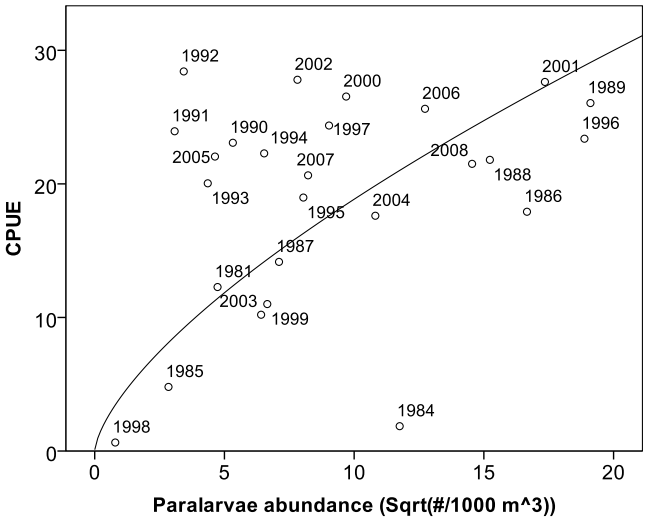

Figure 5. Scatterplot of market squid CPUE from the southern California fishery (mt/landing) and paralarvae abundance ((#/1000 $m^3)^{0.5}$). The fit of a power function is shown: $y = 4.03\ x^{0.67}$, $R^2 = 0.30$, $p < 0.01$.

CPUE data, but not the paralarval data, exhibited significant trend, increasing with time ($p < 0.05$). The linear correlation between the time series was marginal ($r = 0.35$, $p = 0.08$). However, the initial sharp increase in CPUE appears to have led to a significant nonlinear relationship between the two time series (fig. 5). Both time series record the precipitous drop in squid spawning stock during the major El Niño events of 1998 and lesser decline during the moderate El Niño of 2003. However, during several periods of moderate El Niño conditions, notably the early 1990s and around 2005, paralarval abundance was reduced but the fishery and CPUE remained high. There was no significant relationship between paralarval abundance and CPUE in the following year, indicating that paralarval abundance is not significantly related to subsequent recruitment.

Environmental Relationships

About half of the environmental variables were significantly correlated with market squid paralarval abundance: temperature, nitrate, phosphate, and silicate, and chlorophyll *a* at 10 m and the ENSO index (table 1). However, the PDO and NPGO indices, as well as upwelling, salinity, oxygen, and zooplankton biomass, were not significantly correlated with the *D. opalescens* time series. None of these variables were significantly autocorrelated.

Most of the local variables significantly correlated with *D. opalescens* paralarval abundance were also significantly correlated with ENSO and with each other (table 2). This is not surprising: upwelling intensity, near-surface ocean temperature, salinity, nutrient and oxygen concentrations, and phytoplankton and zooplankton abundance are interrelated ocean properties influenced by the ENSO cycle. We therefore carried out a princi-

TABLE 1

Pearson correlations of market squid (*Doryteuthis opalescens*) paralarval abundance, square-root transformed with local environmental variables measured at 10 m depth: temperature (T), salinity (S), oxygen (O_2), nitrate (NO_3), phosphate (PO_4), silicate (SiO_3),chlorophyll *a* (chl), and square-root transformed zooplankton displacement volume (Zoo); also, upwelling at 33°N, 119°W, and the ENSO, PDO, and NPGO environmental indices. The temperature, nitrate, and zooplankton time series were detrended. *: $p < 0.05$; **: $p < 0.01$; ***: $p < 0.001$ (two-tailed significance). N = 26.

	T	S	O_2	NO_3	PO_4	SiO_3	Chl	Zoo	Upwell	ENSO	PDO	NPGO
Doryteuthis opalescens paralarvae	0.47*	0.06	0.33	0.49*	0.49*	0.53**	0.51**	0.29	0.17	0.71***	0.09	0.25

TABLE 2

Pearson correlations for mean values (January–May) of the ENSO index, upwelling at 33°N, 119°W and local environmental variables measured at 10 m depth: temperature (T), salinity (S), oxygen (O_2), nitrate (NO_3), phosphate (PO_4), silicate (SiO_3), chlorophyll *a* (chl), and square-root transformed zooplankton displacement volume (Zoo). The local variables are averaged over all CalCOFI stations shown in Figure 1. The temperature, nitrate, and zooplankton time series were detrended. The correlation coefficients are shown in the right upper part of the table and the significance levels in the lower left (n = 27–28). *: $p < 0.05$; **: $p < 0.01$; ***: $p < 0.001$ (two-tailed significance).

	ENSO	T	S	O_2	NO_3	PO_4	SiO_3	Chl	Zoo	Upwell
ENSO		.79	.20	.55	.67	.55	.58	.48	.49	.49
T	***		–.32	–.60	–.79	–.56	–.70	-.47	–.53	–.60
S				.16	.36	.20	.29	.02	.26	.49
O_2	**	**			.43	.45	.07	.21	.55	.32
NO_3	***	***		*		.86	.82	.61	.28	.43
PO_4	**	**		*	***		.30	.52	.17	.18
SiO_3	**	***			***			.52	.09	.43
Chl	*	*			**	**	**		.20	.01
Zoo	**	**		**						.47
Upwell	**	**	**		*		*		*	

TABLE 3
Variable loadings on principal component 1 (PC1). The variables were transformed and detrended as in Table 2.

Variable	PC1
Temperature (C)	–0.92
Salinity (PSU)	0.50
O_2 (ml/L)	0.71
NO_3 (uM/L)	0.81
Chl *a* (mg/m^3)	0.49
Zooplankton Biomass	0.68
Upwelling	0.71
Variance Explained	49.6%

pal component (PC) analysis of the local oceanographic variables, including upwelling intensity, to reduce the dimensionality of the data set prior to further analysis. We also considered it unlikely that any single variable, except possibly zooplankton availability or temperature, influenced squid abundance in isolation. Because the nutrient variables were closely intercorrelated (r = 0.82–0.86 for the correlation of NO_3 with PO_4 and SiO_3), only NO_3 was entered into the PCA to avoid biasing the analysis toward the nutrients.

The first PC explained 49.6% of the variance of the seven environmental variables entered into the analysis (eigenvalue (λ) = 3.5), more than twice the explanatory power (18.7%) of PC2 (λ = 1.3). All seven variables had factor loadings on PC1, equal to the correlation of the PC1 time series with the time series of the individual variables, of 0.49 or greater (table 3). Temperature and nitrate concentration at 10 m depth were most closely linked to PC1 (loadings = –0.92 and 0.81, respectively), followed by upwelling and oxygen concentration at 10 m (loadings = 0.71). PC1 was significantly correlated with the abundance of market squid paralarvae (r = 0.43, n = 26, p < 0.05), as well as with ENSO, the PDO, and NPGO, but not with the squid fishery CPUE (table 4). The strongest correlation was with ENSO (r = 0.77, p < 0.001). The strong relationship between ENSO and the market squid paralarval abundance is seen in Figure 6. The apparent outliers to the relationship (1985, 1999, 2000) followed the strong El Niño events of 1983 and 1998. It is apparent that although the fishery recovered within a year of these El Niño events (fig. 4), paralarval abundance (and by implication, the squid stock biomass) required more than two years to recover.

Stepwise regression was used to examine the explanatory power of PC1 and the ENSO, PDO, and NPGO

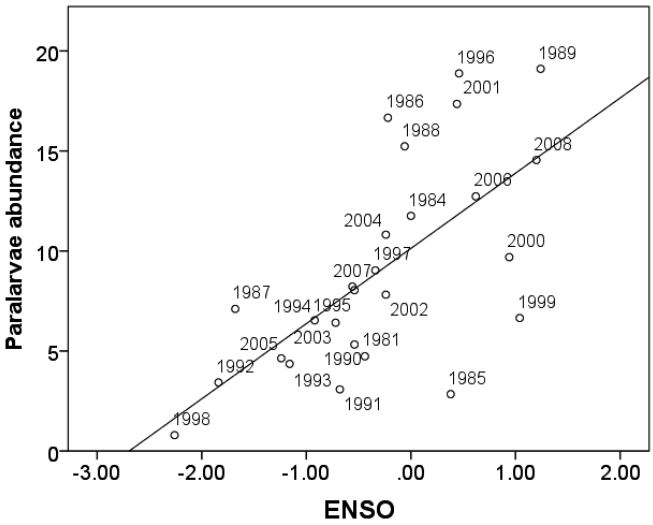

Figure 6. Scatterplot of the ENSO index and market squid paralarval abundance per 1000m³, square-root transformed. El Niños correspond with periods when the index is negative, La Niñas with when it is positive. The three years that appear to be outliers to the linear relationship (1985, 1999, 2000) followed the strong El Niño events of 1983 and 1998. (1982, 1983 not shown because CalCOFI did not sample those years.) The linear relationship is shown: $y = 10.13 + 3.76$*ENSO, $R^2 = 0.43$, $p < 0.001$.

TABLE 5
Results of stepwise regression analysis with market squid paralarvae abundance as dependent variable and PC1, ENSO, PDO, and NPGO as independent variables. ENSO and PDO entered significantly into the regression in that order. *: p < 0.05; **: p < 0.01; ***: p < 0.001 (two-tailed significance).

Regression Components	Unstandardized Coefficients		Standardized Coefficients	
	R^2	B	β	t
Constant		9.15		10.52***
ENSO	0.43	4.94	0.87	5.20***
PDO	0.54	2.46	0.39	2.35*

indices in explaining the variance in market squid paralarval abundance. ENSO was most highly correlated with paralarval variance and entered the regression first. Once ENSO entered the regression, only the PDO contributed significantly to explaining the remaining variance in paralarval abundance (table 5). ENSO explained 43% of the variance in the paralarval data; adding the PDO explained a further 11% of the variance, for a total of 54%. The standardized regression coefficients (β) indicate that ENSO explained more than twice the variance in paralarval abundance than the PDO (table 5). Time

TABLE 4
Correlations of PC1 with market squid paralarval abundance (Paralarvae), ENSO, PDO, NPGO and the detrended CPUE for the squid fishery. *: p < 0.05; **: p < 0.01; ***: p < 0.001 (two-tailed significance).

Variables	Paralarvae	ENSO	PDO	NPGO	CPUE
PC1	0.43*	0.77***	0.45*	0.43*	0.10

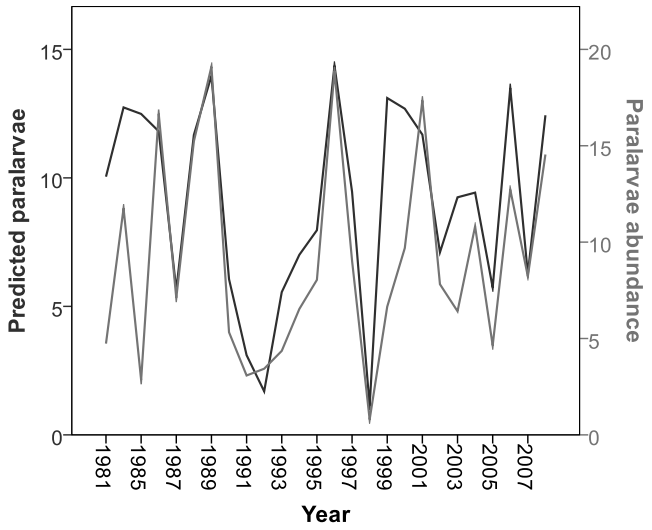

Figure 7. Market squid paralarval abundance and its abundance predicted based on a stepwise regression with ENSO and PDO.

series of the observed paralarval abundance and that predicted by this regression indicate a strong relationship, with most high-frequency variability (rapid shifts in abundance) explained (fig. 7).

DISCUSSION

Several studies have examined the vertical distribution of *D. opalescens* paralarvae, based on plankton tows at discrete depths from 5 or 10 m to several hundred meters depth (Okutani and McGowan 1969; Zeidberg and Hamner 2002). However, previous studies did not sample the neuston. The exceptionally high relative concentration of the paralarvae in the night manta tows (>500-fold more abundant in the manta tows at night than in the day) indicates that a substantial fraction of the paralarvae migrate into the neuston at night. This was critical to our study, since their density from the CalCOFI integrated water-column sampling appeared too low and patchy to allow successful analysis. The nighttime manta tow data provide a readily accessible fishery-independent time series for this key species in the California Current.

We were not surprised that ENSO and the PDO, rather than the local environmental variables synthesized in PC1, entered the regression to explain paralarval abundance. There was high collinearity between PC1 and the ENSO index (a correlation of 0.71), so the two indices explained a highly overlapping component of the variability. Once ENSO had entered the regression, PC1 no longer explained a significant portion of the variability. However, the PDO, which was not significantly correlated with paralarval abundance on its own, explained a significant portion of the remaining variability after ENSO entered the regression. The mechanism underlying this relationship is uncertain but may be related to loss of suitable spawning habitat during El Niño events. Zeidberg et al. (2011) have shown that *D. opalescens* exhibits a narrow temperature range for its preferred spawning habitat (optimum ~12°C, range+ 9–14°C), which is generally found at 20–70 m depth. Depression of isotherms during strong El Niño events deepens the squid's spawning habitat to depths where diminished currents may affect oxygen availability on the dense spawning beds.

Several authors have previously noted the dramatic impact of strong El Niño events on the southern California market squid fishery (Reiss et al. 2004; Zeidberg et al. 2006). This may result from enhanced mortality or deepening of squid spawning beyond the range of the fishery's purse seine gear. Decreased incidence of market squid in the diet of sea lions, a major squid predator, during El Niño events also indicates a major decline of the squid population at those times (Lowry and Carretta 1997). However, more remarkable than the dramatic decline of the squid fishery during an El Niño event has been its recovery, often within a year (fig. 4) (Reiss et al. 2004). Without a fishery-independent time series or other means to assess stock size, it has not been possible to assess whether the stock had in fact recovered to the extent that the improved fishery indicated. The fishery is conducted on nearshore spawning aggregations (Vojkovich 1998). As a result, landings and CPUE likely provide only crude indices of stock abundance, revealing only extreme fluctuations (or possibly changes in availability), such as during major El Niño events. The fishery-independent paralarval time series suggests that the *D. opalescens* spawning stock may recover more slowly than the fishery, consistent with focused spawning ground paralarval surveys following the 1997–98 El Niño event (Zeidberg and Hamner 2002).

Although the CalCOFI surveys were designed to sample the extensive spawning habitat of the Pacific sardine within the southern California Current, rather than the nearshore spawning habitat of the market squid, the sampling grid is extensive, with transects extending to the 20 m isobaths, and consistent over almost 30 years of manta-tow sampling. This provides a fishery-independent paralarval-based index of *D. opalescens* spawning stock size that may be used for research purposes and management of the fishery.

Our data indicate that the squid fishery CPUE is not significantly linearly correlated with the time series of paralarval abundance. In part this is due to apparently a rapid enhancement in the fishery's CPUE as the fishery adopted more efficient gear in the 1980s, switching to purse and drum seines from brail nets (Vojkovich 1998). However, our data based on paralarval abundance also suggest that the population requires several years to recover

from major El Niño events, such as 1983 and 1998 (fig. 6), and is depressed during moderate El Niños, such as prevailed during the early 1990s and around 2005. These fluctuations are not reflected in the fishery CPUE, suggesting that CPUE may not provide a valid index of squid spawning stock (fig. 4, 5). Bias in CPUE-based indices of stock biomass is commonly observed, particularly for aggregating species (Hilborn and Walters 2001).

Paralarval abundance may also be biased as an index of stock biomass, if paralarval mortality is enhanced or squid fecundity is diminished during El Niño events. Field studies indicate a marked decrease in mantle length of *D. opalescens* during El Niño events, apparently due to the interaction of higher temperatures and decreased zooplankton prey on growth and maturity (Lowry and Carretta 1997; Zeidberg and Hamner 2002; Jackson and Domeier 2003). This could influence fecundity, although the weight-specific relationship for fecundity in *D. opalescens* has not been determined. Laboratory experiments indicate that the increased water temperatures and decreased food availability during El Niño events could also lead to increased mortality during the early life history (Vidal et al. 2002), but this needs to be confirmed in the field.

Further research on the reproductive biology and early life history of the squid is required to develop egg production estimates of market squid spawning stock biomass. However, until such research is carried out, the incidence of relatively high CPUE during the early 1990s and 2005–2007 (fig. 4) indicate that it may provide a positively (i.e., optimistically) biased indicator of spawning stock. Paralarval abundance is fishery-independent and may provide a more parsimonious and precautionary representation of stock biomass than CPUE.

Our results suggest that the squid fishery could be more actively managed based on the relationship of ENSO and the PDO with paralarval abundance. The ENSO and PDO indices are known in the months leading up to the fishing season and can therefore be used to modulate catch quotas. Furthermore, given the extended squid spawning season, paralarval abundance estimates from CalCOFI or targeted surveys in the first part of the spawning season could be used to manage fishing activity in the latter part of the season.

ACKNOWLEDGMENTS

We thank Karen Baker, Mason Kortz, and James Connor who assisted with the database; Dale Sweetnam and Briana Brady of California Department of Fish and Game, who provided catch and effort data; and project members Art Miller, Sam McClatchie, Lou Zeidberg, John McGowan, and Ed Weber for valuable discussions. We are grateful to the NOAA Integrated Ocean Observing System program for funding.

LITERATURE CITED

California Department of Fish and Game. 2005. Market Squid Fishery Management Plan. California Department of Fish and Game, Marine Region. Available from: www.dfg.ca.gov/mrd/marketsquid/index.html.

Butler, J. L., D. Fuller, and M. Yaremko. 1999. Age and growth of market squid (*Loligo opalescens*) off California during 1998. Calif. Coop. Oceanic Fish. Invest. Rep. 40: 191–195.

Fields, W. G. 1950. A preliminary report on the fishery and on the biology of the squid *Loligo opalescens*. Calif Fish Game 36: 366–377.

Fields, W. G. 1965. The structure, development, food relations, reproduction, and life history of the squid *Loligo opalescens* Berry. Calif. Dept. Fish Game Fish. Bull. 131: 1–108.

Hilborn, R. and C. Walters. 2001. Quantitative Fisheries Stock Assessment: Choice, Dynamics, and Uncertainty, Kluwer Academic Publishers, Norwell, MA.

Jackson, G. D. and M. L. Domeier. 2003. The effects of an extraordinary El Niño/La Niña event on the age and growth of the squid *Loligo opalescens* off southern California. Mar. Biol. 142: 925–935

Karpov, K. A. and G. M. Caillet. 1978. Feeding dynamics of *Loligo opalescens.* Calif. Dept. Fish. Game, Fish. Bull. 169: 45–66.

Koslow, J. A., R. Goericke, A. Lara-Lopez & W. Watson. In press. Impact of declining intermediate-water oxygen on deepwater fishes in the California Current. Mar. Ecol. Prog. Ser.

Lasker, R. 1985. An egg production method for estimating spawning biomass of pelagic fish: application to the northern anchovy, *Engraulis mordax*. NOAA Tech. Rept. NMFS 36.

Legendre, L. and P. Legendre. 1983. *Numerical Ecology.* New York: Elsevier, pp: 268–288.

Lowry, M. S. and J. V. Carretta. 1999. Market squid (*Loligo opalescens*) in the diet of California sea lions (*Zalophus californianus*) in southern California (1981–1995). Calif. Coop. Oceanic Fish. Invest. Rep. 40: 196–207.

Morejohn, G. V., J. T. Harvey and L. T. Krasnow. 1978. The importance of *Loligo opalescens* in the food web of marine vertebrates in Monterey Bay, California. Calif. Dept. Fish Game Fish. Bull. 169: 67–98.

Moser, H. G., R. L. Charter, W. Watson, D. A. Ambrose, J. L. Butler, S. R. Charter and E. M. Sandknop. 2000. Abundance and distribution of rockfish (*Sebastes*) larvae in the Southern Californbia Bight in relation to environmental conditions and fishery exploitation. Calif. Coop. Oceanic Fish. Invest. Rep. 41: 32–47.

Moser, H. G., R. L. Charter, W. Watson, D. A. Ambrose, K. T. Hill, P. E. Smith, J.L. Butler, E.M. Sandknop and S.R. Charter. 2001. The CalCOFI ichthyoplankton time series: potential contributions to the management of rocky-shore fishes. Calif. Coop. Oceanic Fish. Invest. Rep. 42: 112–128.

Moser, H.G. & W. Watson. 1990. Distribution and abundance of early life history stages of the California halibut, *Paralichthys californicus* and comparisons with the fantail sole, *Xystreurys liolepis*. Calif. Dept. Fish Game Fish. Bull. 174: 31–84.

Okutani, T. and J. A. McGowan. 1969. Systematics, distribution, and abundance of the epiplanktonic squid (Cephalopoda, Decapoda) larvae of the California Current April, 1954–March, 1957. Bull. Scripps Institution of Oceanography 14: 1–90.

Porzio, D. and B. Brady. 2007. Status of the Fisheries Report on Market Squid. Los Alamitos, California: California Department of Fish and Game: http://www.dfg.ca.gov/marine/status/report2006/squid.pdf .

Pyper, B.J. and R.M. Peterman. 1998. Comparison of methods to account for autocorrelation in correlation analyses of fish data. Can. J. Fish. Aquat. Sci. 55: 2127–2140.

Recksiek, C.W. and J. Kashiwada. 1979. Distribution of larval squid, *Loligo opalescens*, in various nearshore locations. Calif. Coop. Oceanic Fish. Invest. Rep. 20: 31–34.

Reiss, S. C., M. R. Maxwell, J. R. Hunter, and A. Henry. 2004. Investigating environmental effects on population dynamics of *Loligo opalescens* in the Southern California Bight. Calif. Coop. Oceanic Fish. Invest. Rep. 45: 87–98.

Sweetnam, D. (ed.). 2010. Review of selected California fisheries for 2009: coastal pelagic finfish, market squid, red abalone, Dungeness crab, Pacific herring, groundfish/nearshore live-fish, highly migratory species, kelp, California halibut, and sandbasses. Calif. Coop. Oceanic Fish. Invest. Rep. 51: 14–38.

Vidal, E.A.G., F.P. DiMarco, J.H. Wormuth and P.G. Lee. 2002. Influence of temperature and food availability on survival, growth and yolk utilization in hatchling squid. Bull. Mar. Sci. 71: 915–931.

Vojkovich, M. 1998. The California fishery for market squid (*Loligo opalesces*). Calif. Coop. Oceanic Fish. Invest. Rep. 39: 55–60.

Zeidberg, L. and W. Hamner. 2002. Distribution of squid paralarvae, *Loligo opalescens* (Cephalopoda: Myopsida), in the Southern California Bight in the three years following the 1997–1998 El Niño. Mar. Biol. 141: 111–122.

Zeidberg, L.D., W.M. Hamner, N.P. Nezlin and A. Henry. 2006. The fishery for California market squid (*Loligo opalescens*) (Cephalopoda: Myopsida), from 1981 through 2003. Fish. Bull. 104: 46–59.

Zeidberg, L.D., G. Isaac, C.L. Widmer, H. Neumeister and W.F. Gilly. 2011. Egg capsule hatch rate and incubation duration of the California market squid, Doryteuthis (*Loligo*) *opalescens*: insights from laboratory manipulations. Mar. Ecol. doi:10.1111/j.1439–0485.2011.00445.x.

INSTRUCTIONS TO AUTHORS

CalCOFI Reports is a peer-reviewed journal. Papers submitted for publication in the "Scientific Contributions" section are read by two or more referees and by arbiters when necessary; "Symposium" papers are invited by the convener of the annual symposium and are reviewed and edited at the convener's discretion. The "Reports, Review, and Publications" section contains newsworthy information on the status of stocks and environmental conditions; the papers in this section are not peer reviewed; the CalCOFI Editorial Board will not consider unsolicited review papers.

The CalCOFI Editorial Board will consider for publication in the "Scientific Contributions" section manuscripts not previously published elsewhere that address the following in relation to the North Pacific, the California Current, and the Gulf of California: marine organisms; marine chemistry, fertility, and food chains; marine fishery modeling, prediction, policy, and management; marine climatology, paleoclimatology, ecology, and paleoecology; marine pollution; physical, chemical, and biological oceanography; and new marine instrumentation and methods.

Submission Guidelines

Submissions must be received no later than January 15 of the year in which publication is sought. Please submit manuscripts as MS word documents in electronic format via email to: calcofi_coordinator@coast.ucsd.edu. (use Word; see "Manuscript Guidelines" below for more details on preparing tables and figures). Manuscript should be submitted to:

CalCOFI Coordinator
Southwest Fisheries Science Center
8604 La Jolla Shores Drive
La Jolla, California 92037-1508 USA
Fax: (858) 546-5656

The manuscript should contain the following parts:

1. A title page containing the manuscript's title, your name, your institutional affiliation and contact information (address, telephone and fax numbers, e-mail address), and a word count
2. An abstract of no more than 150 words that succinctly expresses only the manuscript's most central points, using the active voice
3. Body of the text, including any footnotes
4. Literature cited, in alphabetical order
5. Acknowledgments, if any
6. Tables
7. Figures and captions

Manuscript Guidelines

Length. Unless previously approved by the Scientific Editor, manuscripts should not exceed 6,000 words, including title page, abstract, text body, footnotes, acknowledgments, and literature cited but excluding figures and tables.

Text. Double-space all elements of the text, allow margins of at least 1 inch on all sides, and use a standard font (such as Times or Times New Roman) no smaller than 12 points. Number the pages consecutively. Eliminate all nonessential formatting. Indicate subordination of heads consistently; for example, use all caps for the main heads, boldface for the next level, and italics for the third level. To indent paragraphs, use the tab key, not the space bar or a "style" feature of any sort. Never use letters for numbers or vice versa; in other words, do not type the lowercase "el" for the number "one" or the capital letter "oh" for zero. Use your word-processor's automatic footnoting feature to insert footnotes. Acknowledgments, if included, should be placed at the end of the text and may include funding sources. Place the entire text (title page, abstract, text body, footnotes, acknowledgments, and literature cited) in one document file, and label it with your name—for example, "Smith text.doc."

Tables. Use your word-processor's *Table* feature, rather than spaces or tabs, to create the columns and rows. Use *minimal* formatting, and do not insert vertical or horizontal rules. Double-space the tables and use a standard font, such as Times or Times New Roman. Number the tables consecutively, and provide a brief title for each. Place explanatory material and sources in a note beneath the table. Place the tables in a separate file labeled, for example, "Smith tables.doc," and place this on the disk with the text file. Provide one printout of each table, gathered together at the end of the text printout submitted. Be sure each table is specifically referred to in the text.

Figures. Figures must be in black and white. Submit figures—whether drawings, graphs, or photographs—as high-resolution electronic files as separate files. Label the files, for example, "Smith fig 1" and "Smith fig 2." The preferred file formats are JPG and PDF. If you are submitting as a PDF, please embed all type. In the printed volume figures will appear in black and white only and may be reduced from their original size. Contributors are advised to make a trial reduction of complex figures to ensure that patterns, shading, and letters will remain distinct when reduced. Include a north arrow and latitude and longitude lines on maps. Use consistent labels and abbreviations and the same style of lettering for all figures if possible. Number figures consecutively, and specifically refer to each in the text. Provide a caption for each figure. Gather the captions together, and place them at the end of the electronic text file, following the "Literature Cited" section; include the captions in the printouts.

Editorial Style

For matters of editorial style, contributors should consult recent editions of *CalCOFI Reports.* Contributors may also refer to *The Chicago Manual of Style*, 15th ed. Whenever possible, write in the first person, and use active verbs. Use the full name of a

person, organization, program, or agency when mentioning it for the first time in your manuscript. Double-check the spelling of non-English words, and include special characters such as accents and umlauts. Use correct SI symbols for *units of measure* in figures, tables, and text (other units may be given in parentheses). Prepare *equations* in accordance with similar expressions in the printed literature.

Cite *sources* in the text as Smith (1999) or Smith and Jones (2000) or (Smith and Jones 2000; Gabriel et al. 1998) (the latter when there are three or more authors). There should be no comma between author and date.

In the "Literature Cited" section, show sources alphabetically by the first author's surname, and secondarily in chronological order with earliest dates first. Provide surnames and first initials of all authors; do not use "et al." for multi-authored works. No source should appear in the "Literature Cited" section unless it is specifically cited in the text, tables, or figure captions. *Personal communications* and *unpublished documents* should not be included in the "Literature Cited" section but may be cited in the text in parentheses; use footnotes only when parentheses will not suffice. Abbreviate journal titles to match BIOSYS usage. Each source must be complete according to the following guidelines:

ARTICLE IN A JOURNAL:

Barnes, J. T., L. D. Jacobson, A. D. MacCall, and P. Wolf. 1992. Recent population trends and abundance estimates for the Pacific sardine (*Sardinops sagax*). Calif. Coop. Oceanic Fish. Invest. Rep. 33:60–75.

BOOK:

Odum, E. P. 1959. Fundamentals of ecology. 2nd ed. Philadelphia: Saunders. 546 pp.

CHAPTER IN A BOOK:

Wooster, W. S., and J. L. Reid Jr. 1963. Eastern boundary currents. *In* The sea, M. N. Hill, ed. New York: Interscience Pub., pp. 253–280.

If your manuscript is accepted for publication, we will provide further guidance regarding preparing it for editing.